Electronic Supporting Information

A Topologically Chiral Catenane that is Not Topologically Chiral

Noel Pairault,[=] Federica Rizzi,[=] David Lozano, Ellen M. G. Jamieson, Graham Tizzard, Stephen M. Goldup*

Department of Chemistry, University of Southampton, Highfield, Southampton, SO17 1BJ

[=]These authors contributed equally
*s.goldup@soton.ac.uk

1. CONTENTS

2. General Experimental Information

Unless otherwise stated, all reagents were purchased from commercial sources (Acros Organics, Alfa Aesar, Fisher Scientific, FluoroChem, Sigma Aldrich and VWR) and used without further purification. $[Cu(CH_3CN)_4]PF_6$ was prepared as described by Pigorsch and Köckerling.[1] Anhydrous solvents were purchased from Acros Organics. Petrol refers to the fraction of petroleum ether boiling in the range 40-60 °C. THF refers to tetrahydrofuran. EDTA-$NH_{3(aq.)}$ solution refers to an aqueous solution of NH_3 (17% w/w) with sodium-ethylenediaminetetraacetate. Rochelle $salt_{(aq.)}$ solution refers to an aqueous solution of potassium sodium tartrate. $CDCl_3$ (without stabilising agent) was distilled over $CaCl_2$ and K_2CO_3 prior to use. Unless otherwise stated, all reaction mixtures were performed in oven dried glassware under an inert N_2 atmosphere with purchased anhydrous solvents. Unless otherwise stated experiments carried out in sealed vessels were performed in CEM microwave vials, with crimped aluminium caps, with PTFE septa.

Flash column chromatography was performed using Biotage Isolera-4 or Isolera-1 automated chromatography system. SiO_2 cartridges were purchased commercially Biotage (SNAP or ZIP (50 μm), or Sfär (60 μm) irregular silica, default flow rates). Analytical TLC was performed on pre-coated silica gel plates on aluminum (0.25 mm thick, 60F254, Merck, Germany) and observed under UV light (254 nm) or visualised with $KMnO_4$, vanilin or ninhydrin stains.

All melting points were determined using a Griffin apparatus. NMR spectra were recorded on Bruker AV400 or AV500 instrument, at a constant temperature of 298 K. Chemical shifts are reported in parts per million from low to high field and referenced to residual solvent. Coupling constants (*J*) are reported in Hertz (Hz). Standard abbreviations indicating multiplicity were used as follows: m = multiplet, quint = quintet, q = quartet, t = triplet, d = doublet, s = singlet, app. = apparent, br = broad, sept = septet. Signal assignment was carried out using 2D NMR methods (COSY, NOESY, ROESY, TOCSY, HSQC or HMBC) where necessary. In some cases, complex multiplets with multiple contributing proton signals, exact assignment was not possible. In interlocked compounds, all proton signals corresponding to axle components are in lower case, and all proton signals corresponding to the macrocycle components are in upper case.

Low resolution mass spectrometry was carried out by the mass spectrometry services at University of Southampton (Waters TQD mass spectrometer equipped with a triple quadrupole analyser with UHPLC injection [BEH C18 column; CH_3CN-H_2O gradient {0.2% formic acid}]). High resolution mass spectrometry was carried out either by the mass spectrometry services at the University of Southampton (MaXis, Bruker Daltonics, with a Time of Flight (TOF) analyser; samples were introduced to the mass spectrometer via a Dionex Ultimate 3000 autosampler and uHPLC pump in a gradient of 20% CH_3CN in ^{n}hexane to 100% acetonitrile (0.2% formic acid) over 5-10 min at 0.6 mL/min; column: Acquity UPLC BEH C18 (Waters) 1.7 micron 50 × 2.1mm).

Circular dichroism spectra were acquired on an Applied Photo-physics Chirascan spectropolarimeter, recorded using Applied Photophysics software Ver. 4.2.0 in dried spectroscopic grade CH_3CN at a concentration range of <50 μM, in a quartz cell of 1 cm path length, at a temperature of 293 K.

Stereochemical purities of COOMe/OH/NH-OTBDMS catenanes were determined by Chiral Stationary Phase HPLC on a Waters Acquity Arc Instrument at 303 K, with ^{n}hexane-EtOH isocratic eluents, employing Regis Technologies (S,S)-Whelk-O1 (1-(3,5-dinitrobenzamido)-1,2,3,4-tetrahydrophenanthrene stationary phase (5 μm, column dimensions 25 cm x 4.6 mm). Samples of catenane **5** were analysed by REACH Separations (Nottingham, UK) using Supercritical Fluid Chromatography, at 313 K and 125 BarG, with isocratic 1:1 MeOH:CO_2 (0.1% v/v NH_3), employing Chiralpak IK tris(3-chloro-5-methylphenyl)carbamate stationary phase (5 μm, column dimensions 25 cm x 4.6 mm).

Compounds **2**[2], **S1**[3,4], **S4**[5], **S7**[6], **S18**[2], **S20**[2], **S21**[7], piperidinium acetate[8], benzyl azide[9] tris[(1-benzyl-1H-1,2,3-triazol-4-yl)methyl]amine (TBTA)[10] were synthesised following literature procedures.

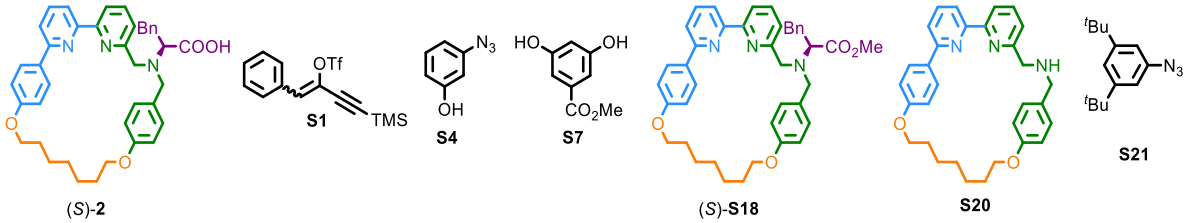

3. Synthesis of Pre-Macrocycle (*Z*)-1

3.1. Synthetic schemes

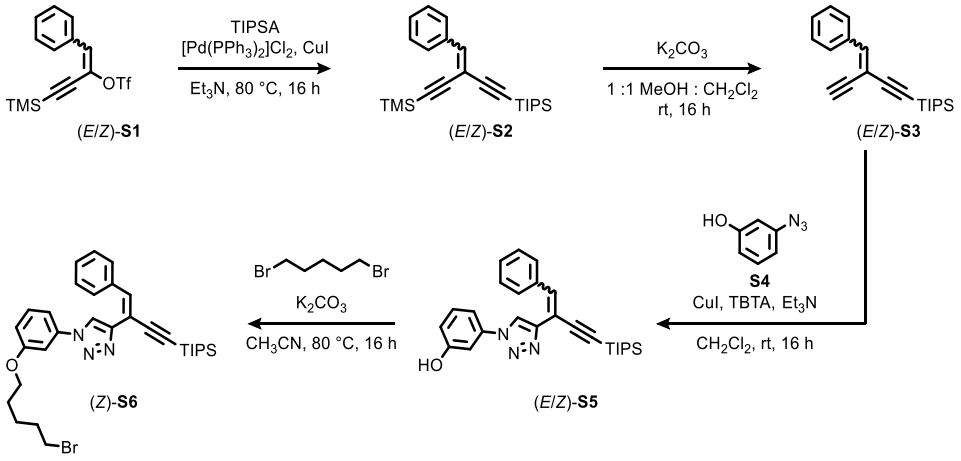

Scheme S1: Synthetic route to compound (*Z*)-**S6**.

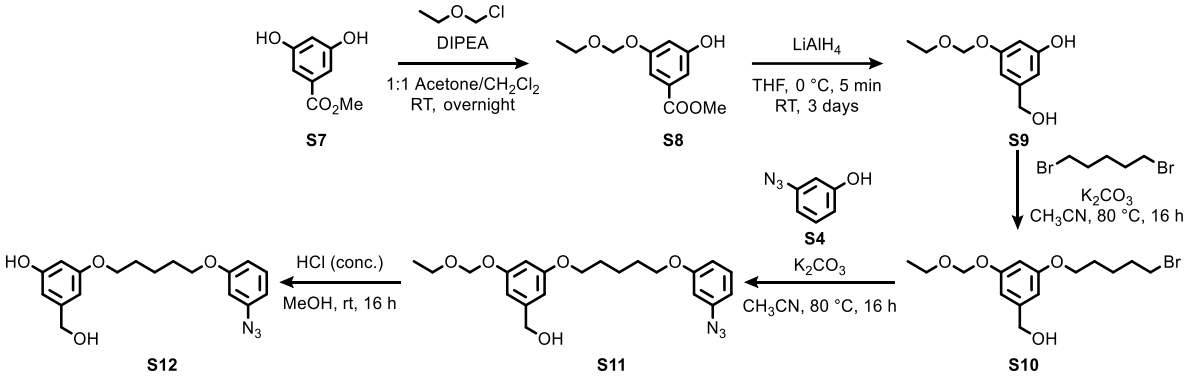

Scheme S2: Synthetic route to compound **S12**.

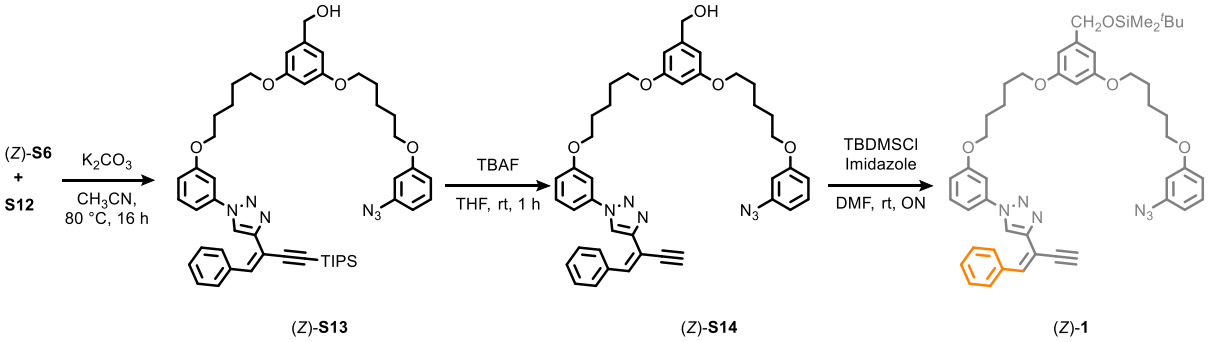

Scheme S3: Synthetic route to compound (*Z*)-**1**.

3.2. compounds leading to (*Z*)-S6

(*E/Z*)-S2

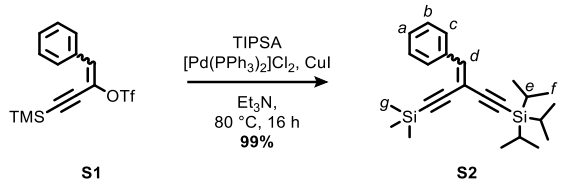

S1 **S2**

To a solution of (*E/Z*)-**S1** (3.52 g, 10.1 mmol), $Pd(PPh_3)_2Cl_2$ (355 mg, 0.506 mmol), and CuI (193 mg, 1.01 mmol) in anhydrous Et_3N (200 mL) at 80 °C was added (triisopropylsilyl)acetylene (2.10 mL, 12.0 mmol) *via* syringe. The solution was stirred for 16 h, then concentrated *in vacuo*. Chromatography (petrol) afforded (*E/Z*)-**S2** (64 : 36 *dr* Figure S1) as a yellow oil (3.83 g, 99%).

^{1}H NMR (400 MHz, $CDCl_3$) δ_H 7.98-7.87 (m, 2H, ***H***$_c$), 7.38-7.28 (m, 6H, ***H***$_a$, ***H***$_b$), 7.04 - 7.02 (2 s, 1H, ***H***$_d$), 1.15-1.09 (m, 21H, ***H***$_e$, ***H***$_f$), 0.26 - 0.23 (2 s, 9H, ***H***$_g$).

^{13}C NMR (101 MHz, $CDCl_3$) δ_C 144.1, 143.7, 135.6, 135.6, 129.3, 129.4, 129.4, 129.3, 129.3, 128.4, 128.3, 106.5, 104.8, 103.8, 103.7, 103.6, 102.1, 101.3, 99.0, 93.4, 90.5, 18.8, 18.8, 11.5, 0.0, -0.2.

HR-EI-MS (+ve): *m/z* = 337.1803 $[M\text{-}^{i}Pr]^{+\bullet}$ (100) calc. for $C_{21}H_{29}Si_2$ 337.1802; *m/z* = 380.2353 $[M]^{+\bullet}$ (32.3) calc. for $C_{24}H_{36}Si_2$ 380.2350.

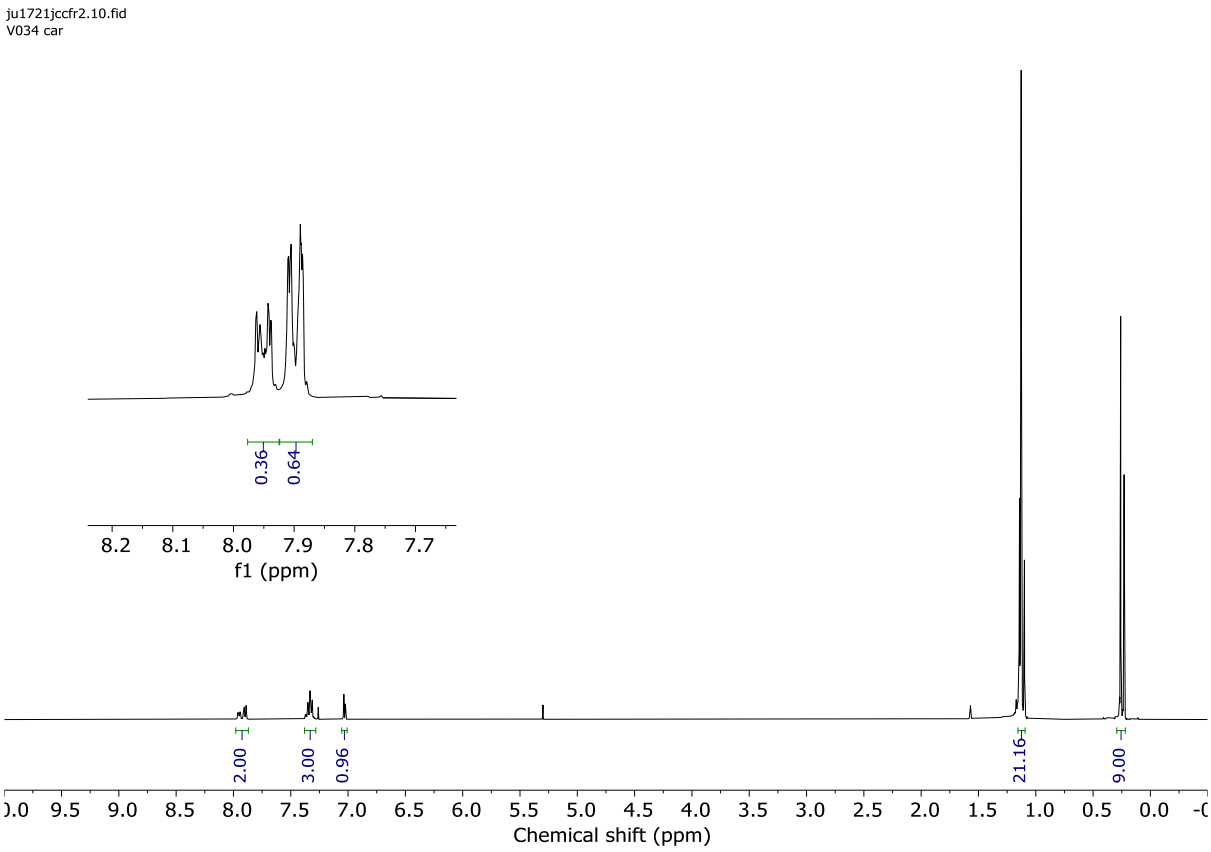

Figure S1: ^{1}H NMR ($CDCl_3$, 400 MHz, 298 K) of (*E/Z*)-**S2**.

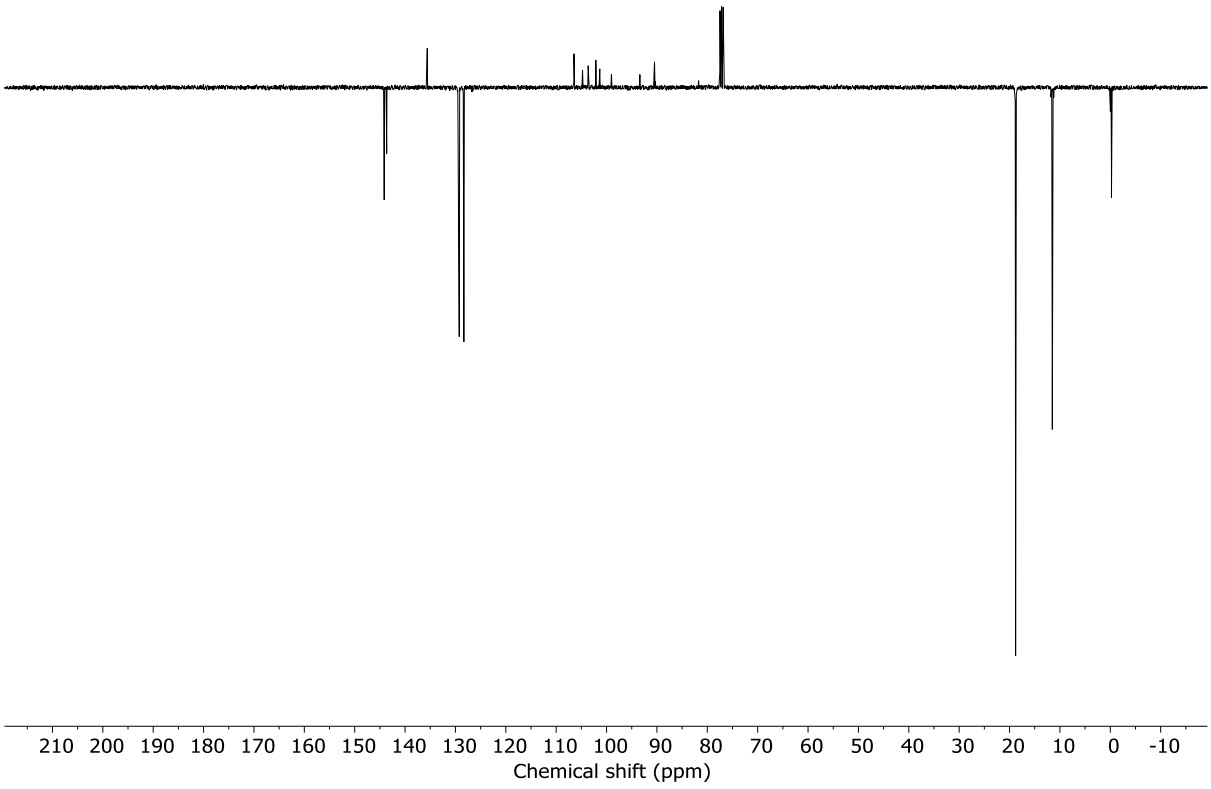

Figure S2: JMOD NMR ($CDCl_3$, 101 MHz, 298 K) of (*E/Z*)-**S2**.

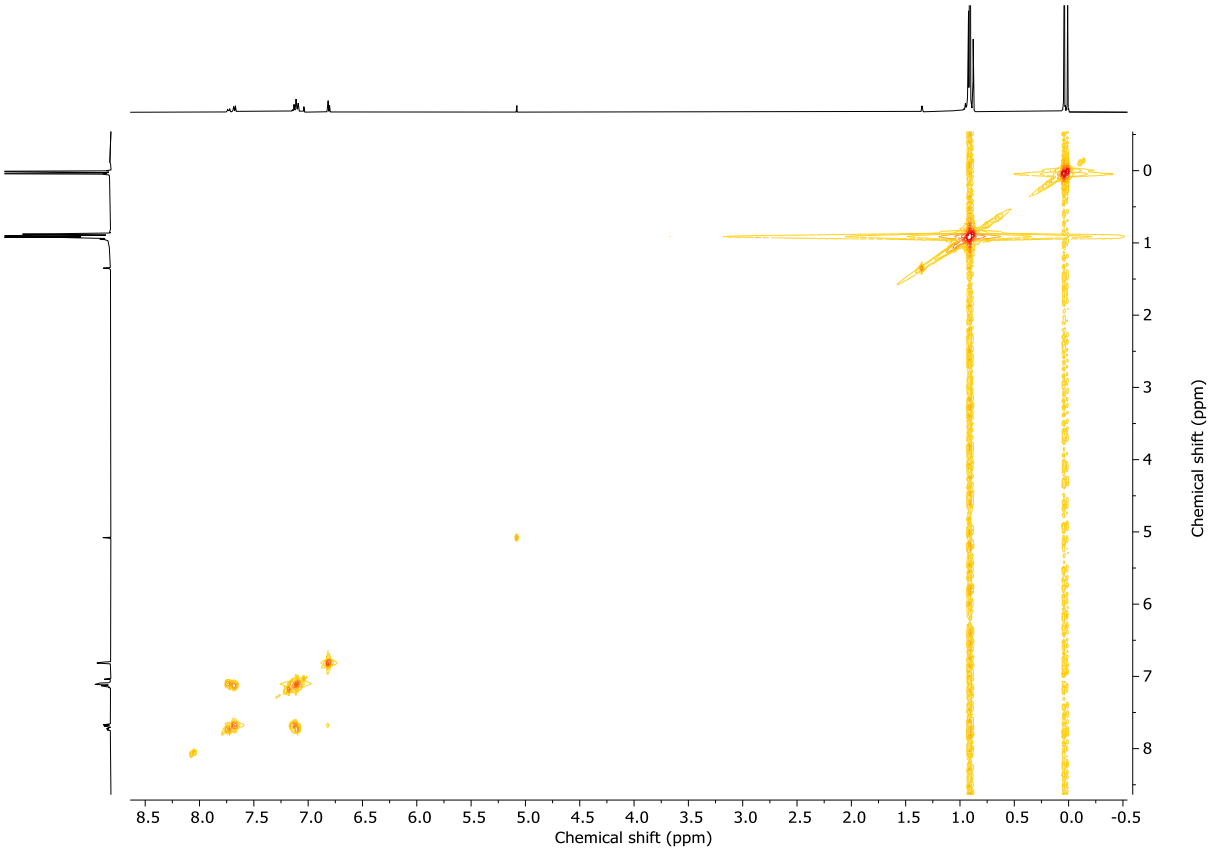

Figure S3: COSY NMR ($CDCl_3$, 298 K) of (*E/Z*)-**S2**.

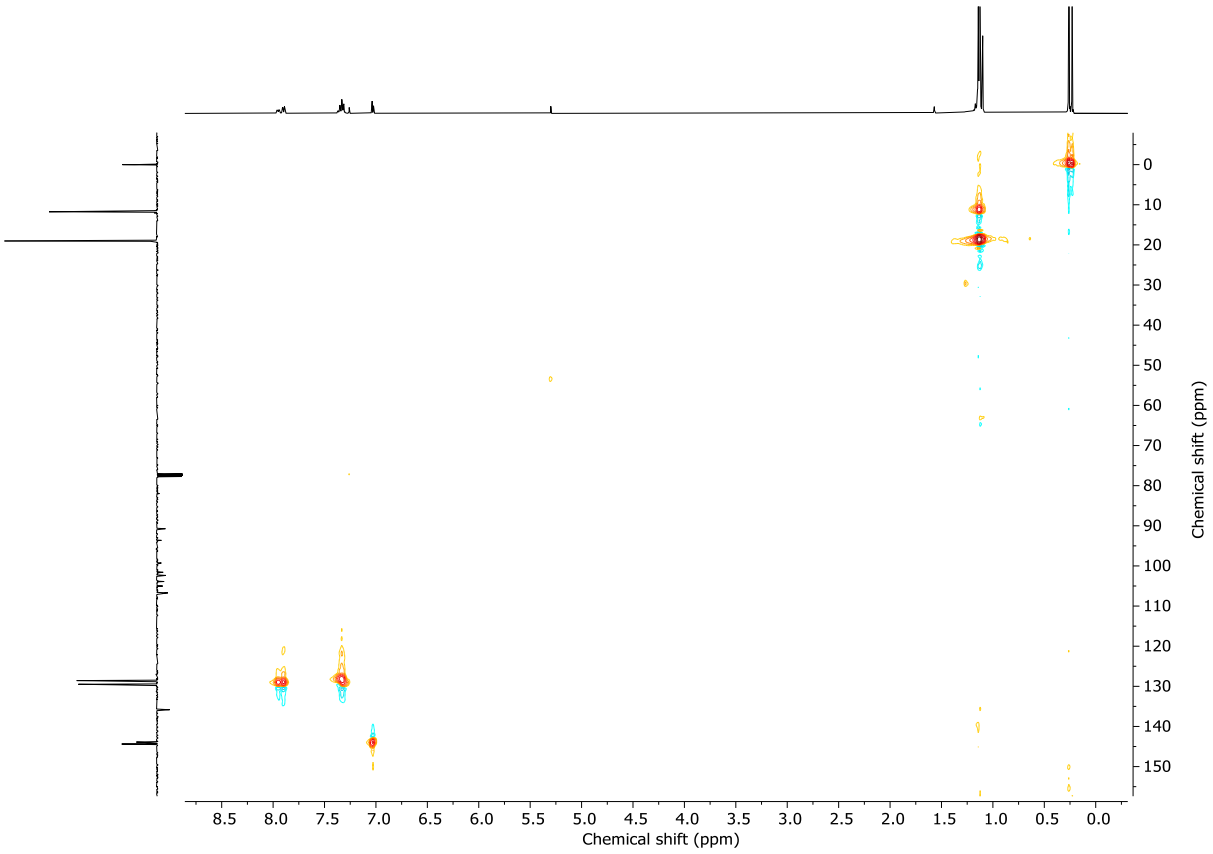

Figure S4: HSQC NMR ($CDCl_3$, 298 K) of (*E/Z*)-**S2**.

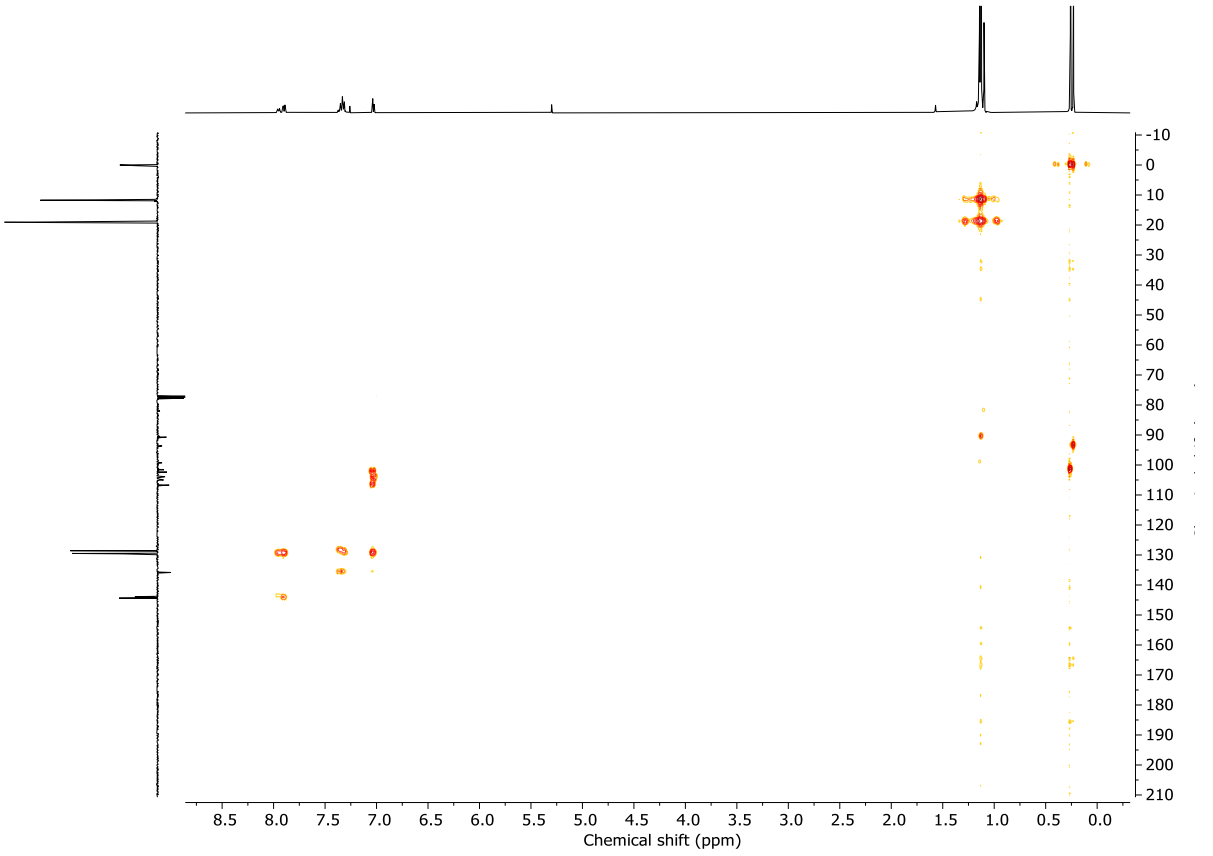

Figure S5: HMBC NMR ($CDCl_3$, 298 K) of (*E/Z*)-**S2**.

Compound (*E/Z*)-S3

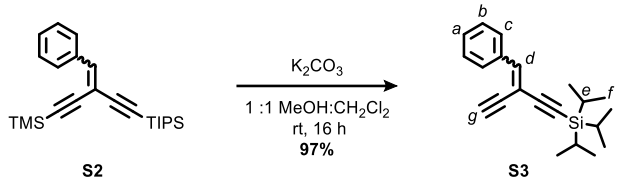

To a stirred solution of (*E/Z*)-**S2** (64 : 36 *dr*, 2.79 g, 7.33 mmol) in a MeOH-CH_2Cl_2 (1 : 1, 74 mL) was added K_2CO_3 (5.07 g, 36.7 mmol). The resulting suspension was stirred for 16 h, then filtered through Celite® and concentrated *in vacuo*. Chromatography (100% petrol) afforded (*E/Z*)-**S3** (52 : 48 *dr* Figure S6) as a pale-yellow oil (2.19 g, 97%).

^{1}H NMR (400 MHz, $CDCl_3$) δ_H 7.99-7.84 (m, 2H, ***H***$_c$), 7.40-7.30 (m, 3H, ***H***$_a$, ***H***$_b$), 7.12 - 7.08 (2 s, 1H, ***H***$_d$), 3.37 - 2.98 (2 s, 1H, ***H***$_g$), 1.17-1.11 (m, 21H, ***H***$_e$, ***H***$_f$).

^{13}C NMR (101 MHz, $CDCl_3$) δc 145.3, 144.9, 135.3, 135.3, 129.6, 129.5, 129.3, 129.1, 128.5, 128.4, 106.2, 103.3, 102.6, 102.5, 99.1, 90.5, 83.5, 83.1, 80.8, 75.8, 18.8, 18.7, 11.5 (x2).

HR-EI-MS (+ve): *m/z* = 195.0626 $[C_{13}H_{11}Si]^{+\bullet}$ (100) calc. for $C_{13}H_{11}Si$ 195.0630; *m/z* = 265.1409 $[M\text{-}^iPr]^{+\bullet}$ (72.1) calc. for $C_{18}H_{21}Si$ 265.1407; *m/z* = 308.1958 $[M]^{+\bullet}$ (15.2) calc. for $C_{21}H_{28}Si$ 308.1955.

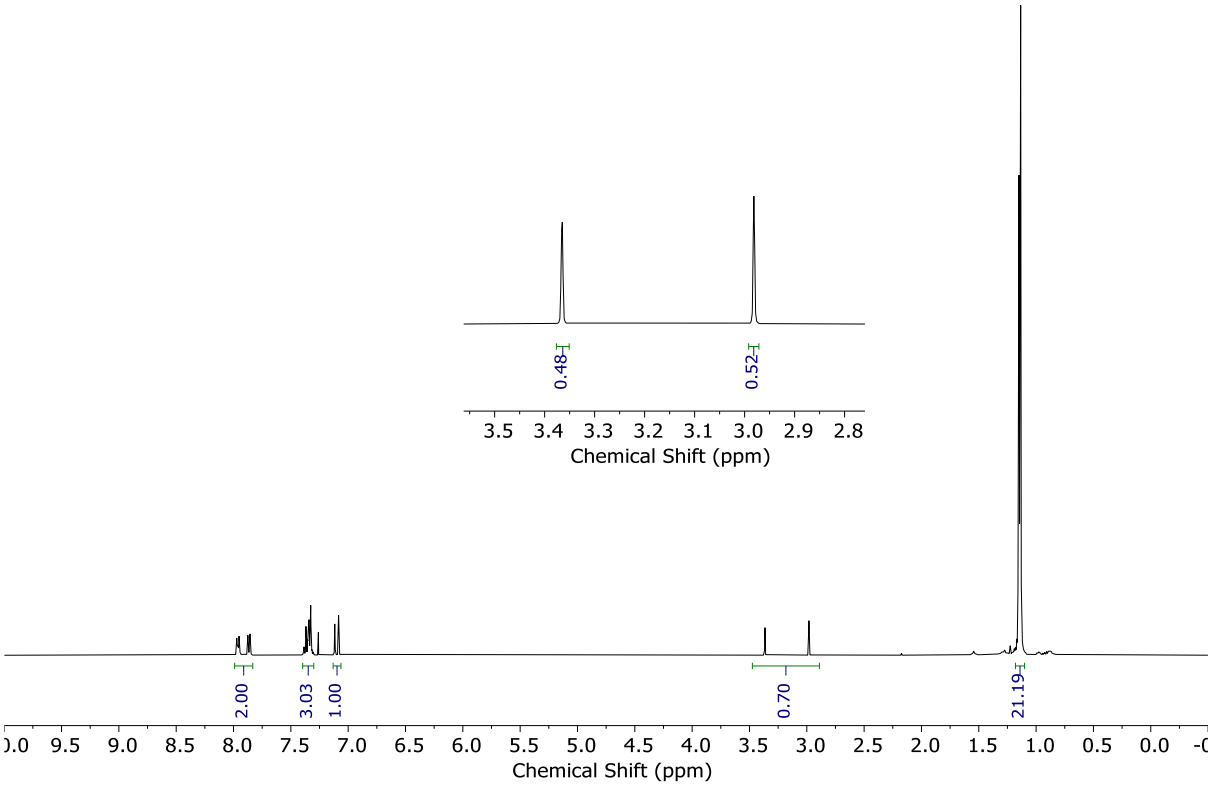

Figure S6: ^{1}H NMR ($CDCl_3$, 400 MHz, 298 K) of (*E/Z*)-**S3**.

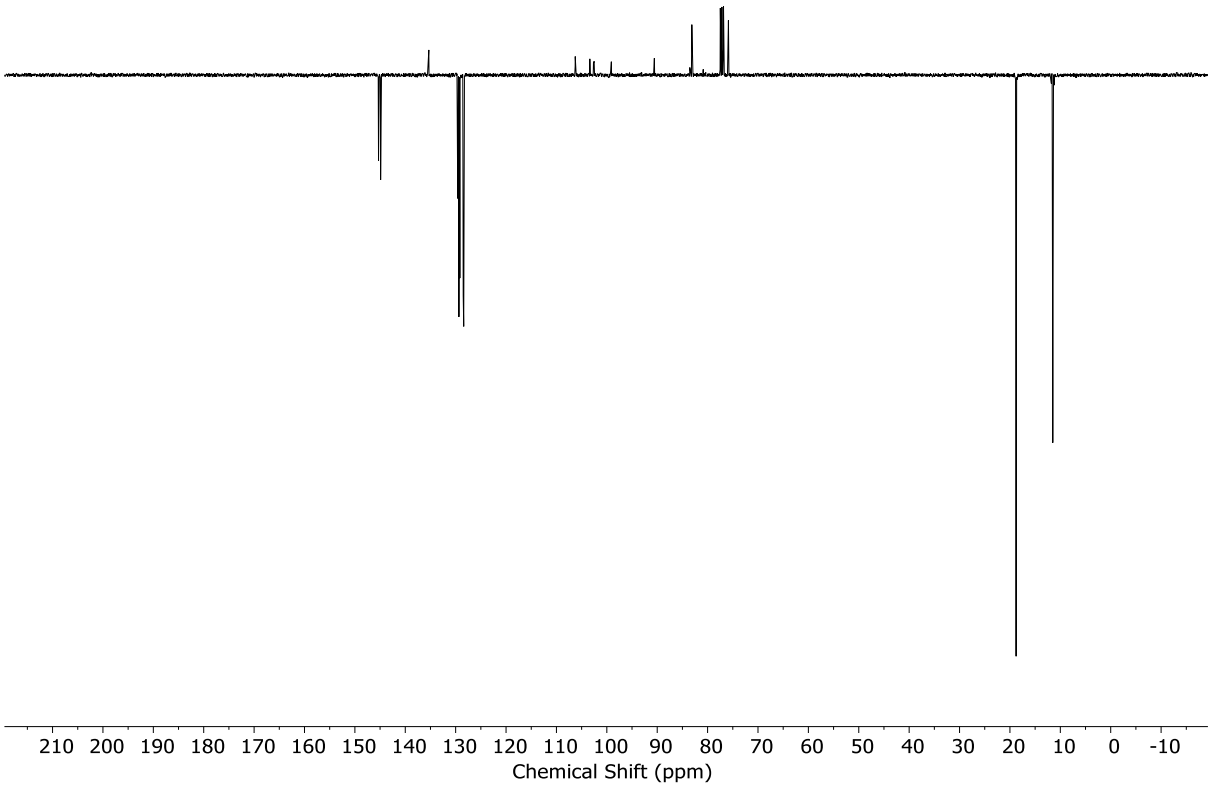

Figure S7: J-MOD NMR ($CDCl_3$, 101 MHz, 298 K) of (*E/Z*)-**S3**.

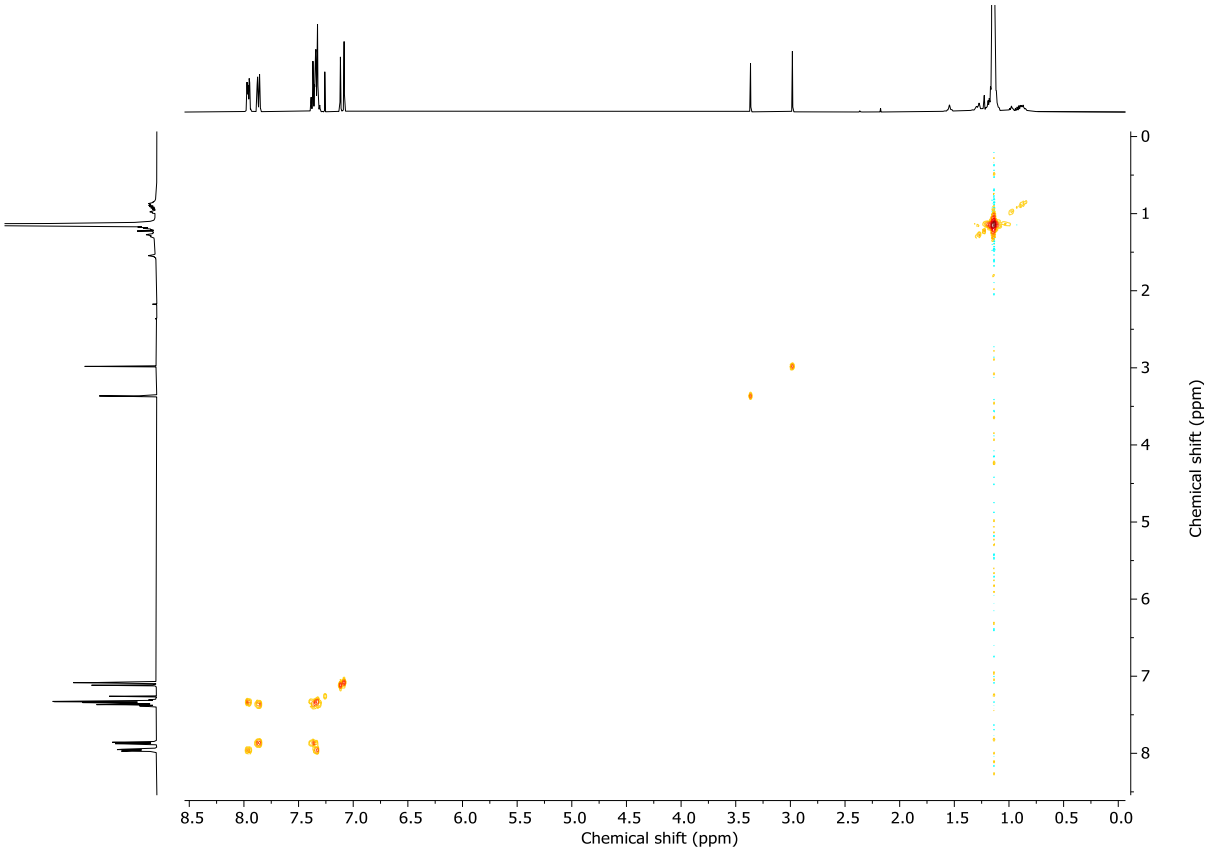

Figure S8: COSY NMR ($CDCl_3$, 298 K) of (*E/Z*)-**S3**.

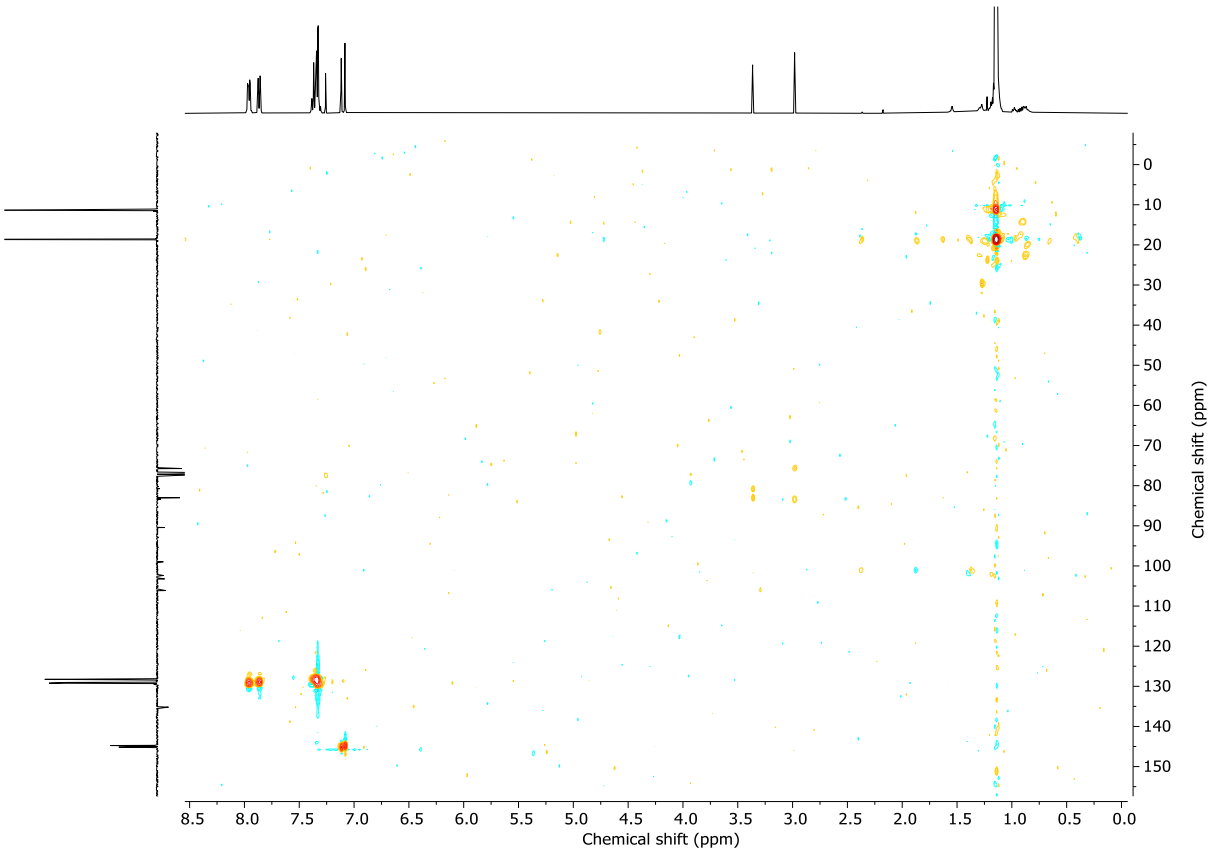

Figure S9: HSQC NMR ($CDCl_3$, 298 K) of (*E/Z*)-**S3**.

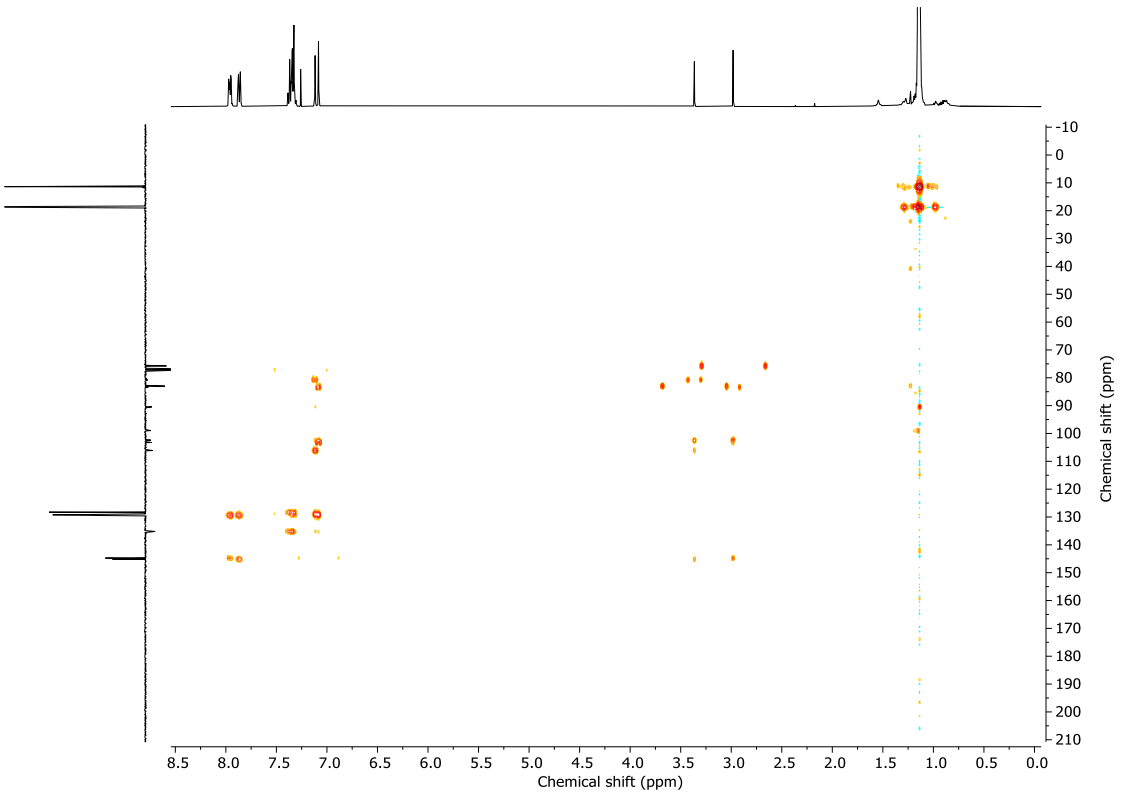

Figure S10: HMBC NMR ($CDCl_3$, 298 K) of (*E/Z*)-**S3**.

Compound S5

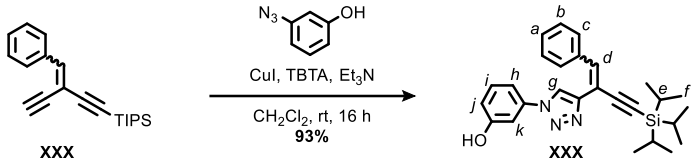

XXX **XXX**

To a solution of **S3** (92 mg, 0.30 mmol), (*E/Z*)-**S4** (48 : 52 *dr*, 62.5 mg, 0.462 mmol), CuI (6 mg, 0.03 mmol) and TBTA (20 mg, 0.037 mmol) in CH_2Cl_2 (3 mL) was added Et_3N (42 μL, 0.30 mmol). The solution was stirred for 16 h, then diluted with CH_2Cl_2 (10 mL), washed with EDTA-$NH_{3(aq)}$ (0.1 M, 20 mL), and the aqueous phase extracted with CH_2Cl_2 (3 x 10 mL). The combined organic layers were dried ($MgSO_4$), filtered, and concentrated *in vacuo*. Chromatography (CH_2Cl_2-acetone 0 : 100 to 5 : 95) afforded (*E/Z*)-**S5** (56 : 44 *dr* Figure S11) as a red oil (123 mg, 93%).

^{1}H NMR (400 MHz, $CDCl_3$) δ_H 9.56 (s, 2H, $\boldsymbol{H}_{OH}$), 8.57 (app. dt, *J* = 8.7, 2.2, 2H, $\boldsymbol{H}_k$), 8.20-8.12 (m, 2H, $\boldsymbol{H}_{c'}$, $\boldsymbol{H}_{g'}$), 7.85 (s, 1H, $\boldsymbol{H}_{d'}$), 7.78 (s, 1H, $\boldsymbol{H}_g$), 7.44-7.23 (m, 6H, $\boldsymbol{H}_a$, $\boldsymbol{H}_b$, $\boldsymbol{H}_c$, $\boldsymbol{H}_d$, $\boldsymbol{H}_i$), 7.02-6.93 (m, 1H, $\boldsymbol{H}_j$), 6.88 (app. dddd, *J* = 48.9, 8.0, 2.3, 0.9, 1H, $\boldsymbol{H}_h$), 1.28-1.12 (m, 42H, $\boldsymbol{H}_e$, $\boldsymbol{H}_{e'}$, $\boldsymbol{H}_f$, $\boldsymbol{H}_{f'}$);

^{13}C NMR (101 MHz, $CDCl_3$) δ_C 159.1, 159.1, 148.4, 144.7, 140.4, 137.6, 137.4, 135.7, 135.6, 135.3, 130.6, 130.5, 129.8, 129.2, 129.0, 128.7, 128.6, 128.4, 120.7, 119.8, 117.1, 117.0, 113.0, 109.6, 109.6, 109.2, 108.9, 108.8, 106.8, 104.1, 99.6, 92.1, 18.9, 18.9, 11.5, 11.5.

HR-ESI-MS (+ve): *m/z* = 444.2476 $[M+H]^+$ calc. for $C_{27}H_{34}N_3OSi$ 443.2466; *m/z* = 466.2295 $[M+Na]^+$ calc. for $C_{27}H_{33}N_3NaOSi$ 466.2285.

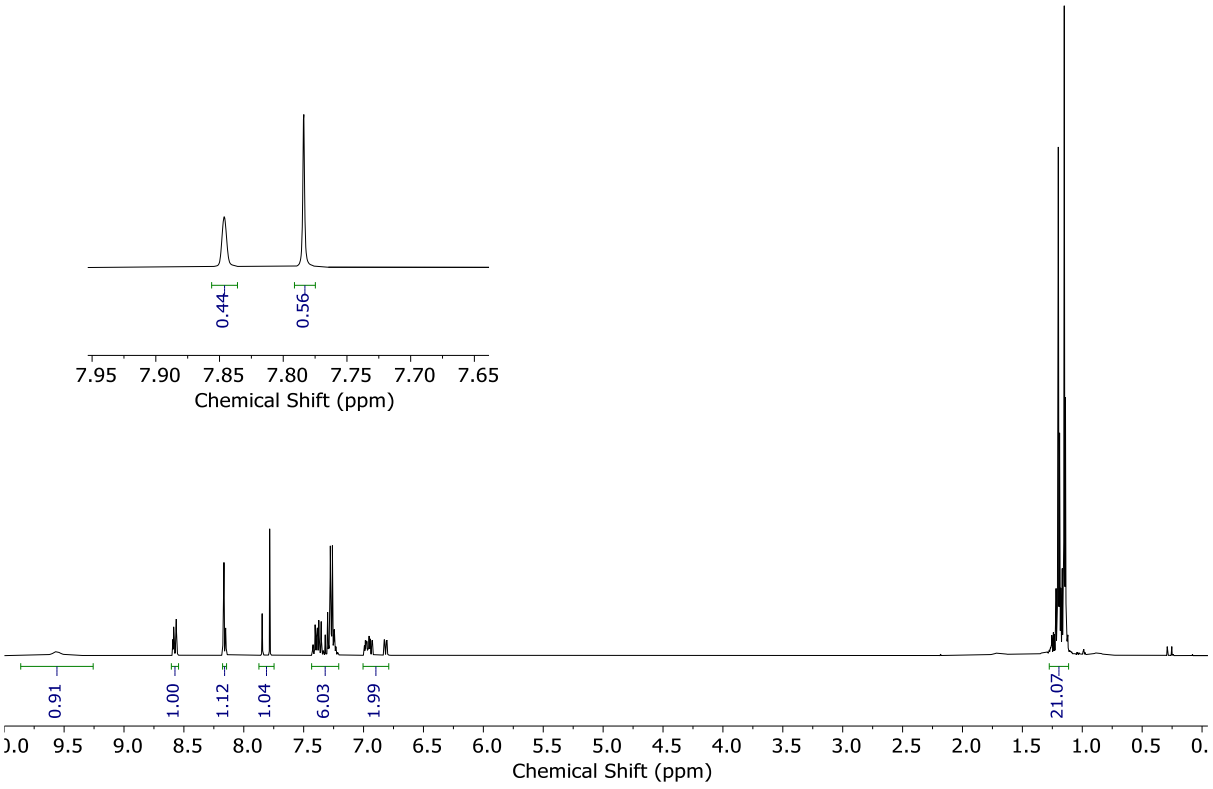

Figure S11: ^{1}H NMR ($CDCl_3$, 400 MHz, 298 K) of (*E/Z*)-**S5**.

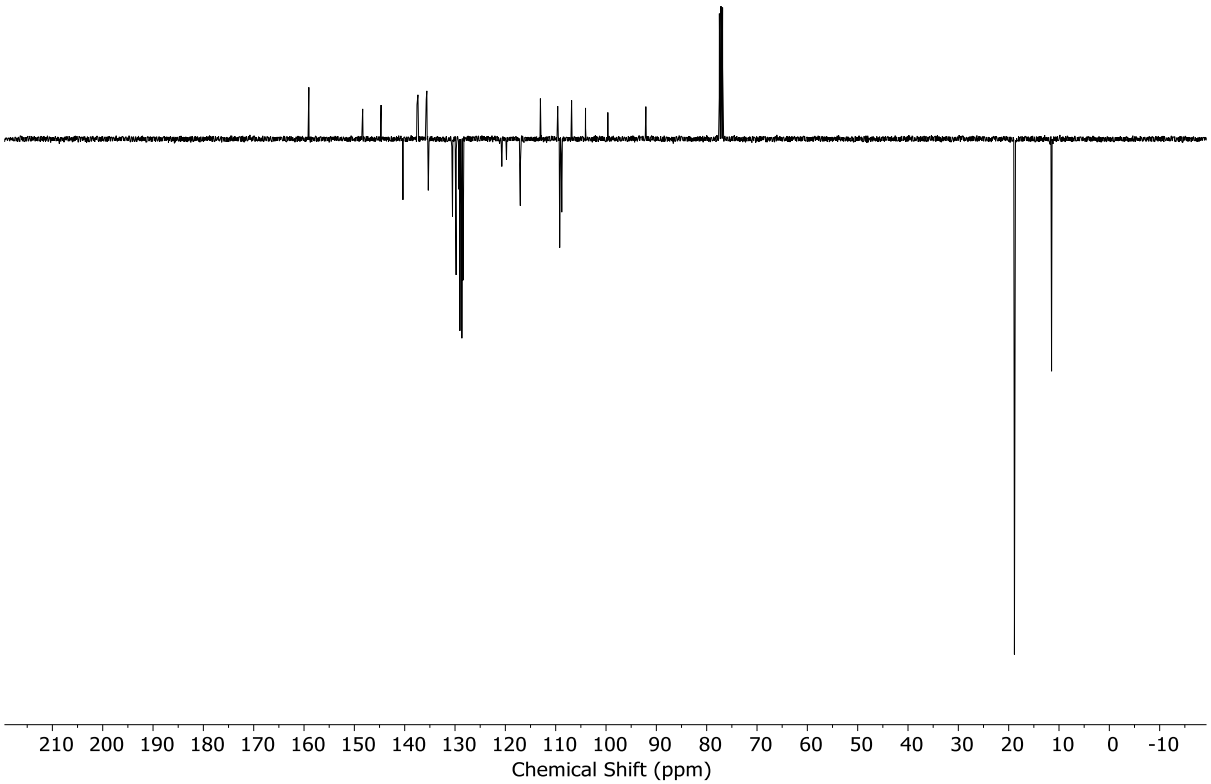

Figure S12: JMOD NMR ($CDCl_3$, 101 MHz, 298 K) of (*E/Z*)-**S5**.

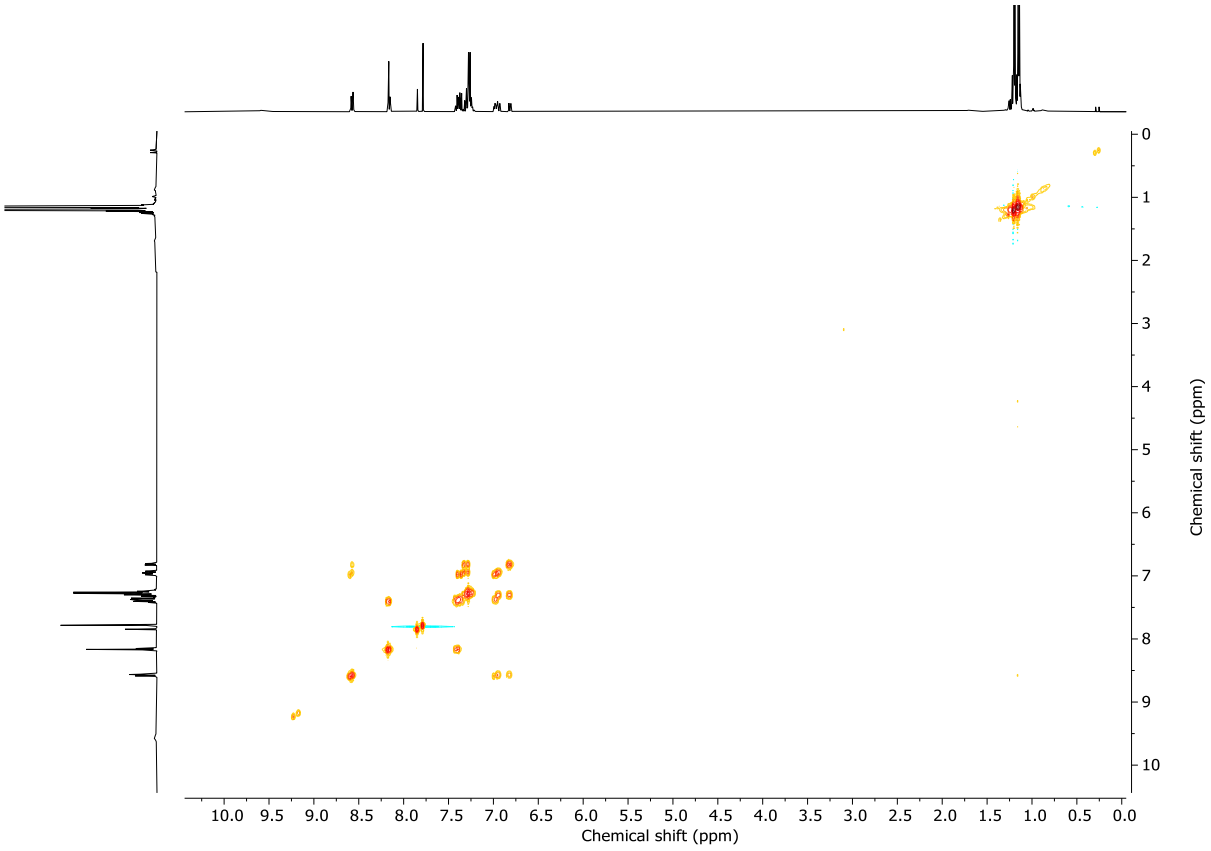

Figure S13: COSY NMR ($CDCl_3$, 298 K) of (*E/Z*)-**S5**.

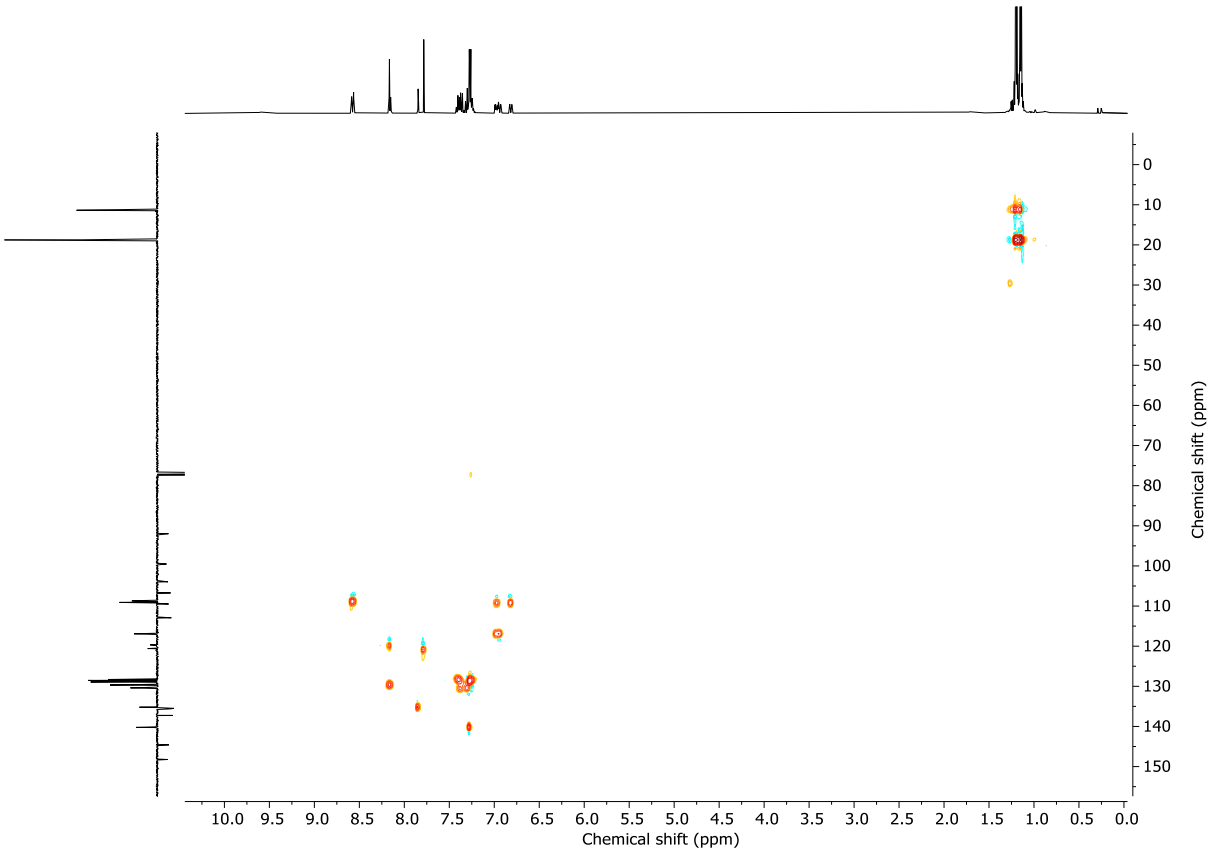

Figure S14: HSQC NMR ($CDCl_3$, 298 K) of (*E*/*Z*)-**S5**.

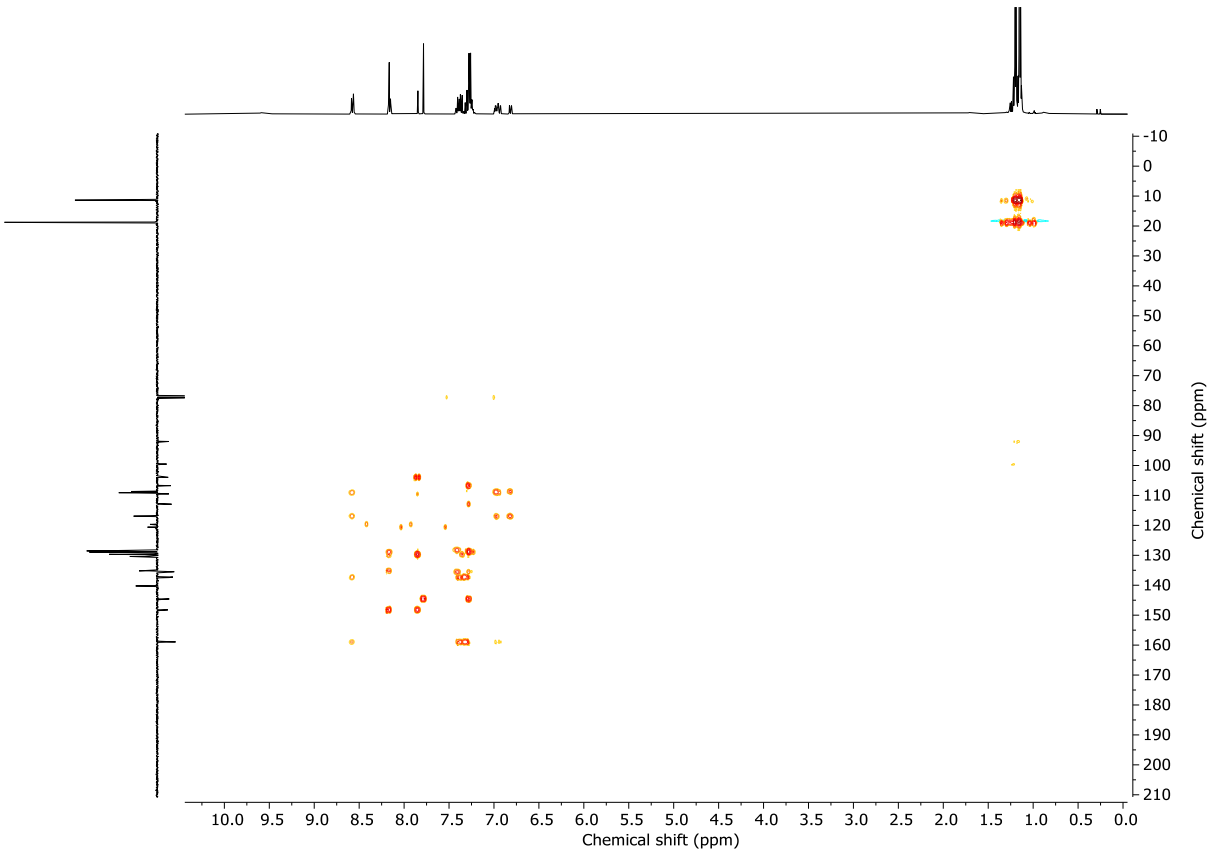

Figure S15: HMBC NMR ($CDCl_3$, 298 K) of (*E*/*Z*)-**S5**.

Compound (*Z*)-S6

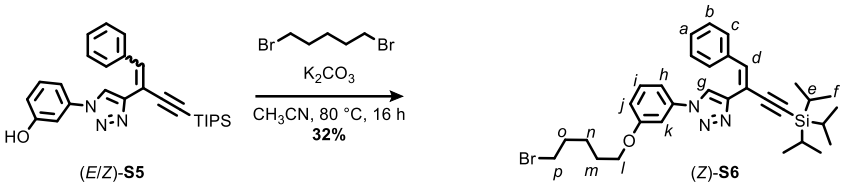

To a stirred solution of (*E/Z*)-**S5** (56 : 44 *dr*, 2.48 g, 5.58 mmol) and 1,5-dibromopentane (1.90 mL, 13.9 mmol) at 80 °C in CH_3CN (28 mL) was added K_2CO_3 (3.89 g, 28.2 mmol), and the resulting solution was stirred for 16 h. The mixture was allowed to cool rt, filtered through Celite® and concentrated *in vacuo*. Chromatography (petrol-CH_2Cl_2 1 : 1) gave (*Z*)-**S6** (>98 : <2 *dr* Figure S16 as a pale yellow oil (1.05 g, 32%). Note: this separation is extremely challenging. It was carried out manually using a 50 cm x 6 cm column of SiO_2.

^{1}H NMR (400 MHz, $CDCl_3$) δ_H 7.81 (s, 1H, ***H***$_g$), 7.44-7.40 (m, 2H, ***H***$_c$), 7.37 (t, *J* = 8.2, 1H, ***H***$_i$), 7.32-7.25 (m, 4H, ***H***$_a$, ***H***$_b$, ***H***$_k$), 7.22 (s, 1H, ***H***$_d$), 7.15 (ddd, *J* = 8.0, 2.0, 0.9, 1H, ***H***$_h$), 6.94 (ddd, *J* = 8.4, 2.5, 0.9, 1H, ***H***$_j$), 4.03 (t, *J* = 6.3, 2H, ***H***$_l$), 3.45 (t, *J* = 6.7, 2H, ***H***$_p$), 1.99-1.91 (m, 2H, ***H***$_o$), 1.90-1.80 (m, 2H, ***H***$_m$), 1.69-1.60 (m, 2H, ***H***$_n$), 1.17-1.13 (m, 21H, ***H***$_e$, ***H***$_f$).

^{13}C NMR (101 MHz, $CDCl_3$) δ_C 160.1, 145.2, 139.5, 138.0, 135.9, 130.6, 129.4, 128.5, 128.4, 121.2, 115.3, 113.3, 112.1, 108.0, 106.7, 90.9, 68.2, 33.6, 32.5, 28.4, 24.9, 18.9, 11.5.

HR-ESI-MS (+ve): *m/z* = 592.2352 $[M+H]^+$ (calc. for $C_{32}H_{43}{}^{79}BrN_3OSi$ 592.2353), 614.2177 $[M+Na]^+$ (calc. for $C_{32}H_{42}BrN_3NaOSi$ 614.2173).

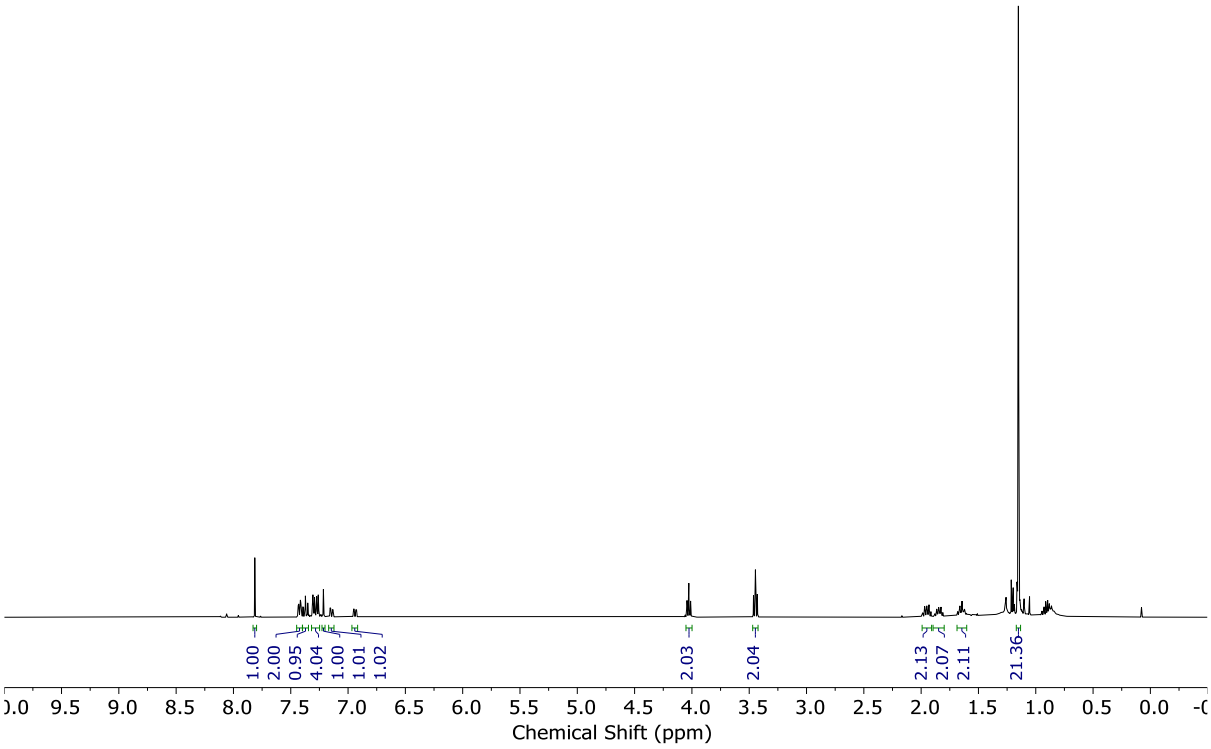

Figure S16: ^{1}H NMR ($CDCl_3$, 400 MHz, 298 K) of (*Z*)-**S6**.

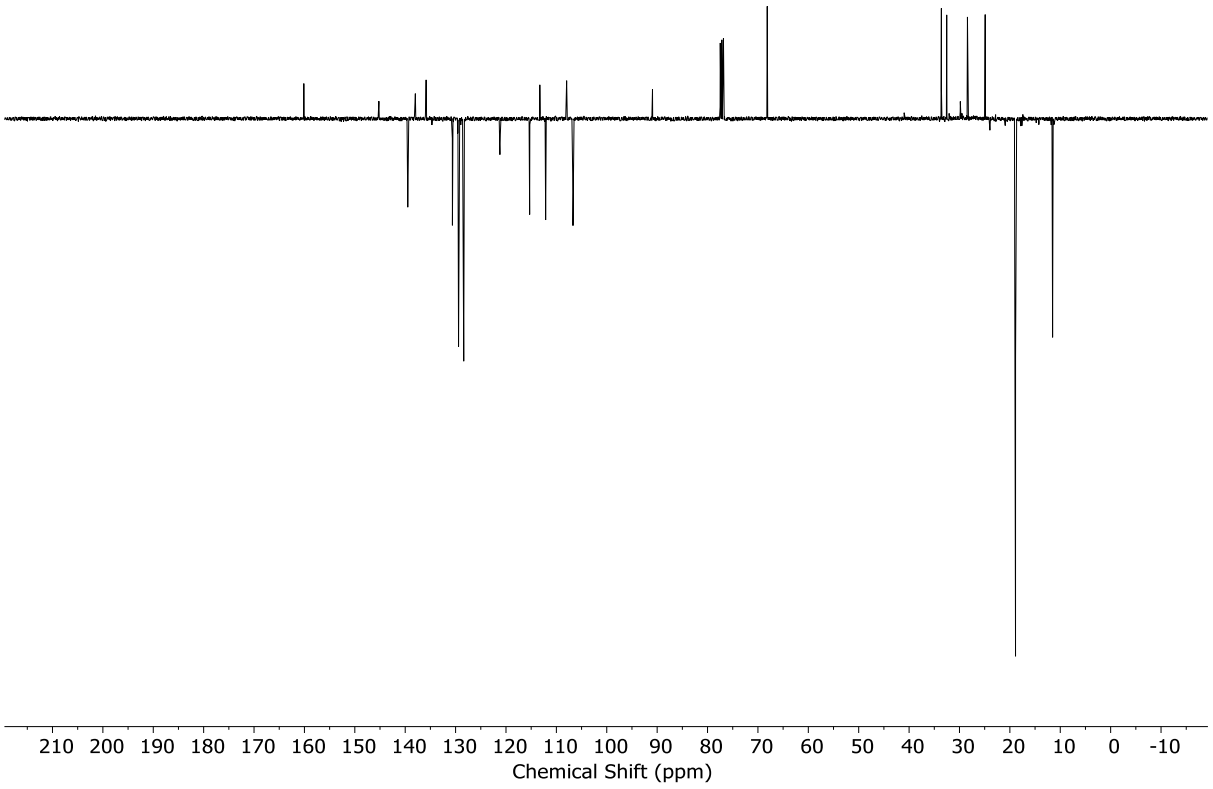

Figure S17: JMOD NMR ($CDCl_3$, 101 MHz, 298 K) of (*Z*)-**S6**.

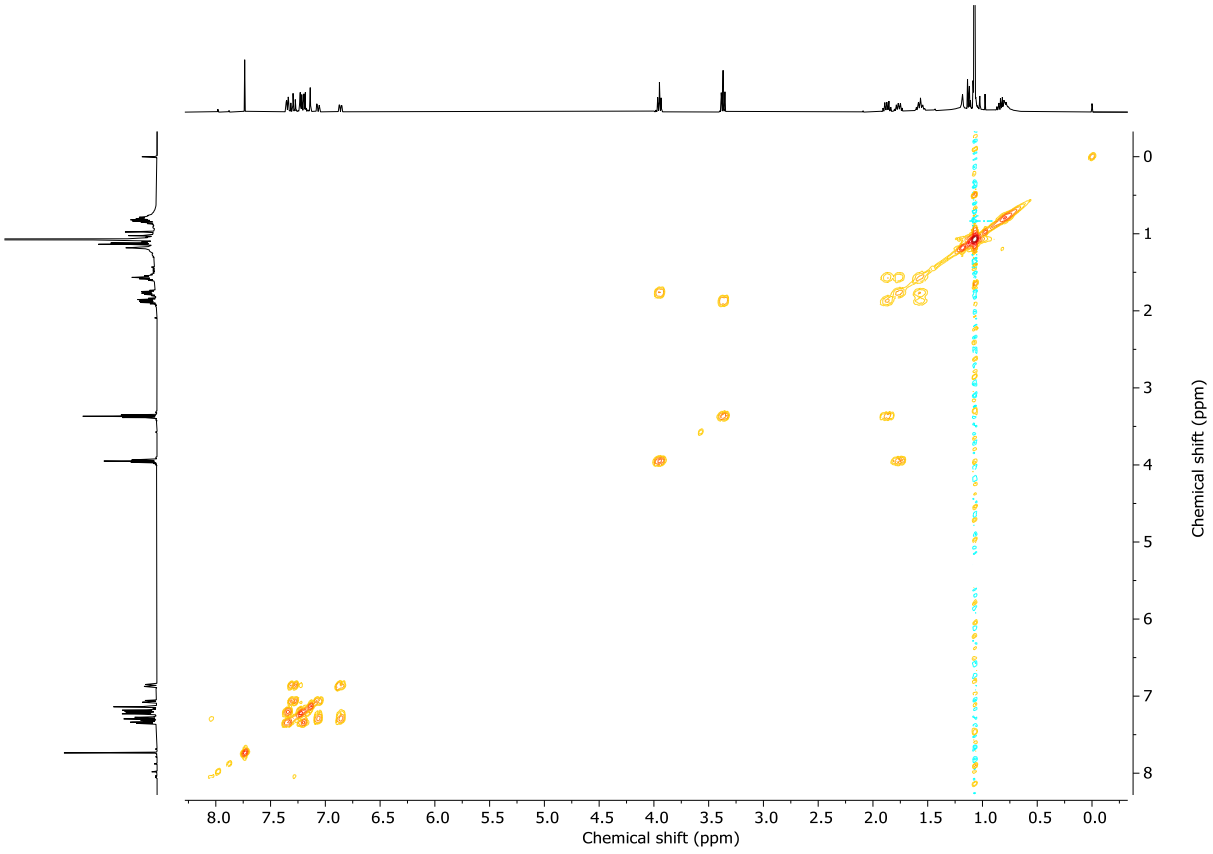

Figure S18: COSY NMR ($CDCl_3$, 298 K) of (*Z*)- **S6**.

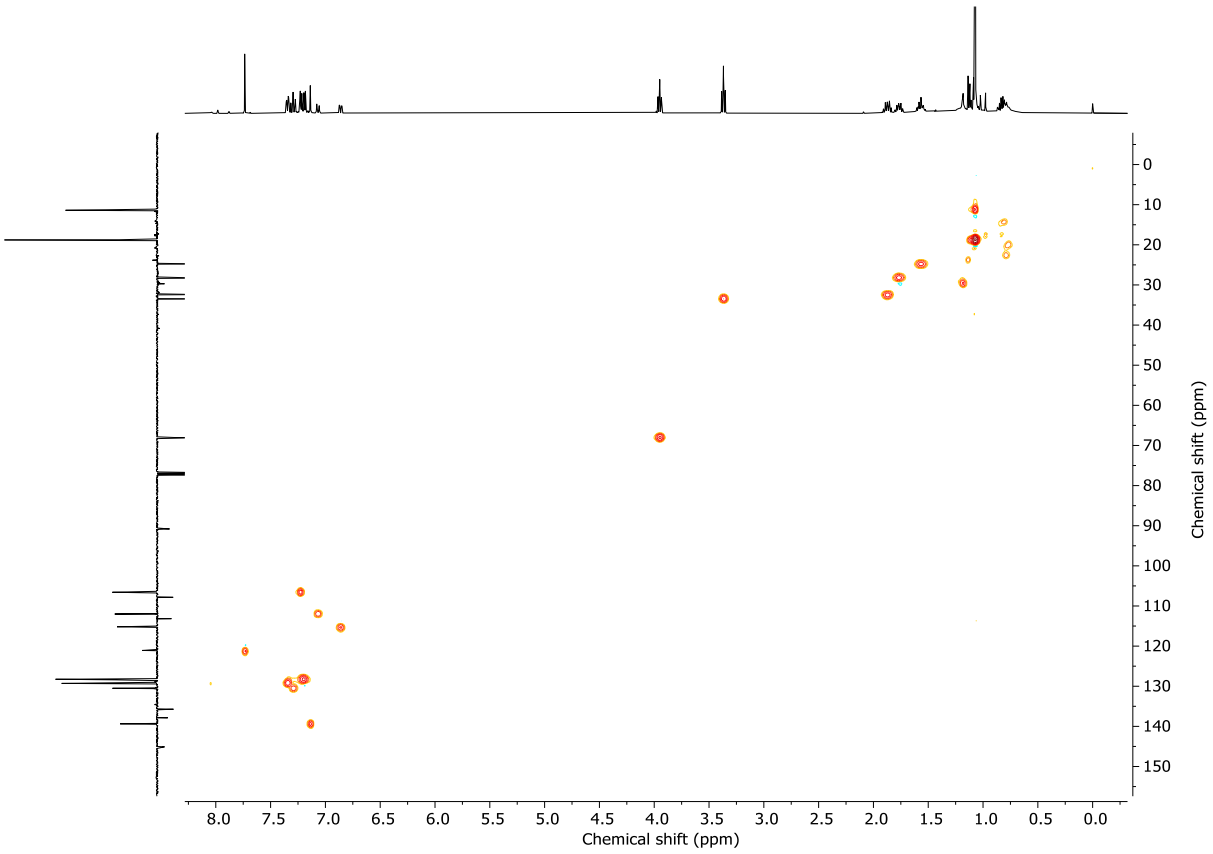

Figure S19: HSQC NMR ($CDCl_3$, 298 K) of (*Z*)- **S6**.

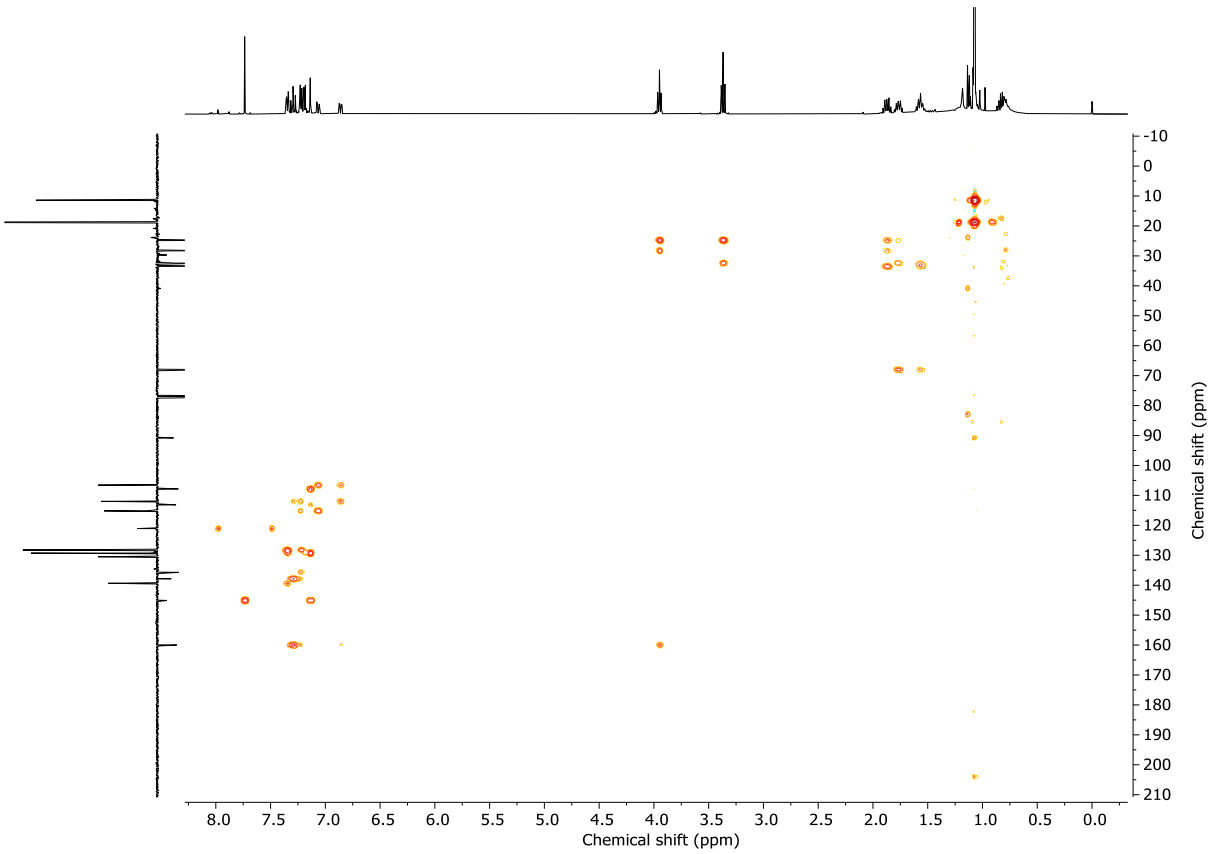

Figure S20: HMBC NMR ($CDCl_3$, 298 K) of (*Z*)- **S6**.

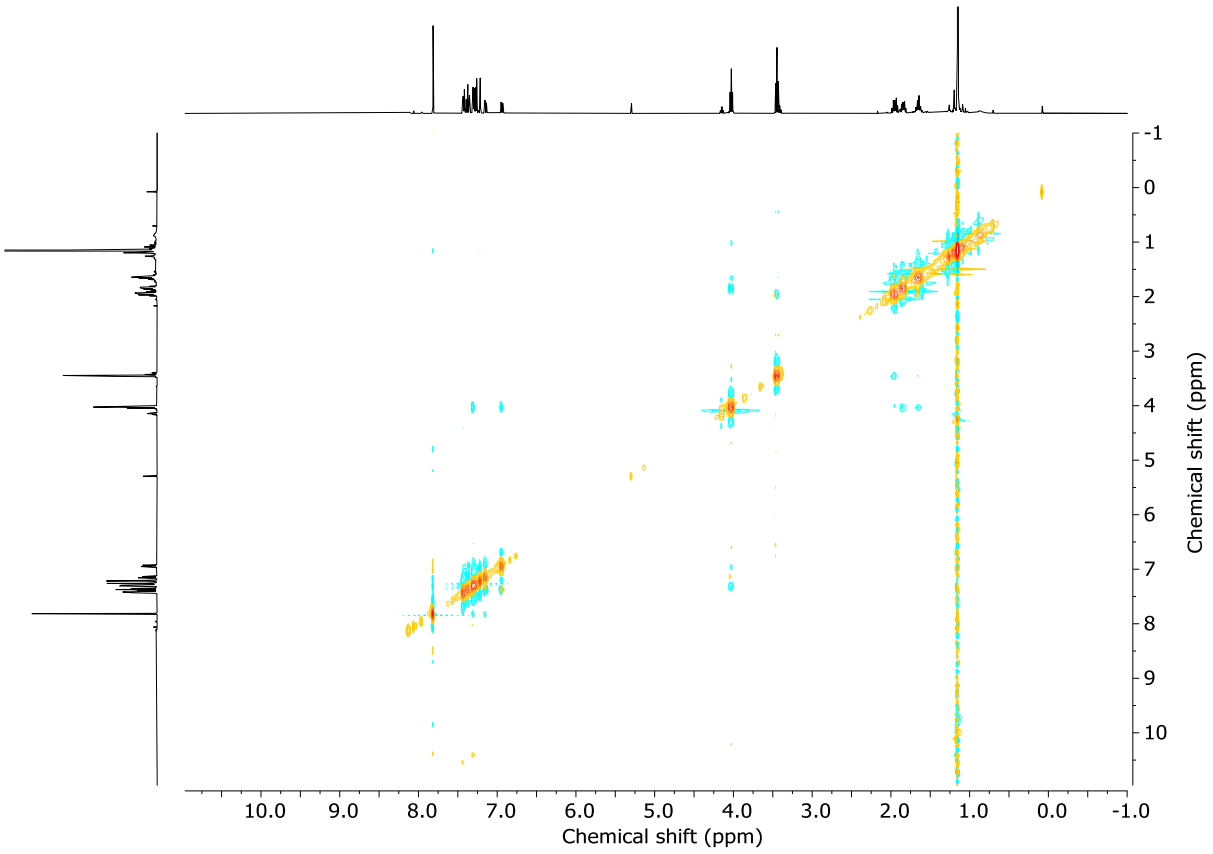

Figure S21: NOESY NMR ($CDCl_3$, 298 K) of (*Z*)- **S6**.

Compound (*E*)-S6

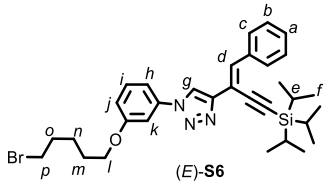

(*E*)-**S6**

^{1}H NMR (400 MHz, $CDCl_3$) δ_H 8.14-8.10 (m, 2H, ***H***$_c$), 8.06 (s, 1H, ***H***$_g$), 7.96 (s, 1H, ***H***$_d$), 7.42 (t, *J* = 8.2, 1H, ***H***$_i$), 7.40-7.30 (m, 4H, ***H***$_a$, ***H***$_b$, ***H***$_k$), 7.23 (ddd, *J* = 8.0, 2.0, 0.9, 1H, ***H***$_h$), 6.97 (ddd, *J* = 8.4, 2.5, 0.9, 1H, ***H***$_j$), 4.05 (t, *J* = 6.3, 2H, ***H***$_l$), 3.45 (t, *J* = 6.7, 2H, ***H***$_p$), 2.01-1.92 (m, 2H, ***H***$_o$), 1.91-1.83 (m, 2H, ***H***$_m$), 1.71-1.62 (m, 2H, ***H***$_n$), 1.22-1.17 (m, 21H, ***H***$_e$, ***H***$_f$).

^{13}C NMR (101 MHz, $CDCl_3$) δ_C 160.2, 148.5, 138.1, 136.0, 134.7, 130.7, 129.6, 129.0, 128.4, 119.8, 115.3, 112.1, 110.1, 106.7, 104.5, 99.2, 68.1, 33.6, 32.5, 28.4, 24.9, 18.9, 11.5.

HR-ESI-MS (+ve): *m/z* = 592.2352 $[M+H]^+$ (calc. for $C_{32}H_{43}{}^{79}BrN_3OSi$ 592.2353), 614.2177 $[M+Na]^+$ (calc. for $C_{32}H_{42}{}^{79}BrN_3NaOSi$ 614.2173).

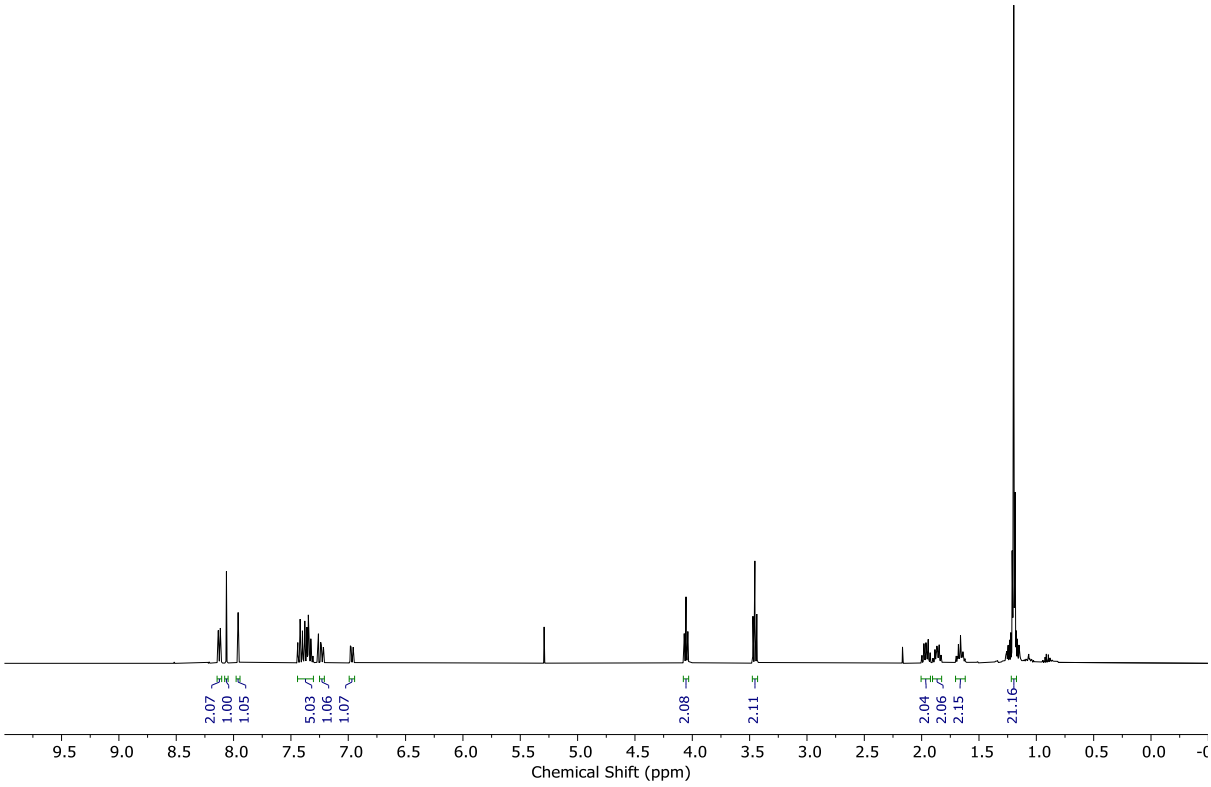

Figure S22: ^{1}H NMR ($CDCl_3$, 400 MHz, 298 K) of (*E*)-**S6**.

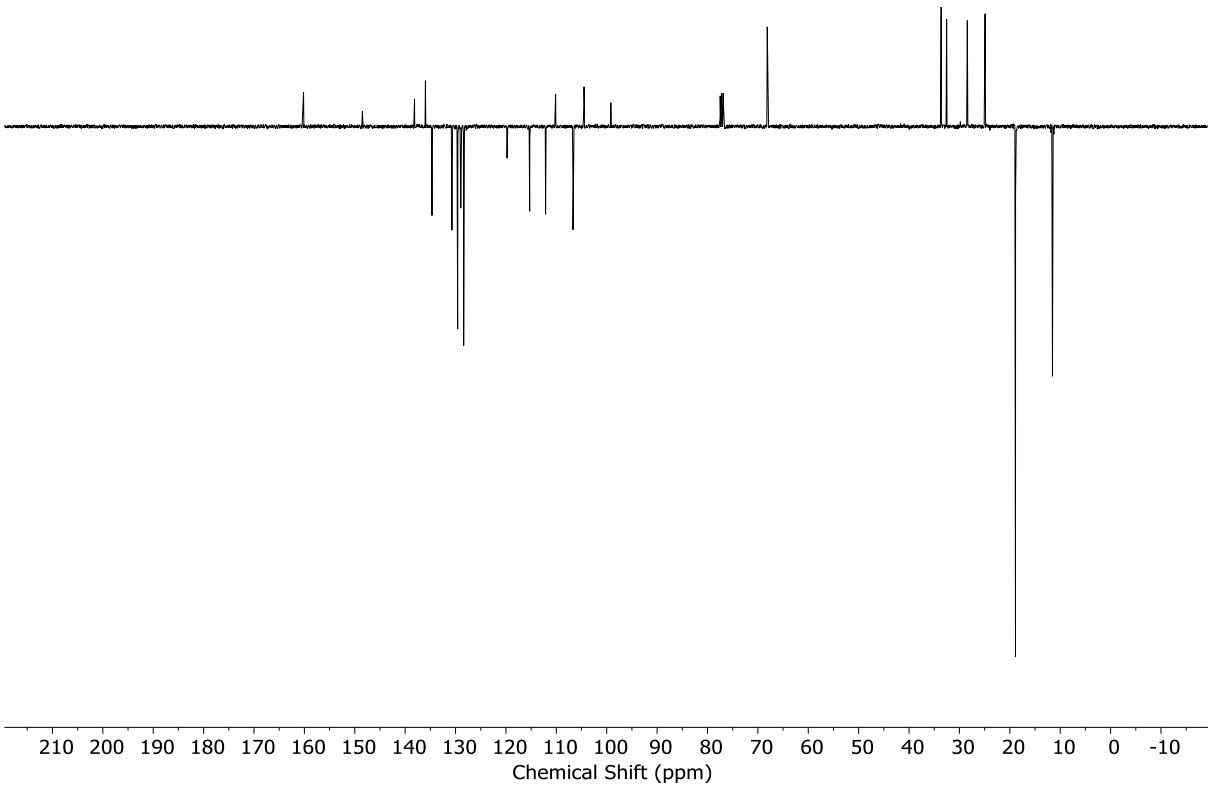

Figure S23: JMOD NMR ($CDCl_3$, 101 MHz, 298 K) of (*E*)-**S6**.

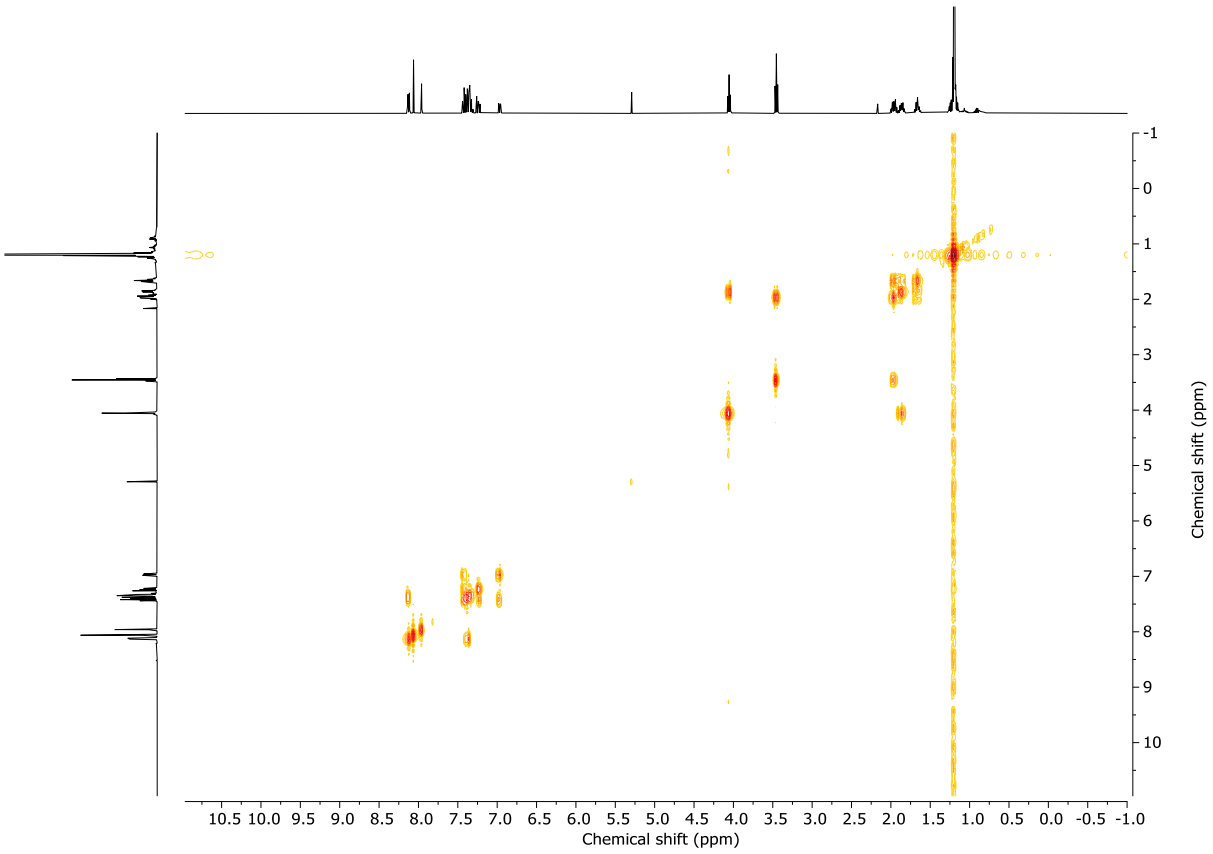

Figure S24: COSY NMR ($CDCl_3$, 298 K) of (*E*)-**S6**.

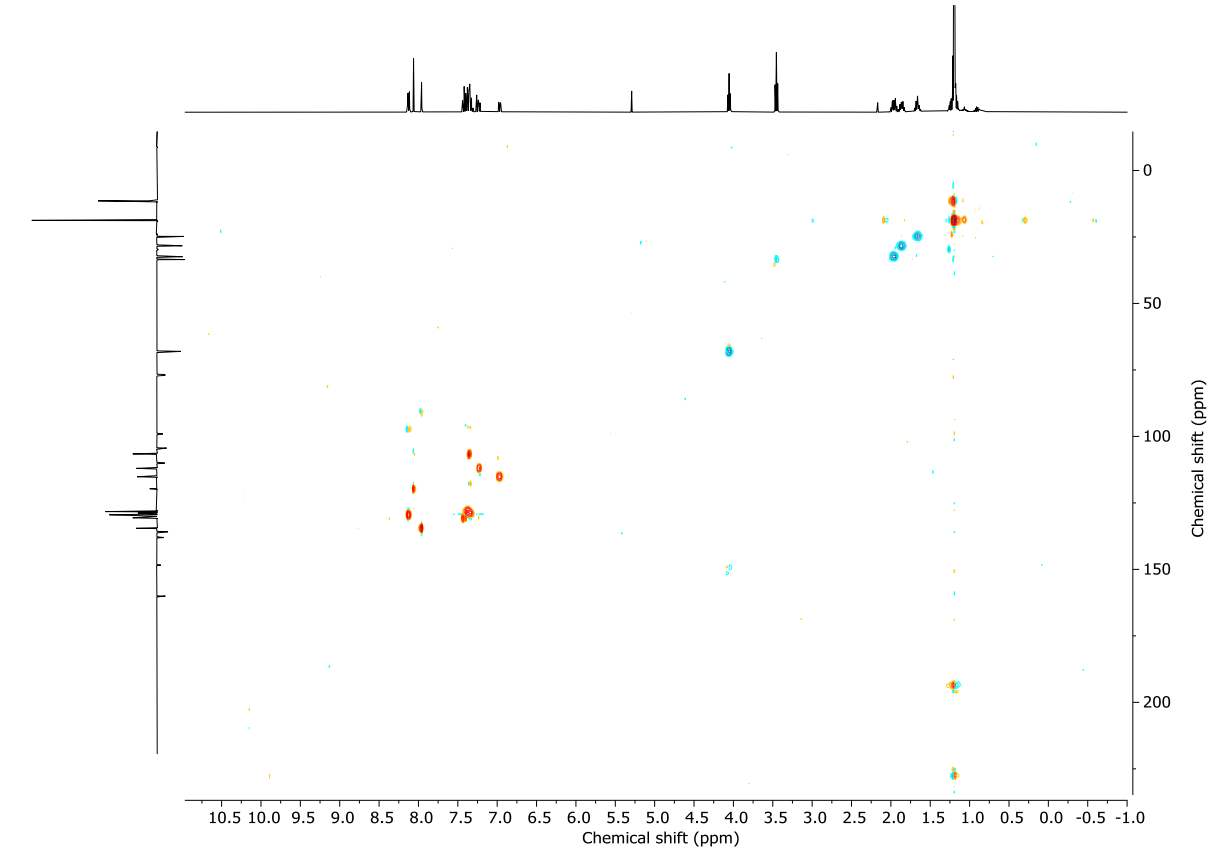

Figure S25: HSQC NMR ($CDCl_3$, 298 K) of (*E*)-**S6**.

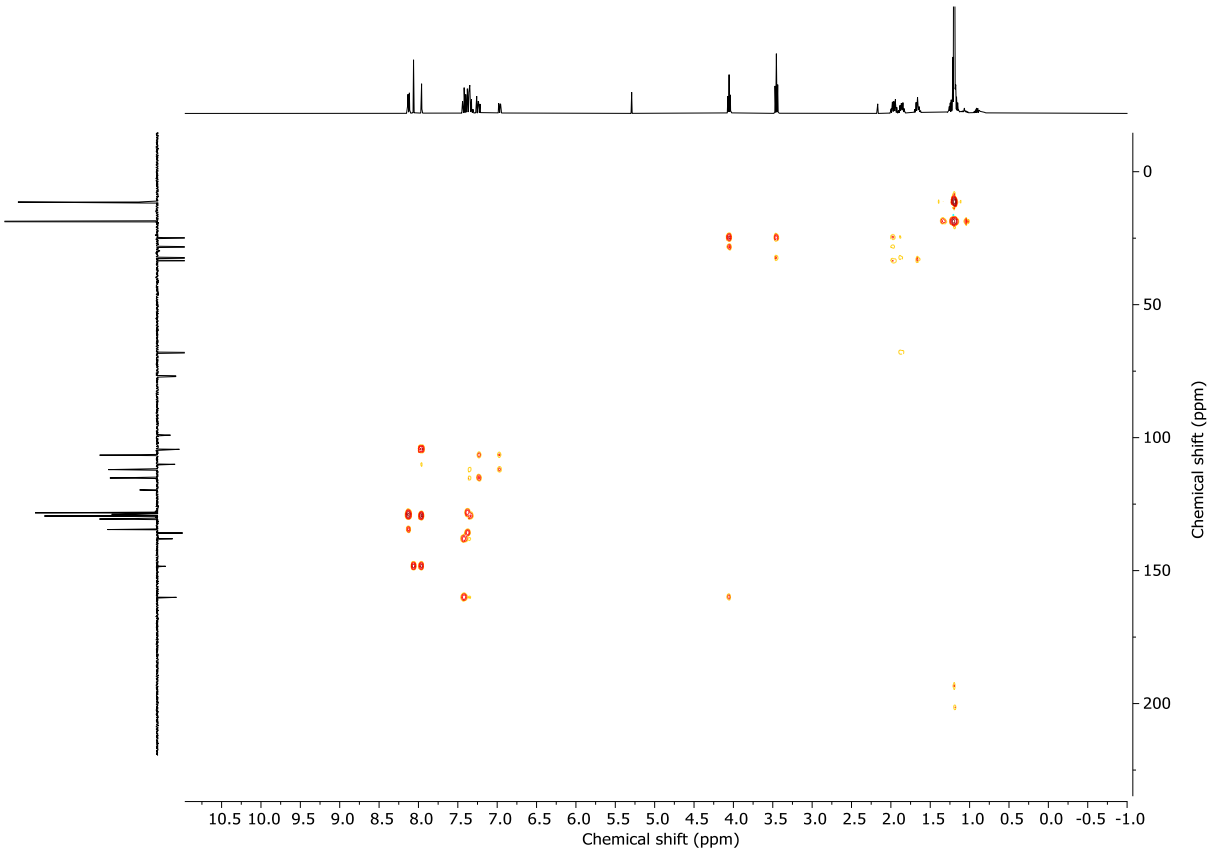

Figure S26: HMBC NMR ($CDCl_3$, 298 K) of (*E*)-**S6**.

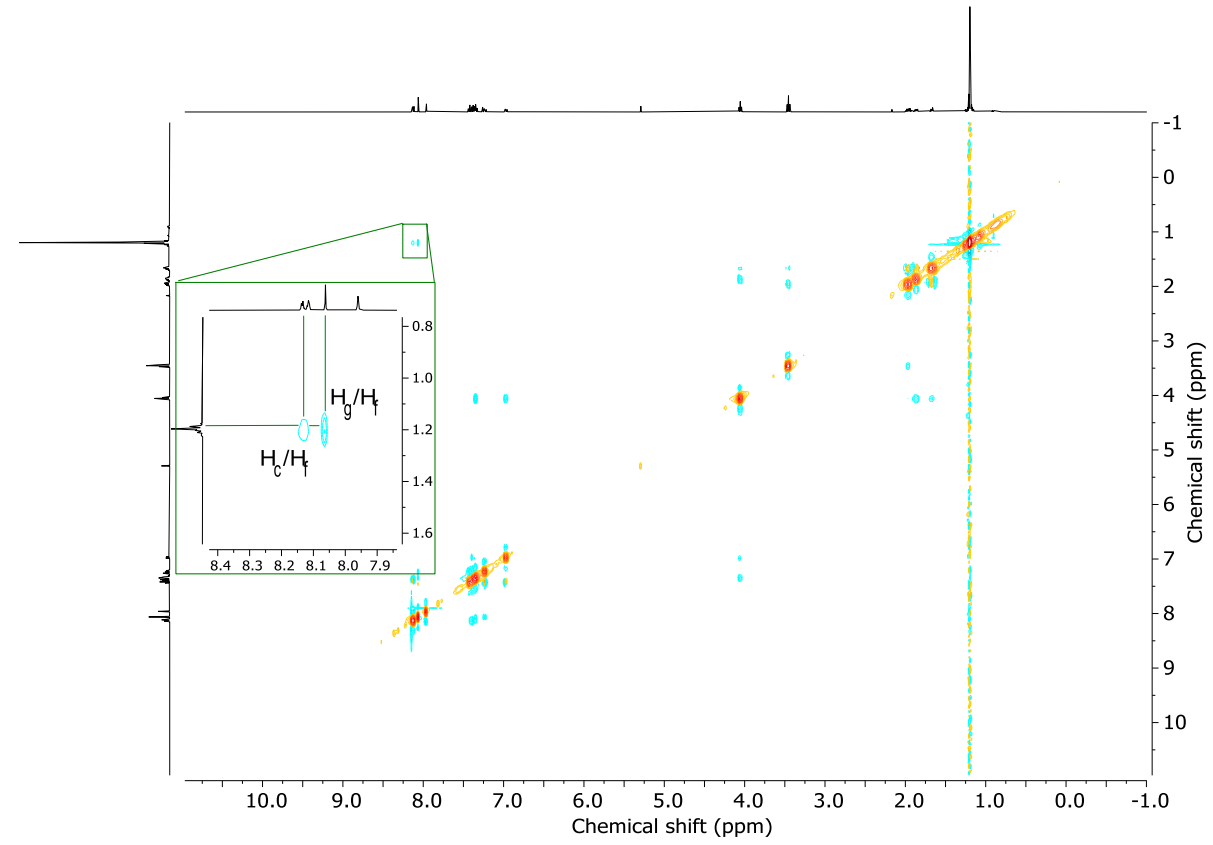

Figure S27: NOESY NMR ($CDCl_3$, 298 K) of (*E*)-**S6**. Inset shows close interactions through space between the phenyl ring of the alkene and the methylenic protons of TIPS protecting group, indicating the presence of (*E*)-isomer.

3.3. Compounds leading to S13

Mono-protected phenol S8

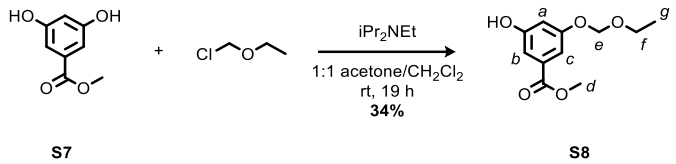

S7 **S8**

Bis-phenol **S7** (0.20 g, 1.2 mmol) was dissolved in acetone-CH_2Cl_2 (1 : 1, 3 mL), under N_2 atmosphere and $^{i}Pr_2NEt$ (0.31 mL, 1.8 mmol) was added at rt. Chloromethyl ethyl ether (0.12 mL, 1.3 mmol) was added and the reaction mixture stirred for 19 h at rt. The reaction mixture was diluted with EtOAc (40 mL), washed with sat. $NH_4Cl_{(aq)}$ (3 x 30 mL), H_2O (30 mL) and brine (30 mL). The organic layer was dried (Na_2SO_4), filtered, and concentrated *in vacuo*. Chromatography (petrol- EtOAc 9 : 1 to 6 : 4) gave mono-protected phenol **S8** as a colourless oil (93 mg, 34%).

^{1}H NMR (400 MHz, $CDCl_3$) δ 7.28 (dd, *J* = 2.3, 1.3, 1H, ***H***$_c$), 7.18 (dd, *J* = 2.4, 1.3, 1H, ***H***$_b$), 6.76 (t, *J* = 2.3, 1H, ***H***$_a$), 5.34 (s, 1H, ***H***$_{OH}$), 5.23 (s, 2H, ***H***$_e$), 3.90 (s, 3H, ***H***$_d$), 3.73 (q, *J* = 7.1, 2H, ***H***$_f$), 1.23 (t, *J* = 7.1, 3H, ***H***$_g$).

^{13}C NMR (101 MHz, $CDCl_3$) δ 166.9, 158.7, 156.9, 132.3, 110.2, 110.0, 108.6, 93.3, 64.7, 52.5, 15.2.

HR-ESI-MS (+ve): *m/z* = 249.0735 $[M + Na]^+$ calc. for $C_{11}H_{14}NaO_5$ 249.0733.

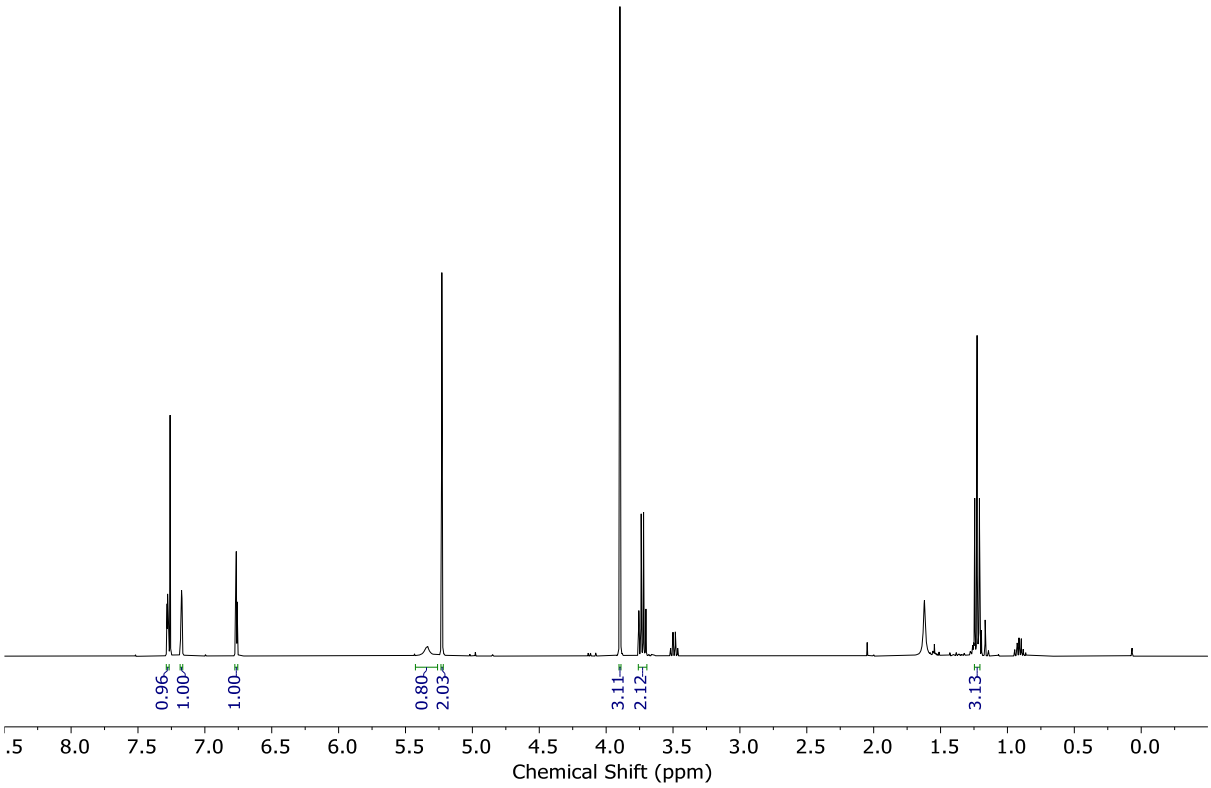

Figure S28: ^{1}H NMR ($CDCl_3$, 400 MHz, 298 K) of **S8**.

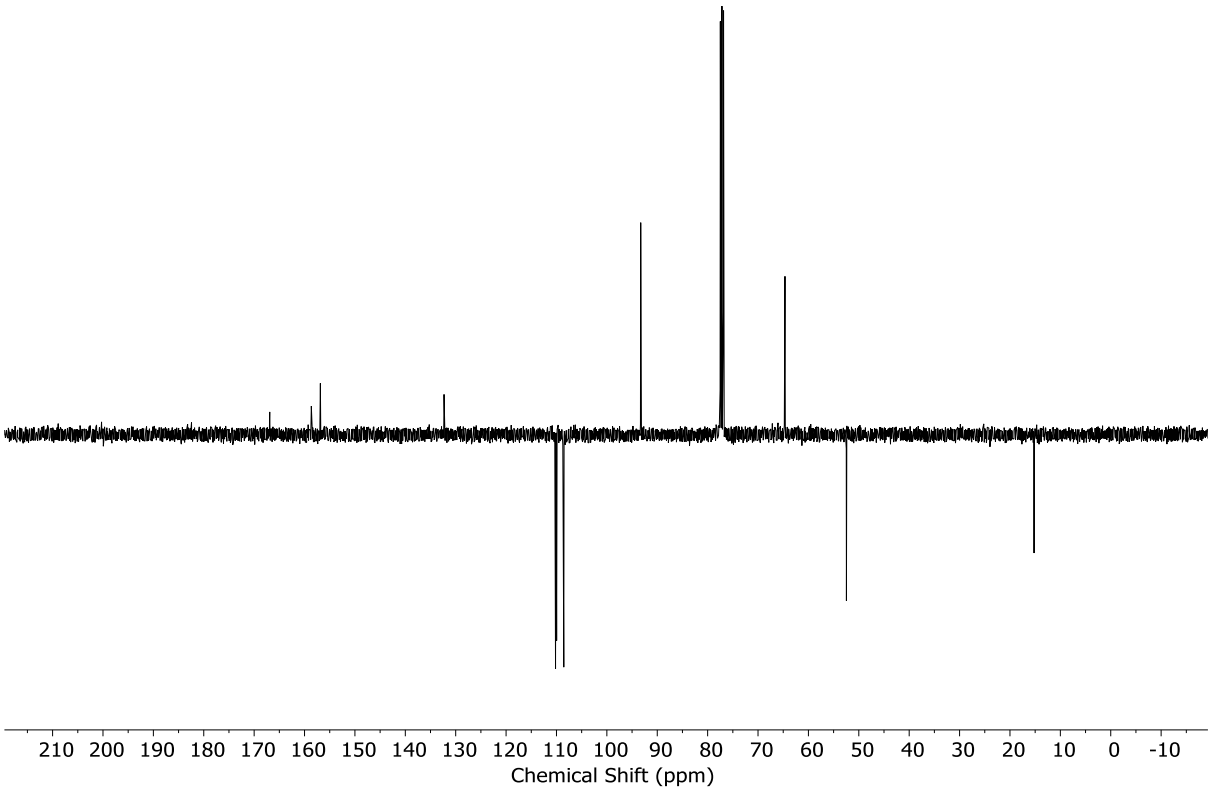

Figure S29: JMOD NMR ($CDCl_3$, 101 MHz, 298 K) of **S8**.

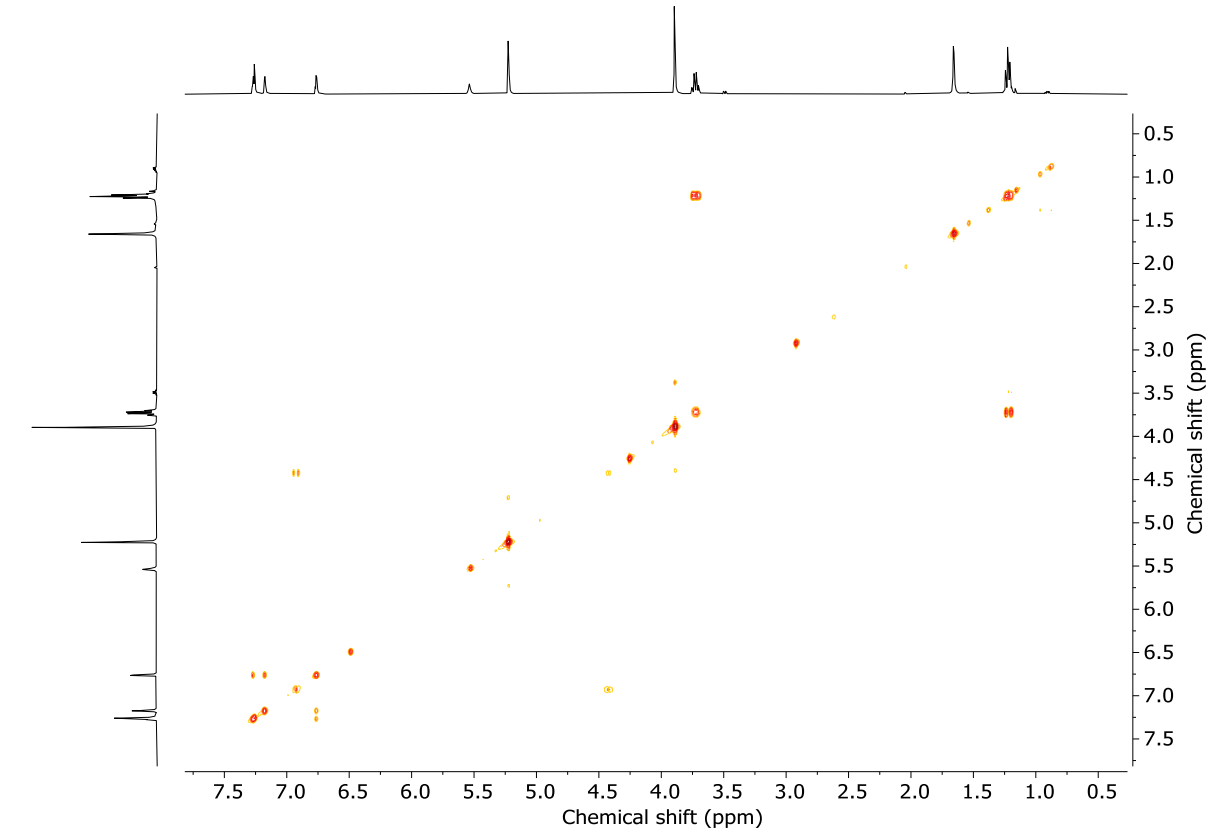

Figure S30: COSY NMR ($CDCl_3$, 298 K) of **S8**.

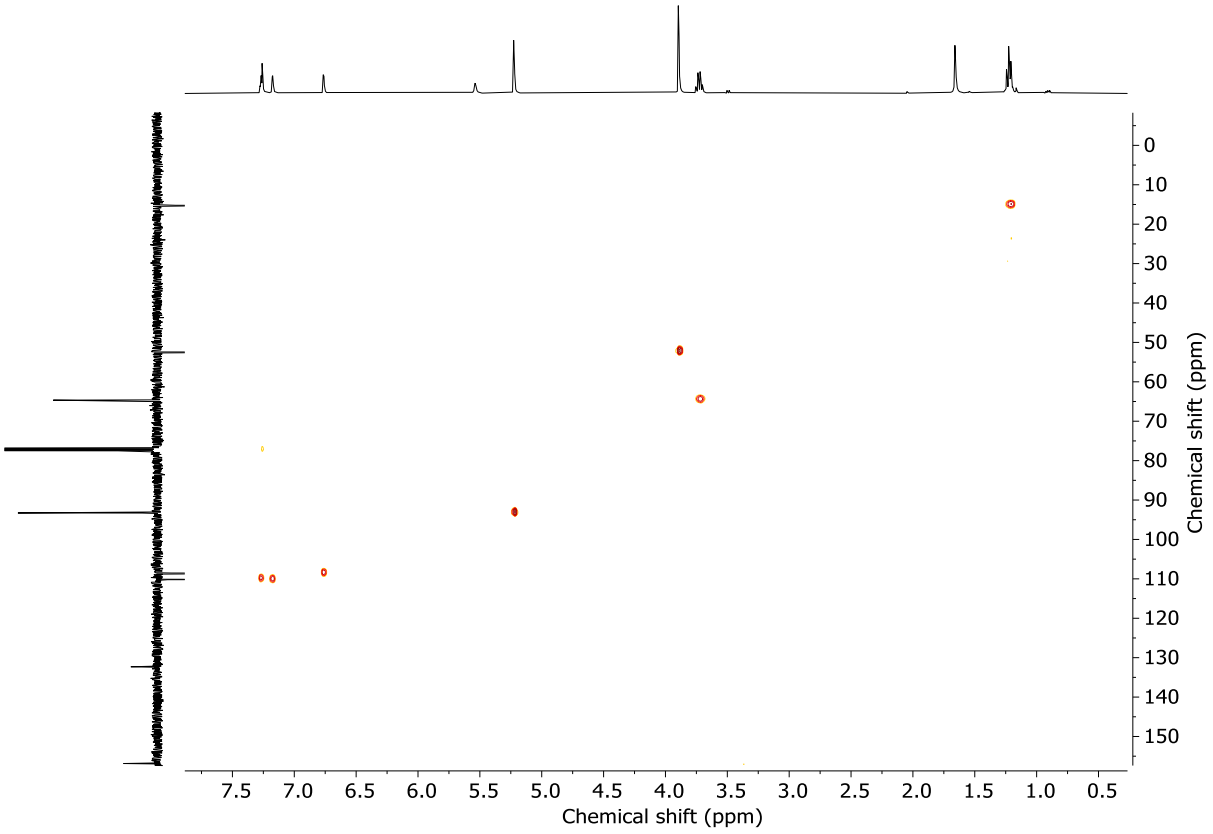

Figure S31: HSQC NMR ($CDCl_3$, 298 K) of **S8**.

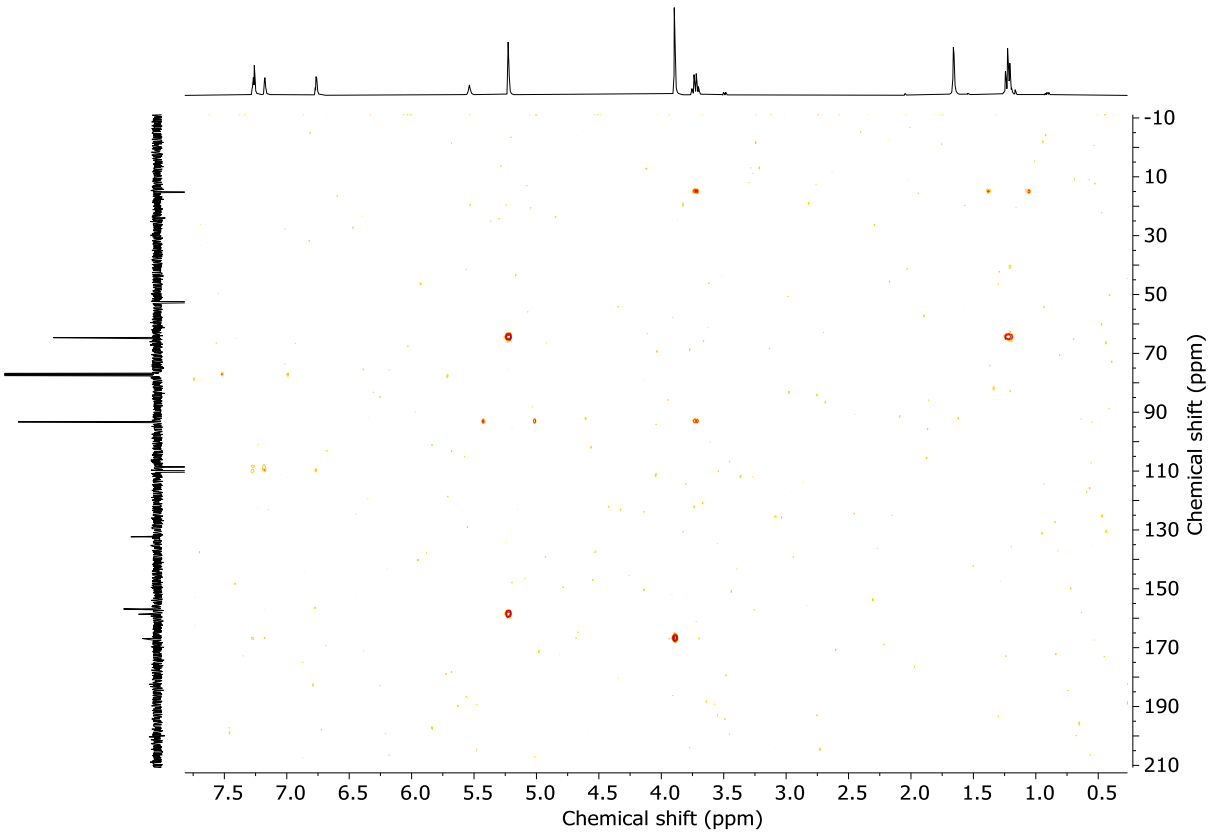

Figure S32: HMBC NMR ($CDCl_3$, 298 K) of **S8**.

Benzylic alcohol S9

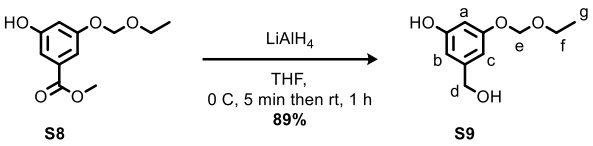

Ester **S8** (2.60 g, 11.5 mmol) was dissolved in THF (50 mL) under an N_2 atmosphere and cooled at 0 °C. $LiAlH_4$ (1 M in THF, 15.0 mL, 15.0 mmol) was added dropwise over 15 min at 0 °C. The reaction mixture was stirred for 5 min at 0 °C then 1 h at rt. The reaction mixture was cooled at 0 °C, quenched with MeOH (2 mL) then partitioned between EtOAc (100 mL) and sat. Rochelle $salt_{(aq.)}$ (150 mL). The layers were separated, and the aqueous layer extracted with EtOAc (4 x 75 mL). The combined organic layers were dried (Na_2SO_4), filtered, and concentrated *in vacuo* to give alcohol **S9** as a yellow oil (2.04 g, 89%). No further purification was required.

^{1}H NMR (400 MHz, $CDCl_3$) δ 6.51 – 6.48 (m, 1H, ***H***$_c$), 6.46 – 6.44 (m, 1H, ***H***$_b$), 6.43 (t, *J* = 2.2, 1H, ***H***$_a$), 5.12 (s, 2H, ***H***$_e$), 4.49 (s, 2H, ***H***$_d$), 3.69 (q, *J* = 7.1, 2H, ***H***$_f$), 1.19 (t, *J* = 7.1, 3H, ***H***$_g$).

^{13}C NMR (101 MHz, $CDCl_3$) δ 158.6, 157.4, 143.2, 107.8, 107.0, 103.2, 93.1, 64.9, 64.6, 15.1.

HR-ESI-MS (+ve): *m/z* = 221.0781 $[M + Na]^+$ calc. for $C_{10}H_{14}NaO_4$ 221.0784.

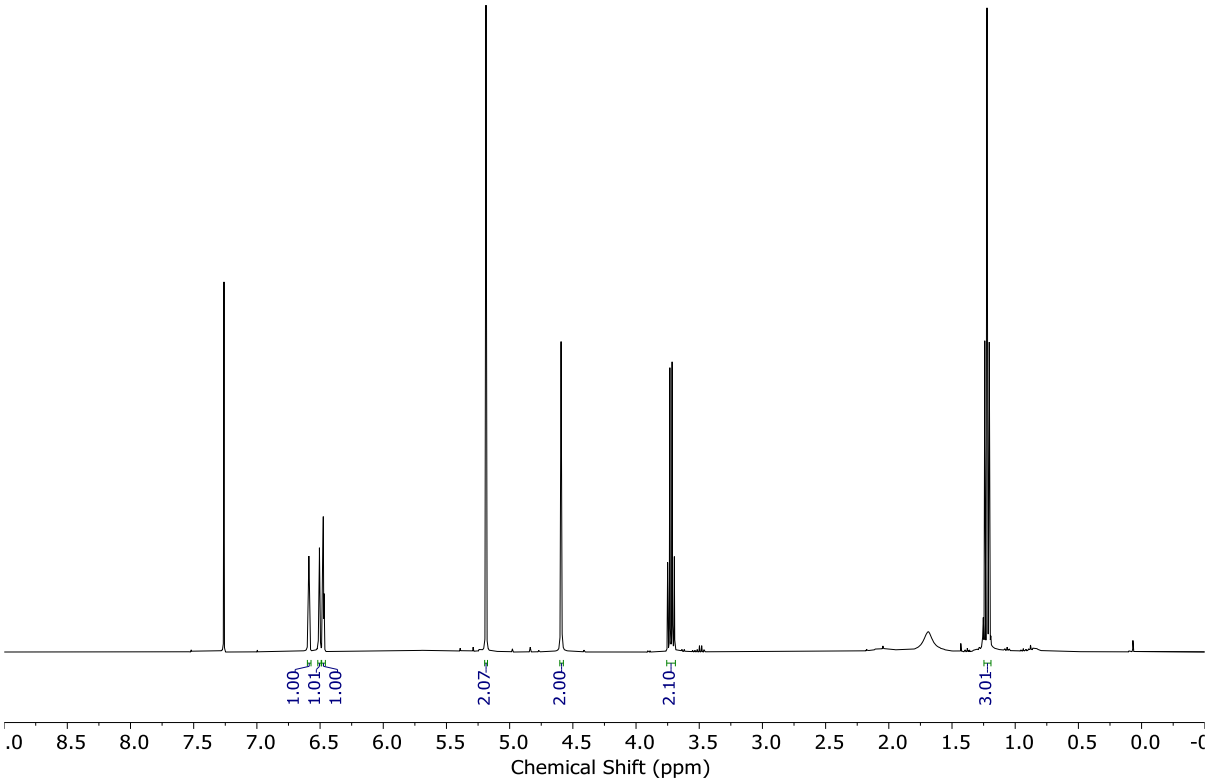

Figure S33: ^{1}H NMR ($CDCl_3$, 400 MHz, 298 K) of **S9**.

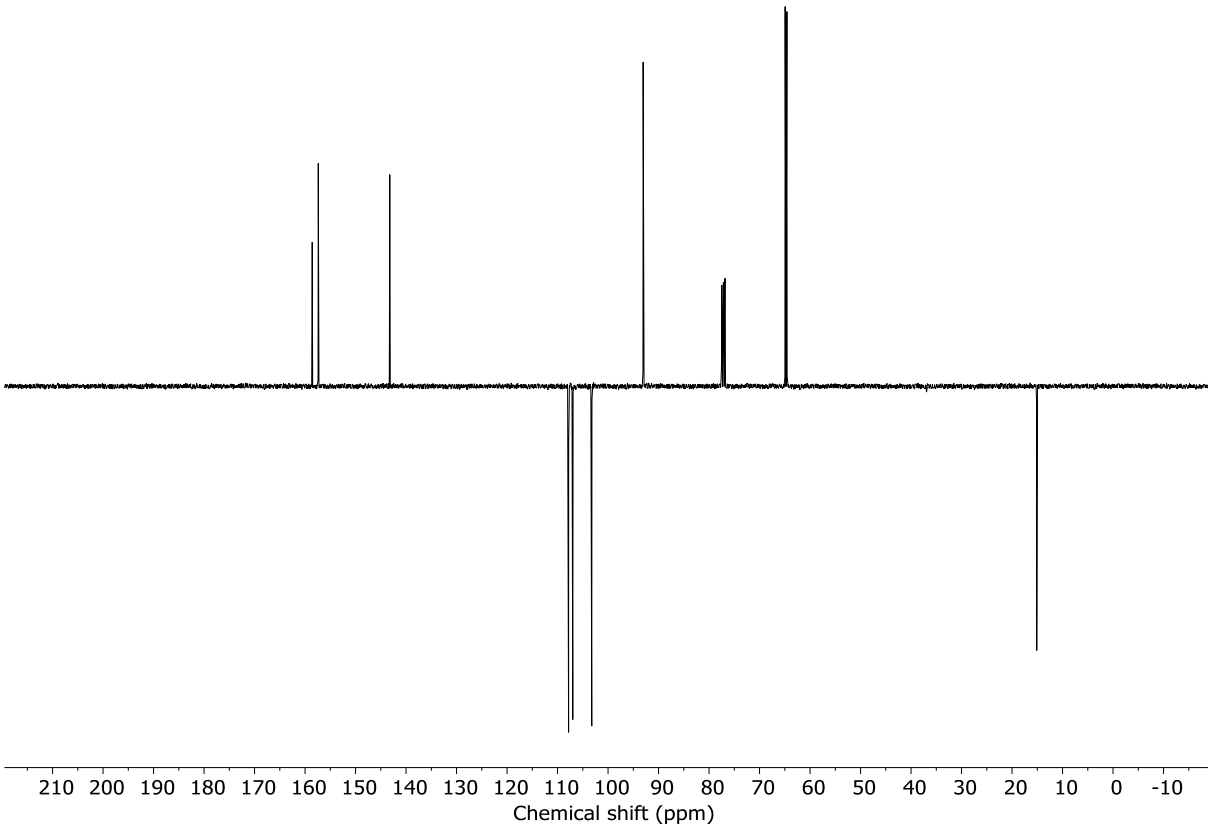

Figure S34: J-MOD NMR ($CDCl_3$, 101 MHz, 298 K) of **S9**.

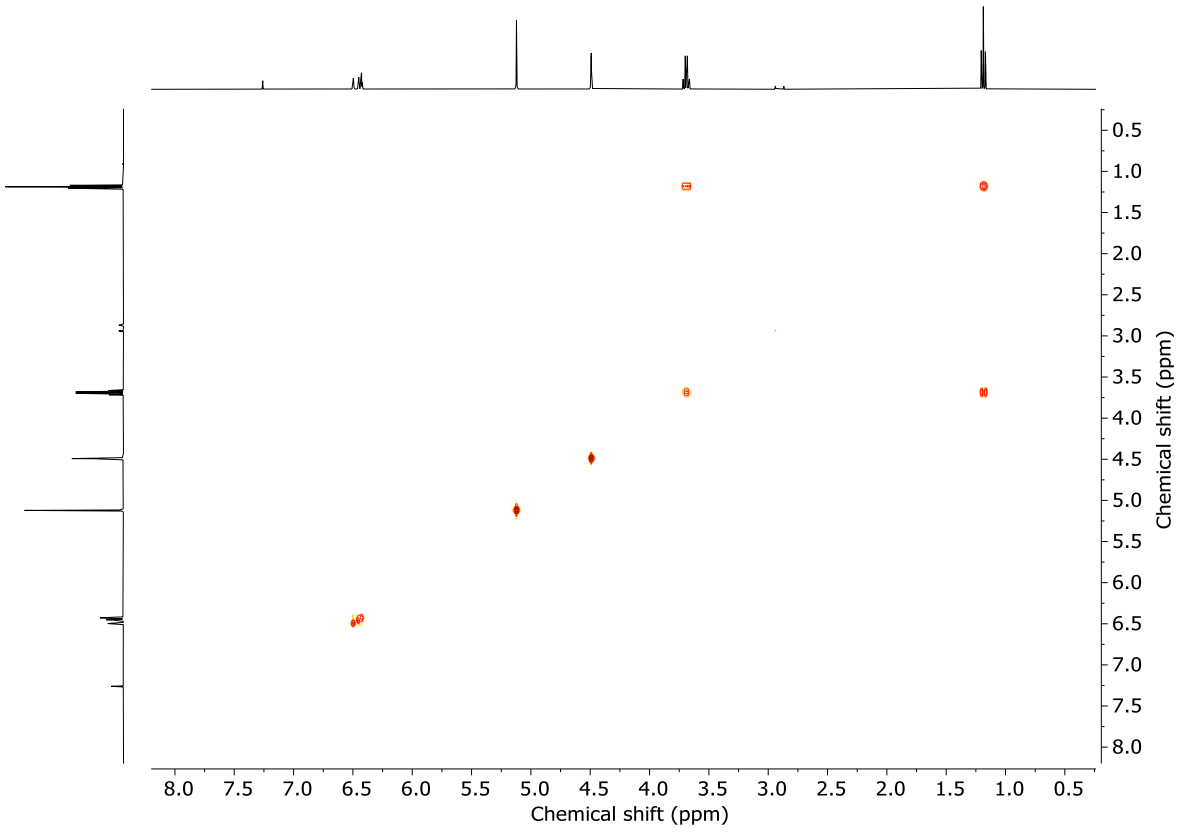

Figure S35: COSY NMR ($CDCl_3$, 298 K) of **S9**.

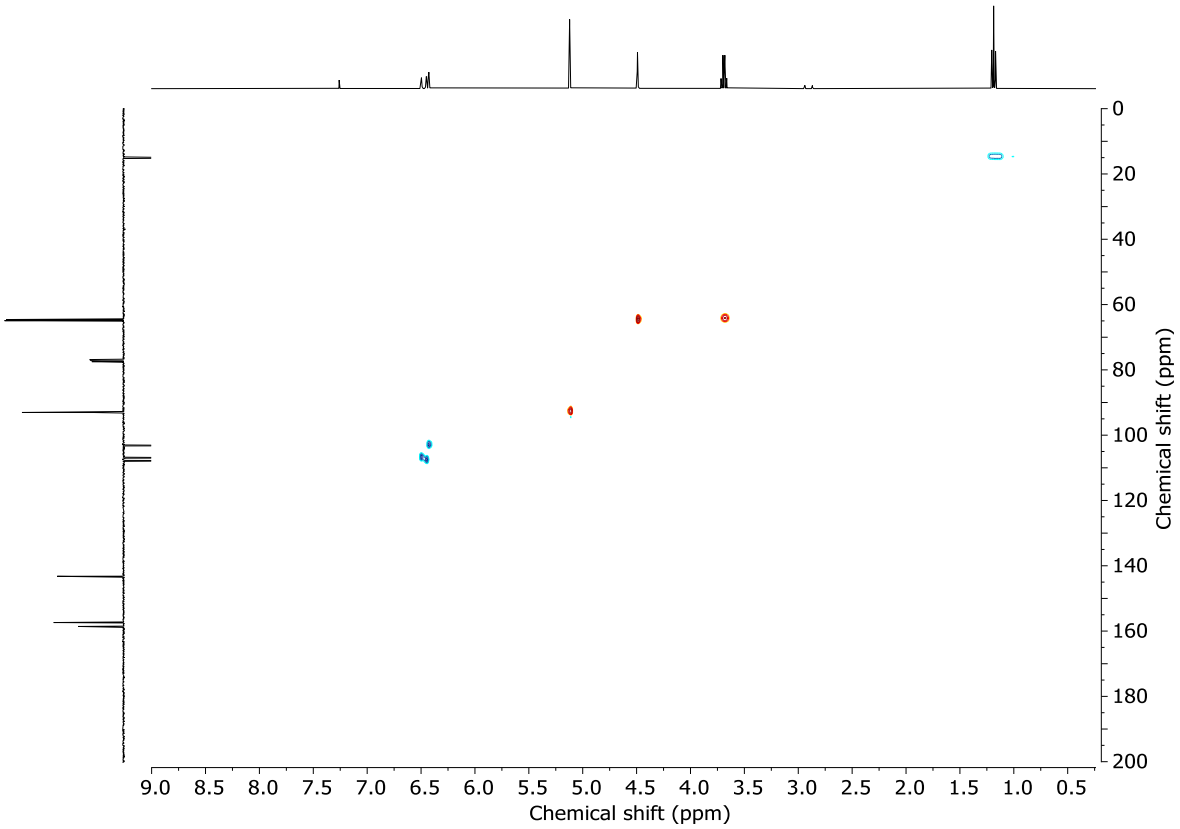

Figure S36: HSQC NMR ($CDCl_3$, 298 K) of **S9**.

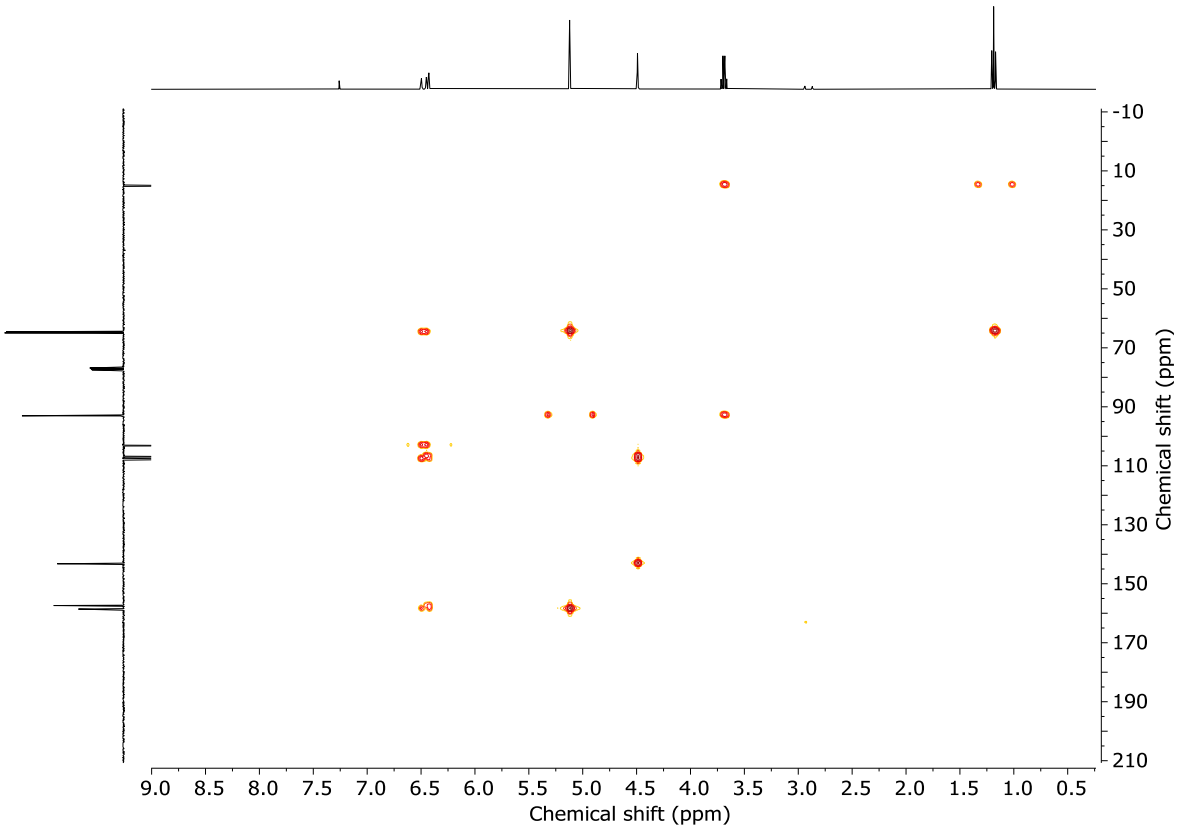

Figure S37: HMBC NMR ($CDCl_3$, 298 K) of **S9**.

Alkyl bromide S10

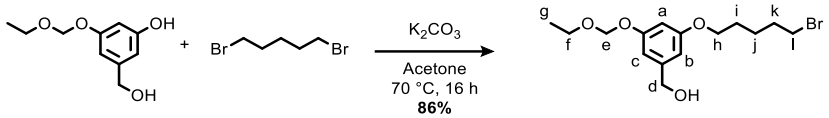

S9 **S10**

Phenol **S9** (260 mg, 1.31 mmol) and K_2CO_3 (905 mg, 6.49 mmol) were suspended in acetone (13 mL). After 5 min of stirring at rt, 1,5-dibromopentane (0.89 mL, 6.6 mmol) was added and the reaction mixture was heated at 70 °C overnight. After being cooled to rt, the reaction mixture was filtered over Celite®, the residue washed with acetone and the filtrate concentrated *in vacuo*. Chromatography (petrol-Et_2O 100 : 0 to 1:1) gave bromide **S10** as a colourless oil (390 mg, 86%).

^{1}H NMR (400 MHz, $CDCl_3$) δ 6.63 (ddt, *J* = 2.0, 1.3, 0.7, 1H, H_c), 6.57 (td, *J* = 1.4, 0.7, 1H, H_b), 6.52 (t, *J* = 2.3, 1H, H_a), 5.21 (s, 2H, H_e), 4.63 (d, *J* = 6.1, 2H, H_d), 3.96 (t, *J* = 6.3, 2H, H_h), 3.73 (q, *J* = 7.1, 2H, H_f), 3.44 (t, *J* = 6.8, 2H, H_l), 1.99 – 1.88 (m, 2H, H_k), 1.86 – 1.75 (m, 2H, H_i), 1.70 – 1.58 (m, 2H, H_J), 1.23 (t, *J* = 7.1, 3H, H_g).

^{13}C NMR (101 MHz, $CDCl_3$) δ 160.5, 158.8, 143.5, 1067.0, 106.4, 102.4, 93.3, 67.8, 65.5, 64.5, 33.7, 32.6, 28.5, 25.0, 15.3.

HR-ESI-MS (+ve): m/z = 369.0675 $[M + Na]^+$ calc. for $C_{15}H_{23}{}^{79}BrNaO_4$ 369.0672.

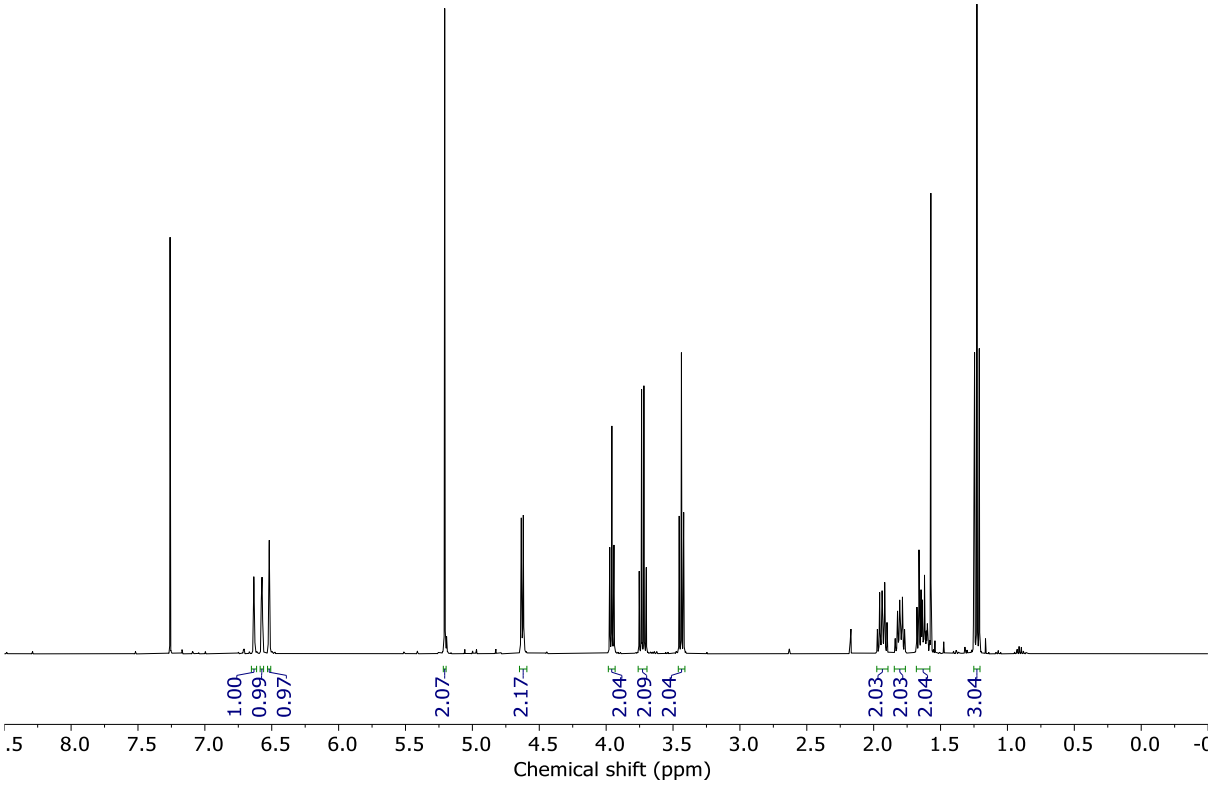

Figure S38: ^{1}H NMR ($CDCl_3$, 400 MHz, 298 K) of **S10**.

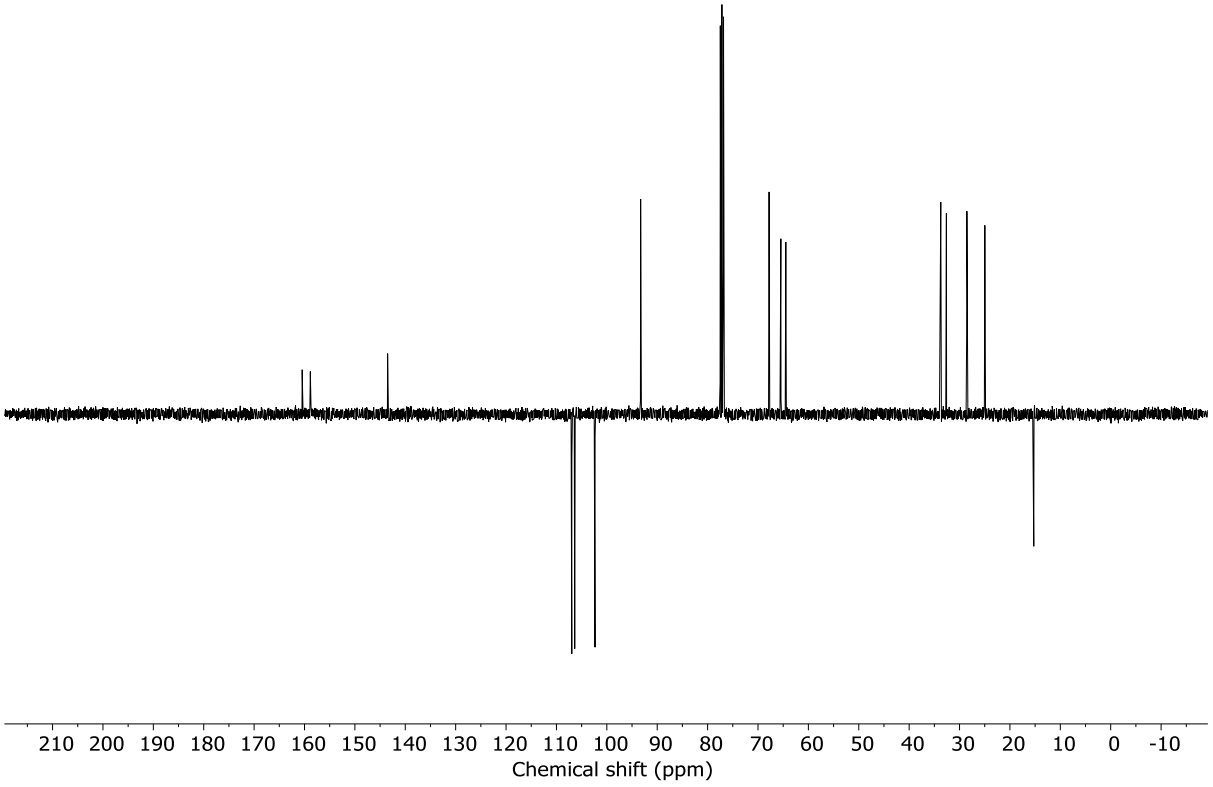

Figure S39: J-MOD NMR ($CDCl_3$, 101 MHz, 298 K) of **S10**.

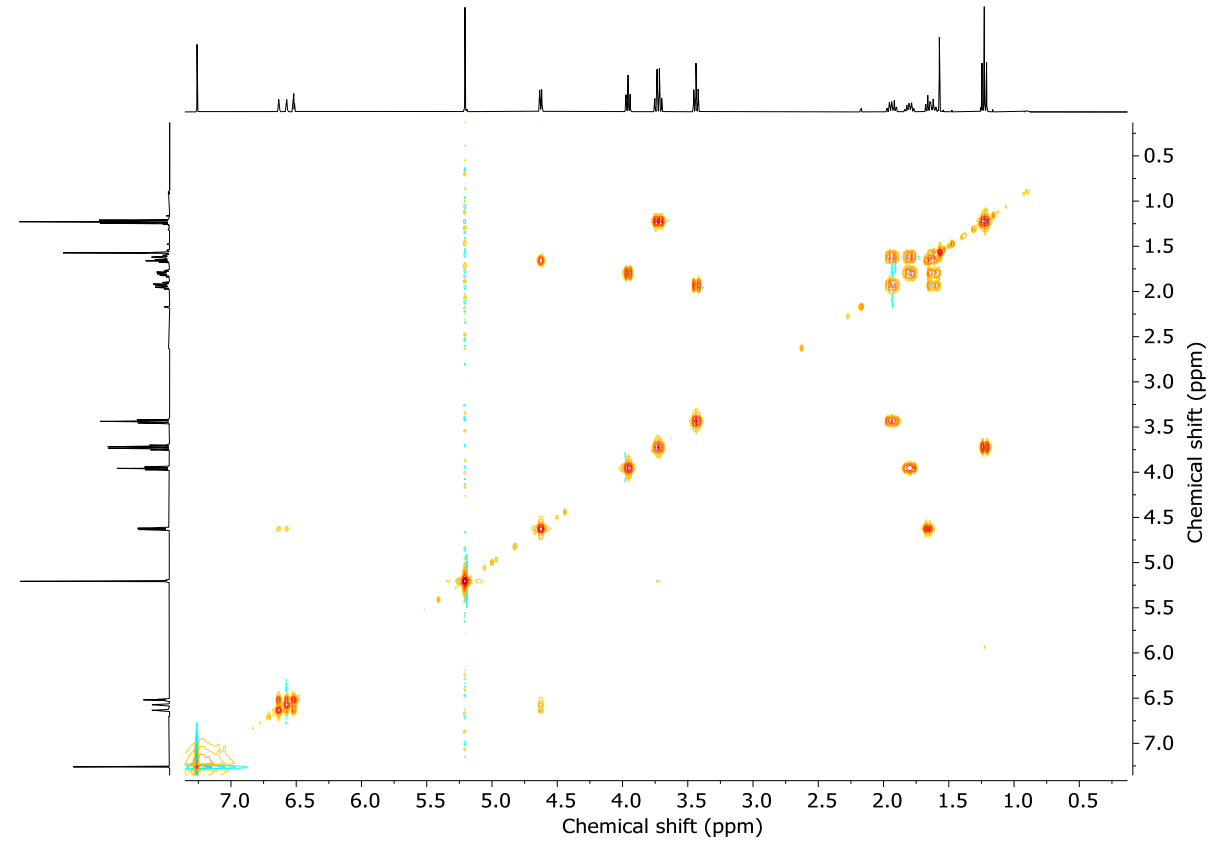

Figure S40: COSY NMR ($CDCl_3$, 298 K) of **S10**.

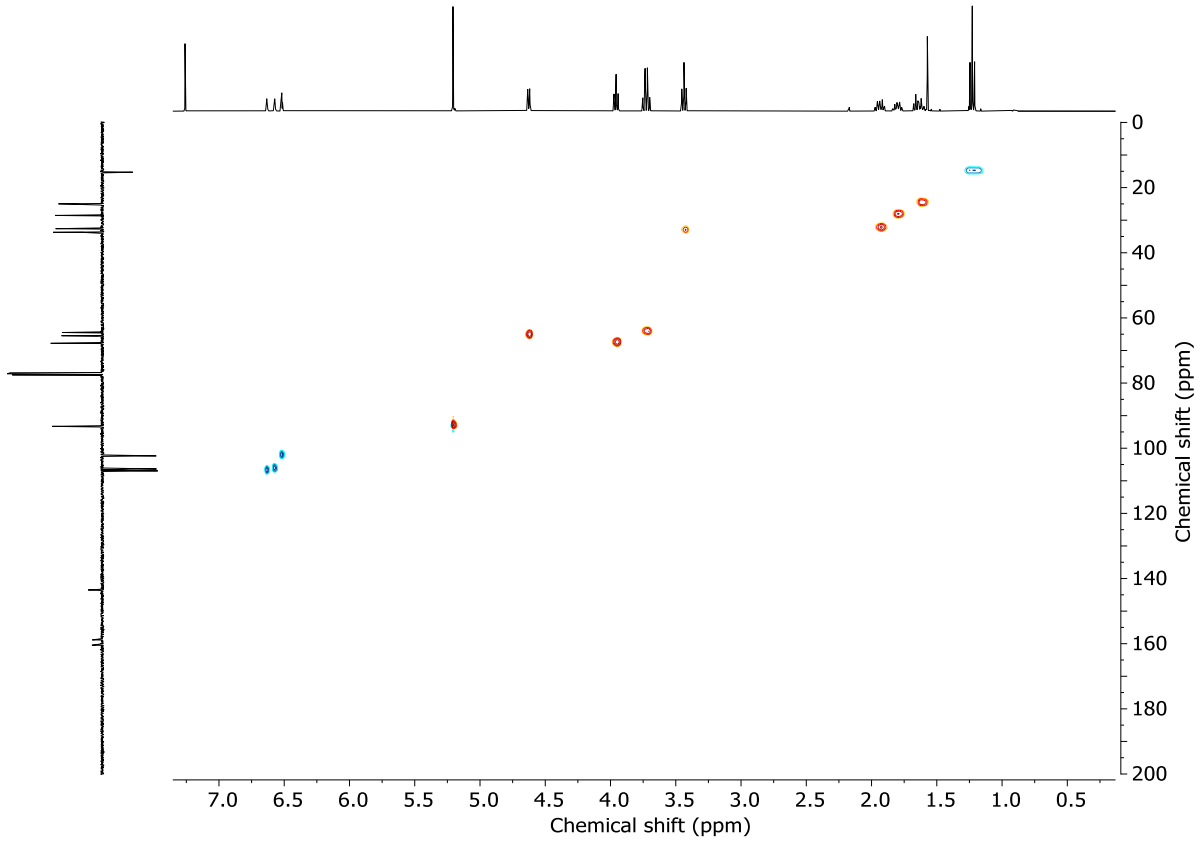

Figure S41: HSQC NMR ($CDCl_3$, 298 K) of **S10**.

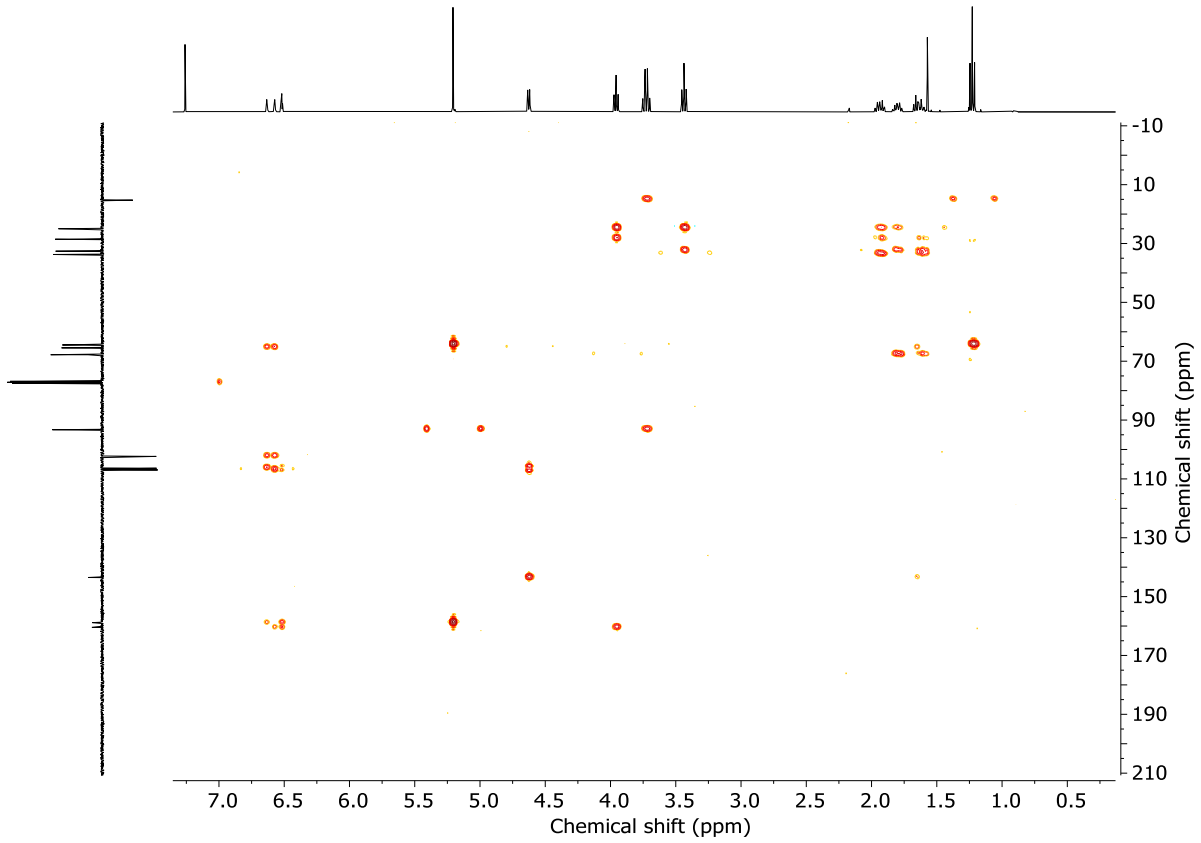

Figure S42: HMBC NMR ($CDCl_3$, 298 K) of **S10**.

Azide S13

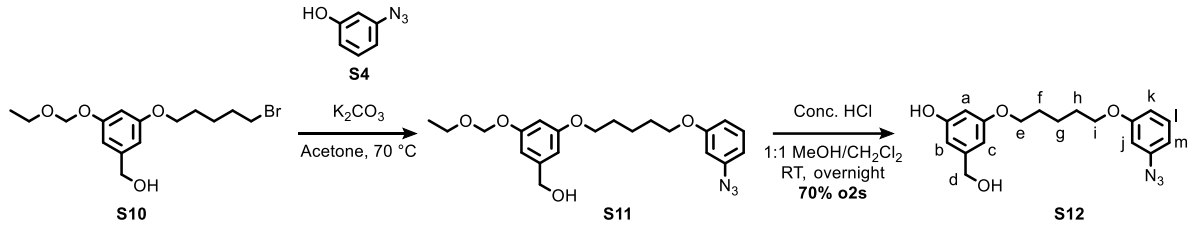

Bromide **S10** (440 mg, 1.27 mmol) and 3-azidophenol **S4** (189 mg, 1.40 mmol) were dissolved in acetone (12 mL) and K_2CO_3 (888 mg, 6.42 mmol) was added. The reaction mixture was heated at 70 °C overnight then cooled to rt. The reaction mixture was filtered over Celite®, the residue washed with acetone and the filtrate concentrated *in vacuo*. The residue containing azide **S11** (

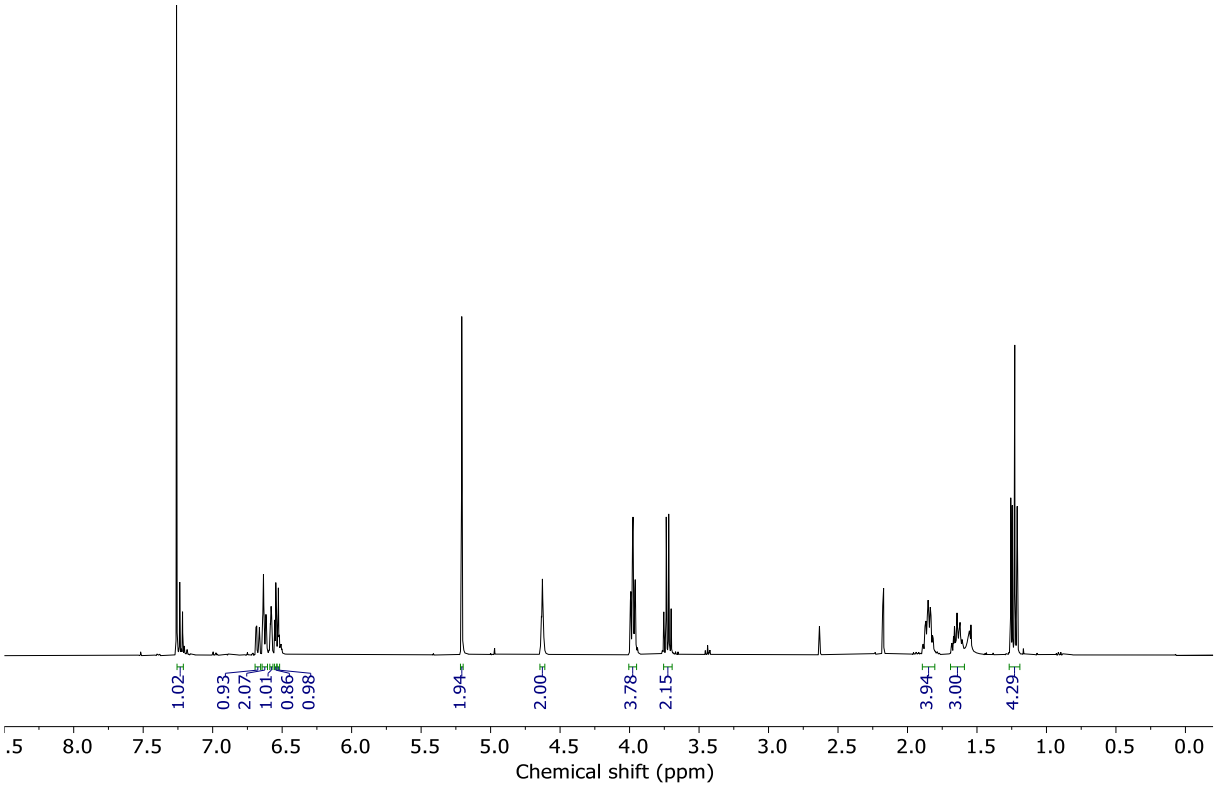

Figure S43) was dissolved in MeOH-CH_2Cl_2 (1 : 1, 13 mL) and conc. HCl (0.25 mL) was added and the reaction mixture was stirred overnight at rt. The reaction mixture was quenched with sat. $NaHCO_{3(aq.)}$ (25 mL), the layers were separated, and the aqueous layer was extracted with CH_2Cl_2 (3 x 10 mL). The combined organic layers were dried (Na_2SO_4), filtered, and concentrated *in vacuo*. Chromatography (petrol-Et_2O 1:1 to 0 : 100) gave azide **S12** as a pale-yellow powder (304 mg, 70% over two steps).

^{1}H NMR (400 MHz, $CDCl_3$) δ 7.24 (t, *J* = 8.2, 1H, ***H***$_j$), 6.68 (ddd, *J* = 8.3, 2.4, 0.9, 1H, ***H***$_k$), 6.63 (ddd, *J* = 7.9, 2.2, 0.8, 1H, ***H***$_m$), 6.54 (t, *J* z= 2.2, 1H, ***H***$_l$), 6.50 (ddt, *J* = 2.1, 1.3, 0.7, 1H, ***H***$_c$), 6.44 (ddt, *J* = 2.0, 1.3, 0.6, 1H, ***H***$_b$), 6.32 (t, *J* = 2.3, 1H, ***H***$_a$), 5.70 (br s, 1H, ***H***$_{OH}$), 4.61 (s, 2H, ***H***$_d$), 3.96 (t, *J* = 6.4, 2H, ***H***$_i$), 3.94 (t, *J* = 6.4, 2H, ***H***$_e$), 2.11 (br s, 1H, ***H***$_{OH}$), 1.90 – 1.77 (m, 4H, ***H***$_f$, ***H***$_h$), 1.70 – 1.54 (m, 2H, ***H***$_g$).

^{13}C NMR (101 MHz, $CDCl_3$) δ 160.7, 160.4, 157.2 (x2), 143.5, 141.4, 130.6, 111.4, 111.3, 106.3 (x2), 105.6, 105.6, 101.4 (x2), 68.0, 68.0, 65.3, 29.1, 29.0, 22.8.

HR-ESI-MS (+ve): m/z = 366.1419 $[M + Na]^+$ calc. for $C_{18}H_{21}N_3NaO_4$ 366.1424.

m.p.: 93 - 94 ˚C

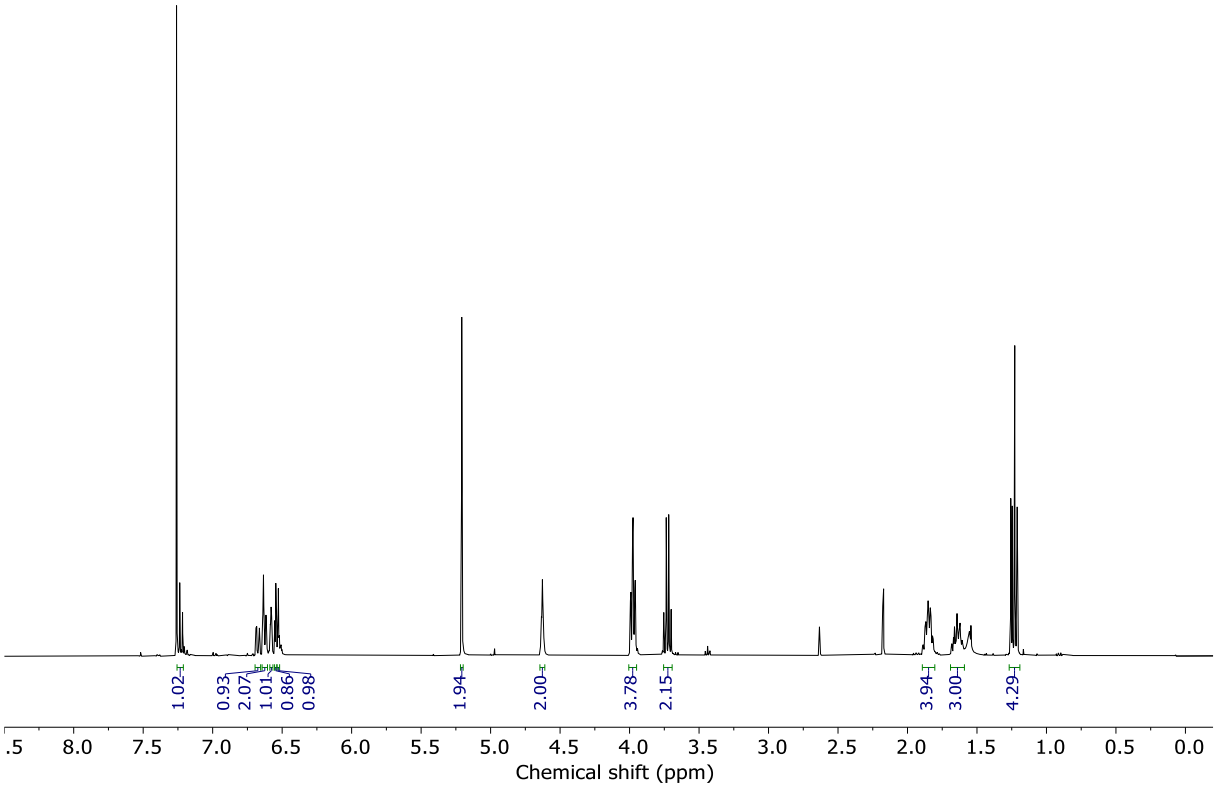

Figure S43: ^{1}H NMR ($CDCl_3$, 400 MHz, 298 K) of the residue containing **S11** prior to ethoxymethyl ether deprotection.

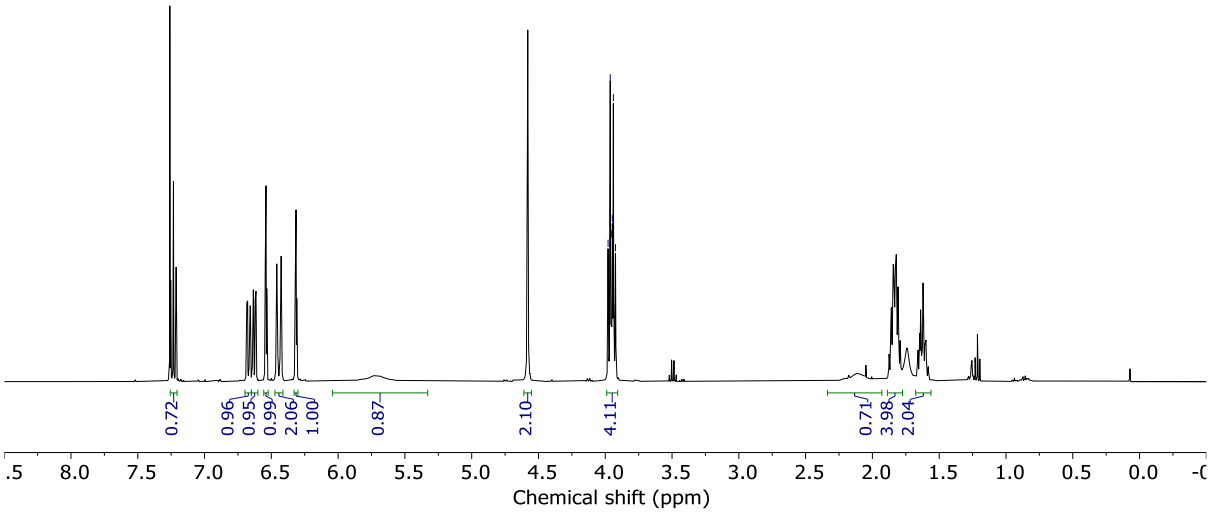

Figure S44: ^{1}H NMR ($CDCl_3$, 400 MHz, 298 K) of **S12**.

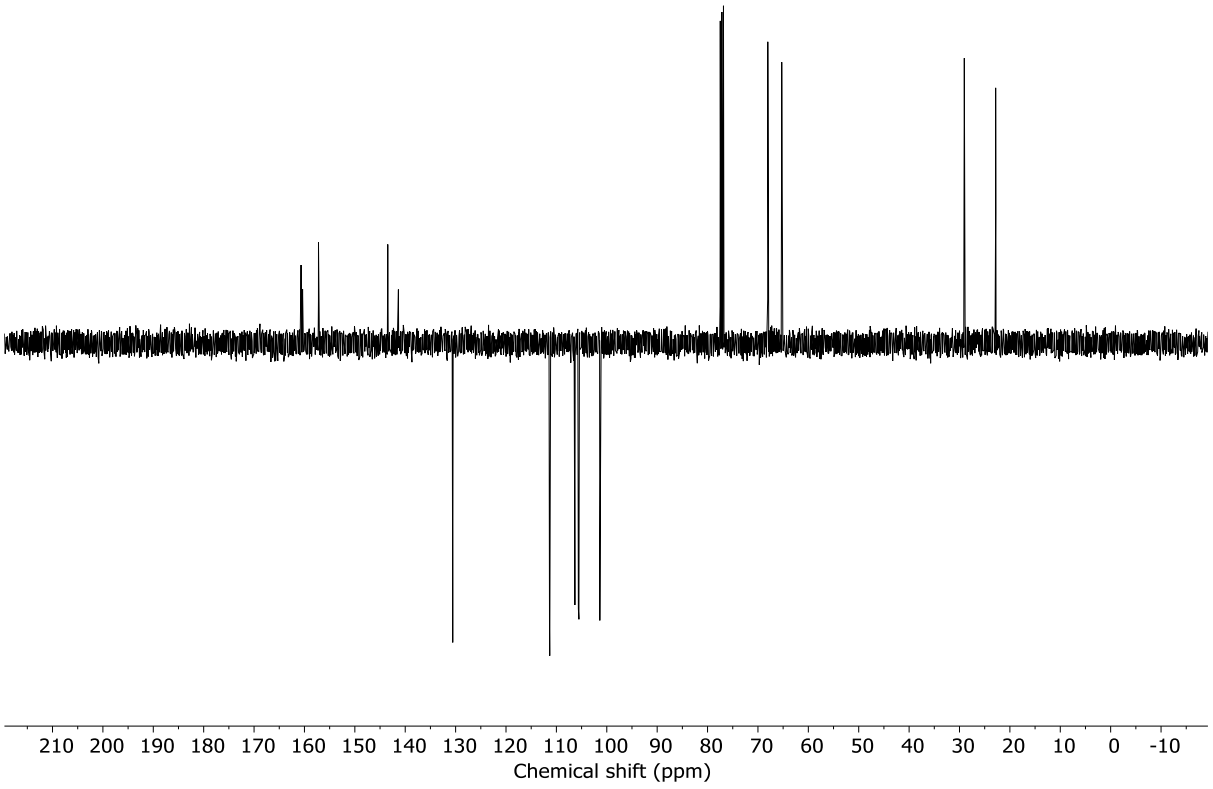

Figure S45: J-MOD NMR ($CDCl_3$, 101 MHz, 298 K) of **S12**.

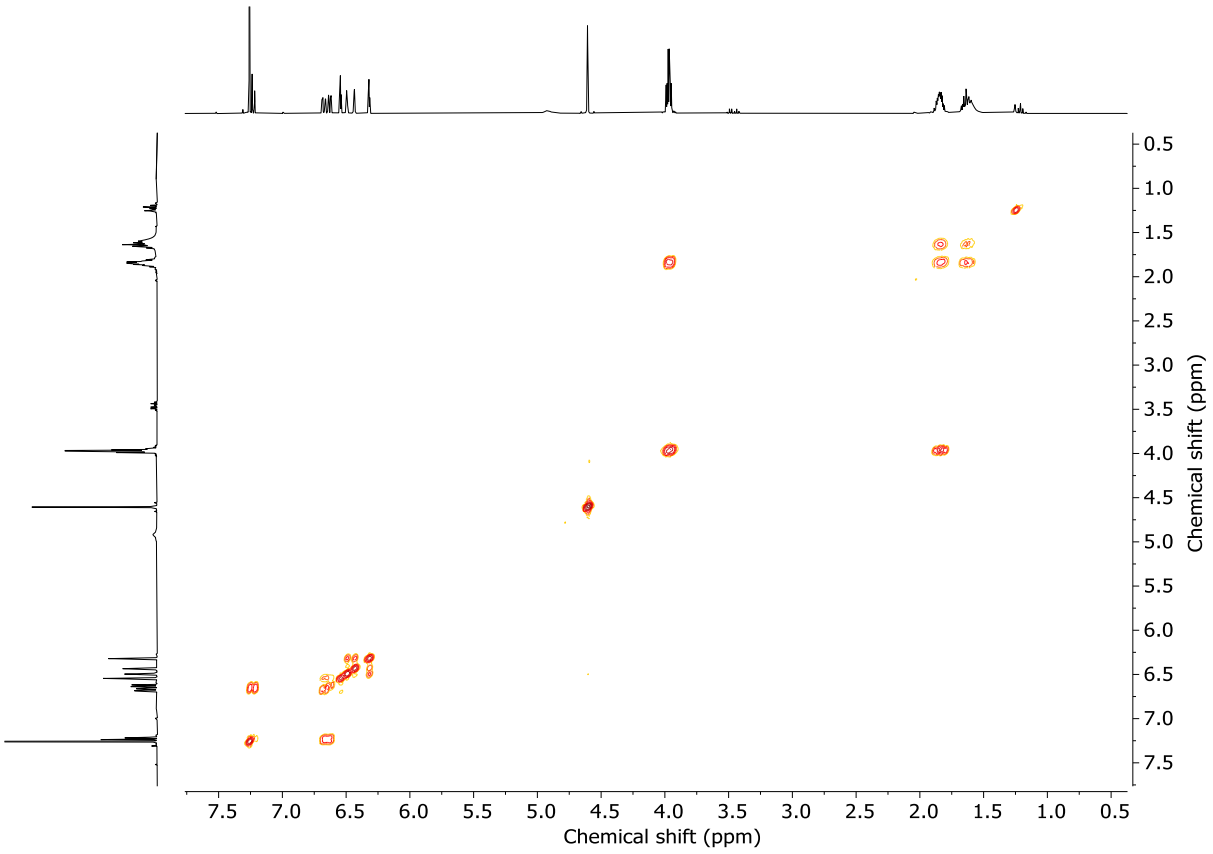

Figure S46: COSY NMR ($CDCl_3$, 298 K) of **S12**.

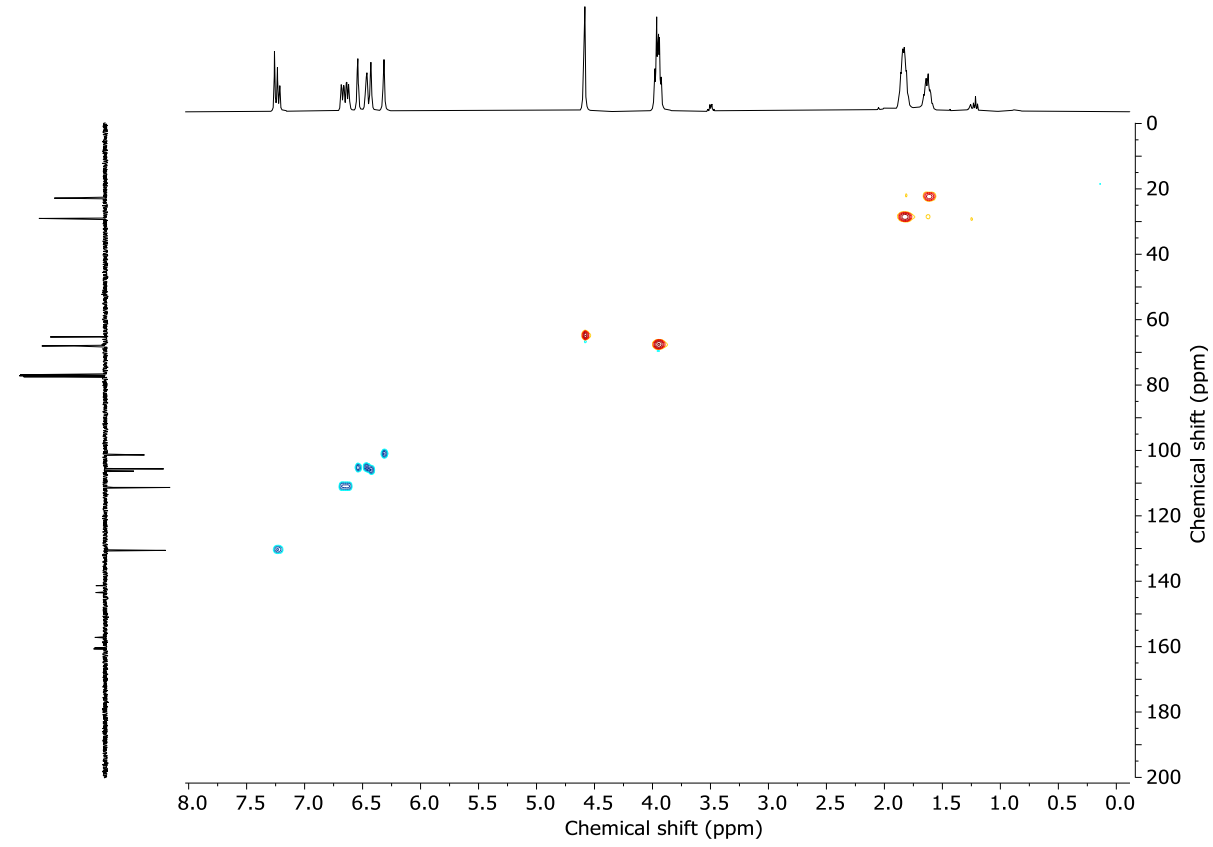

Figure S47: HSQC NMR ($CDCl_3$, 298 K) of **S12**.

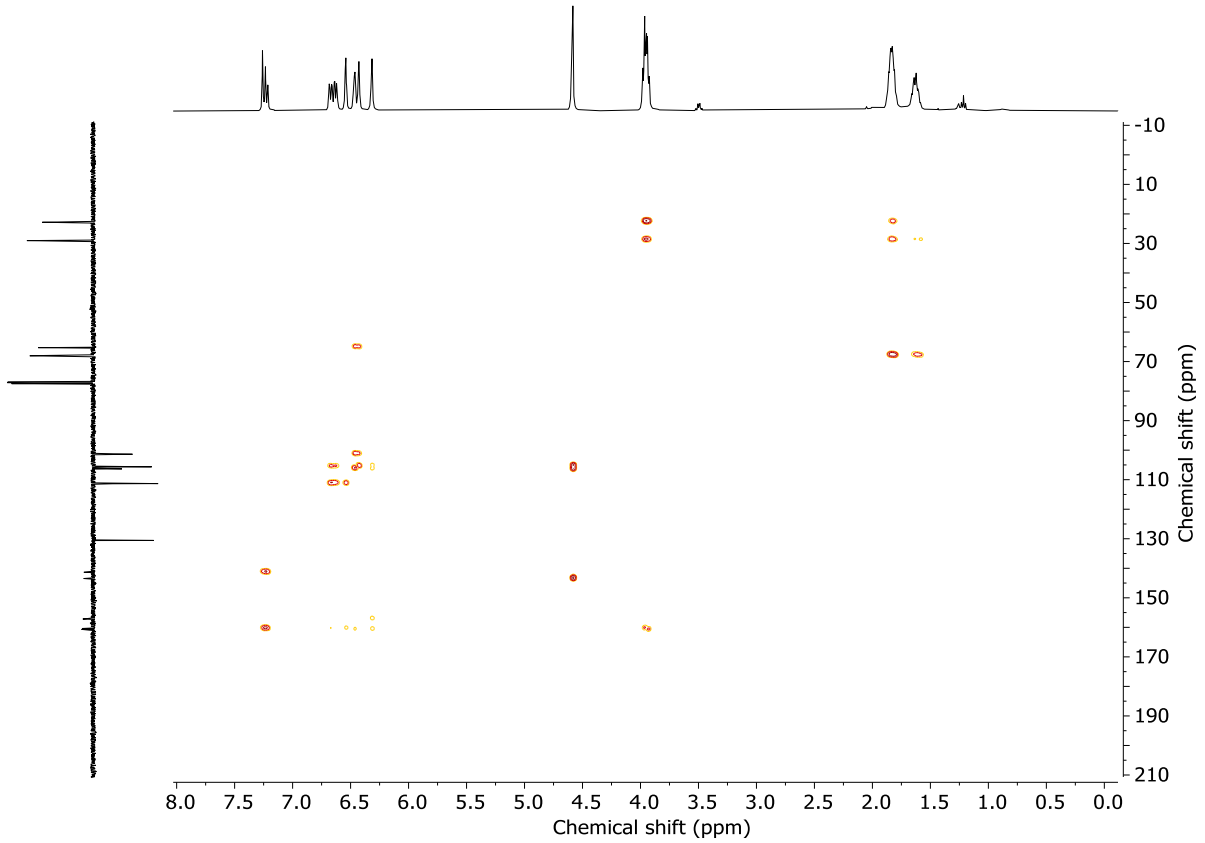

Figure S48: HMBC NMR ($CDCl_3$, 298 K) of **S12**.

3.4. Compounds leading to (*Z*)-1

Protected pre-macrocycle (*Z*)-S14

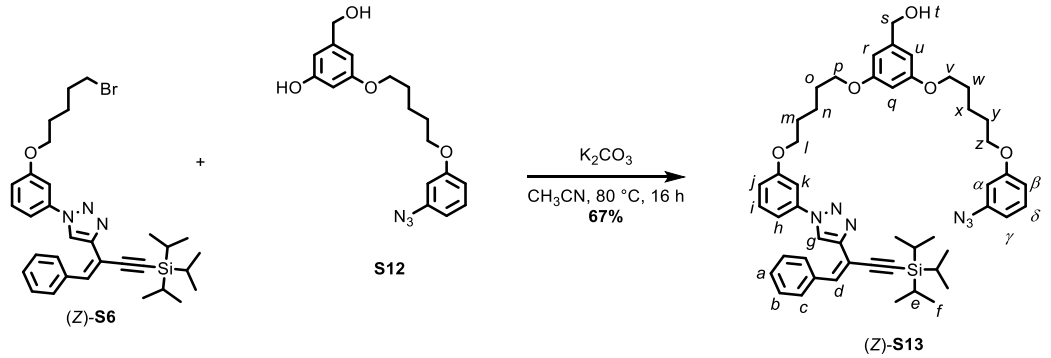

To a stirred solution of (*Z*)-**S6** (220 mg, 0.371 mmol) and **S12** (127mg, 0.371 mmol) at 80 °C in CH_3CN (3.5 mL) was added K_2CO_3 (213 mg, 1.54mmol), and the resulting mixture stirred for 18 h. The mixture was cooled to rt and filtered through Celite®. The residue was washed with EtOAc and the filtrate was concentrated *in vacuo*. Chromatography (petrol-Et_2O 100 : 0 to 8 : 2) gave (*Z*)-**S13** as a pale-yellow oil (246 mg, 78%).

^{1}H NMR (400 MHz, acetone-d_6) δ 8.35 (s, 1H, $\boldsymbol{H}_g$), 7.50-7.36 (m, 5H, $\boldsymbol{H}_c$, $\boldsymbol{H}_h$, $\boldsymbol{H}_i$, $\boldsymbol{H}_k$), 7.32-7.25 (m, 5H, $\boldsymbol{H}_a$, $\boldsymbol{H}_b$, $\boldsymbol{H}_d$, $\boldsymbol{H}_\delta$), 7.05 (ddd, *J* = 8.3, 2.4, 1.0, 1H, $\boldsymbol{H}_j$), 6.76 (ddd, *J* = 8.3, 2.4, 0.9, 1H, $\boldsymbol{H}_\beta$), 6.66 (ddd, *J* = 7.9, 2.2, 0.8, 1H, $\boldsymbol{H}_\gamma$), 6.61 (t, *J* = 2.2, 1H, $\boldsymbol{H}_\alpha$), 6.56 – 6.50 (m, 2H, $\boldsymbol{H}_r$, $\boldsymbol{H}_u$), 6.36 (t, *J* = 2.3, 1H, $\boldsymbol{H}_q$), 4.55 (dq, *J* = 5.9, 0.6, 2H, $\boldsymbol{H}_s$), 4.14 (t, *J* = 6.4, 2H, $\boldsymbol{H}_l$), 4.11 (t, *J* = 5.9, 1H, $\boldsymbol{H}_t$), 4.05 (t, *J* = 6.4, 2H, $\boldsymbol{H}_z$), 4.01 (t, *J* = 6.4, 2H, $\boldsymbol{H}_p$ or $\boldsymbol{H}_v$),3.99 (t, *J* = 6.4, 2H, $\boldsymbol{H}_p$ or $\boldsymbol{H}_v$), 1.94-1.79 (m, 8H, $\boldsymbol{H}_m$, $\boldsymbol{H}_o$, $\boldsymbol{H}_w$, $\boldsymbol{H}_y$), 1.73-1.61 (m, 4H, $\boldsymbol{H}_n$, $\boldsymbol{H}_x$), 1.16-1.13 (m, 21H, $\boldsymbol{H}_e$, $\boldsymbol{H}_f$)

^{13}C NMR (101 MHz, acetone-d_6) δ 161.4, 161.3 (x2), 161.1, 145.9, 145.3, 142.0, 140.4, 138.9, 136.6, 131.6, 131.5, 130.2, 129.3, 129.1, 122.4, 115.9, 114.5, 112.9, 112.3, 111.8, 109.3, 107.3, 106.2, 105.5 (x2), 100.5, 91.0, 69.0, 68.7, 68.4 (x2), 64.7, 29.8 (x2), 29.6 (x2), 23.4 (x2), 19.1, 12.1.

HR-ESI-MS (+ve): *m/z* = 855.4635 $[M + H]^+$ calc. for $C_{50}H_{63}N_6O_5Si$ 855.4624.

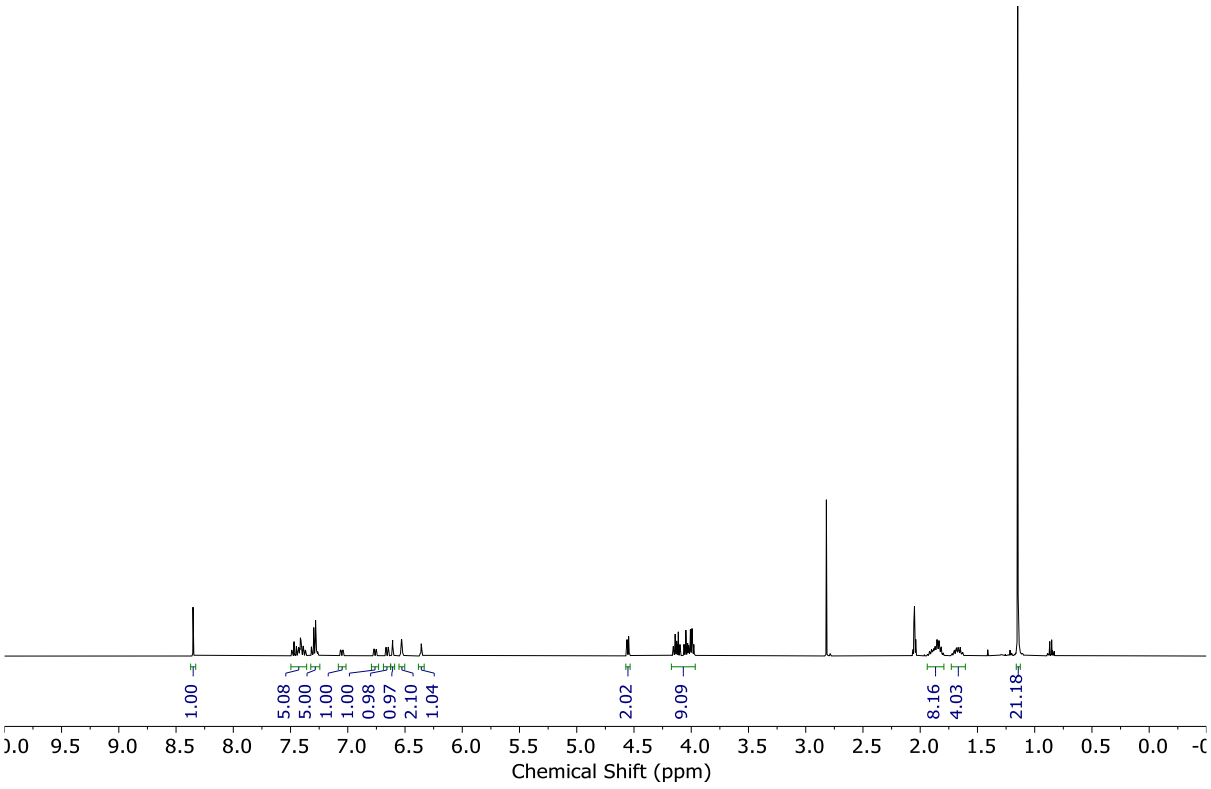

Figure S49: ^{1}H NMR (acetone-d_6, 400 MHz, 298 K) of (*Z*)-**S13**.

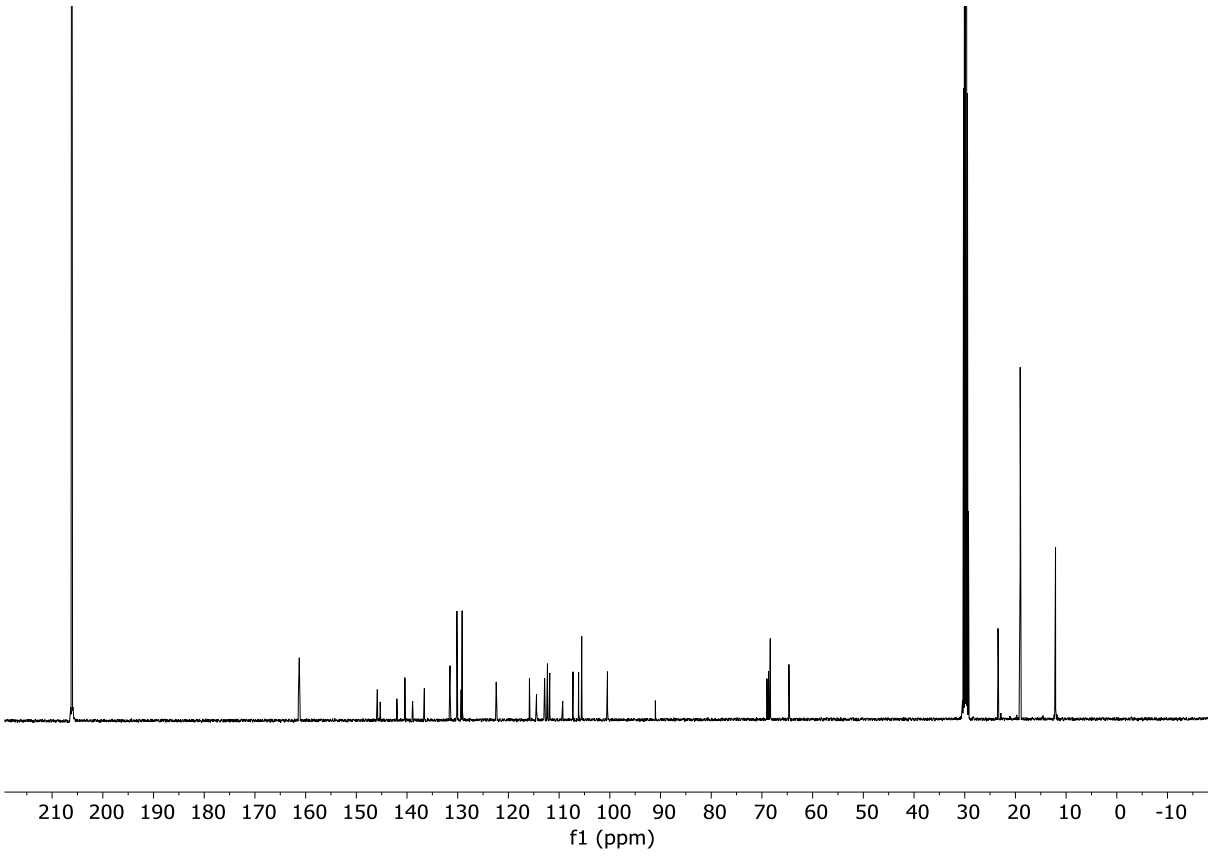

Figure S50: ^{13}C NMR (acetone-d_6, 101 MHz, 298 K) of (*Z*)-**S13**.

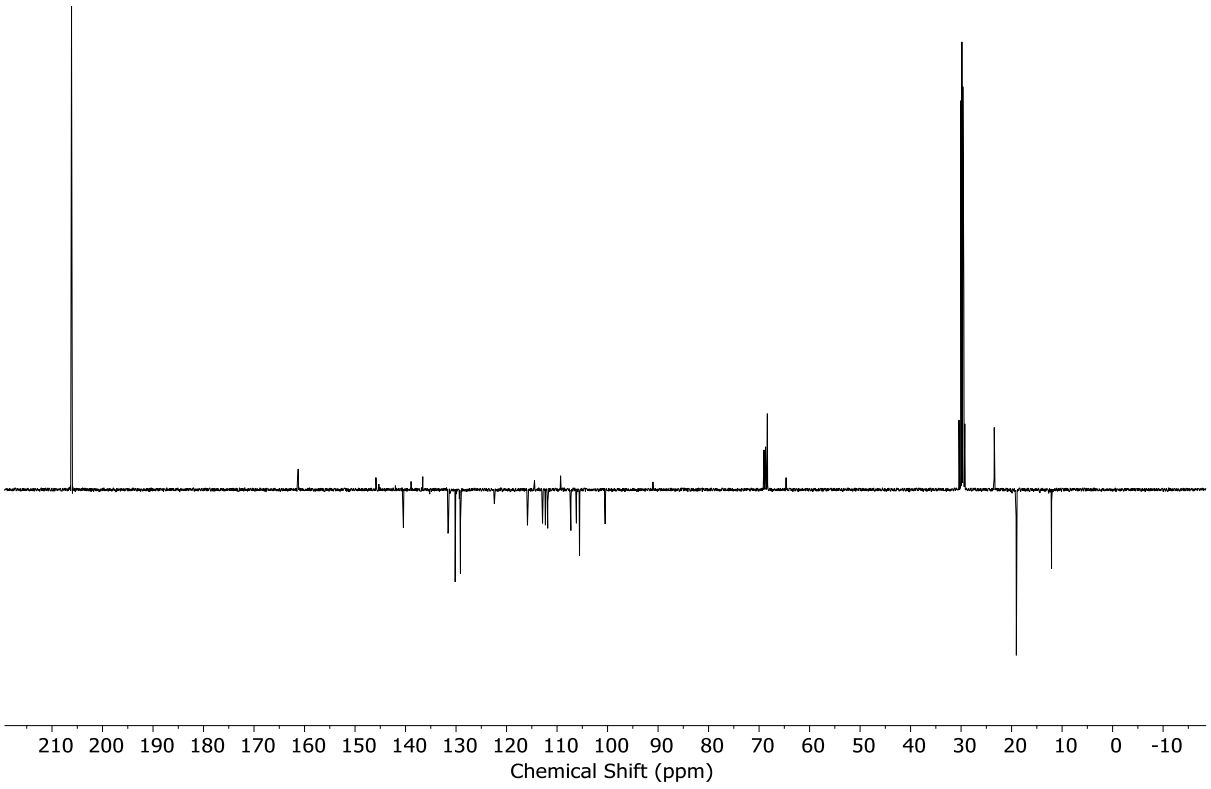

Figure S51: JMOD NMR (acetone-d_6, 101 MHz, 298 K) of (*Z*)-**S13**.

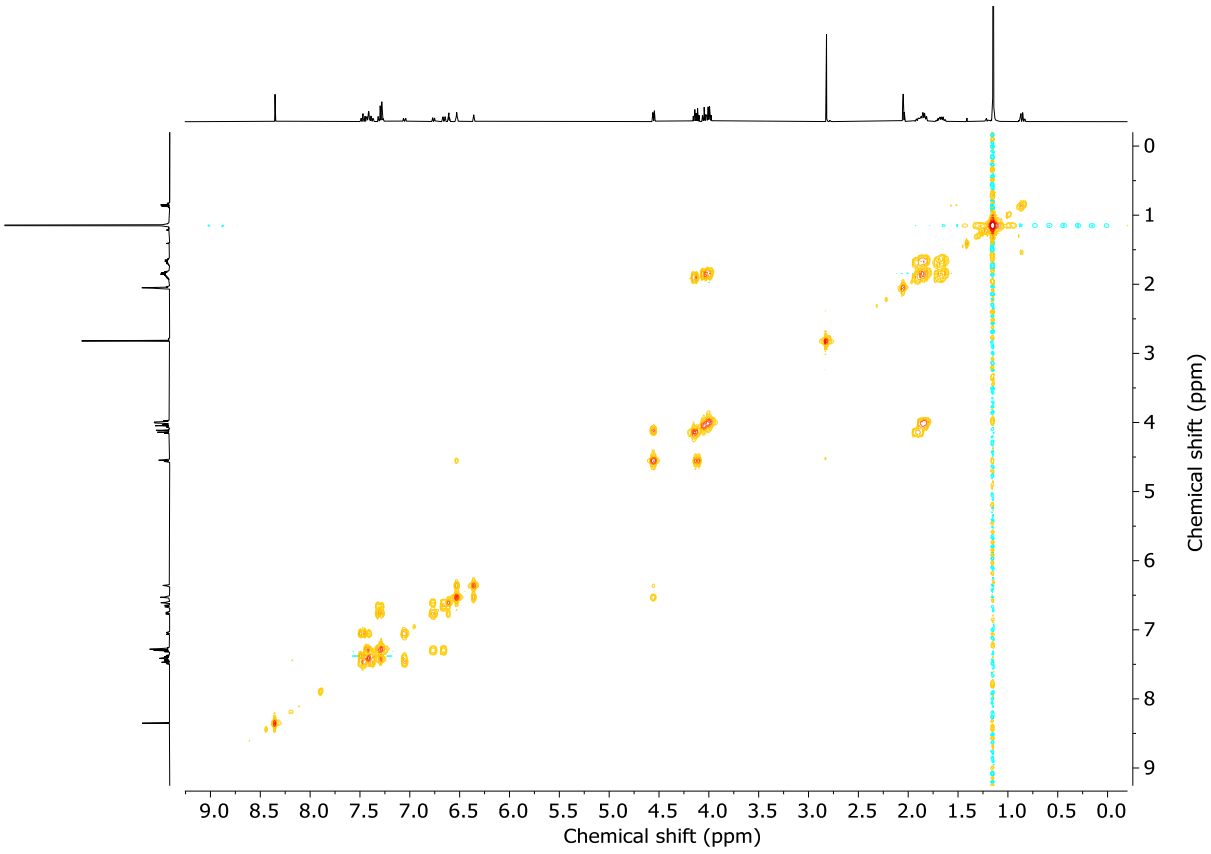

Figure S52: COSY NMR (acetone-d_6, 298 K) of (*Z*)-**S13**.

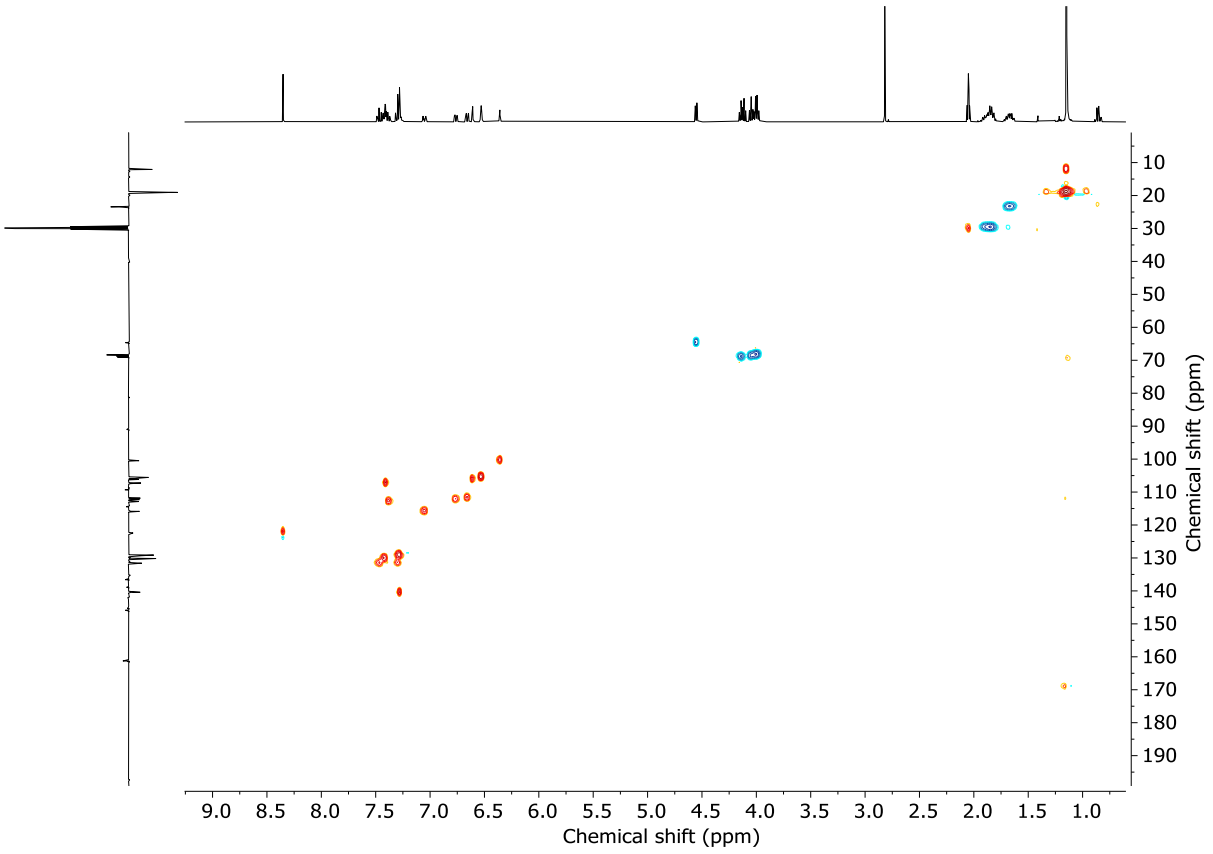

Figure S53: HSQC NMR (acetone-d_6, 298 K) of (*Z*)-**S13**.

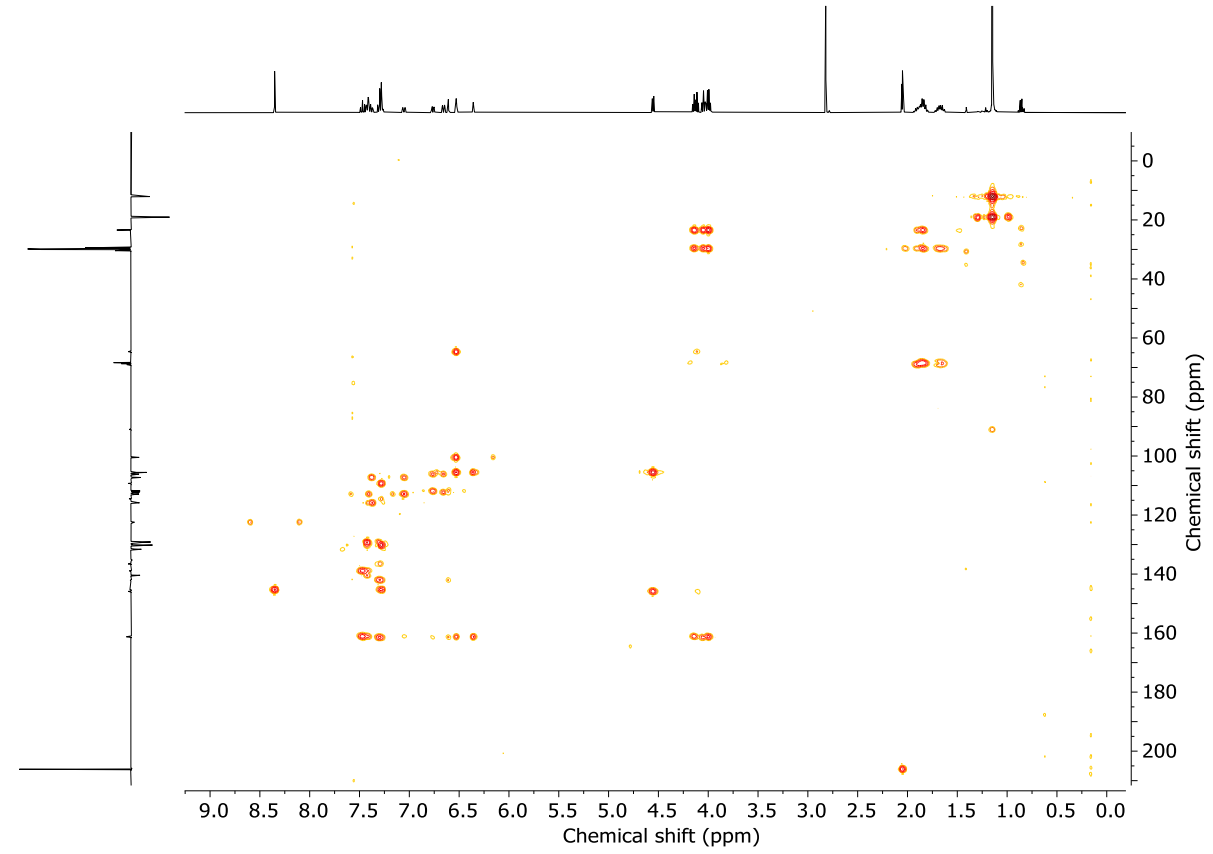

Figure S54: HMBC NMR (acetone-d_6, 298 K) of (*Z*)-**S14**.

Benzylic alcohol pre-macrocycle (*Z*)-S14

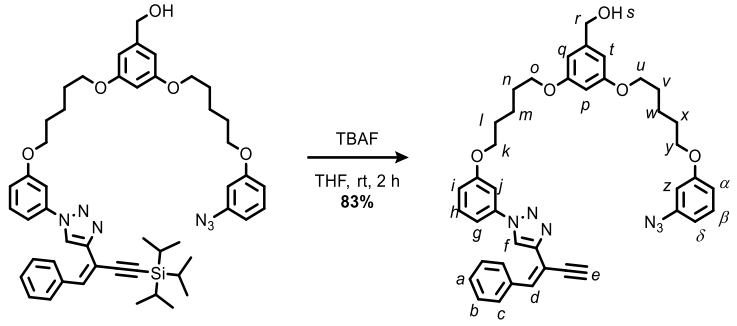

(*Z*)-**S13** (*Z*)-**S14**

To a stirred solution of (*Z*)-**S13** (220 mg, 0.257 mmol) in THF (2.5 mL) was added TBAF (1.0 M in THF, 1.3 mL, 1.3 mmol) and the resulting solution was stirred at rt for 2 h. The solution was diluted with sat. $NH_4Cl_{(aq.)}$ and extracted with Et_2O (3 x 20 mL). The combined organic phases were dried ($MgSO_4$), filtered, and concentrated *in vacuo*. Chromatography (^{n}hexane-acetone 100:0 to 1 : 1) gave benzylic alcohol pre-macrocycle (*Z*)-**S14** as a pale yellow oil (149 mg, 83%).

^{1}H NMR (400 MHz, acetone-d_6) δ 8.44 (s, 1H, $\boldsymbol{H}_f$), 7.51-7.40 (m, 5H, $\boldsymbol{H}_c$, $\boldsymbol{H}_g$, $\boldsymbol{H}_h$, $\boldsymbol{H}_j$), 7.35-7.23 (m, 5H, $\boldsymbol{H}_a$, $\boldsymbol{H}_b$, $\boldsymbol{H}_d$, $\boldsymbol{H}_\beta$), 7.05 (ddd, *J* = 7.7, 2.6, 1.4, 1H, $\boldsymbol{H}_i$), 6.76 (ddd, *J* = 8.3, 2.4, 0.9, 1H, $\boldsymbol{H}_\alpha$), 6.66 (ddd, *J* = 7.9, 2.1, 0.8, 1H, $\boldsymbol{H}_\delta$), 6.61 (t, *J* = 2.2, 1H, $\boldsymbol{H}_z$), 6.53 (ddq, *J* = 2.6, 1.7, 0.9, 2H, $\boldsymbol{H}_q$), 6.36 (t, *J* = 2.3, 1H, $\boldsymbol{H}_p$), 4.55 (d, *J* = 5.5, 2H, $\boldsymbol{H}_r$), 4.14 (t, *J* = 6.4, 2H, $\boldsymbol{H}_k$), 4.11 (t, *J* = 6.2, 1H, $\boldsymbol{H}_s$), 4.05 (t, *J* = 6.4, 2H, $\boldsymbol{H}_y$), 4.01 (t, *J* = 6.4, 2H, $\boldsymbol{H}_o$ or $\boldsymbol{H}_u$), 3.99 (t, *J* = 6.4, 2H, $\boldsymbol{H}_o$ or $\boldsymbol{H}_u$), 3.67 (d, *J* = 0.6, 1H, $\boldsymbol{H}_e$), 1.94-1.79 (m, 8H, $\boldsymbol{H}_l$, $\boldsymbol{H}_n$, $\boldsymbol{H}_v$, $\boldsymbol{H}_x$), 1.73-1.60 (m, 4H, $\boldsymbol{H}_m$, $\boldsymbol{H}_w$).

^{13}C NMR (101 MHz, acetone-d_6) δ 161.4, 161.3 (x2), 161.1, 145.9, 145.1, 142.0, 140.8, 138.9, 136.5, 131.6, 131.5, 130.2, 129.4, 129.1, 122.6, 115.8, 113.4, 112.9, 112.3, 111.9, 107.3, 106.2, 105.6 (x2), 100.5, 85.4, 79.1, 69.0, 68.7, 68.4 (x2), 64.7, 29.8 (x2), 29.6 (x2), 23.4 (x2).

HR-ESI-MS (+ve): *m/z* = 721.3120 $[M + Na]^+$ calc. for $C_{41}H_{42}N_6NaO_5$ 721.3109.

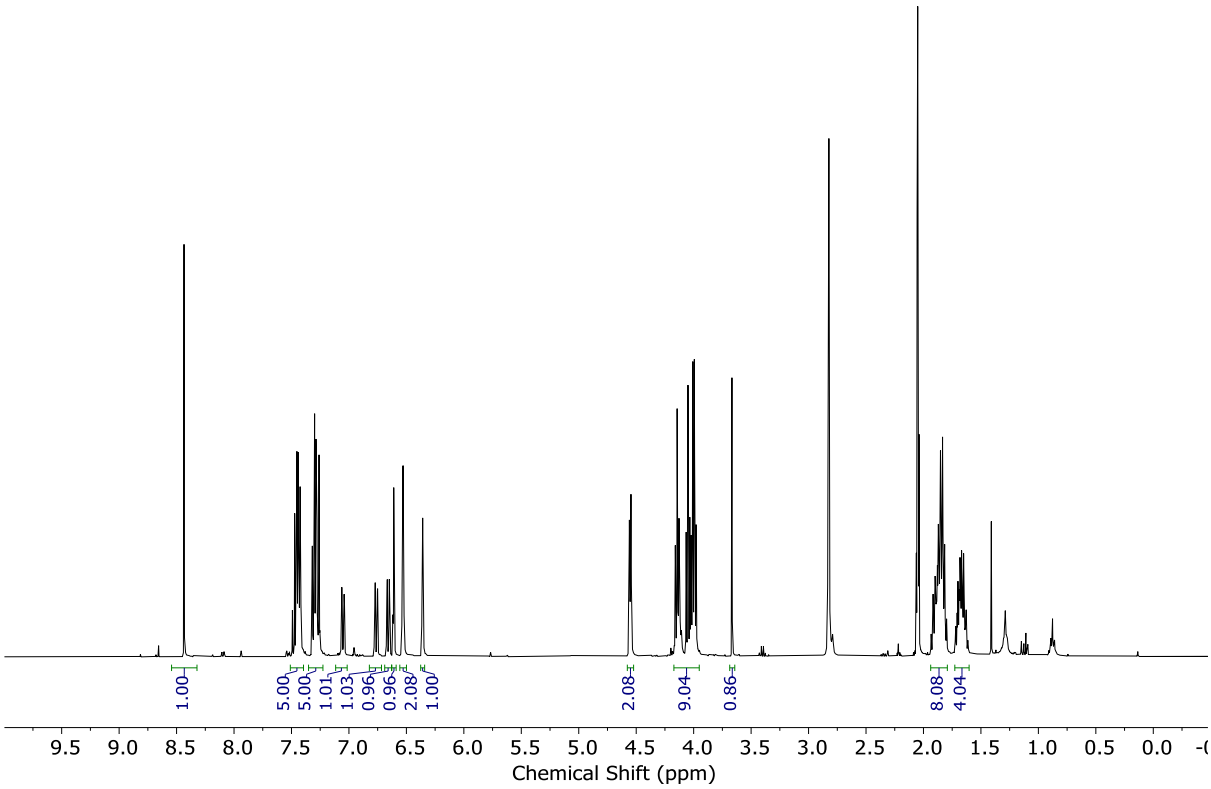

Figure S55: ^{1}H NMR (acetone-d_6, 400 MHz, 298 K) of (*Z*)-**S14**.

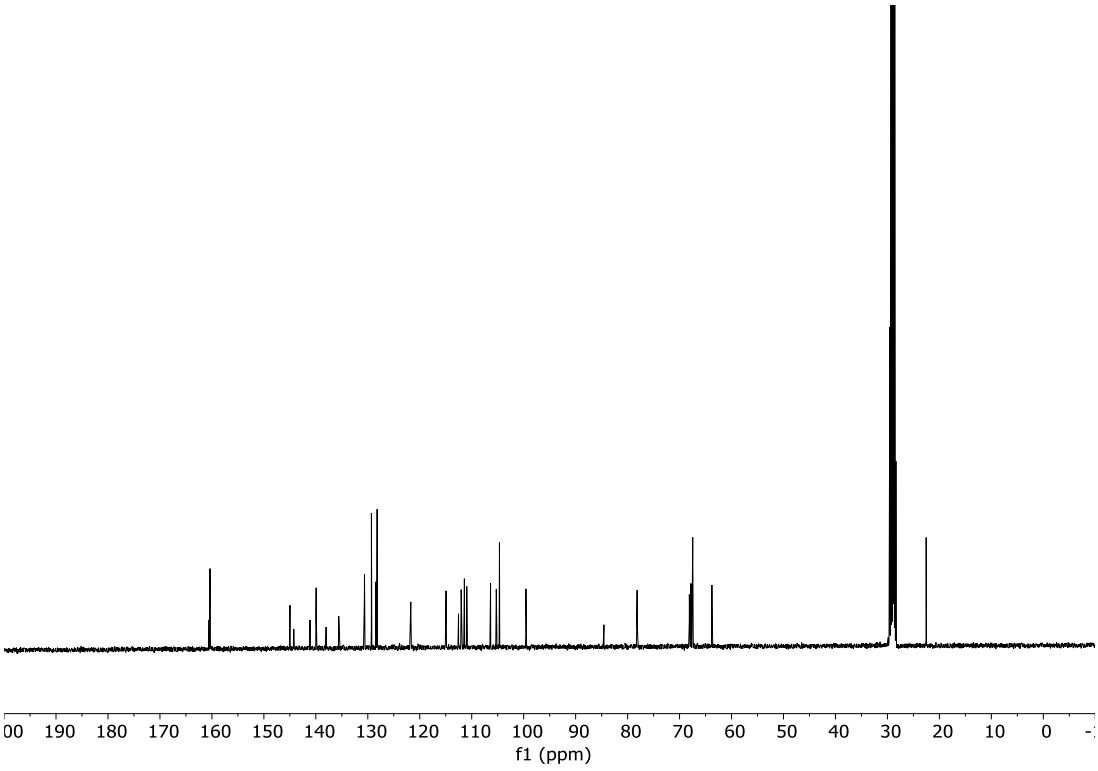

Figure S56: ^{13}C NMR (acetone-d_6, 101 MHz, 298 K) of (*Z*)-**S14**.

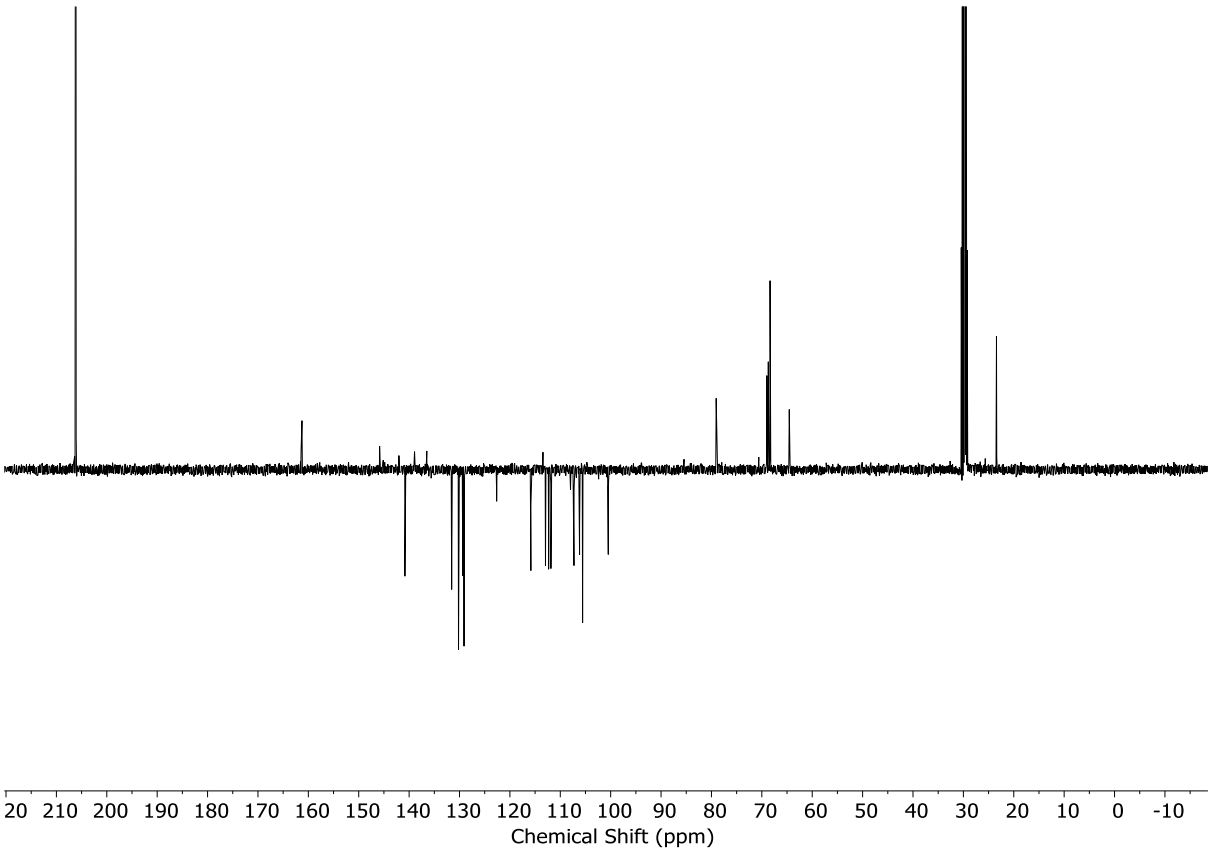

Figure S57: JMOD NMR (acetone-d_6, 101 MHz, 298 K) of (*Z*)-**S14**.

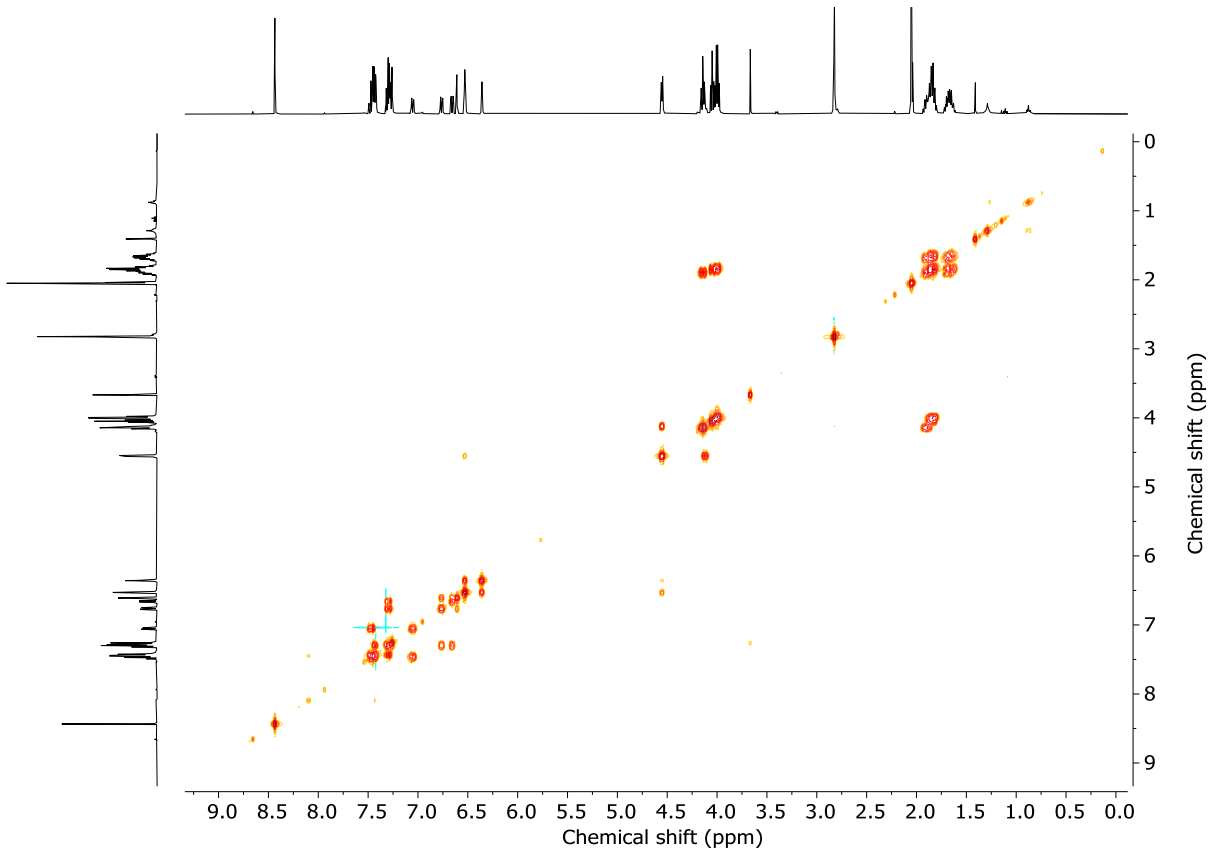

Figure S58: COSY NMR (acetone-d_6, 298 K) of (*Z*)-**S14**.

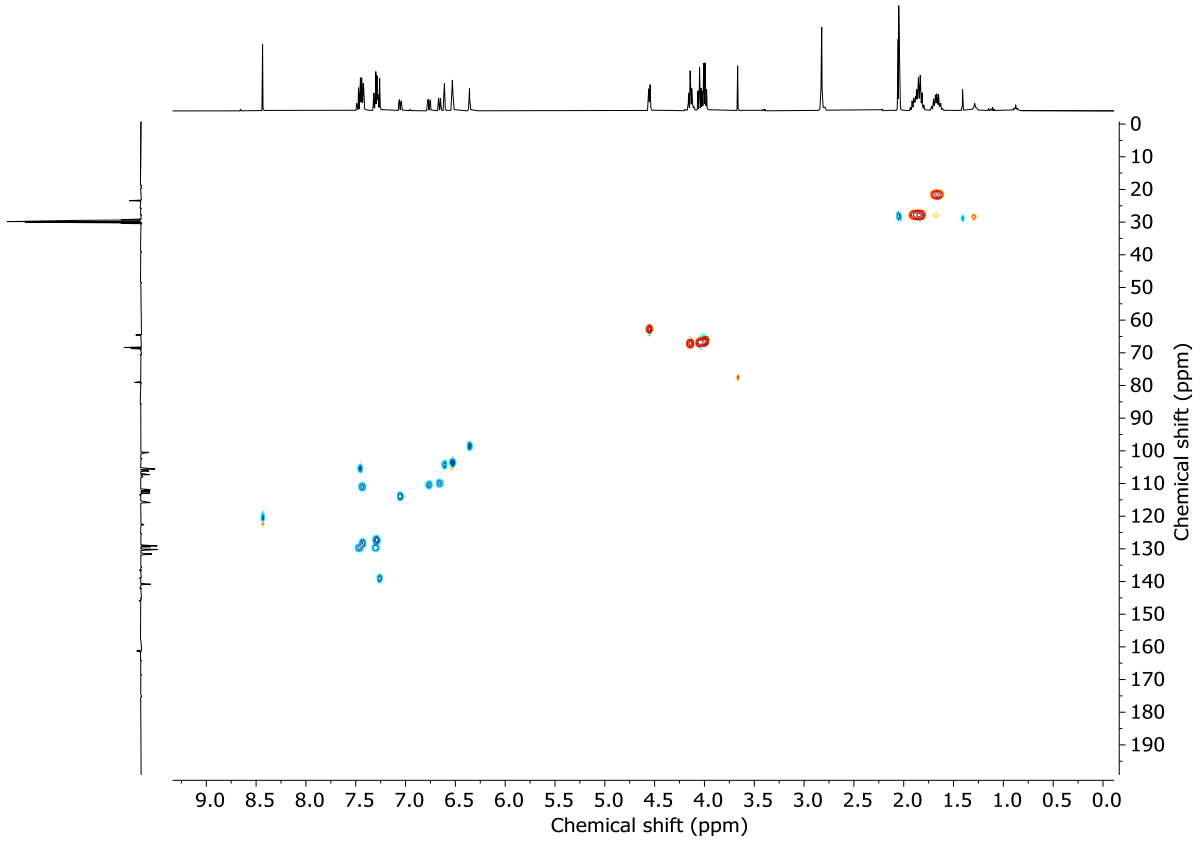

Figure S59: HSQC NMR (acetone-d_6, 298 K) of (*Z*)-**S14**.

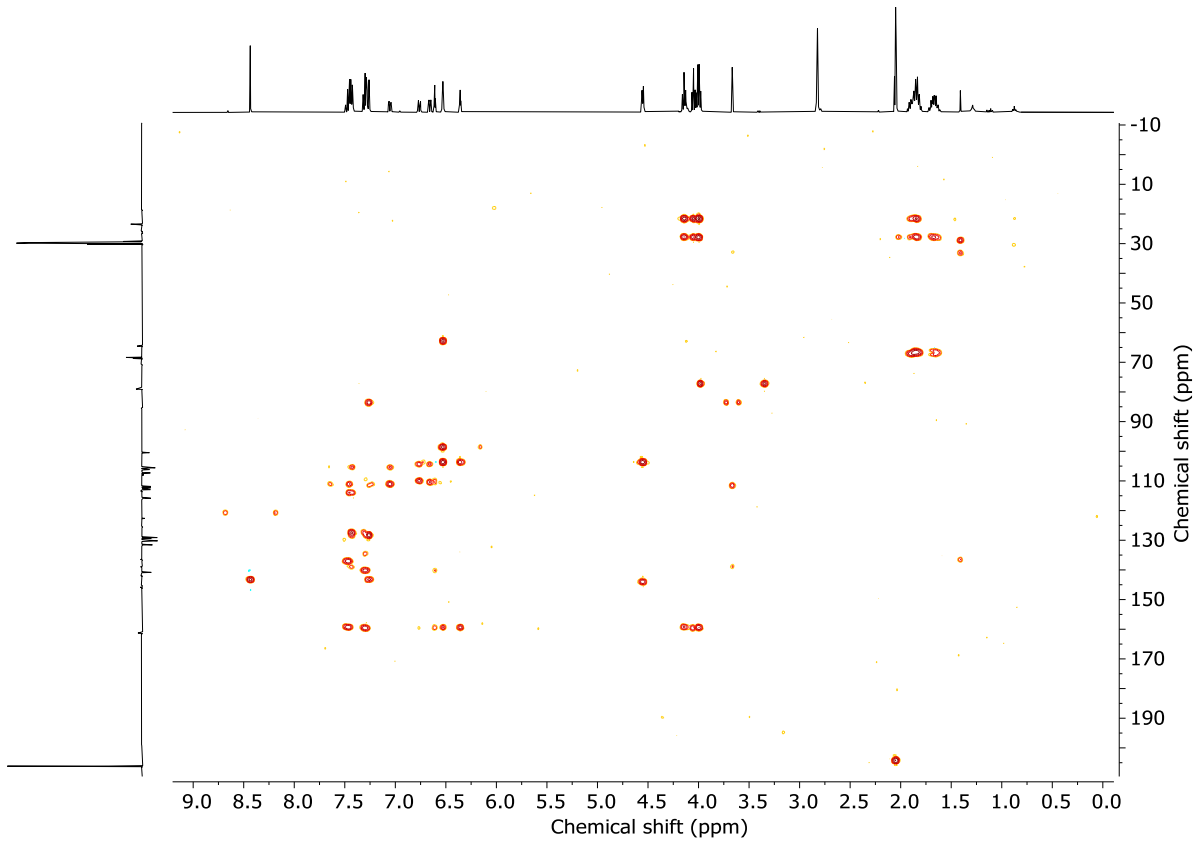

Figure S60: HMBC NMR (acetone-d_6, 298 K) of (*Z*)-**S14**.

Pre-macrocycle (*Z*)-1

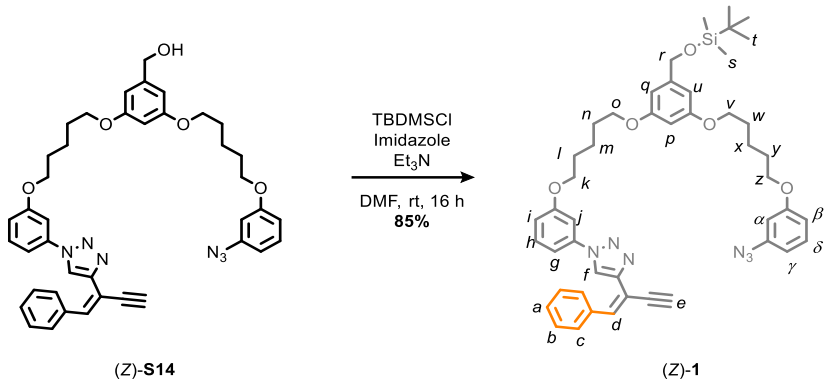

(*Z*)-**S14** (*Z*)-**1**

To a stirred solution of (*Z*)-**S14** (147 mg, 0.211 mmol), imidazole (70 mg, 1.0 mmol) and TBDMSCl (316 mg, 2.10 mmol) in DMF (2.0 mL) was added Et_3N (60 μL, 0.43 mmol) and the resulting solution was stirred at rt for 16 h. H_2O (15 mL) was added and the mixture was extracted with EtOAc (3 x 20 mL). The combined organic layers were washed with brine (2 x 20 mL), dried ($MgSO_4$), filtered, and concentrated *in vacuo*. Chromatography (^{n}hexane-acetone 100:0 to 1 : 1) gave (*Z*)-**1** as a pale yellow oil (146.3 mg, 85%).

^{1}H NMR (400 MHz, acetone-d_6) δ 8.43 (s, 1H, ***H***$_f$), 7.50-7.40 (m, 5H, ***H***$_c$, ***H***$_g$, ***H***$_h$, ***H***$_j$), 7.34-7.23 (m, 5H, ***H***$_a$, ***H***$_b$, ***H***$_d$, ***H***$_\delta$), 7.05 (ddd, *J* = 7.5, 2.7, 1.5, 1H, ***H***$_i$), 6.76 (ddd, *J* = 8.3, 2.4, 0.9, 1H, ***H***$_\beta$), 6.66 (ddd, *J* = 7.9, 2.1, 0.9, 1H, ***H***$_\gamma$), 6.61 (t, *J* = 2.2, 1H, ***H***$_\alpha$), 6.52 (dq, *J* = 2.4, 0.8, 2H, ***H***$_q$, ***H***$_u$), 6.37 (t, *J* = 2.3, 1H, ***H***$_p$), 4.69 (d, *J* = 0.7, 2H, ***H***$_r$), 4.14 (t, *J* = 6.4, 2H, ***H***$_k$), 4.05 (t, *J* = 6.4, 2H, ***H***$_z$), 4.01 (t, *J* = 6.4, 2H, ***H***$_y$), 4.00 (t, *J* = 6.4, 2H, ***H***$_o$ or ***H***$_u$), 3.66 (d, *J* = 0.7, 1H, ***H***$_e$), 1.93-1.79 (m, 8H, ***H***$_l$, ***H***$_n$, ***H***$_w$, ***H***$_y$), 1.73-1.60 (m, 4H, ***H***$_m$, ***H***$_x$), 0.94 (s, 9H, ***H***$_t$), 0.11 (s, 6H, ***H***$_s$).

^{13}C NMR (101 MHz, acetone-d_6) δ 161.4, 161.3 (x2), 161.1, 145.1, 144.9, 142.0, 140.8, 138.9, 136.5, 131.5, 131.5, 130.2, 129.3, 129.1, 122.6, 115.8, 113.4, 112.9, 112.3, 111.8, 107.3, 106.2, 105.1 (x2), 100.5, 85.5, 79.0, 69.0, 68.7, 68.4 (x2), 65.4, 29.7 (x2), 29.6 (x2), 26.3, 23.4 (x2), 18.9, -5.1.

HR-ESI-MS (+ve): *m/z* = 813.4173 $[M + H]^+$ calc. for $C_{47}H_{57}N_6O_5Si$ 813.4154.

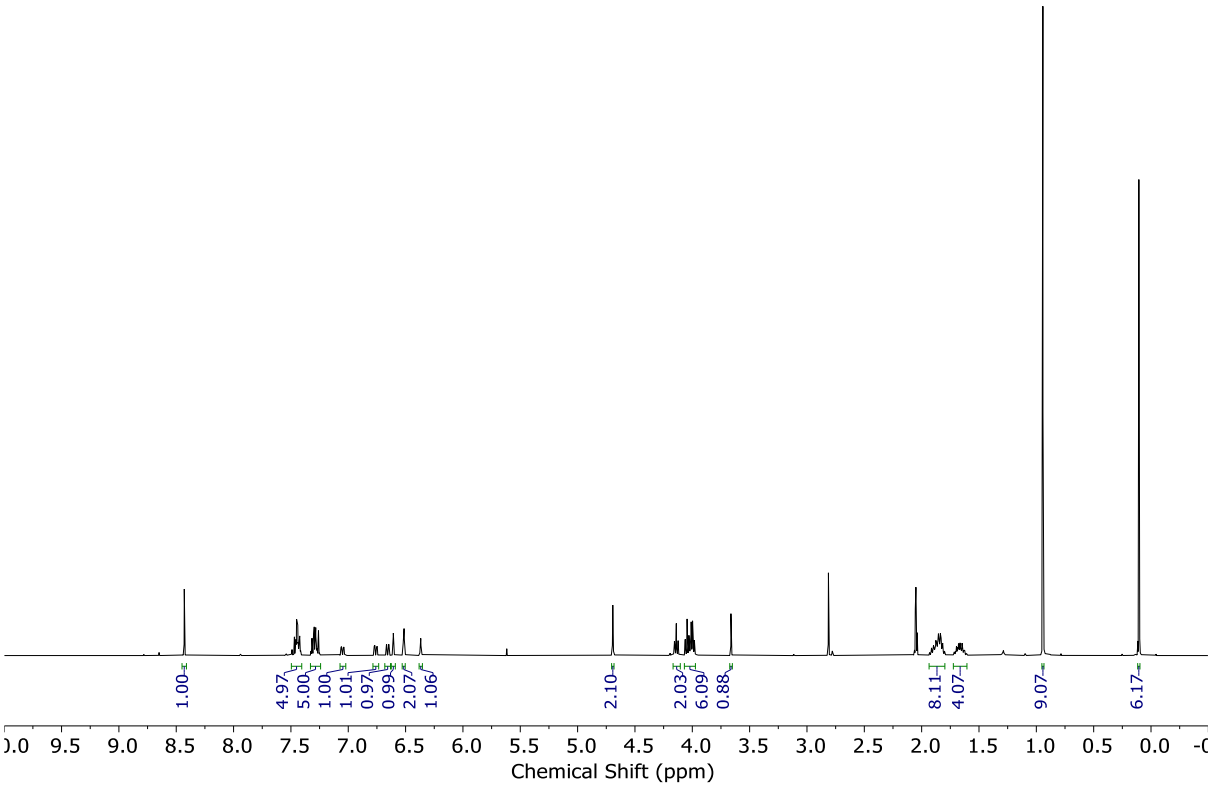

Figure S61: ^{1}H NMR (acetone-d_6, 400 MHz, 298 K) of (*Z*)-**1**.

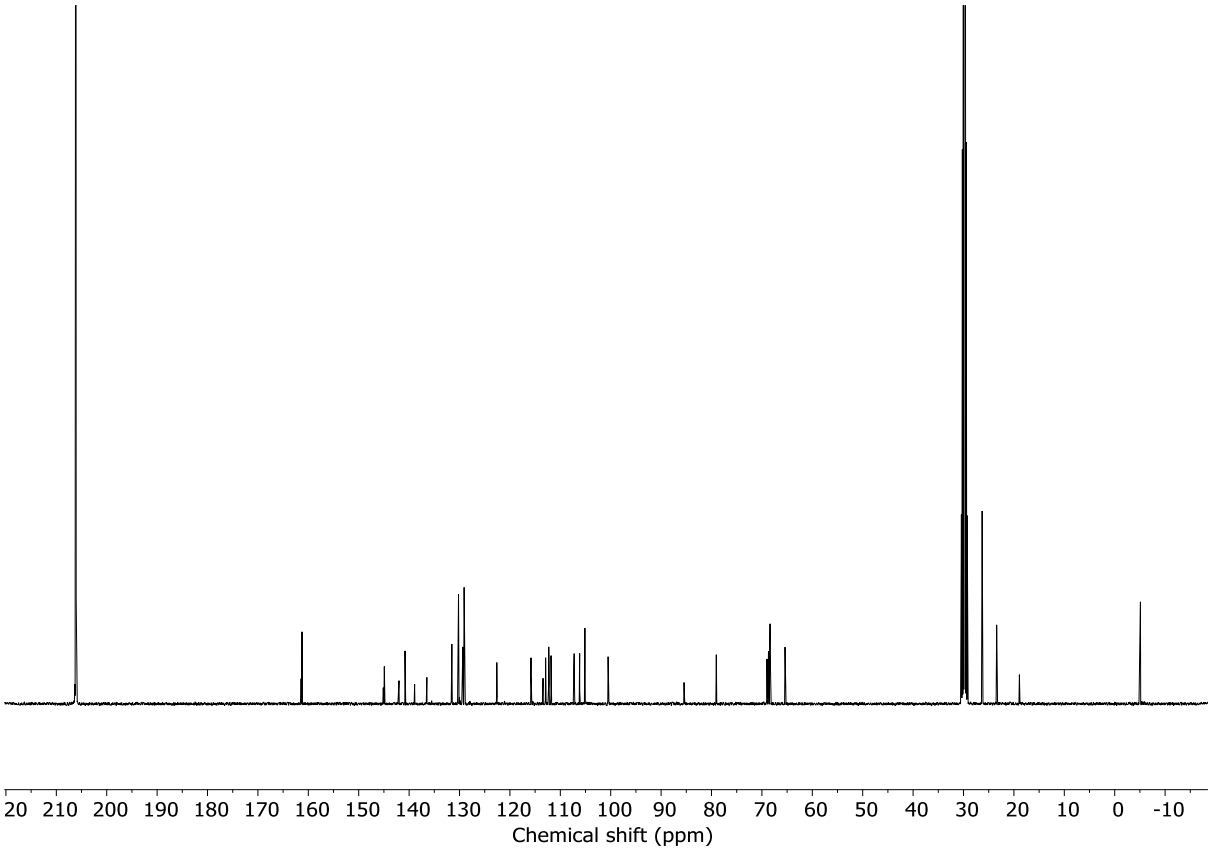

Figure S62: ^{13}C NMR (acetone-d_6, 101 MHz, 298 K) of (*Z*)-**1**.

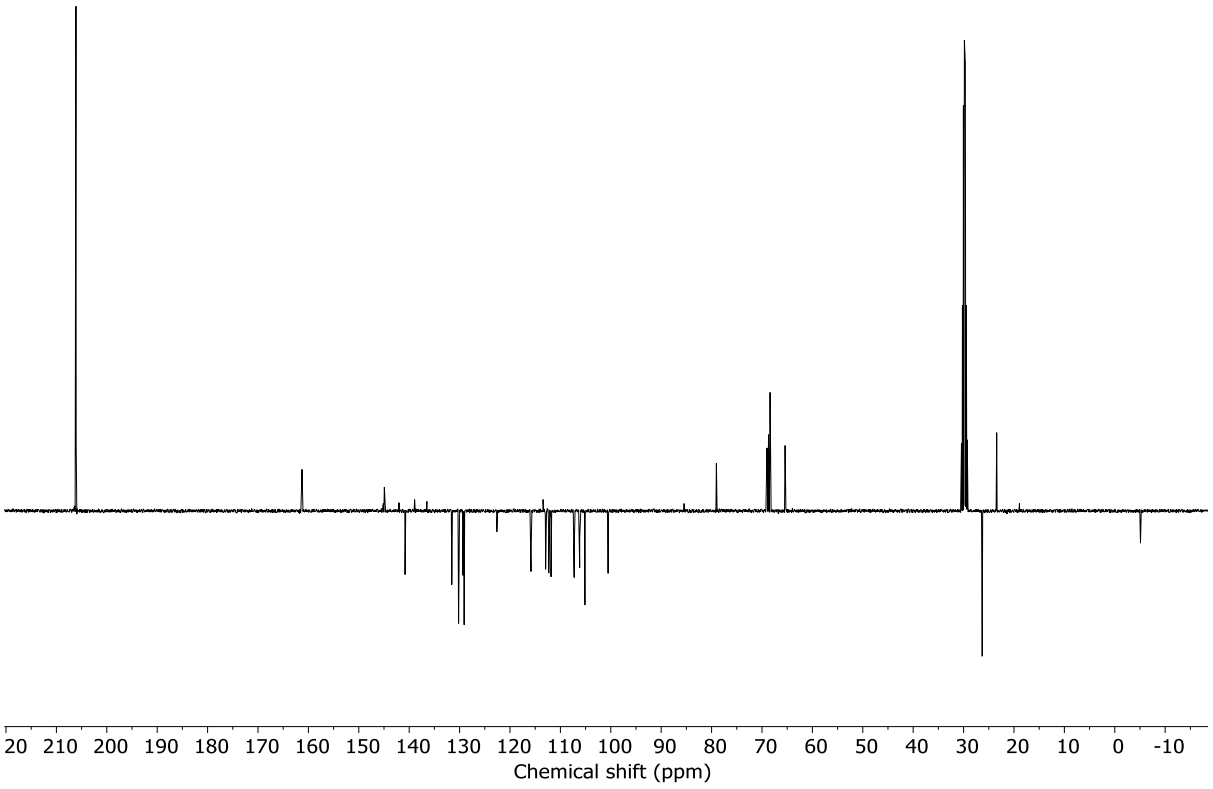

Figure S63: JMOD NMR (acetone-d_6, 101 MHz, 298 K) of (*Z*)-**1**.

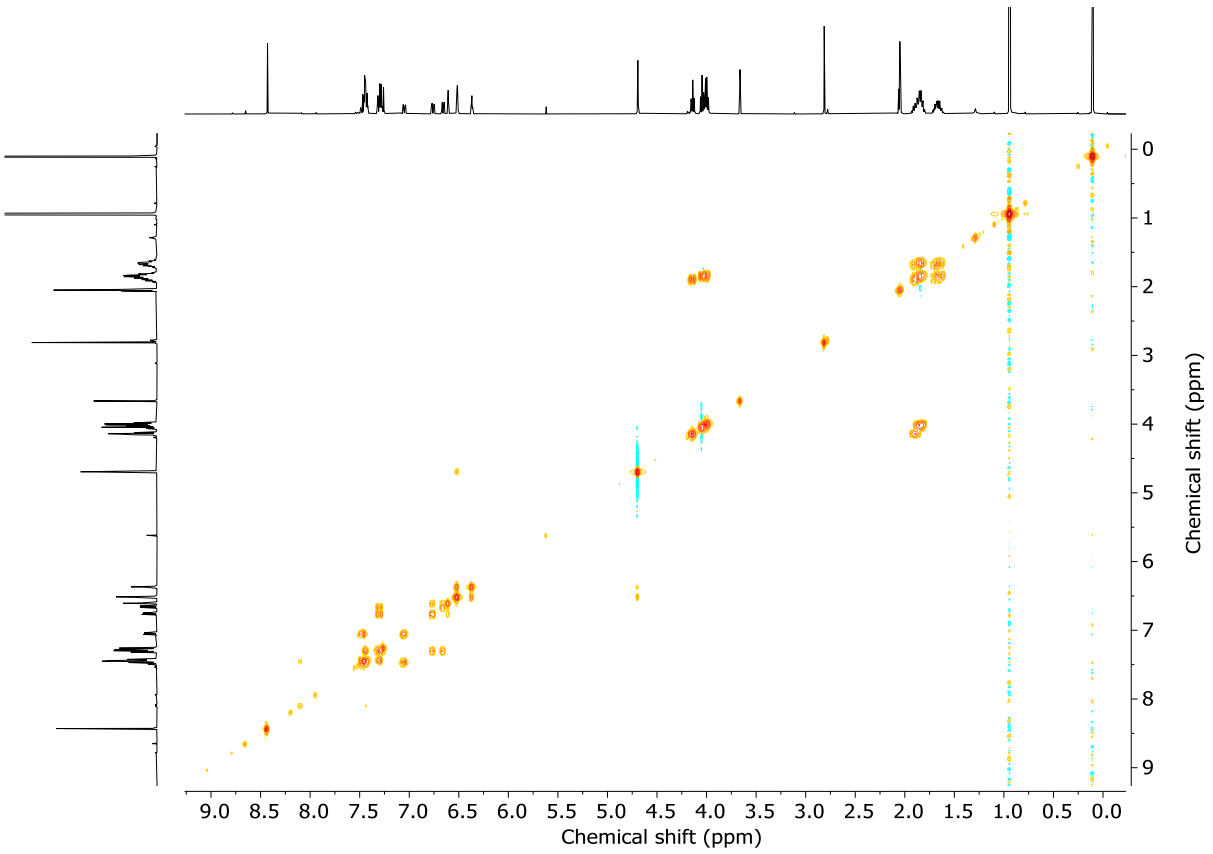

Figure S64: COSY NMR (acetone-d_6, 298 K) of (*Z*)-**1**.

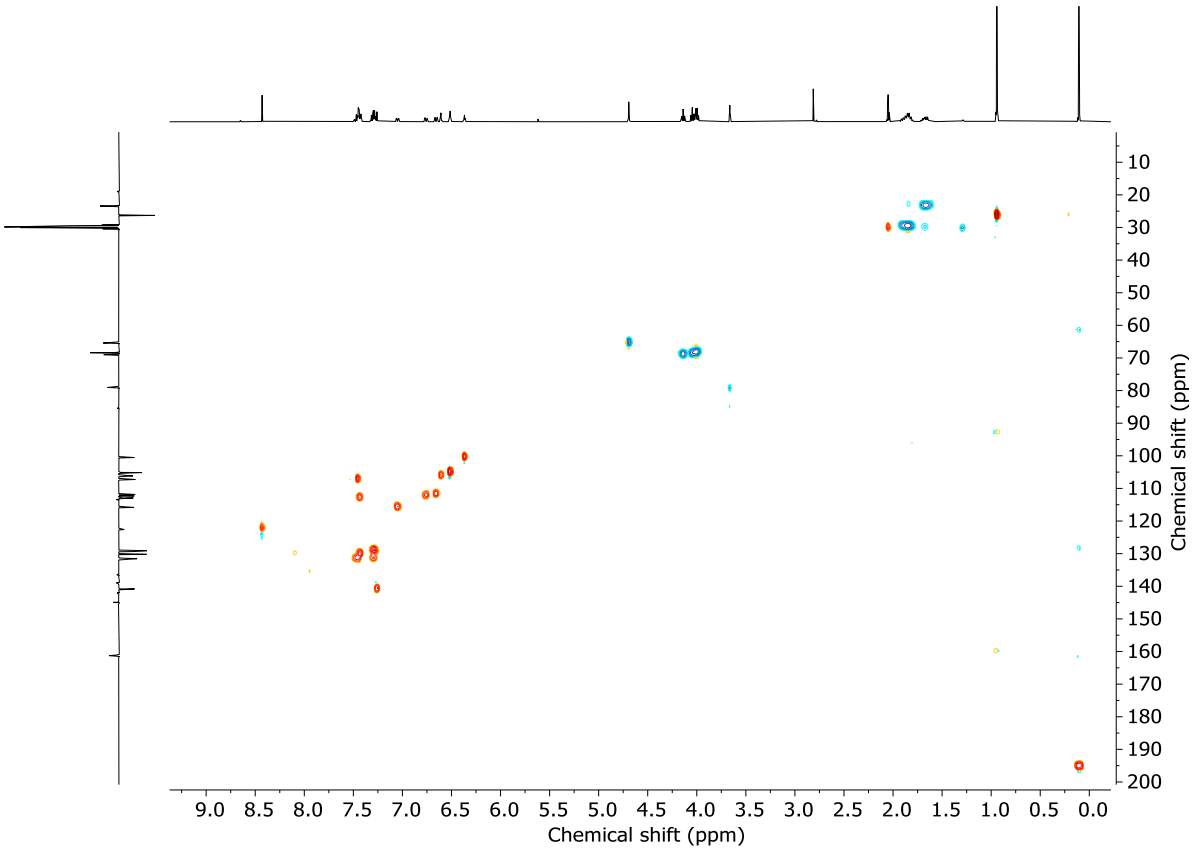

Figure S65: HSQC NMR (acetone-d_6, 298 K) of (*Z*)-**1**.

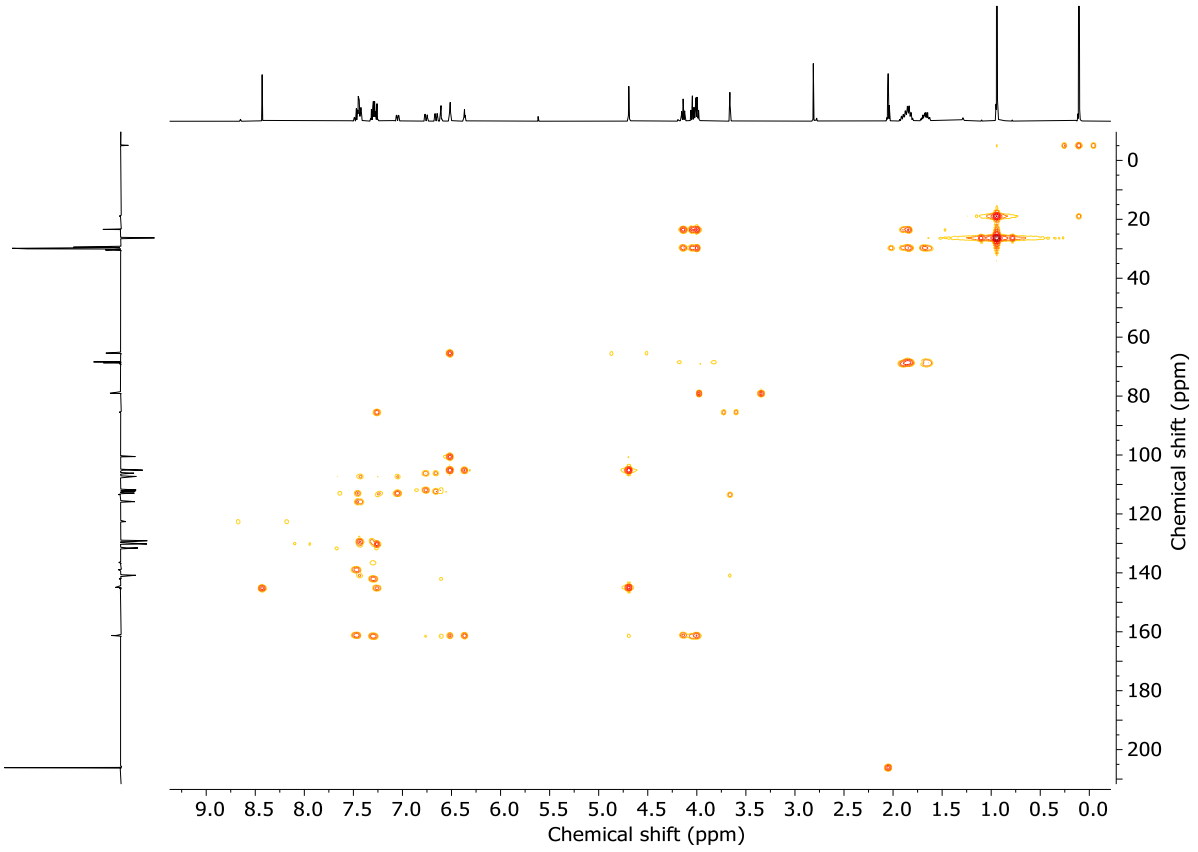

Figure S66: HMBC NMR (acetone-d_6, 298 K) of (*Z*)-**1**.

4. Synthesis of Catenane (R_{MP})-5 (Figure 2 in Main Text)

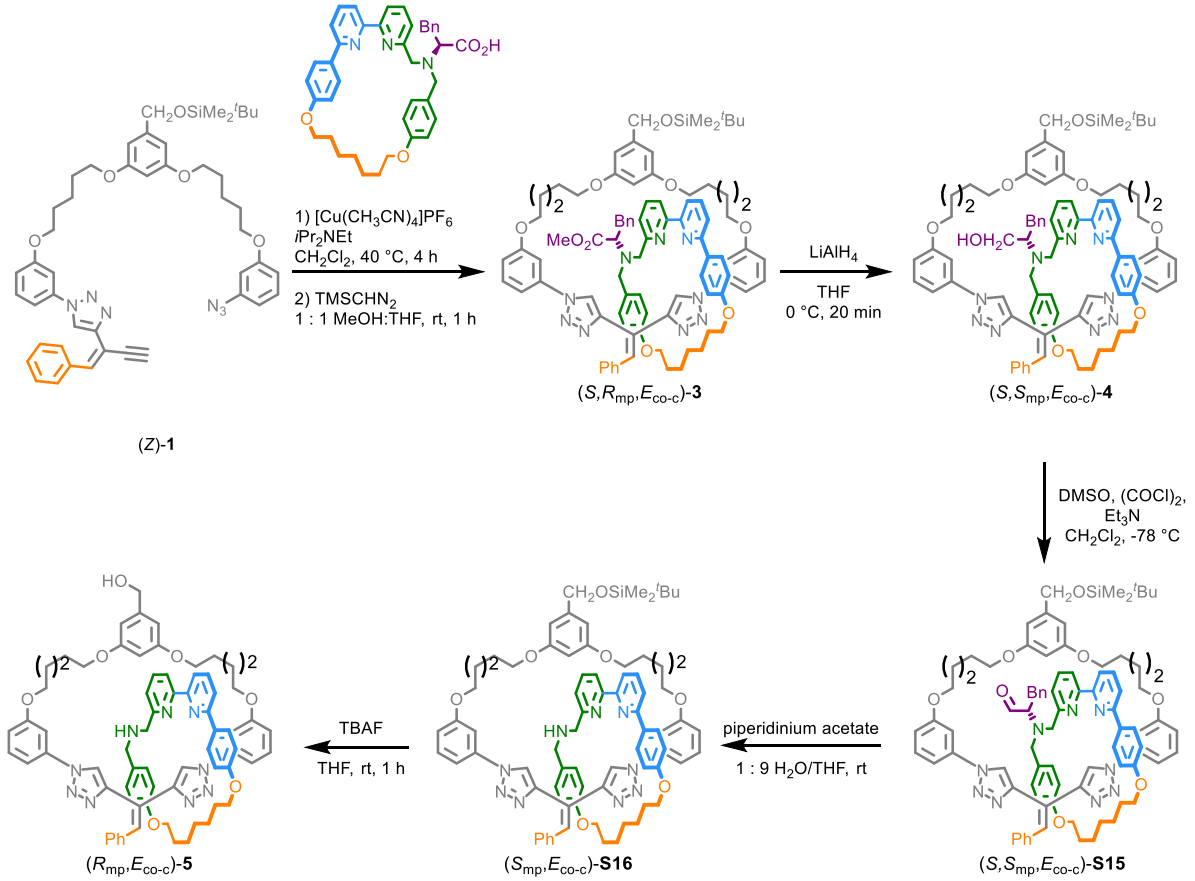

Scheme S4: Synthetic route to compound (R_{mp},$E_{co\text{-}c}$)-**5**.

Catenane (S,R_{mp},$E_{co\text{-}c}$)-3

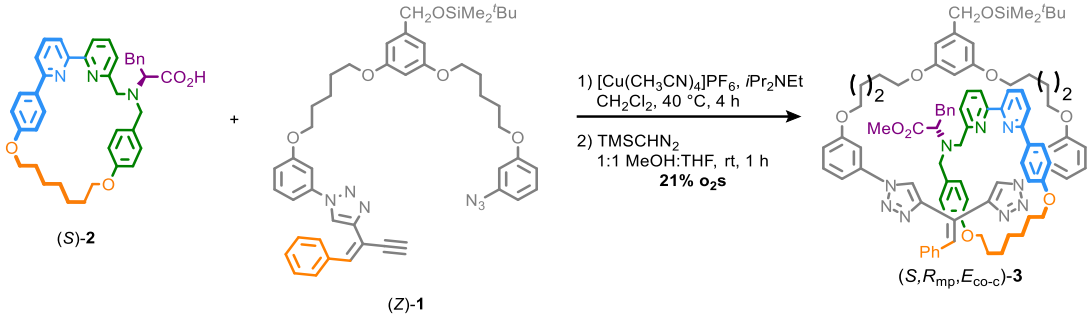

To a stirred solution of (S)-**2** (10 mg, 0.016 mmol), $[Cu(CH_3CN)_4]PF_6$ (5.7 mg, 0.15 mmol), and $^{i}Pr_2NEt$ (11.5 µL, 0.0660 mmol) in CH_2Cl_2 (1.6 mL) at 35 °C was added (*Z*)-**1** (29 mg, 0.035 mmol) in CH_2Cl_2 (0.7 mL) at a constant rate using a syringe pump over 4 h. The reaction mixture was stirred for 10 min after the addition had completed, cooled to rt and sat. EDTA-$NH_{3(aq)}$ (2 mL) was added with stirring. After 17 h, the mixture was diluted with H_2O (20 mL), the layers were separated and the aqueous layer extracted with CH_2Cl_2 (3 x 10 mL). The combined organic layers were dried (Na_2SO_4), filtered, and concentrated *in vacuo*. The residue was redissolved in THF-MeOH (1 : 1, 1.0 mL), and $TMSCHN_2$ (2.0 M in hexanes, 0.05 mL, 0.1 mmol) was added and the resulting solution stirred at rt for 1 h then concentrated *in vacuo*. Chromatography (^{n}hexane-CH_2Cl_2-Et_2O 1 : 1 : 0 to 0 : 0 : 1) afforded (S,R_{mp},$E_{co\text{-}c}$)-**3** as an colorless film (5 mg, 21% over two steps).

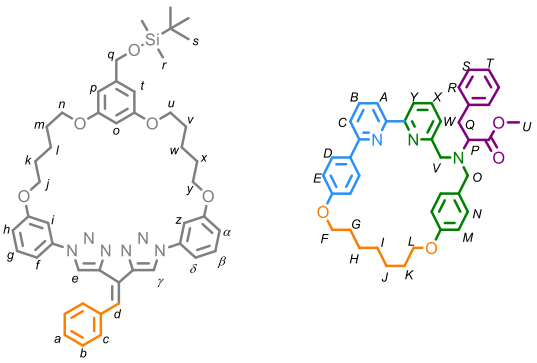

^{1}H NMR (400 MHz, CD_2Cl_2) δ_H 9.37 (s, 1H, H_γ), 8.59 (s, 1H, H_e), 7.71 (s, 1H, H_d), 7.56 (t, J = 7.8, 1H, H_B), 7.35 – 7.15 (m, 12H, H_a, H_b, H_c, H_f, H_g, H_δ,H_A, H_C, H_T, H_X), 7.15 – 7.04 (m, 6H, H_D, H_W, H_Y, H_S), 6.97 (t, J = 8.2, 1H, H_β), 6.88 (t, J = 2.2, 1H, H_z), 6.87-6.82 (m, 2H, H_R), 6.79 (ddd, J = 7.9, 2.4, 1.4, 1H, H_h), 6.65 (d, J = 8.5, 2H, H_N), 6.60 (t, J = 2.2, 1H, H_i), 6.58-6.52 (m, 4H, H_p, H_t, H_E), 6.50 (ddd, J = 8.2, 2.4, 0.9, 1H, H_α), 6.43 (t, J = 2.4, 1H, H_o), 6.16 (d, J = 8.5, 2H, H_M), 4.72 (s, 2H, H_q), 4.25-4.11 (m, 2H, H_F), 4.05-3.74 (m, 8H, 1 of H_j, H_n, 1 of H_O, H_u, H_L), 3.62 (s, 3H, H_U), 3.61-3.55 (m, 1H, 1 of H_j), 3.42-3.22 (m, 5H, H_y, H_P, H_V), 3.11 (dd, J = 13.9, 10.7, 1H, 1 of H_Q), 2.80 (d, J = 13.3, 1H, 1 of H_O), 2.59 (dd, J = 14.0, 4.2, 1H, 1 of H_Q), 2.04-1.50 (m, 18H, H_k, H_l, H_m, H_v, H_G, H_H, H_I, H_J, H_K), 1.39-1.22 (m, 3H, H_x, 1 of H_w), 1.17-1.04 (m, 1H, 1 of H_w), 0.98 (app d, J = 0.4, 9H, H_s), 0.14 (app d, J = 0.4, 6H, H_r).

^{13}C NMR (101 MHz, CD_2Cl_2) δ 171.7, 160.7, 160.7, 160.0, 159.7, 159.5, 159.3, 158.2, 158.0, 157.9 (x2), 147.1, 145.0, 144.8, 138.8, 138.3, 137.9, 137.8, 137.5, 136.6, 131.5, 130.4, 130.2, 129.9, 129.3, 129.1, 128.9 (x2), 128.5, 128.3, 128.1, 127.4, 126.5, 126.4, 123.0, 122.0, 121.6, 121.3, 120.7, 120.2, 115.3, 114.2, 113.7, 113.0, 112.0, 111.7, 106.3, 105.6, 104.4, 104.3, 101.2, 68.2, 68.2, 68.1, 68.0, 67.6, 65.3, 65.1, 62.4, 57.2, 55.1, 51.2, 37.4, 29.8, 29.3, 29.2, 29.1, 29.1, 29.0, 28.4, 26.1, 26.1, 26.0, 23.5, 23.2, 18.7, -5.2.

LR-ESI-MS (+ve): m/z = 1454.7 $[M + H]^+$ calc. for $C_{88}H_{100}N_9O_9Si$ 1454.7.

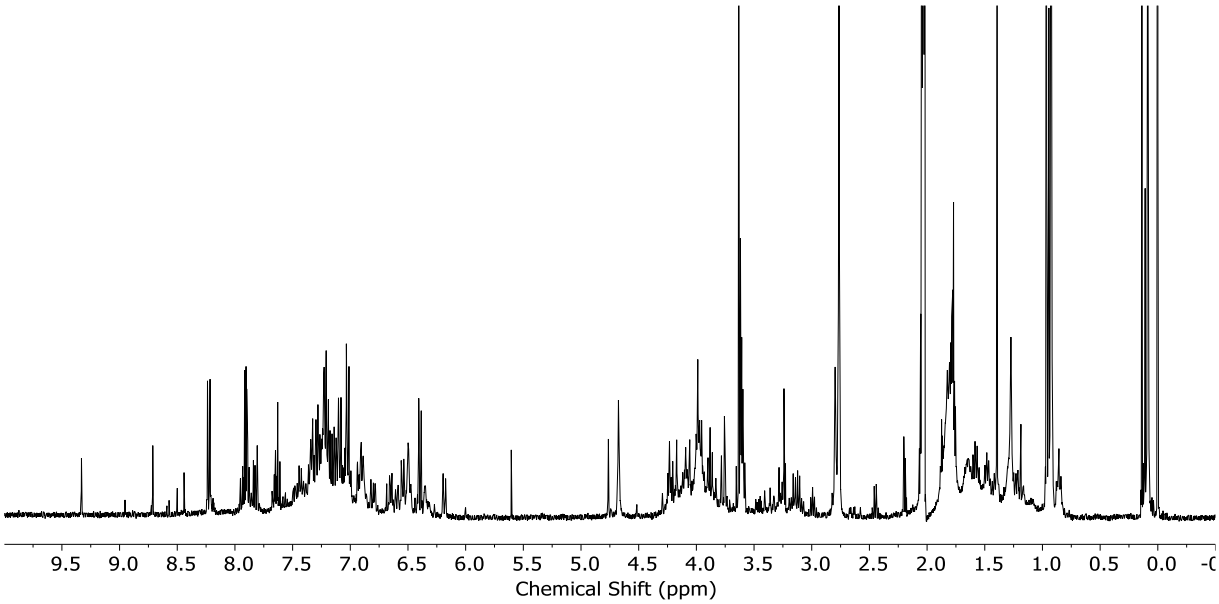

Figure S67: ^{1}H NMR (acetone-d_6, 400 MHz, 298 K) of the residue containing (S,R_{mp},$E_{co\text{-}c}$)-**3** prior to chromatography.

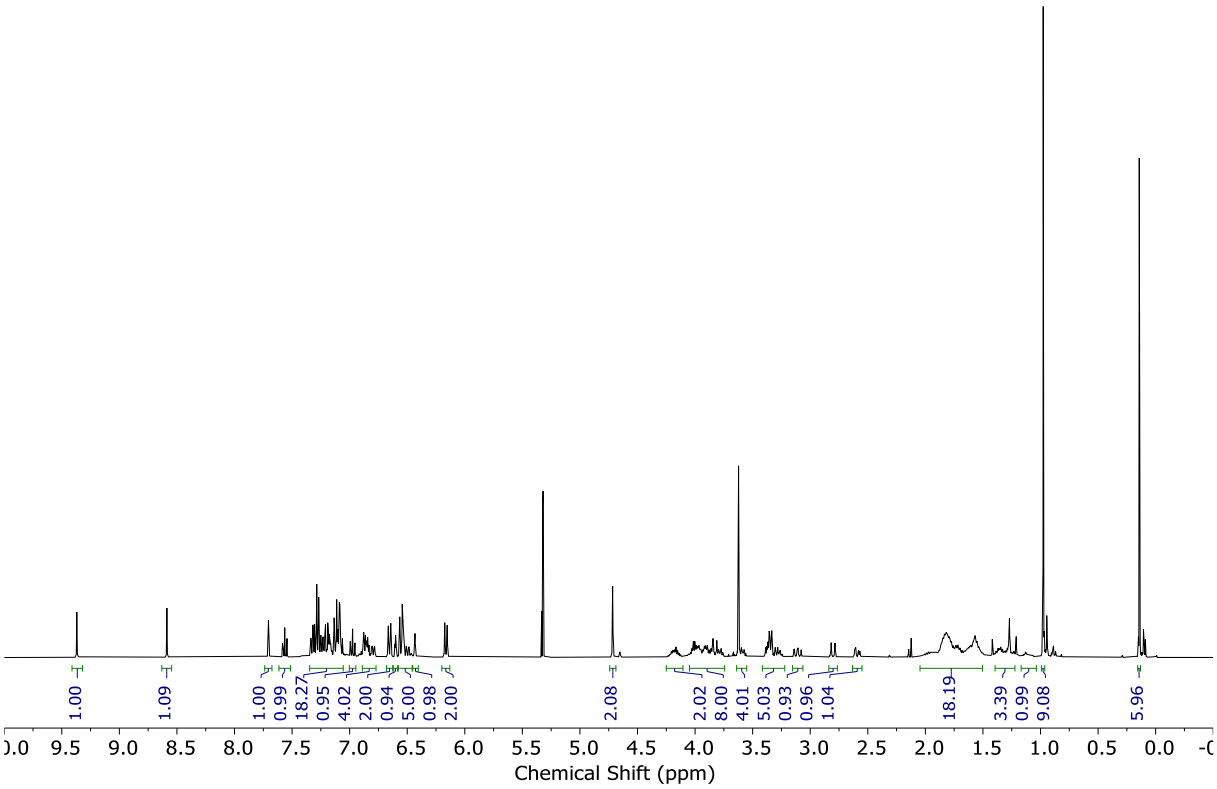

Figure S68: ^{1}H NMR (CD_2Cl_2, 400 MHz, 298 K) of (S,R_{mp},$E_{co\text{-}c}$)-**3**.

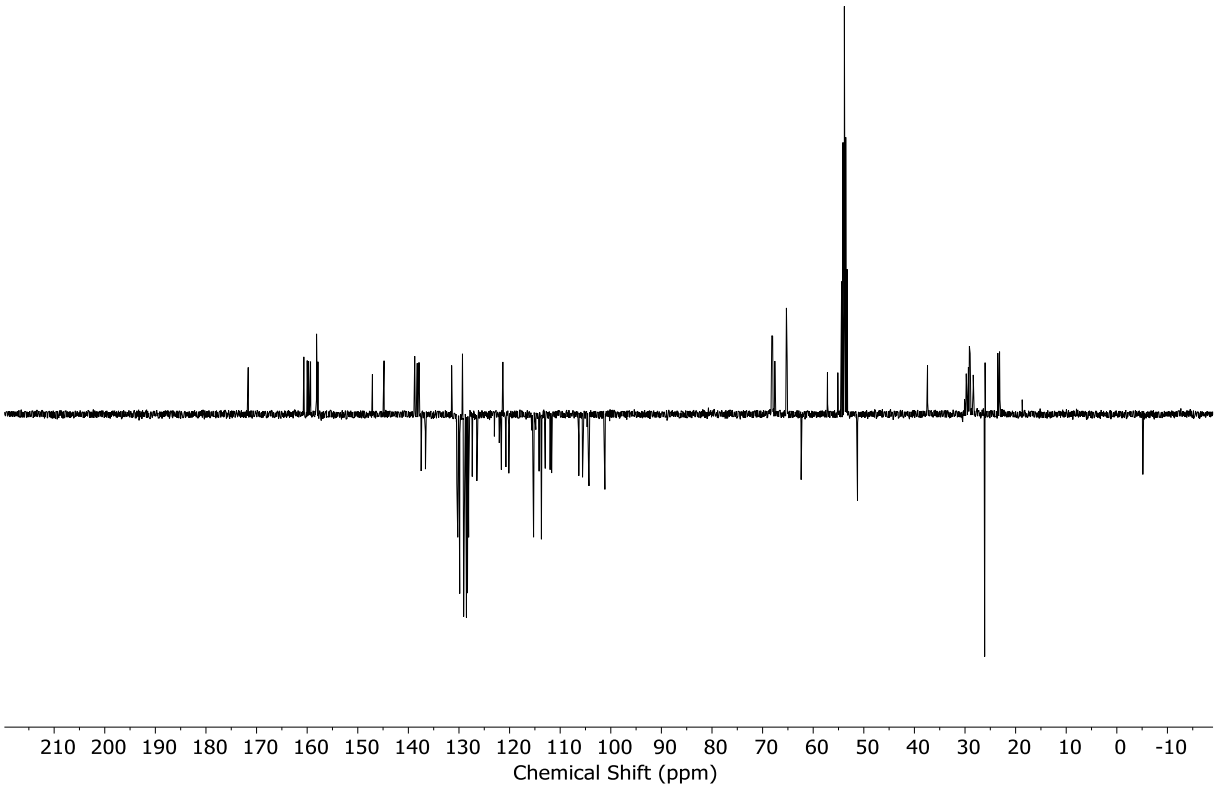

Figure S69: J-MOD NMR (CD_2Cl_2, 101 MHz, 298 K) of (S,R_{mp},$E_{co\text{-}c}$)-**3**.

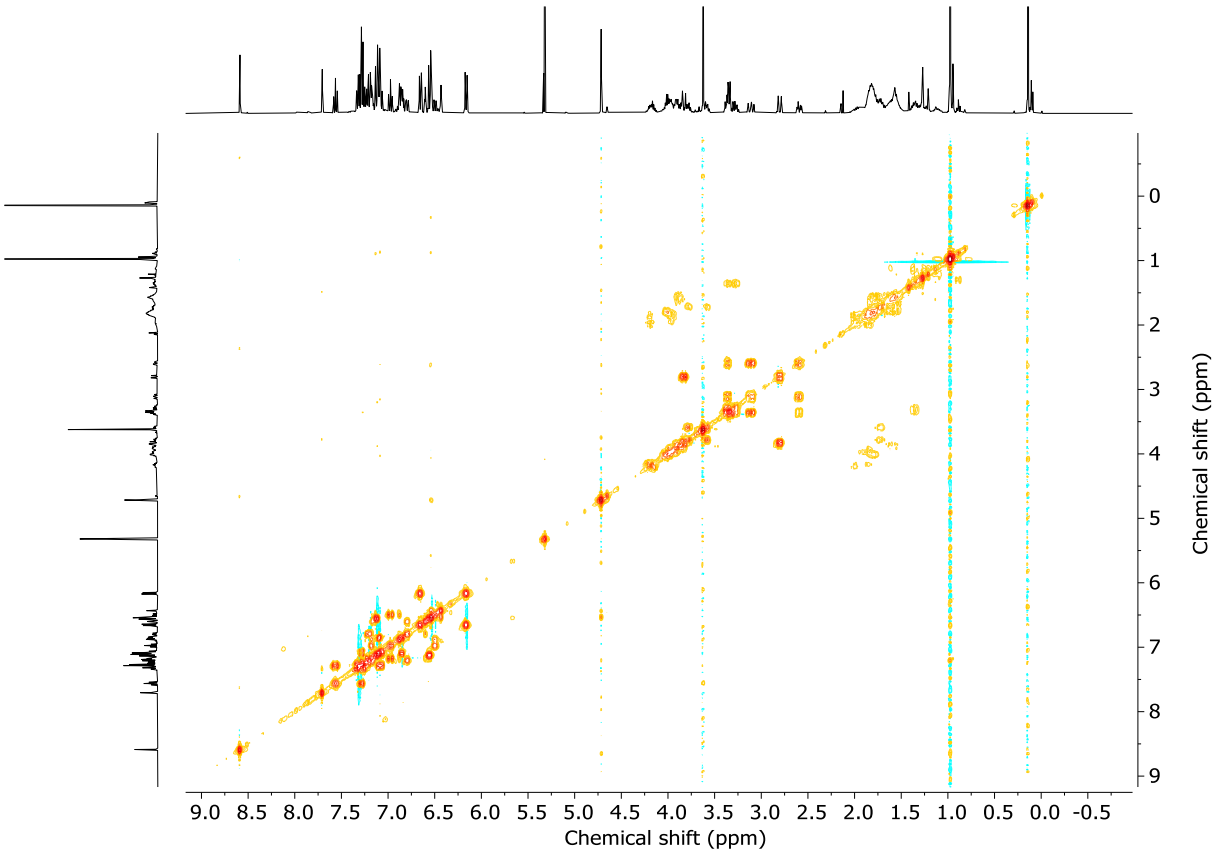

Figure S70: COSY NMR (CD_2Cl_2, 298 K) of (S,R_{mp},$E_{co\text{-}c}$)-**3**.

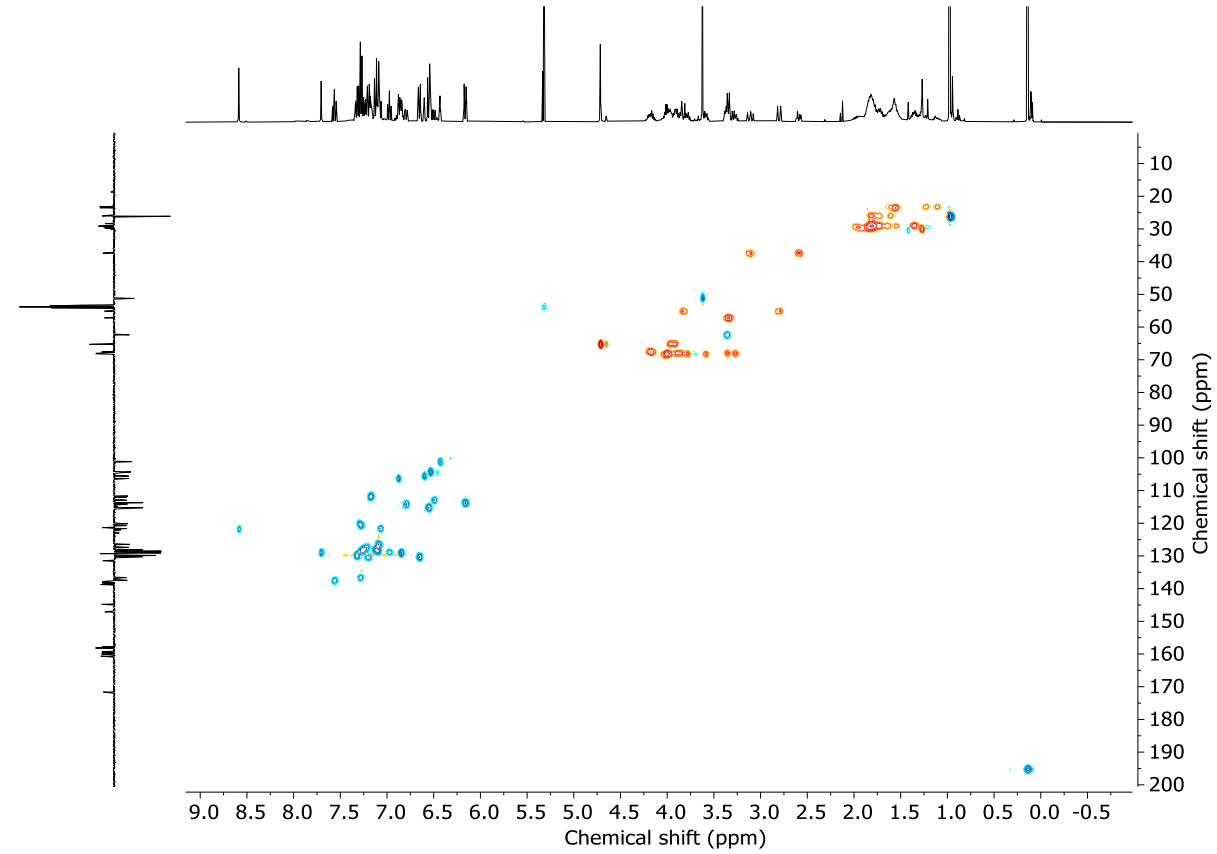

Figure S71 HSQC NMR (CD_2Cl_2, 298 K) of (S,R_{mp},$E_{co\text{-}c}$)-**3**.

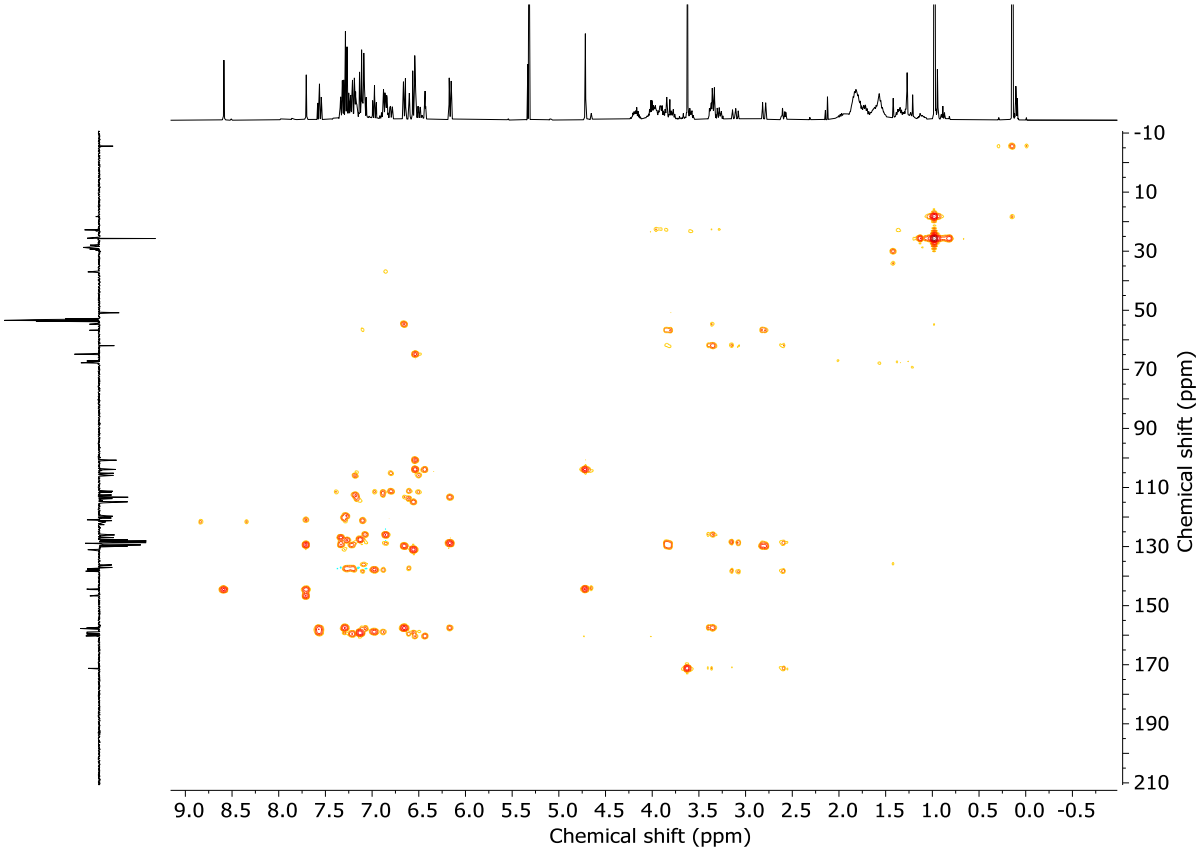

Figure S72: HMBC NMR (CD_2Cl_2, 298 K) of (S,R_{mp},$E_{co\text{-}c}$)-**3**.

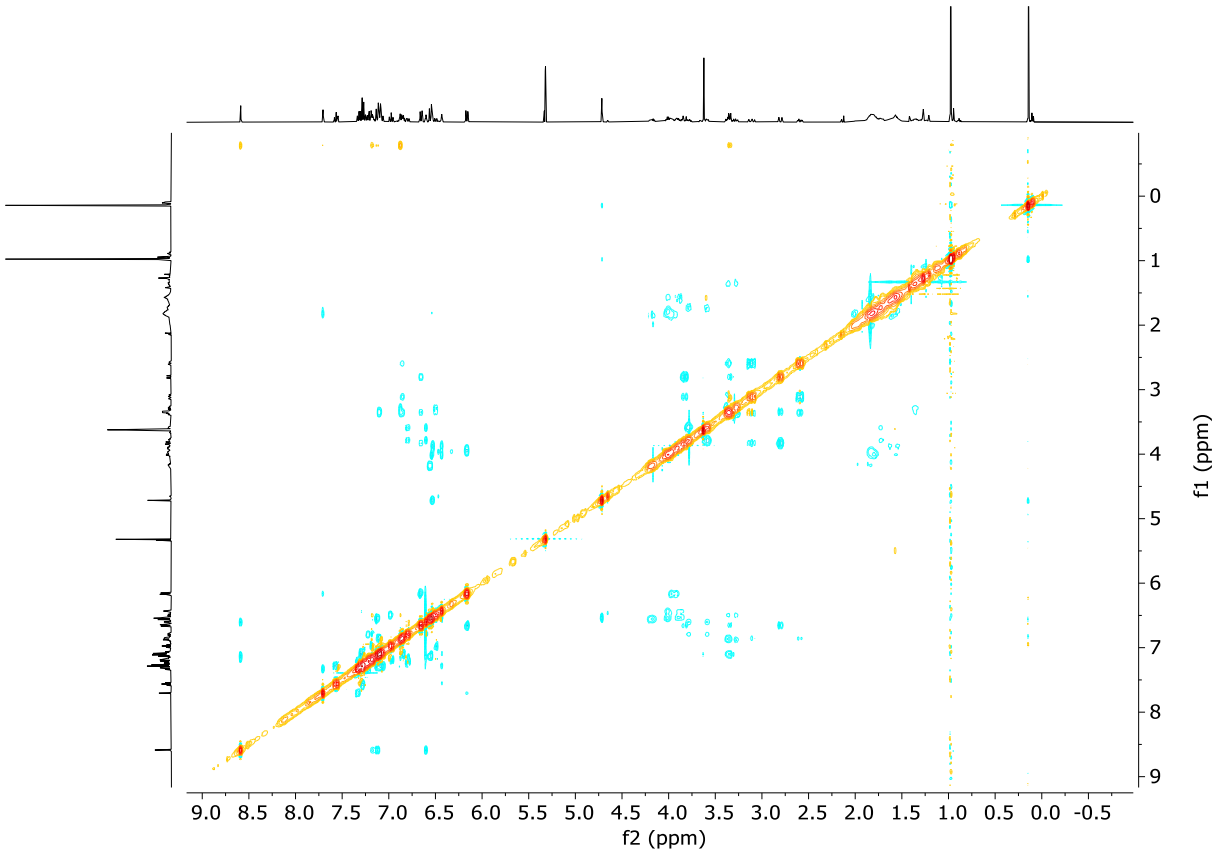

Figure S73: NOESY NMR (CD_2Cl_2, 298 K) of (S,R_{mp},$E_{co\text{-}c}$)-**3**.

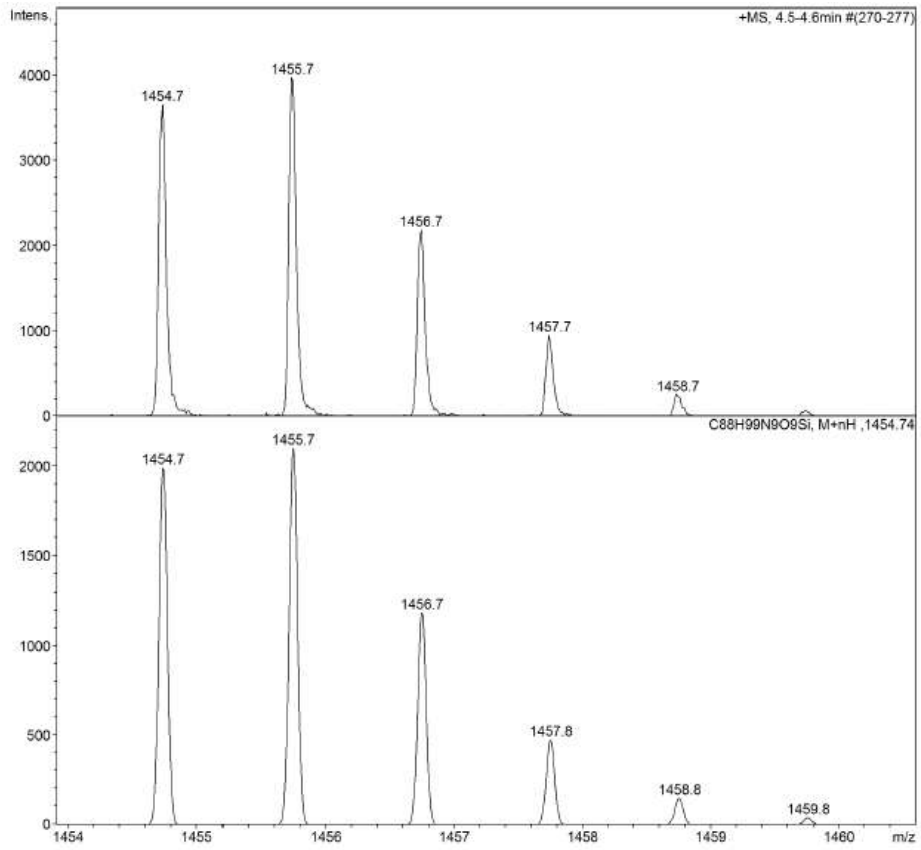

Figure S74: LRMS - Observed (top) and calculated (bottom) isotopic pattern for (S,R_{mp},$E_{co\text{-}c}$)-**3** $C_{88}H_{100}N_9O_9Si$.

Catenanes (*R*,S_{mp},$E_{co\text{-}c}$)-3 and *rac*-(*S*,R_{mp},$E_{co\text{-}c}$)-3

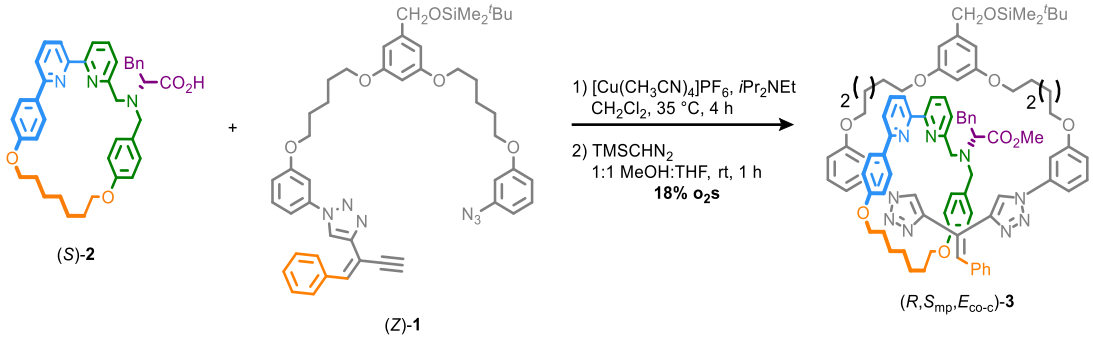

To a stirred solution of (*R*)-**2** (27 mg, 0.044 mmol), $[Cu(CH_3CN)_4]PF_6$ (16 mg, 0.042 mmol), and $^{i}Pr_2NEt$ (30.0 μL, 0.17 mmol) in CH_2Cl_2 (4.2 mL) at 35 °C was added (*Z*)-**1** (39 mg, 0.048 mmol) in CH_2Cl_2 (1.7 mL) at a constant rate using a syringe pump over 4 h. The reaction mixture was stirred for 10 min after the addition had completed, cooled to rt and sat. EDTA-$NH_{3(aq)}$ (3 mL) was added with stirring. After 17 h, the mixture was diluted with H_2O (30 mL), the layers were separated and the aqueous layer extracted with CH_2Cl_2 (3 x 15 mL). The combined organic layers were dried (Na_2SO_4), filtered, and concentrated *in vacuo*. The residue was redissolved in THF-MeOH (1 : 1, 2.0 mL), and $TMSCHN_2$ (2.0 M in hexanes, 0.2 mL, 0.4 mmol) was added and the resulting solution stirred at rt for 1 h then concentrated *in vacuo*. Chromatography (^{n}hexane-CH_2Cl_2-Et_2O 1 : 1 : 0 to 0 : 0 : 1) afforded (*R*,S_{mp},$E_{co\text{-}c}$)-**3** as an white foam (11 mg, 18% over two steps).

rac-(*S*,R_{mp},$E_{co\text{-}c}$)-**3** (26 mg, 23% over two steps) was synthesised starting from rac-**2** (50 mg, 0.080 mmol) using the same procedure.

rac-(*S*,R_{mp},$E_{co\text{-}c}$)-**3** and (*R*,S_{mp},$E_{co\text{-}c}$)-**3** produced identical analytical data to (*S*,R_{mp},$E_{co\text{-}c}$)-**3** (e.g., Figure S75) with the exception of their CSP-HPLC (Figure S76) and circular dichroism spectra (Figure S77).

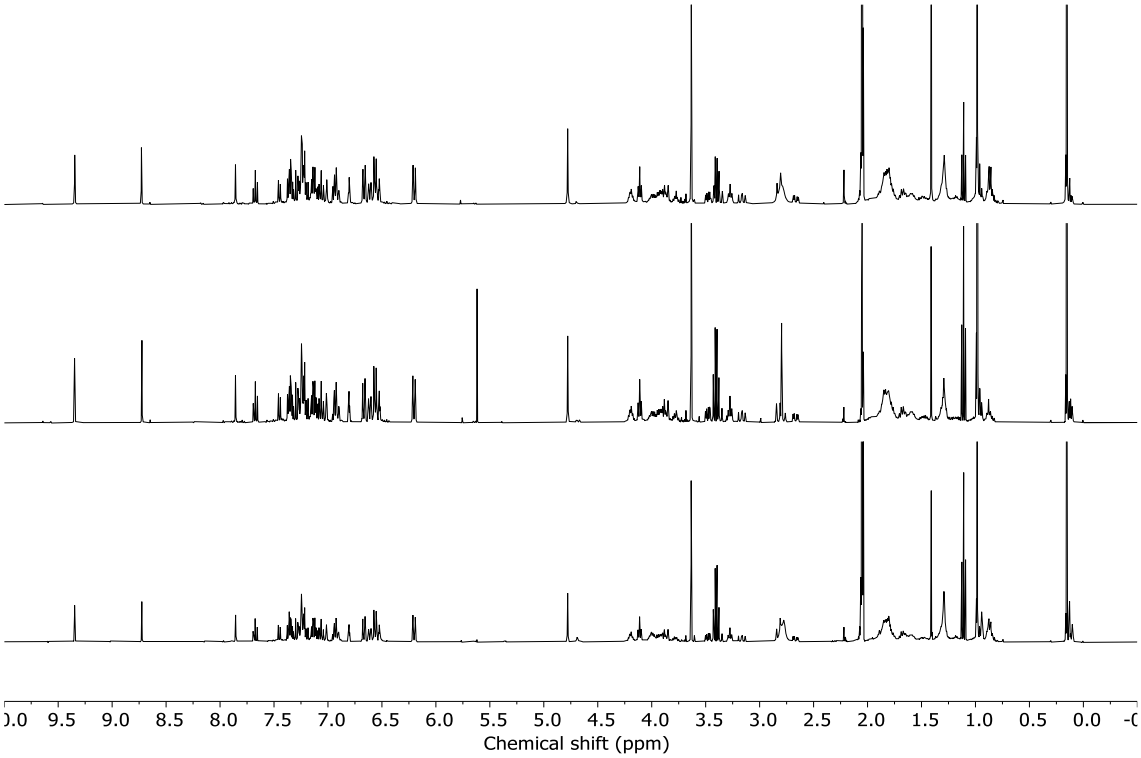

Figure S75: Stack plot ^{1}H NMR (acetone-d_6, 400 MHz, 298 K). (Top) (*R*,S_{mp},$E_{co\text{-}c}$)-**3**; (Middle) *rac*-(*S*,R_{mp},$E_{co\text{-}c}$)-**3**; (Bottom) (*S*,R_{mp},$E_{co\text{-}c}$)-**3**.

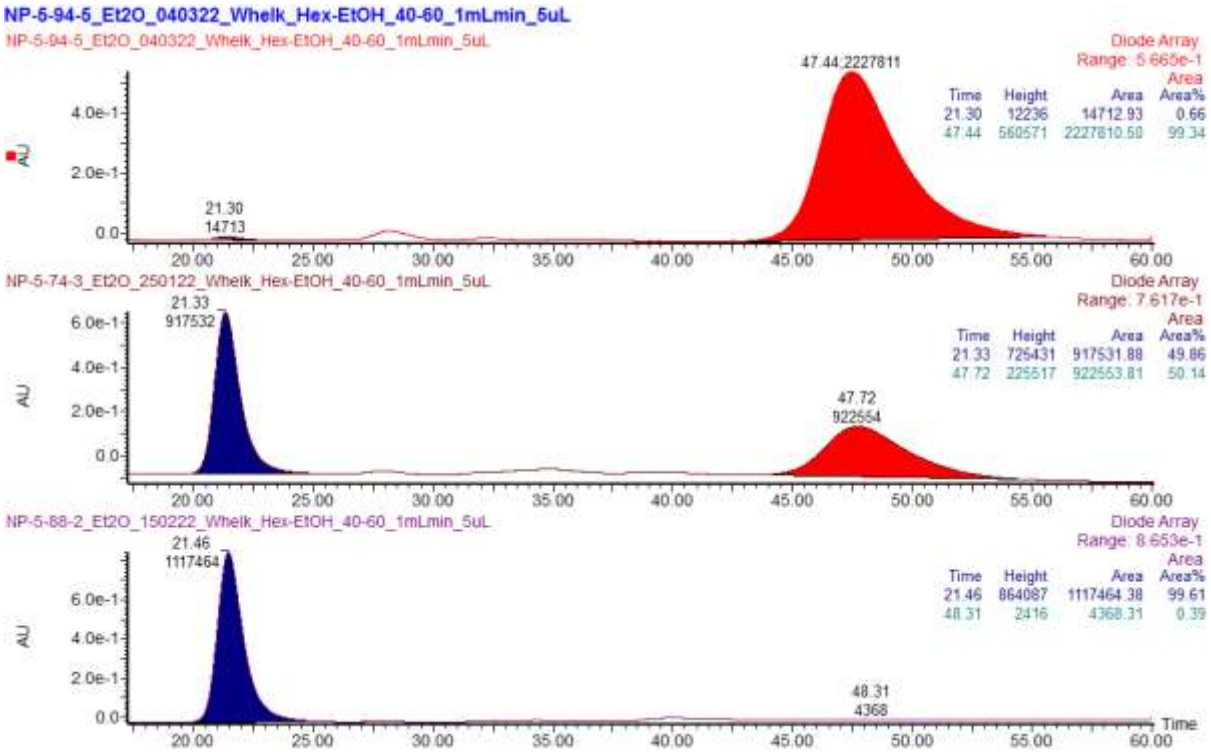

Figure S76: CSP-HPLC (loaded in Et_2O, SSWhelk, ^{n}hexane-EtOH 40 : 60, flowrate 1 mLmin^{-1}) of (*R*,S_{mp},$E_{co\text{-}c}$)-**3** (98.7% *ee*) (top); *rac*-(*S*,R_{mp},$E_{co\text{-}c}$)-**3** ([*S*,R_{mp},$E_{co\text{-}c}$]-**3** @ 21.33 min, 49.9%; [*R*,S_{mp},$E_{co\text{-}c}$]-**3** @ 47.72 min, 50.1%) (middle); (*S*,R_{mp},$E_{co\text{-}c}$)-**3** (99.2% *ee*).

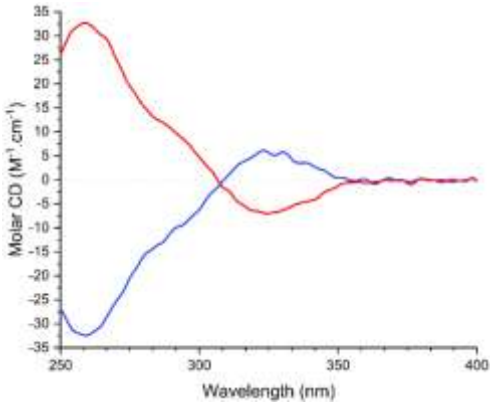

Figure S77: Circular dichroism spectra (3.23 μM in CH_3CN, 293 K) of (R,S_{mp},$E_{co\text{-}c}$)-**3** (red) and (S,R_{mp},$E_{co\text{-}c}$)-**3** (blue).

Catenanes (S,S_{mp},$E_{co\text{-}c}$)-4 and (R,R_{mp},$E_{co\text{-}c}$)-4

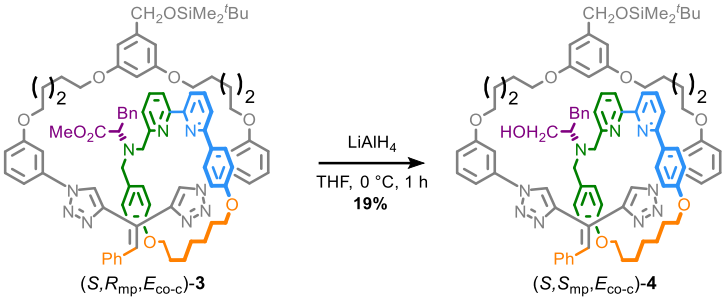

Ester catenane (S,R_{mp},$E_{co\text{-}c}$)-**3** (16 mg, 0.011 mmol) was dissolved in THF (1.0 mL), cooled to 0 °C and $LiAlH_4$ (1 M in THF, 0.05 mL, 0.05 mmol) was added dropwise. After 5 min at 0 °C, the flask was removed from the ice-bath. After 90 min at rt, the reaction mixture was cooled down at 0 °C, diluted with Et_2O (10 mL) and water (0.08 mL), $NaOH_{(aq)}$ (15% w/v, 0.08 mL) and H_2O (0.24 mL) were successively added. The flask was removed from the ice-bath and the reaction mixture was stirred at rt for 15 min. Solid $MgSO_4$ was added and the reaction mixture stirred for 15 min at rt. The reaction mixture was filtered over Celite®, the solids washed with Et_2O and the filtrate concentrated *in vacuo*. Two rounds of chromatography (1st: ^{n}hexane-CH_2Cl_2-Et_2O 1 : 1 : 0 to 2 : 2 : 1; 2nd CH_2Cl_2-MeOH 100 : 0 to 97 : 3) gave catenane (S,S_{mp},$E_{co\text{-}c}$)-**4** as a colorless film (3 mg, 19%).

(R,R_{mp},$E_{co\text{-}c}$)-**4** (3 mg, 40%) was synthesised using a similar procedure starting from (R,S_{mp},$E_{co\text{-}c}$)-**3** (8 mg, 0.005 mmol) but purified using a single round of chromatography (CH_2Cl_2-MeOH 100 : 0 to 98 : 2 and ^{n}hexane-CH_2Cl_2-Et_2O 1 : 1 : 0 to 3 : 3 : 4).

Analytical data of (S,S_{mp},$E_{co\text{-}c}$)-**4** and (R,R_{mp},$E_{co\text{-}c}$)-**4** were identical (e.g., Figure S84) with the exception of their CSP-HPLC (Figure S84) and circular dichroism spectra (Figure S86).

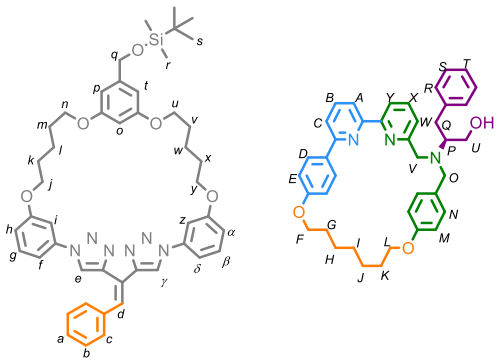

^{1}H NMR (400 MHz, CD_2Cl_2) δ 8.98 (s, 1H, $\boldsymbol{H}_{\gamma}$), 7.83 (s, 1H, $\boldsymbol{H}_{e}$), 7.63 (t, *J* = 7.8, 1H, $\boldsymbol{H}_{B}$), 7.47 (t, *J* = 7.8, 1H, $\boldsymbol{H}_{X}$), 7.46 (s, 1H, $\boldsymbol{H}_{d}$), 7.40 (ddd, *J* = 8.1, 2.1, 1.0, 1H, $\boldsymbol{H}_{\delta}$), 7.35 – 7.25 (m, 6H, $\boldsymbol{H}_{g}$, $\boldsymbol{H}_{A,}$ $\boldsymbol{H}_{W,}$ $\boldsymbol{H}_{z,}$ $\boldsymbol{H}_{S}$), 7.25 – 7.02 (m, 13H, $\boldsymbol{H}_{a}$, $\boldsymbol{H}_{b}$, $\boldsymbol{H}_{c}$, $\boldsymbol{H}_{f}$, $\boldsymbol{H}_{C}$, $\boldsymbol{H}_{D,}$ $\boldsymbol{H}_{R}$, $\boldsymbol{H}_{T}$, $\boldsymbol{H}_{\beta}$), 6.99 (d, *J* = 7.9, 1H, $\boldsymbol{H}_{Y}$), 6.93 (t, *J* = 2.1, 1H, $\boldsymbol{H}_{i}$), 6.91 (ddd, *J* = 8.2, 2.4, 0.9, 1H, $\boldsymbol{H}_{h}$), 6.78 (d, *J* = 8.5, 2H, $\boldsymbol{H}_{N}$), 6.68 (ddd, *J* = 8.2, 2.5, 0.9, 1H, $\boldsymbol{H}_{\alpha}$), 6.52 (dd, *J* = 2.3, 1.2, 1H, $\boldsymbol{H}_{p}$), 6.46 (dd, *J* = 2.3, 1.2, 1H, $\boldsymbol{H}_{t}$), 6.41 (d, *J* = 8.7, 2H, $\boldsymbol{H}_{E}$), 6.33 (t, *J* = 2.3, 1H, $\boldsymbol{H}_{o}$), 6.26 (d, *J* = 8.5, 2H, $\boldsymbol{H}_{M}$), 4.67 (s, 2H, $\boldsymbol{H}_{q}$), 4.06 (m, 5H, $\boldsymbol{H}_{n}$, $\boldsymbol{H}_{F}$, 1 of $\boldsymbol{H}_{L}$), 3.99 – 3.79 (m, 4H, $\boldsymbol{H}_{j}$, 1 of $\boldsymbol{H}_{L}$, 1 of $\boldsymbol{H}_{V}$), 3.78 – 3.67 (m, 3H, $\boldsymbol{H}_{u}$, 1 of $\boldsymbol{H}_{O}$), 3.68 – 3.58 (m, 1H, 1 of $\boldsymbol{H}_{y}$), 3.55 (d, *J* = 12.8, 1H, 1 of $\boldsymbol{H}_{V}$), 3.44 (t, *J* = 9.7, 1H, 1 of $\boldsymbol{H}_{U}$), 3.36 – 3.23 (m, 2H, 1 of $\boldsymbol{H}_{O,}$ 1 of $\boldsymbol{H}_{U}$), 3.09 – 2.94 (m, 3H, $\boldsymbol{H}_{P}$, 1 of $\boldsymbol{H}_{Q}$, 1 of $\boldsymbol{H}_{y}$), 2.52 (dd, *J* = 12.8, 8.4, 1H, 1 of $\boldsymbol{H}_{Q}$), 1.95 – 1.47 (m, 18H, $\boldsymbol{H}_{k}$, $\boldsymbol{H}_{l}$, $\boldsymbol{H}_{m}$, $\boldsymbol{H}_{v}$, $\boldsymbol{H}_{G}$, $\boldsymbol{H}_{H}$, $\boldsymbol{H}_{I}$, $\boldsymbol{H}_{J}$, $\boldsymbol{H}_{K}$), 1.41 (app. quint, *J* = 7.1, 2H, $\boldsymbol{H}_{x}$), 1.17 – 1.08 (m, 2H, $\boldsymbol{H}_{w}$), 0.95 (s, 9H, $\boldsymbol{H}_{s}$), 0.11 (s, 6H, $\boldsymbol{H}_{r}$).

^{13}C NMR (101 MHz, CD_2Cl_2) δ 160.7, 160.6, 160.3, 159.6, 159.3, 159.2, 159.1, 159.0, 158.2, 157.7, 147.1, 144.7, 144.4, 140.2, 138.4, 138.2, 137.4, 137.4, 137.3, 131.9, 130.6, 130.4, 129.9, 129.8, 129.7, 129.7, 129.3, 128.9, 128.5, 128.3, 127.5, 126.6, 125.2, 122.3, 121.9, 121.6, 121.2, 120.1, 120.1, 115.0, 114.5, 114.1, 114.0, 112.2, 112.1, 107.2, 106.4, 104.9, 103.8, 100.8, 68.6, 68.2, 68.0 (x2), 67.7, 65.8, 65.3, 62.2, 61.3, 56.6, 53.2, 33.0, 29.7, 29.4, 29.3, 29.2, 29.1, 29.0, 28.7, 26.2, 26.2, 26.1, 23.8, 22.8, 18.7, -5.2.

LR-ESI-MS (+ve): *m/z* = 1427.7 $[M + H]^+$ 100%, calc. for $C_{87}H_{100}N_9O_8Si$ 1427.7.

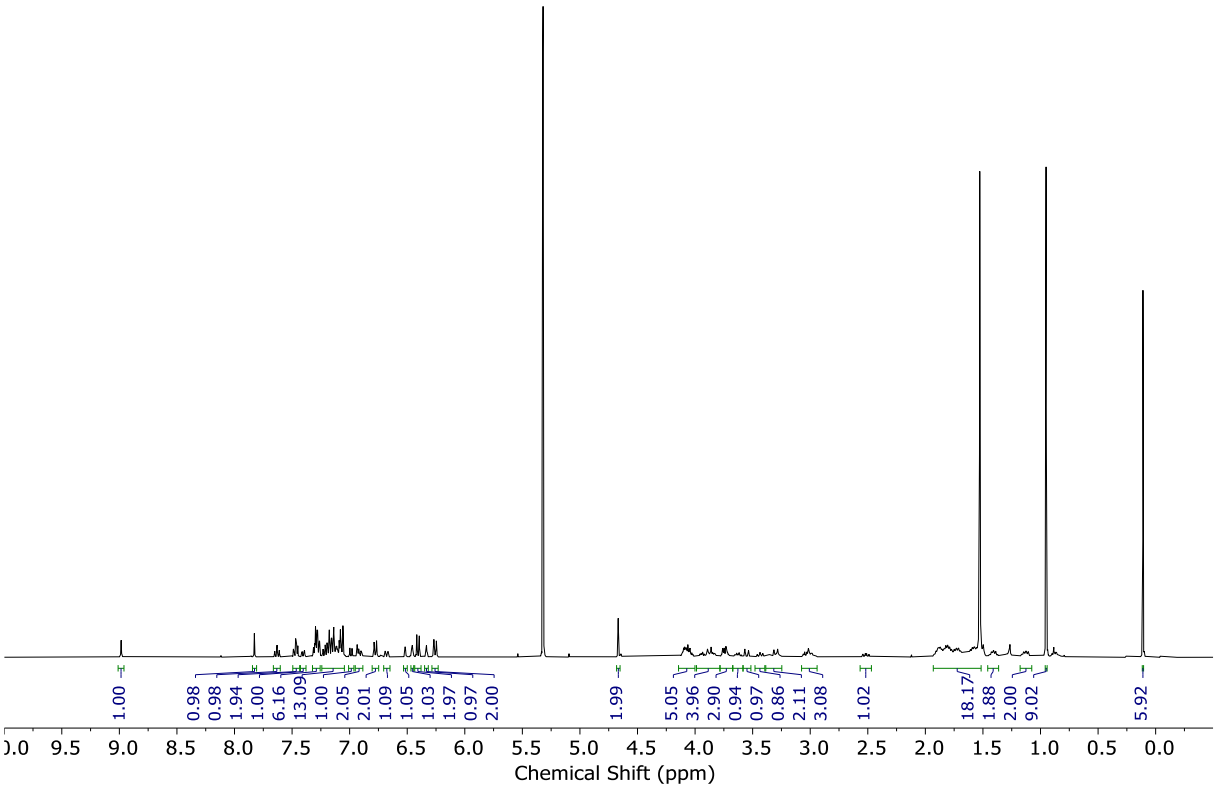

Figure S78: ^{1}H NMR (CD_2Cl_2, 400 MHz, 298 K) of (S,S_{mp},$E_{co\text{-}c}$)-**4**.

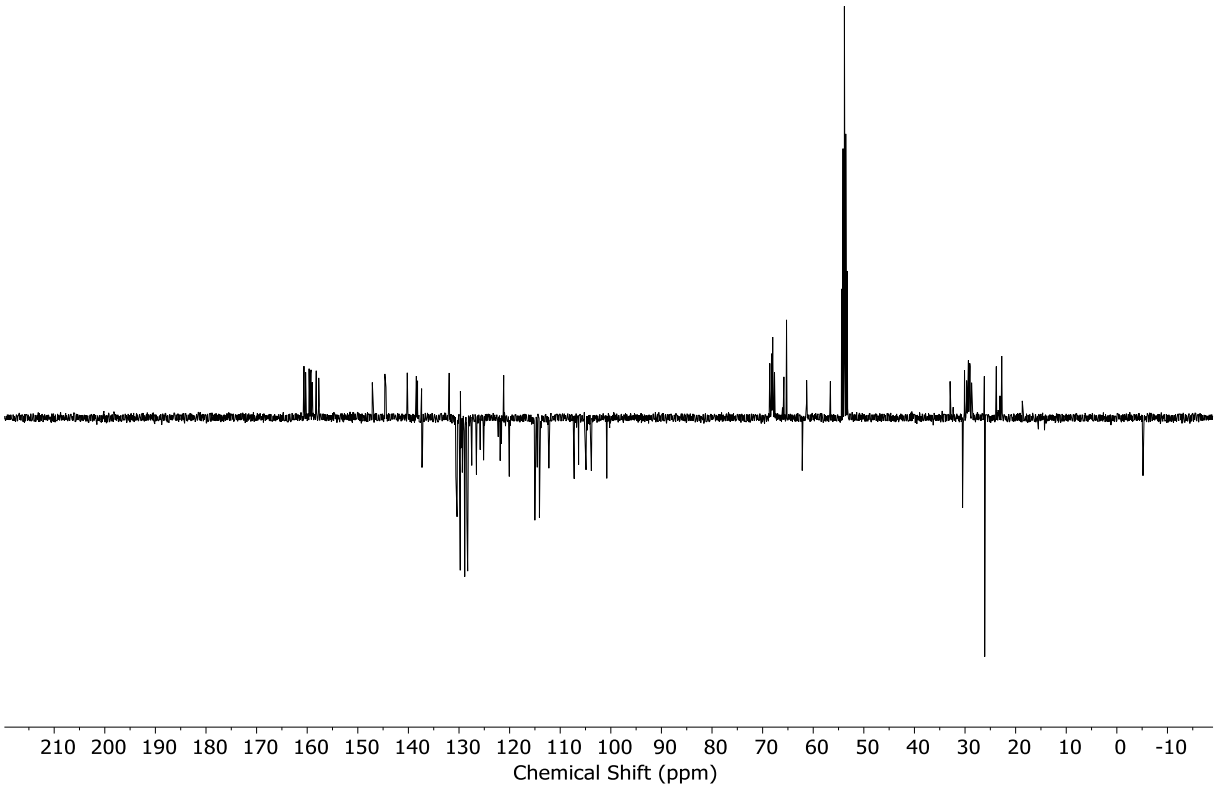

Figure S79: JMOD NMR (CD_2Cl_2, 101 MHz, 298 K) of (S,S_{mp},$E_{co\text{-}c}$)-**4**.

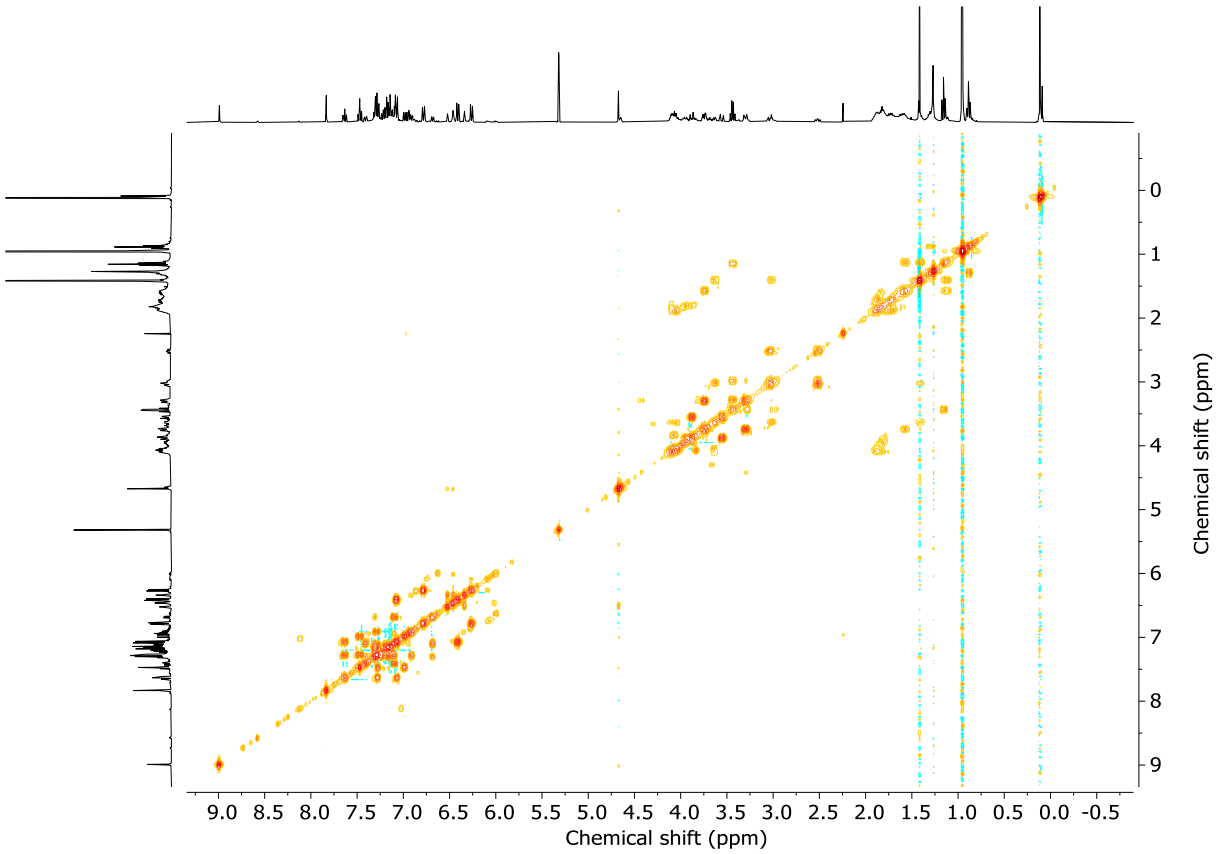

Figure S80: COSY NMR (CD_2Cl_2, 298 K) of (S,S_{mp},$E_{co\text{-}c}$)-**4**.

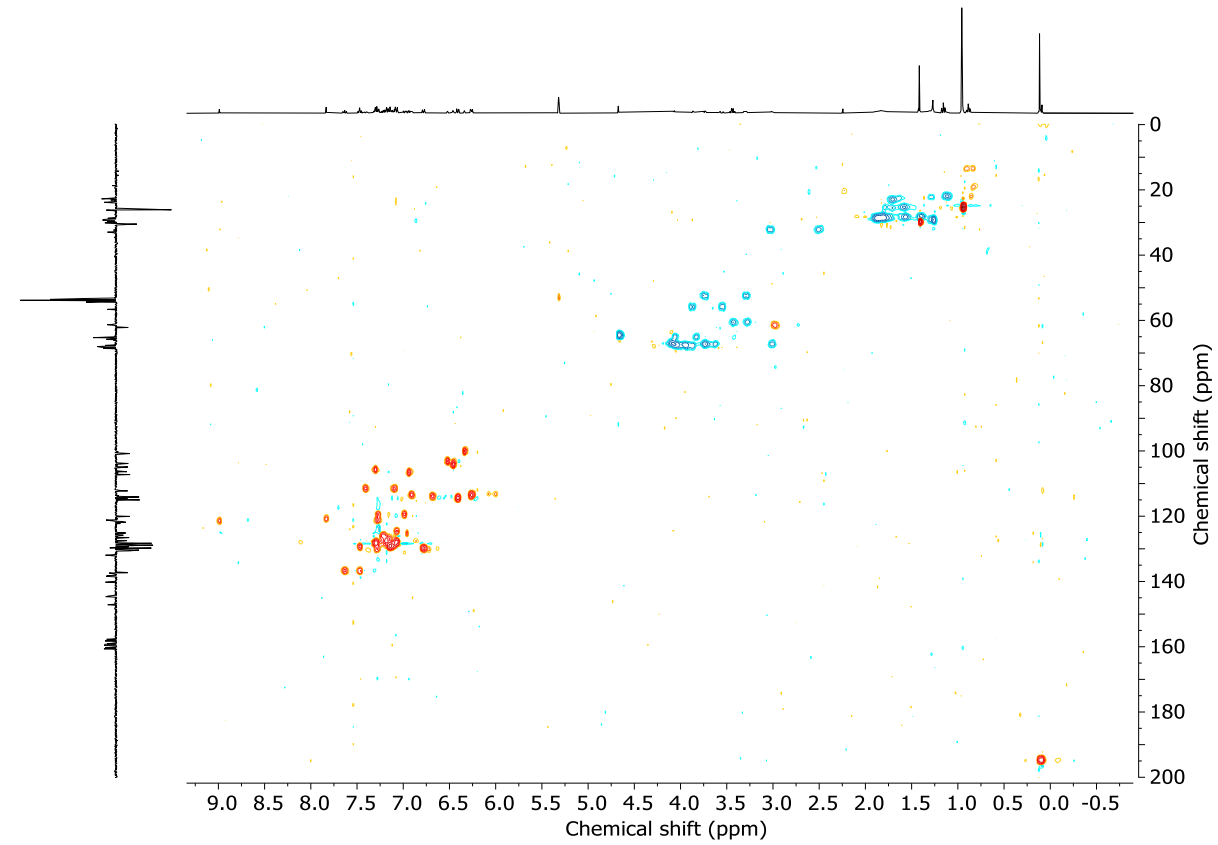

Figure S81: HSQC NMR (CD_2Cl_2, 298 K) of (S,S_{mp},$E_{co\text{-}c}$)-**4**.

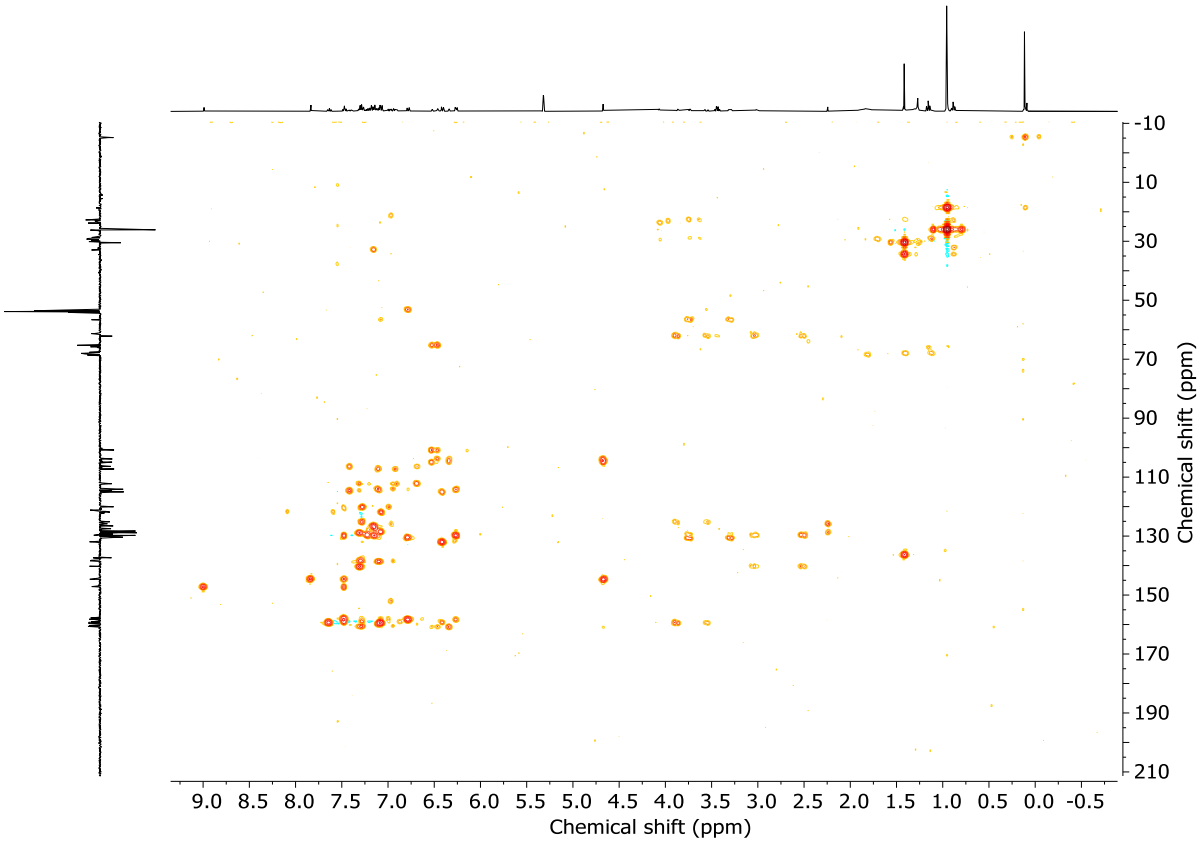

Figure S82: HMBC NMR (CD_2Cl_2, 298 K) of (S,S_{mp},$E_{co\text{-}c}$)-**4**.

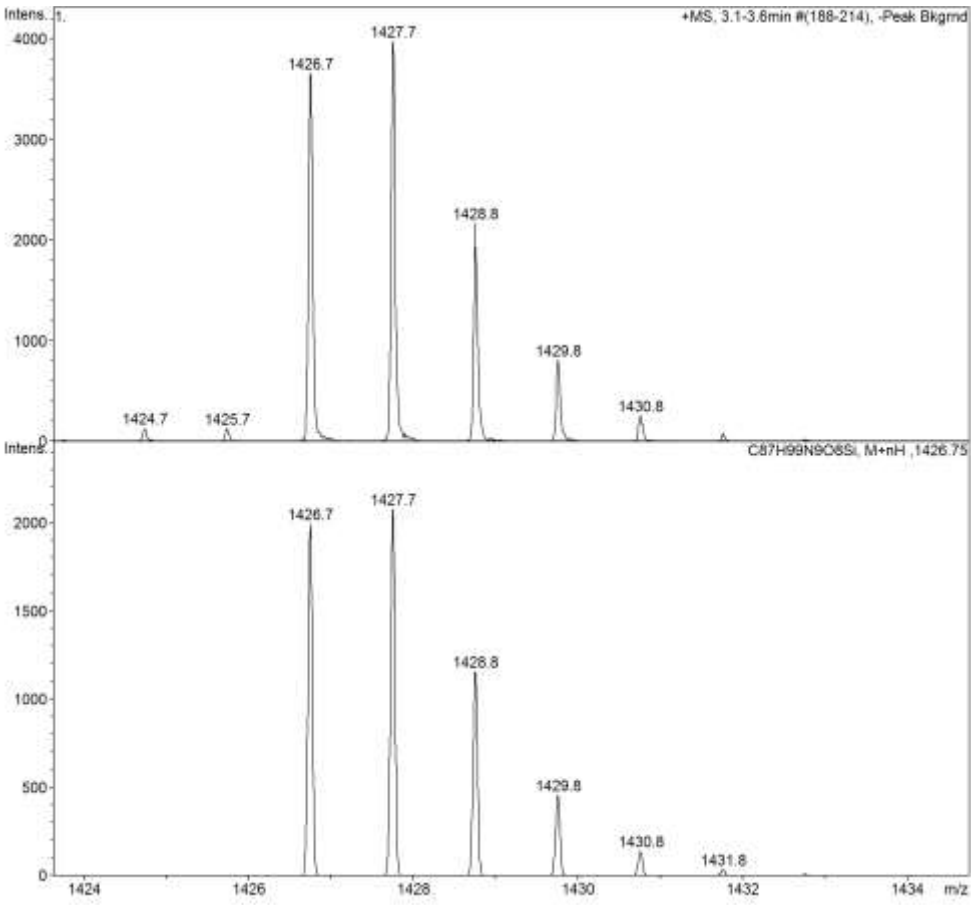

Figure S83: LRMS - Observed (top) and calculated (bottom) isotopic pattern for (S,S_{mp},$E_{co\text{-}c}$)-**4** $C_{87}H_{100}N_9O_9Si$.

Catenane *rac*-($S,S_{mp},E_{co\text{-}c}$)-4

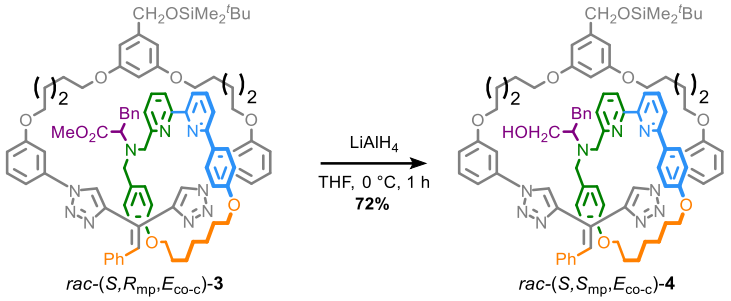

Ester catenane *rac*-($S,R_{mp},E_{co\text{-}c}$)-**3** (33 mg, 0.023 mmol) was dissolved in THF (1.8 mL), cooled to 0 °C and $LiAlH_4$ (1 M in THF, 0.09 mL, 0.09 mmol) was added dropwise. After 15 min, the reaction mixture was quenched by slow addition of EtOAc (0.2 mL), stirred at 0 °C for 5 min and warmed to rt. Sat. Rochelle $salt_{(aq)}$ (2 mL) was added and the mixture stirred for 10 min. H_2O (20 mL) was added, the layers separated, and the aqueous layer extracted with CH_2Cl_2 (3 x 10 mL). The combined organic layers were dried (Na_2SO_4) and concentrated *in vacuo*. Chromatography (^{n}hexane-Et_2O 100:0 to 3 : 7) gave catenane *rac*-($S,S_{mp},E_{co\text{-}c}$)-**4** as an off-white foam (23 mg, 72%).

Analytical data of *rac*-($S,S_{mp},E_{co\text{-}c}$)-**4** were identical to those of ($S,S_{mp},E_{co\text{-}c}$)-**4** and ($R,R_{mp},E_{co\text{-}c}$)-**4** (*e.g.*, Figure S84) with the exception of their CSP-HPLC (Figure S85) and circular dichroism spectra (Figure S86).

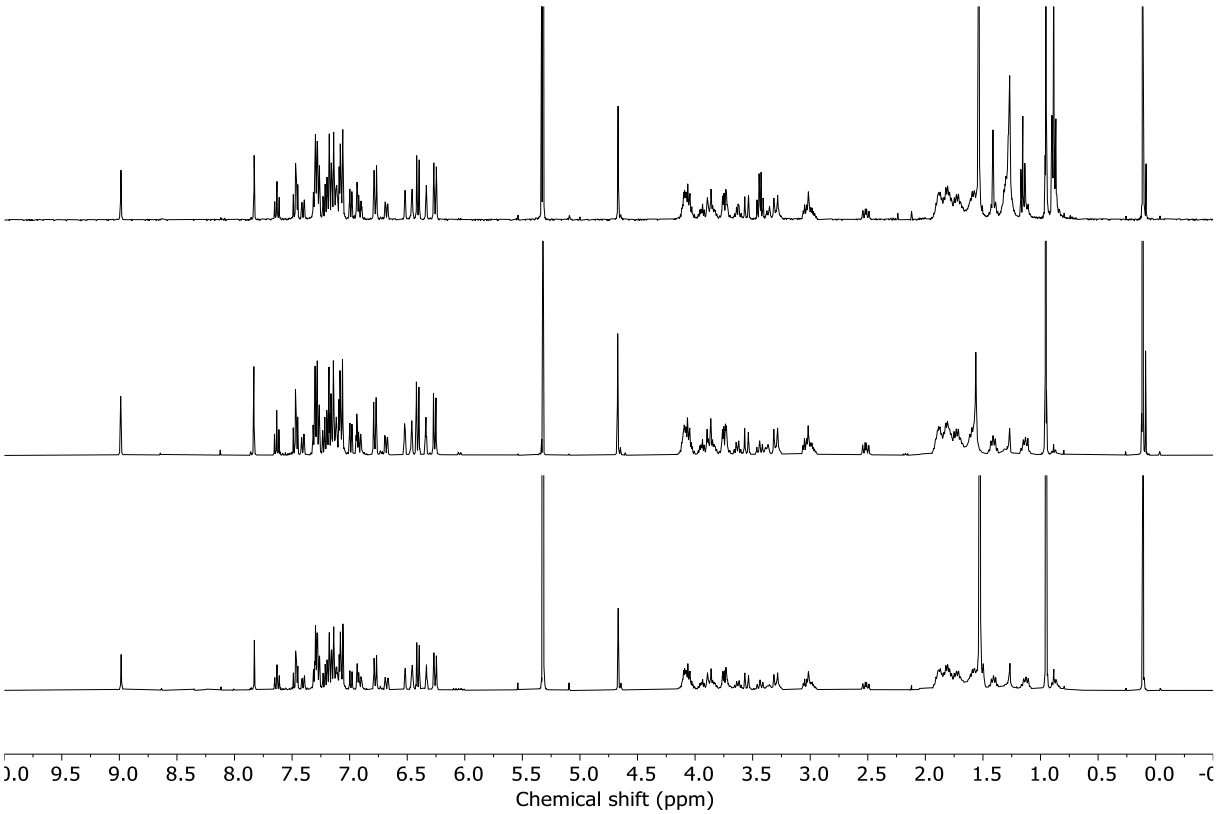

Figure S84: Stack plot ^{1}H NMR (CD_2Cl_2, 400 MHz, 298 K) of ($R,R_{mp},E_{co\text{-}c}$)-**4** (top), *rac*-($S,S_{mp},E_{co\text{-}c}$)-**4** (middle) and ($S,S_{mp},E_{co\text{-}c}$)-**4** (bottom).

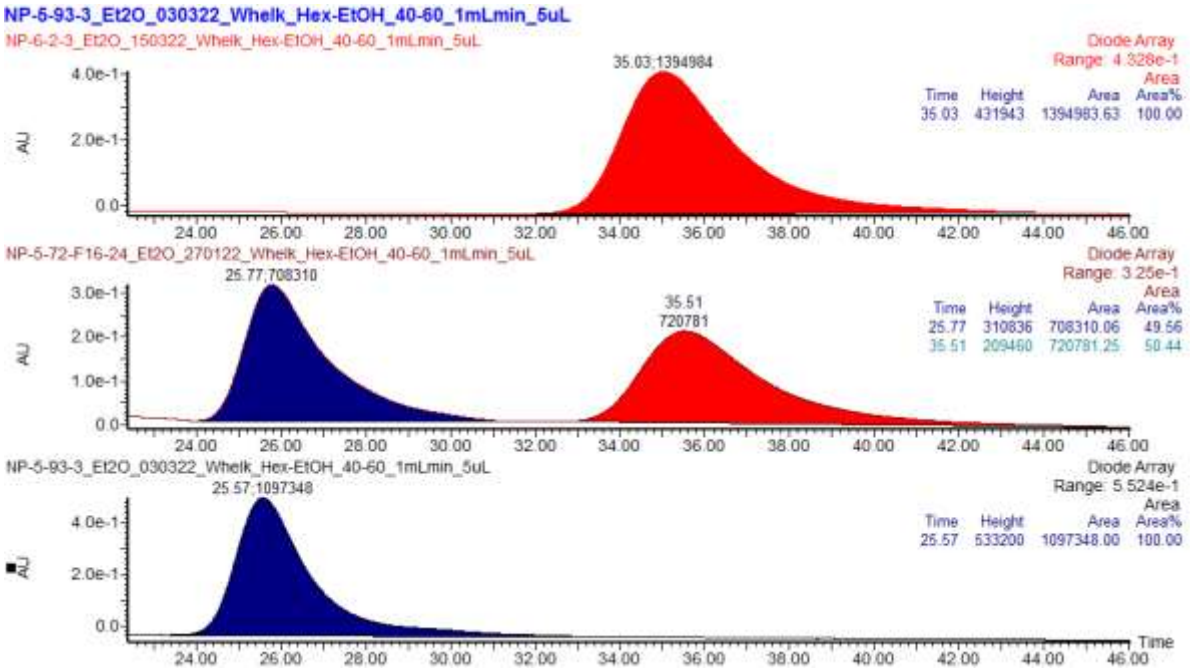

Figure S85: CSP-HPLC (loaded in Et_2O, SSWhelk, ^{n}hexane-EtOH 40 : 60, flowrate 1 mLmin^{-1}) of (R,R_{mp},$E_{co\text{-}c}$)-**4** (>99% *ee*) (top); *rac*-(S,S_{mp},$E_{co\text{-}c}$)-**4** ([S,S_{mp},$E_{co\text{-}c}$]-**4** @ 25.77 min, 49.6%; [R,R_{mp},$E_{co\text{-}c}$]-**4** @ 35.51 min, 50.4%) (middle); (S,S_{mp},$E_{co\text{-}c}$)-**4** (>99% *ee*) (bottom).

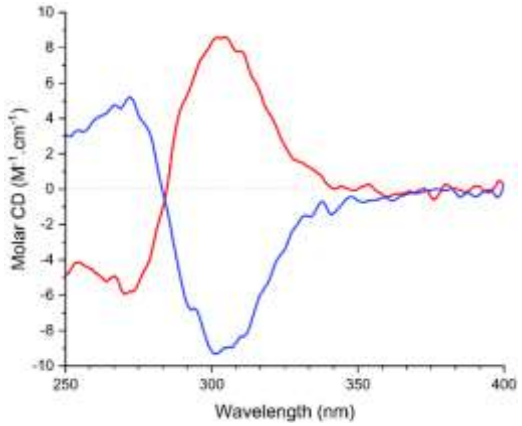

Figure S86: Circular dichroism spectra (4.20 μM in CH_3CN, 293 K) of (R,R_{mp},$E_{co\text{-}c}$)-**4** (red) and (S,S_{mp},$E_{co\text{-}c}$)-**4** (blue).

Catenanes (S_{mp},$E_{co\text{-}c}$)-S16 and (R_{mp},$E_{co\text{-}c}$)-S16 (telescoped procedure)

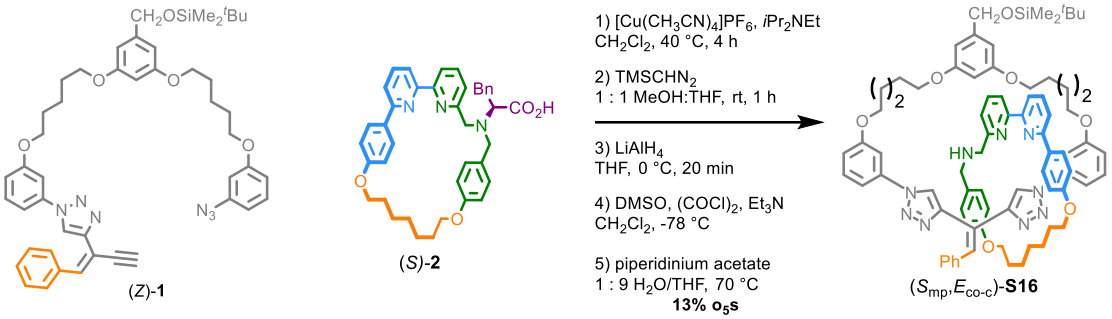

For convenience, enantioenriched catenanes (S_{mp},$E_{co\text{-}c}$)-**S16** and (R_{mp},$E_{co\text{-}c}$)-**S16** were obtained using a telescoped procedure from (*Z*)-**1** and macrocycle **2** without purification of the intermediate products:

Step 1: To a stirred solution of (*S*)-**2** (35 mg, 0.056 mmol), $[Cu(CH_3CN)_4]PF_6$ (20 mg, 0.053 mmol), and $^{i}Pr_2NEt$ (39.0 µL, 0.224 mmol) in CH_2Cl_2 (5.6 mL) at 38 °C was added (*Z*)-**1** (99 mg, 0.122 mmol) in CH_2Cl_2 (2.5 mL) at a constant rate using a syringe pump over 4 h. The reaction mixture was stirred for 10 min after the addition had completed, cooled to rt and sat. EDTA-$NH_{3(aq)}$ (4 mL) was added with stirring. After 15 min, the mixture was diluted with H_2O (40 mL), the layers were separated, and the aqueous layer extracted with CH_2Cl_2 (3 x 20 mL). The combined organic layers were washed with brine (50 mL), dried (Na_2SO_4), filtered, and concentrated *in vacuo*. The residue was redissolved in THF-MeOH (1 : 1, 3.6 mL), and $TMSCHN_2$ (2.0 M in hexanes, 0.18 mL, 0.36 mmol) was added and the resulting solution stirred at rt for 1 h then concentrated *in vacuo* to give a residue containing methyl ester catenane (*S*,R_{mp},$E_{co\text{-}c}$)-**3**.

Step 2: The residue was dissolved in THF (5.0 mL), cooled to 0 °C and $LiAlH_4$ (1 M in THF, 0.22 mL, 0.22 mmol) was added dropwise. After 15 min at 0 °C, the reaction mixture was diluted with Et_2O (20 mL) and water (0.05 mL), $NaOH_{(aq)}$ (15% w/v, 0.05 mL) and water (0.15 mL) were successively added. The mixture was allowed to warm up at rt and the reaction mixture was stirred at rt for 15 min. Solid $MgSO_4$ was added and the reaction mixture stirred for 15 min at rt. The reaction mixture was filtered over Celite®, the solids rinced with Et_2O and the filtrate concentrated in vacuo to give a residue containing alcohol catenane (*S*,S_{mp},$E_{co\text{-}c}$)-**S4**.

Step 3: DMSO (0.12 mL, 1.7 mmol) was added dropwise to a solution of oxalyl chloride (0.07 mL, 0.8 mmol) in CH_2Cl_2 (3.0 mL) at -78 °C and the reaction mixture was stirred for 10 min. An aliquot of this solution (1.0 mL) was added to the previous residue in CH_2Cl_2 (5.0 mL) at -78 °C followed by Et_3N (0.22 mL, 1.6 mmol) and the reaction mixture was stirred for 5 min before the flask was removed from the -78 °C bath. After 3 hours at rt, the reaction was quenched by addition of sat. $NaHCO_{3(aq)}$ (50 mL), the phases separated, and the aqueous layer extracted with CH_2Cl_2 (3 x 15 mL). The combined organic layers were dried (Na_2SO_4), filtered and concentrated *in vacuo* to give a residue containing the corresponding aldehyde catenane.

Step 4: Piperidinium acetate (40 mg, 0.28 mmol) was added to the residue and the flask purged with N_2 for 10 min. THF-H_2O (9 : 1, 3.3 mL) was sparged with N_2 for 5 min, added to the mixture, and the resulting solution was stirred at 70 °C for 42 h. The reaction mixture was cooled to rt, quenched by addition of sat. $NaHCO_{3(aq)}$ (50 mL), the phases separated, and the aqueous layer extracted with CH_2Cl_2 (3 x 20 mL). The combined organic layers were dried (Na_2SO_4), filtered and concentrated *in vacuo*. Successive chromatographies (^{n}hexane-acetone 100 : 0 to 0 : 100; CH_2Cl_2-acetone 100 : 0 to 0 : 100; CH_2Cl_2-MeOH-Et_3N 99.5 : 0 : 0.5 to 98.5 : 1 : 0.5) gave NH-catenane (S_{mp},$E_{co\text{-}c}$)-**S16** as a white foam (9 mg, 98% *ee*, 13% over five steps).

(R_{mp},$E_{co\text{-}c}$)-**S16** (8 mg, 98% *ee*, 12% over five steps) was synthesised using an identical procedure starting from (*R*)-**2** (35 mg, 0.056 mmol). Analytical data for (S_{mp},$E_{co\text{-}c}$)-**S16** and (R_{mp},$E_{co\text{-}c}$)-**S16** were identical (e.g., Figure S95) with the exception of their CSP-HPLC (Figure S96) and circular dichroism spectra (Figure S97).

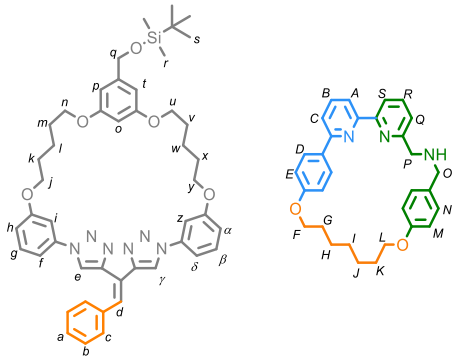

^{1}H NMR (500 MHz, CD_2Cl_2) δ 9.17 (s, 1H, H_γ), 7.66 (s, 1H, H_d), 7.55 (t, *J* = 7.8, 1H, H_B), 7.51 (t, *J* = 7.7, 1H, H_R), 7.46 (s, 1H, H_e), 7.43 (ddd, *J* = 8.1, 2.0, 1.0, 1H, H_δ), 7.34 – 7.29 (m, 2H, H_C, H_z), 7.28 – 7.13 (m, 9, H_a, H_b, H_c, H_g, H_β, H_A, H_S), 7.02 (d, *J* = 8.7, 2H, H_D), 6.96 (d, *J* = 7.7, 1H, H_Q), 6.84 (ddd, *J* = 8.4, 2.5, 0.9, 1H, H_h), 6.75 (dd, *J* = 8.1, 1.2, 1H, H_f), 6.72 (d, *J* = 8.4, 2H, H_N), 6.68 (ddd, *J* = 8.2, 2.4, 0.9, 1H, H_α), 6.63 (t, *J* = 2.2, 1H, H_i), 6.56 (dd, *J* = 2.2, 1.2, 1H, H_p), 6.46 (dd, *J* = 2.3, 1.2, 1H, H_t), 6.40 (t, *J* = 2.3, 1H, H_o), 6.36 (d, *J* = 8.7, 2H, H_E), 6.25 (d, *J* = 8.5, 2H, H_M), 4.69 (s, 2H, H_q), 4.22 (dt, *J* = 10.1, 5.1, 1H, 1 of H_L), 4.18 – 4.04 (m, 4H, H_n, H_F), 3.99 – 3.88 (m,3H, H_J,1 of H_L), 3.79 – 3.71 (m, 3H, H_u 1 of H_O), 3.56 (d, *J* = 12.2, 1H, 1 of H_P), 3.47 (d, *J* = 12.2, 1H, 1 of H_O), 3.43 (d, *J* = 13.1, 1H, 1 of H_P), 3.22 (dt, *J* = 9.0, 6.4, 1H, 1 of H_y), 3.01 (dt, *J* = 9.0, 6.6, 1H, 1 of H_y), 2.13 – 1.45 (m, 18H, H_k, H_l, H_m, H_v, H_G, H_H, H_I, H_J, H_K), 1.40 – 1.21 (m, 2H, H_x), 1.15 – 1.01 (m, 2H, H_w), 0.96 (s, 9H, H_s), 0.13 (s, 6H, H_r).

^{13}C NMR (126 MHz, CD_2Cl_2) δ 160.7, 160.6, 160.1, 160.1, 159.6, 159.5, 158.0, 156.9, 156.9, 156.7, 147.1, 144.8, 144.6, 138.6, 137.8, 137.6, 137.4, 137.2, 132.1, 130.3, 129.7, 129.6, 129.3, 129.3, 128.7, 128.5 (x2), 127.5, 123.1, 121.4, 121.1, 120.8, 120.6, 120.3, 114.6, 114.6, 114.0, 113.9, 112.0, 111.8, 107.0, 105.3, 105.1, 103.8, 101.0, 68.6, 68.2, 67.8, 67.6, 67.4, 65.5, 65.3, 54.4 (x2), 29.7, 29.5, 29.3, 29.2, 28.8, 28.7, 28.4, 26.2, 26.1, 26.1, 23.8, 22.6, 18.7, -5.2.

LR-ESI-MS (+ve): *m/z* = 1292.7 (100%) $[M + H]^+$ calc. for $C_{78}H_{90}N_9O_7Si$ 1292.7.

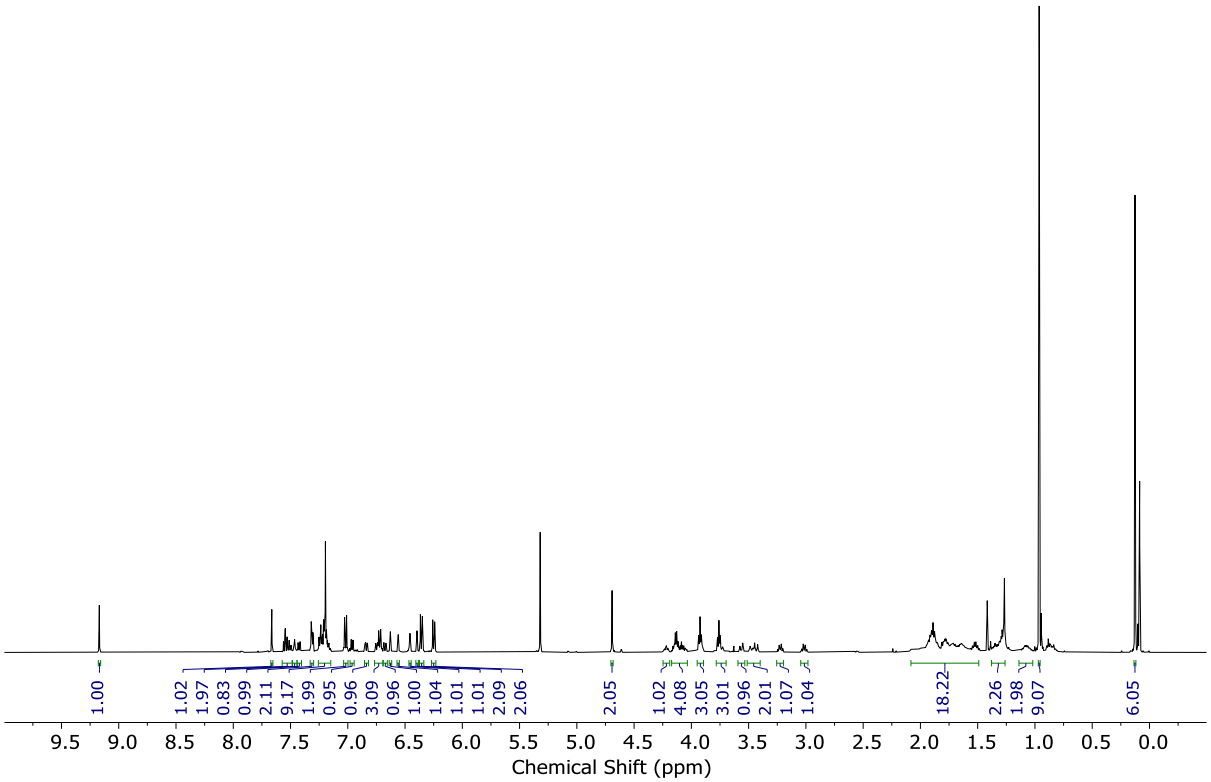

Figure S87: ^{1}H NMR (CD_2Cl_2, 500 MHz, 298 K) of (S_{mp},$E_{co\text{-}c}$)-**S16**.

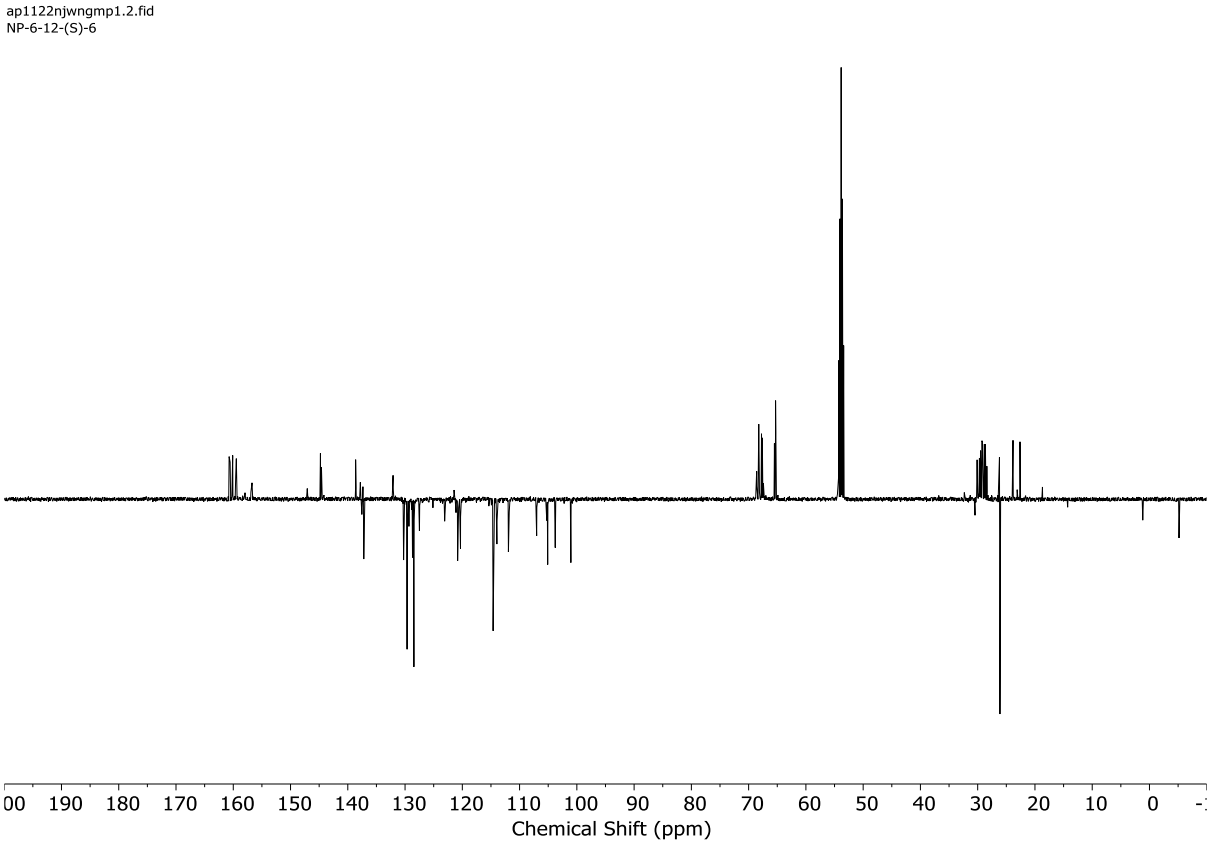

Figure S88: ^{1}H NMR (CD_2Cl_2, 126 MHz, 298 K) of (S_{mp},$E_{co\text{-}c}$)-**S16** .

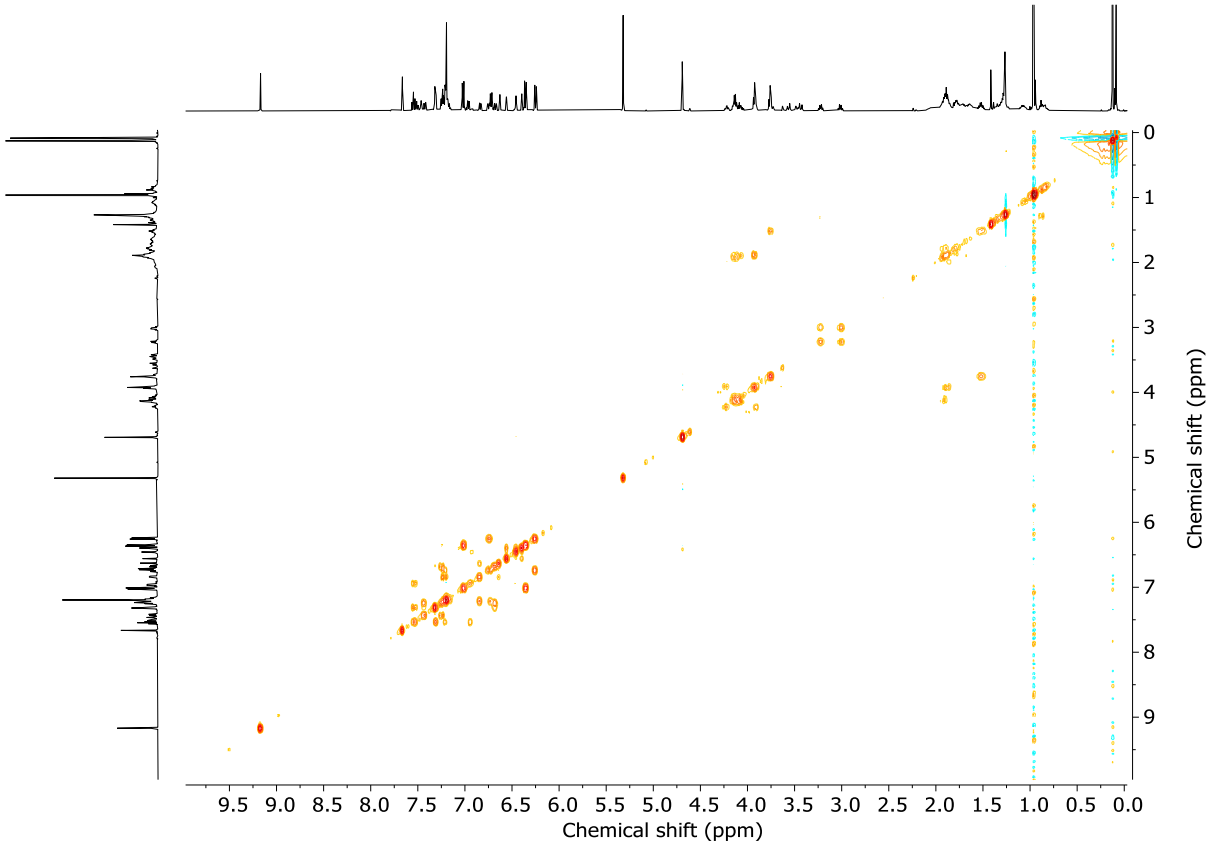

Figure S89: COSY NMR (CD_2Cl_2, 298 K) of (S_{mp},$E_{co\text{-}c}$)-**S16** .

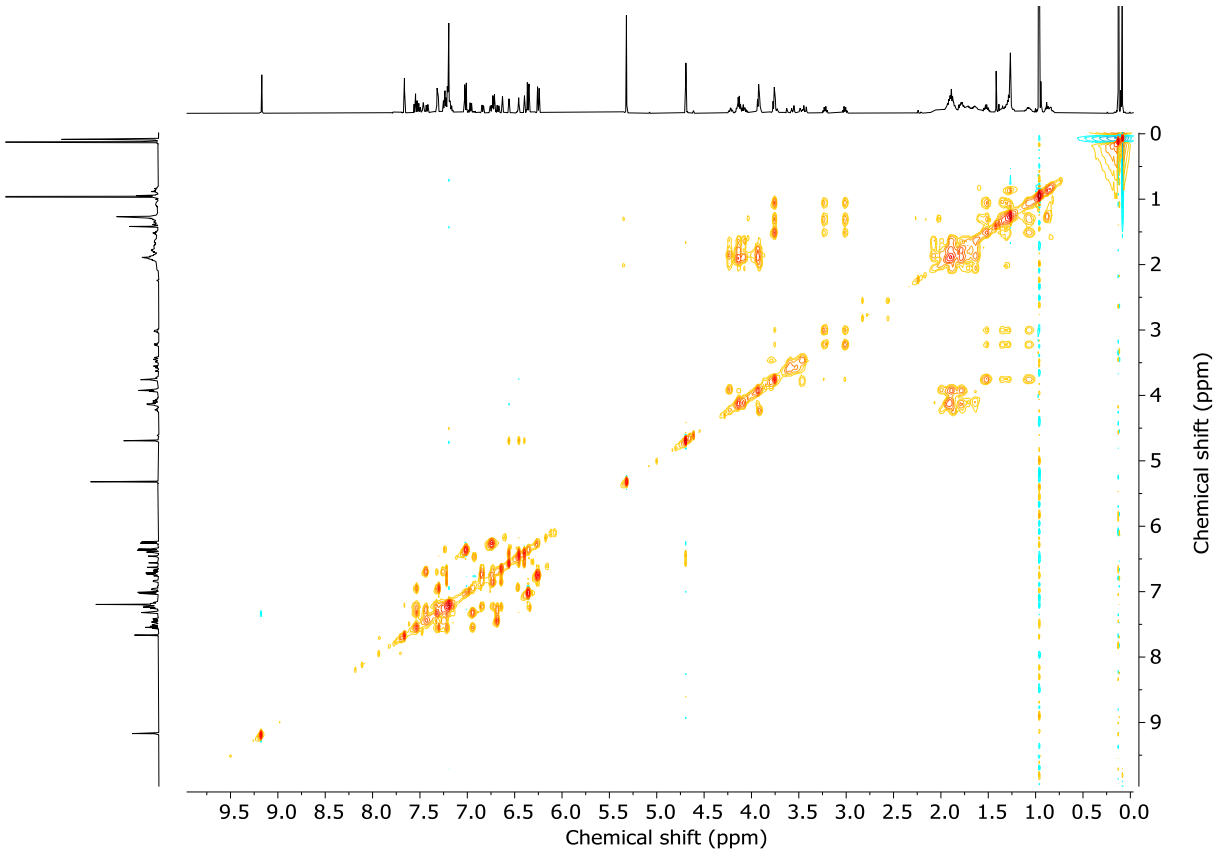

Figure S90: TOCSY NMR (CD_2Cl_2, 298 K) of (S_{mp},$E_{co\text{-}c}$)-**S16**.

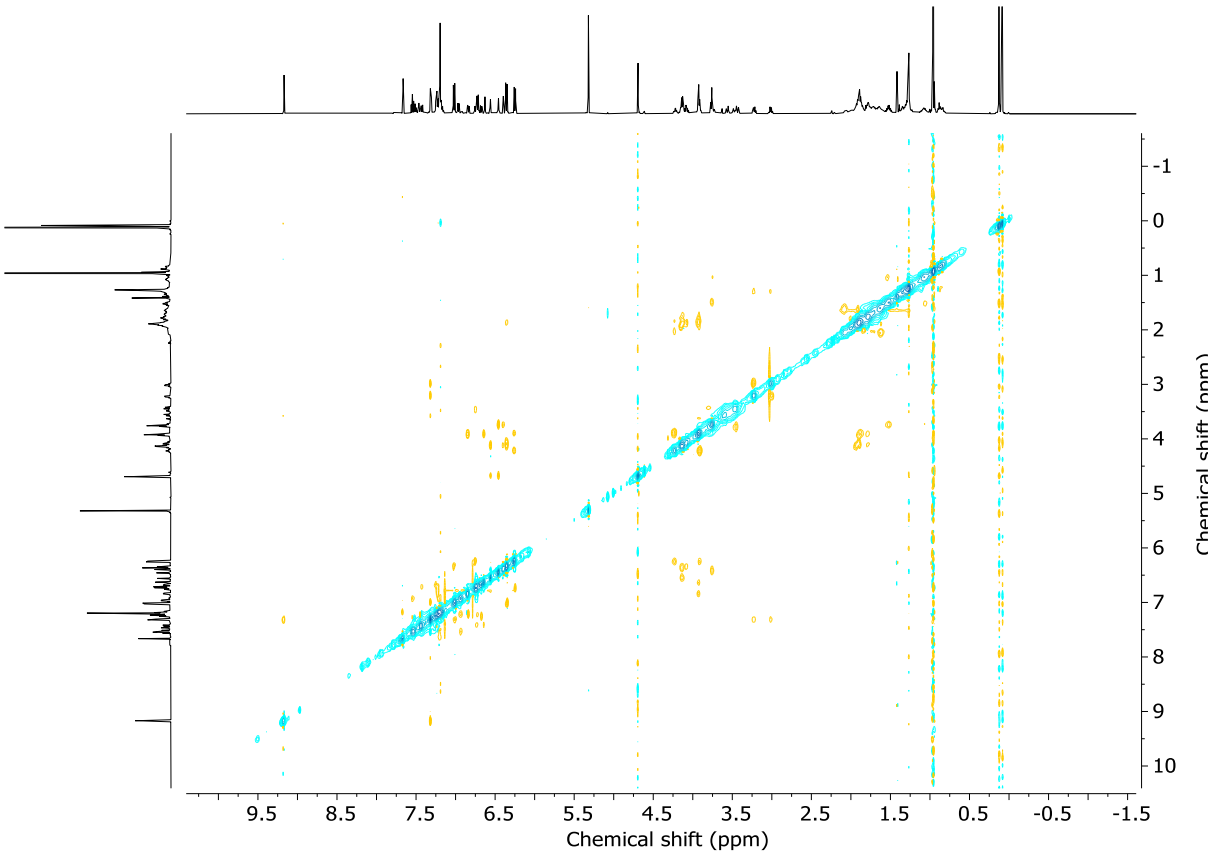

Figure S91: NOESY NMR (CD_2Cl_2, 298 K) of (S_{mp},$E_{co\text{-}c}$)-**S16** .

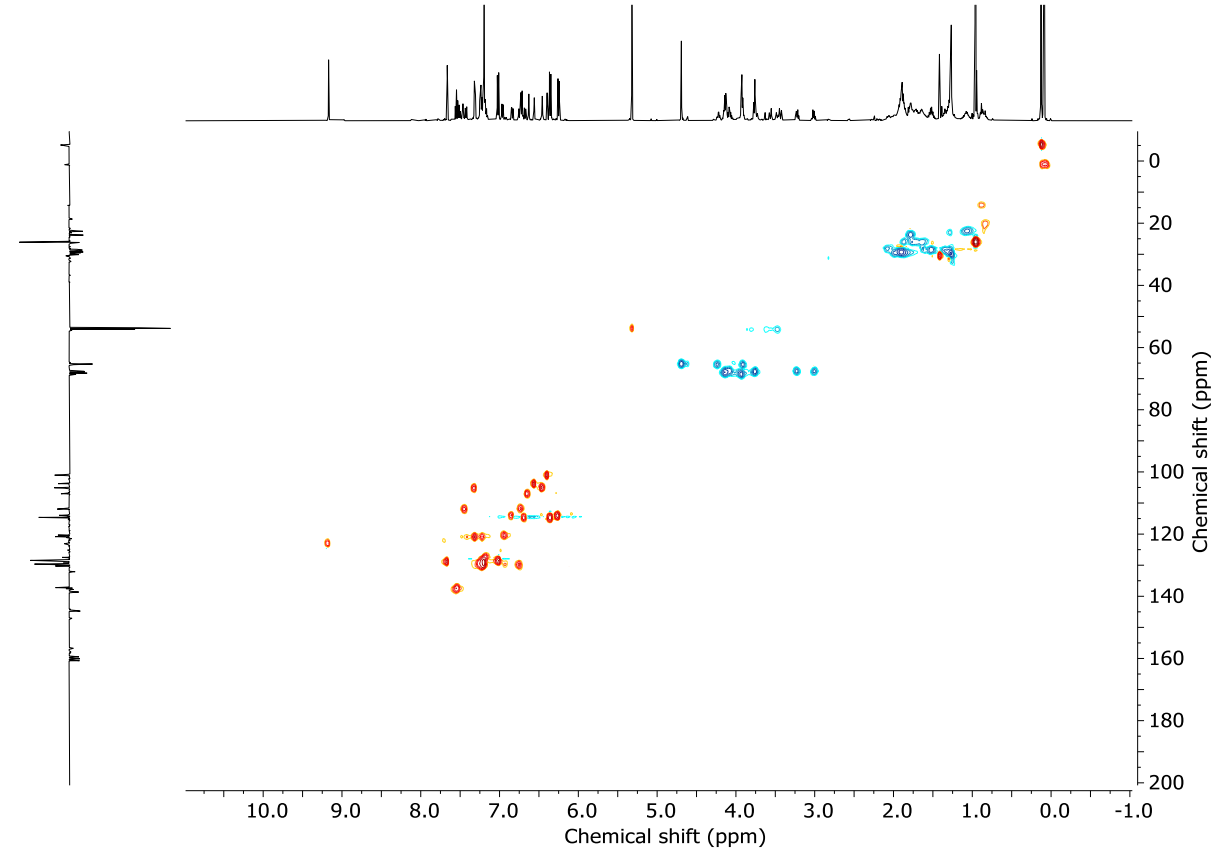

Figure S92: HSQC NMR (CD_2Cl_2, 298 K) of (S_{mp},$E_{co\text{-}c}$)-**S16** .

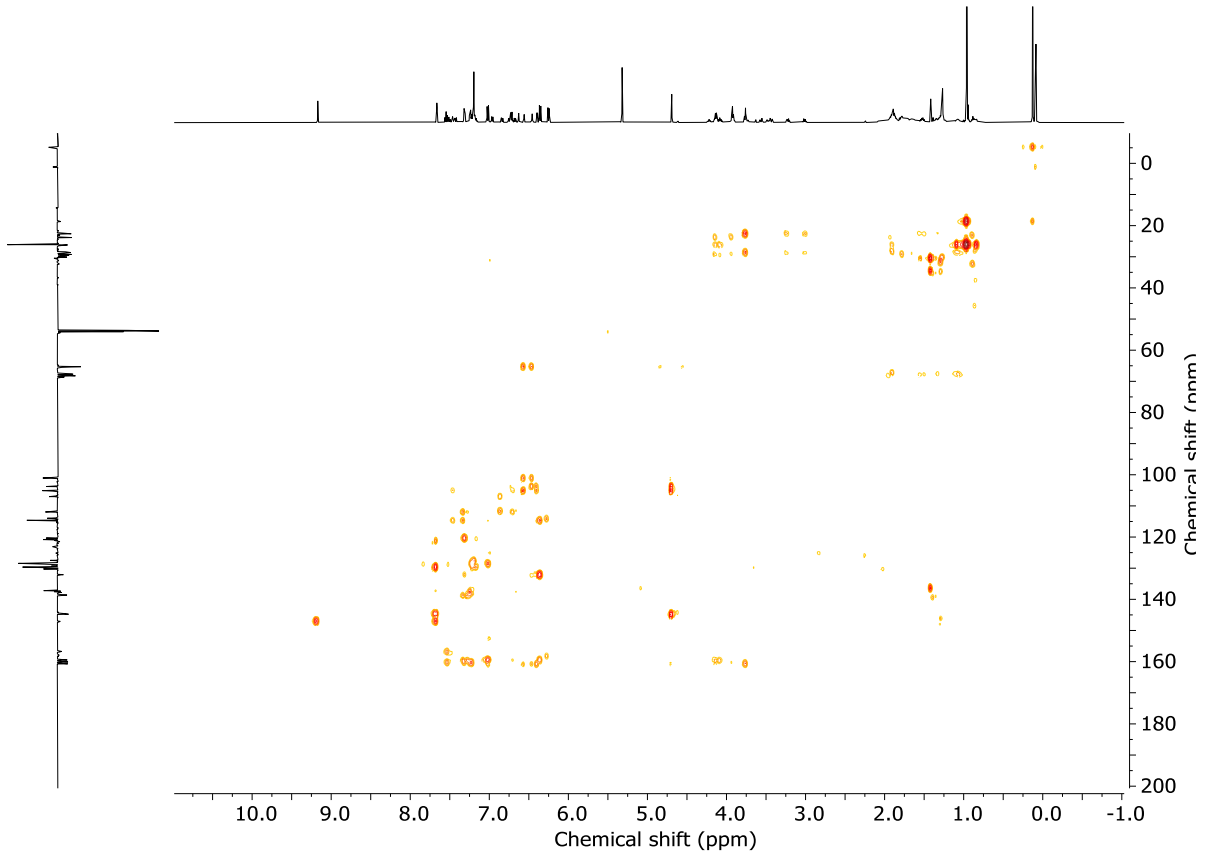

Figure S93: HMBC NMR (CD_2Cl_2, 298 K) of (S_{mp},$E_{co\text{-}c}$)-**S16** .

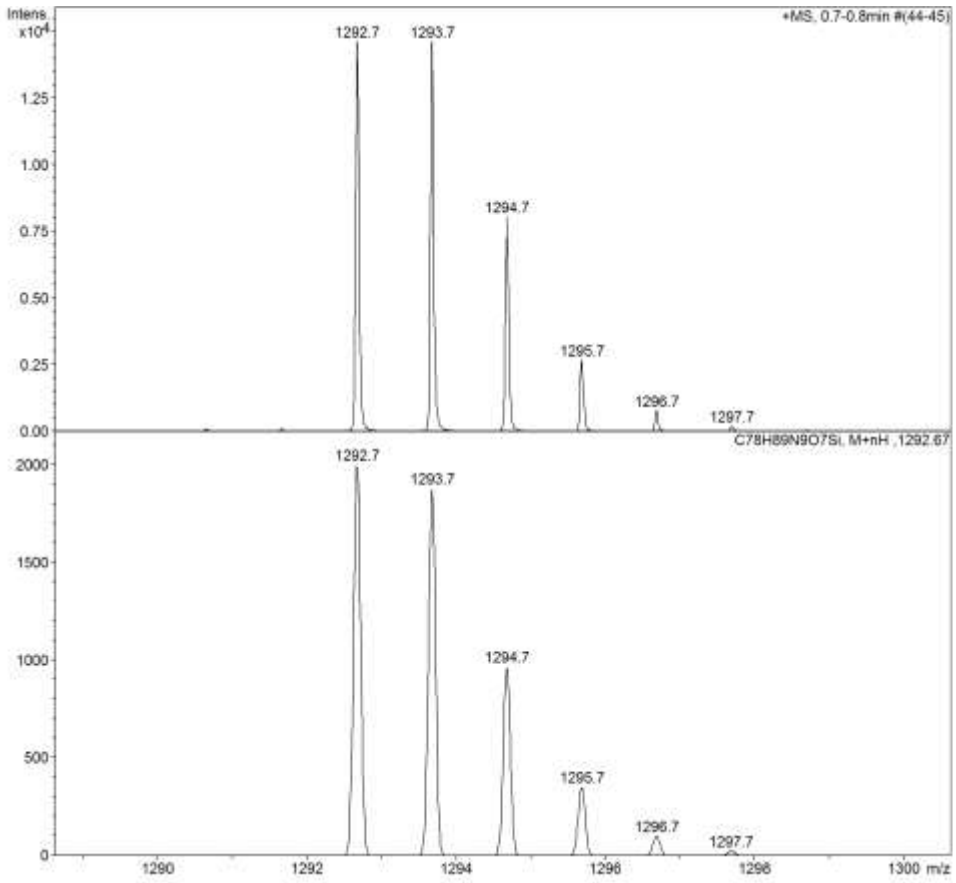

Figure S94: LRMS - Observed (top) and calculated (bottom) isotopic pattern for (S_{mp},$E_{co\text{-}c}$)-**S16** $C_{78}H_{90}N_9O_7Si$.

Amine catenane *rac*-(S_{mp},$E_{co\text{-}c}$)-S16

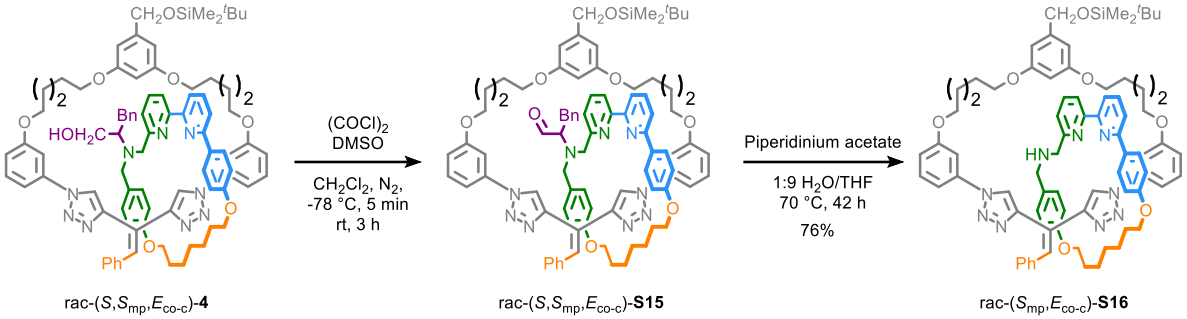

rac-(S,S_{mp},$E_{co\text{-}c}$)-**4** rac-(S,S_{mp},$E_{co\text{-}c}$)-**S15** rac-(S_{mp},$E_{co\text{-}c}$)-**S16**

DMSO (0.12 mL, 1.7 mmol) was added dropwise to a solution of oxalyl chloride (0.07 mL, 0.8 mmol) in CH_2Cl_2 (3.0 mL) at -78 °C and the reaction mixture was stirred for 10 min. An aliquot of this solution (0.53 mL) was added to a stirred solution of catenane *rac*-(S,S_{mp},$E_{co\text{-}c}$)-**4** (41 mg, 0.029 mmol) in CH_2Cl_2 (1.8 mL) at -78 °C followed by Et_3N (0.11 mL, 0.79 mmol) and the reaction mixture was stirred for 5 min before the flask was removed from the -78 °C bath. After 3 hours at rt, the reaction was quenched by addition of sat. $NaHCO_{3(aq)}$ (30 mL), the phases separated, and the aqueous layer extracted with CH_2Cl_2 (3 x 15 mL). The combined organic layers were dried (Na_2SO_4), filtered and concentrated *in vacuo* to give a residue containing aldehyde catenane (S,S_{mp},$E_{co\text{-}c}$)-**S15**. Piperidinium acetate (21 mg, 0.14 mmol) was added to the residue and the flask purged with N_2 for 10 min. THF-H_2O (9 : 1, 1.8 mL) was sparged with N_2 for 5 min, added to the mixture, and the resulting solution was stirred at 70 °C for 44 h. The reaction mixture was cooled to rt, quenched by addition of sat. $NaHCO_{3(aq)}$ (40 mL), the phases separated, and the aqueous layer extracted with CH_2Cl_2 (3 x 15 mL). The combined organic layers were dried (Na_2SO_4), filtered and concentrated *in vacuo*. Chromatography (CH_2Cl_2-MeOH 100 : 0 to 94 : 6) gave NH-catenane *rac*-(S_{mp},$E_{co\text{-}c}$)-**S16** as a white foam (22 mg). Impure product fractions were combined and repurified using the same chromatography conditions to afford additional material (6 mg, 28 mg in total, 76% over two steps).

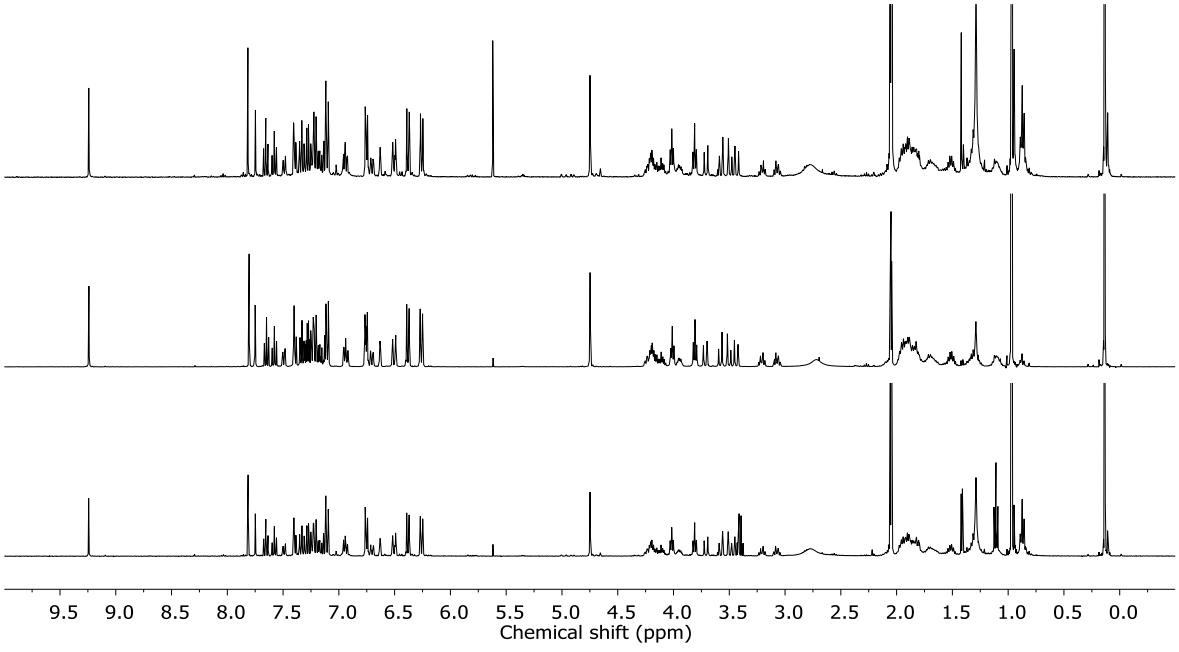

Figure S95: Stack plot ^{1}H NMR (acetone-d_6, 400 MHz, 298 K) of (S_{mp},$E_{co\text{-}c}$)-**S18** (top), *rac*-(S_{mp},$E_{co\text{-}c}$)-**S18** (middle), and (R_{mp},$E_{co\text{-}c}$)-**S18** (bottom).

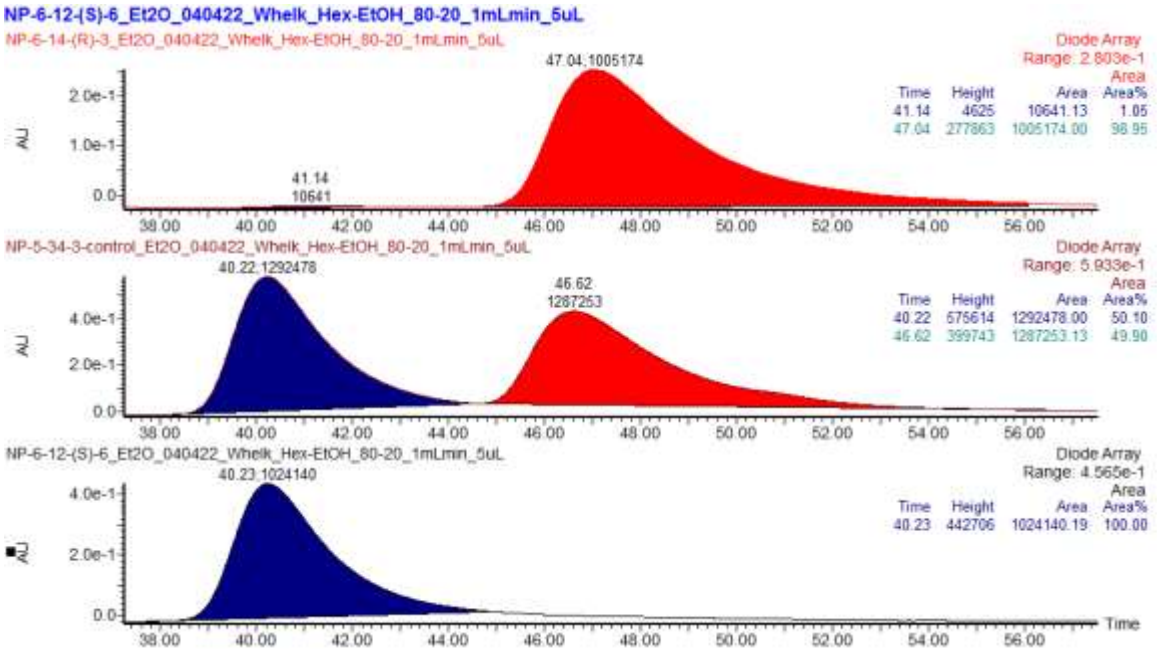

Figure S96: CSP-HPLC (loaded in Et_2O, SSWhelk, ^{n}hexane-EtOH 80 : 20, flowrate 1 mLmin^{-1}) of (S_{mp},$E_{co\text{-}c}$)-**S18** (97.8% *ee*) (top); *rac*-(R_{mp},$E_{co\text{-}c}$)-**S18** ([R_{mp},$E_{co\text{-}c}$]-**S18** @ 40.22 min, 50.1%; [S_{mp},$E_{co\text{-}c}$]-**S18** @ 46.62 min, 49.9%) (middle); (R_{mp},$E_{co\text{-}c}$)-**S18** (>99% *ee*) (bottom).

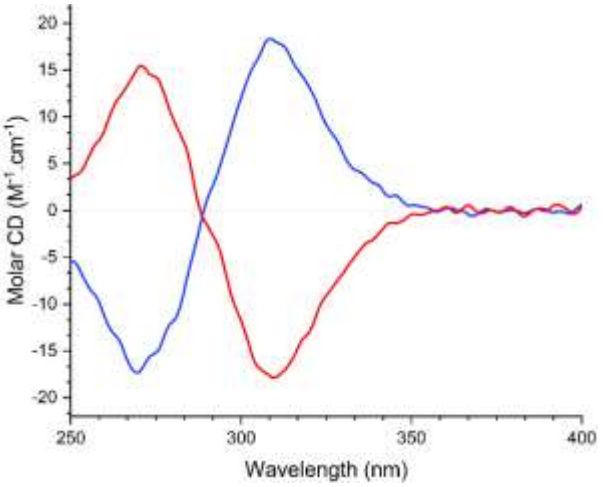

Figure S97: Circular dichroism spectra (3.12 mM mM in CH_3CN, 293 K) of (S_{mp},$E_{co\text{-}c}$)-**S16** (red) and (R_{mp},$E_{co\text{-}c}$)-**S16** (blue).

Catenanes 5

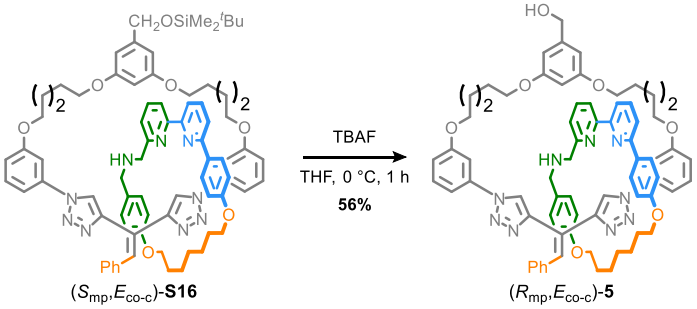

TBDMS catenane (S_{mp},$E_{co\text{-}c}$)-**S16** (9 mg, 0.007 mmol) was dissolved in THF (1.0 mL) and cooled to 0 °C. TBAF (1 M in THF, 0.07 mL, 0.07 mmol) was added dropwise and the reaction mixture was stirred at 0 °C for 20 min. $NH_4Cl_{(aq)}$ (0.1 M, 0.4 mL) was added dropwise at 0 °C and the mixture was stirred for 2 min. EtOAc (50 mL) was added, the phases separated, and the organic layer was washed with H_2O (3 x 30 mL) and brine (50 mL). The combined organic layers were dried (Na_2SO_4), and concentrated *in vacuo*. Chromatography (CH_2Cl_2-MeOH 100:0 to 92 : 8) gave amino-alcohol catenane (R_{mp})-**5** as white foam (4 mg, 43%). Catenane (R_{mp})-**5** was initially isolated and characterised as its (R_{mp},$E_{co\text{-}c}$)-**5** co-conformational isomer but on standing in solution this evolved to an equilibrium mixture of (R_{mp},$E_{co\text{-}c}$)-**5** and (R_{mp},$Z_{co\text{-}c}$)-**5** (see section S6).

Catenanes *rac*-**4** (11 mg, 56%) and (S_{mp})-**5** (3 mg, 38%) were synthesised using an identical procedure starting from *rac*-(R_{mp},$E_{co\text{-}c}$)-**S16** (22 mg, 0.017 mmol) or (R_{mp},$E_{co\text{-}c}$)-**S16** (8 mg, 0.006 mmol) respectively. Their analytical data were identical to (R_{mp})-**5** (e.g., Figure S107) with the exception of their CSP-HPLC (Figure S108) and CD spectra (Figure S109).

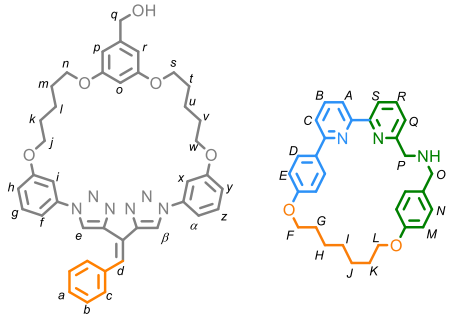

^{1}H NMR (500 MHz, CD_2Cl_2) δ 9.15 (s, 1H, $\boldsymbol{H}_{\beta}$), 7.66 (s, 1H, $\boldsymbol{H}_{d}$), 7.51 (t, *J* = 7.8, 1H, $\boldsymbol{H}_{R}$), 7.49 (t, *J* = 7.8, 1H, $\boldsymbol{H}_{B}$), 7.45 (d, *J* = 7.9, 1H, $\boldsymbol{H}_{\alpha}$), 7.34 – 7.28 (m, 2H, $\boldsymbol{H}_{x,}$ $\boldsymbol{H}_{C}$), 7.26 (app. t, *J* = 8.2, 2H, $\boldsymbol{H}_{z}$, $\boldsymbol{H}_{e}$), 7.25 – 7.13 (m, 7H, $\boldsymbol{H}_{a}$, $\boldsymbol{H}_{b}$, $\boldsymbol{H}_{c}$, $\boldsymbol{H}_{g,}$ $\boldsymbol{H}_{A}$), 7.10 (d, *J* = 7.6, 1H, $\boldsymbol{H}_{S}$), 7.00 (d, *J* = 8.6, 2H, $\boldsymbol{H}_{D}$), 6.86 (app. ddd , *J* = 8.3, 2.4, 0.9 H z, 2H, $\boldsymbol{H}_{h}$, $\boldsymbol{H}_{Q}$), 6.77 (d, *J* = 8.0, 2H, $\boldsymbol{H}_{N}$), 6.70 (dd, *J* = 8.2, 1.5, 1H, $\boldsymbol{H}_{y}$), 6.69 – 6.60 (m, 3H, $\boldsymbol{H}_{i}$, $\boldsymbol{H}_{p}$, $\boldsymbol{H}_{f}$), 6.51 (s, 1H, $\boldsymbol{H}_{r}$), 6.43 (t, *J* = 2.3, 1H, $\boldsymbol{H}_{o}$), 6.35 (d, *J* = 8.6, 2H, $\boldsymbol{H}_{E}$), 6.25 (d, *J* = 8.5, 2H, $\boldsymbol{H}_{M}$), 4.63 (d, *J* = 13.0, 1H, 1 of $\boldsymbol{H}_{q}$), 4.60 (d, *J* = 13.0, 1H, 1 of $\boldsymbol{H}_{q}$), 4.29 – 4.17 (m, 2H, 1 of $\boldsymbol{H}_{n}$, 1 of $\boldsymbol{H}_{L}$), 4.18 – 4.09 (m, 2H, 1 of $\boldsymbol{H}_{n}$, 1 of $\boldsymbol{H}_{F}$), 4.07 (dt, *J* = 10.1, 5.7, 1H, 1 of $\boldsymbol{H}_{F}$), 3.98 – 3.68 (m, 4H, $\boldsymbol{H}_{j}$, 1 of $\boldsymbol{H}_{O,}$ 1 of $\boldsymbol{H}_{L}$), 3.86 – 3.73 (m, 2H, $\boldsymbol{H}_{s}$), 3.68 – 3.41 (m, 3H, $\boldsymbol{H}_{P,}$ 1 of $\boldsymbol{H}_{O}$), 3.25 (dt, *J* = 8.9, 6.1, 1H, $\boldsymbol{H}_{w}$), 2.98 (dt, *J* = 9.0, 6.7, 1H, 1 of $\boldsymbol{H}_{w}$), 2.16 – 1.45 (m, 18H, $\boldsymbol{H}_{k}$, $\boldsymbol{H}_{l}$, $\boldsymbol{H}_{m}$, $\boldsymbol{H}_{t}$, $\boldsymbol{H}_{G}$, $\boldsymbol{H}_{H}$, $\boldsymbol{H}_{I}$, $\boldsymbol{H}_{J}$, $\boldsymbol{H}_{K}$), 1.43 – 1.18 (m, 2H, $\boldsymbol{H}_{v}$), 1.17 – 0.99 (m, 2H, $\boldsymbol{H}_{u}$).

^{13}C NMR (126 MHz, CD_2Cl_2) δ 160.9, 160.7, 160.3 (x2), 160.1, 159.7, 159.5, 158.2 (HMBC), 156.8 (x3), 147.0, 144.9, 144.6, 138.6, 137.7, 137.7, 137.2, 137.2, 132.0, 130.3, 129.6, 129.4, 128.7, 128.5, 128.4, 127.6, 123.1, 121.3, 120.9, 120.8 (x2), 120.2, 114.7, 114.5 (x2), 114.1, 114.0, 111.9, 111.5, 106.8, 106.4, 105.2, 104.5, 101.4, 68.7, 68.2, 67.7, 67.7, 67.4, 65.5, 65.4, 53.5 (x2, HSQC/HMBC), 30.1, 29.7, 29.5, 29.2, 29.2, 28.8, 28.6, 28.4, 26.2, 26.1, 23.7, 22.6.

LR-ESI-MS (+ve): *m/z* = 1178.6 (100%) $[M+H]^+$ calc. for $C_{72}H_{76}N_9O_7$ 1178.6.

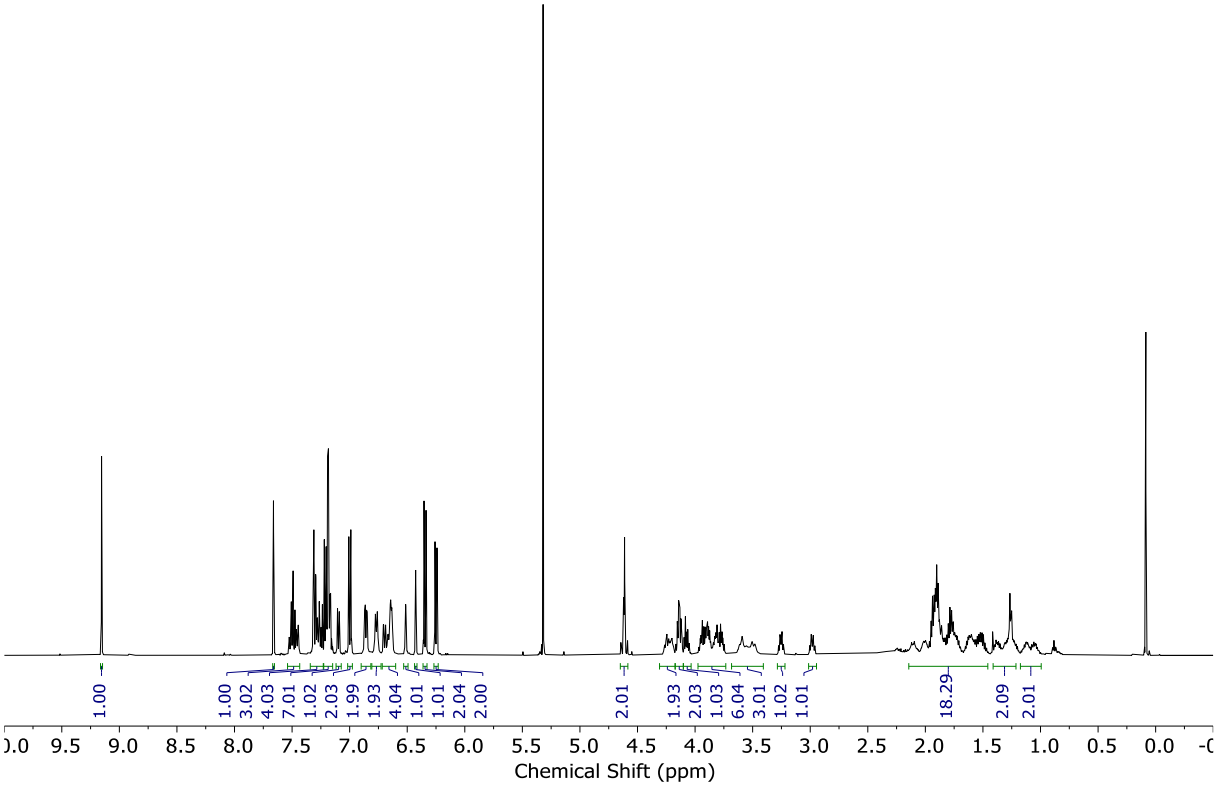

Figure S98: ^{1}H NMR (CD_2Cl_2, 500 MHz, 298 K) of (R_{mp})-**5**.

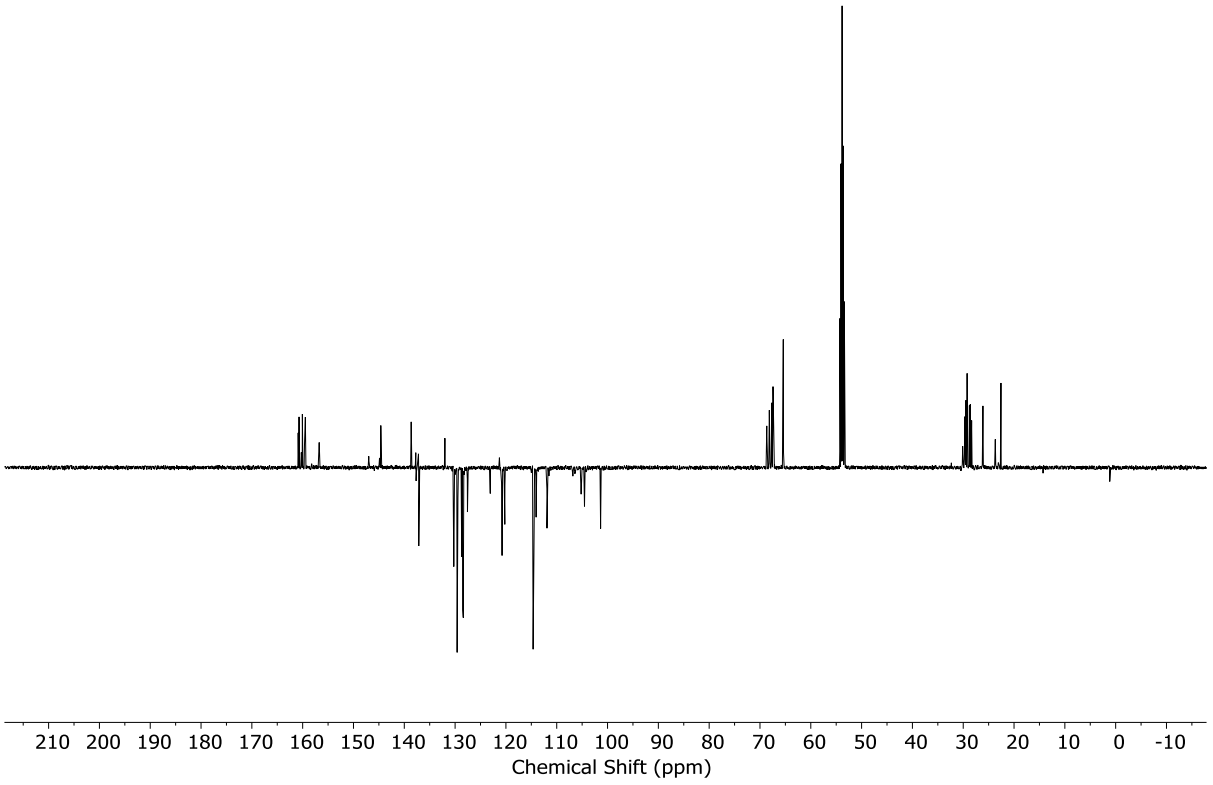

Figure S99: JMOD NMR (CD_2Cl_2, 126 MHz, 298 K) of (R_{mp})-**5**.

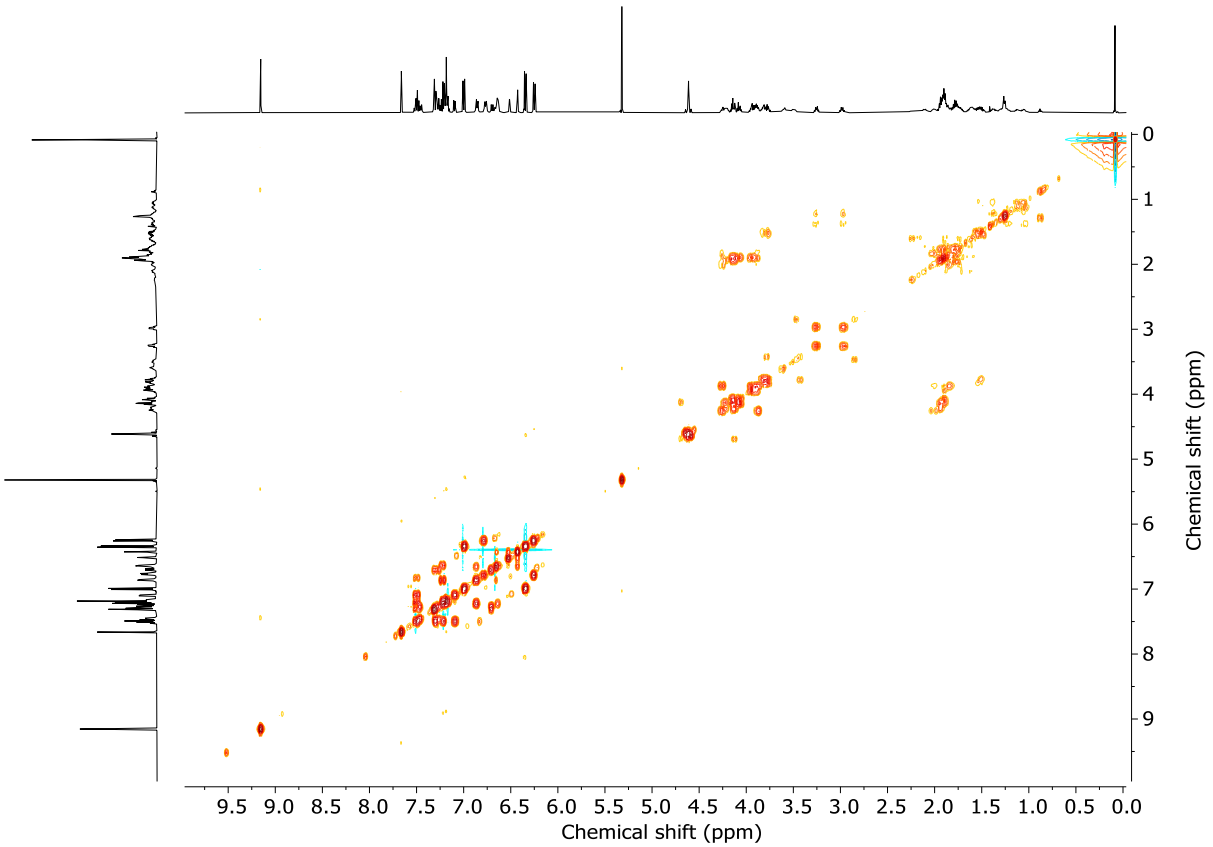

Figure S100: COSY NMR (CD_2Cl_2, 298 K) of (R_{mp})-**5**.

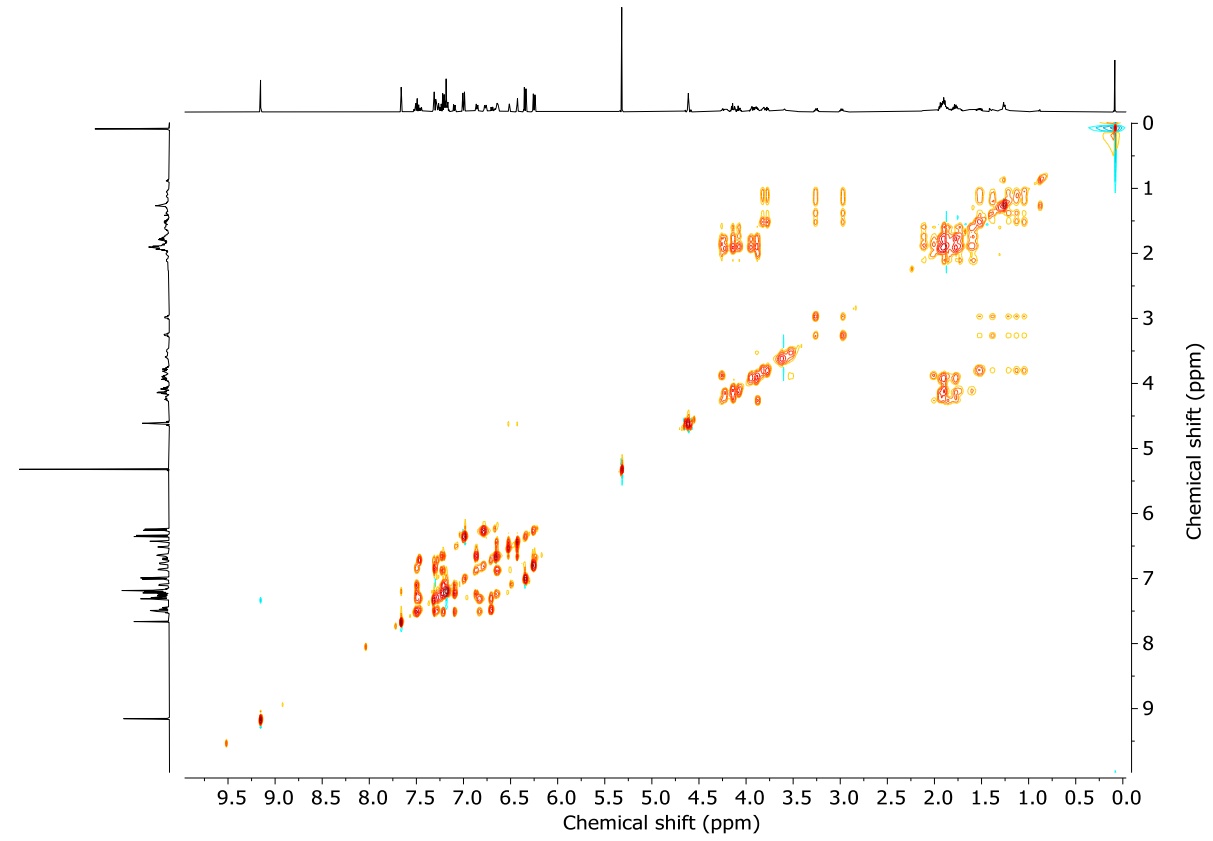

Figure S101: TOCSY NMR (CD_2Cl_2, 298 K) of (R_{mp})-**5**.

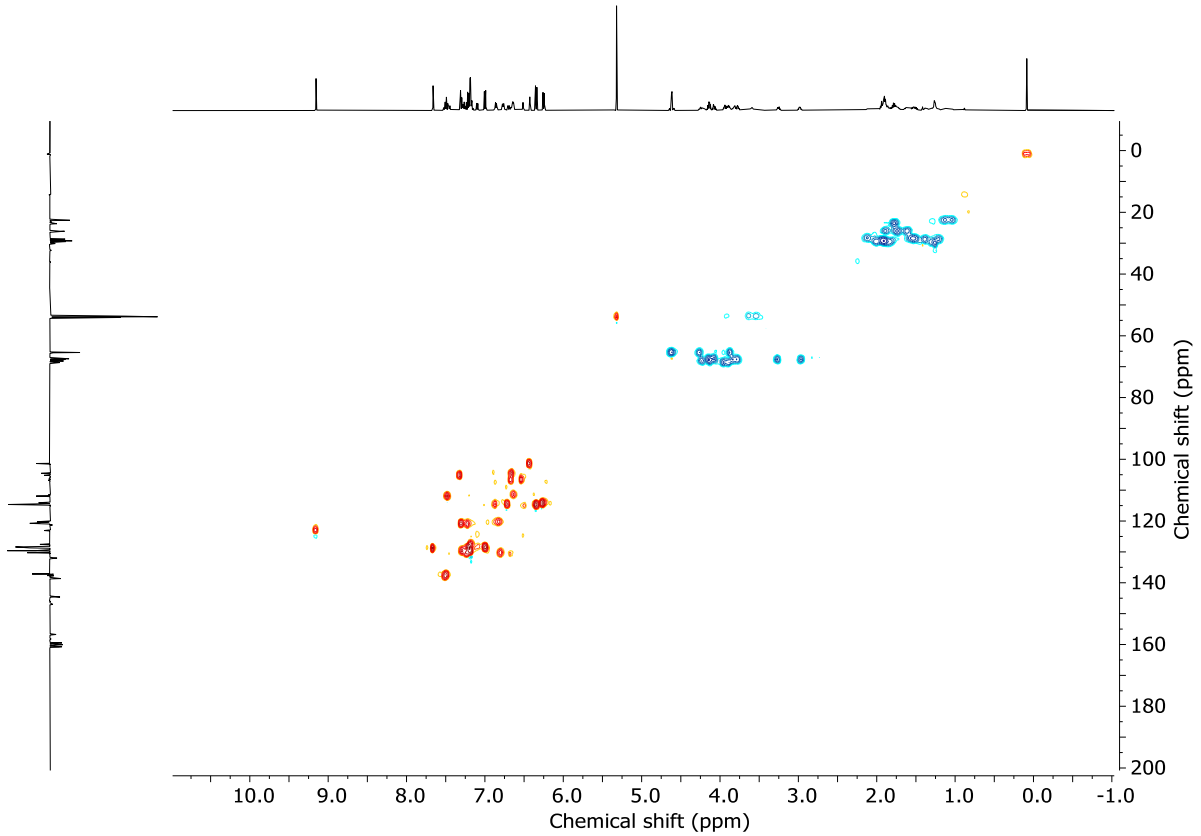

Figure S102: HSQC NMR (CD_2Cl_2, 298 K) of (R_{mp})-**5**.

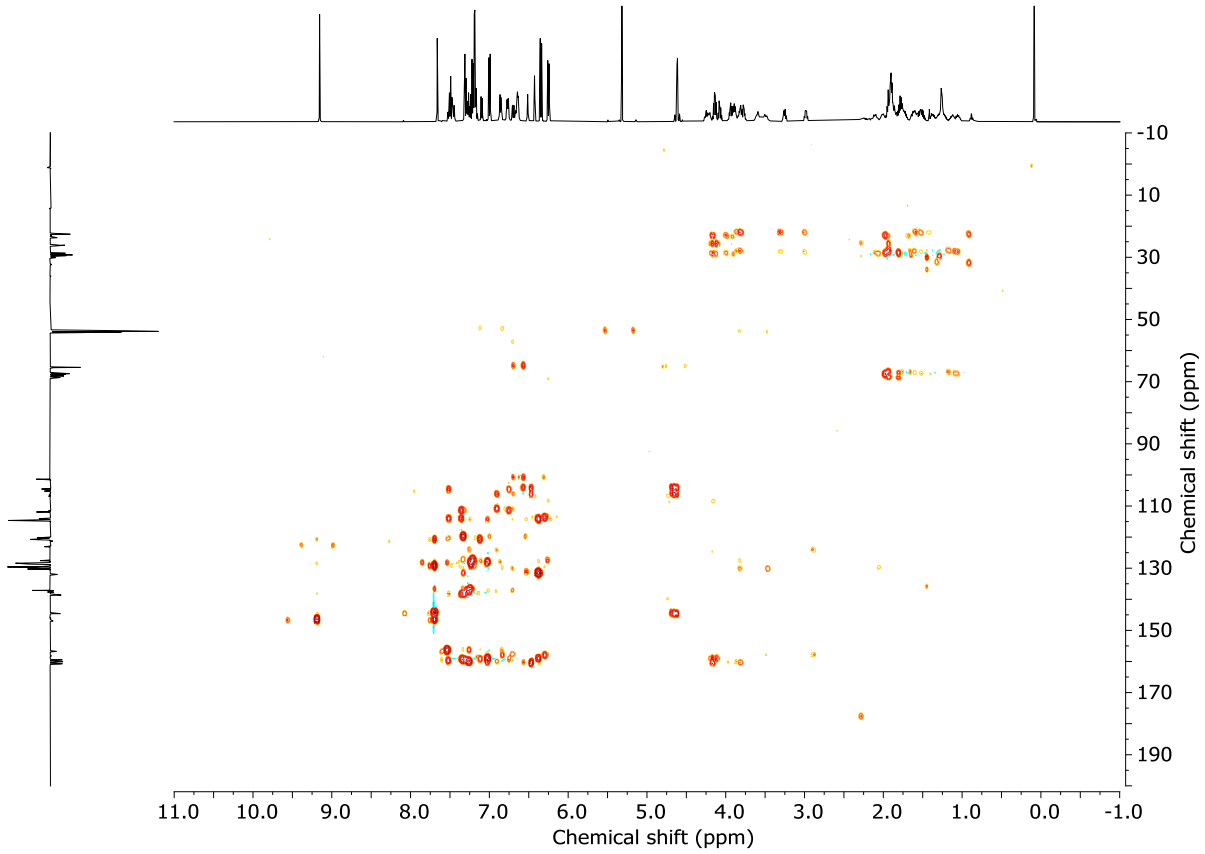

Figure S103: HMBC NMR (CD_2Cl_2, 298 K) of (R_{mp})-**5**.

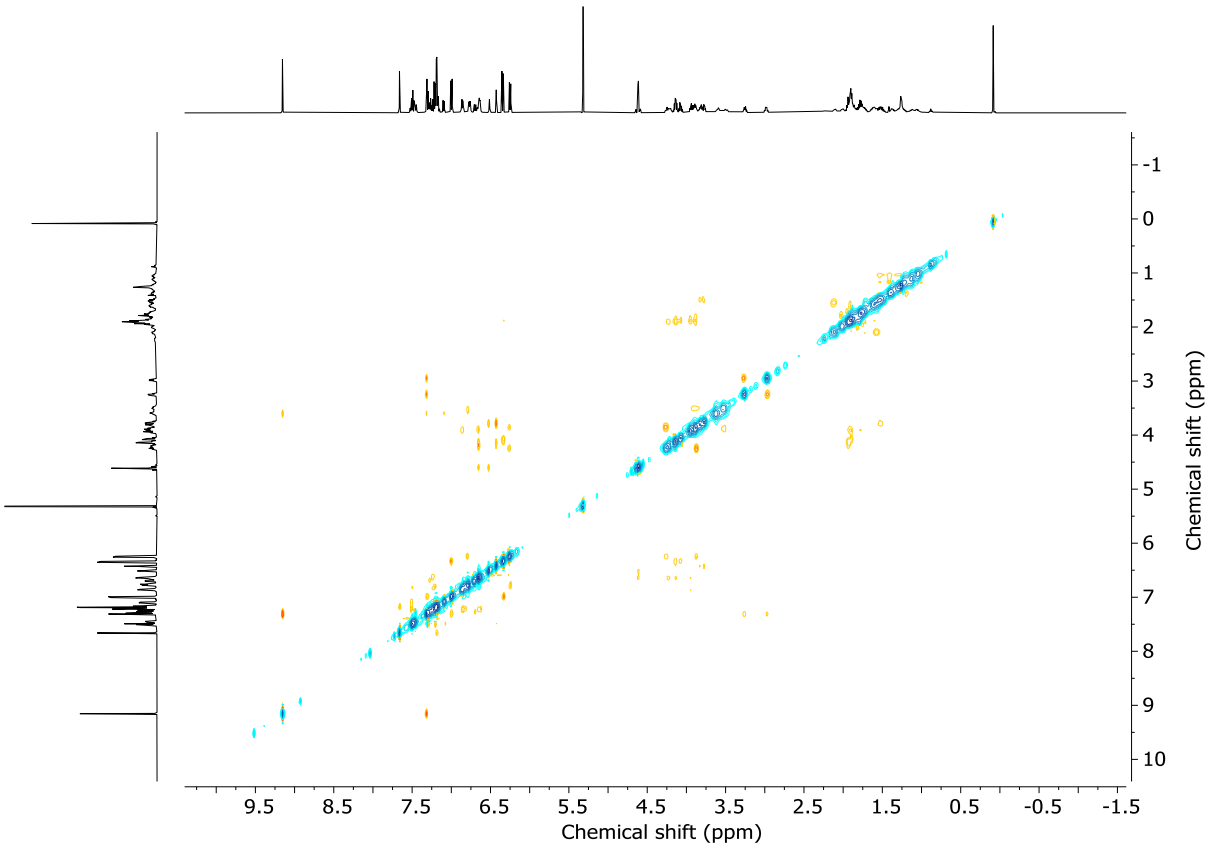

Figure S104: NOESY NMR (CD_2Cl_2, 298 K) of (R_{mp})-**5**.

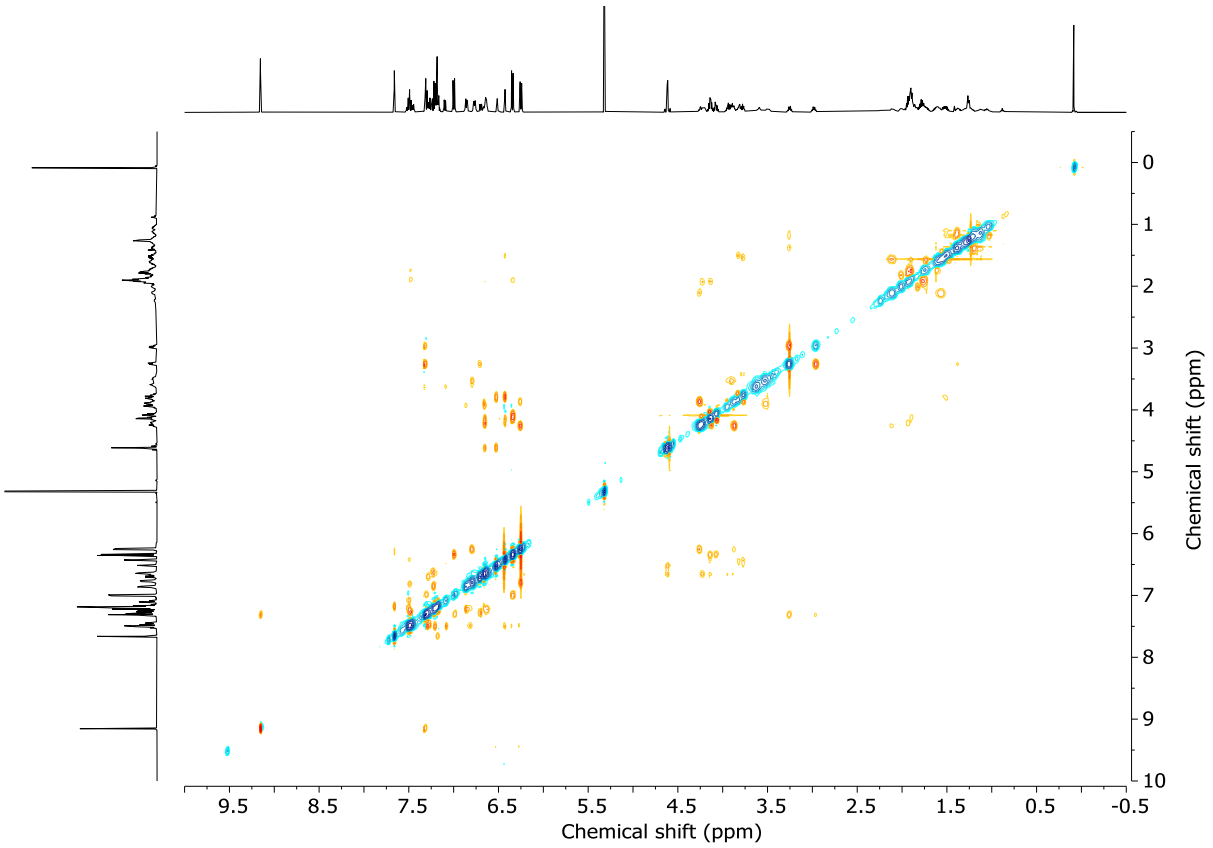

Figure S105: ROESY NMR (CD_2Cl_2, 298 K) of (R_{mp})-**5**.

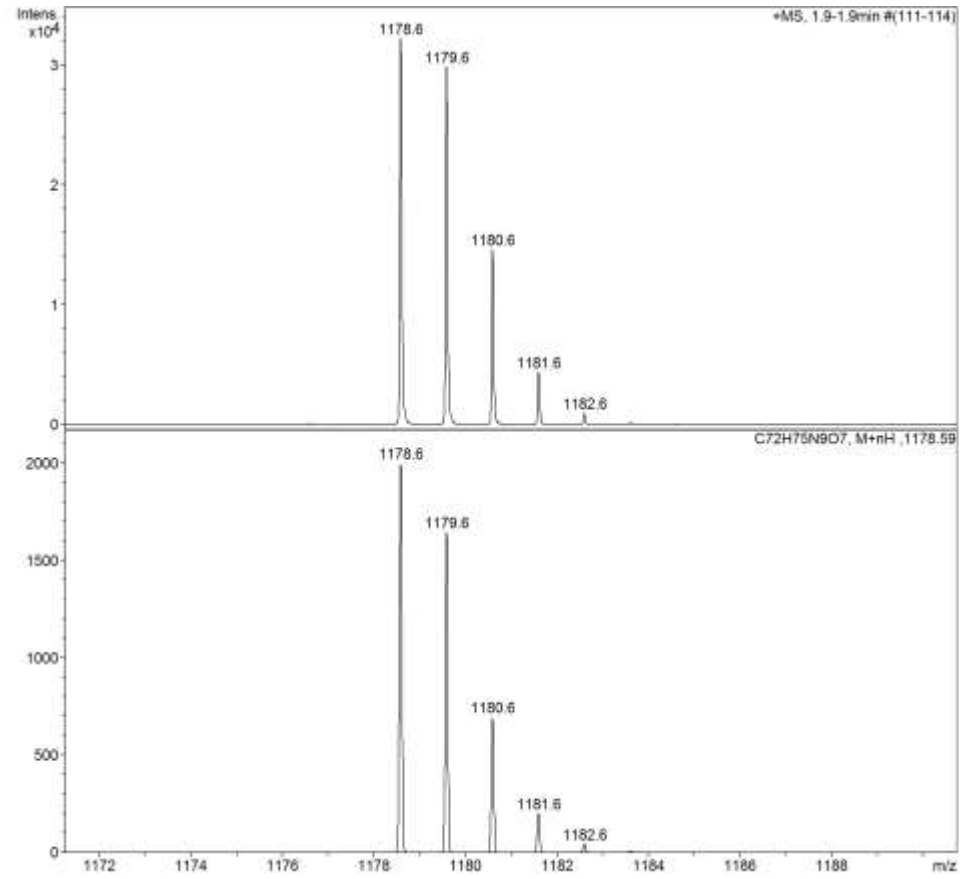

Figure S106: LRMS - Observed (top) and calculated (bottom) isotopic pattern for (R_{mp})-**5** $C_{72}H_{75}N_9O_7$.

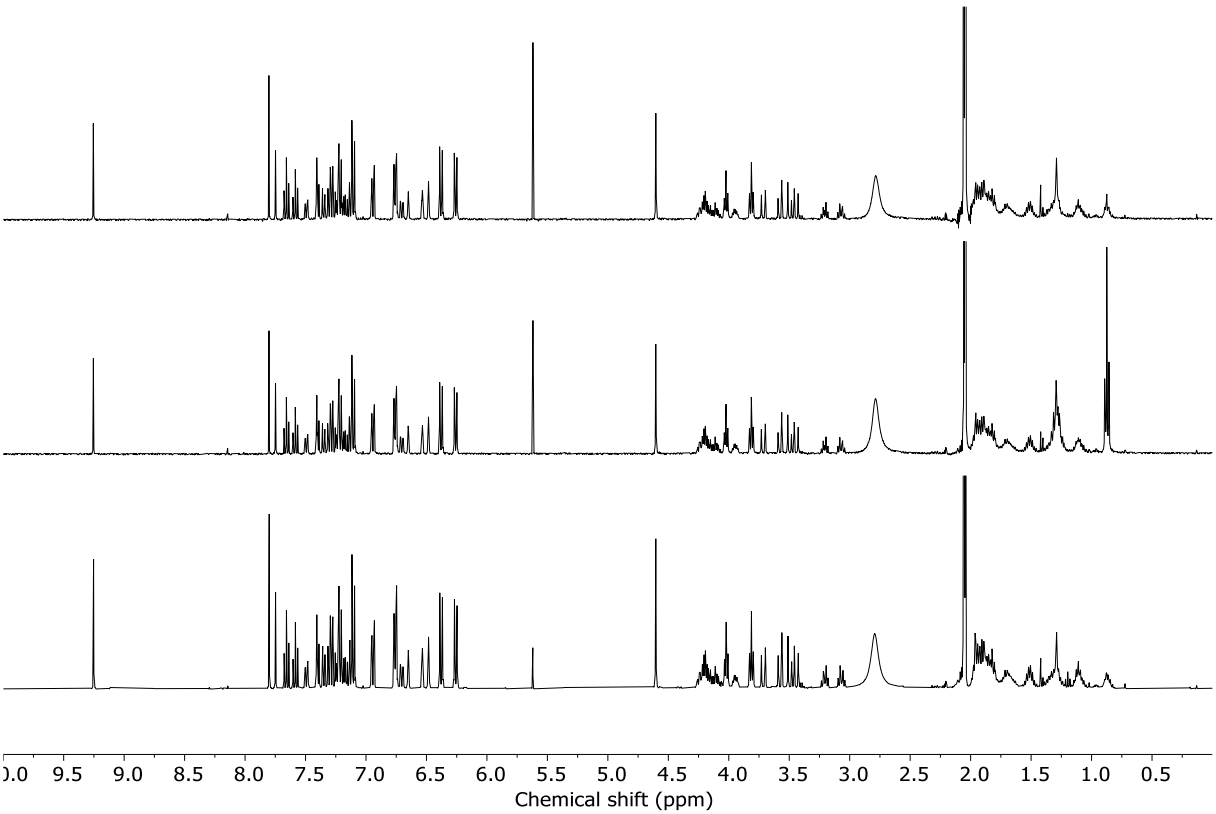

Figure S107: ^{1}H NMR (acetone-d_6, 400 MHz, 298 K) stack plot of (S_{mp})-**5** (top), *rac*-**5** (middle) and (R_{mp})-**5** (bottom).

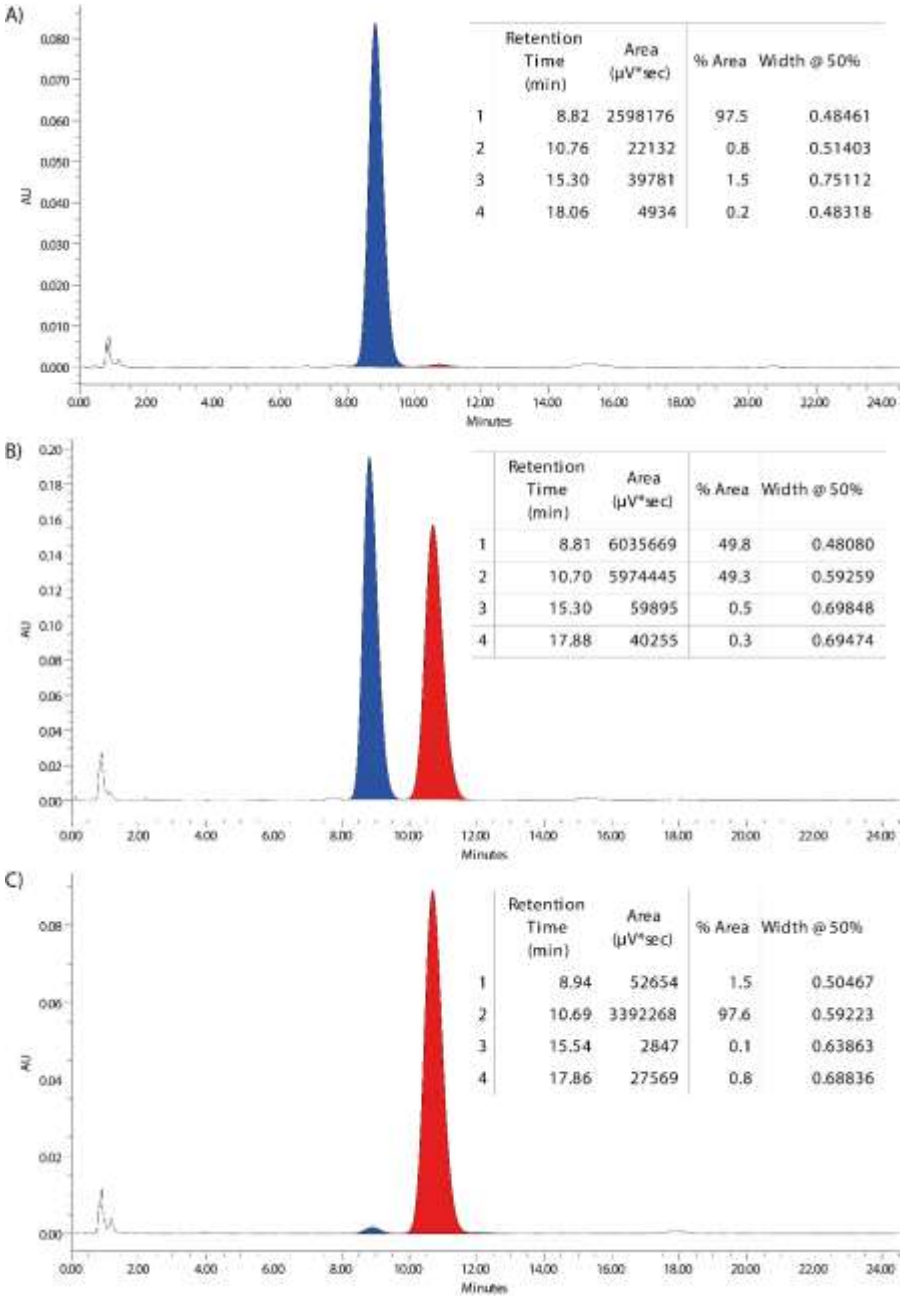

Figure S108: CSP-HPLC (1 mL loaded in Et_2O, Chiralpak IK, 40 ˚C, 125 BarG, isocratic 50 : 50 MeOH : CO_2 [0.1% v/v NH_3], 4 mL.min^{-1}) of (R_{mp},$E_{co\text{-}c}$)-**5** (97.5% *ee*) (top); *rac*-(R_{mp},$E_{co\text{-}c}$)-**4** ([R_{mp},$E_{co\text{-}c}$]-**5** @ 8.81 min, 50.2%; [S_{mp},$E_{co\text{-}c}$]-**5** @ 10.70 min, 49.8%) (middle); (S_{mp},$E_{co\text{-}c}$)-**5** (97.5% *ee*) (bottom).

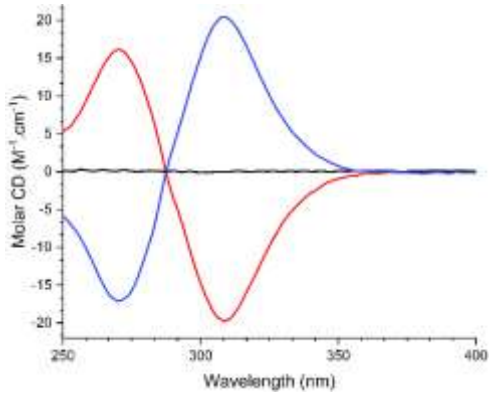

Figure S109: Circular dichroism spectra (3.23 μM in CH_3CN, 293 K) of (S_{mp},$E_{co\text{-}c}$)-**5** (red), (R_{mp},$E_{co\text{-}c}$)-**5** (blue) and *rac*-($E_{co\text{-}c}$)-**5** (black).

5. ^{1}H NMR Spectra of Catenanes 3 and 4 and their Non-Interlocked Components

5.1. ^{1}H NMR stack plot comparing catenane 3 and the component non-interlocked macrocycles

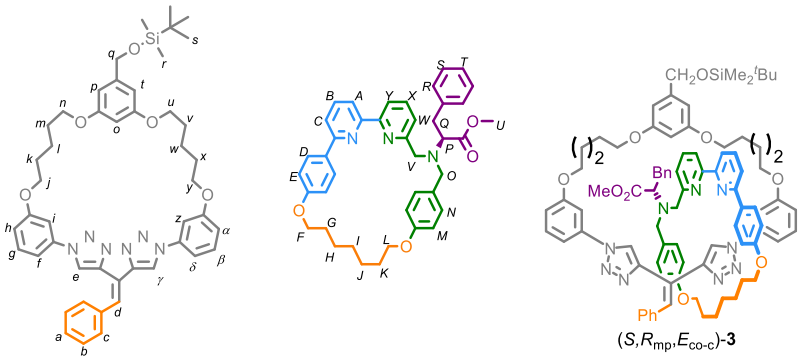

Figure S110: The structures of catenane **3**, triazole macrocycle **S17** and bipyridine macrocycle (*S*)-**S18** with key proton environments labelled.

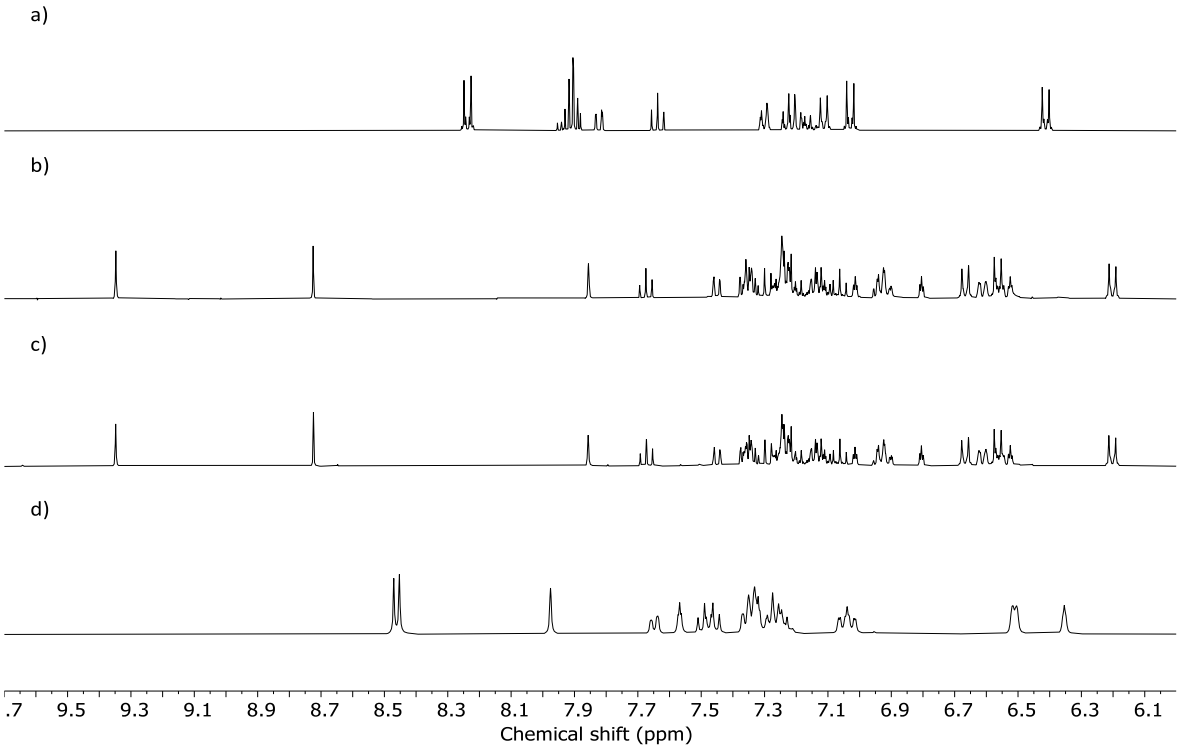

Figure S111: Partial ^{1}H NMR (acetone-d_6, 400 MHz, 298 K) of (a) bipyridine macrocycle (*S*)-**S18**, (b) (*S*,R_{mp},$E_{co\text{-}c}$)-**3**, (c) *rac*-(*S*,R_{mp},$E_{co\text{-}c}$)-**3**, (d) triazole macrocycle **S17**.

5.2. ^{1}H NMR stack plot comparing catenane 5 and the component non-interlocked macrocycles

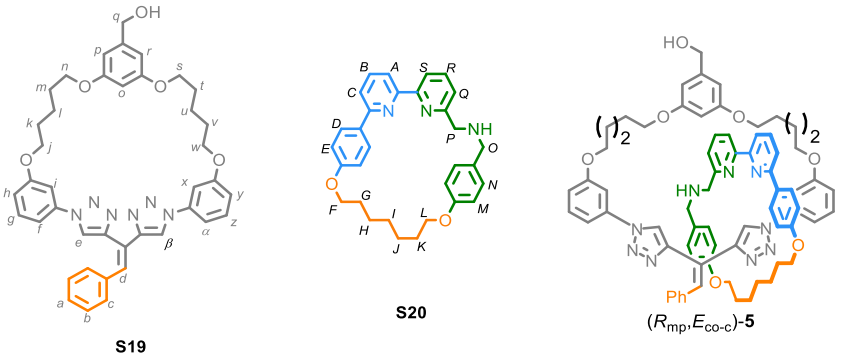

Figure S112: The structures of catenane **5**, triazole macrocycle **S19** and bipyridine macrocycle **S20** with key proton environments labelled.

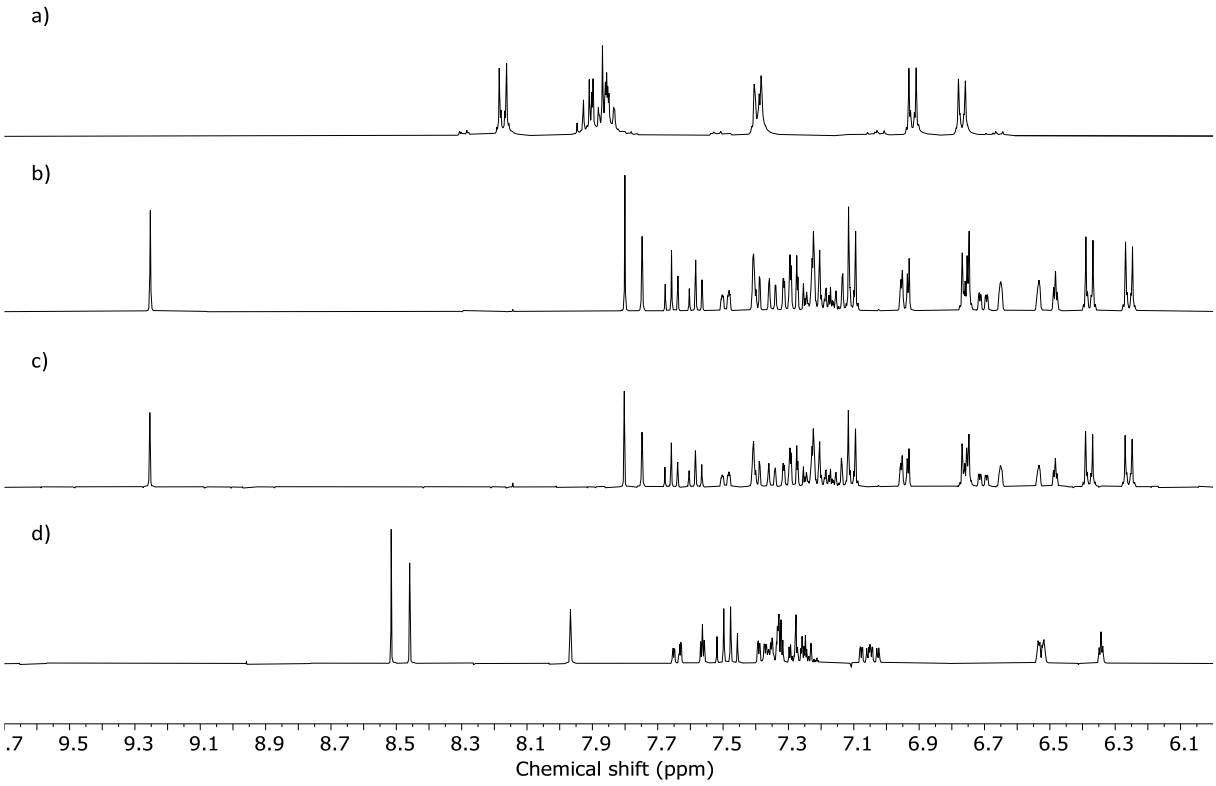

Figure S113: Partial ^{1}H NMR (acetone-d_6, 400 MHz, 298 K) of (a) bipyridine macrocycle **S20**, (b) (R_{mp},$E_{co\text{-}c}$)-**5**, (c) *rac*-($E_{co\text{-}c}$)-**5**, (d) triazole macrocycle **S19**.

5.3. Synthesis of non-interlocked macrocycles S17 and S19

Non-interlocked macrocycle S17

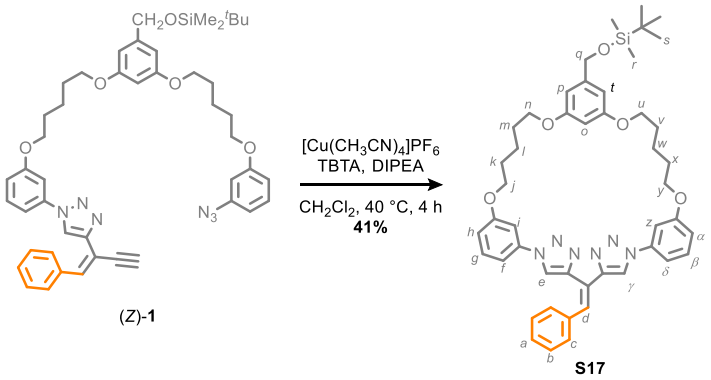

To a stirred solution of TBTA (5 mg, 0.01 mmol), $[Cu(CH_3CN)_4]PF_6$ (4 mg, 0.01 mmol) and $^{i}Pr_2NEt$ (17 µL, 0.097 mmol) in CH_2Cl_2 (1.0 mL) at 40 °C was added (*Z*)-**1** (39 mg, 0.048 mmol) in CH_2Cl_2 (1.9 mL) at a constant rate using a syringe pump over 4 h. The reaction mixture was stirred for 15 min after the addition had completed, cooled to rt and diluted with CH_2Cl_2 (5 mL). The solution was washed with EDTA-NH_3 solution (0.1 M, 2 x 5 mL) then brine (10 mL), dried ($MgSO_4$) and concentrated *in vacuo*. Chromatography (petrol-Et_2O 100 : 0 to 100 : 0) gave macrocycle **S17** (16 mg, 41%) as a white foam.

^{1}H NMR (500 MHz, CD_2Cl_2) δ 8.15 (s, 1H, $\boldsymbol{H}_{\gamma}$), 8.04 (s, 1H, $\boldsymbol{H}_{d}$), 7.73 (s, 1H, $\boldsymbol{H}_{e}$), 7.61 (ddd, *J* = 8.1, 2.1, 0.9, 1H, $\boldsymbol{H}_{f}$), 7.52 (t, *J* = 2.2, 1H, $\boldsymbol{H}_{i}$), 7.45 (t, *J* = 8.2, 1H, $\boldsymbol{H}_{g}$), 7.37 (t, *J* = 8.2, 1H, $\boldsymbol{H}_{\beta}$), 7.36 – 7.24 (m, 5H, $\boldsymbol{H}_{a,}$ $\boldsymbol{H}_{b,}$ $\boldsymbol{H}_{c}$), 7.04 (t, *J* = 2.2, 1H, $\boldsymbol{H}_{z}$), 7.00 – 6.93 (m, 2H, $\boldsymbol{H}_{h,}$ $\boldsymbol{H}_{\alpha}$), 6.97 – 6.91 (m, 1H, $\boldsymbol{H}_{\delta}$), 6.45 (dt, *J* = 2.3, 0.8, 2H, $\boldsymbol{H}_{p,}$ $\boldsymbol{H}_{t}$), 6.35 (t, *J* = 2.3, 1H, $\boldsymbol{H}_{o}$), 4.65 (s, 2H, $\boldsymbol{H}_{q}$), 4.09 (t, *J* = 6.2, 2H, $\boldsymbol{H}_{j}$), 4.04 (t, *J* = 6.2, 2H, $\boldsymbol{H}_{y}$), 3.97 (app q, *J* = 6.2, 4H, $\boldsymbol{H}_{n,}$ $\boldsymbol{H}_{u}$), 1.94 – 1.78 (m, 8H, $\boldsymbol{H}_{k,}$ $\boldsymbol{H}_{m,}$ $\boldsymbol{H}_{v,}$ $\boldsymbol{H}_{x}$), 1.72 – 1.63 (m, 4H, $\boldsymbol{H}_{l,}$ $\boldsymbol{H}_{w}$), 0.94 (s, 9H, $\boldsymbol{H}_{s}$), 0.10 (s, 6H, $\boldsymbol{H}_{r}$).

^{13}C NMR (126 MHz, CD_2Cl_2) δ 160.7, 160.7, 160.6, 160.4, 148.3, 145.0, 144.4, 138.5, 138.2, 136.9, 131.1, 130.9, 130.9, 129.6, 128.8, 128.3, 122.0, 121.0, 120.8, 115.2, 114.2, 113.3, 112.1, 107.8, 107.0, 105.2, 103.8, 100.6, 68.8, 68.8, 68.3, 68.2, 65.3, 65.2, 29.4, 29.4, 29.3, 29.1, 23.4, 23.3, 18.7, -5.2.

HR-ESI-MS (+ve): *m/z* = 835.3956 $[M + Na]^+$ calc. for $C_{47}H_{56}N_6NaO_5Si$ 835.3974.

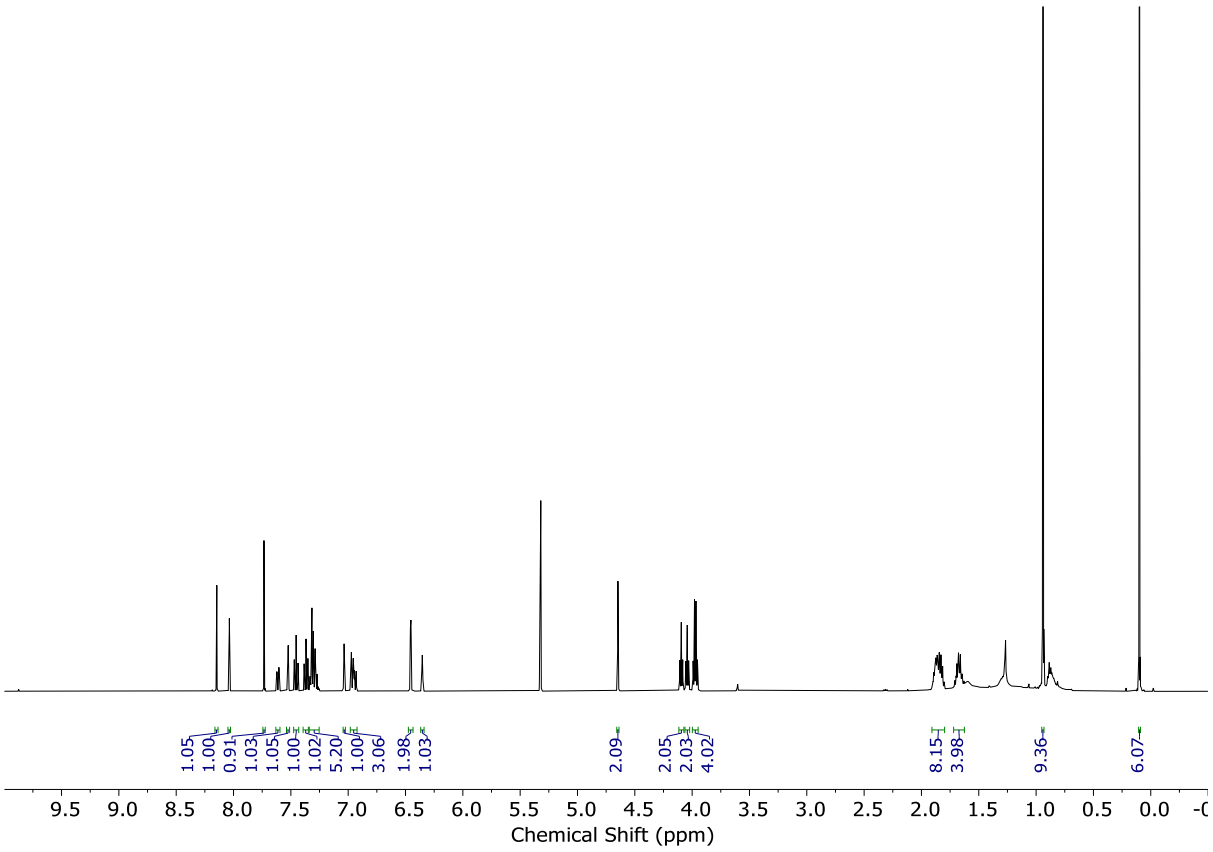

Figure S114: ^{1}H NMR (CD_2Cl_2, 500 MHz, 298 K) of **S17**.

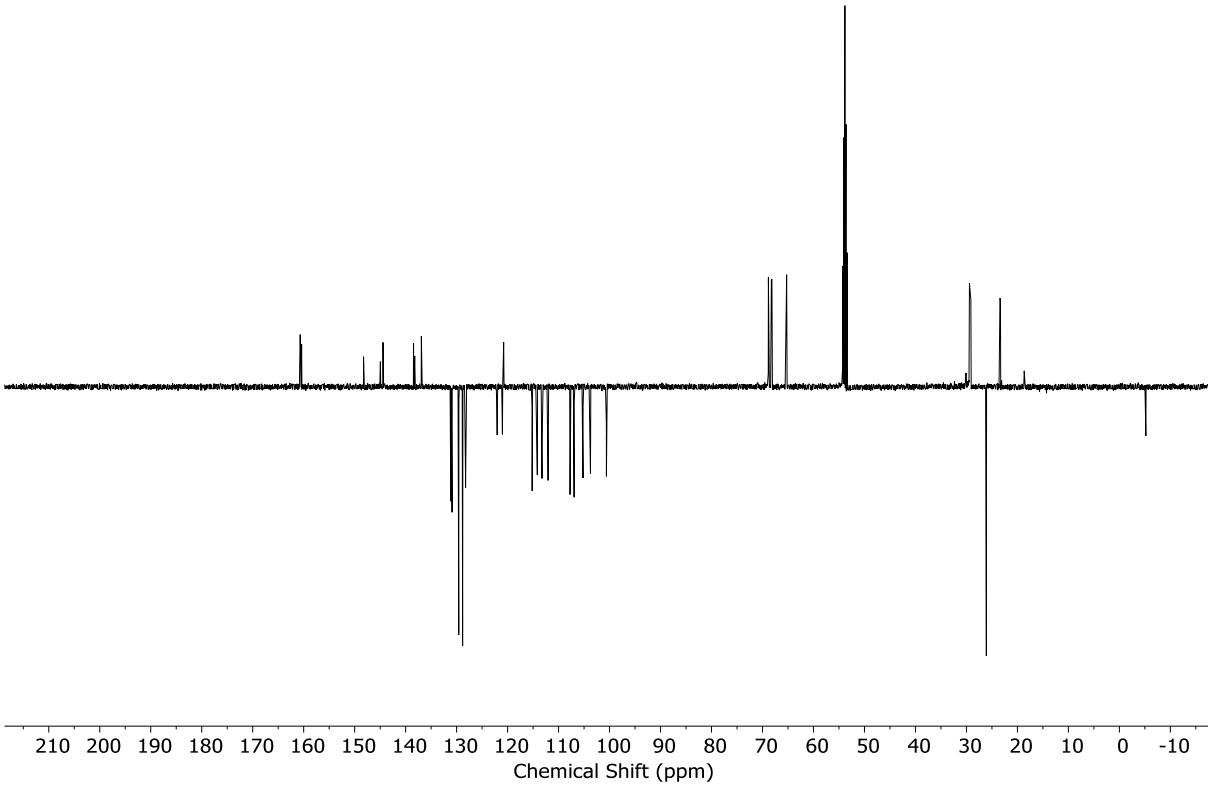

Figure S115: JMOD NMR (CD_2Cl_2, 126 MHz, 298 K) of **S17**.

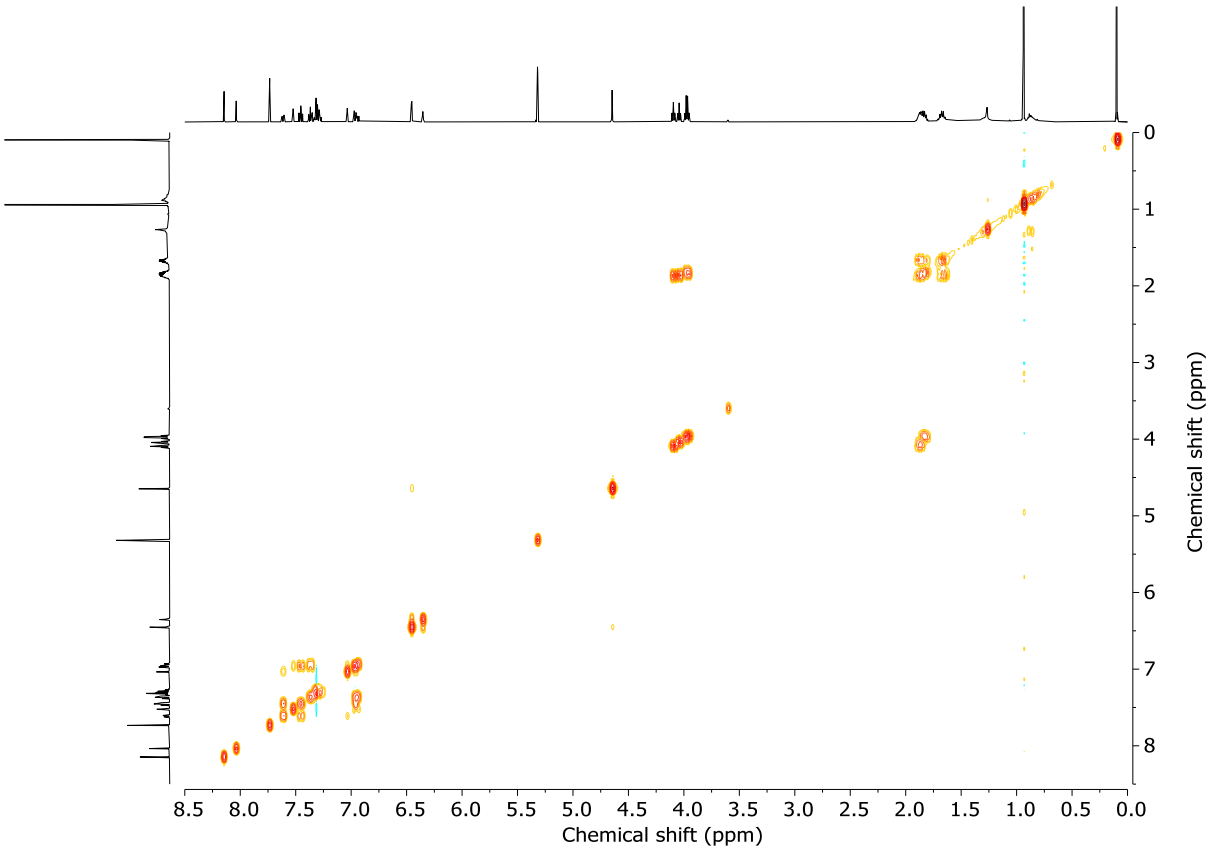

Figure S116: COSY NMR (CD_2Cl_2, 298 K) of **S17**.

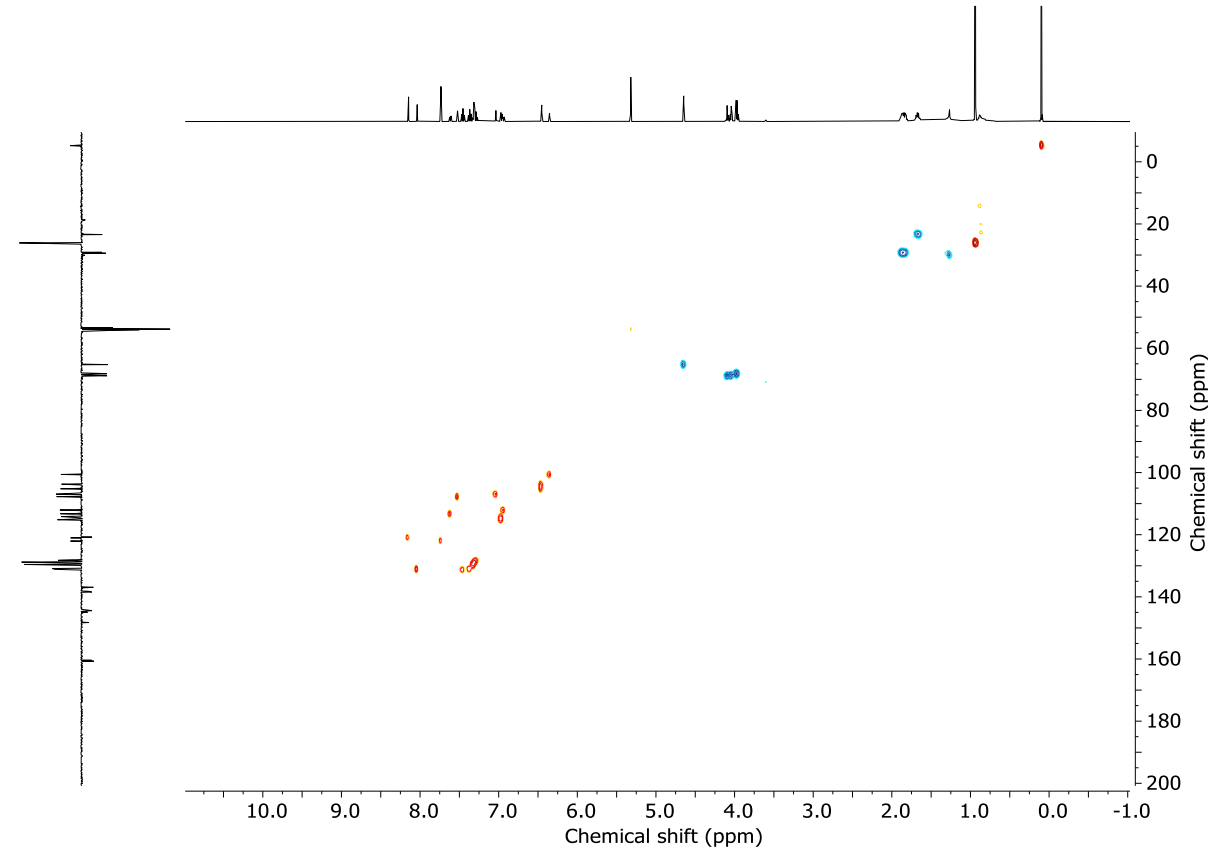

Figure S117: HSQC NMR (CD_2Cl_2, 298 K) of **S17**.

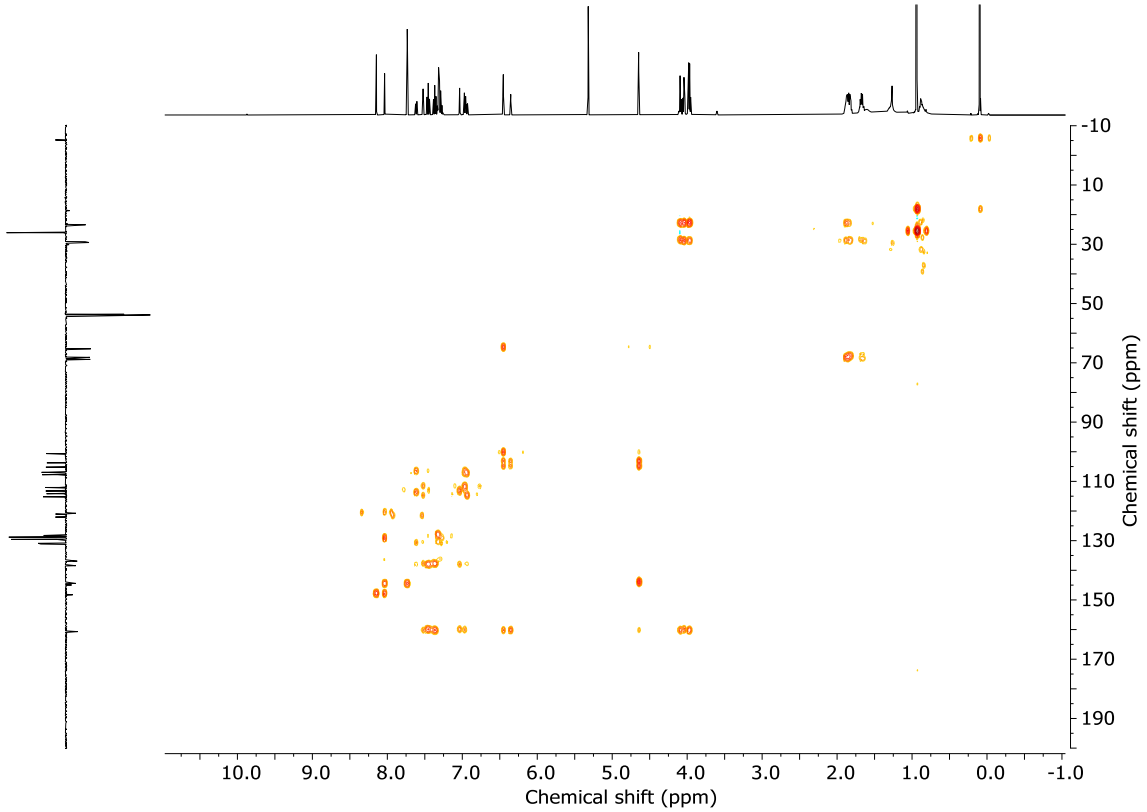

Figure S118: HMBC NMR (CD_2Cl_2, 298 K) of S**17**.

Non-Interlocked macrocycle S19

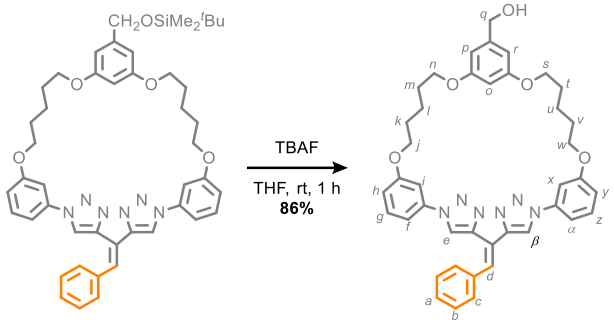

S17 **S19**

To a solution of macrocycle **S17** (16 mg, 0.020 mmol, 1 eq.) in THF (0.3 mL) at 0 ˚C was added TBAF (1 M in THF, 30 µL, 0.030 mmol) and the reaction mixture stirred at rt for 1 h. The solution was diluted with EtOAc (5 mL), washed with H_2O (2 x 5 mL) then brine (5 mL), dried ($MgSO_4$) and concentrated *in vacuo*. Chromatography (petrol-EtOAc 100 : 0 to 0 : 100) gave macrocycle **S19** (12 mg, 86%) as a white foam.

^{1}H NMR (500 MHz, CD_2Cl_2) δ 8.15 (s, 1H, $\boldsymbol{H}_\beta$), 8.03 (s, 1H, $\boldsymbol{H}_d$), 7.73 (s, 1H, $\boldsymbol{H}_e$), 7.61 (ddd, *J* = 8.0, 2.1, 0.9, 1H, $\boldsymbol{H}_f$), 7.52 (t, *J* = 2.2, 1H, $\boldsymbol{H}_i$), 7.45 (t, *J* = 8.2, 1H, $\boldsymbol{H}_g$), 7.37 (t, *J* = 8.2, 1H, $\boldsymbol{H}_z$), 7.34 – 7.25 (m, 5H, $H_{a,b,c}$), 7.04 (t, *J* = 2.2, 1H, $\boldsymbol{H}_x$), 6.97 (dtd, *J* = 8.4, 2.3, 0.9, 2H, $\boldsymbol{H}_h$, $\boldsymbol{H}_y$), 6.93 (ddd, *J* = 8.0, 2.1, 0.9, 1H, $\boldsymbol{H}_\alpha$), 6.49 – 6.47 (m, 2H, $\boldsymbol{H}_p$, $\boldsymbol{H}_r$), 6.39 (app t, *J* = 2.3, 1H, $\boldsymbol{H}_o$), 4.58 (s, 2H, $\boldsymbol{H}_q$), 4.09 (t, *J* = 6.3, 2H, $\boldsymbol{H}_j$), 4.04 (t, *J* = 6.2, 2H, $\boldsymbol{H}_w$), 3.99 (t, *J* = 6.0, 2H, $\boldsymbol{H}_n$ or $\boldsymbol{H}_s$), 3.98 (t, *J* = 6.4, 2H, $\boldsymbol{H}_n$ or $\boldsymbol{H}_s$), 1.92 – 1.80 (m, 8H, $\boldsymbol{H}_k$, $\boldsymbol{H}_m$, $\boldsymbol{H}_t$, $\boldsymbol{H}_v$), 1.71 – 1.63 (m, 4H, $\boldsymbol{H}_l$, $\boldsymbol{H}_u$).

^{13}C NMR (126 MHz, CD_2Cl_2) δ 160.9, 160.8, 160.7, 160.4, 148.2, 145.0, 144.1, 138.5, 138.2, 136.9, 131.2, 131.0, 130.9, 129.6, 128.8, 128.3, 122.1, 121.0, 120.8, 115.2, 114.2, 113.3, 112.1, 107.8, 107.0, 105.9, 104.4, 101.1, 68.8, 68.7, 68.3, 68.2, 65.5, 29.34, 29.3, 29.3, 29.1, 23.4, 23.3.

HR-ESI-MS (+ve): *m/z* = 699.3293 $[M + H]^+$ calc. for $C_{41}H_{43}N_6O_5$ 699.3289.

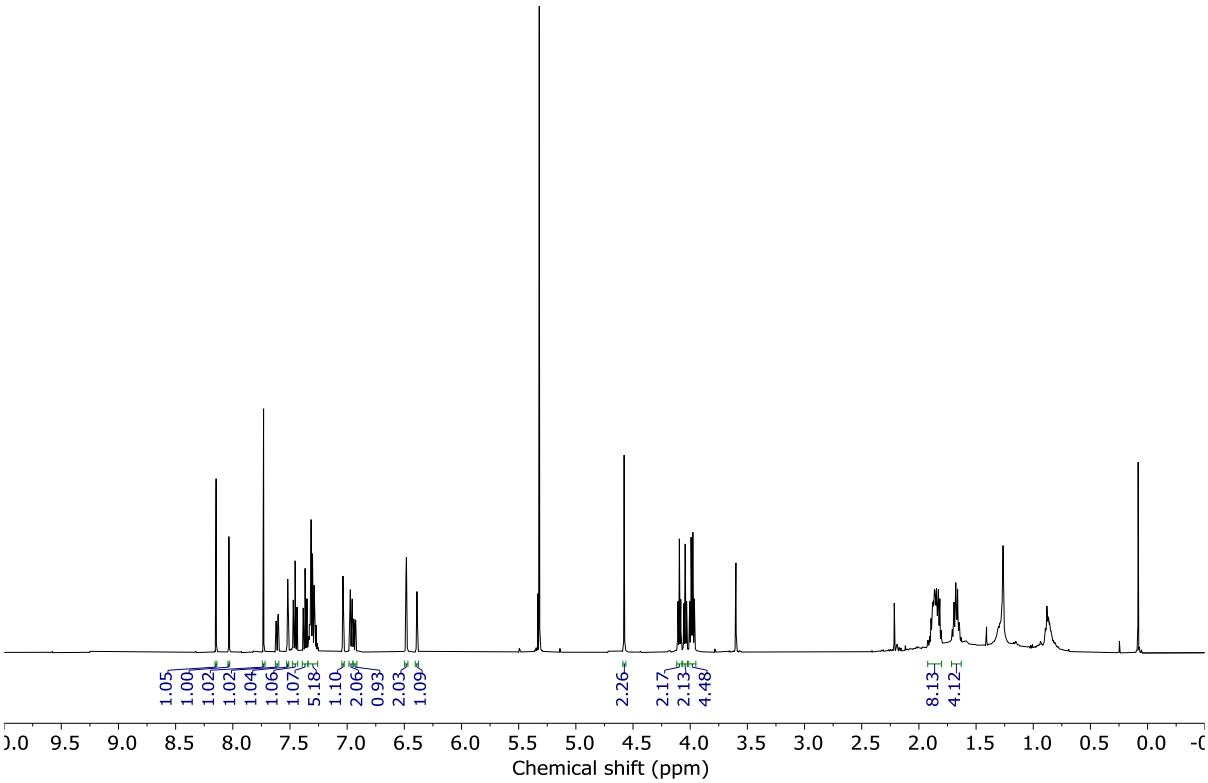

Figure S119: ^{1}H NMR (CD_2Cl_2, 500 MHz, 298 K) of **S19**.

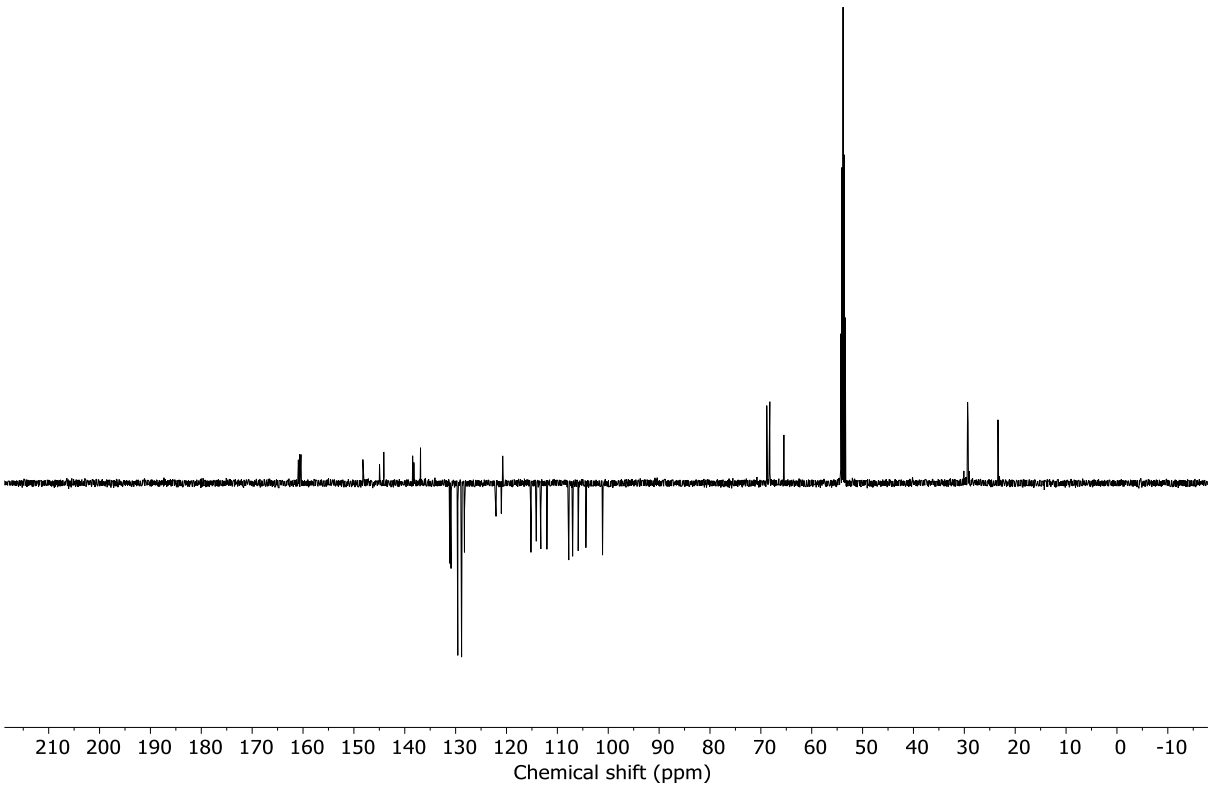

Figure S120: JMOD NMR (CD_2Cl_2, 126 MHz, 298 K) of **S19**.

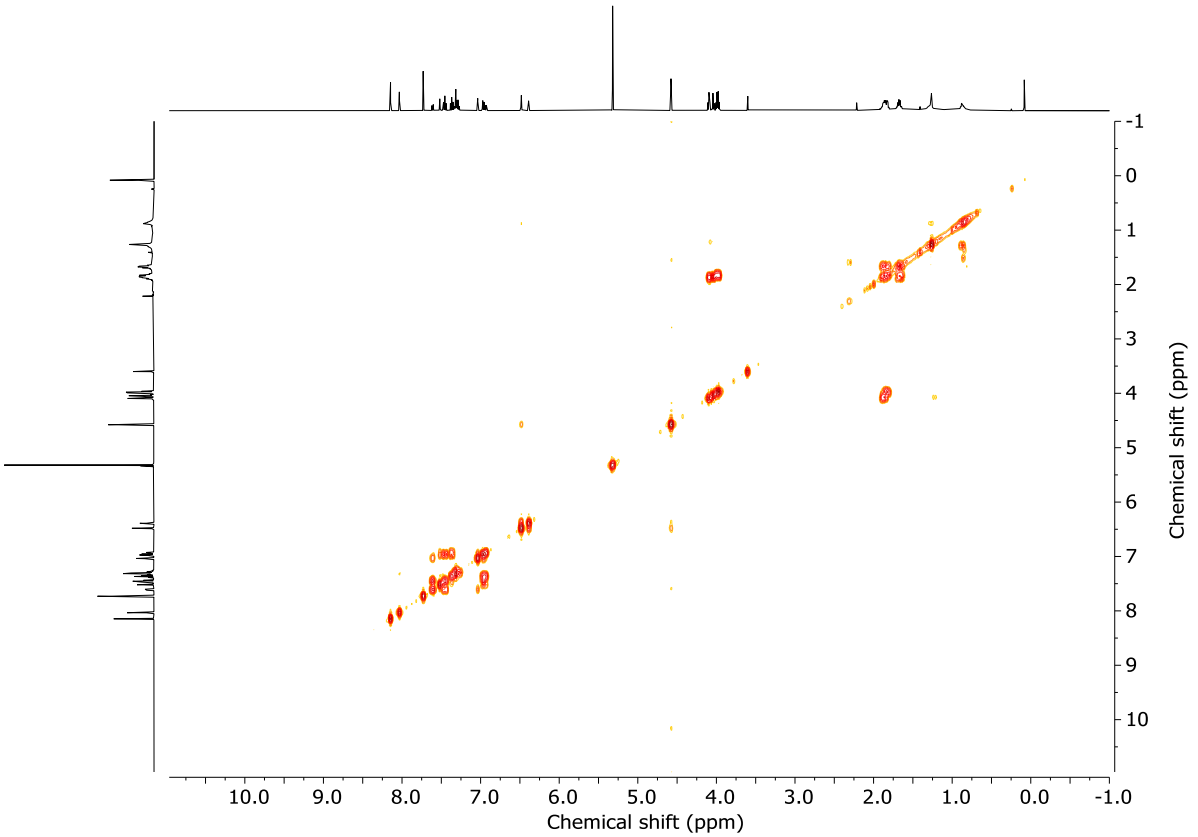

Figure S121: COSY NMR (CD_2Cl_2, 298 K) of **S19**.

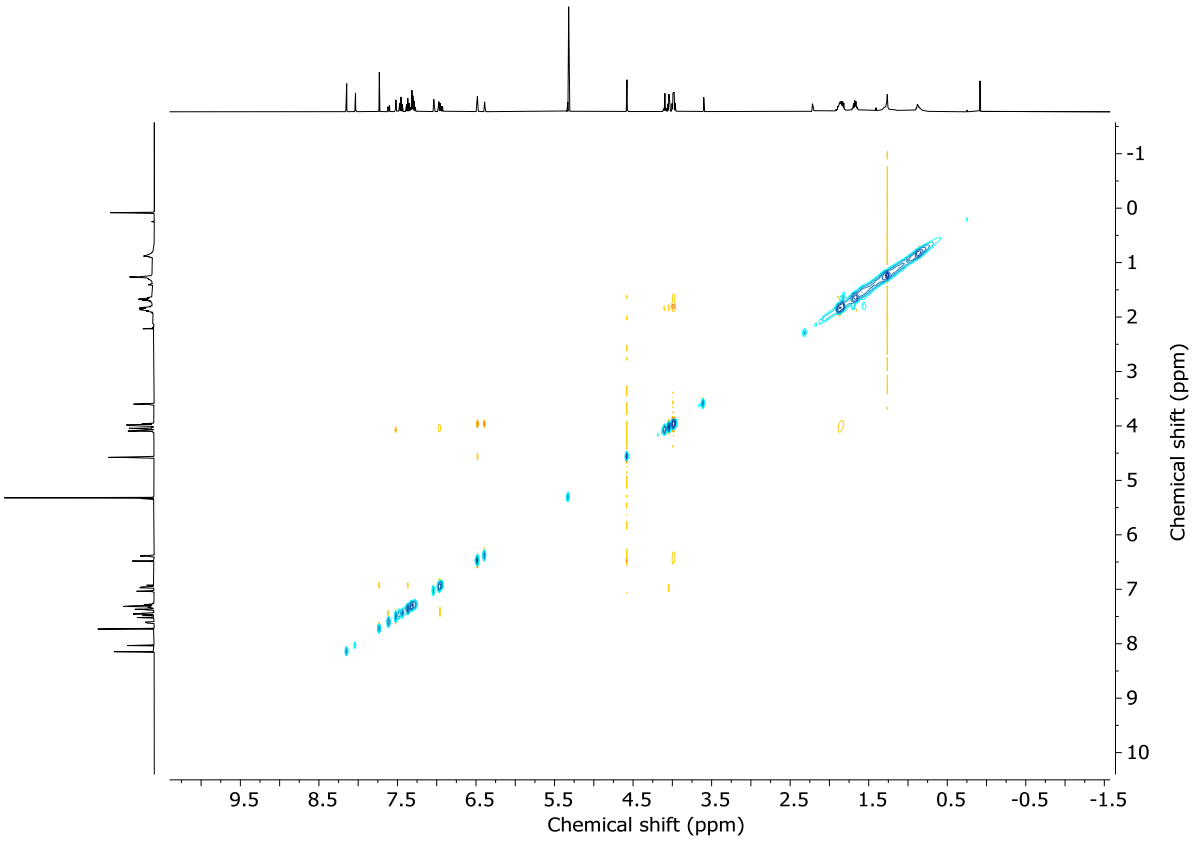

Figure S122: NOESY NMR (CD_2Cl_2, 298 K) of **S19**.

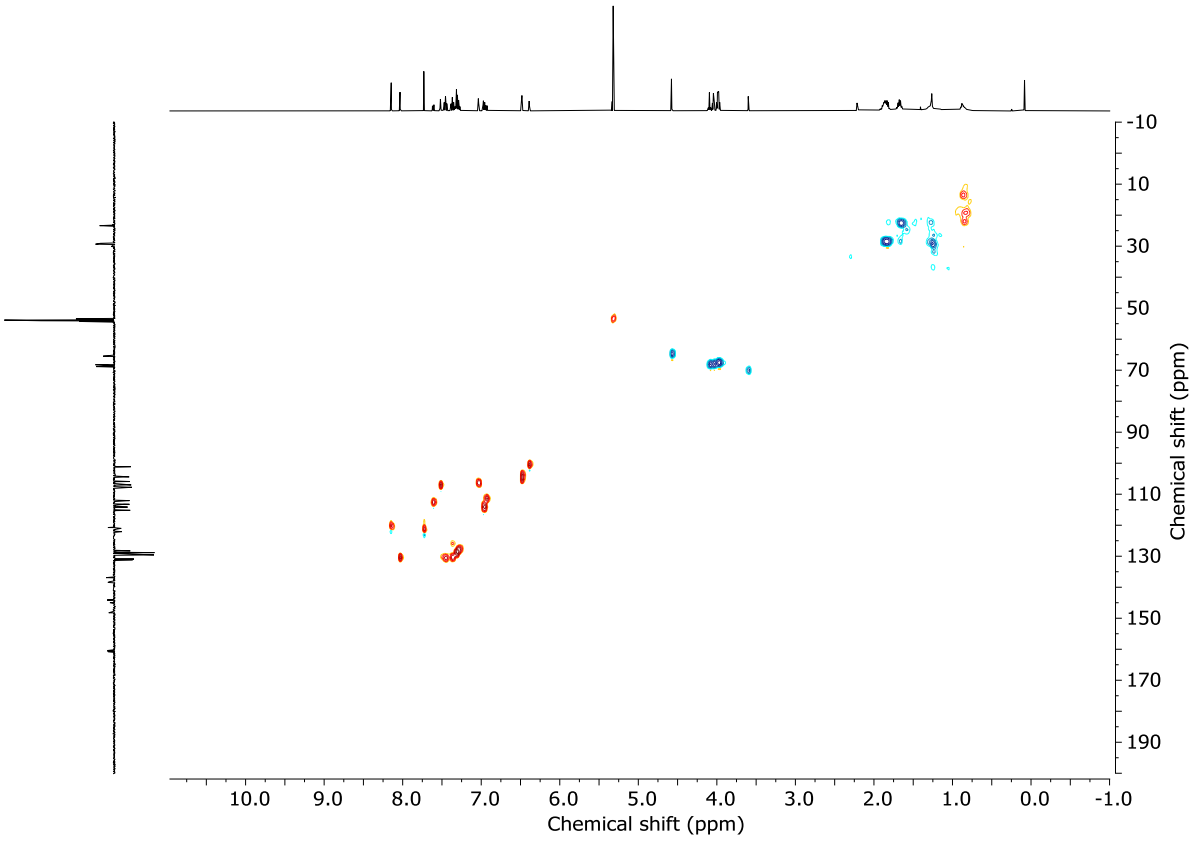

Figure S123: HSQC NMR (CD_2Cl_2, 298 K) of **S19**.

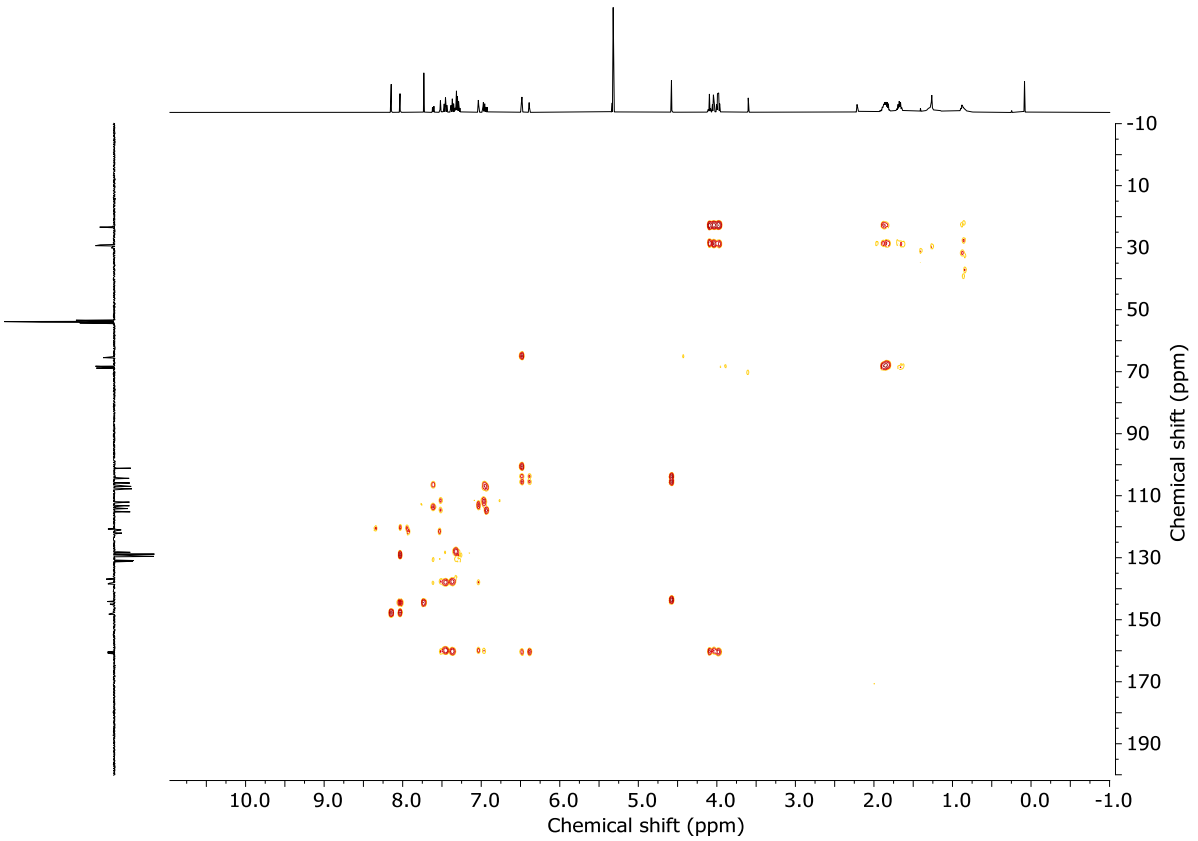

Figure S124: HMBC NMR (CD_2Cl_2, 298 K) of **S19**.

6. Co-Conformational Isomerism of Catenane 5

6.1. Co-Conformational Exchange Between ($E_{co\text{-}c}$)-5 and ($Z_{co\text{-}c}$)-5

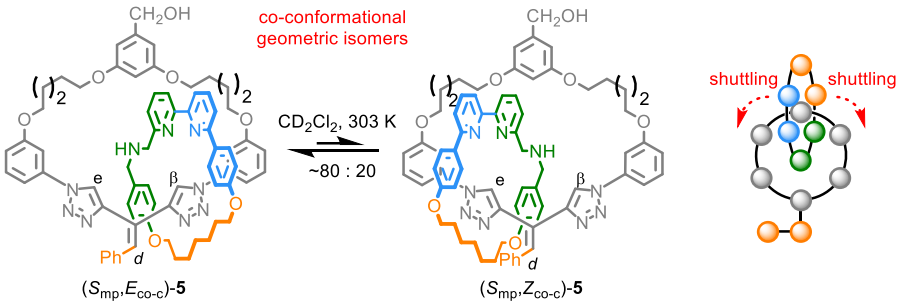

Scheme S4: Proposed co-conformational exchange process.

^{1}H NMR analysis of the as-synthesised samples of catenane **5** (*e.g.*, Figure S125a) revealed a single set of signals that could be assigned to a single co-conformational isomer of the product. This was assigned as the $E_{co\text{-}c}$ isomer on the basis of the solid-state structure of catenane **4**. However, on standing at rt overnight in CD_2Cl_2, additional signals consistent with catenane **5** appeared (Figure S125b), which suggested the appearance of the $Z_{co\text{-}c}$ co-conformational isomer in slow exchange with the as-synthesised $E_{co\text{-}c}$ isomer (Figure S125).

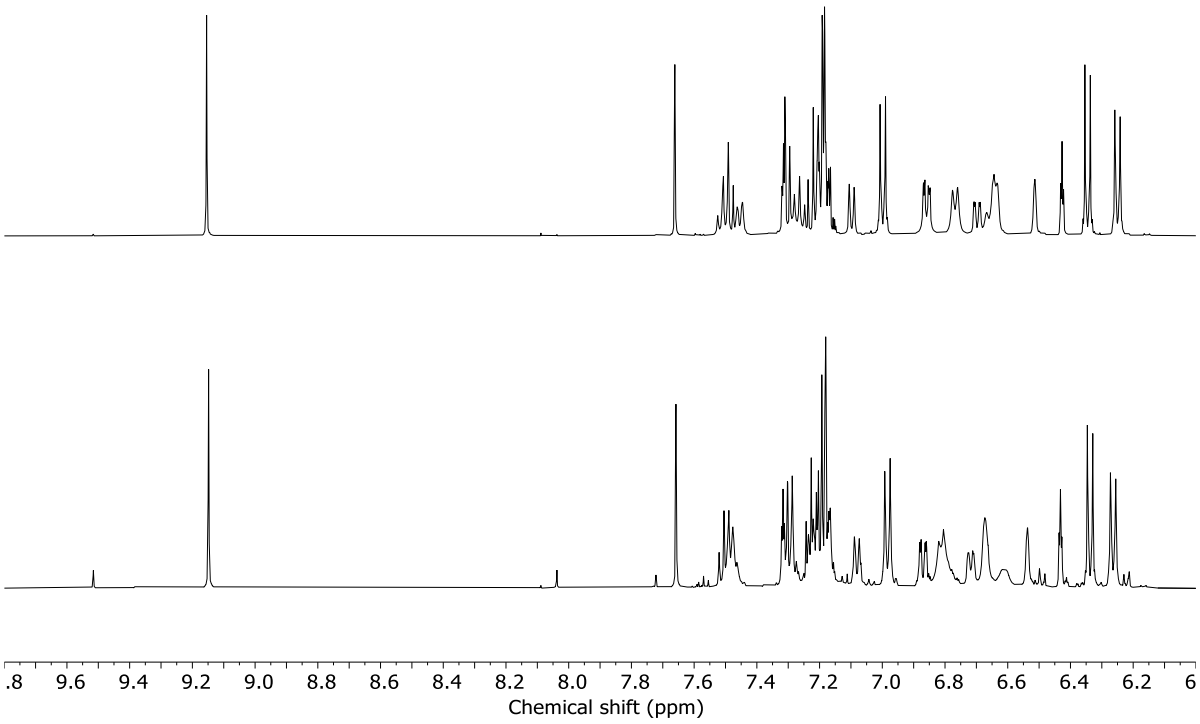

Figure S125: ^{1}H NMR (CD_2Cl_2, 500 MHz, 298 K) of **5** (Top) t = 0 h after dissolution; (Bottom) t = 18.5 h after dissolution.

To monitor the isomerisation process more accurately, catenane (S_{mp})-**5** (3 mg) was dissolved in CD_2Cl_2 (0.6 mL) and transferred to an NMR tube, which was capped and further sealed with Parafilm. The ^{1}H NMR spectrum of the sample was recorded over 68 hours with the probe held at a constant temperature of 303 K, after which no further change was observed (Figure S126). The same experiment was repeated for (R_{mp})-**5** and *rac*-**5** with consistent results.

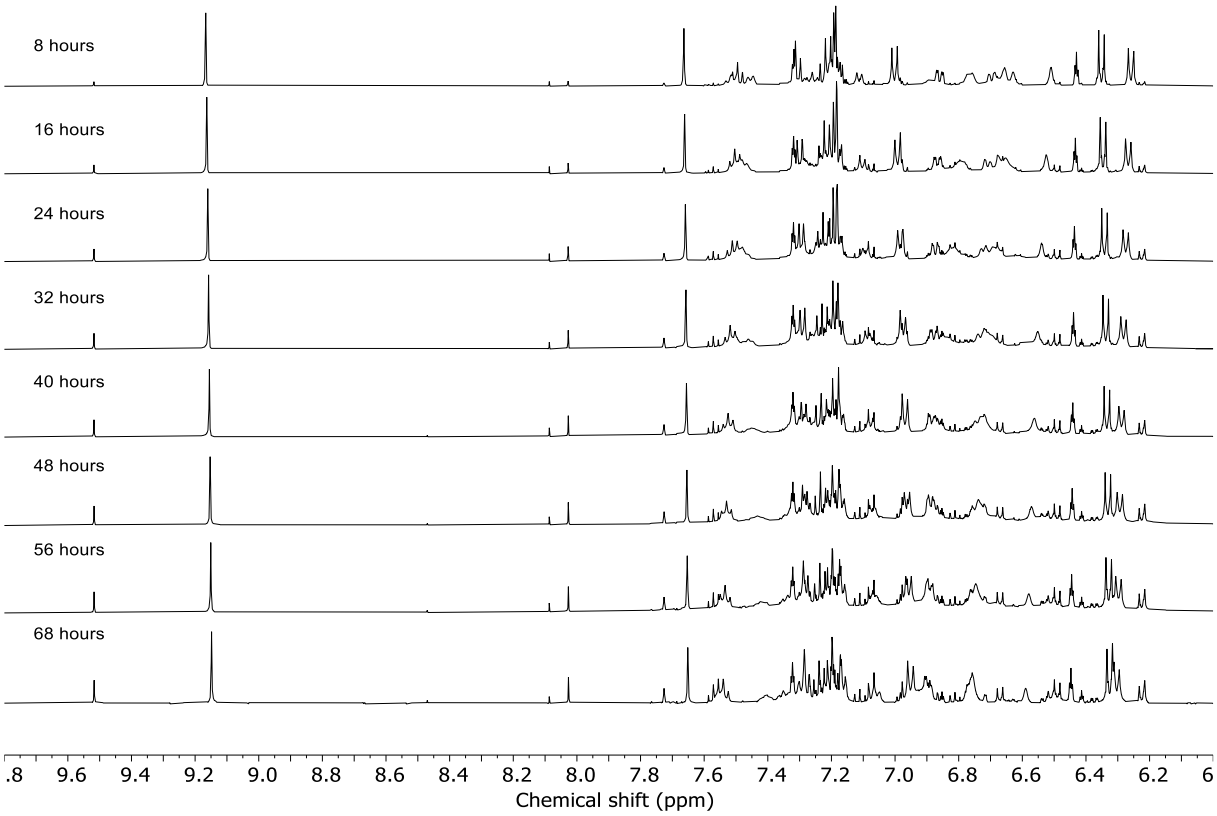

Figure S126: Stack plot of ^{1}H NMR (CD_2Cl_2, 500 MHz, 303 K) of (S_{mp})-**5** measured over 68 h.

We tentatively assigned the new signal that appears at 9.52 ppm (Figure S127) to H_e of ($Z_{co\text{-}c}$)-**5** on the basis of HSQC- and HMBC-NMR analysis (Figure S128). Similarly, the new signal observed at 7.73 ppm (Figure S127) can be tentatively assigned as H_d of ($Z_{co\text{-}c}$)-**5** (Figure S128). Both sets of signals allowed the ratio of ($E_{co\text{-}c}$)-**5** and ($Z_{co\text{-}c}$)-**5** at steady state to be assigned as approximately 4 : 1 (Figure S127). We note that, although there is evidence of decomposition (additional small signals similar to catenane **5**), LC-MS analysis confirmed that catenane **5** remained intact (no non-interlocked macrocycles or fragments thereof were observed).

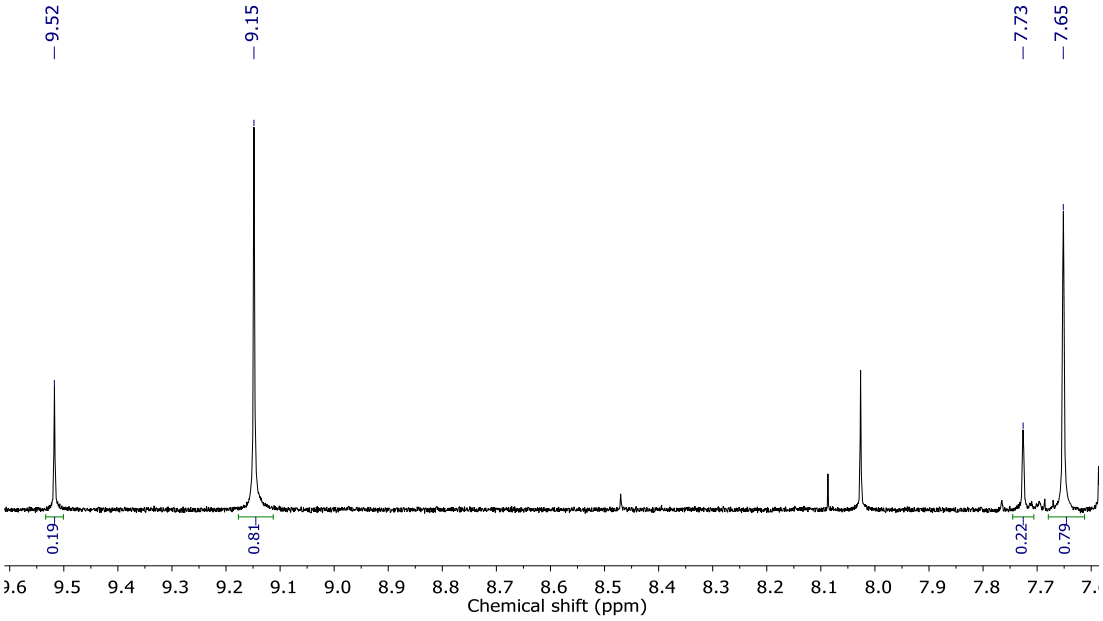

Figure S127: Example of ^{1}H NMR (CD_2Cl_2, 500 MHz, 303 K) of (S_{mp})-**5** measured 68 h after dissolution.

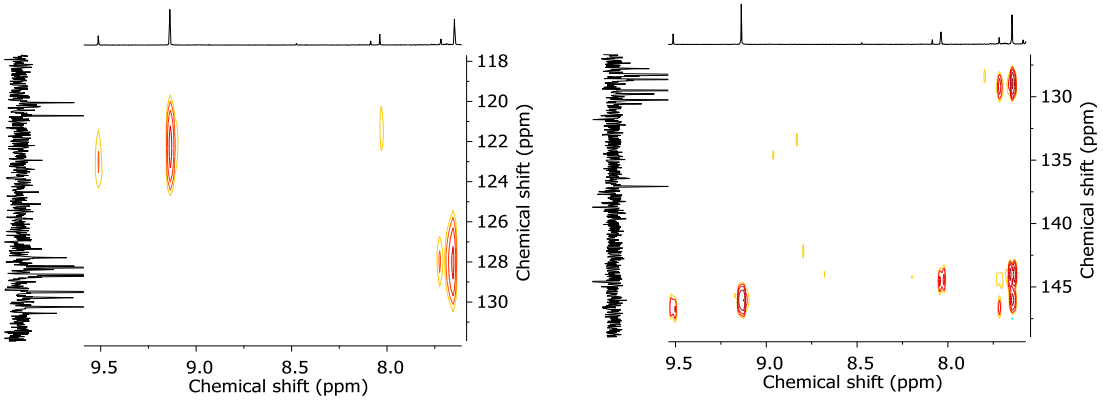

Figure S128: Partial HSQC-NMR (left) and HMBC-NMR (right) (CD_2Cl_2, 298 K) spectra of the mixture obtained by heating catenane **5** at 303 K for 68 h demonstrating that the pairs of signals at 9.52 and 9.15 ppm correlate to the same ^{13}C signals, consistent their assignment as H_e of ($Z_{co\text{-}c}$)-**5** and H_β of ($E_{co\text{-}c}$)-**5** respectively. Similarly, the signals at 7.73 and 7.65 ppm correlate with the same ^{13}C, consistent with their assignment as H_d of ($Z_{co\text{-}c}$)-**5** and ($E_{co\text{-}c}$)-**5** respectively.

Further evidence for the assignment of the new species observed by ^{1}H NMR as the $Z_{co\text{-}c}$ isomer of **5** was obtained by CSP-HPLC. Analysis of the samples of (S_{mp})-**5** and (R_{mp})-**5** that had been heated until a steady state was achieved revealed a new minor peak with the same value of m/z as observed for the as-synthesised catenane but different retention times in each enantiomeric samples. Furthermore, the heated sample of rac-**5** revealed the appearance of two new minor peaks that correspond to the two new minor peaks observed in the enantiomeric products. We note that the ratio of ($E_{co\text{-}c}$)-**5** and ($Z_{co\text{-}c}$)-**5** obtained by CSP-HPLC analysis (9 : 1) differs from that obtained by ^{1}H NMR (80 : 20). However, these measurements were conducted under very different conditions (solvent, temperature, presence of base in the case of the CSP-HPLC), which will affect both the rate of co-conformational isomerisation and position of the co-conformational equilibrium itself. We also note that although the UV-vis extinction coefficients of enantiomers are necessarily identical, those of diastereomers are not (although they are expected to be similar). Thus, uncalibrated CSP-HPLC is not accurate for assessment of ratios and so we choose to rely on ^{1}H NMR analysis for the determination of ($E_{co\text{-}c}$)-**5** and ($Z_{co\text{-}c}$)-**5**, which is quantitative.

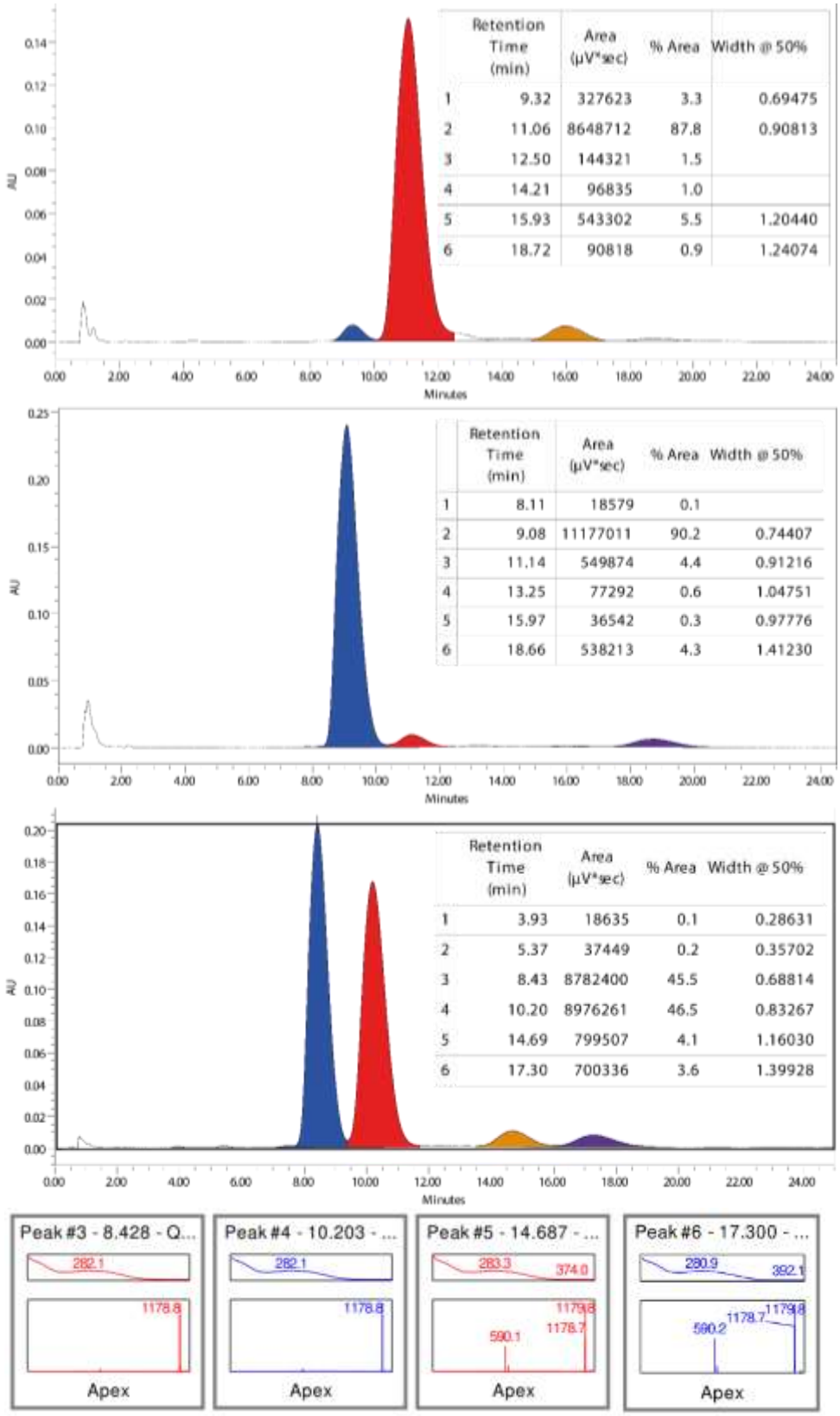

Figure S129: CSP-HPLC (loaded in Et_2O, Chiralpak IK, 40 ˚C, 125 BarG, isocratic 50 : 50 MeOH : CO_2 [0.1% v/v NH_3], 4 mL.min^{-1}, 1 mL injected) of (S_{mp})-**5** (top), (R_{mp})-**5** (middle) and *rac*-**5** (bottom) after heating at 30 ℃ showing the appearance of new peaks (15.95, 18.66, and 14.69 and 17.30 min respectively) which contain species with same m/z as the major isomer (larger peaks) of (*E*)-**5** (example MS spectra included at bottom for *rac*-**5**).

CSP-HPLC analysis also indicated that the enantiopurity of (S_{mp})-**5** and (R_{mp})-**5** was reduced after heating (93% and 91% *ee* respectively based on the peaks assigned as $E_{co\text{-}c}$) compared to the as-synthesised compounds (both 98% *ee*). This suggests that catenane **5** undergoes a slow racemisation process under these conditions, which is consistent with double bond isomerisation. This could also account for the appearance of the $Z_{co\text{-}c}$ isomer, although the appearance of the enantiomer of $E_{co\text{-}c}$, as observed by CSP-HPLC requires both double bond isomerism and co-conformational exchange (see section 5 for a more detailed discussion). Furthermore, the degree of co-conformational exchange is much larger than the degree of racemisation, suggesting that although double bond isomerisation could account for the appearance of the $Z_{co\text{-}c}$ isomer, it cannot be the dominant process.

To unambiguously demonstrate that macrocycle **S20** can shuttle over the benzylic alcohol moiety (*i.e.*, that ($E_{co\text{-}c}$)-**5** and ($Z_{co\text{-}c}$)-**5** can exchange by shuttling) we synthesised pseudo-rotaxane *rac*-(*E*)-**S29**, which, as expected disassembled slowly under the same conditions (Figure S130). Although signals corresponding to the non-interlocked axle clearly appear during the disassembly process, those corresponding to non-interlocked macrocycle **S20** were not observed. Filtration of the sample over K_2CO_3 revealed the expected mixture of axle (*E*)-**S32** and macrocycle **S20**, suggesting that, as with catenane **5**, solvent decomposition to produce acidic biproducts takes place under these conditions.

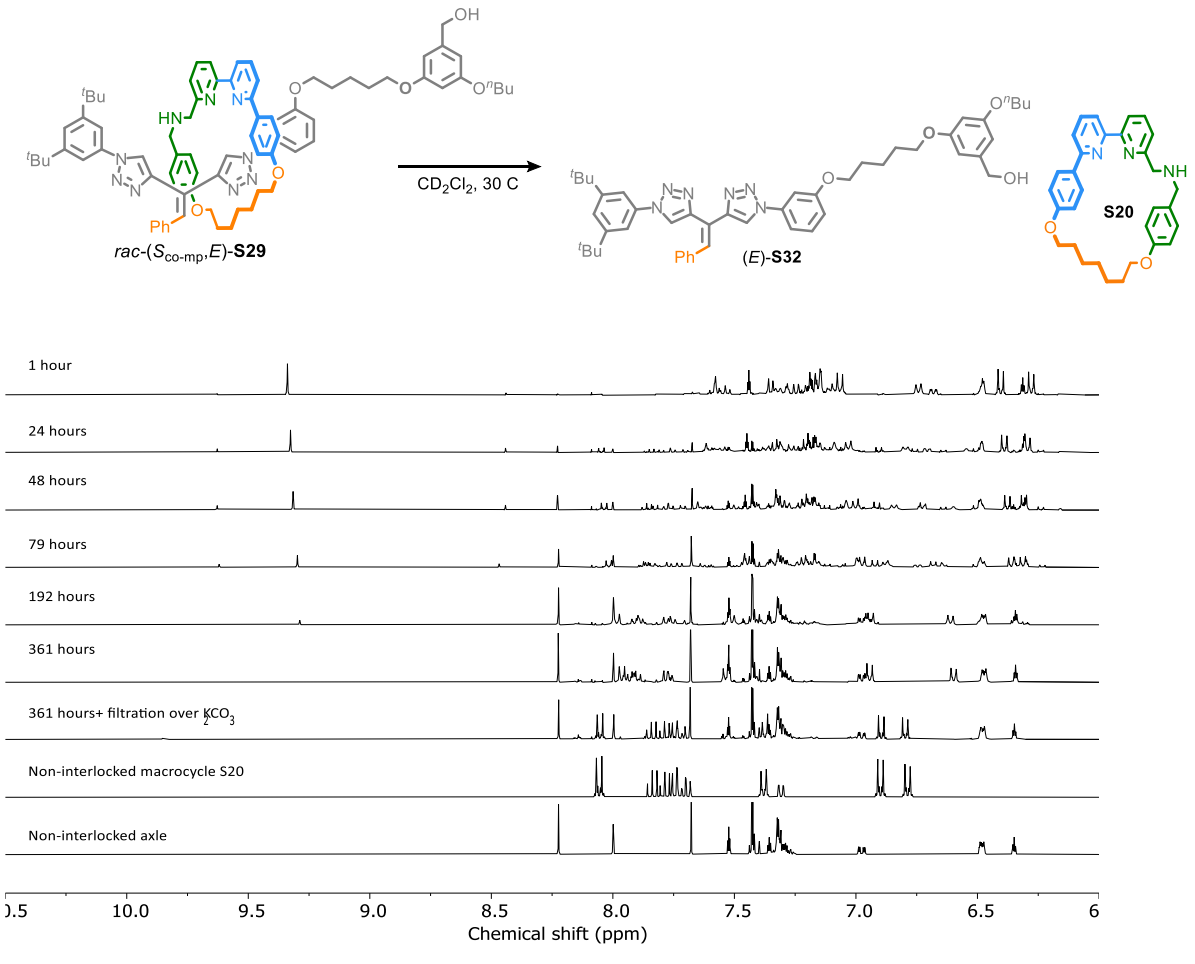

Figure S130: a. Disassembly process of pseudo-rotaxane *rac*-(*E*)-**S29**. b. Stack plot of ^{1}H NMR (CD_2Cl_2, 500 MHz, 303 K) of the reaction mixture containing pseudo-rotaxane *rac*-**S29** at the time points indicated, after filtration over K_2CO_3 and the corresponding non-interlocked components.

6.2. Compounds leading to pseudo-rotaxane *rac*-(*E*)-S29

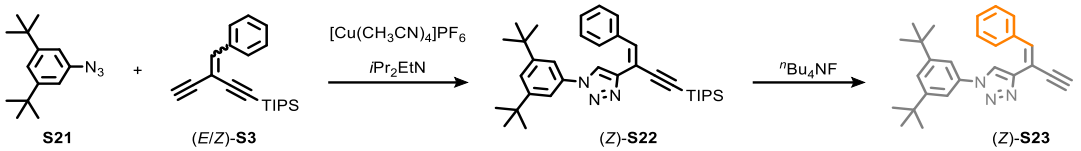

Scheme S5: Synthetic route to compound (*Z*)-**S23**.

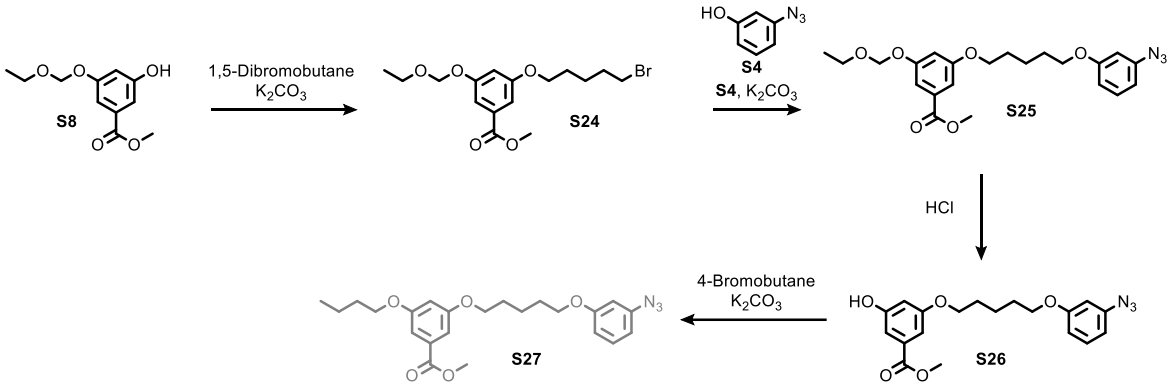

Scheme S6: Synthetic route to compound **S26**.

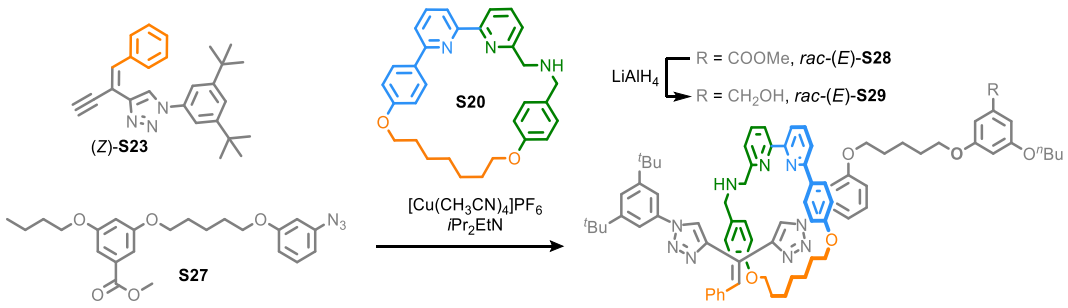

Scheme S7: Synthetic route to compound rac-(*E*)-**S29**.

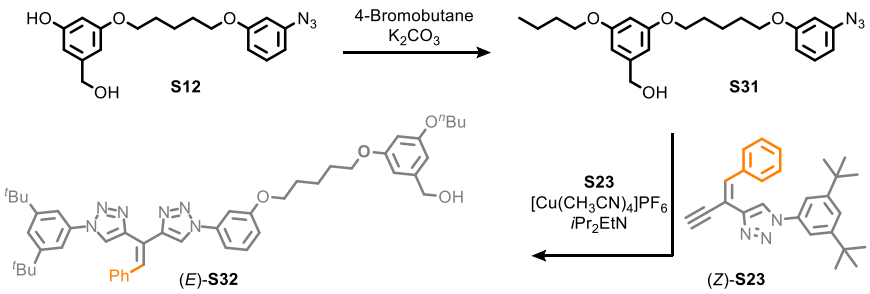

Scheme S8: Synthetic route to compound (*E*)-**S32**.

Triazole S22

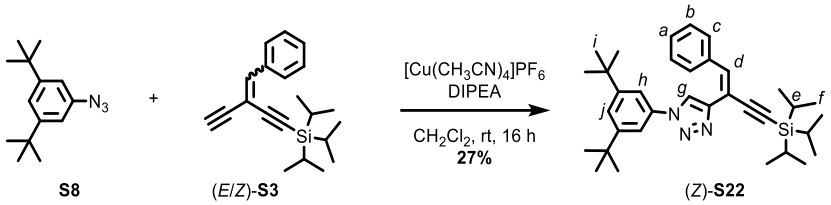

To a solution of (*E*/*Z*)-**S3** (349 mg, 1.13 mmol), azide **S8** (267 mg, 1.15 mmol), $[Cu(CH_3CN)_4]PF_6$ (103 mg, 0.276 mmol) in CH_2Cl_2 (6 mL) was added DIPEA (1.5 mL, 8.9 mmol). The solution was stirred for 16 h at rt, then diluted with CH_2Cl_2 (50 mL), washed with EDTA-NH_3 solution (0.1 M, 30 mL), and the aqueous phase extracted with CH_2Cl_2 (3 x 40 mL). The combined organic phases were dried ($MgSO_4$) and concentrated *in vacuo*. Chromatography (petrol-CH_2Cl_2 100:0 to 4:6) afforded (*Z*)-**S22** as a yellow oil (167 mg, 27%).

^{1}H NMR (400 MHz, $CDCl_3$) δ_H 7.87 (s, 1H, $\boldsymbol{H}_g$), 7.54-7.50 (m, 2H, $\boldsymbol{H}_c$), 7.49 (s, 3H, $\boldsymbol{H}_h$, $\boldsymbol{H}_j$), 7.35-7.25 (m, 3H, $\boldsymbol{H}_a$, $\boldsymbol{H}_b$), 7.22 (s, 1H, $\boldsymbol{H}_d$), 1.37 (s, 18H, $\boldsymbol{H}_i$), 1.19-1.15 (m, 21H, $\boldsymbol{H}_e$, $\boldsymbol{H}_f$).

^{13}C NMR (101 MHz, $CDCl_3$) δ 153.0, 145.2, 139.1, 136.7, 136.0, 129.6, 128.5, 128.3, 123.0, 121.8, 115.2, 113.3, 108.3, 90.6, 35.3, 31.4, 18.9, 11.5.

HR-ESI-MS (+ve): m/z = 540.3764 $[M + H]^+$ (calc. for $C_{35}H_{50}N_3Si$ 530.3769).

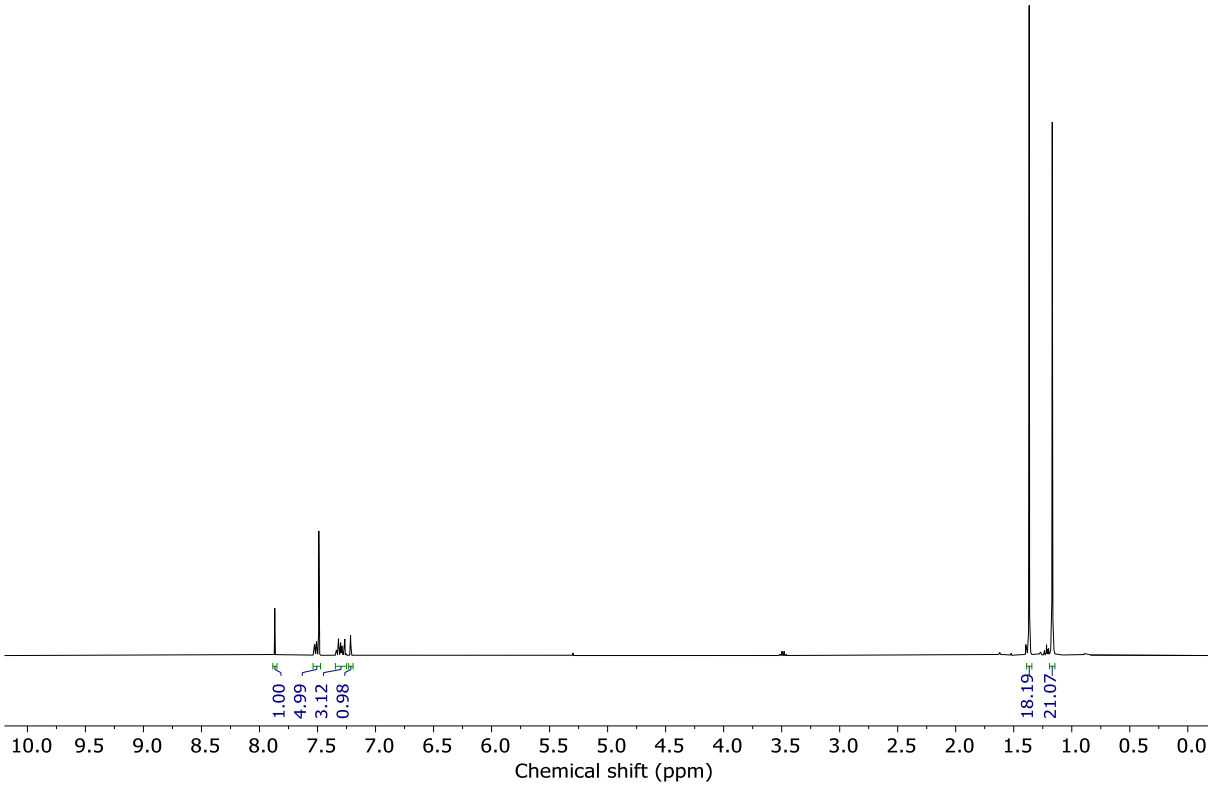

Figure S131: ^{1}H NMR ($CDCl_3$, 400 MHz, 298 K) of (*Z*)-**S22**.

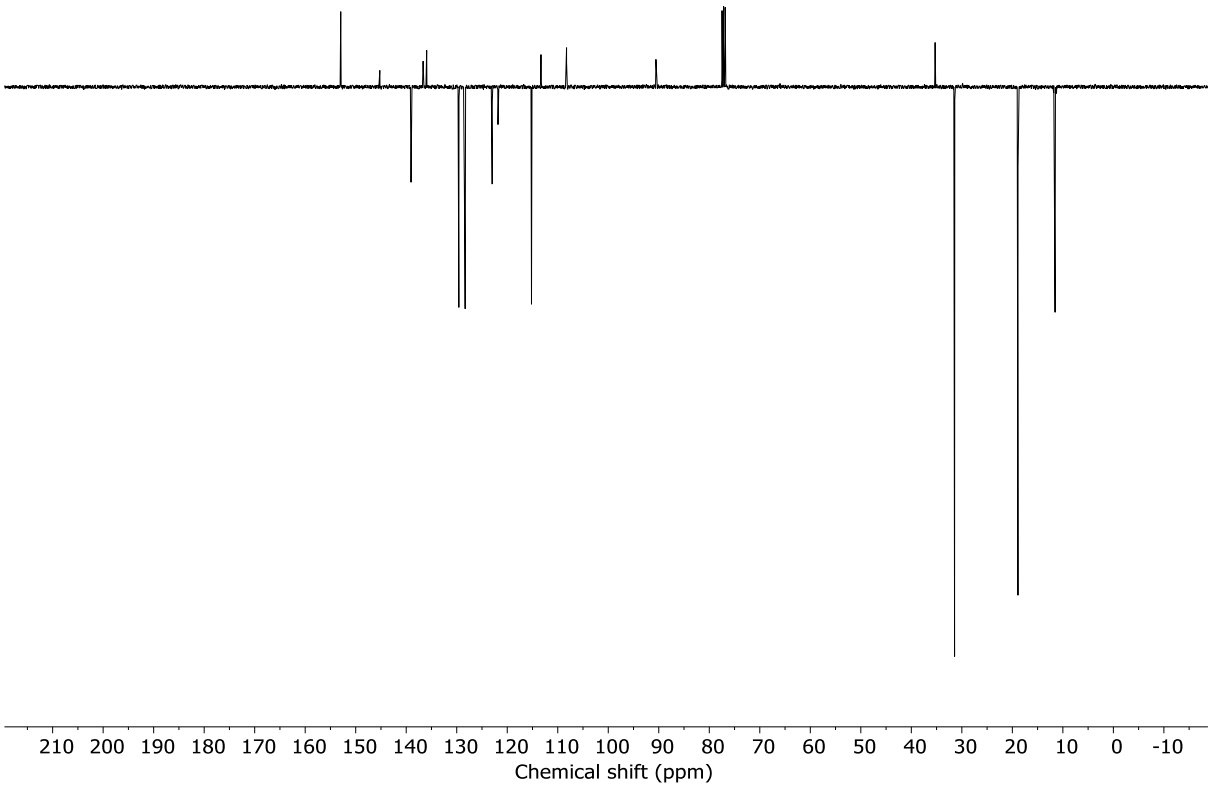

Figure S132: JMOD NMR ($CDCl_3$, 101 MHz, 298 K) of (*Z*)-**S22**.

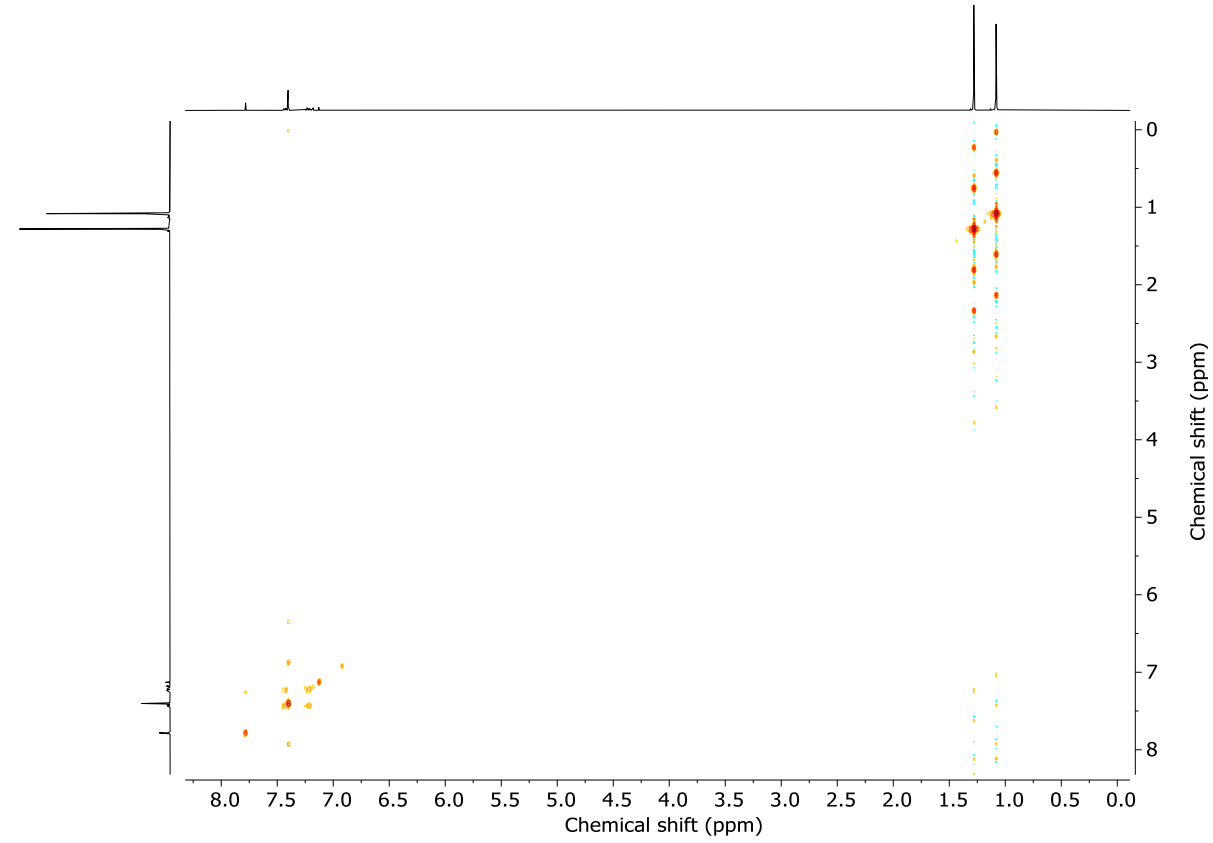

Figure S133: COSY NMR ($CDCl_3$, 298 K) of (*Z*)-**S22**.

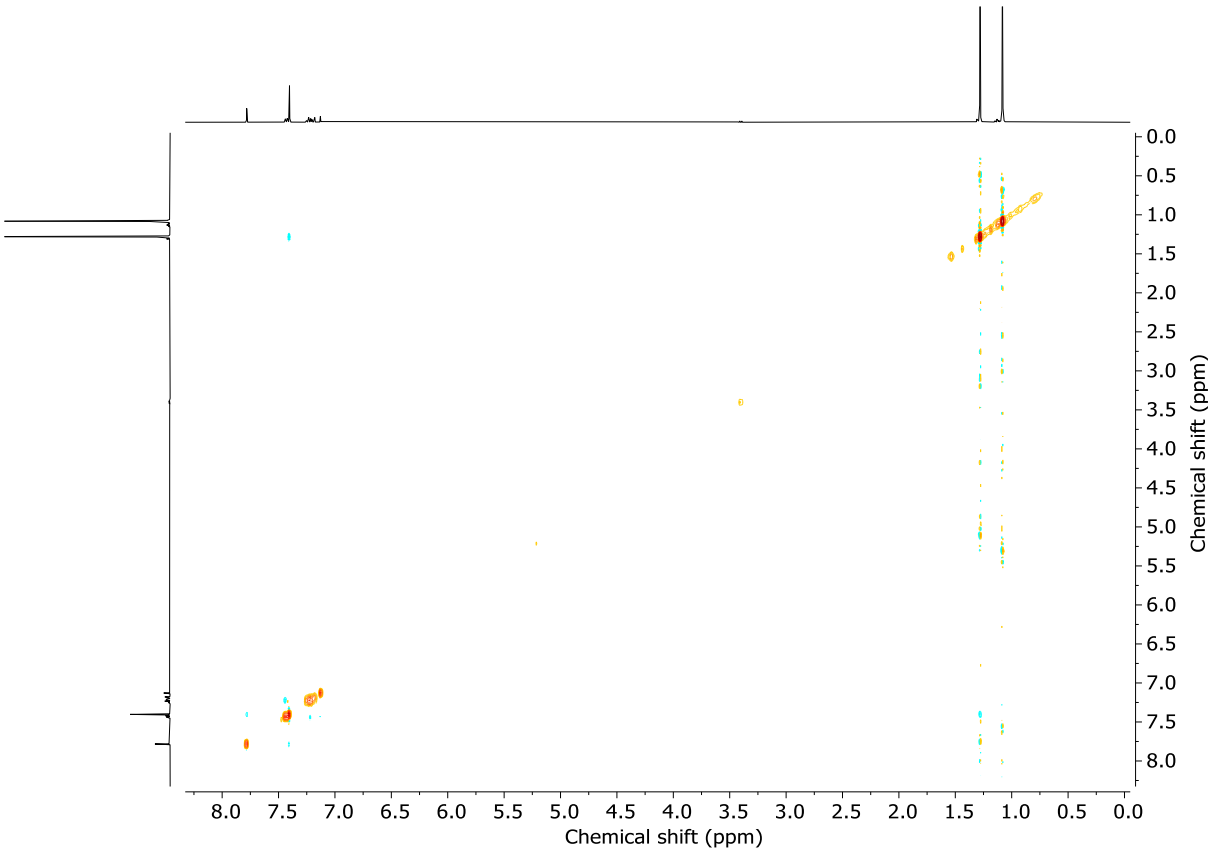

Figure S134: NOESY NMR ($CDCl_3$, 298 K) of (*Z*)-**S22**.

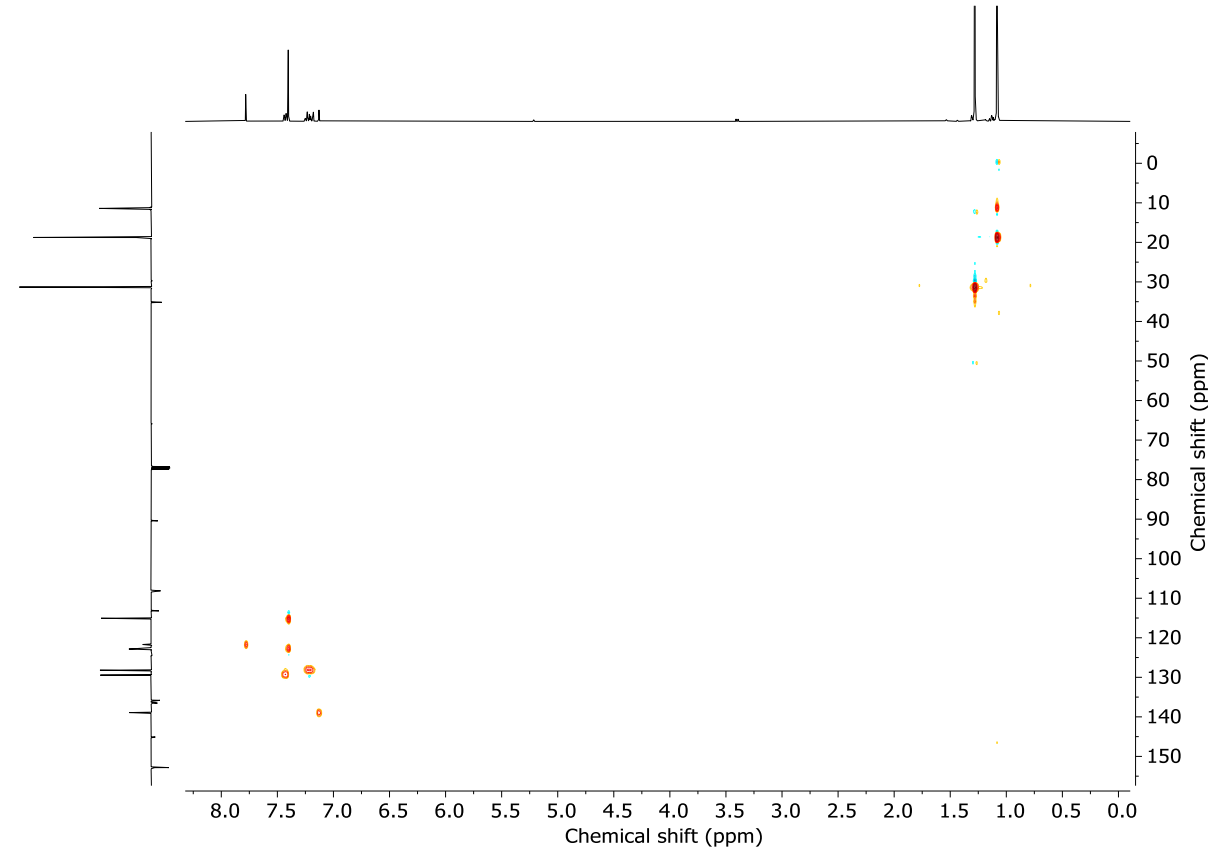

Figure S135: HSQC NMR ($CDCl_3$, 298 K) of (*Z*)-**S22**.

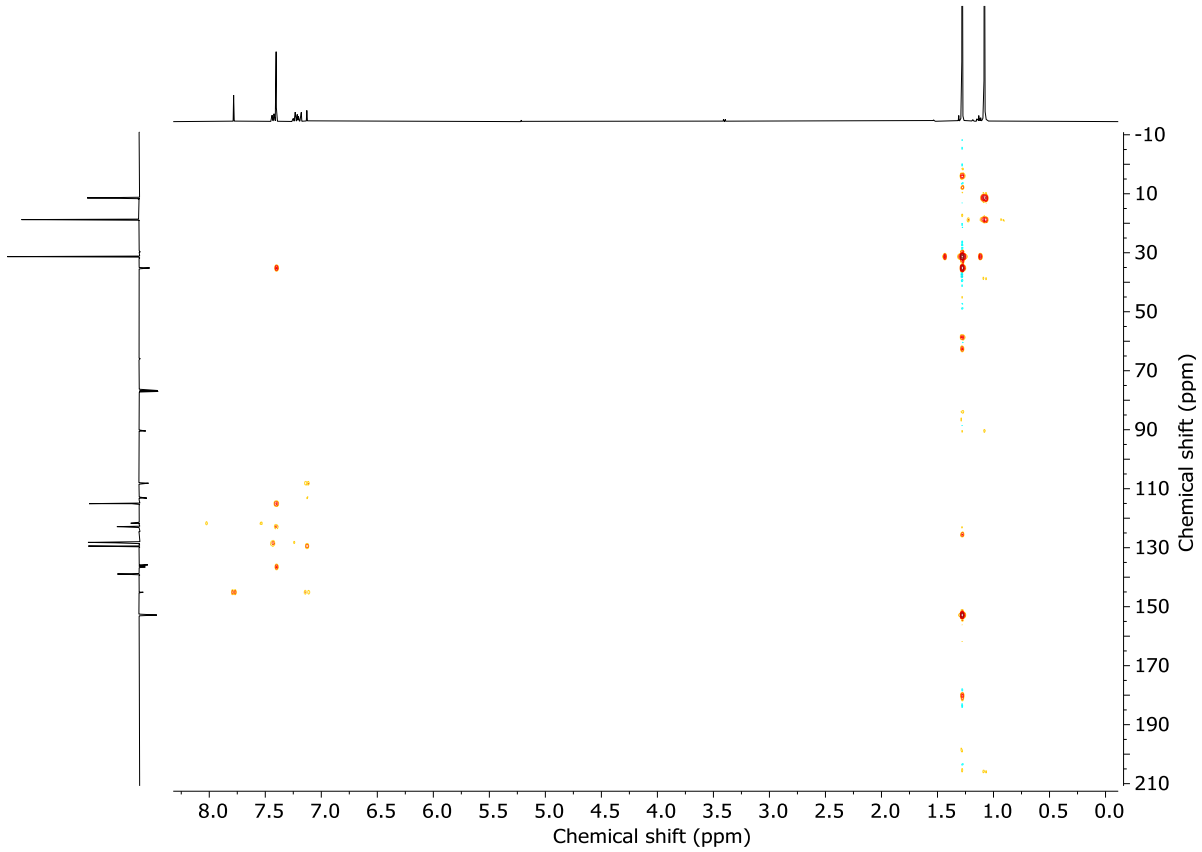

Figure S136: HMBC NMR ($CDCl_3$, 298 K) of (*Z*)-**S22**.

Alkyne S23

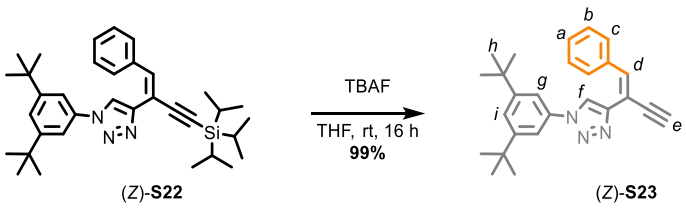

To a stirred solution of (*Z*)-**S22** (68 mg, 0.13 mmol) in anhydrous THF (1.7 mL) was added TBAF (1 M in THF, 0.25 mL, 0.25 mmol) and the resulting solution stirred for 16 h at rt. Sat. $NH_4Cl_{(aq)}$ was added, and the aqueous phase was extracted with Et_2O (3 x 20 mL). The combined organic phases were dried ($MgSO_4$) and concentrated *in vacuo*. Chromatography (petrol-CH_2Cl_2 100:0 to 0:100) gave (*Z*)-**S23** as a yellow oil (48 mg, 99%).

^{1}H NMR (400 MHz, CD_2Cl_2) δ 7.75 (s, 1H, ***H***$_f$), 7.52 (t, *J* = 1.7, 1H, ***H***$_i$), 7.44 (d, *J* = 1.7, 2H, ***H***$_g$), 7.41 – 7.37 (m, 2H, ***H***$_c$), 7.35 – 7.27 (m, 3H, ***H***$_a$, ***H***$_b$, ***H***$_d$), 3.19 (d, *J* = 0.6, 1H, ***H***$_e$), 1.36 (s, 18H, ***H***$_h$).

^{13}C NMR (101 MHz, CD_2Cl_2) δ 153.3, 144.4, 140.4, 136.9, 136.2, 129.5, 128.9, 128.8, 123.6, 122.1, 115.8, 113.1, 84.6, 77.4, 35.5, 31.4.

HR-ESI-MS (+ve): m/z = 384.2438 $[M + H]^+$ calc. for $C_{26}H_{30}N_3$ 384.2434.

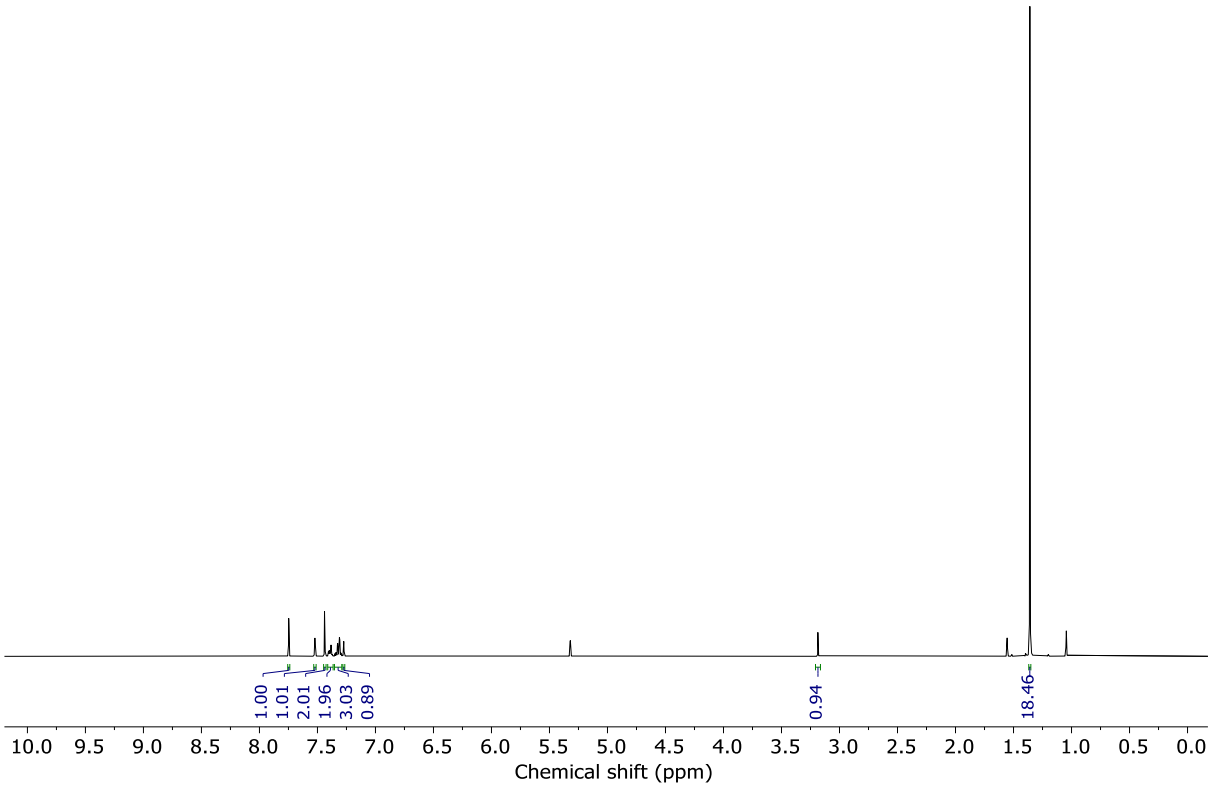

Figure S137: ^{1}H NMR (CD_2Cl_2, 400 MHz, 298 K) of (*Z*)-**S23**.

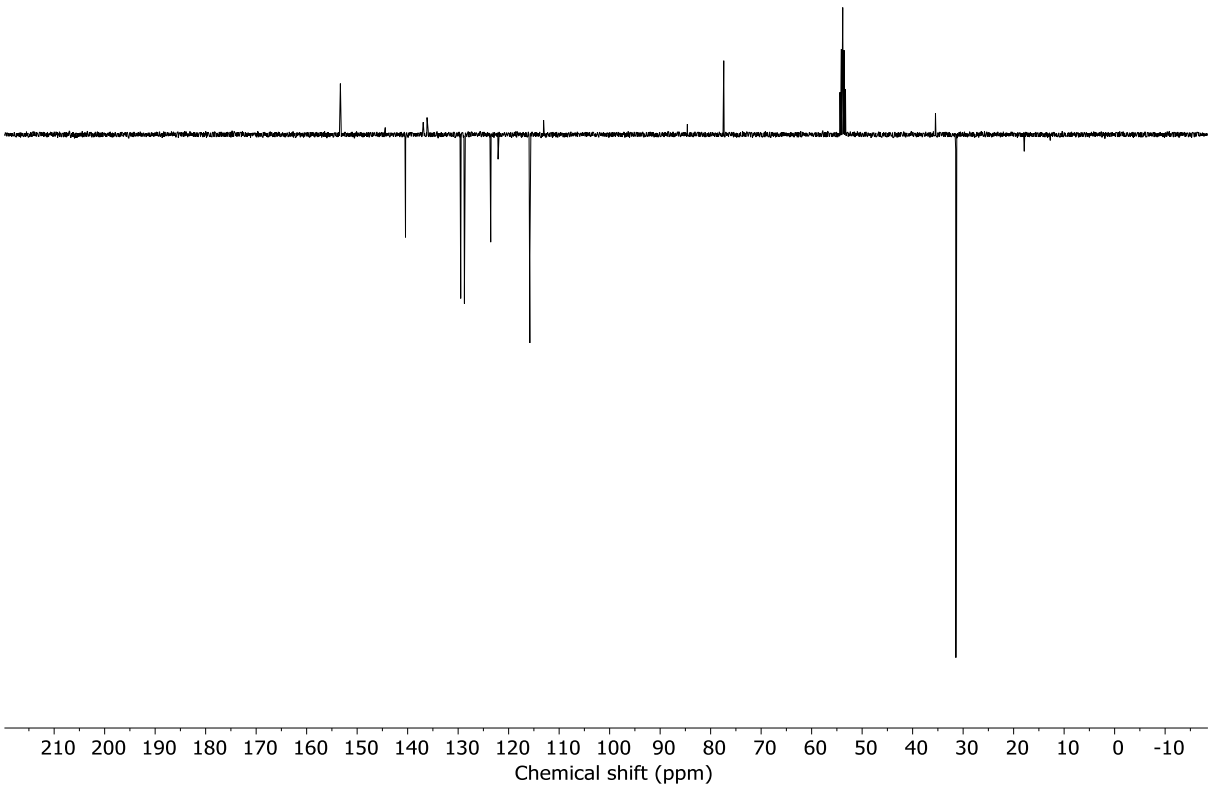

Figure S138: JMOD NMR (CD_2Cl_2, 101 MHz, 298 K) of (*Z*)-**S23**.

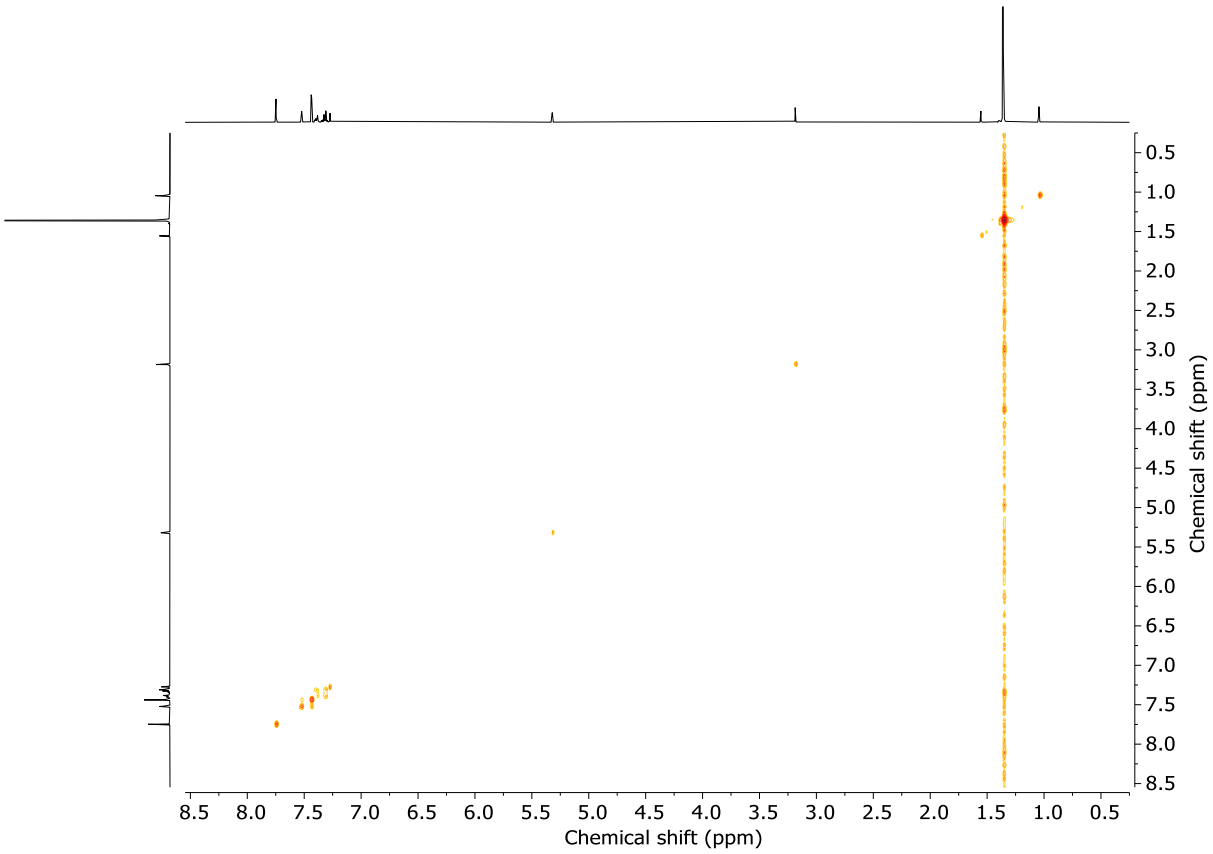

Figure S139: COSY NMR (CD_2Cl_2, 298 K) of (*Z*)-**S23**.

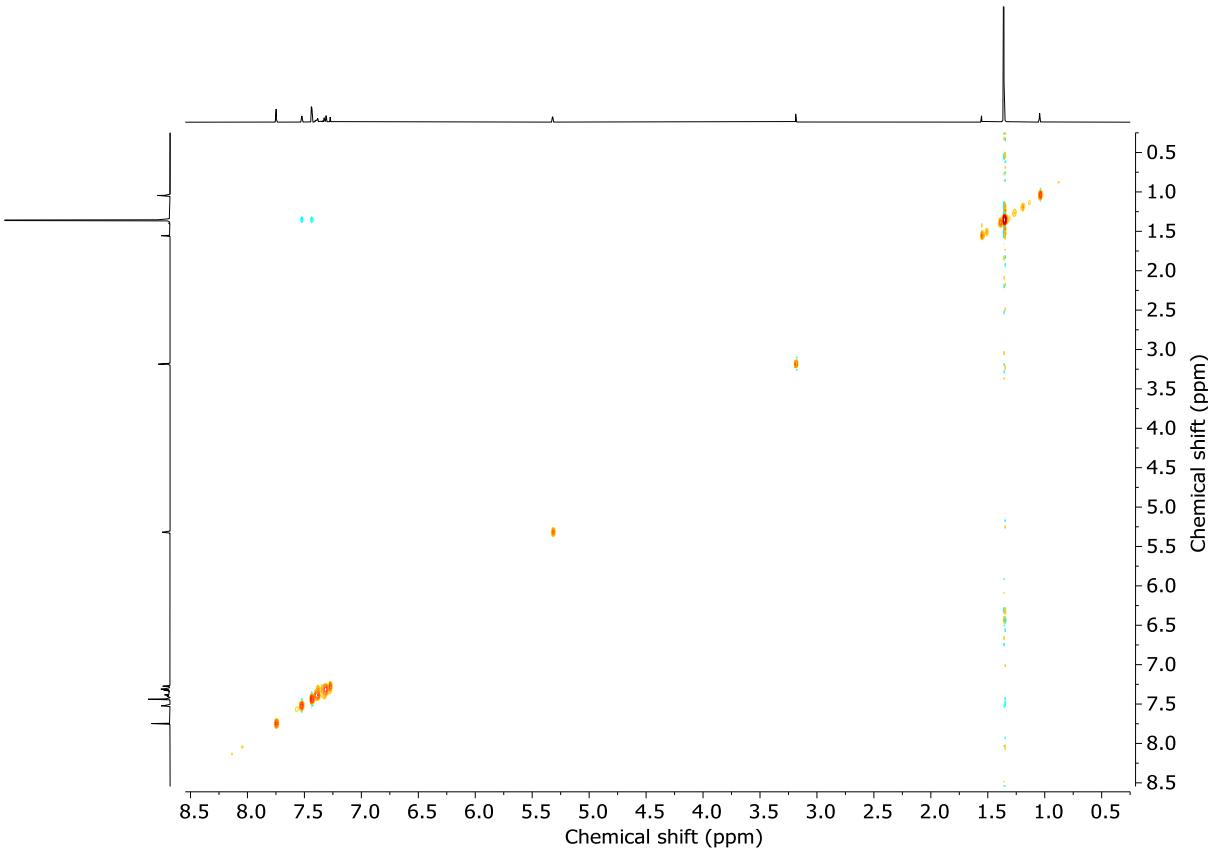

Figure S140: NOESY NMR (CD_2Cl_2, 298 K) of (*Z*)-**S23**.

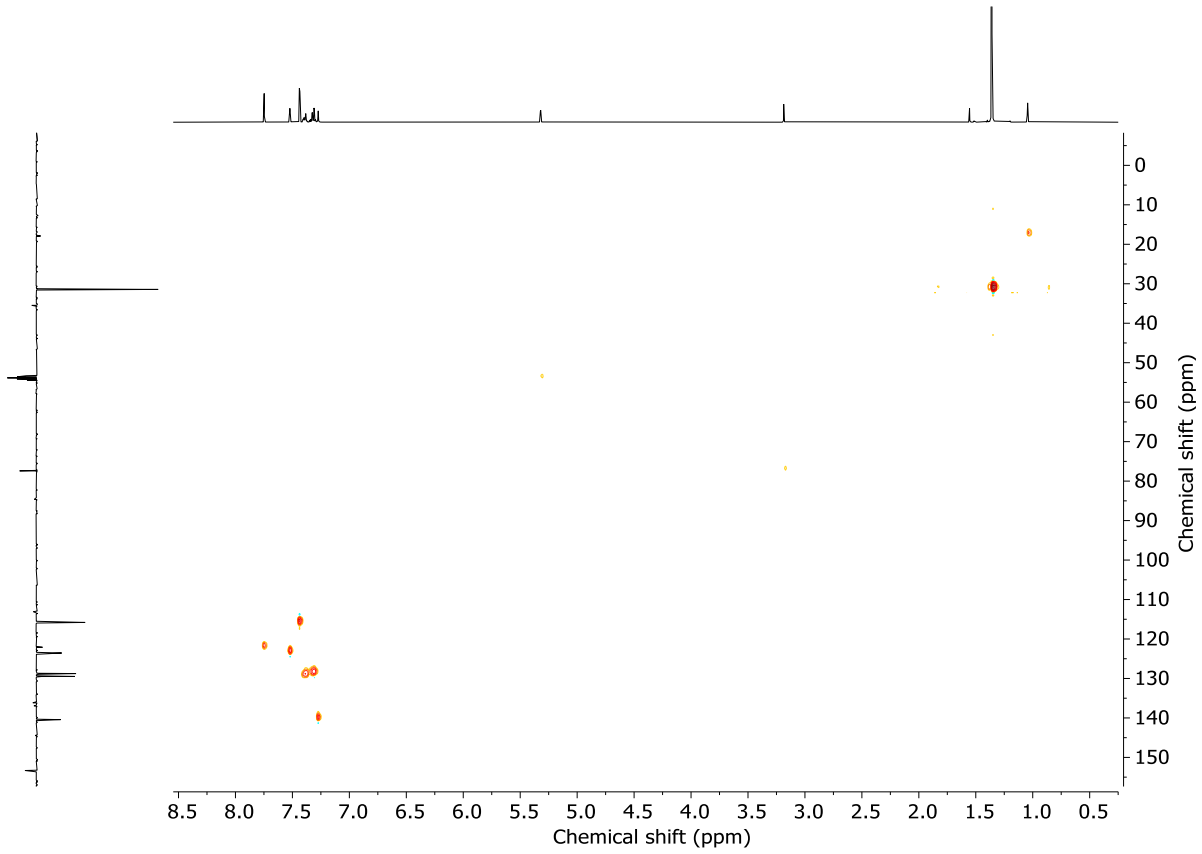

Figure S141: HSQC NMR (CD_2Cl_2, 298 K) of (*Z*)-**S23**.

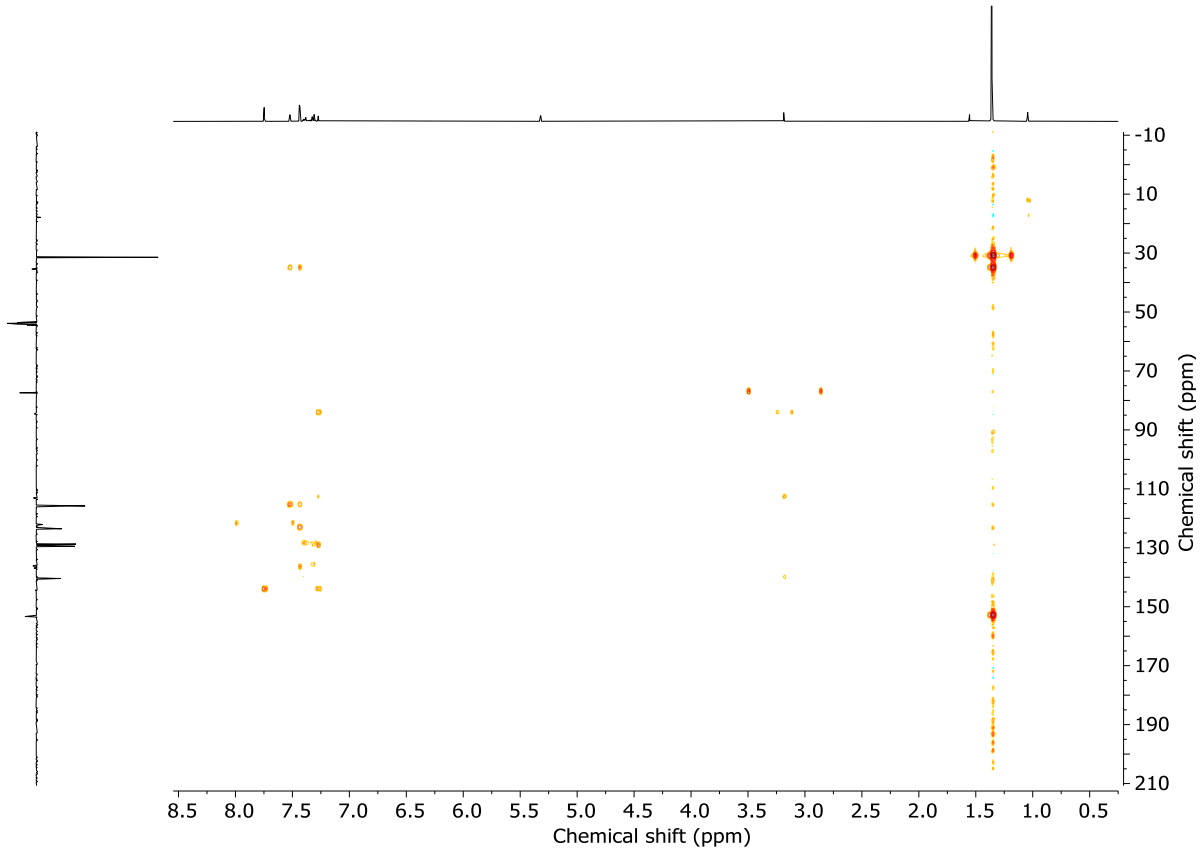

Figure S142: HMBC NMR (CD_2Cl_2, 298 K) of (*Z*)-**S23**.

Compound S24

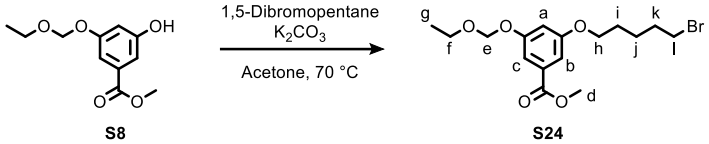

S8 **S24**

Phenol **S8** (93 mg, 0.41 mmol) and K_2CO_3 (0.28 g, 2.1 mmol) were suspended in acetone (4 mL). After 10 min of stirring at rt, 1,5-dibromopentane (0.17 mL, 1.2 mmol) was added and the reaction mixture was heated at 70 °C overnight. After being cooled at rt, the reaction mixture was filtered over Celite®, the solids washed with acetone and the filtrate concentrated *in vacuo*. Chromatography (petrol-Et_2O 100 : 0 to 7 : 3) afforded compound **S24** as a colorless oil (123 mg, 80%).

^{1}H NMR (400 MHz, $CDCl_3$) δ 7.30 (dd, *J* = 2.3, 1.3, 1H, H, H_c), 7.21 (dd, *J* = 2.4, 1.4, 1H, H_b), 6.78 (t, *J* = 2.3, 1H, H_a), 5.23 (s, 2H, H_e), 3.99 (t, *J* = 6.3, 2H, H_h), 3.90 (s, 3H, H_d), 3.73 (q, *J* = 7.1, 2H, H_f), 3.44 (t, *J* = 6.8, 2H, H_l), 1.94 (dq, *J* = 7.9, 6.8, 2H, H_k), 1.87 – 1.78 (m, 2H, H_i), 1.67 – 1.59 (m, 2H, H_j), 1.23 (t, *J* = 7.1, 3H, H_g).

^{13}C NMR (101 MHz, $CDCl_3$) δ 166.9, 160.1, 158.4, 132.2, 110.0, 108.6, 108.3, 93.3, 68.1, 64.6, 52.4, 33.7, 32.6, 28.5, 25.0, 15.3.

HR-ESI-MS (+ve): *m/z* = 397.0620 $[M + Na]^+$ calc. for $C_{16}H_{23}BrNaO_5$ 397.0621.

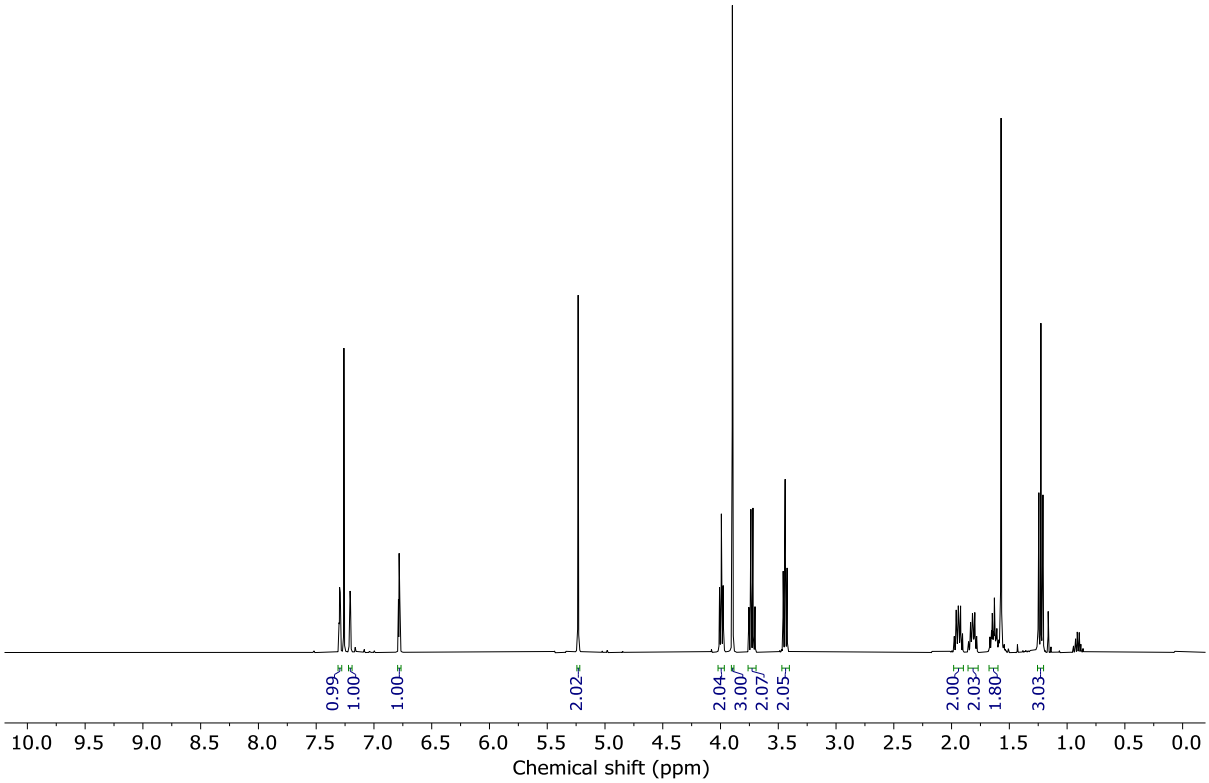

Figure S143: ^{1}H NMR ($CDCl_3$, 400 MHz, 298 K) of **S24**.

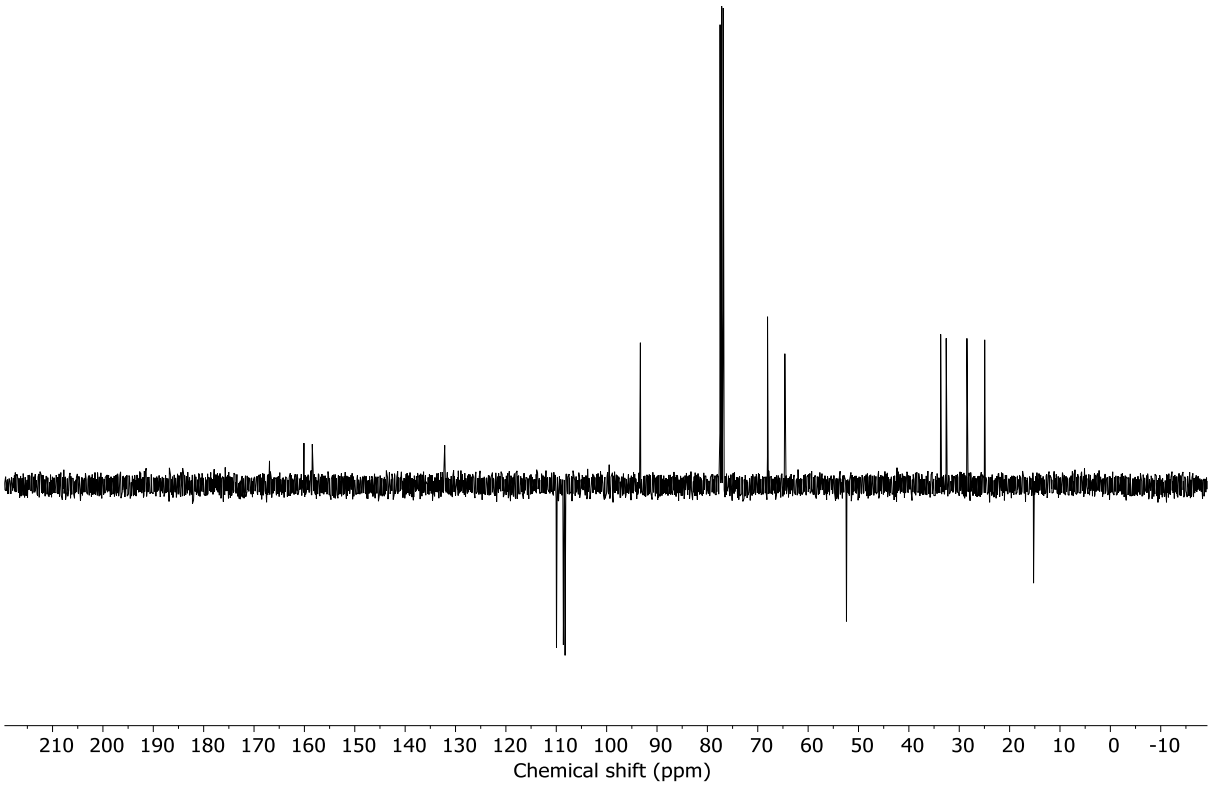

Figure S144: JMOD NMR ($CDCl_3$, 101 MHz, 298 K) of **S24.**

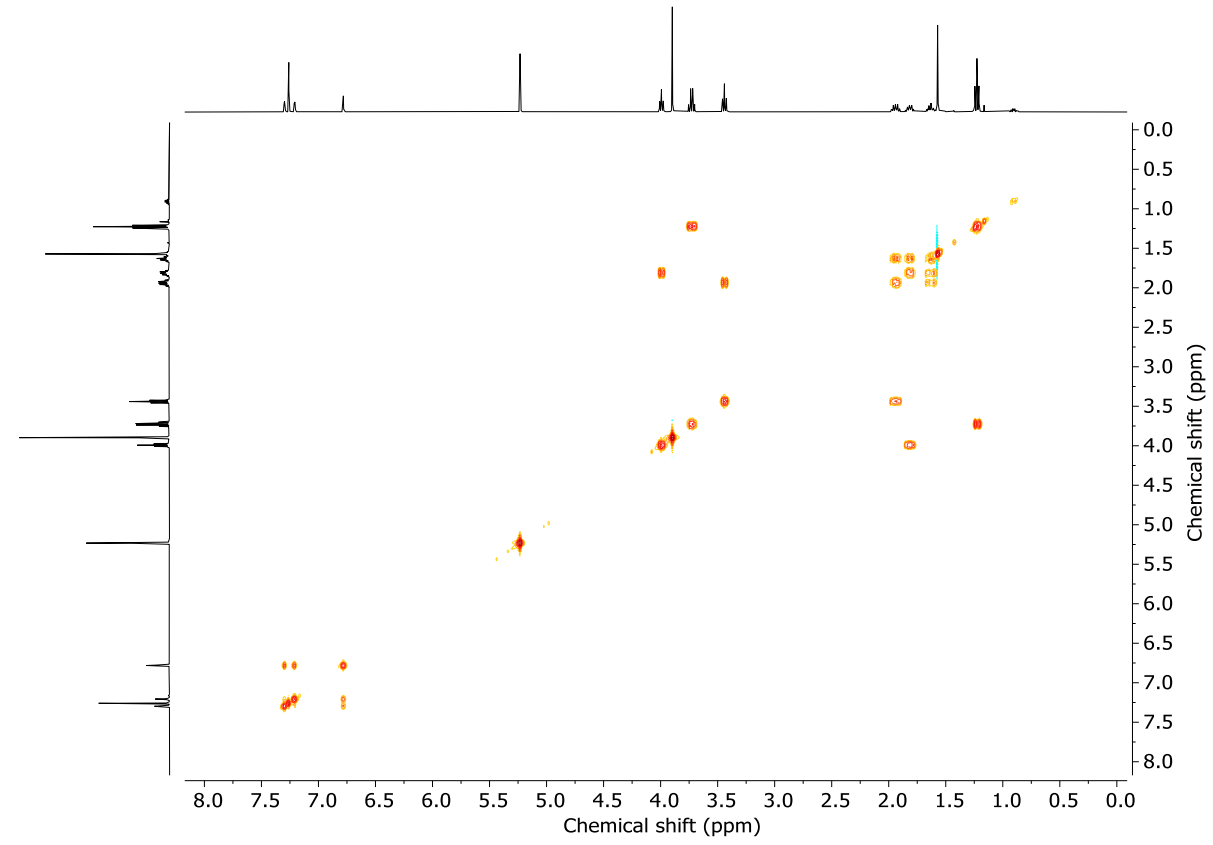

Figure S145: COSY NMR ($CDCl_3$, 298 K) of **S24.**

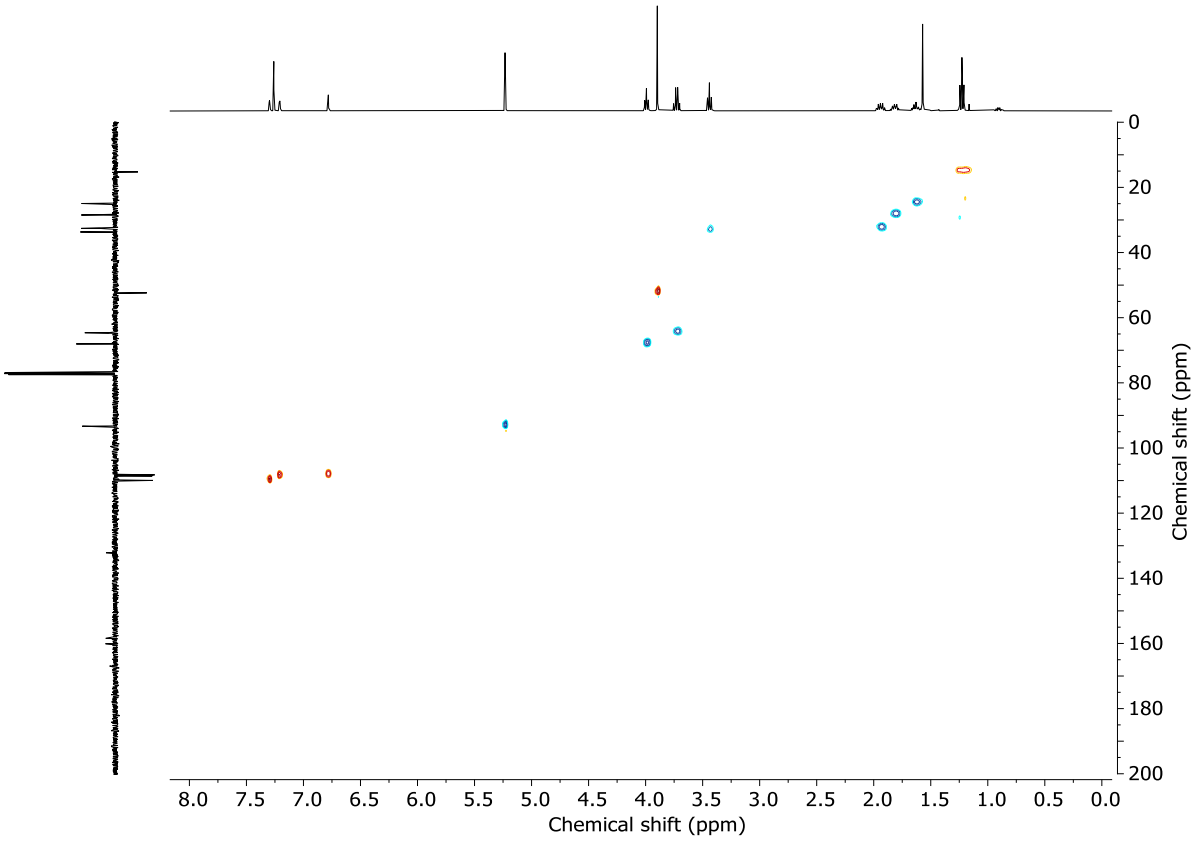

Figure S146: HSQC NMR ($CDCl_3$, 298 K) of **S24**.

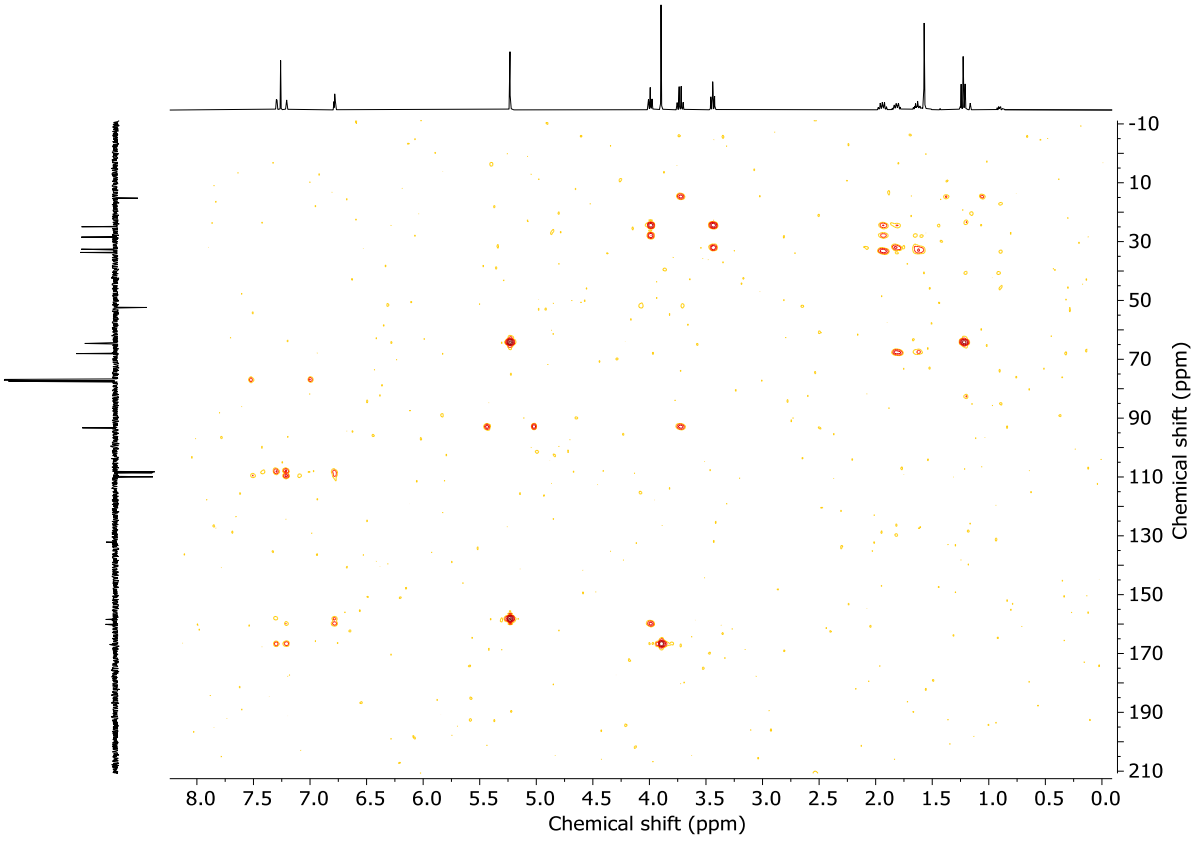

Figure S147: HMBC NMR ($CDCl_3$, 298 K) of **S24.**

Compound S26

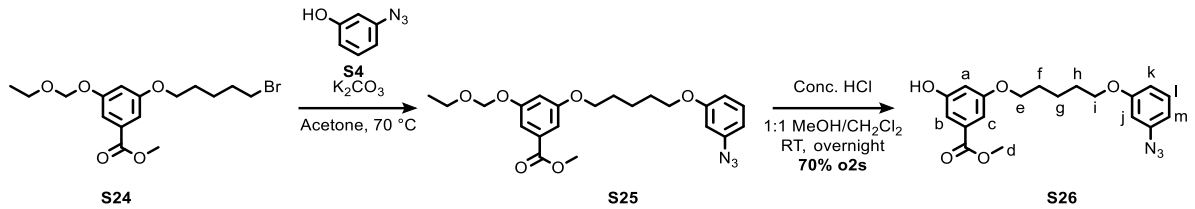

Phenol **S4** (49 mg, 0.37 mmol) was dissolved in acetone (0.5 mL) and K_2CO_3 (225 mg, 1.63 mmol) was added. After 5 min of stirring at rt, bromide **S24** (123 mg, 0.33 mmol), dissolved in acetone (2.5 mL), was added and the reaction mixture was heated at 70 °C overnight. After being cooled at rt, the reaction mixture was filtered over Celite®, the solids washed with acetone and the filtrate concentrated *in vacuo*. Chromatography (petrol-Et_2O 100 : 0 to 3 : 1) afforded compound **S25** which was contaminated with excess phenol **S4**.

This material was dissolved in 1:1 MeOH/CH_2Cl_2 (3 mL) and concentrated HCl (0.05 mL) was added. The reaction mixture was stirred overnight at rt. The reaction mixture was quenched with sat. $NaHCO_{3(aq)}$ (20 mL). The aqueous phase was extracted with CH_2Cl_2 (3 x 15 mL), the combined organic layers dried (Na_2SO_4), and concentrated *in vacuo*. Chromatography (petrol-Et_2O 100 : 0 to 6 : 4) gave **S26** as a yellow oil that solidified on standing over three days at rt (90.5 mg, 75%).

^{1}H NMR (400 MHz, $CDCl_3$) δ 7.24 (t, *J* = 8.2, 1H, H_l), 7.15 (dd, *J* = 2.3, 1.3, 1H, H_b), 7.10 (dd, *J* = 2.4, 1.3, 1H, H_c), 6.68 (ddd, *J* = 8.3, 2.4, 0.9, 1H, $H_{k\ or\ m}$), 6.63 (ddd, *J* = 8.0, 2.1, 0.9, 1H, $H_{k\ or\ m}$), 6.60 (t, *J* = 2.3, 1H, H_a), 6.55 (t, *J* = 2.2, 1H, H_j), 4.00 (t, *J* = 6.3, 2H, H_e), 3.98 (t, *J* = 6.4, 2H, H_i), 3.90 (s, 3H, H_d), 1.86 (dq, *J* = 8.1, 6.5, 4H, $H_{f,\ h}$), 1.66 (m, 2H, H_g).

^{13}C NMR (101 MHz, $CDCl_3$) δ 166.9, 160.5, 160.4, 156.8, 141.4, 132.3, 130.6, 111.4, 111.3, 109.2, 108.0, 107.1, 105.7, 68.2, 68.0, 52.4, 29.0, 29.0, 22.8.

HR-ESI-MS (-ve): *m/z* = 370.1413 $[M - H]^-$ calc. for $C_{19}H_{20}N_3O_5$ 370.1408.

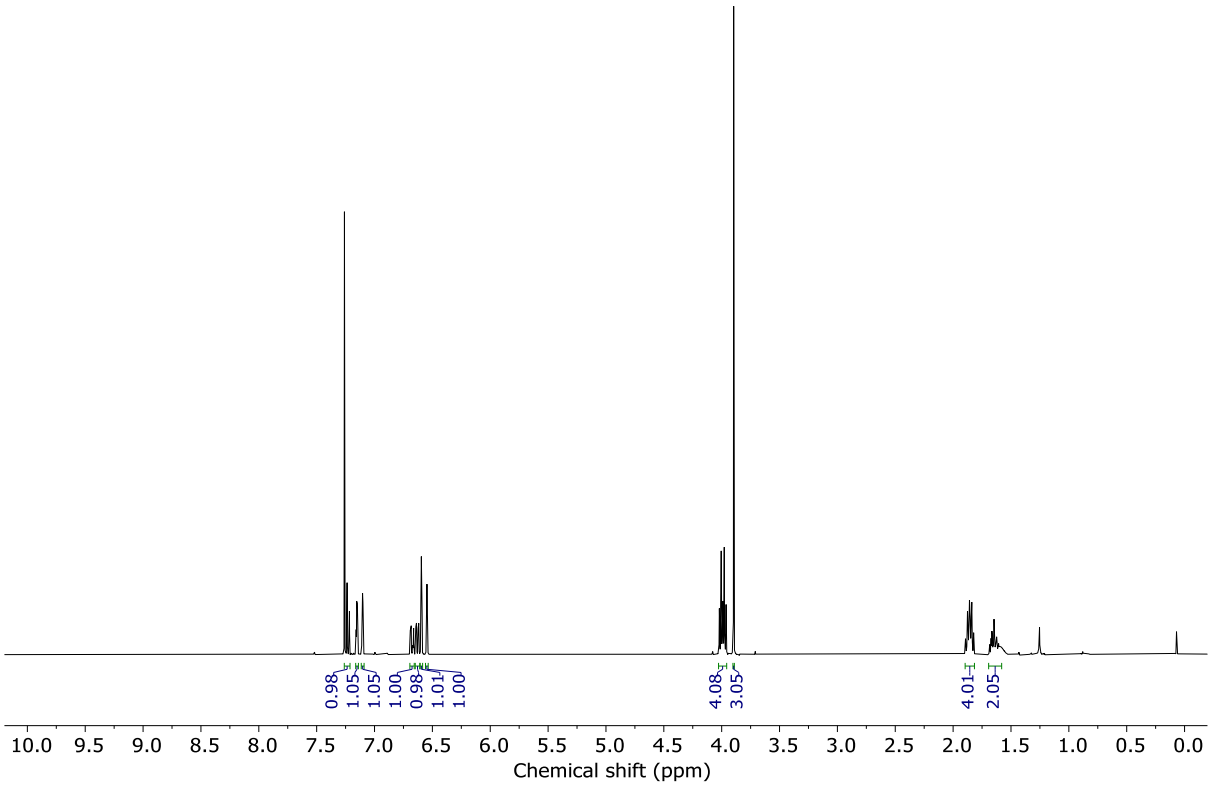

Figure S148: ^{1}H NMR ($CDCl_3$, 400 MHz, 298 K) of **S26**.

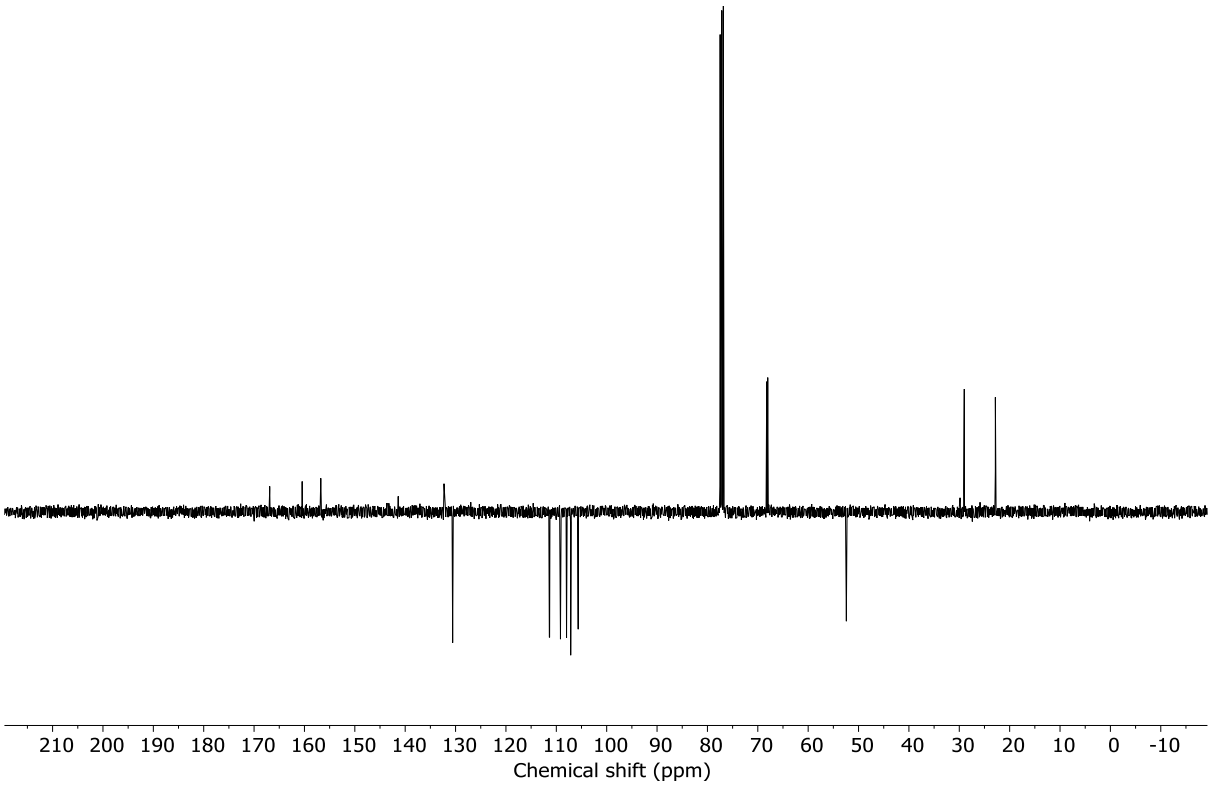

Figure S149: JMOD NMR ($CDCl_3$, 101 MHz, 298 K) of **S26.**

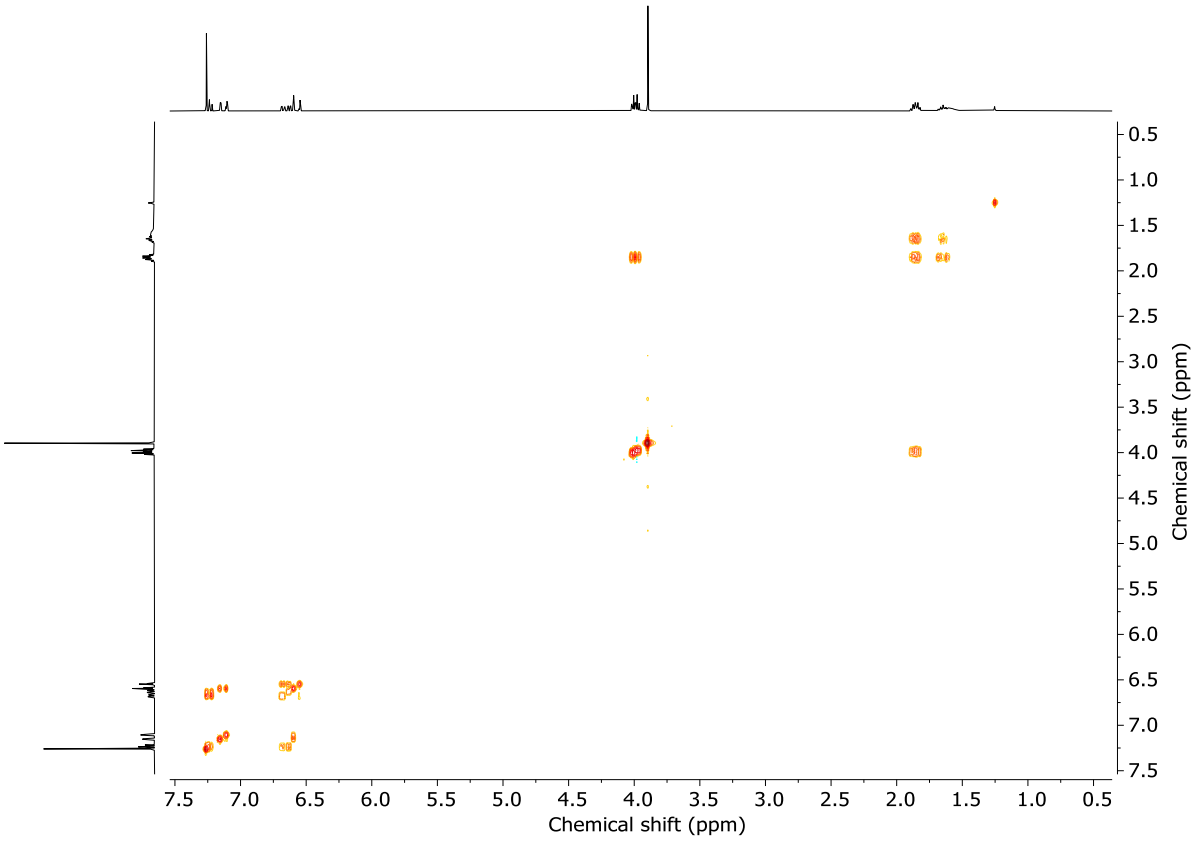

Figure S150: COSY NMR ($CDCl_3$, 298 K) of **S26.**

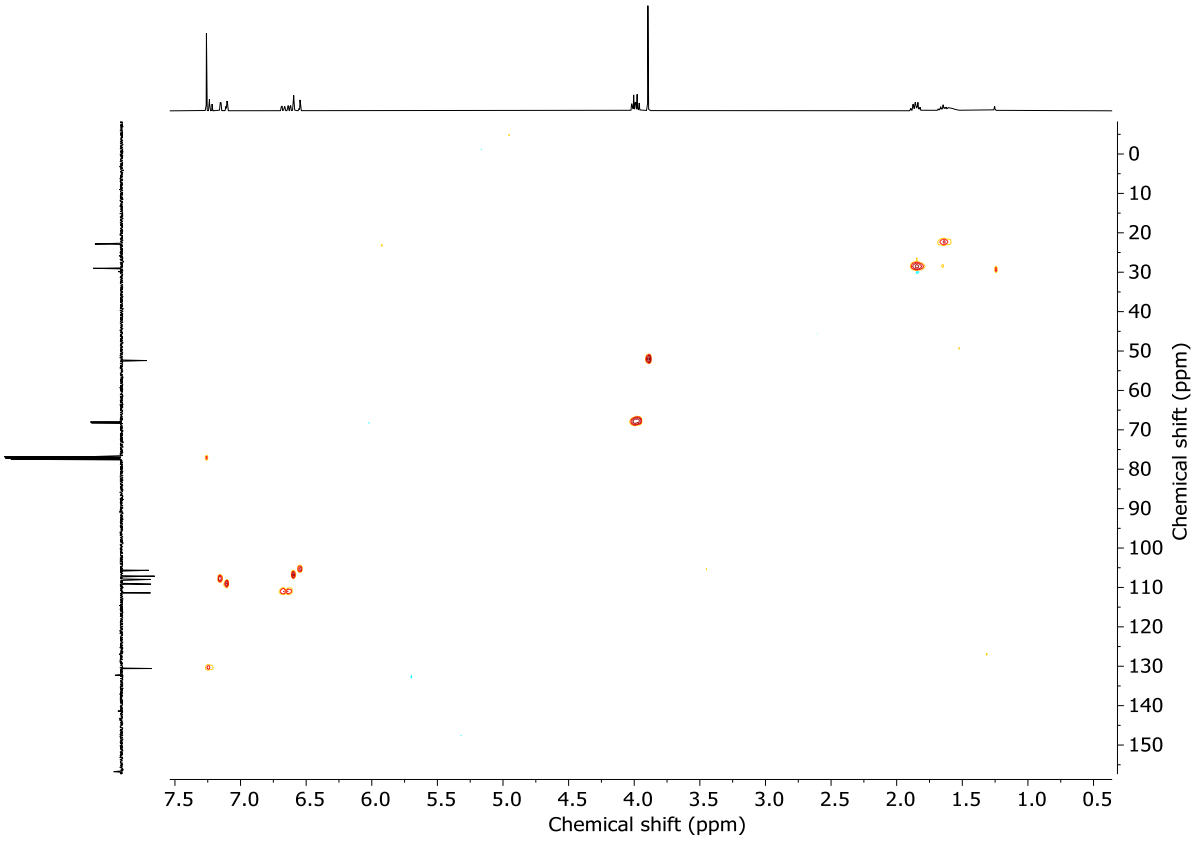

Figure S151: HSQC NMR ($CDCl_3$, 298 K) of **S26**.

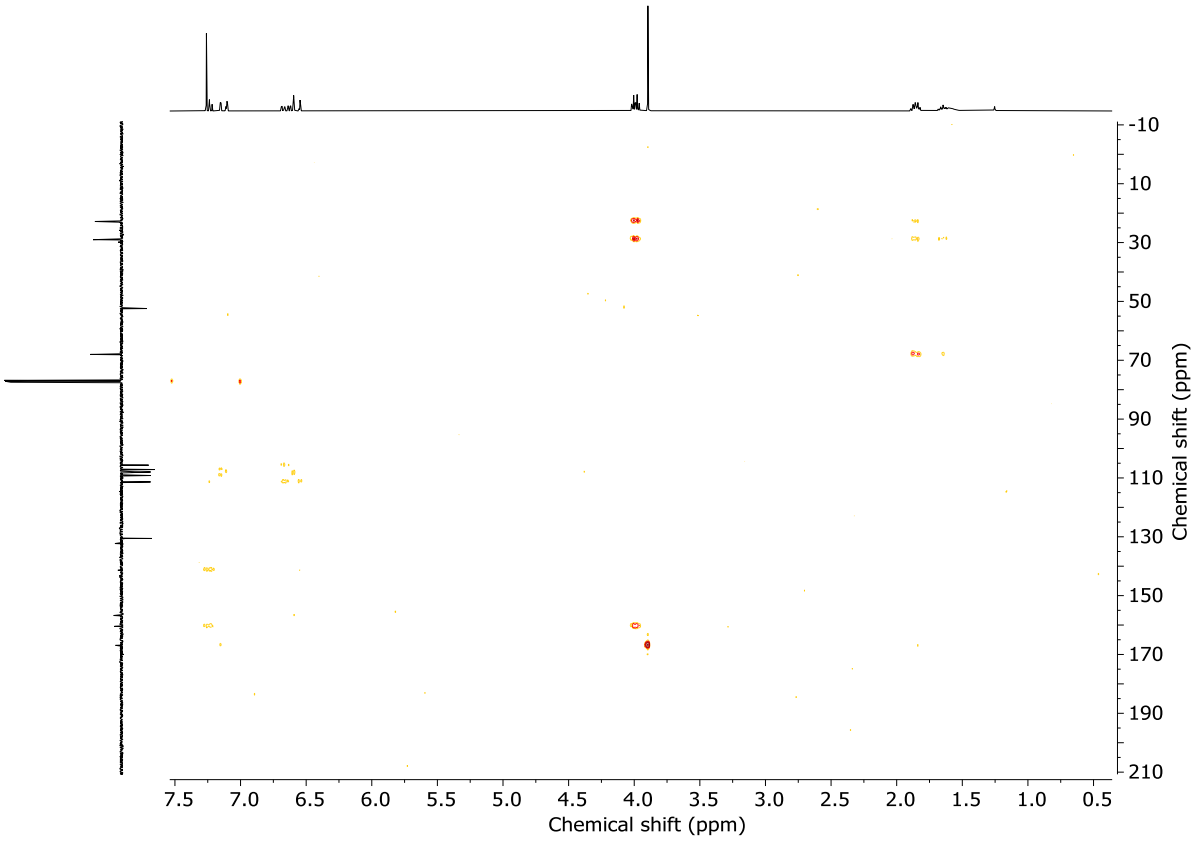

Figure S152: HMBC NMR ($CDCl_3$, 298 K) of **S26.**

Compound S27

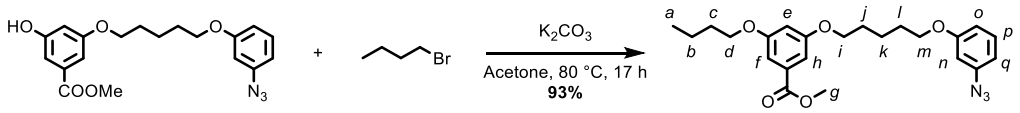

To a stirred solution of **S26** (0.30 g, 0.81 mmol) and 1-bromobutane (0.26 mL, 2.4 mmol) at 80 °C in acetone (8.0 mL) was added K_2CO_3 (0.56 g, 4.1 mmol), and the resulting mixture stirred for 17 h. The mixture was cooled to rt, filtered through Celite® and concentrated *in vacuo*. Chromatography (petrol-Et_2O 100 : 0 to 89 : 11) gave **S27** as a pale-yellow oil (322 mg, 93%).

^{1}H NMR (400 MHz, $CDCl_3$) δ 7.23 (t, *J* = 8.1, 1H, ***H***$_p$), 7.19 – 7.13 (m, 2H, ***H***$_f$, ***H***$_h$), 6.68 (ddd, *J* = 8.3, 2.4, 0.8, 1H, ***H***$_q$), 6.66 – 6.59 (m, 2H, ***H***$_e$, ***H***$_o$), 6.55 (t, *J* = 2.2, 1H, ***H***$_n$), 4.02 (t, *J* = 6.3, 2H, ***H***$_m$), 3.98 (t, *J* = 6.4, 4H, ***H***$_d$, ***H***$_j$), 3.90 (s, 3H, ***H***$_g$), 1.90 – 1.81 (m, 4H, ***H***$_j$, ***H***$_i$), 1.80 – 1.72 (m, 2H, ***H***$_c$), 1.69 – 1.60 (m, 2H, ***H***$_k$), 1.54 – 1.44 (m, 2H, ***H***$_b$), 0.97 (t, *J* = 7.4, 3H, ***H***$_a$).

^{13}C NMR (101 MHz, $CDCl_3$) δ 167.1, 160.4, 160.3, 160.2, 141.4, 132.0, 130.6, 111.4, 111.3, 107.9, 107.7, 106.8, 105.6, 68.2 (x2), 68.0, 52.3, 31.4, 29.1 (x2), 22.9, 19.4, 14.0.

HR-ESI-MS (+ve): *m/z* = 450.1997 $[M + Na]^+$ calc. for $C_{23}H_{29}N_3NaO_5$ 450.1999.

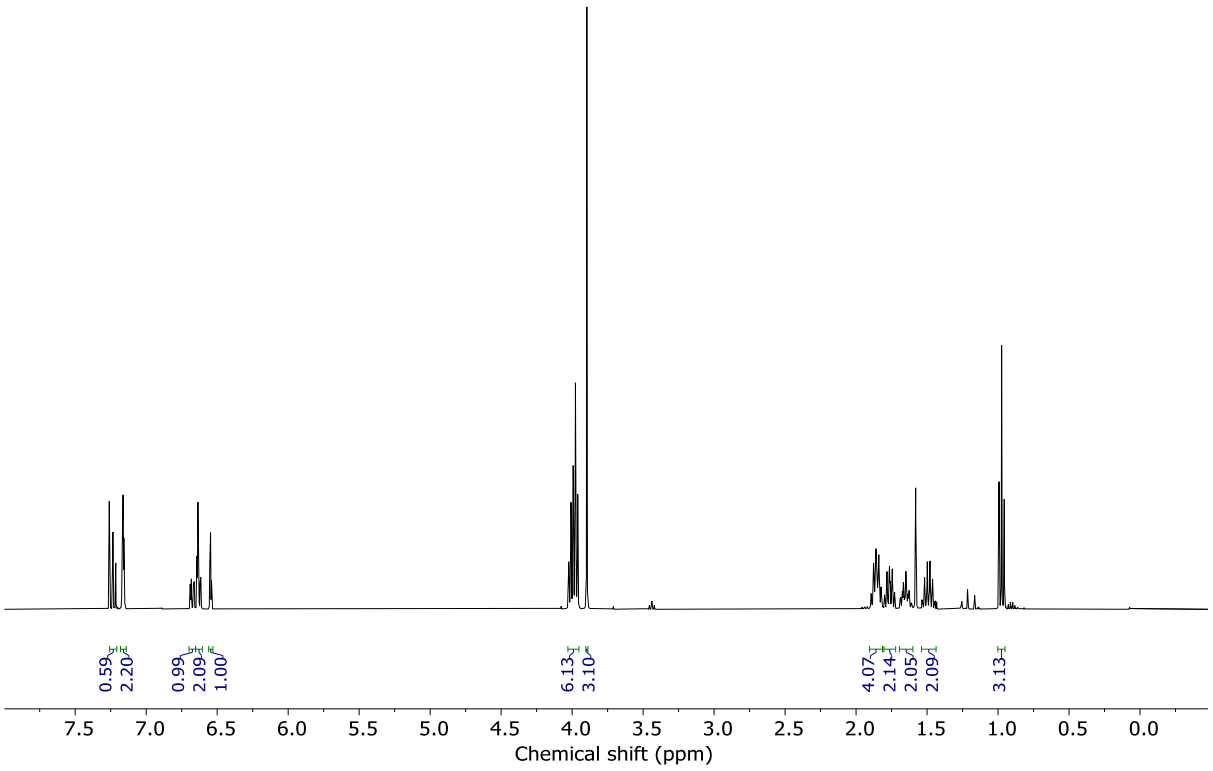

Figure S153: ^{1}H NMR ($CDCl_3$, 400 MHz, 298 K) of **S27**.

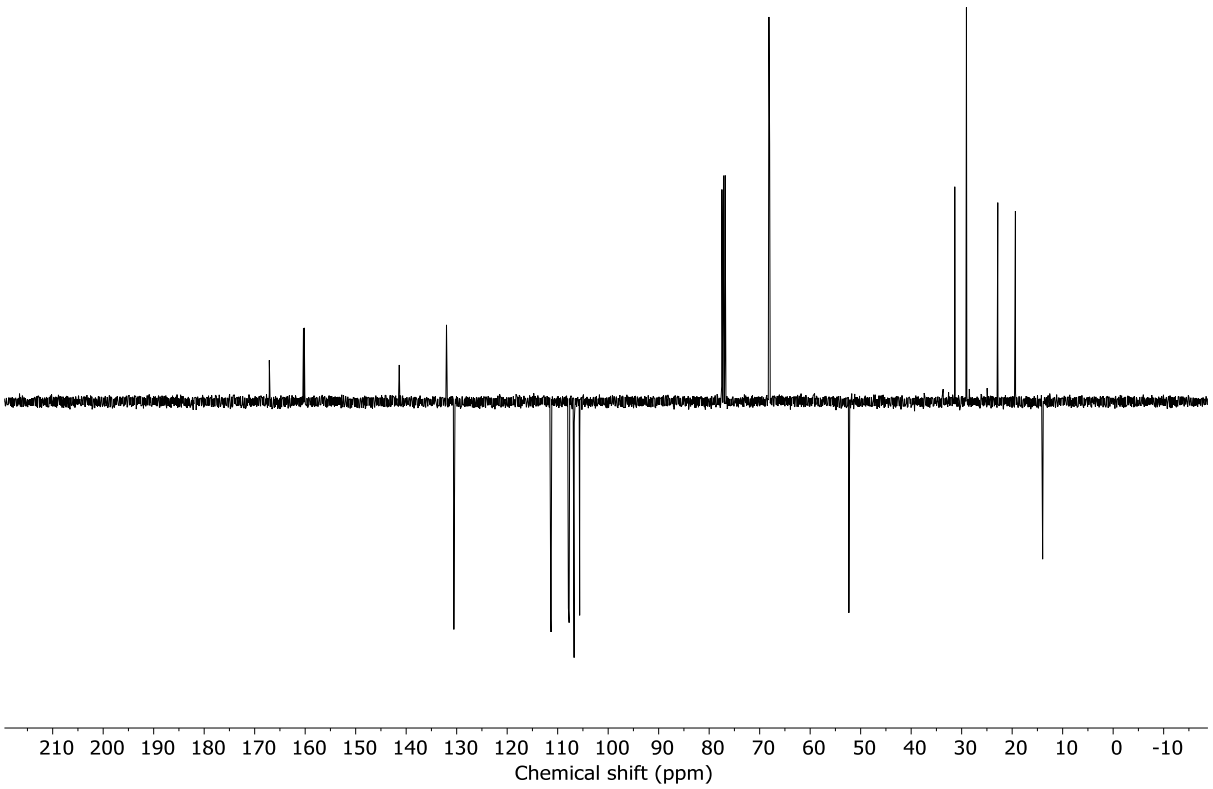

Figure S154: JMOD NMR ($CDCl_3$, 101 MHz, 298 K) of **S27**.

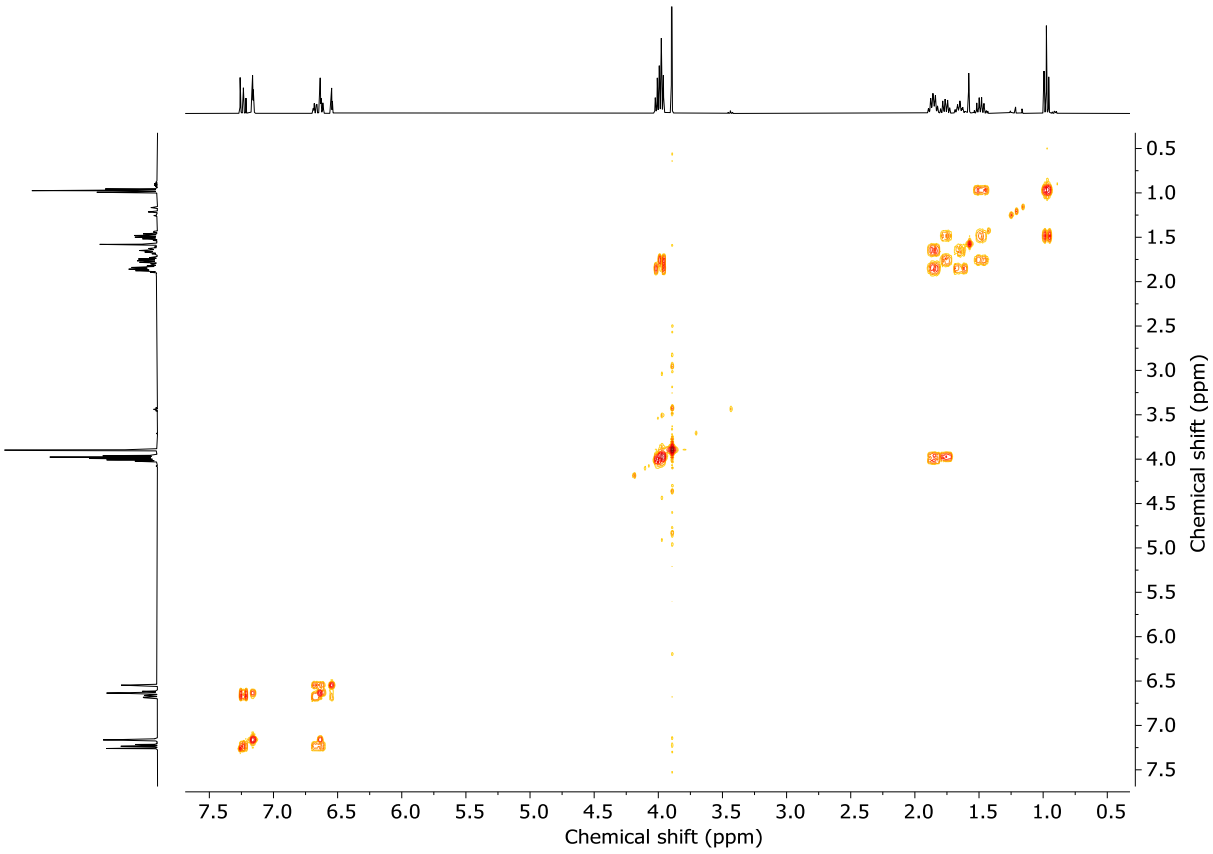

Figure S155: COSY NMR ($CDCl_3$, 298 K) of **S27**.

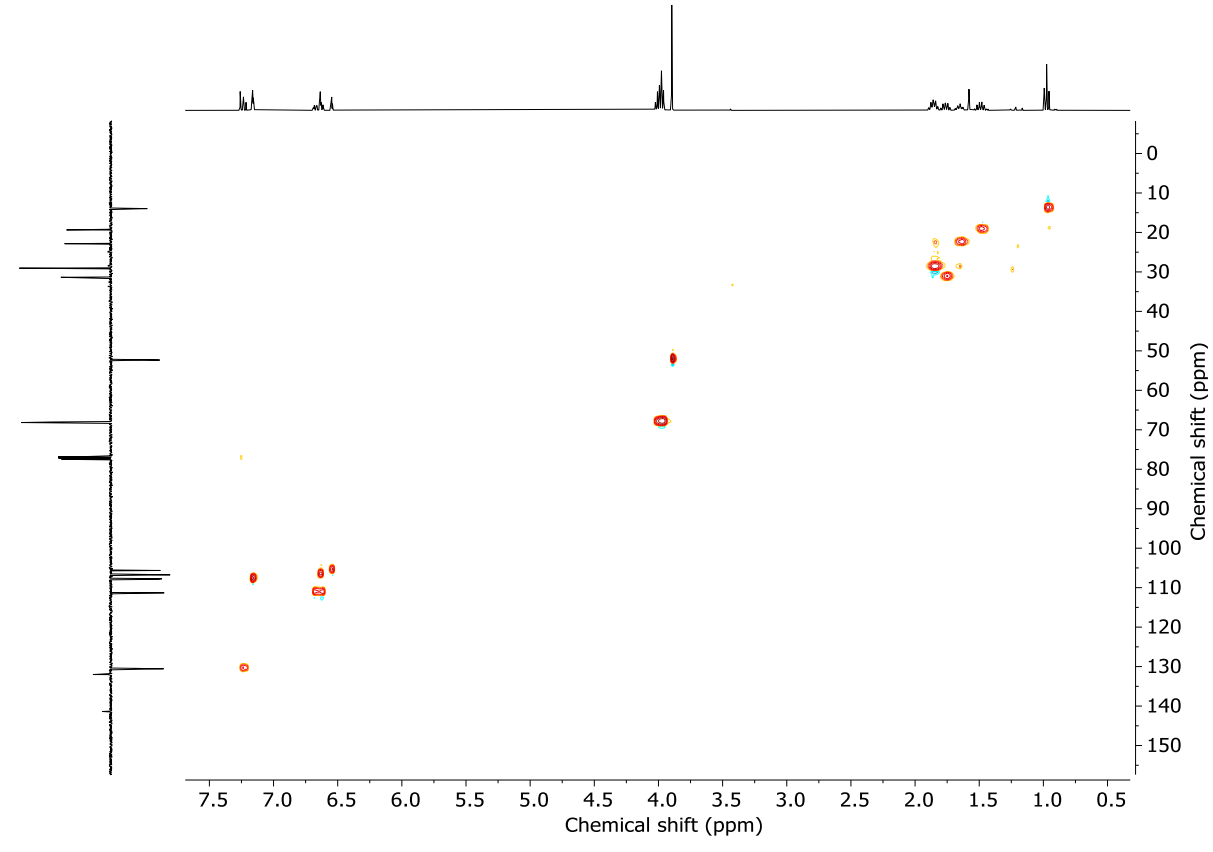

Figure S156: HSQC NMR ($CDCl_3$, 298 K) of **S27**.

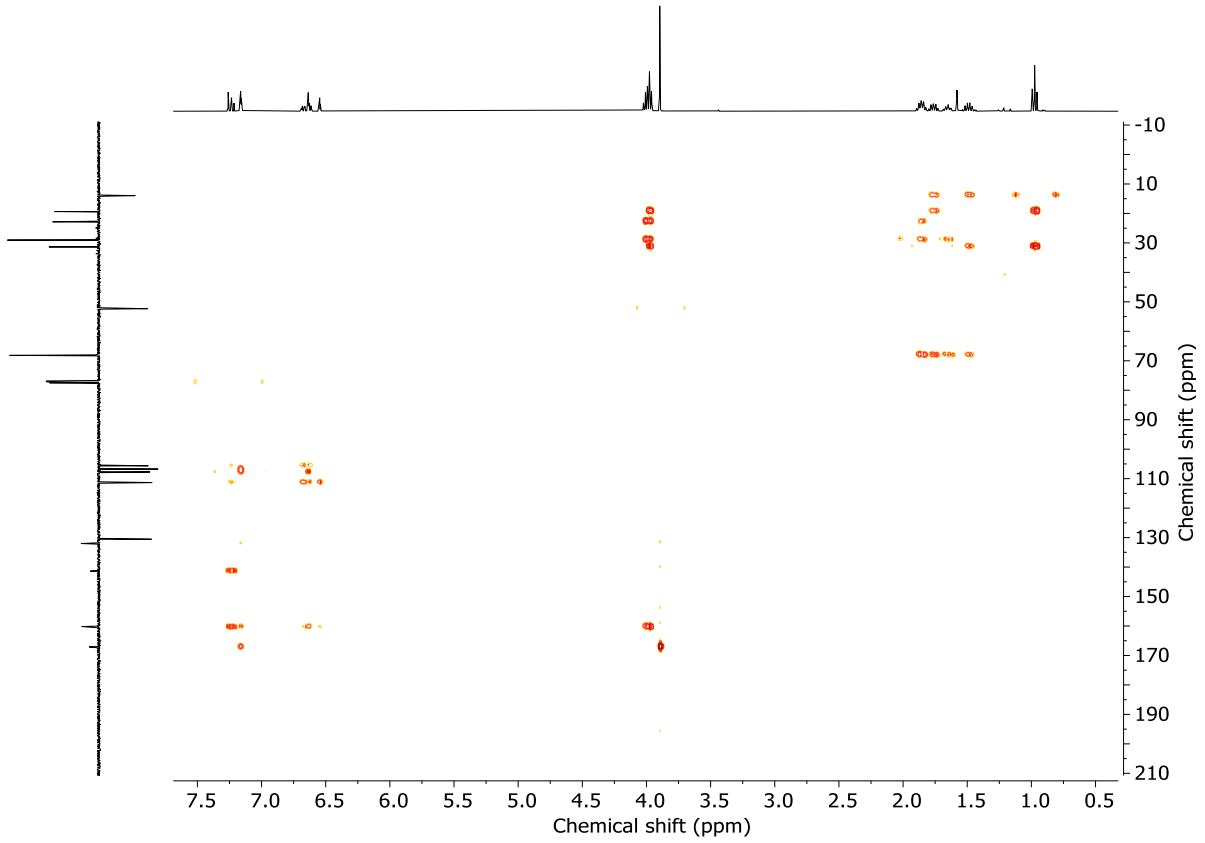

Figure S157: HMBC NMR ($CDCl_3$, 298 K) of **S27**.

Rotaxane *rac*-($R_{co\text{-}mp}$,*E*)-S28

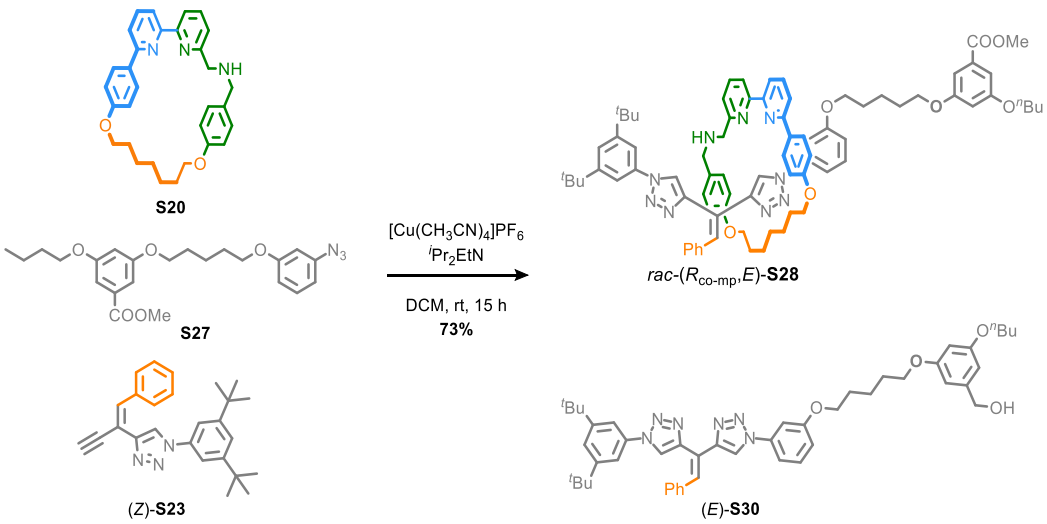

To a stirred solution of macrocycle **S20** (12 mg, 0.025 mmol), $[Cu(CH_3CN)_4]PF_6$ (8.7 mg, 0.023 mmol), alkyne (*Z*)-**S23** (24 mg, 0.062 mmol) and $^{i}Pr_2EtN$ (21.5 µL, 0.123 mmol) at rt in CH_2Cl_2 (0.4 mL) was added azide **S27** (26 mg, 0.062 mmol) in CH_2Cl_2 (0.6 mL) and the resulting mixture stirred at rt for 15 h. Sat. EDTA-$NH_{3(aq)}$ (2 mL) was added and the mixture stirred for 1 h at rt. The mixture was diluted with H_2O (20 mL) and the aqueous layer extracted with CH_2Cl_2 (3 x 10 mL). The combined organic layers were dried (Na_2SO_4) and concentrated *in vacuo*. Chromatography (CH_2Cl_2-MeOH 100 : 0 to 9 : 1) afforded *rac*-($R_{co\text{-}mp}$,*E*)-**S28** as an off-white foam (23 mg, 73%). An analytical sample of axle (*E*)-**S30** was also obtained as a yellow oil.

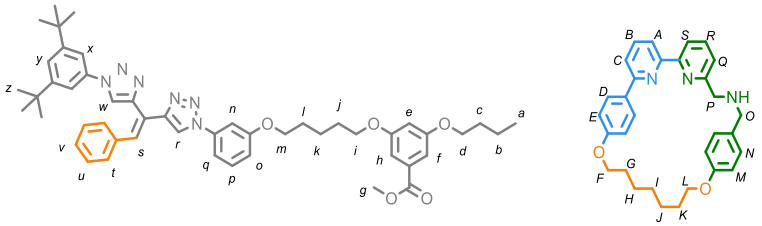

^{1}H NMR (400 MHz, CD_2Cl_2) δ 9.37 (s, 1H, H_r), 7.73 (s, 1H, H_w), 7.62 – 7.55 (m, 2H, H_B, H_S), 7.52 (t, *J* = 7.7, 1H, H_R), 7.43 (t, *J* = 1.7, 1H, H_y), 7.38 – 7.03 (m, 19H, H_f, H_q, H_n, H_p, H_h, H_t, H_u, H_v, H_A, H_C, H_Q, H_R, H_D, H_x), 6.73 (d, *J* = 8.3, 2H, H_N), 6.67 (ddd, *J* = 8.2, 2.4, 1.0, 1H, H_o), 6.61 (t, *J* = 2.3, 1H, H_e), 6.40 (d, *J* = 8.8, 2H, H_E), 6.27 (d, *J* = 8.5, 2H, H_M), 4.22 – 4.02 (m, 3H, H_F, 1 of H_L), 3.97 (t, *J* = 6.5, 2H, H_d), 3.95 – 3.83 (m, 6H, H_g, H_i, 1 of H_L), 3.71 (d, *J* = 13.3, 1H, 1 of H_O or $_P$), 3.65 – 3.48 (m, 3H, 1 of H_O or $_P$, $H_{O\ or\ P}$), 3.44 (dt, *J* = 9.2, 6.5, 1H, 1 of H_m), 3.33 (dt, *J* = 9.2, 6.5, 1H, 1 of H_m), 2.09 – 1.55 (m, 14H, H_c, H_j, H_k, H_G, H_H, H_J, H_K), 1.56 – 1.41 (m, 4H, H_b, H_l), 1.38 – 1.22 (m, 20H, H_l, H_z), 0.98 (t, *J* = 7.4, 3H, H_a).

^{13}C NMR (101 MHz, CD_2Cl_2) δ 167.1, 160.7, 160.6, 160.5, 160.0, 159.6, 159.5, 158.2, 157.3 (X2), 157.0, 152.8, 147.3, 144.4, 138.5, 137.6, 137.4, 137.2, 136.6, 132.4, 132.0, 129.7 (X2), 129.3, 129.1, 128.4, 128.4 (x2), 127.5, 123.2, 123.0, 121.6, 121.4, 120.8, 120.6, 120.3, 114.7, 114.5 (X2), 114.1, 111.8, 108.4, 107.9, 107.8, 106.6, 105.3, 68.5, 68.5, 67.9, 67.5, 65.7, 54.0 (x2,HMBC), 52.5, 35.4, 31.7, 31.5, 29.7, 29.4, 29.2, 28.4, 26.2, 26.1, 22.8, 19.6, 14.0.

LR-ESI-MS (+ve): *m/z* = 1290.7 $[M + H]^+$ calc. for $C_{80}H_{92}N_9O_7$ 1290.7.

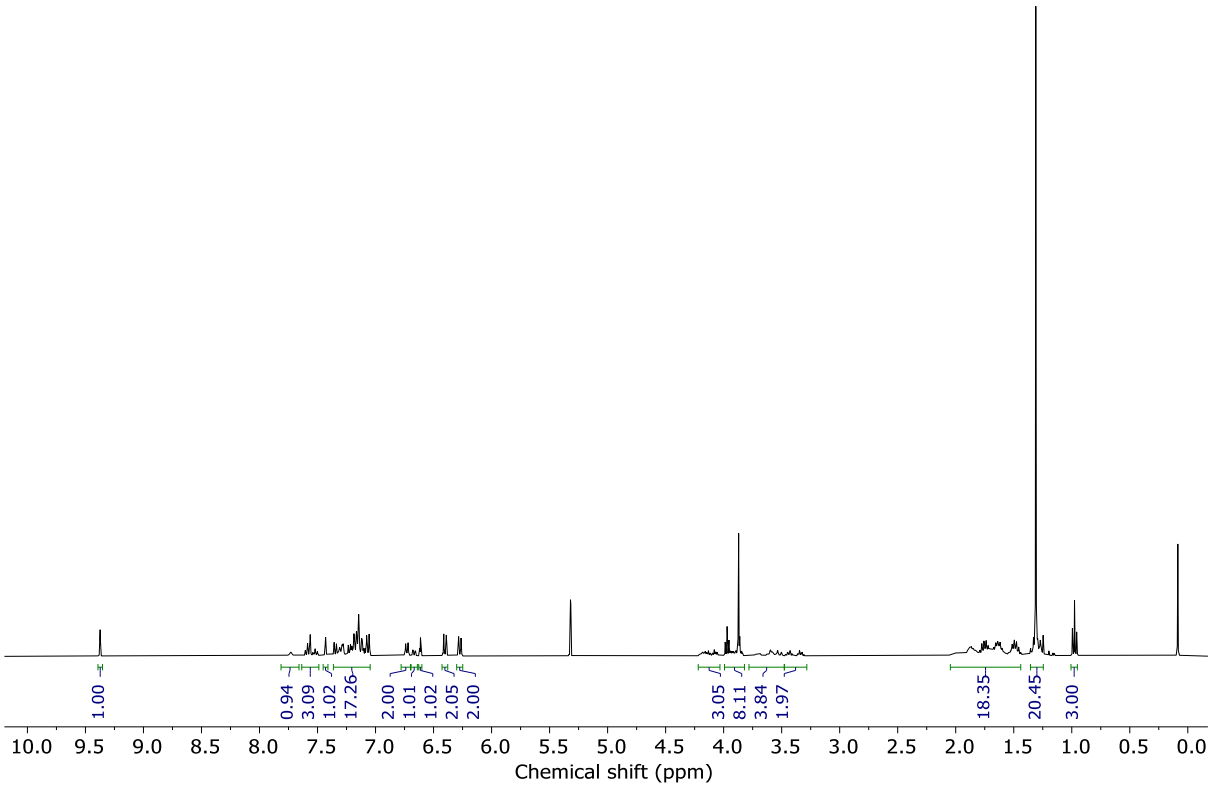

Figure S158: ^{1}H NMR (CD_2Cl_2, 400 MHz, 298 K) of *rac-(E)*-**S28**.

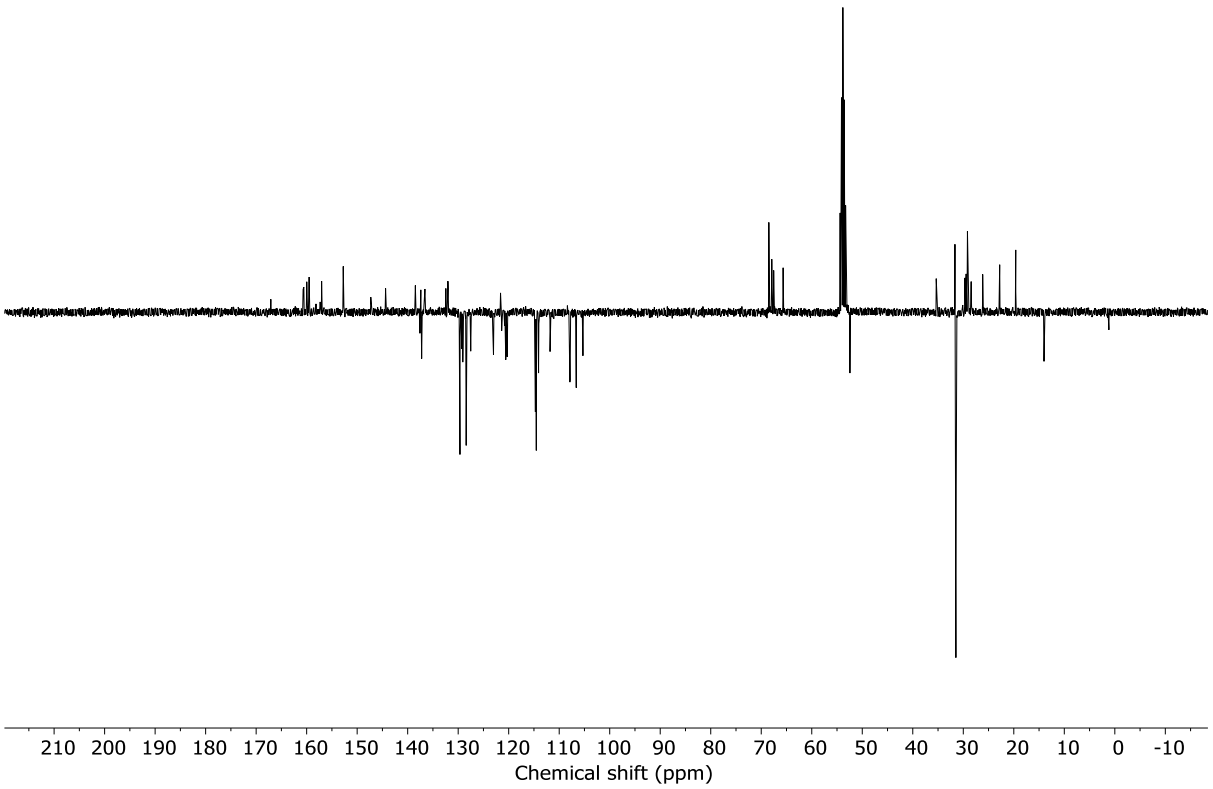

Figure S159: JMOD NMR (CD_2Cl_2, 101 MHz, 298 K) of *rac-(E)*-**S28**.

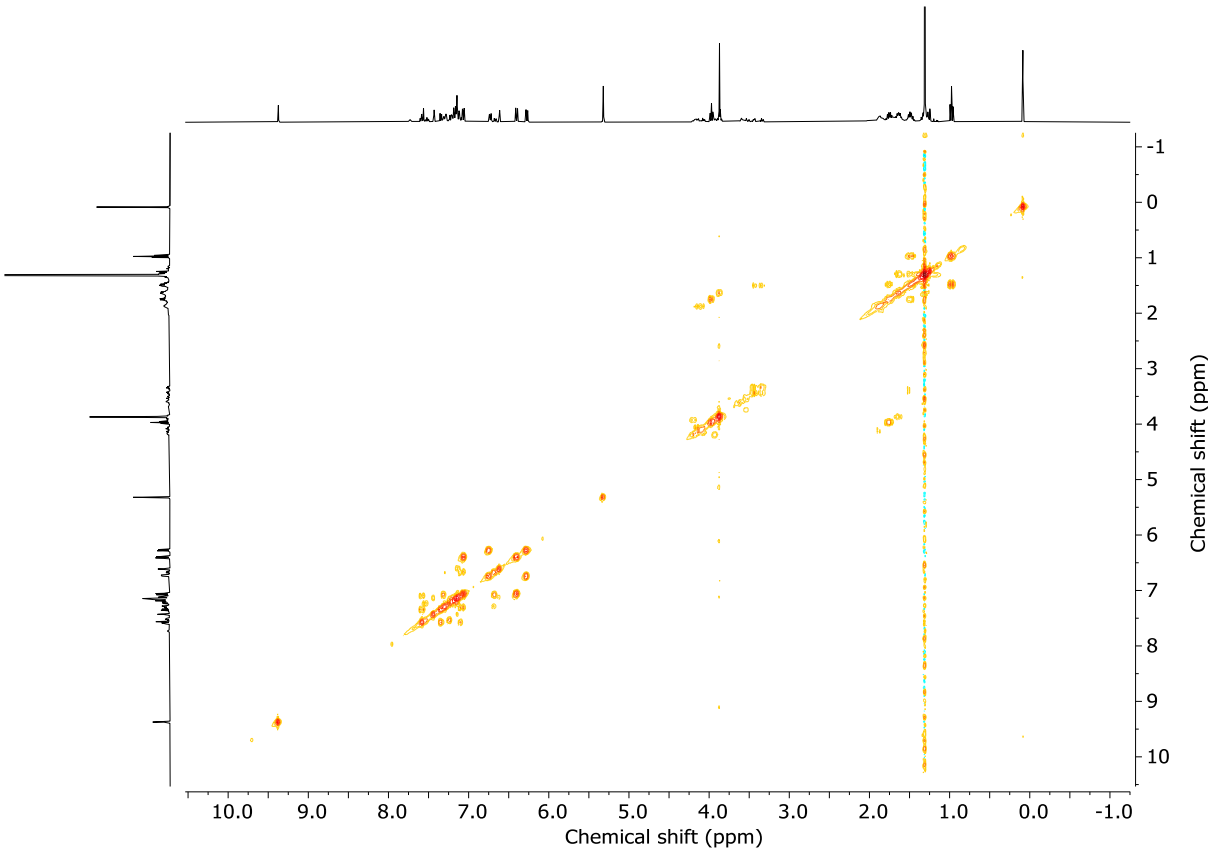

Figure S160: COSY NMR (CD_2Cl_2, 298 K) of *rac-(E)*-**S28**.

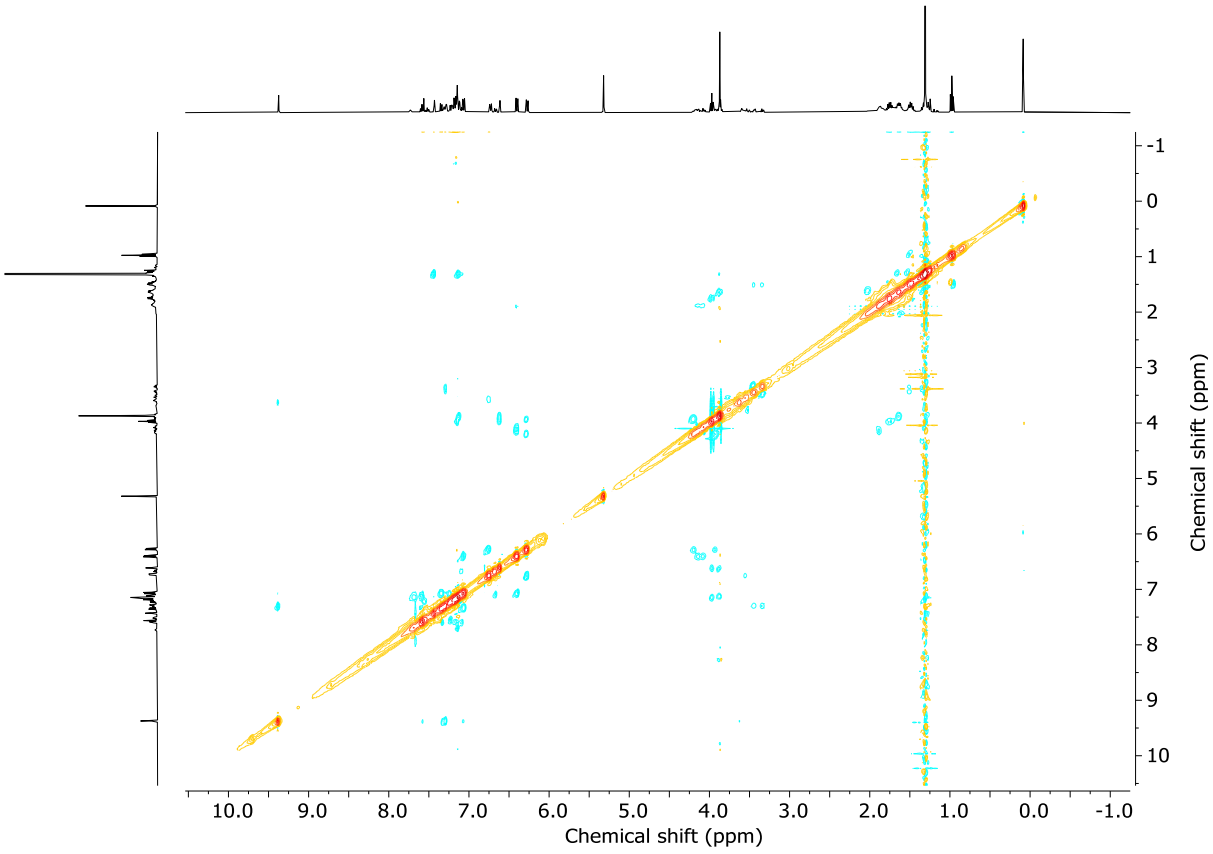

Figure S161: NOESY NMR (CD_2Cl_2, 298 K) of *rac-(E)*-**S28**.

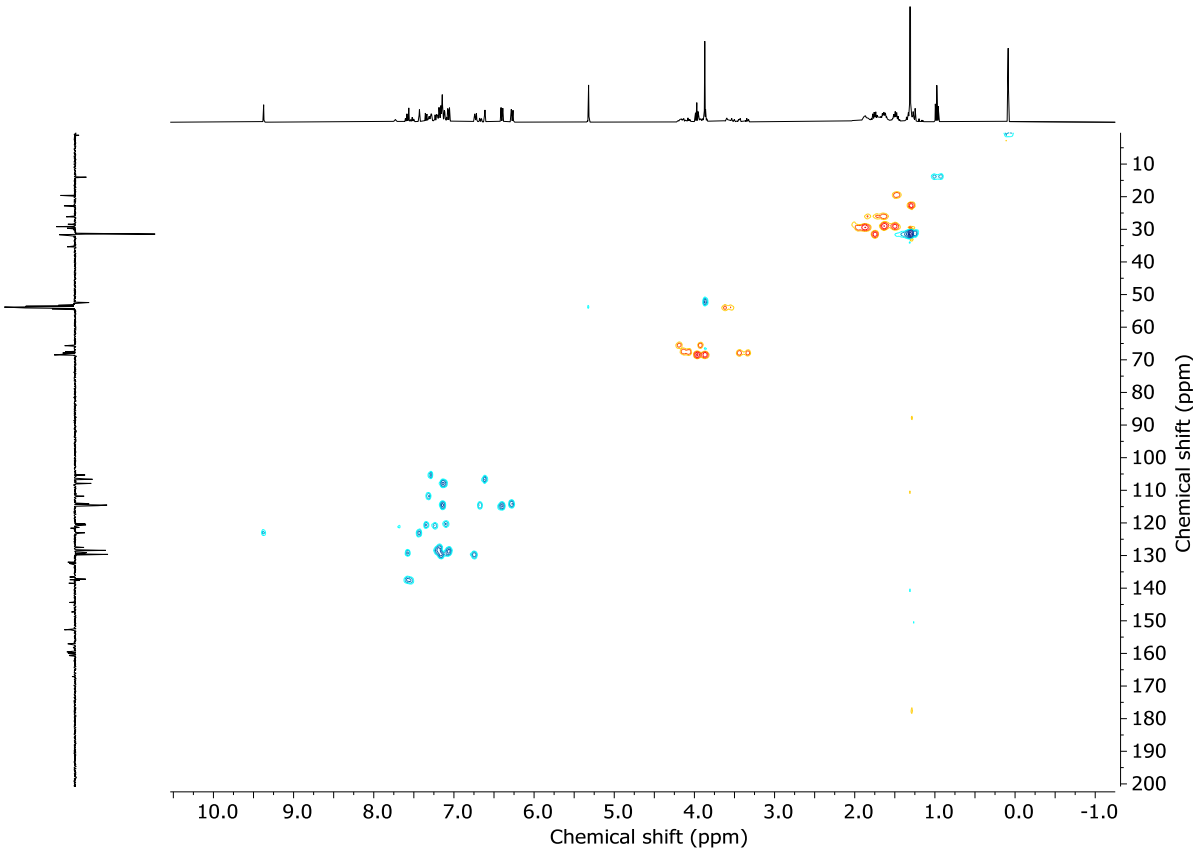

Figure S162: HSQC NMR (CD_2Cl_2, 298 K) of *rac-(E)*-**S28**.

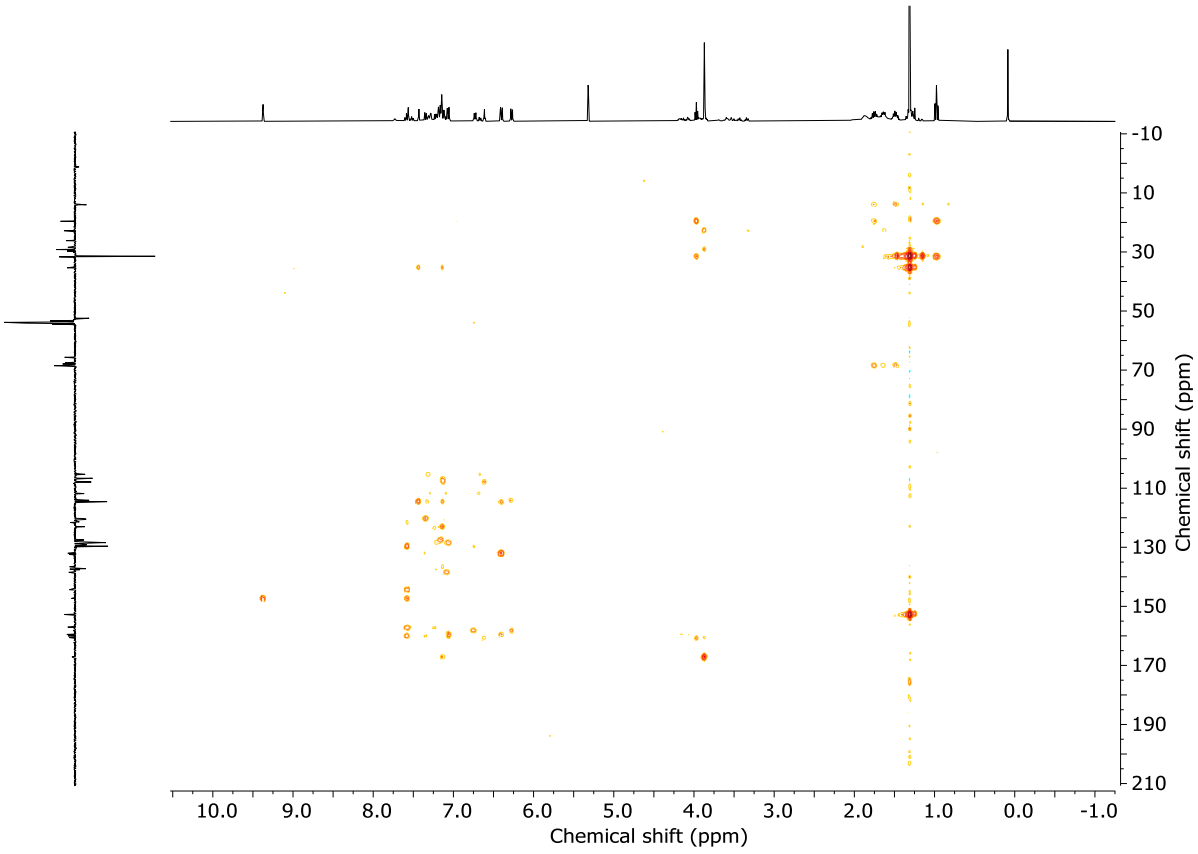

Figure S163: HMBC NMR (CD_2Cl_2, 298 K) of *rac-(E)*-**S28**.

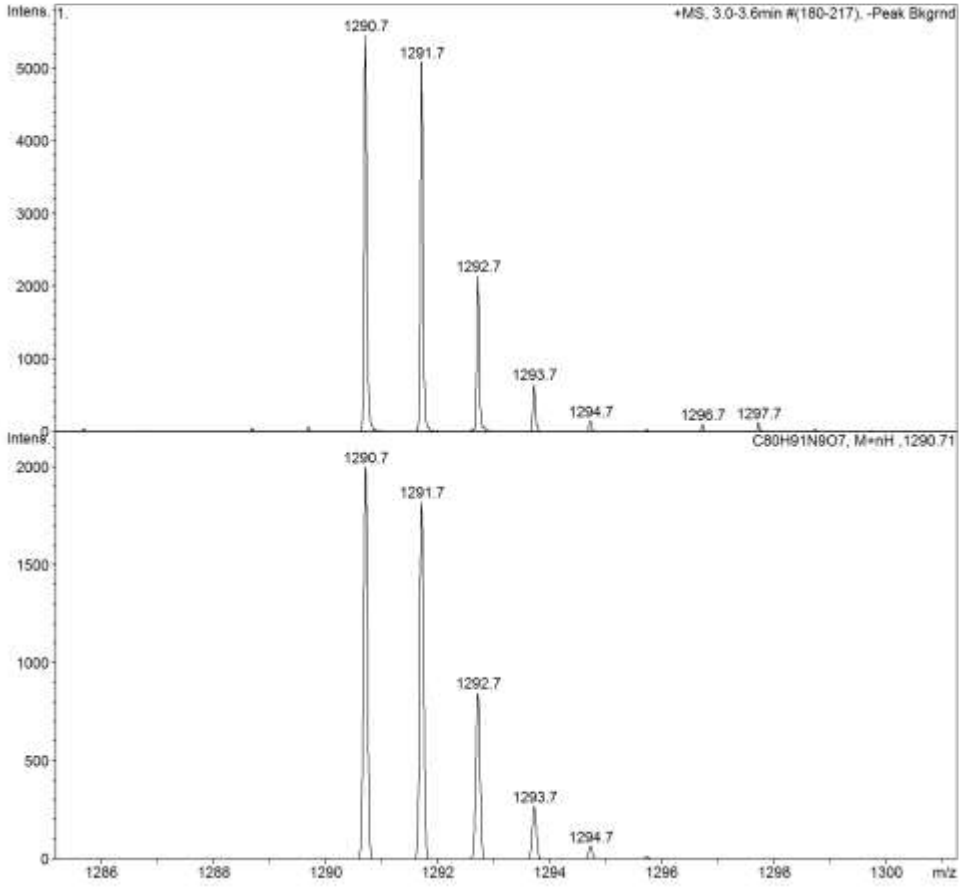

Figure S164: LRMS - Observed (top) and calculated (bottom) isotopic pattern for *rac-(E)*-**S28** $C_{80}H_{92}N_9O_7$.

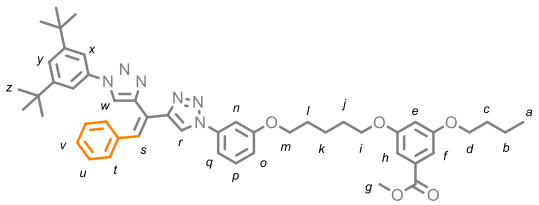

^{1}H NMR (400 MHz, CD_2Cl_2) δ 8.24 (s, 1H, $\boldsymbol{H}_r$), 8.00 (s, 1H, $\boldsymbol{H}_s$), 7.70 – 7.69 (s, 1H, $\boldsymbol{H}_w$), 7.53 (t, *J* = 1.8, 1H, $\boldsymbol{H}_y$), 7.44 – 7.43 (m, 2H, $\boldsymbol{H}_x$), 7.42 (t, *J* = 8.1, 1H, $\boldsymbol{H}_p$), 7.37 (t, *J* = 2.3, 1H, $\boldsymbol{H}_n$), 7.35 – 7.25 (m, 6H, $\boldsymbol{H}_q$, $\boldsymbol{H}_t$, $\boldsymbol{H}_u$, $\boldsymbol{H}_v$), 7.14 (dq, *J* = 2.5, 1.4, 2H, $\boldsymbol{H}_f$, $\boldsymbol{H}_h$), 6.98 (ddd, *J* = 8.3, 2.5, 1.0, 1H, $\boldsymbol{H}_o$), 6.65 (t, *J* = 2.4, 1H, $\boldsymbol{H}_e$), 4.09 (t, *J* = 6.4, 2H, $\boldsymbol{H}_m$), 4.02 (t, *J* = 6.4, 2H, $\boldsymbol{H}_i$), 3.98 (t, *J* = 6.5, 2H, $\boldsymbol{H}_d$), 3.86 (s, 3H, $\boldsymbol{H}_g$), 1.94 – 1.83 (m, 4H, $\boldsymbol{H}_j$, $\boldsymbol{H}_l$), 1.80 – 1.60 (m, 4H, $\boldsymbol{H}_c$, $\boldsymbol{H}_k$), 1.54 – 1.43 (m, 2H, $\boldsymbol{H}_b$), 1.36 (s, 18H, $\boldsymbol{H}_z$), 0.97 (t, *J* = 7.4, 3H, $\boldsymbol{H}_a$).

^{13}C NMR (101 MHz, CD_2Cl_2) δ 167.1, 160.7, 160.6, 160.6, 153.3, 148.3, 144.7, 138.5, 137.2, 136.9, 132.4, 131.0, 130.9, 129.6, 128.8, 128.2, 123.6, 122.6, 121.2, 121.1, 115.8, 115.2, 112.6, 108.0, 107.9, 107.1, 106.6, 68.7, 68.6, 68.5, 52.4, 35.5, 31.6, 31.4, 29.3, 29.3, 23.0, 19.6, 14.0.

HR-ESI-MS (+ve): m/z = 811.4538 $[M + H]^+$ calc. for $C_{49}H_{59}N_6O_5$ 811.4541; m/z = 833.4359 $[M + Na]^+$ calc. for $C_{49}H_{58}N_6NaO_5$ 833.4361

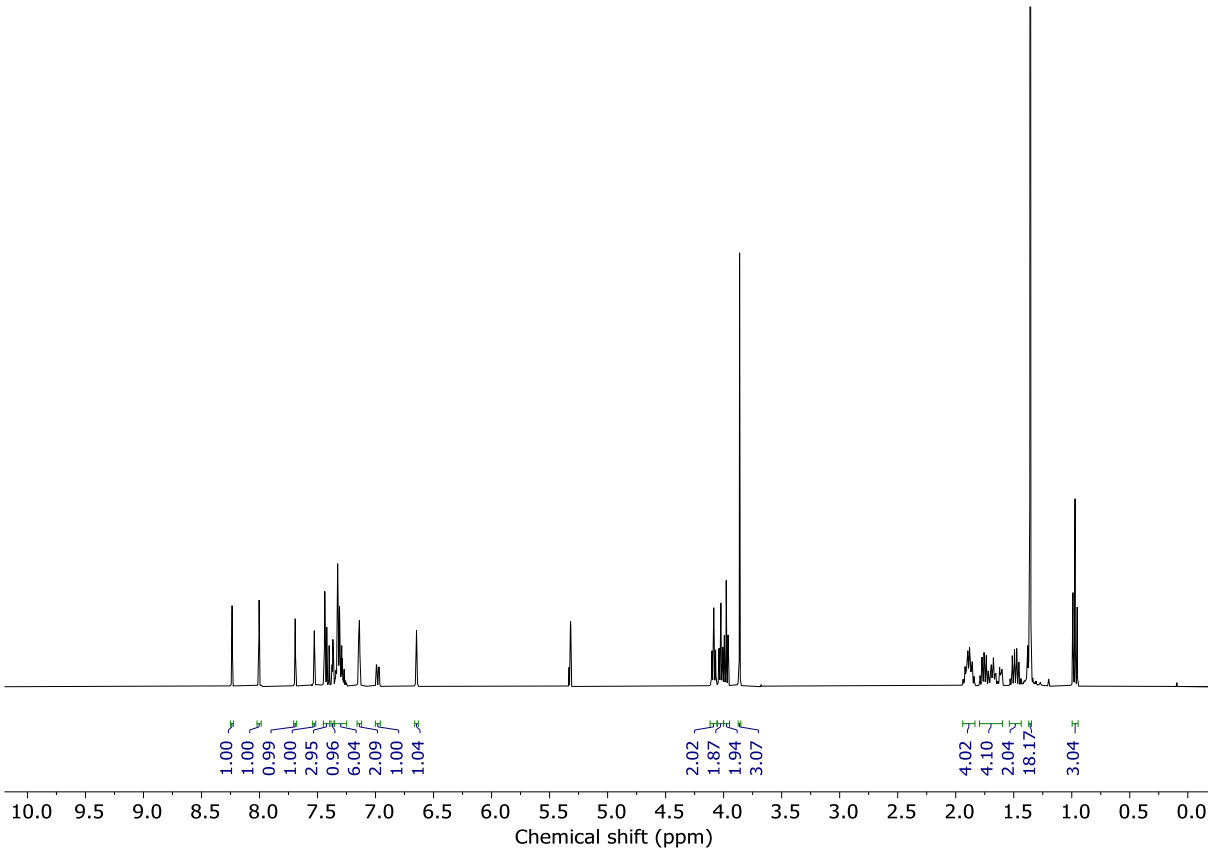

Figure S165: ^{1}H NMR (CD_2Cl_2, 400 MHz, 298 K) of *(E)*-**S30.**

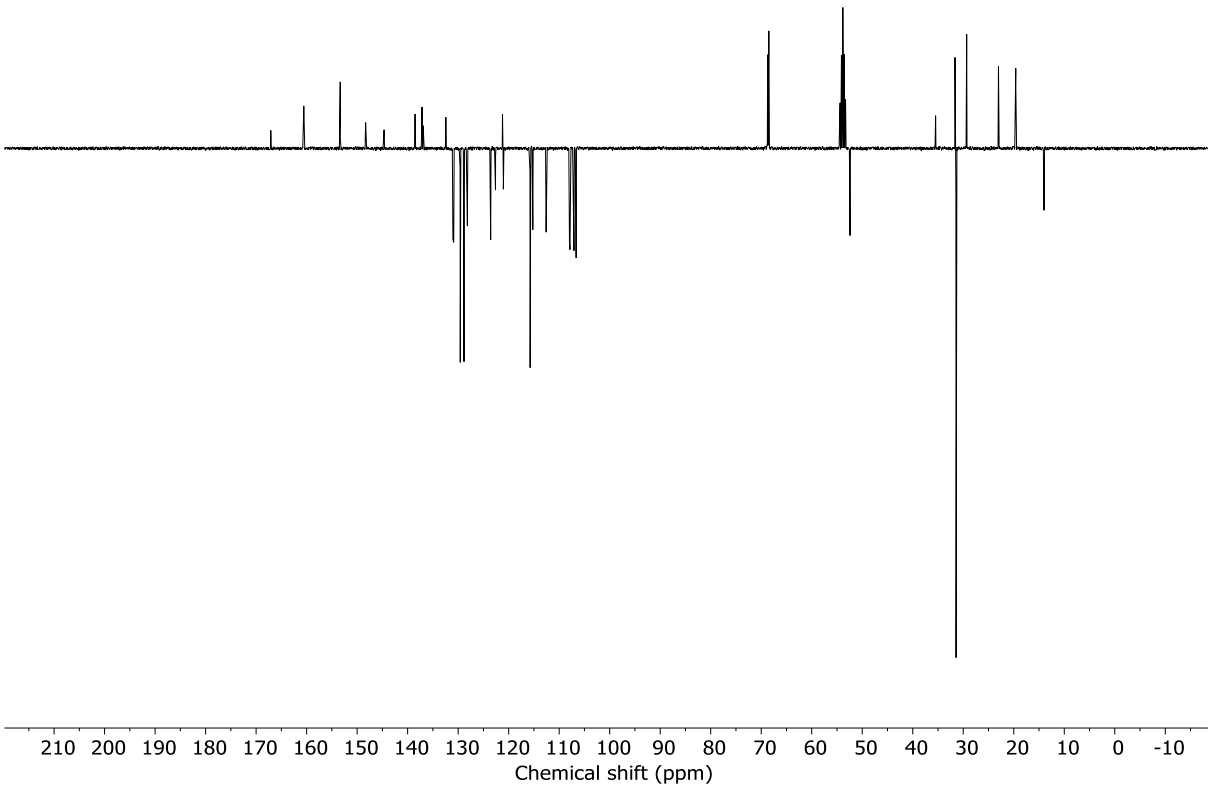

Figure S166: JMOD NMR (CD_2Cl_2, 101 MHz, 298 K) of *(E)*-**S30**.

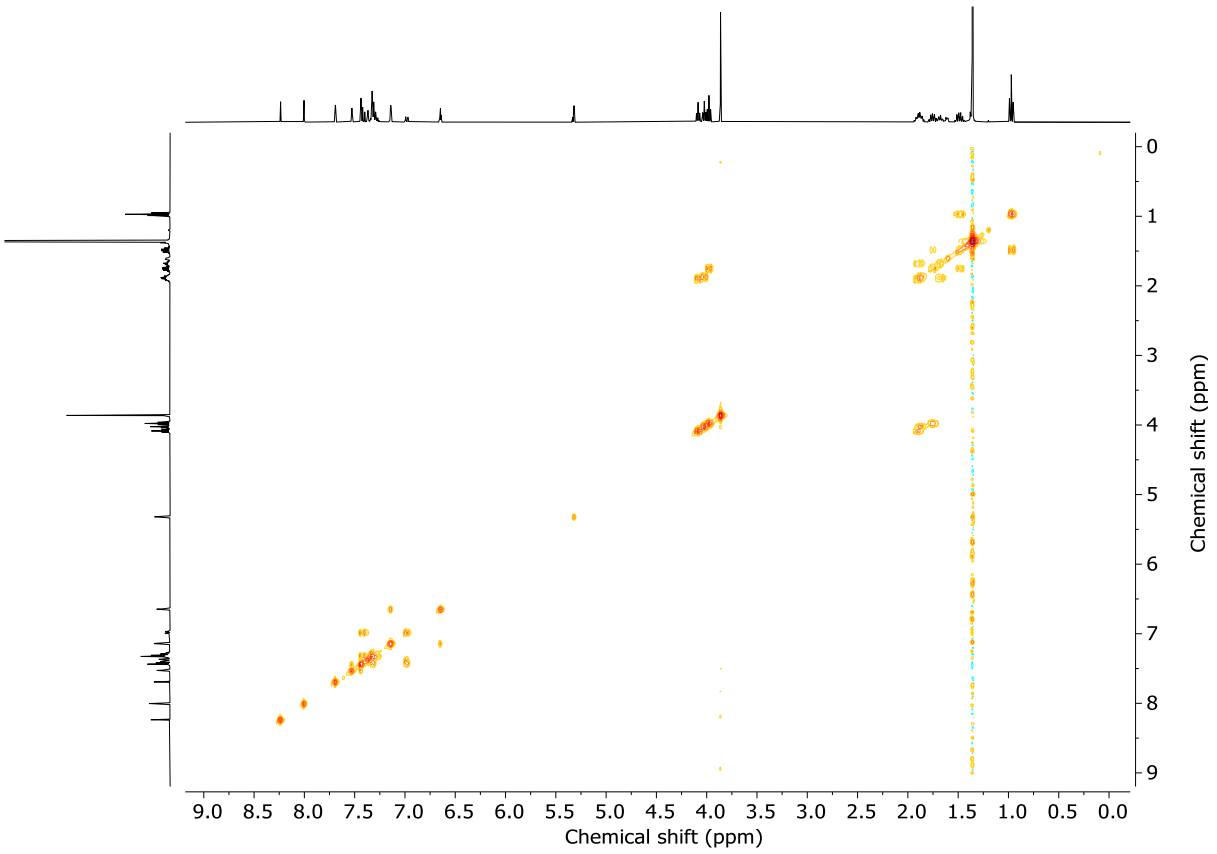

Figure S167: COSY NMR (CD_2Cl_2, 298 K) of *(E)*-**S30**.

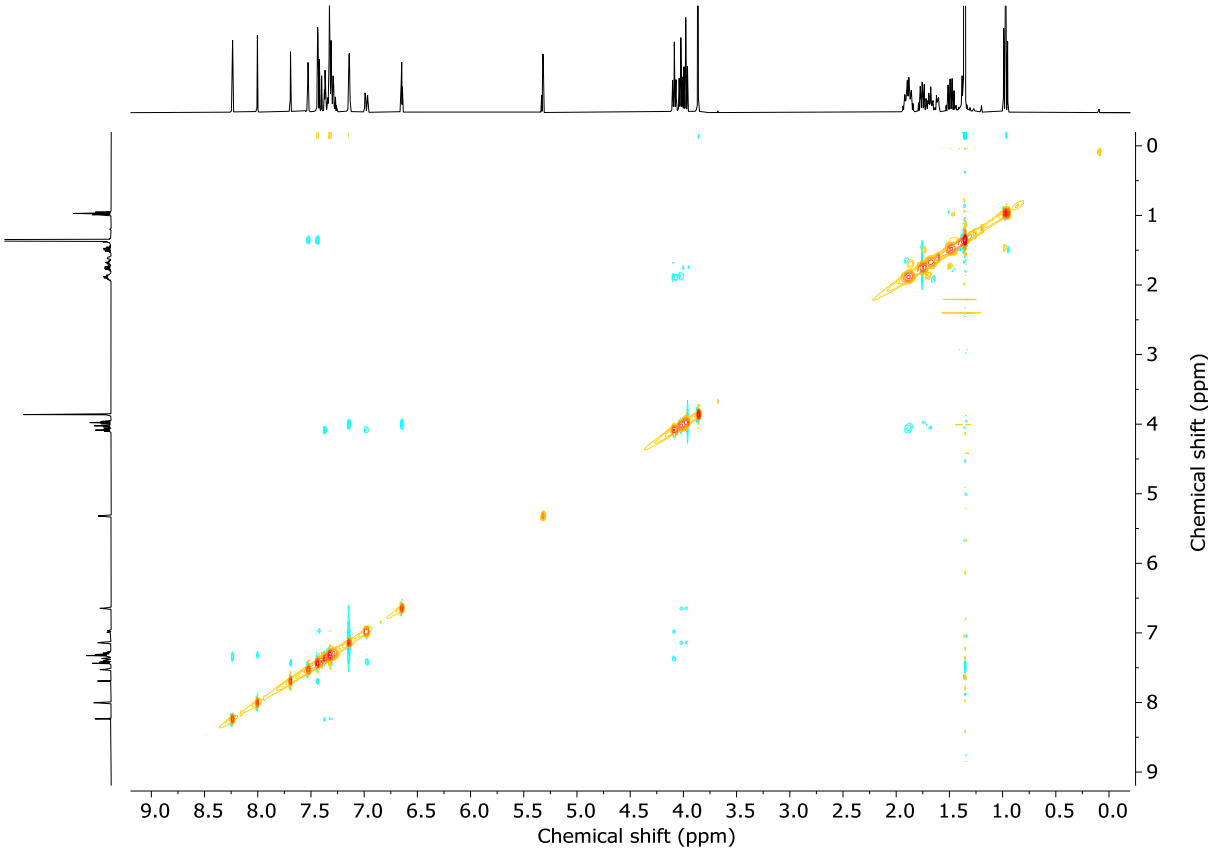

Figure S168: NOESY NMR (CD_2Cl_2, 298 K) of *(E)*-**S30**.

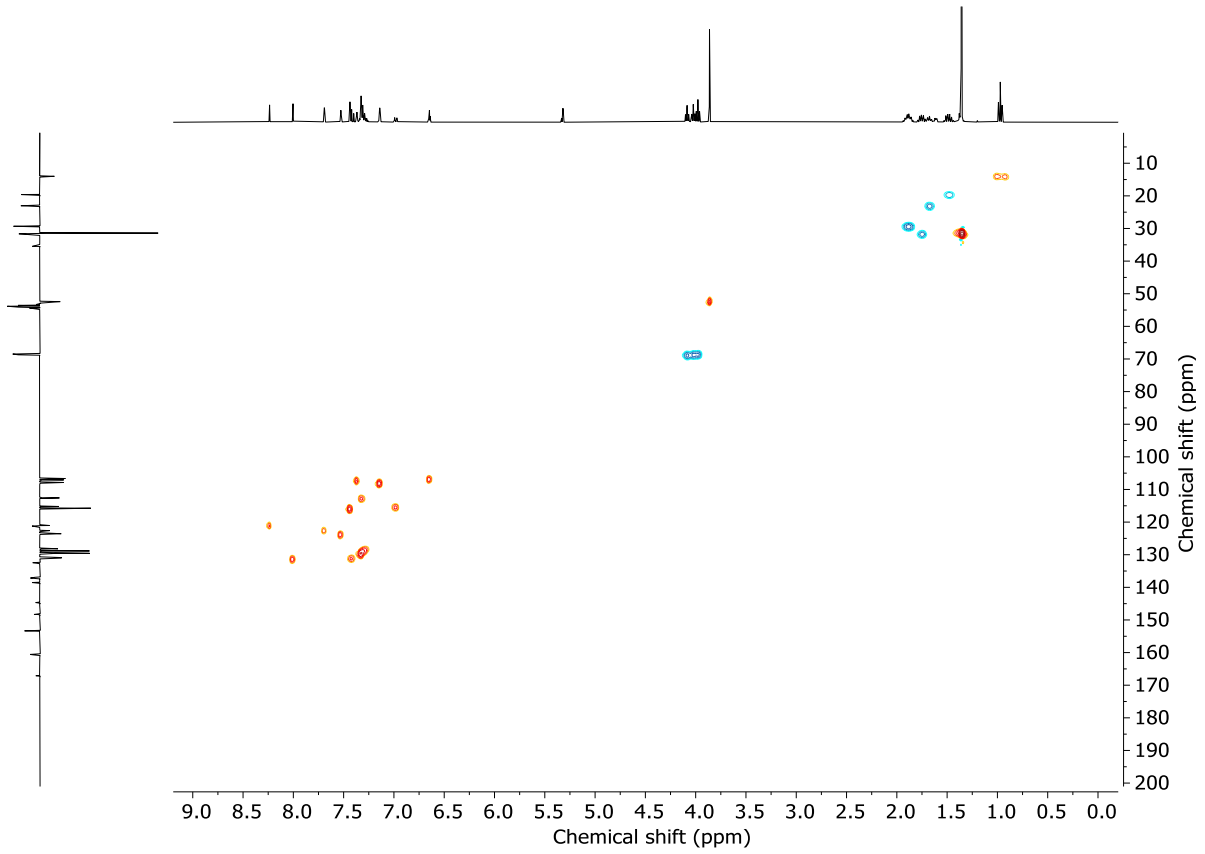

Figure S169: HSQC NMR (CD_2Cl_2, 298 K) of *(E)*-**S30**.

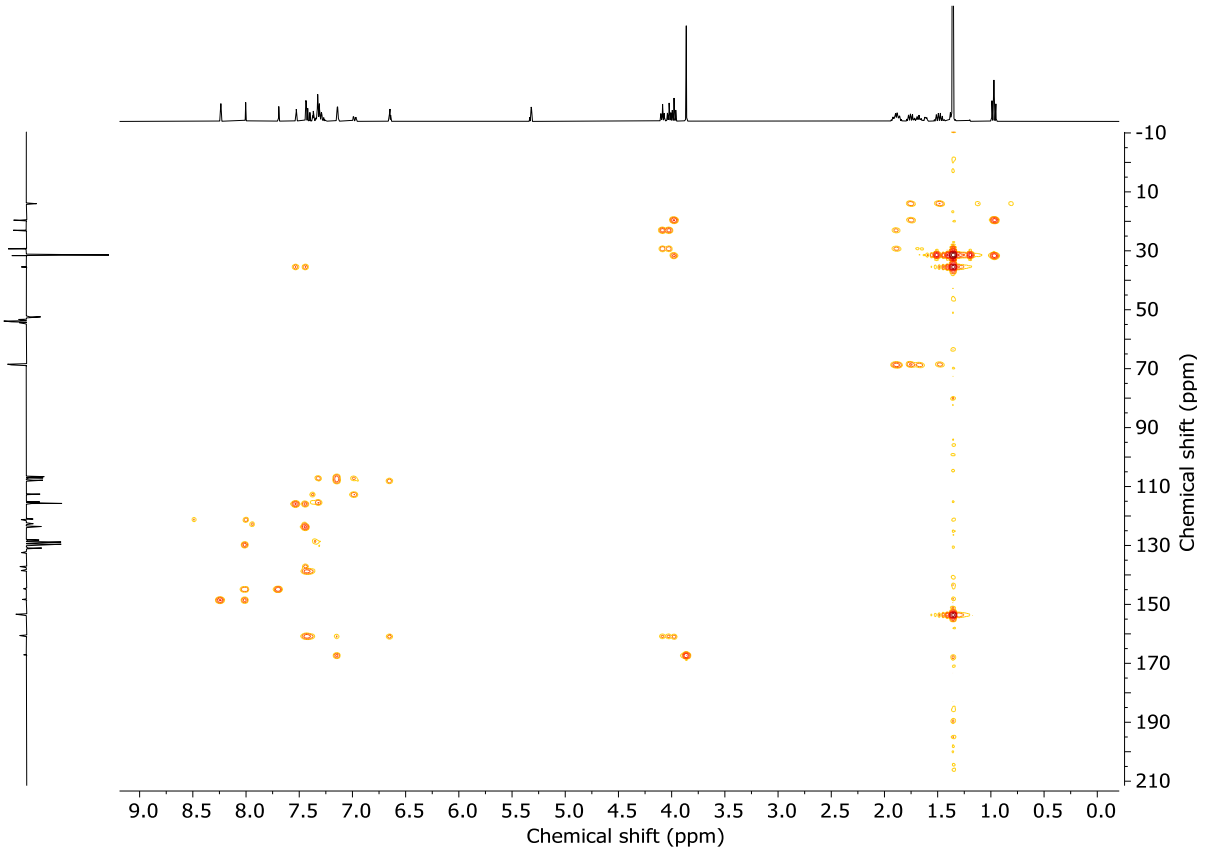

Figure S170: HMBC NMR (CD_2Cl_2, 298 K) of *(E)*-**S30**.

Pseudo-rotaxane *rac*-(*E*)-S29

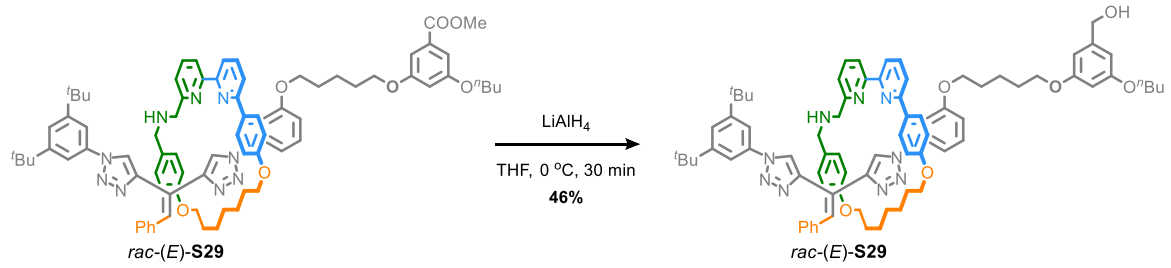

Methyl ester-rotaxane *rac*-(*E*)-**S28** (11 mg, 0.0085 mmol) was dissolved in THF (1.0 mL), cooled to 0 °C and $LiAlH_4$ (1 M in THF, 0.08 mL, 0.08 mmol) was added dropwise. After 30 min, the reaction mixture was quenched by slow addition of EtOAc (0.2 mL), stirred at 0 °C for 5 min and warmed to rt. Sat. Rochelle $salt_{(aq)}$ (1 mL) was added and the mixture stirred for 10 min. H_2O (10 mL) was added, the layers separated, and the aqueous layer extracted with CH_2Cl_2 (3 x 10 mL). The combined organic layers were dried (Na_2SO_4) and concentrated *in vacuo*. Chromatography (CH_2Cl_2-MeOH 99:1 to 9:1) gave kinetically trapped pseudorotaxane *rac*-(*E*)-**S29** as a colourless film (5 mg, 46%).

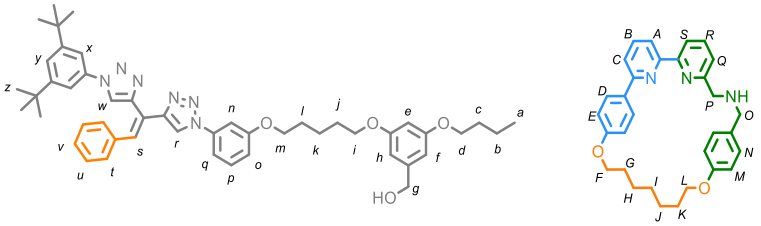

^{1}H NMR (400 MHz, CD_2Cl_2) δ 9.34 (s, 1H, H_r), 7.72 (s, 1H, H_w), 7.60 (t, *J* = 7.8, 1H, H_B), 7.57 (s, 1H, H_s), 7.52 (t, *J* = 7.7, 1H, H_R), 7.43 (t, *J* = 1.7, 1H, H_y), 7.35 (dd, *J* = 7.8, 0.9, 1H, H_C), 7.32 – 7.25 (m, 3H, H_q, H_n, H_Q), 7.25 – 7.10 (m, 9H, H_t, H_u, H_v, H_x, H_A, H_S), 7.12 - 7.03 (d, 3H, H_p, H_D), 6.72 (d, *J* = 8.5, 2H, H_N), 6.67 (ddd, *J* = 8.3, 2.4, 0.9, 1H, H_o), 6.48 – 6.45 (m, 2H, H_f, H_h), 6.41 (d, *J* = 8.8, 2H, H_E), 6.31 (t, *J* = 2.3, 1H, H_e), 6.27 (d, *J* = 8.6, 2H, H_M), 4.54 (s, 2H, H_g), 4.20 – 4.03 (m, 3H, H_F, 1 of H_L), 3.95 – 3.90 (m, 3H, H_d, 1 of H_L,), 3.83 (dt, *J* = 9.3, 6.4, 1H, 1 of H_i), 3.76 (dt, *J* = 9.3, 6.4, 1H, 1 of H_i) 3.68 (d, *J* = 13.3, 1H, 1 of H_O), 3.63 – 3.46 (m, 3H, 1 of H_O, H_P), 3.44 (dt, *J* = 9.3, 6.5, 1H, 1 of H_m), 3.33 (dt, *J* = 9.3, 6.5, 1H, 1 of H_m), 2.05 – 1.40 (m, 16H, H_b, H_c, H_j, H_l, H_G, H_H, H_J, H_K), 1.37 – 1.25 (m, 22H, H_k, H_z, H_l), 0.97 (t, *J* = 7.4, 3H, H_a).

^{13}C NMR (101 MHz, CD_2Cl_2) δ 160.9, 160.8, 160.0, 159.6, 159.5, 158.1, 157.5 (x2), 157.1, 152.8, 147.4, 145.8, 144.4, 144.3, 138.5, 137.6, 137.4, 137.3, 136.6, 132.1, 129.7 (x2), 129.4, 129.2, 128.5, 128.4, 127.5, 123.5, 123.1, 123.0, 121.7, 121.4, 120.8, 120.6, 120.3, 114.8, 114.6, 114.5, 114.1, 111.9, 105.4 (x2), 105.3, 100.7, 68.2, 68.1, 67.9, 67.6, 65.7, 65.4, 54.1 (x2), 35.4, 31.8, 31.5, 29.7, 29.5, 29.2, 29.2, 28.5, 26.2, 26.1, 22.8, 19.7, 14.0.

LR-ESI-MS (+ve): *m/z* = 1262.7 $[M + H]^+$ calc. for $C_{79}H_{92}N_9O_6$ 1262.7.

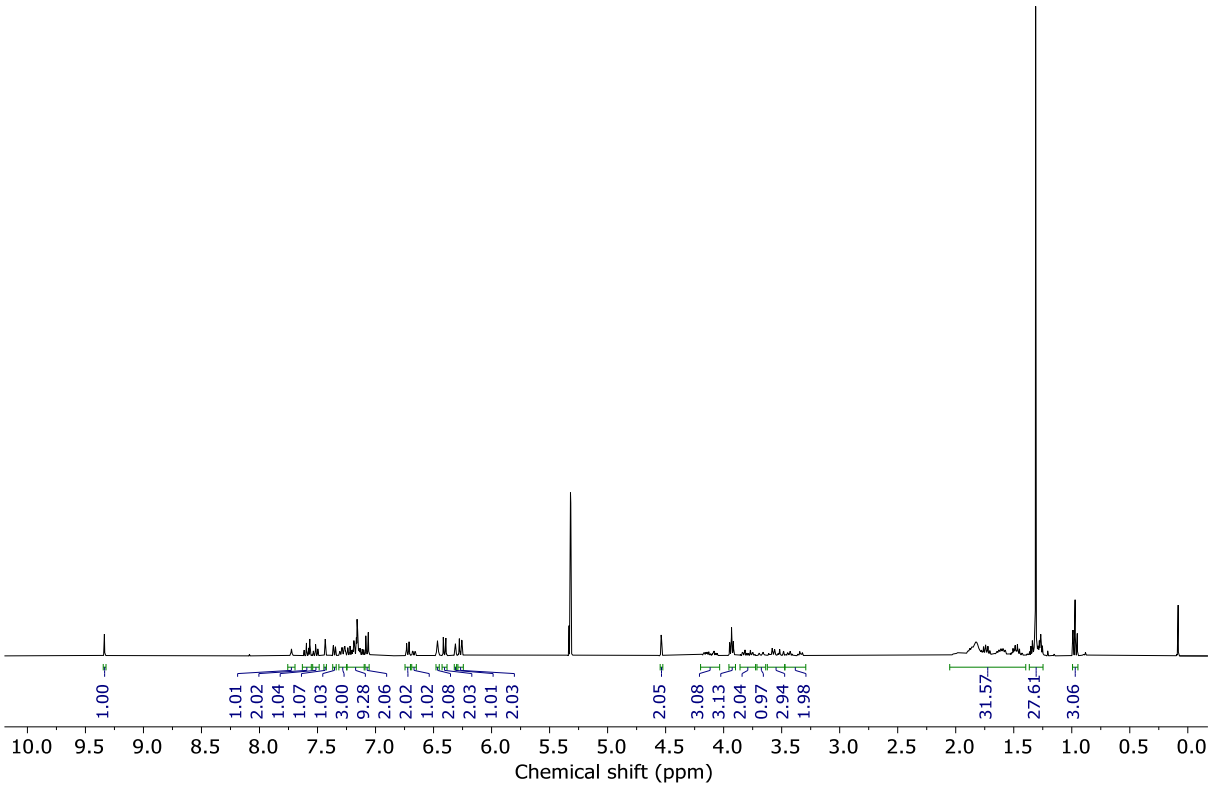

Figure S171: ^{1}H NMR (CD_2Cl_2, 400 MHz, 298 K) of *rac*-(*E*)-**S29**.

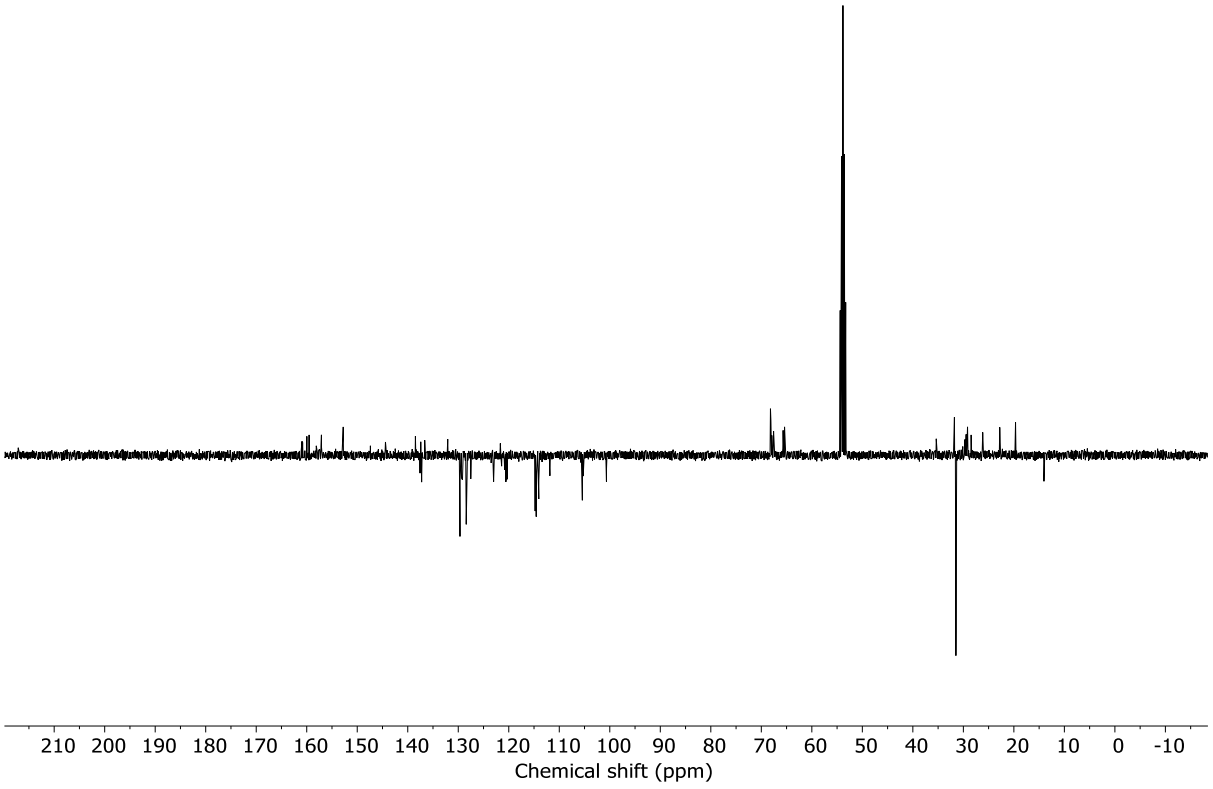

Figure S172: JMOD NMR (CD_2Cl_2, 101 MHz, 298 K) of *rac*-(*E*)-**S29**.

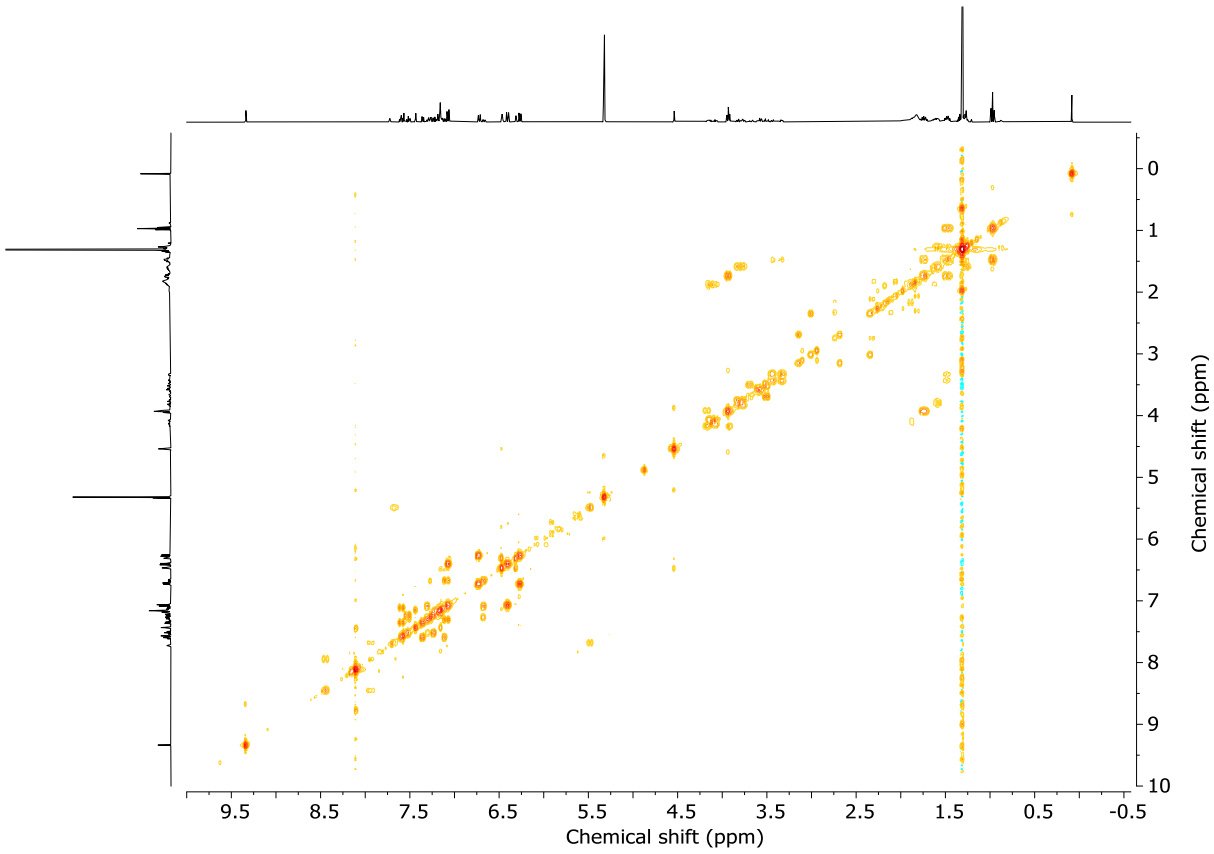

Figure S173: COSY NMR (CD_2Cl_2, 298 K) of *rac*-(*E*)-**S29**.

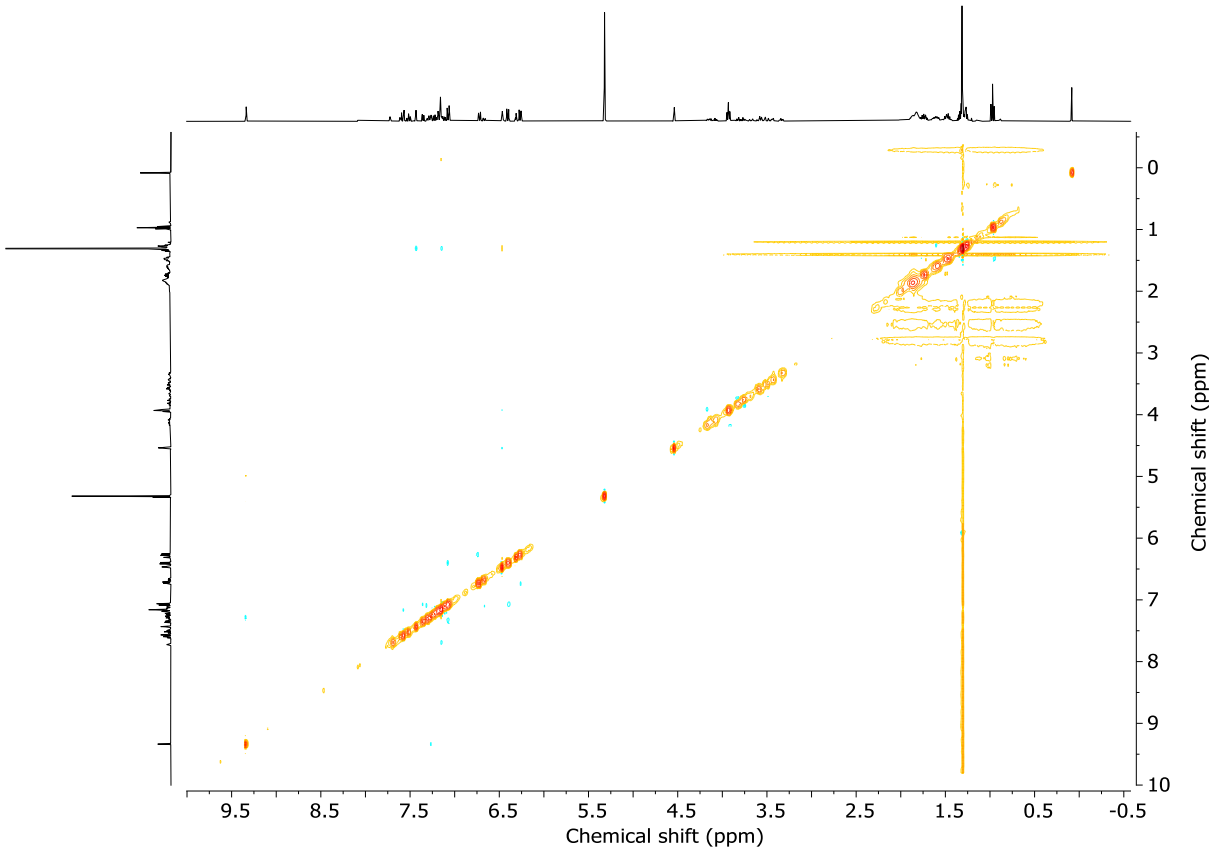

Figure S174: NOESY NMR (CD_2Cl_2, 298 K) of *rac*-(*E*)-**S29**.

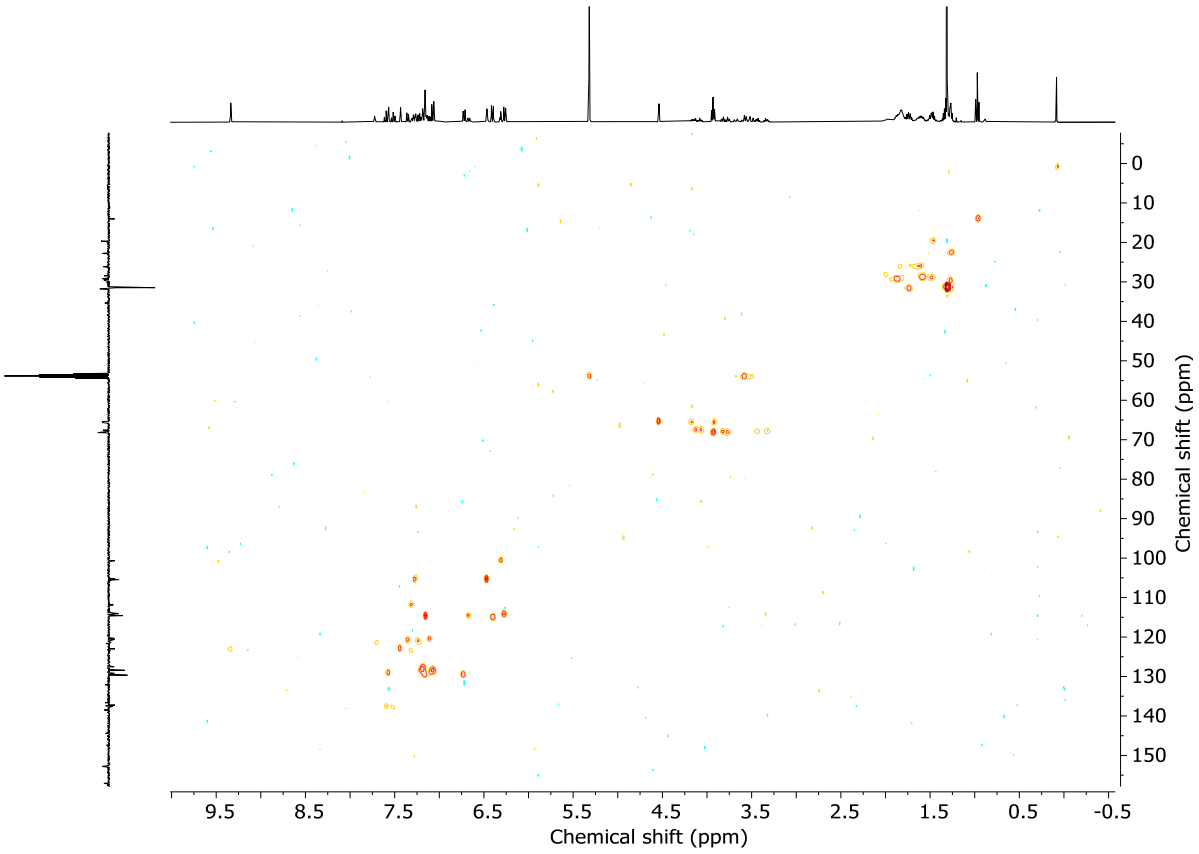

Figure S175: HSQC NMR (CD_2Cl_2, 298 K) of *rac*-(*E*)-**S29**.

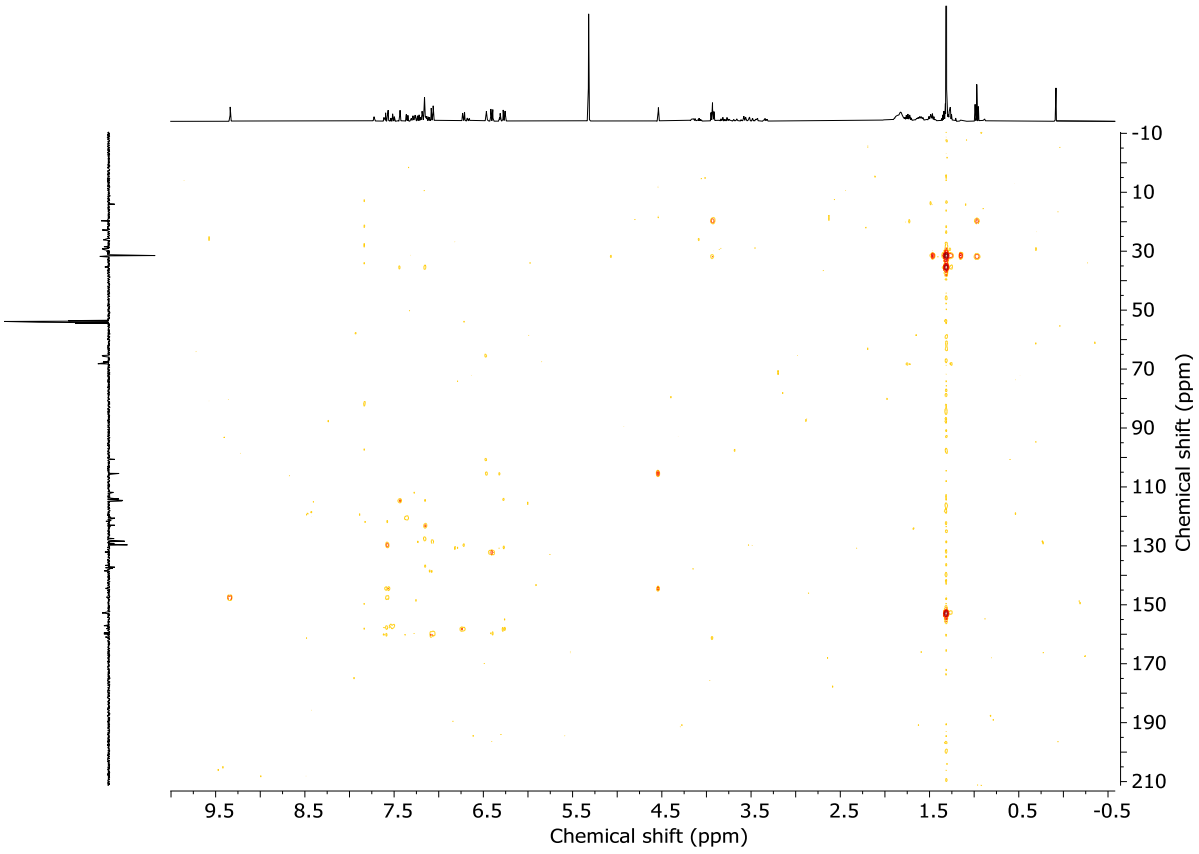

Figure S176: HMBC NMR (CD_2Cl_2, 298 K) of *rac*-(*E*)-**S29**.

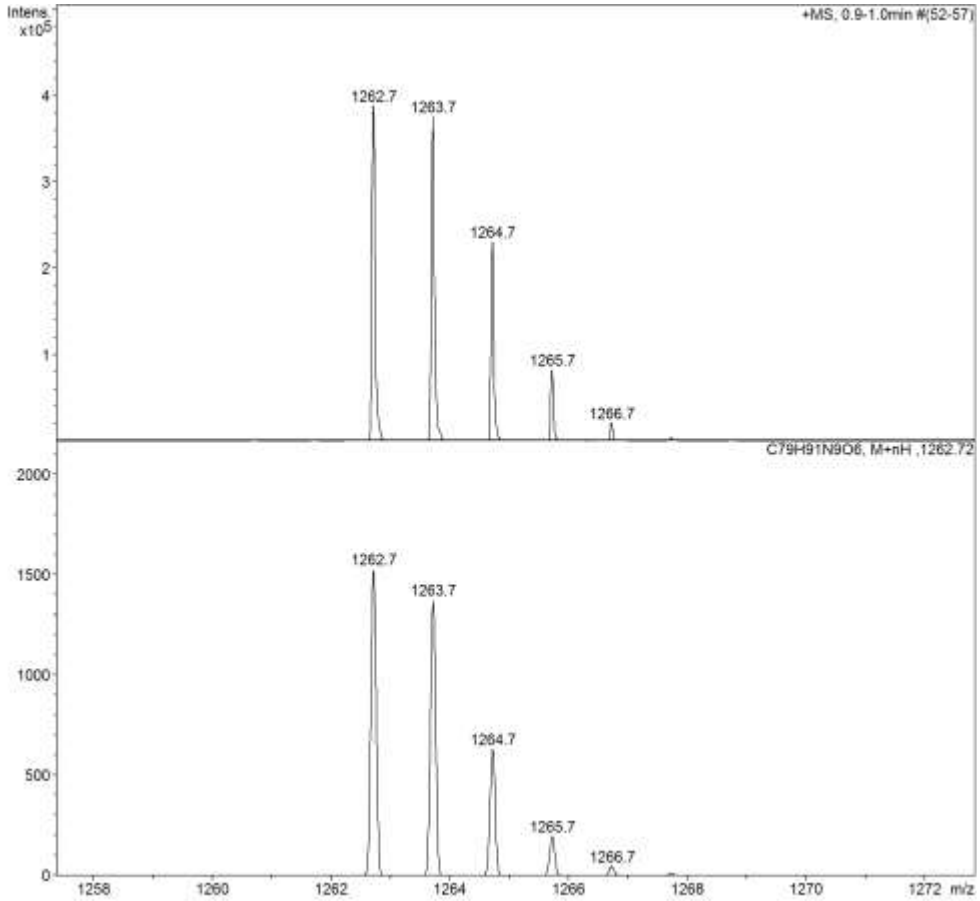

Figure S177: LRMS - Observed (top) and calculated (bottom) isotopic pattern for *rac*-(*E*)-**S29** $C_{79}H_{91}N_9O_6$.

Azide S31

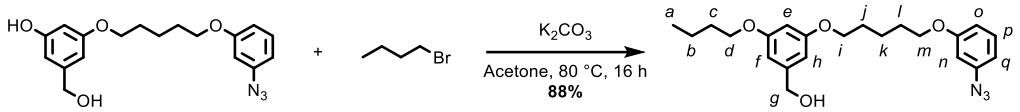

To a stirred solution of **S12** (0.15 g, 0.44 mmol) and 1-bromobutane (0.14 mL, 1.3 mmol) at 80 °C in acetone (4.4 mL) was added K_2CO_3 (0.30 g, 2.2 mmol), and the resulting mixture stirred for 29 h. The mixture was cooled to rt, filtered through Celite® and concentrated *in vacuo*. Chromatography (*n*hexane-Et_2O 100:0 to 1:1) gave compound **S31** as a pale yellow oil (153 mg, 88%).

^{1}H NMR (400 MHz, $CDCl_3$) δ 7.24 (t, *J* = 8.2, 1H, ***H***$_p$), 6.68 (ddd, *J* = 8.3, 2.4, 0.9, 1H, ***H***$_q$), 6.63 (ddd, *J* = 8.1, 2.2, 0.9, 1H, ***H***$_o$), 6.55 (t, *J* = 2.2, 1H, ***H***$_n$), 6.52 – 6.49 (m, 2H, ***H***$_f$, ***H***$_h$), 6.38 (t, *J* = 2.3, 1H, ***H***$_e$), 4.62 (d, *J* = 4.1, 2H, ***H***$_g$), 3.98 (app. td, *J* = 6.4, 1.3, 4H, ***H***$_i$, ***H***$_m$), 3.95 (t, *J* = 6.5, 2H, ***H***$_d$), 1.89 – 1.81 (m, 4H, ***H***$_j$, ***H***$_l$), 1.79 – 1.70 (m, 2H, ***H***$_c$), 1.68 – 1.60 (m, 2H, ***H***$_k$), 1.53 – 1.44 (m, 2H, ***H***$_b$), 0.97 (t, *J* = 7.4, 3H, ***H***$_a$).

^{13}C NMR (101 MHz, $CDCl_3$) δ 160.7, 160.6, 160.4, 143.4, 141.4, 130.6, 111.4, 111.3, 105.7, 105.3, 105.2, 100.7, 68.1, 67.9 (x2), 65.6, 31.5, 29.1, 29.1, 22.9, 19.4, 14.0.

HR-ESI-MS (+ve): *m/z* = 422.2045 $[M + Na]^+$ calc. for $C_{22}H_{29}N_3NaO_4$ 422.2050.

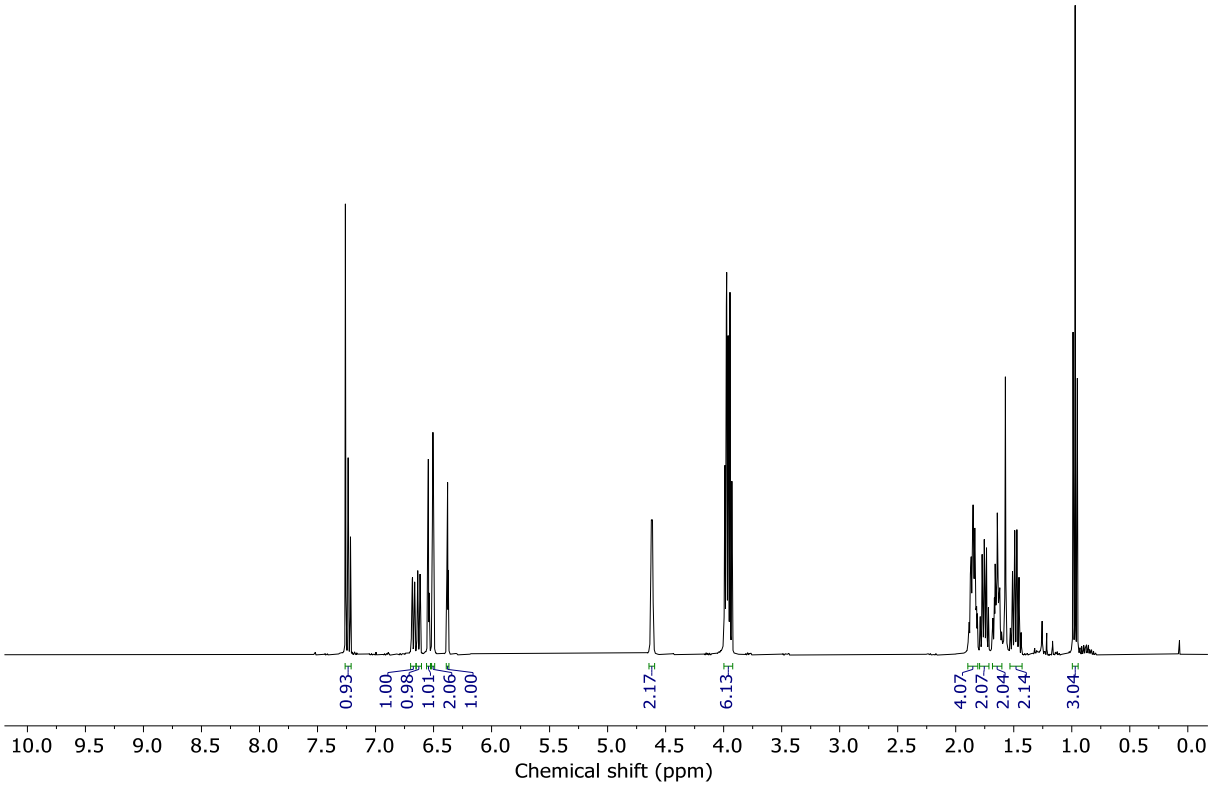

Figure S178: ^{1}H NMR ($CDCl_3$, 400 MHz, 298 K) of **S31**.

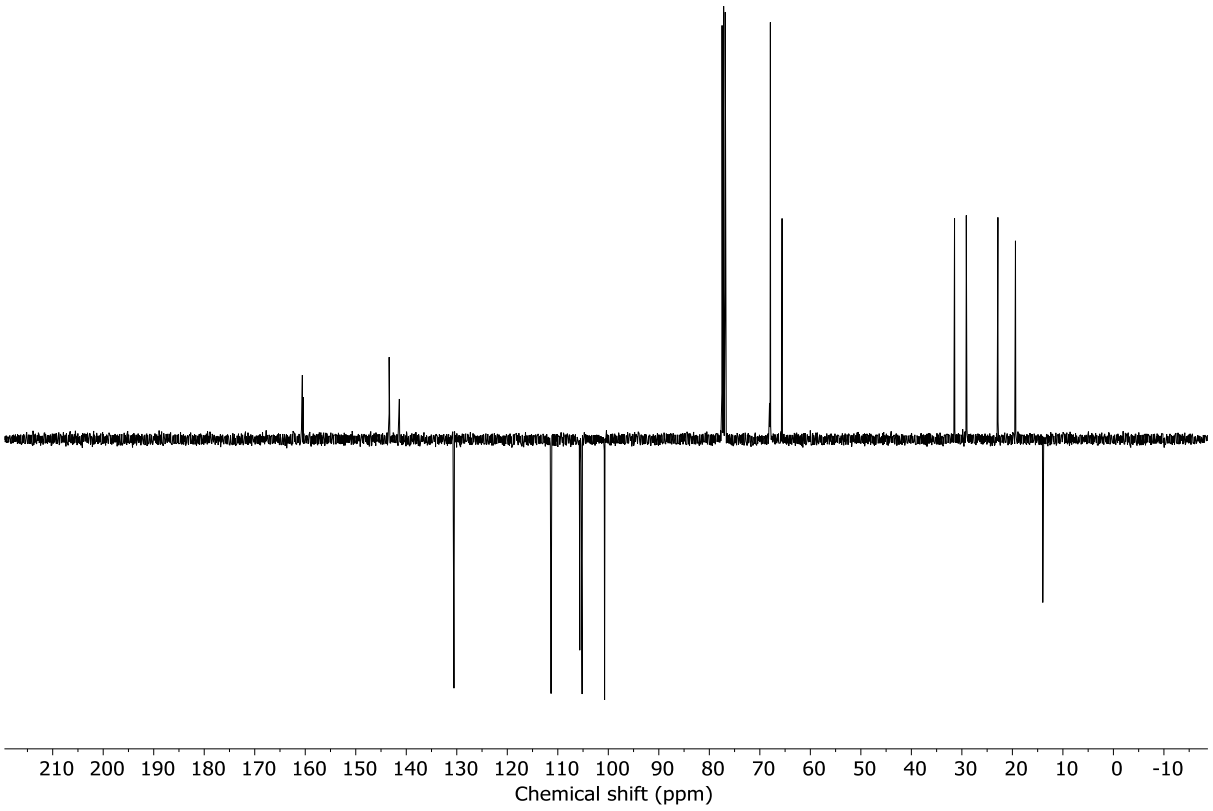

Figure S179: JMOD NMR ($CDCl_3$, 101 MHz, 298 K) of **S31**.

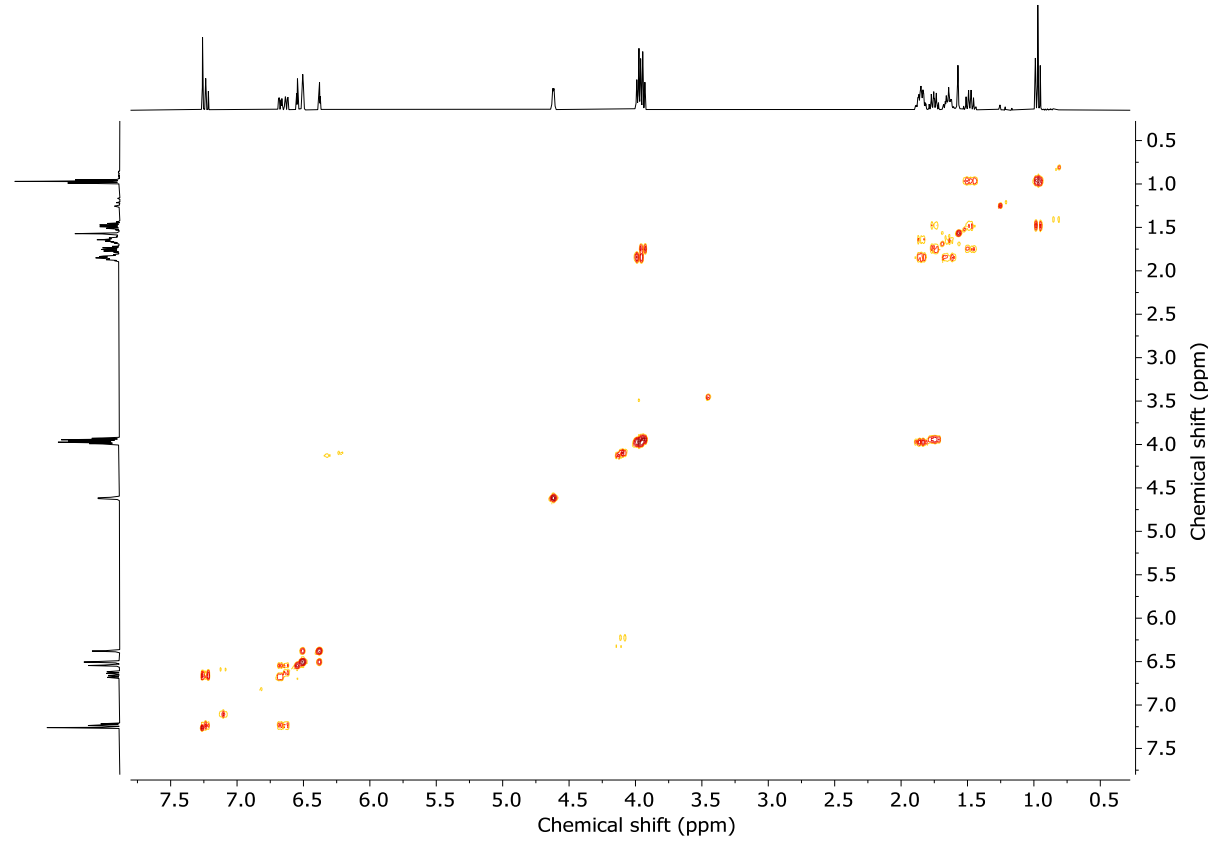

Figure S180: COSY NMR ($CDCl_3$, 298 K) of **S31**.

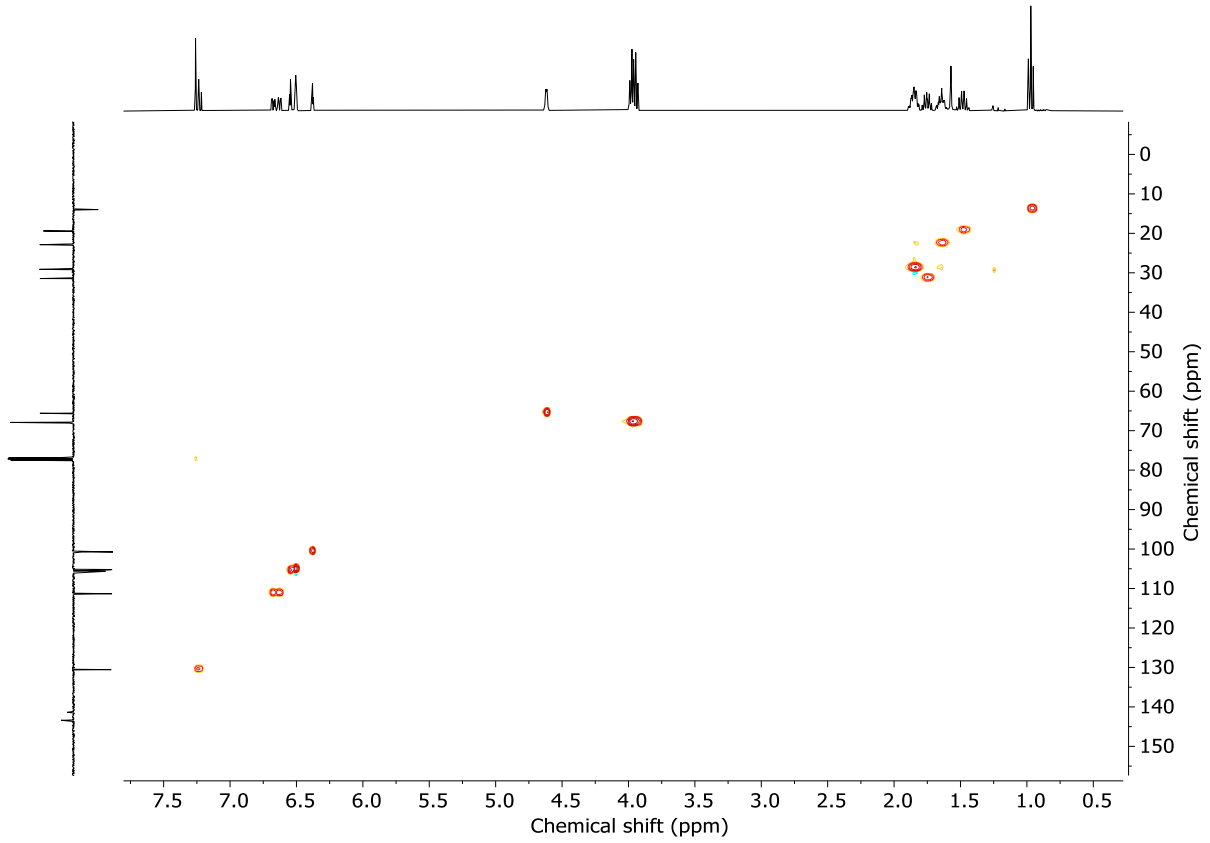

Figure S181: HSQC NMR ($CDCl_3$, 298 K) of **S31**.

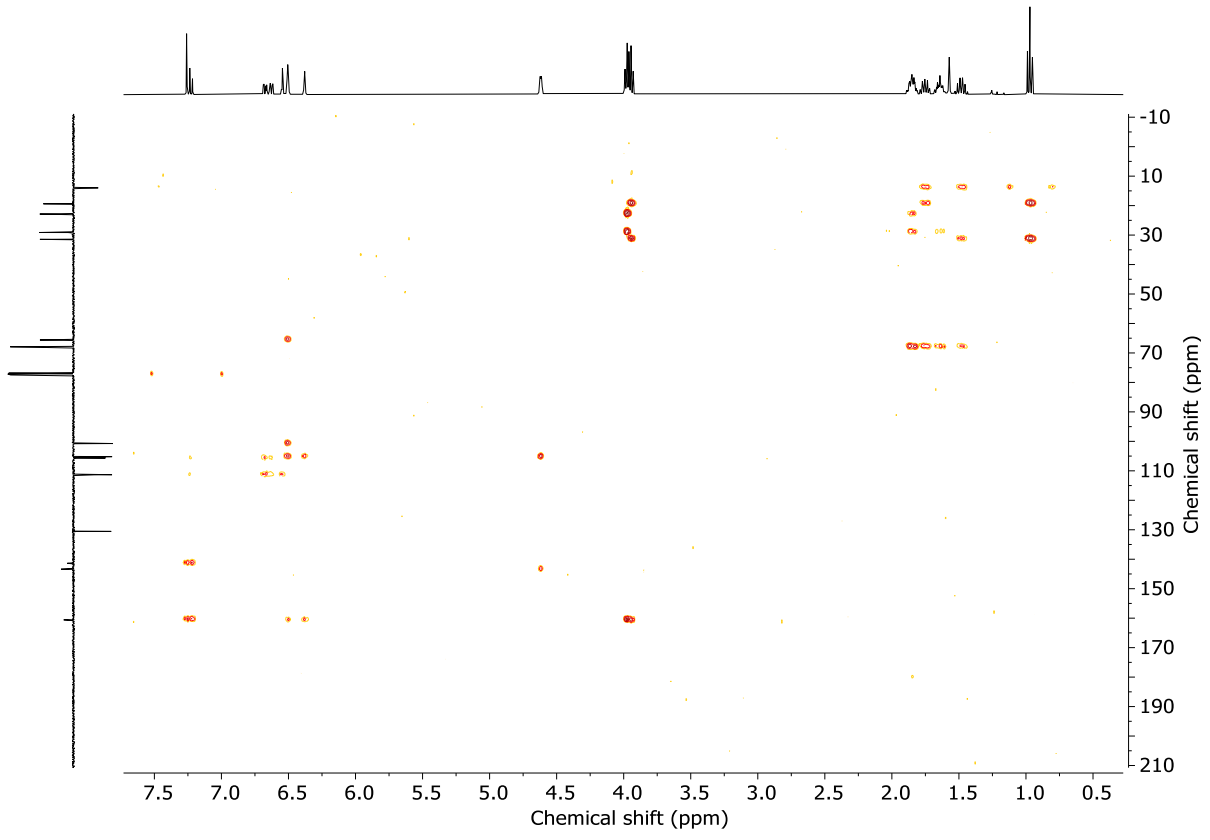

Figure S182: HMBC NMR ($CDCl_3$, 298 K) of **S31**.

Non-interlocked axle (*E*)-S32

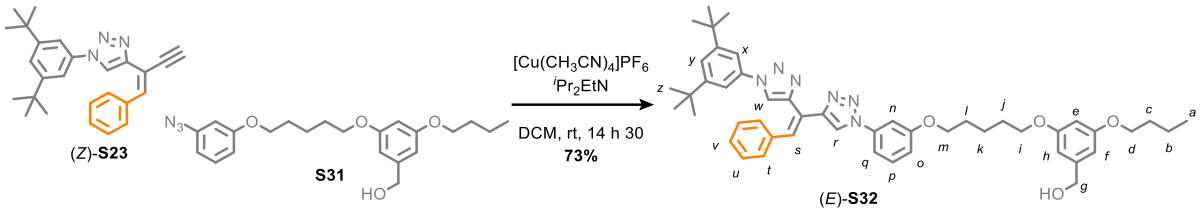

Alkyne (*Z*)-**S23** (25 mg, 0.065 mmol), azide **S31** (24 mg, 0.059 mmol), $[Cu(CH_3CN)_4]PF_6$ (4 mg, 0.01 mmol) and TBTA (4 mg, 0.008 mmol) were dissolved in CH_2Cl_2 (1.0 mL), Et_3N (41 μL, 0.24 mmol) was added and the reaction mixture stirred at 30˚C for 15 h. The reaction mixture was diluted in EtOAc (40 mL) and the organic layer washed with EDTA-$NH_{3(aq)}$ (0.1 M, 3 x 40 mL), H_2O (40 mL), NH_4Cl (1 M, 3 x 40 mL) and brine (40 mL). The organic layer was dried (Na_2SO_4) and concentrated *in vacuo*. Chromatography (^{n}hexane-Et_2O 100 : 0 to 8 : 2) afforded (*E*)-**S32** as a pale red powder (42 mg, 90%).

^{1}H NMR (400 MHz, CD_2Cl_2) δ 8.22 (s, 1H, $\boldsymbol{H}_r$), 8.00 (s, 1H, $\boldsymbol{H}_s$), 7.68 (s, 1H, $\boldsymbol{H}_w$), 7.52 (t, *J* = 1.7, 1H, $\boldsymbol{H}_y$), 7.43 (d, *J* = 1.7, 2H, $\boldsymbol{H}_x$), 7.42 (t, *J* = 8.2, 1H, $\boldsymbol{H}_p$), 7.36 (t, *J* = 2.2, 1H, $\boldsymbol{H}_n$), 7.35 – 7.24 (m, 6H, $\boldsymbol{H}_q$, $\boldsymbol{H}_t$, $\boldsymbol{H}_u$, $\boldsymbol{H}_v$), 6.98 (ddd, *J* = 8.3, 2.5, 1.0, 1H, $\boldsymbol{H}_o$), 6.50 - 6.46 (m, 2H, $\boldsymbol{H}_f$, $\boldsymbol{H}_h$), 6.35 (t, *J* = 2.3, 1H, $\boldsymbol{H}_e$), 4.58 (d, *J* = 5.5, 2H, $\boldsymbol{H}_g$), 4.08 (t, *J* = 6.4, 2H, $\boldsymbol{H}_m$), 3.98 (t, *J* = 6.4, 2H, $\boldsymbol{H}_i$), 3.93 (t, *J* = 6.5, 2H, $\boldsymbol{H}_d$), 1.93 – 1.81 (m, 5H, $\boldsymbol{H}_{OH}$, $\boldsymbol{H}_j$, $\boldsymbol{H}_l$), 1.77 – 1.62 (m, 4H, $\boldsymbol{H}_c$, $\boldsymbol{H}_k$), 1.52 – 1.42 (m, 2H, $\boldsymbol{H}_b$), 1.35 (s, 18H, $\boldsymbol{H}_z$), 0.96 (t, *J* = 7.4, 3H, $\boldsymbol{H}_a$).

^{13}C NMR (101 MHz, CD_2Cl_2) δ 161.0, 160.9, 160.6, 153.4, 148.3, 144.7, 144.1, 138.6, 137.2, 137.0, 131.1, 130.9, 129.6, 128.9, 128.2, 123.6, 122.6, 121.2, 121.1, 115.8, 115.3, 112.6, 107.2, 105.3, 105.3, 100.7, 68.8, 68.2, 68.2, 65.5, 35.5, 31.7, 31.4, 29.4, 29.3, 23.0, 19.7, 14.0.

HR-ESI-MS (+ve): *m/z* = 783.4593 $[M + H]^+$ calc. for $C_{48}H_{59}N_6O_4$ 783.4592.

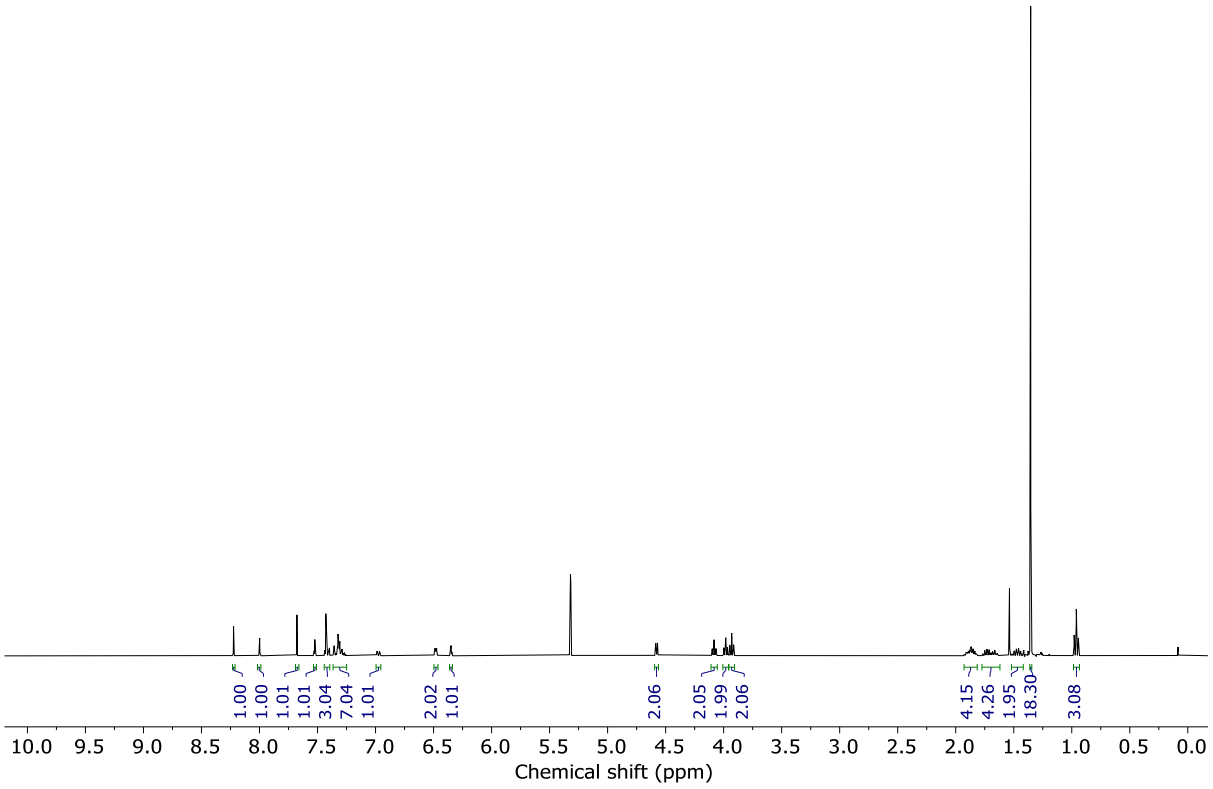

Figure S183: ^{1}H NMR (CD_2Cl_2, 400 MHz, 298 K) of (*E*)-**S32**.

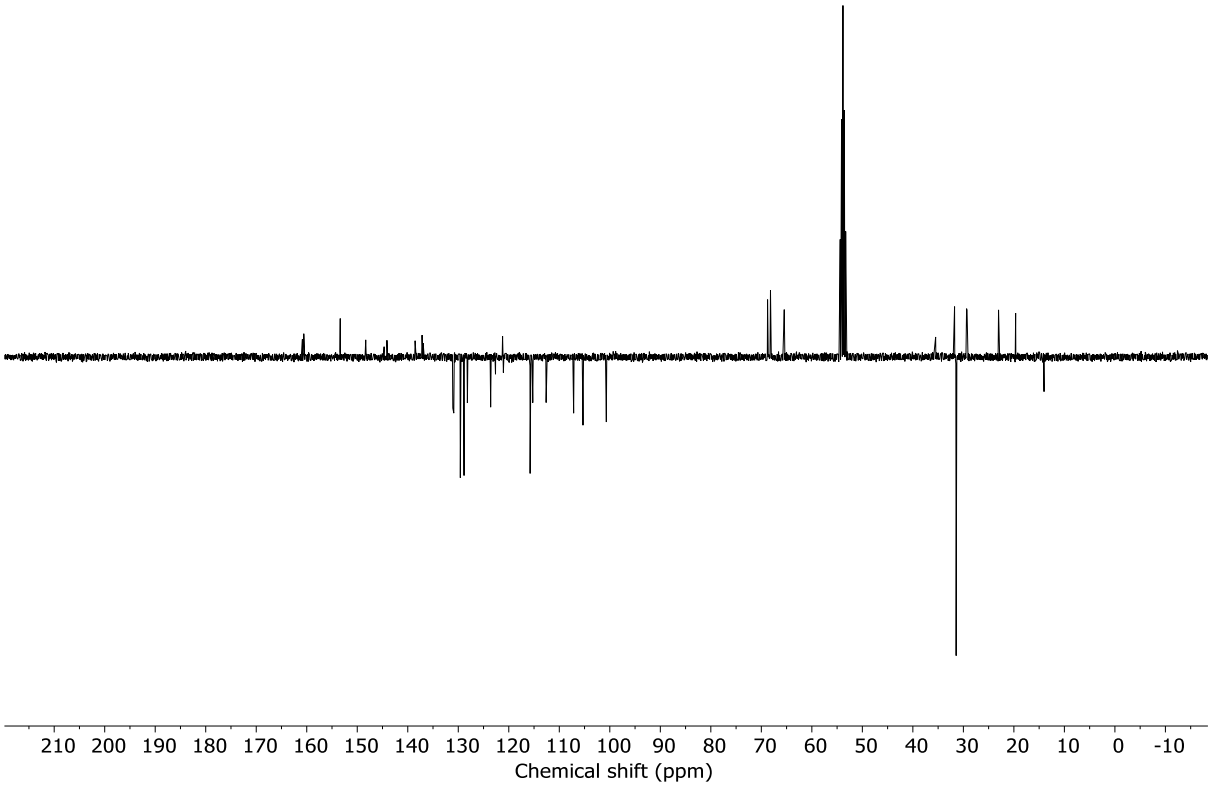

Figure S184: JMOD NMR (CD_2Cl_2, 101 MHz, 298 K) of (*E*)-**S32**.

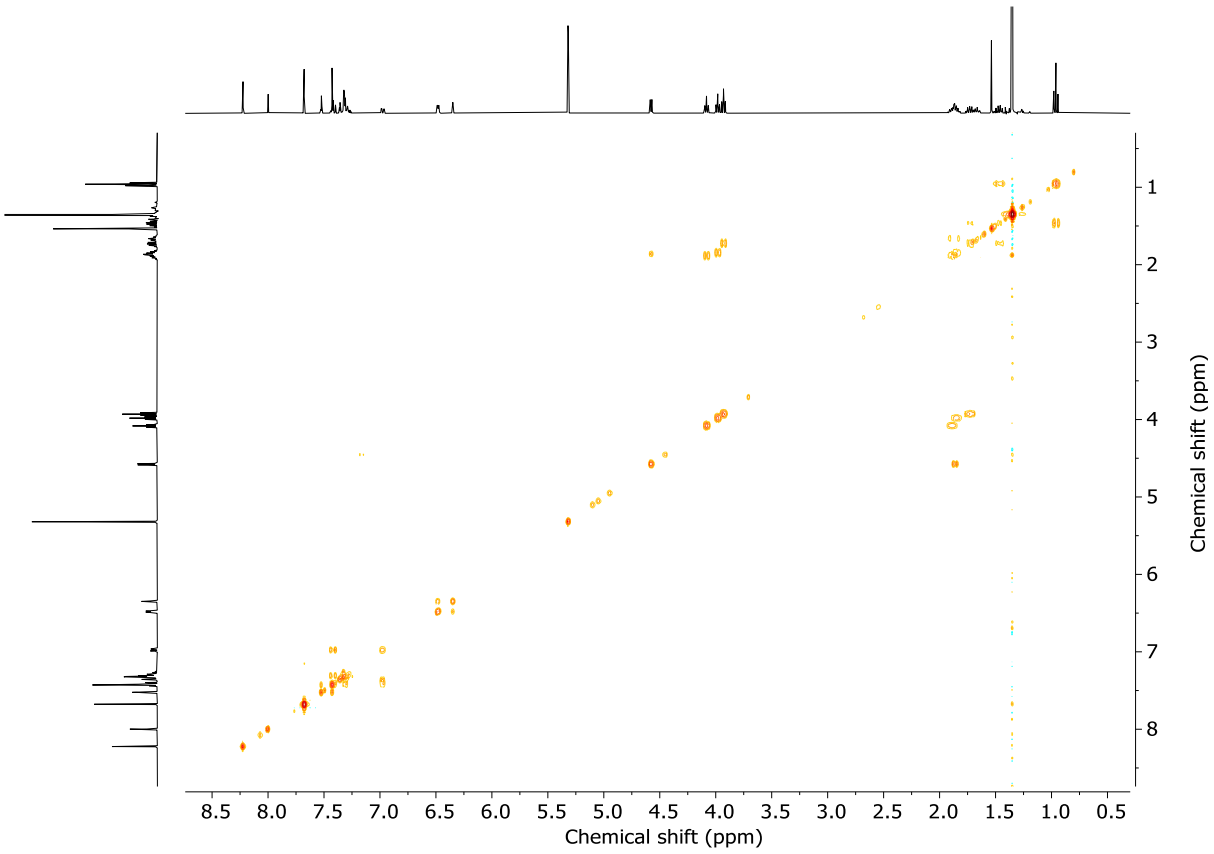

Figure S185: COSY NMR (CD_2Cl_2, 298 K) of (*E*)-**S32**.

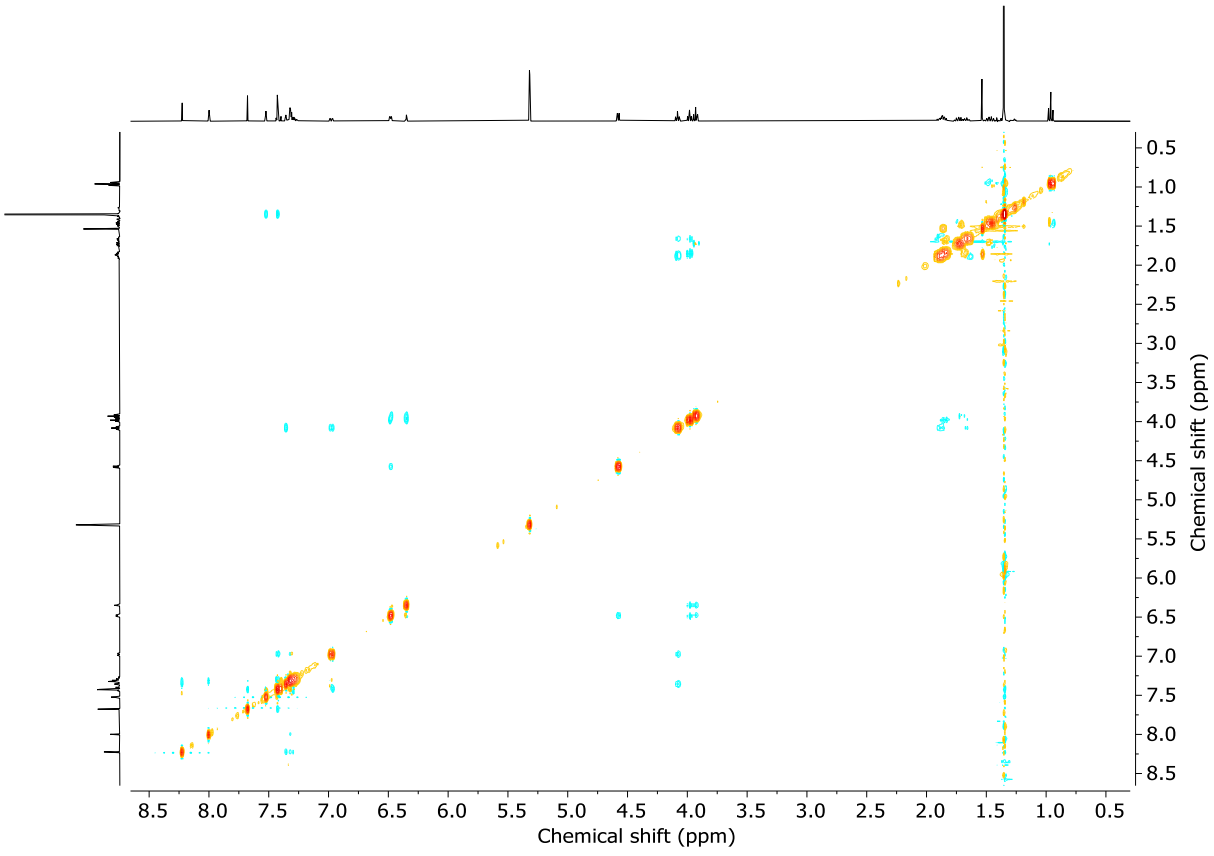

Figure S186: NOESY NMR (CD_2Cl_2, 298 K) of (*E*)-**S32**.

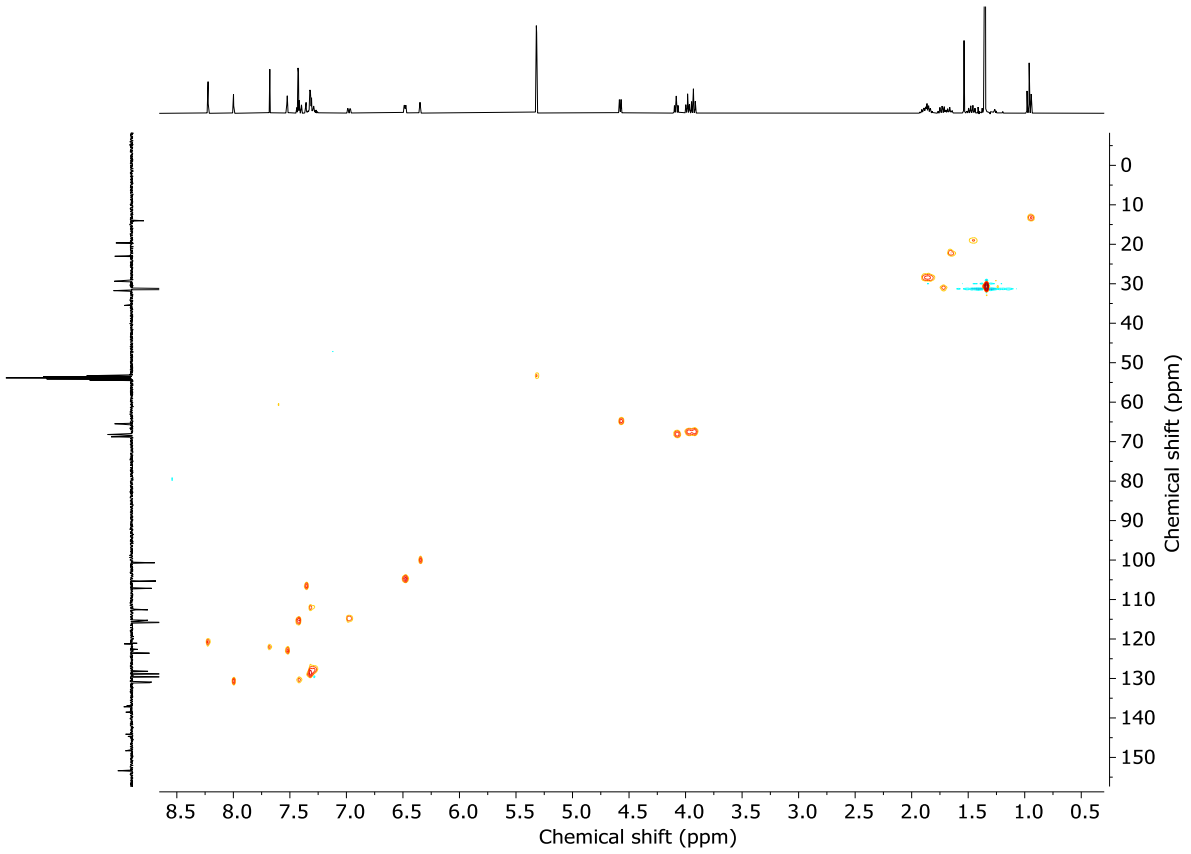

Figure S187: HSQC NMR (CD_2Cl_2, 298 K) of (*E*)-**S32**.

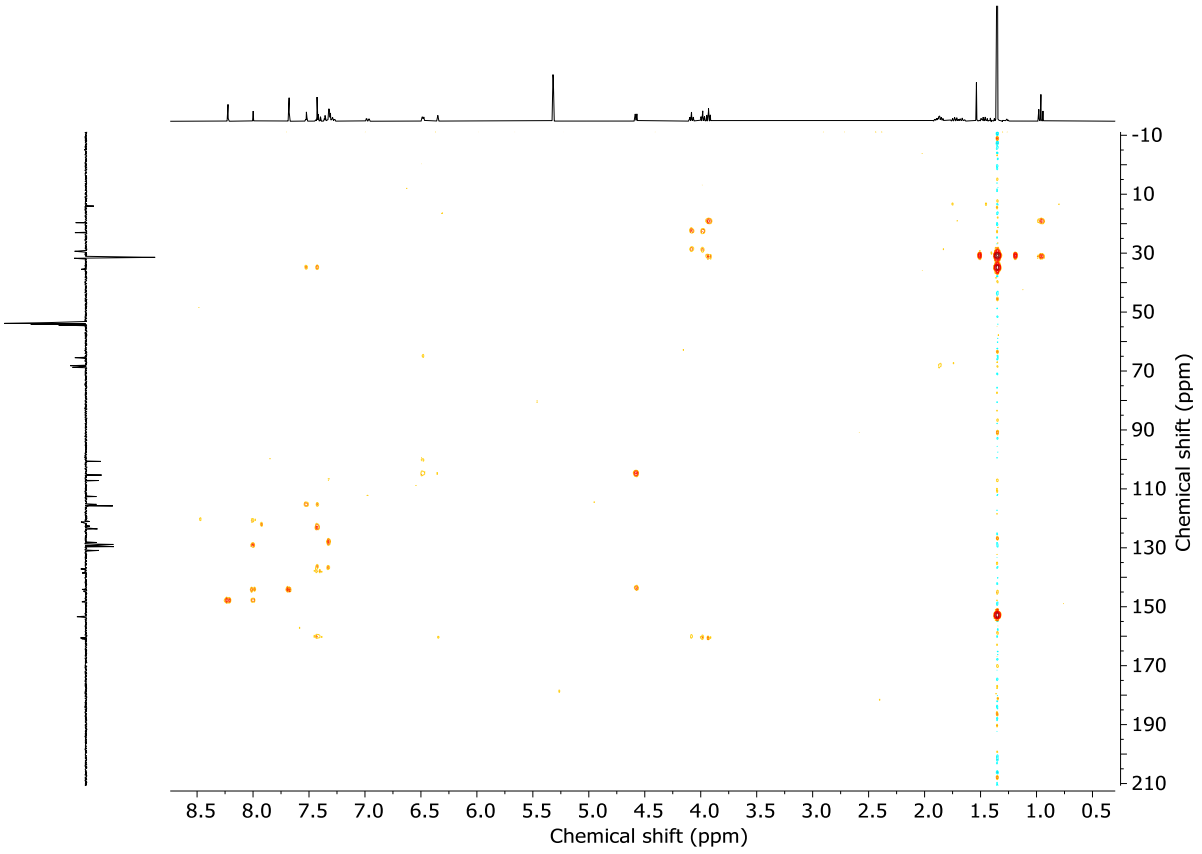

Figure S188: HMBC NMR (CD_2Cl_2, 298 K) of (*E*)-**S32**.

7. Racemisation of Catenane 5

7.1. Racemisation of catenane 5

As noted above, the enantiomers of catenane **5** underwent racemisation when heated in CD_2Cl_2 (Scheme S9); CSP-HPLC analysis indicated that the enantiopurity fell from 98% *ee* for both to (S_{mp})-**5** and (R_{mp})-**5** to 93% and 91% *ee* respectively, based on the peaks assigned as $E_{co\text{-}c}$ (Figure S129). Further heating of (R_{mp})-**5** (323 K, CD_2Cl_2) in an NMR tube fitted with a J Young tap sealed NMR tube led to further erosion of stereopurity; after 4 days the stereopurity of ($E_{co\text{-}c}$)-**5** was found to fall to 86% *ee* from 91% *ee* and after a further 6 days a value of 83% *ee* was obtained (Figure 189). The loss of enantipurity was accompanied by noticeable decomposition; a small but significant peak was observed that contains the molecular ion corresponding to non-interlocked bipyridine macrocycle **S20**.

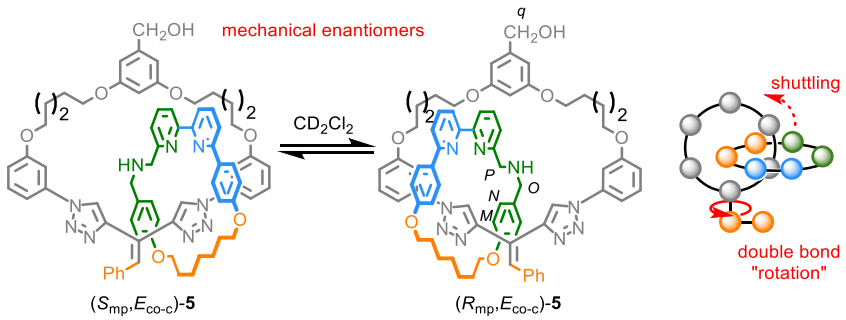

Scheme S9: The racemisation process observed and schematic of the processes that must take place for this to occur.

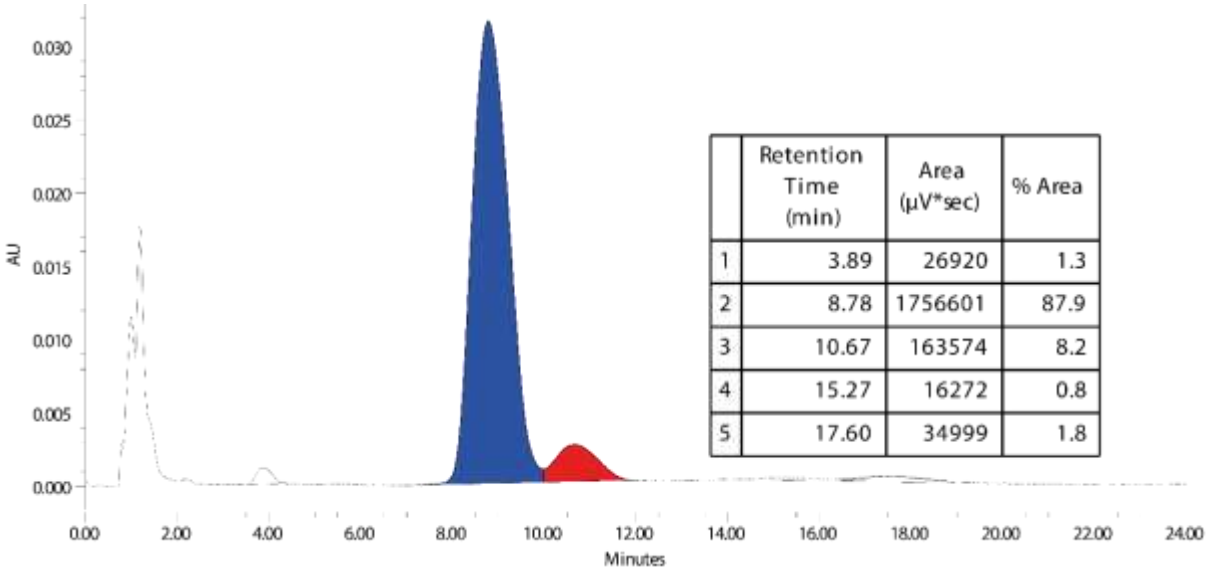

	Retention Time (min)	Area (µV*sec)	% Area
1	3.89	26920	1.3
2	8.78	1756601	87.9
3	10.67	163574	8.2
4	15.27	16272	0.8
5	17.60	34999	1.8

Figure 189: CSP-HPLC (loaded in Et_2O, Chiralpak IK, 40 ˚C, 125 BarG, isocratic 50 : 50 MeOH : CO_2 (0.1% v/v NH_3), 4 mL.min^{-1}, 1 mL injected) of (R_{mp},$E_{co\text{-}c}$)-**5** after heating for 10 days at 323 K. The peak at 3.89 was found to contain a mass ion whose m/z corresponds to non-interlocked macrocycle **S20**.

Interestingly, CSP-HPLC analysis of the samples heated at 323 K also indicated the disappearance of the minor $Z_{co\text{-}c}$ diastereomer (Figure 189). ^{1}H NMR analysis of samples after heating at 323 K corroborated the disappearance of ($Z_{co\text{-}c}$)-**5** (Figure S190); signals attributed to this species were present after heating the sample at 303 K but largely absent after heating at 323 K. We also observed changes in the chemical shift of the protons in the bipyridine macrocycle (e.g. H_M, H_N, H_O, H_P) close to the amine unit, as well as changes

in the signal attributed to benzylic protons H_q of the triazole containing ring. We hypothesised that the observed changes may be due to the slow evolution of DCl by decomposition of the solvent. In keeping with this, filtration of the sample obtained after 10 days heating at 323 K through solid K_2CO_3 restored the appearance of the ^{1}H NMR spectrum of catenane **5**.

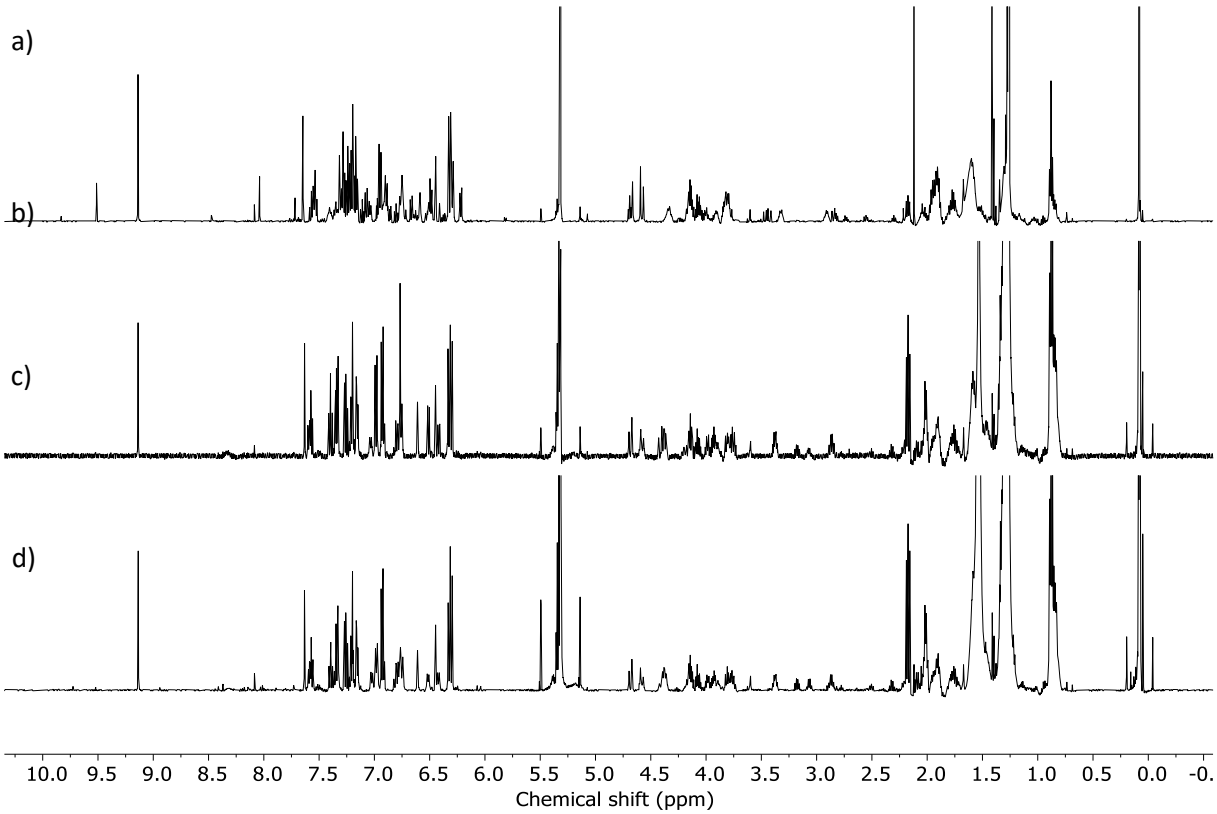

Figure S190: Stack plot of ^{1}H NMR (CD_2Cl_2, 500 MHz, 298 K) of (R_{mp},$E_{co\text{-}c}$)-**4** measured a) before heating at 30 ℃, b) the same sample after 144 h at 30 ℃, c) the same sample after 10 days at 50 ℃ and d) the same sample after filtration over K_2CO_3.

CD analysis of the samples of (R_{mp})-**5** after heating at 303 K for 6 days followed by 4 and 6 further days of heating at 323 K showed the expected slow decrease in the CD intensity (Figure S191). However, counterintuitively, the intensity of the CD signal obtained for the as-synthesised sample (98% *ee*) was lower than these samples assessed to have lower enantiopurity. Once again, this contradiction was explained by the protonation of catenane **5** on heating in CD_2Cl_2; when the sample obtained after heating at 323 K for 10 days was filtered through solid K_2CO_3 its intensity fell, suggesting that protonation of **5** increases its CD response. Furthermore, addition of AcOH (1 drop) to this sample led to a significant increase in its CD signal, which was once again reversed on addition of NEt_3 (2 drops).

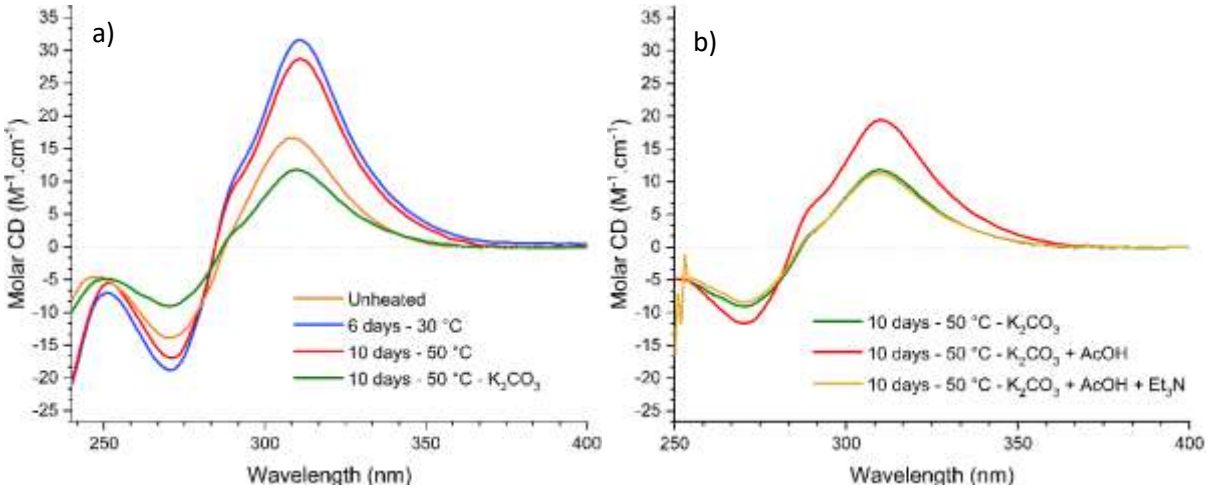

Figure S191: a) Evolution of the circular dichroism spectrum of (R_{mp},$E_{co\text{-}c}$)-**4** (Orange curve) unheated, (Blue curve) after 6 days at 30 °C, (Red curve) after 10 days at 50 °C and (Green curve) after 10 days at 50 °C and filtration over K_2CO_3, 21 µM in CH_3CN, 293 K; b) Evolution of the circular dichroism spectrum of (R_{mp},$E_{co\text{-}c}$)-**4** (Green curve) after 10 days at 50 °C and filtration over K_2CO_3, followed by successive addition of (Red curve) acetic acid and (Orange curve) triethylamine, 21 µM in CH_3CN, 293 K.

Taken together, the above experimental data confirms that catenane **5** undergoes a slow racemisation process on heating in CD_2Cl_2. This process slows over time and the co-conformational equilibrium also shifts to favour the $E_{co\text{-}c}$ isomer. We tentatively propose that all of these observations can be attributed to the evolution of DCl by decomposition of the solvent. The racemisation process itself can be rationalised by the reversible protonation of the alkene to produce a cation what can undergo single bond rotation to generate the opposite geometric isomer (Scheme S10). This could occur with or without reversible trapping of the stabilised cation by adventitious H_2O (see below). The shift in the co-conformational equilibrium can also be attributed to protonation of catenane **5**, which would also alter the rate of racemisation; protonation of the amine unit, which is expected to be thermodynamically favourable, can also be expected to alter the kinetics of double bond protonation.

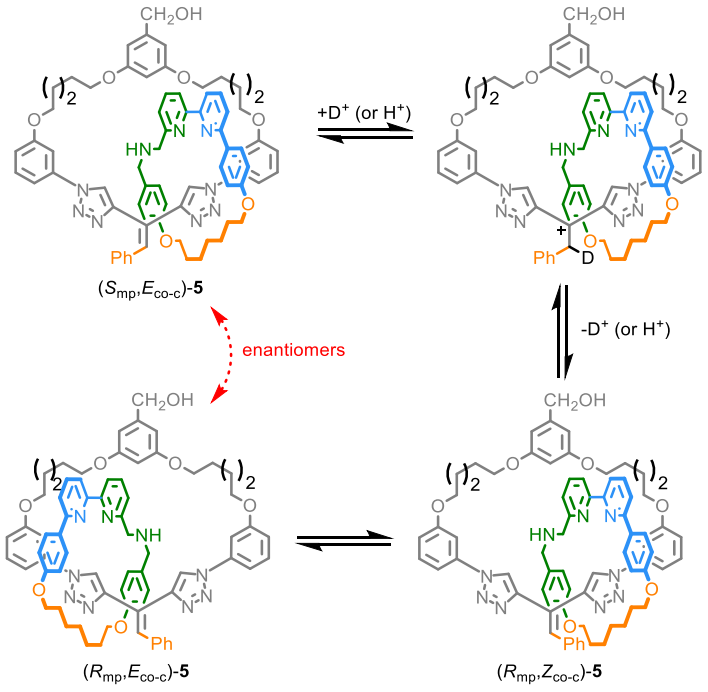

Scheme S10: Tentative mechanism of isomerisation for catenane **5**

In addition to the evidence presented above for the evolution of DCl *in situ* (changes in the ^{1}H NMR and CD spectra of catenane **5** after filtration through K_2CO_3), further support for this proposal was found through the synthesis and analysis of model rotaxane (R_{mp},$E_{co\text{-}c}$)-**S36** (Scheme S11) The bipyridine macrocycle of (R_{mp},$E_{co\text{-}c}$)-**S36** cannot exchange between the triazole compartments of the axle due to the steric bulk of the styrene moiety. However, on standing in $CDCl_3$ a second set of signals that are consistent with the (R_{mp},$Z_{co\text{-}c}$)-**S36** isomer were observed to appear, which is consistent with double bond isomerisation, which interestingly corresponds to inversion of both the co-conformational covalent stereogenic unit and the mechanical stereogenic unit. Further heating of this sample did not cause any further change, consistent with an equilibrium having been established.

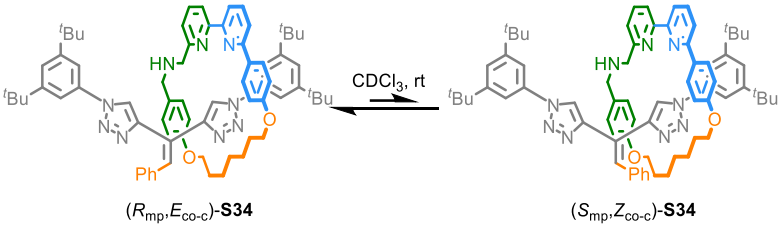

Scheme S11: Tentative mechanism of isomerisation for catenane **5**

Furthermore, during attempts to grow crystals suitable for x-ray diffraction from (S,R_{mp},$E_{co\text{-}c}$)-**S34**, the precursor to (R_{mp},$E_{co\text{-}c}$)-**S36**, we were surprised to obtain a structure that contains the product of double bond isomerisation (S,S_{mp},$Z_{co\text{-}c}$)-**S34** and hydration (S,$S_{co\text{-}mp}$)-**S39**) (see Section 3 for further details). The observation of these species lends support to the proposal that racemisation of catenane **5** may occur via reversible double bond hydration.

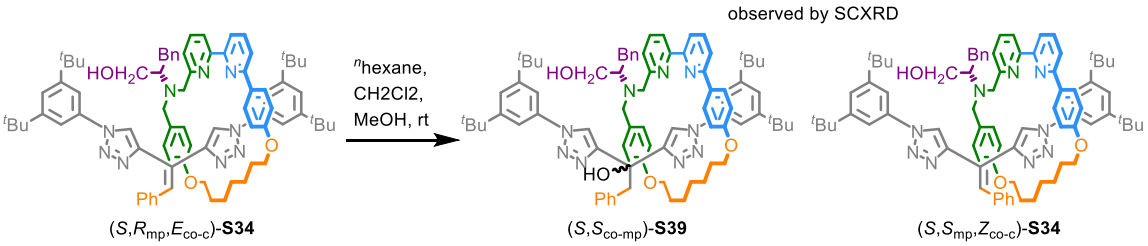

Scheme S12: Observed conversion of (S,R_{mp},$E_{co\text{-}c}$)-**S34** to (S,S_{mp},$Z_{co\text{-}c}$)-**S34** and (S,$R_{co\text{-}mp}$)-**S39**.

7.2. Synthesis of rotaxane (R_{mp},$E_{co\text{-}c}$)-S36

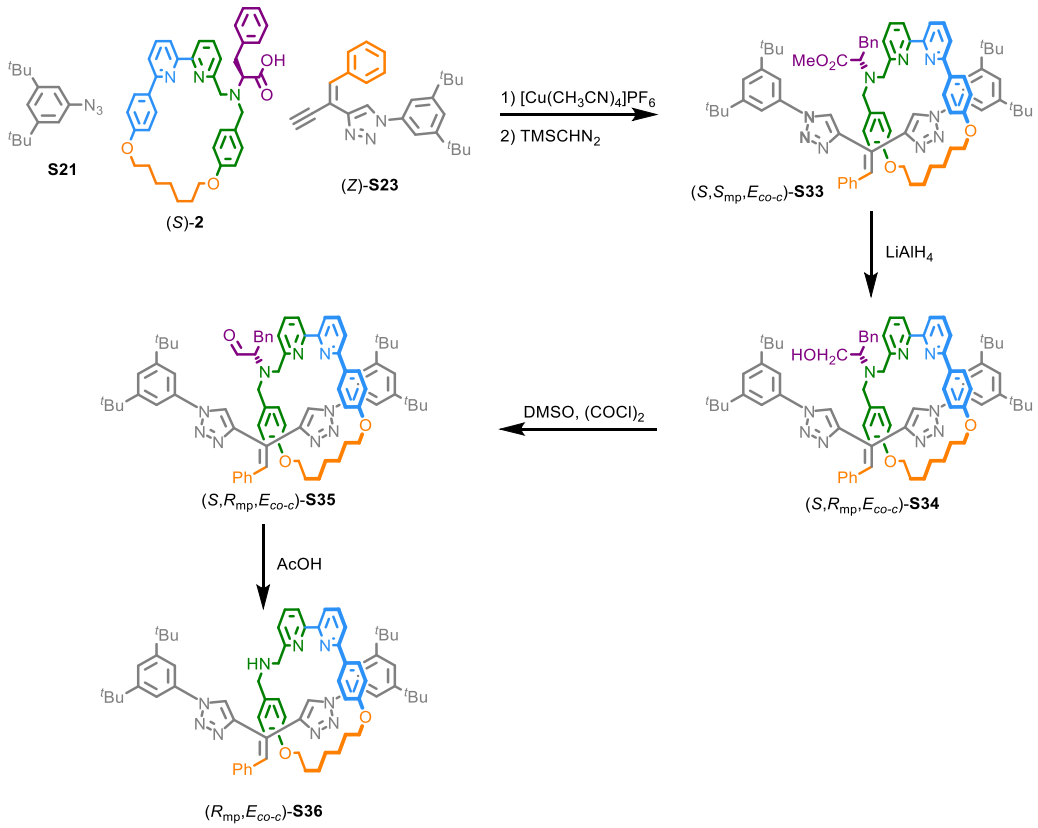

Scheme S13: Synthesis of rotaxane (R_{mp},$E_{co\text{-}c}$)-**S36**

Rotaxane (S,S_{mp},$E_{co\text{-}c}$)-S33

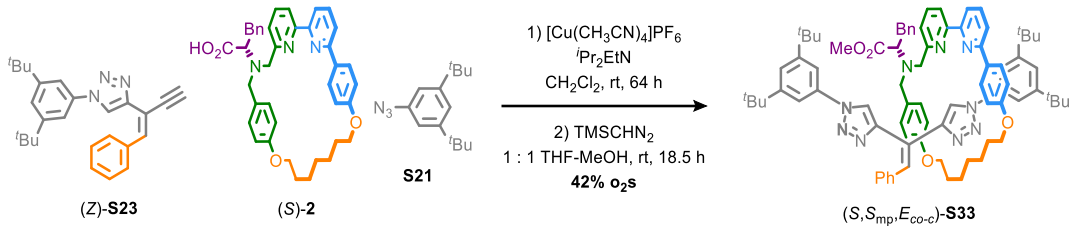

Macrocycle (*S*)-**2** (50 mg, 0.080 mmol), alkyne (*Z*)-**S23** (51 mg, 0.13 mmol), azide **S21** (28 mg, 0.12 mmol) and $[Cu(CH_3CN)_4]PF_6$ (28 mg, 0.075 mmol) were dissolved in CH_2Cl_2 (3.0 mL) and $^{i}Pr_2EtN$ (69.5 µL, 0.399 mmol) was added. The dark orange solution was stirred 64 h at rt before being quenched by addition of sat. EDTA-$NH_{3(aq.)}$ (3 mL) and stirring in air for 3.5 h. The reaction mixture was diluted with H_2O (30 mL) and the aqueous layer extracted with CH_2Cl_2 (3 x 15 mL). The combined organic layers were dried (Na_2SO_4) and concentrated *in vacuo*. The residue was dissolved in THF-MeOH (1 : 1, 5.0 mL) and $TMSCHN_2$ (2 M in hexanes, 0.21 mL, 0.42 mmol) was added. The reaction mixture was stirred at rt for 18.5 h then concentrated *in vacuo*. Chromatography (petrol-acetone 100 : 0 to 9 : 1) gave [2]rotaxane (S,S_{mp},$E_{co\text{-}c}$)-**S33** as a yellow foam (42 mg, 42%, 95 : 5 *dr* Figure S193).

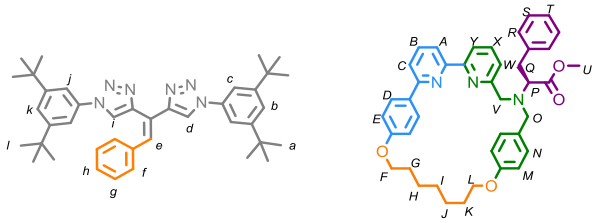

^{1}H NMR (400 MHz, $CDCl_3$) δ 9.88 (s, 1H, $\boldsymbol{H}_d$), 8.42 (s, 1H, $\boldsymbol{H}_i$), 7.63 (t, *J* = 7.8, 1H, $\boldsymbol{H}_B$), 7.43 (s, 1H, $\boldsymbol{H}_e$), 7.39 – 7.35 (m, 2H, $\boldsymbol{H}_k$, $\boldsymbol{H}_A$), 7.34 – 7.28 (m, 6H, $\boldsymbol{H}_c$, $\boldsymbol{H}_j$, $\boldsymbol{H}_C$, $\boldsymbol{H}_X$), 7.25 (dd, *J* = 7.8, 1.1, 1H, $\boldsymbol{H}_Y$), 7.23 – 7.09 (m, 9H, $\boldsymbol{H}_b$, $\boldsymbol{H}_f$, $\boldsymbol{H}_g$, $\boldsymbol{H}_h$, $\boldsymbol{H}_S$, $\boldsymbol{H}_T$), 7.02 (dd, *J* = 7.7, 1.1, 1H, $\boldsymbol{H}_W$), 6.96 (d, *J* = 8.8, 2H, $\boldsymbol{H}_D$), 6.87 (dd, *J* = 7.8, 1.7, 2H, $\boldsymbol{H}_R$), 6.72 (d, *J* = 8.4, 2H, $\boldsymbol{H}_N$), 6.49 (d, *J* = 8.8, 2H, $\boldsymbol{H}_E$), 6.00 (d, *J* = 8.5, 2H, $\boldsymbol{H}_M$), 4.40 (td, *J* = 9.2, 8.7, 4.5, 1H, 1 of $\boldsymbol{H}_L$), 4.06 (m, 2H, 1 of $\boldsymbol{H}_F$, 1 of $\boldsymbol{H}_L$), 3.93 – 3.85 (m, 2H, 1 of $\boldsymbol{H}_F$, 1 of $\boldsymbol{H}_O$), 3.75 (d, *J* = 11.8, 1H, 1 of $\boldsymbol{H}_V$), 3.65 (s, 3H, $\boldsymbol{H}_U$), 3.38 (dd, *J* = 11.6, 3.0, 1H, $\boldsymbol{H}_P$), 3.33 (d, *J* = 11.9, 1H, 1 of $\boldsymbol{H}_V$), 3.20 (t, *J* = 12.3, 1H, 1 of $\boldsymbol{H}_Q$), 2.87 (d, *J* = 13.2, 1H, 1 of $\boldsymbol{H}_O$), 2.68 (dd, *J* = 13.1, 3.0, 1H, 1 of $\boldsymbol{H}_Q$), 2.32 – 2.19 (m, 1H, 1 of $\boldsymbol{H}_I$), 2.15 – 2.03 (m, 1H, 1 of $\boldsymbol{H}_K$), 2.02 – 1.58 (m, 7H, $\boldsymbol{H}_G$, $\boldsymbol{H}_H$, 1 of $\boldsymbol{H}_K$), 1.58 – 1.45 (m, 1H, 1 of $\boldsymbol{H}_I$), 1.25 (s, 18H, $\boldsymbol{H}_I$), 1.14 (s, 18H, $\boldsymbol{H}_a$).

^{13}C NMR (101 MHz, $CDCl_3$) δ 171.5, 159.8, 159.4, 158.3, 157.9, 157.8, 157.7, 152.3, 150.5, 147.2, 144.8, 138.3, 137.3, 137.0, 136.5, 136.3, 136.1, 131.0, 130.1, 129.9, 129.6, 129.1, 129.0, 128.4, 127.9, 127.6, 127.1, 126.6, 126.3, 122.7, 122.2, 121.5, 121.2, 121.0, 120.6, 120.5, 120.1, 114.8, 113.8, 113.3, 113.2, 67.4, 65.1, 63.2, 57.2, 55.3, 51.1, 37.6, 35.1, 35.0, 31.6, 31.4, 29.7, 29.1, 28.1, 25.7, 25.7.

LR-ESI-MS (+ve): *m/z* = 1256.8 $[M + H]^+$ calc. for $C_{81}H_{93}N_9O_4$ 1256.7.

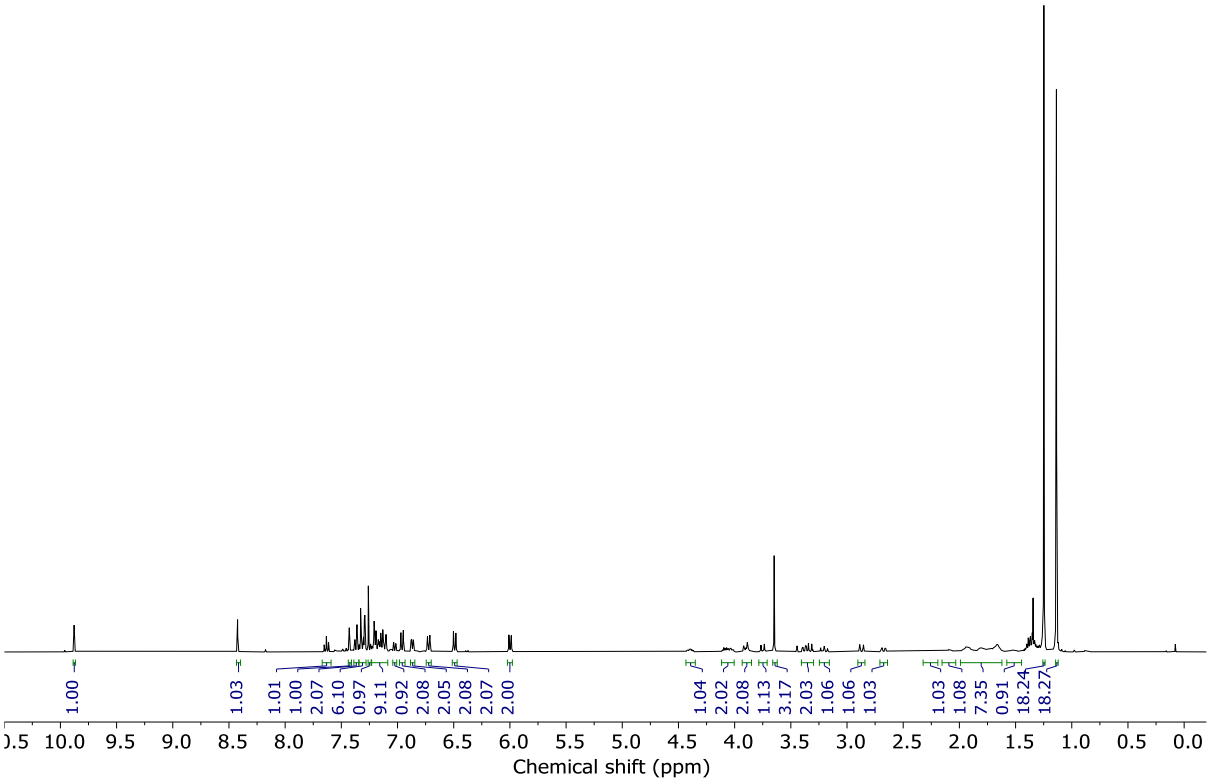

Figure S192: ^{1}H NMR ($CDCl_3$, 400 MHz, 298 K) of (S,S_{mp},$E_{co\text{-}c}$)-**S33** (95 : 5 *dr*).

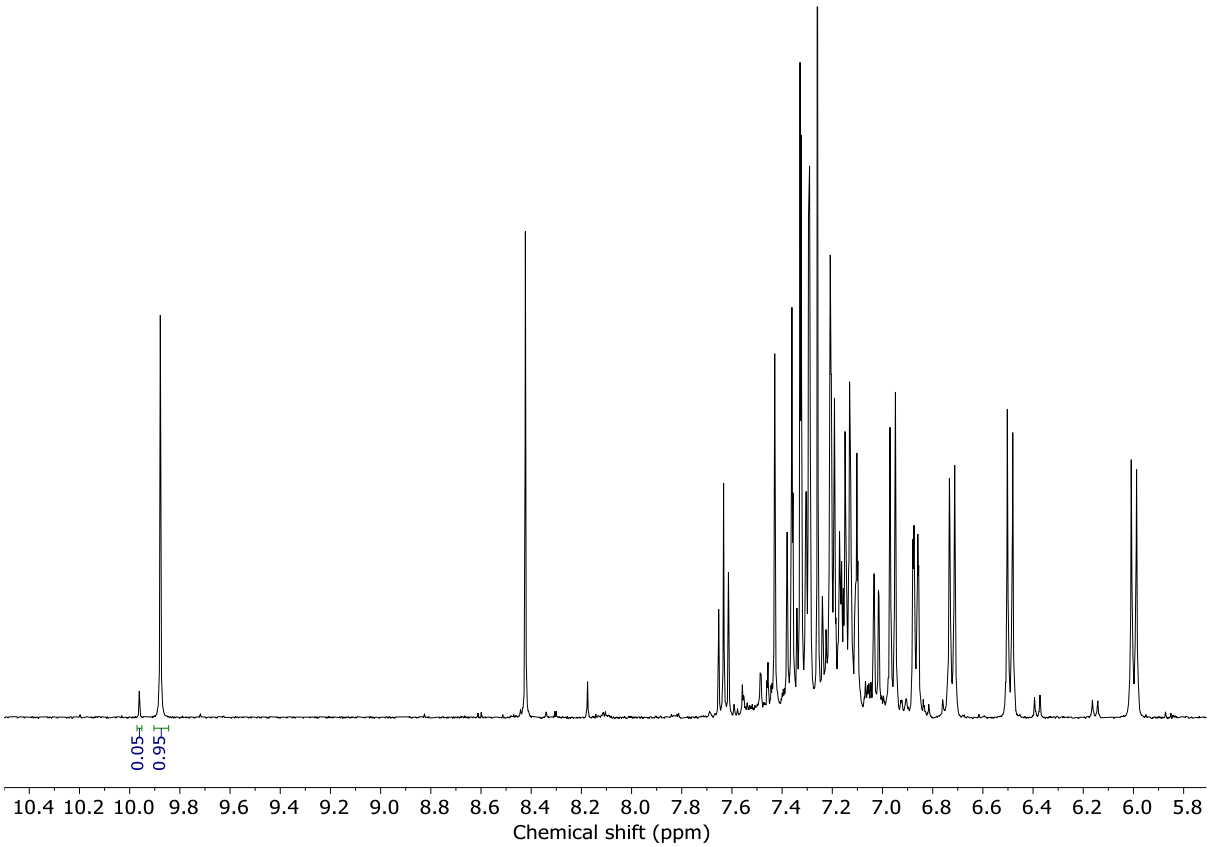

Figure S193: Partial ^{1}H NMR ($CDCl_3$, 400 MHz, 298 K) of (S,S_{mp},$E_{co\text{-}c}$)-**S33** (95 : 5 d.r.).

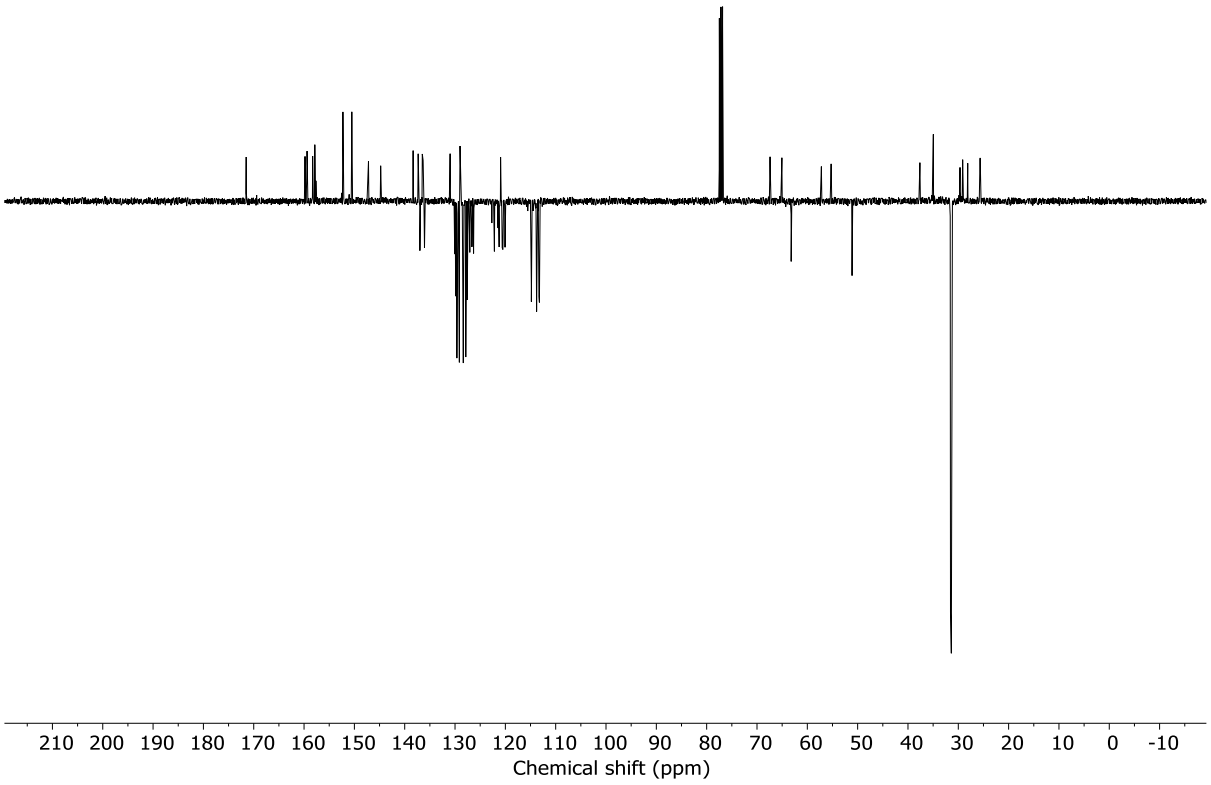

Figure S194: JMOD NMR ($CDCl_3$, 101 MHz, 298 K) of (S,S_{mp},$E_{co\text{-}c}$)-**S33** (95 : 5 d.r.).

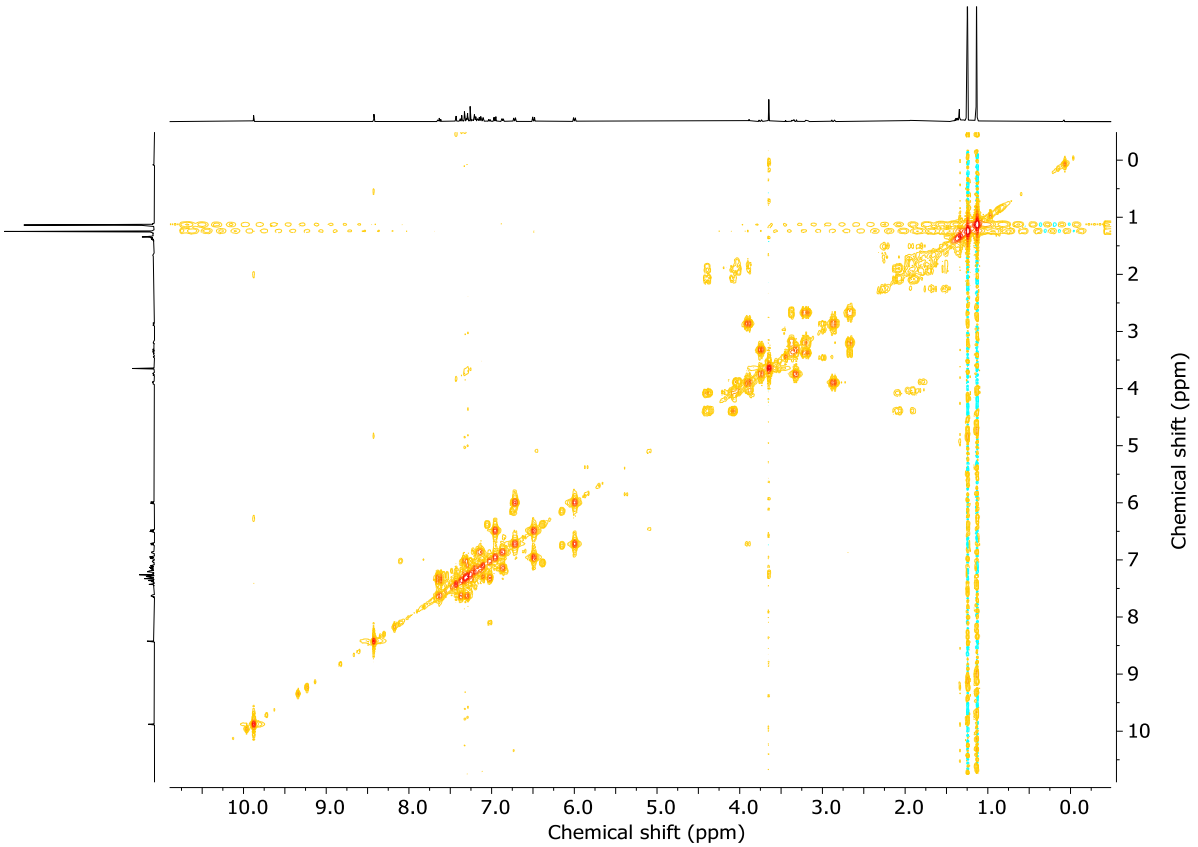

Figure 195: COSY NMR ($CDCl_3$, 298 K) of (S,S_{mp},$E_{co\text{-}c}$)-**S33** (95 : 5 d.r.).

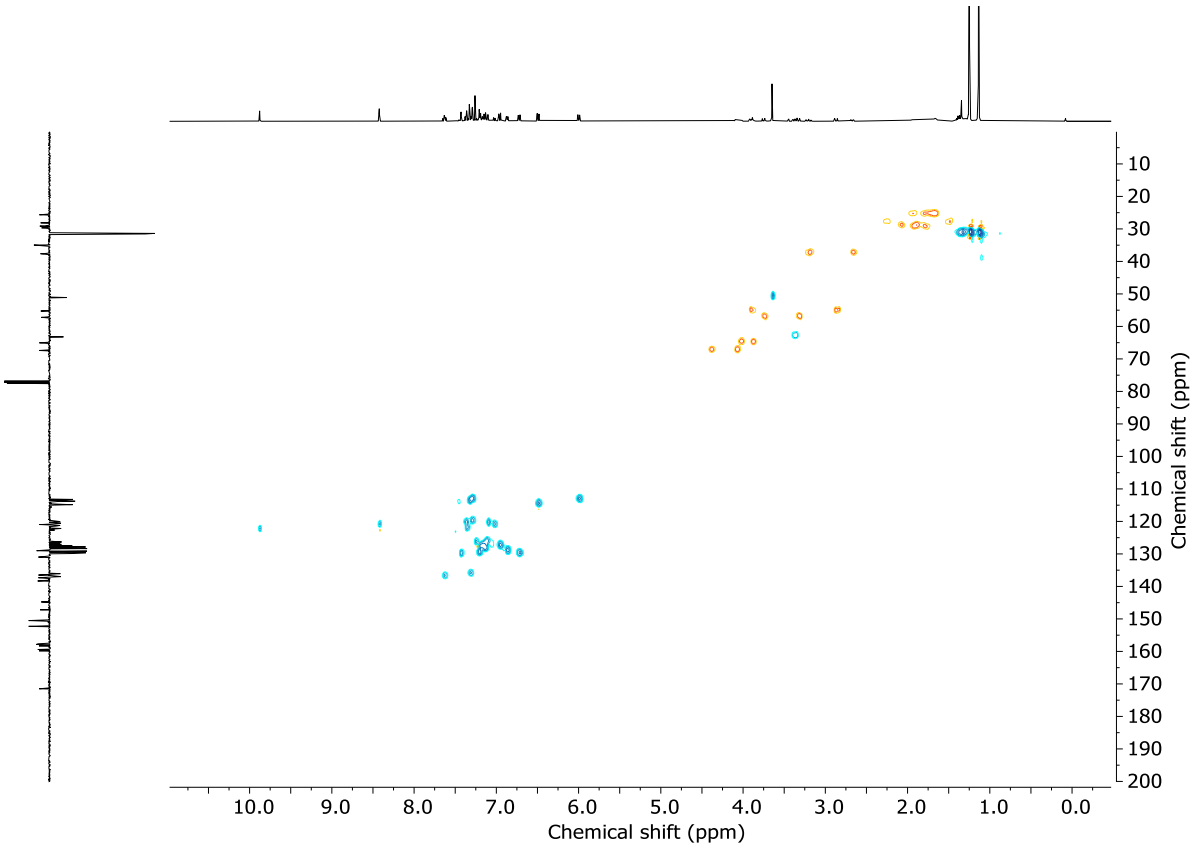

Figure 196: HSQC NMR ($CDCl_3$, 298 K) of (S,S_{mp},$E_{co\text{-}c}$)-**S33** (95 : 5 d.r.).

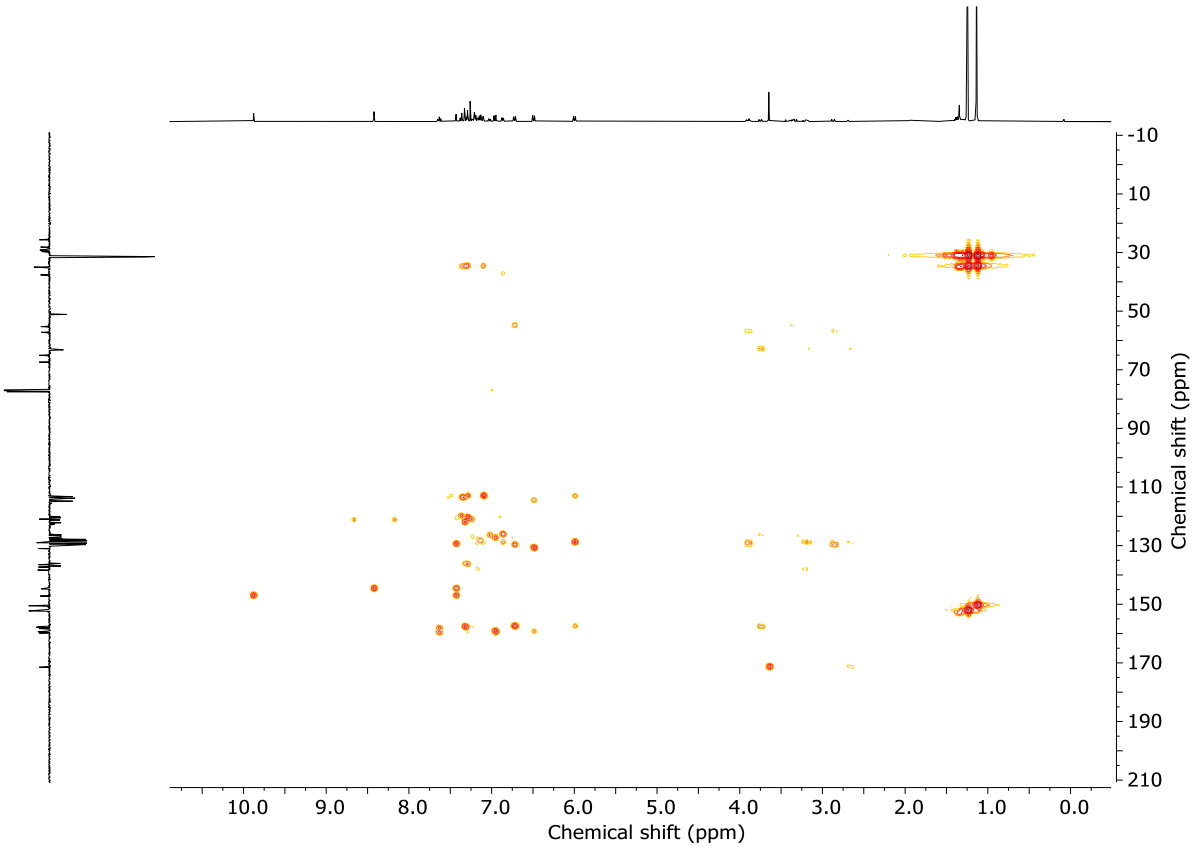

Figure 197: HMBC NMR ($CDCl_3$, 298 K) of (S,S_{mp},$E_{co\text{-}c}$)-**S33** (95 : 5 d.r.).

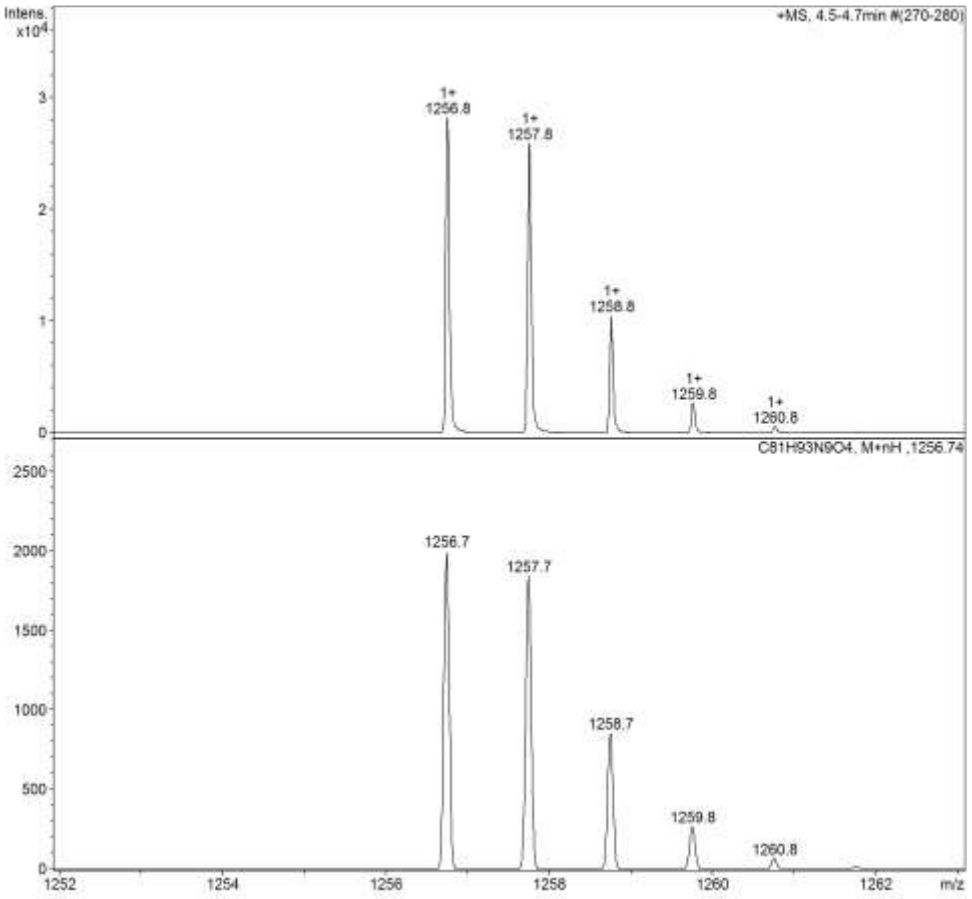

Figure 198: LRMS - Observed (top) and calculated (bottom) isotopic pattern for (S,S_{mp},$E_{co\text{-}c}$)-**S33** $C_{81}H_{93}N_9O_4$.

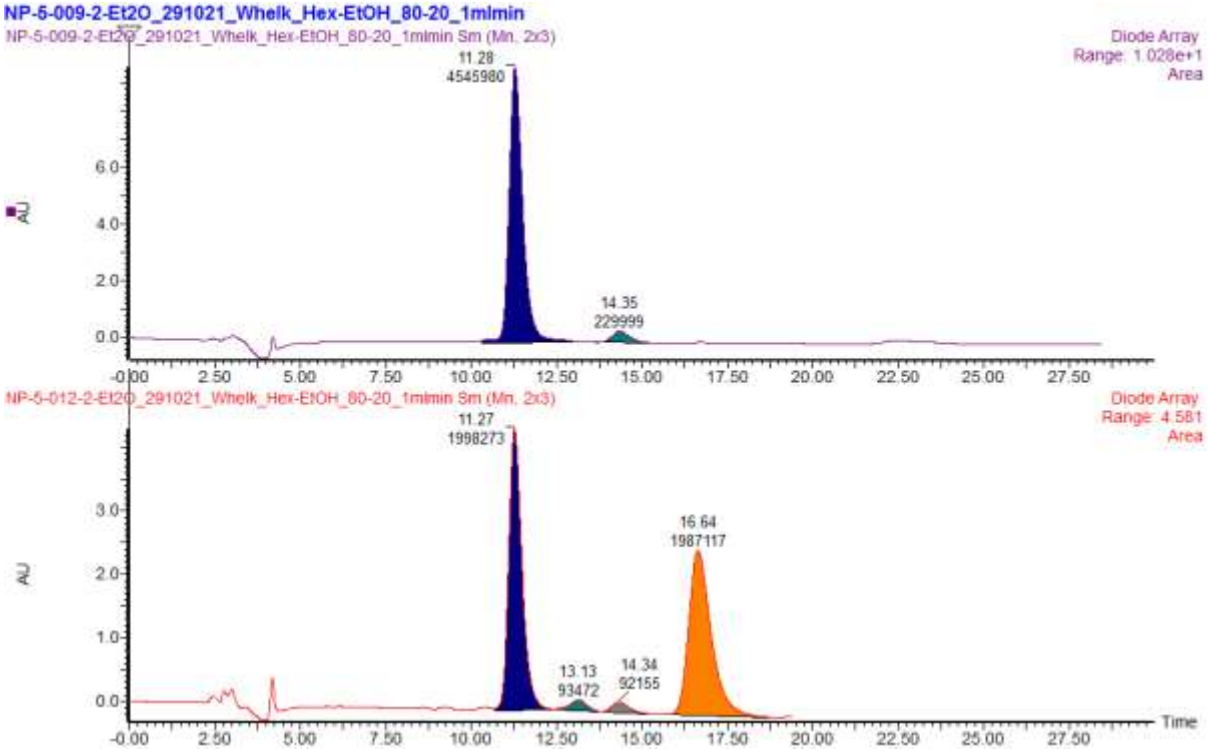

Figure 199: CSP-HPLC of **S33** (loaded in Et_2O). SSWhelk, ^{n}hexane-EtOH 80 : 20, flowrate 1 mLmin^{-1}. (top) (S,S_{mp},$E_{co\text{-}c}$)-**S33** (11.28 min, 95.2%), (S,R_{mp},$E_{co\text{-}c}$)-**S33** (14.34 min, 4.8%); (bottom) (*Rac*)-(S,S_{mp},$E_{co\text{-}c}$)-**S33:** (S,S_{mp},$E_{co\text{-}c}$)-**S33** (11.27 min, 47.9%), (R,S_{mp},$E_{co\text{-}c}$)-**S33** (13.13 min, 2.2%), (S,R_{mp},$E_{co\text{-}c}$)-**S33**(14.34 min, 2.2%), (R,R_{mp},$E_{co\text{-}c}$)-**S33** (16.64 min, 47.7%).

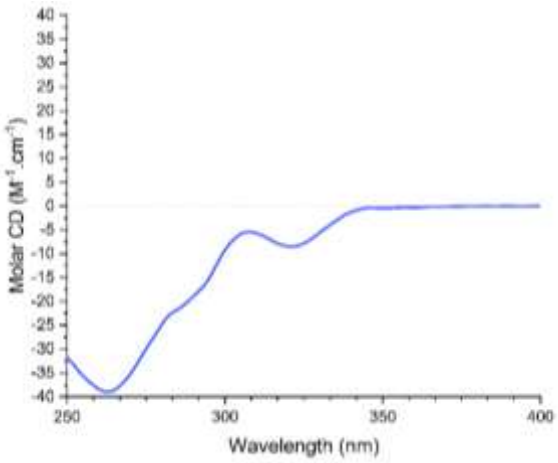

Figure 200: Circular dichroism spectra (23.9 μM in $CHCl_3$, 298 K) of (S,S_{mp},$E_{co\text{-}c}$)-**S33** (95:5 d.r.).

Rotaxane (S,R_{mp},$E_{co\text{-}c}$)-S34

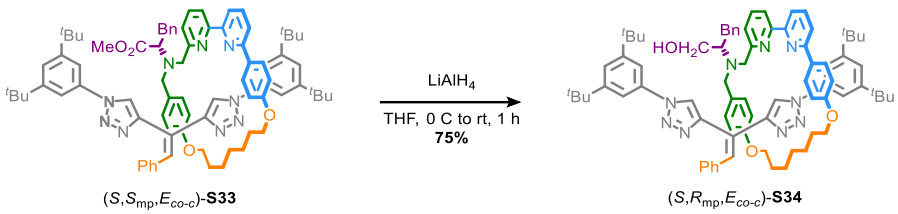

Rotaxane (S,S_{mp},$E_{co\text{-}c}$)-**S33** (61 mg, 0.048 mmol) was dissolved in THF (5.0 mL), the solution cooled to 0 °C before a $LiAlH_4$ (1 M in THF, 0.15 mL, 0.15 mmol) was added dropwise. The reaction mixture was stirred at 0 °C for 5 min then 1 h at rt. The reaction mixture was cooled at 0 °C before addition of H_2O (20 mL). The aqueous layer was extracted with CH_2Cl_2 (3 x 10 mL) and the combined organic layers dried (Na_2SO_4) and concentrated *in vacuo*. Chromatography (^{n}hexane-EtOAc 100 : 0 to 7 : 3) gave (S,R_{mp},$E_{co\text{-}c}$)-**S34** as a beige foam (44 mg, 75%).

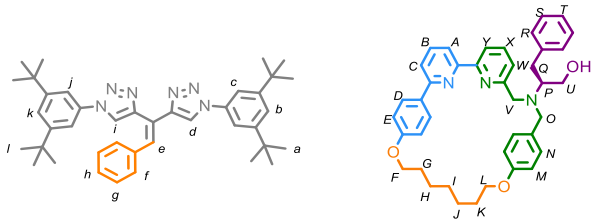

^{1}H NMR (400 MHz, $CDCl_3$) δ 9.84 (s, 1H, H_d), 7.99 (s, 1H, H_i), 7.74 (t, J = 7.7, 1H, H_B), 7.66 (d, J = 1.7, 2H, H_c), 7.54 (d, J = 1.7, 2H, H_j), 7.52 (dd, J = 7.9, 0.9, 1H, H_A), 7.50 (t, J = 7.8, 1H, H_X), 7.46 (t, J = 1.7, 1H, H_k), 7.36 (dd, J = 7.9, 0.9, 1H, H_W), 7.31 – 7.18 (m, 6H, H_b, H_Y, H_C, H_S, H_T), 7.15 (d, J = 8.7, 2H, H_D), 7.09 – 6.96 (m, 5H, H_f, H_h H_R), 6.87 – 6.83 (m, 2H, H_g), 6.76 (d, J = 8.5, 2H, H_N), 6.71 (s, 1H, H_e), 6.35 (d, J = 8.7, 2H, H_E), 6.29 (d, J = 8.6, 2H, H_M), 4.14 – 4.02 (m, 3H, H_F, 1 of H_L), 3.86 (d, J = 12.1, 1H, 1 of H_V), 3.84 – 3.79 (m, 2H, 1 of H_L, 1 of H_O), 3.59 (d, J = 12.0, 1H, 1 of H_V), 3.35 (t, J = 10.0, 1H, 1 of H_U), 3.20 (dt, J = 17.1, 7.1, 2H, H_{OH}, 1 of H_U), 3.13 (d, J = 13.1, 1H, H_O), 3.04 (dd, J = 13.2, 4.1, 1H, 1 of H_Q), 3.01 – 2.89 (m, 1H, H_P), 2.41 (dd, J = 13.2, 10.0, 1H, 1 of H_Q), 1.98 – 1.47 (m, 10H, H_G, H_H, H_I, H_J, H_K), 1.38 (s, 18H, H_L), 1.17 (s, 18H, H_A).

^{13}C NMR (101 MHz, $CDCl_3$) δ 159.5, 159.3, 159.2, 158.9, 157.9, 157.6, 152.6, 151.4, 147.0, 144.0, 139.5, 137.6, 137.2, 137.1, 137.0, 136.8, 131.4, 129.9, 129.8, 129.5, 129.2, 128.6, 128.5, 128.1, 127.6, 126.7, 126.3, 125.6, 122.5, 122.3 (x2), 122.0, 121.6, 121.0, 120.2, 120.0, 114.9, 114.7, 114.6, 114.0, 67.8, 65.4, 61.4, 60.5, 56.7, 53.3, 35.3, 35.1, 31.8, 31.6, 31.4, 29.2, 29.1, 28.1, 25.6, 25.5.

LR-ESI-MS (+ve): m/z = 1228.8 $[M + H]^+$ calc. for $C_{80}H_{93}N_9O_4$ 1228.7.

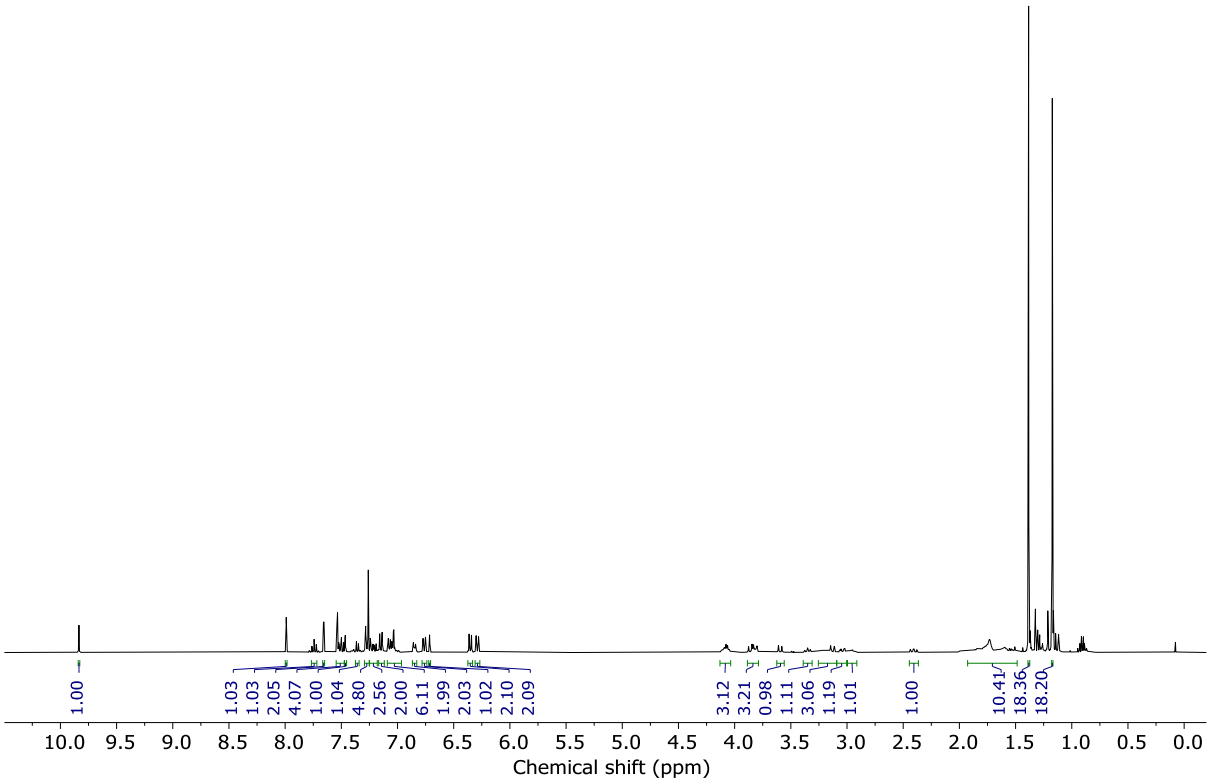

Figure 201: ^{1}H NMR ($CDCl_3$, 400 MHz, 298 K) of (S,R_{mp},$E_{co\text{-}c}$)-**S34**.

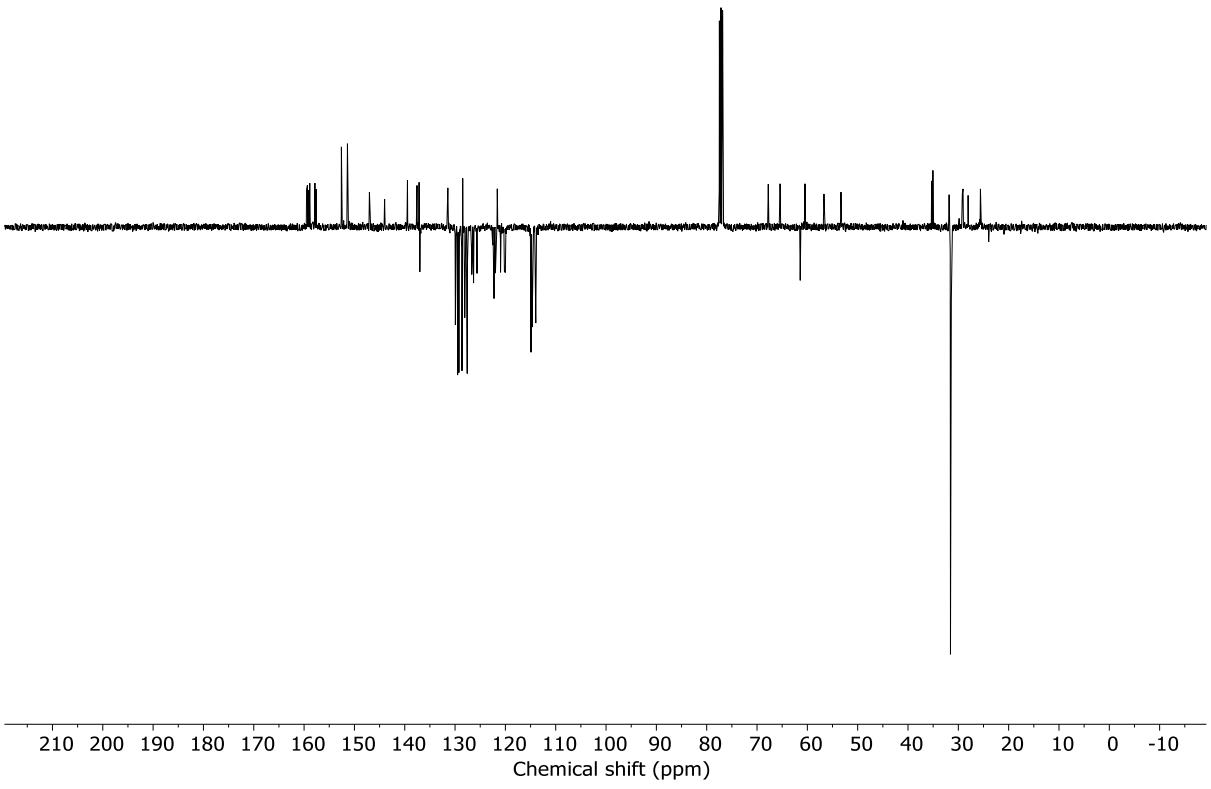

Figure 202: JMOD NMR ($CDCl_3$, 101 MHz, 298 K) of (S,R_{mp},$E_{co\text{-}c}$)-**S34**.

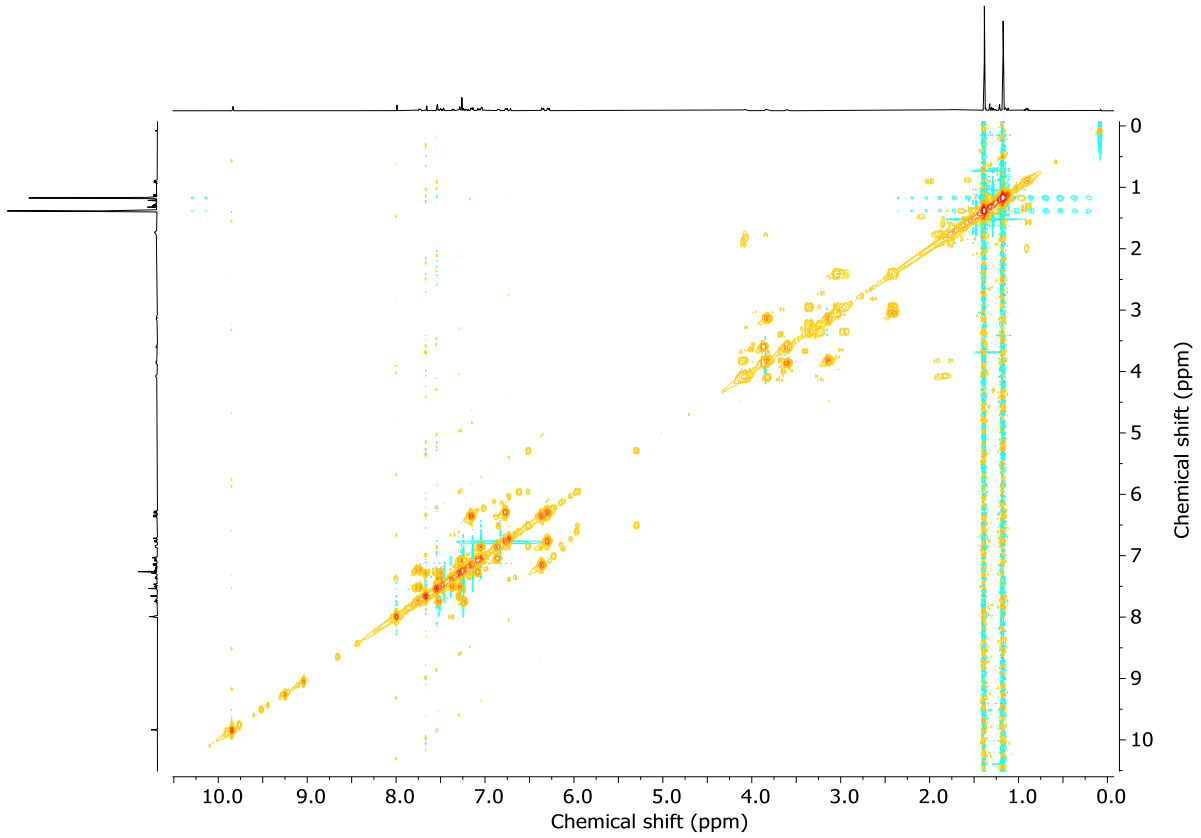

Figure 203: COSY NMR ($CDCl_3$, 298 K) of (S,R_{mp},$E_{co\text{-}c}$)-**S34**.

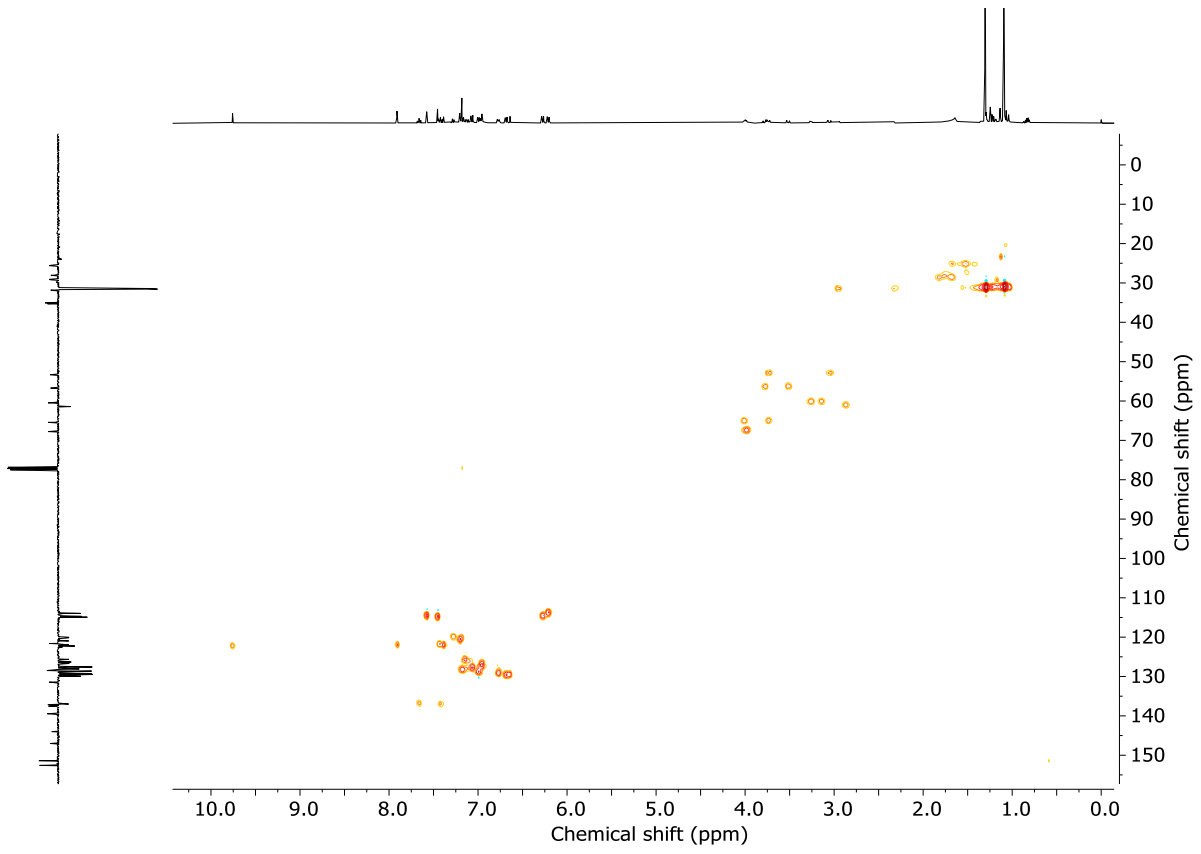

Figure 204: HSQC NMR ($CDCl_3$, 298 K) of (S,R_{mp},$E_{co\text{-}c}$)-**S34**.

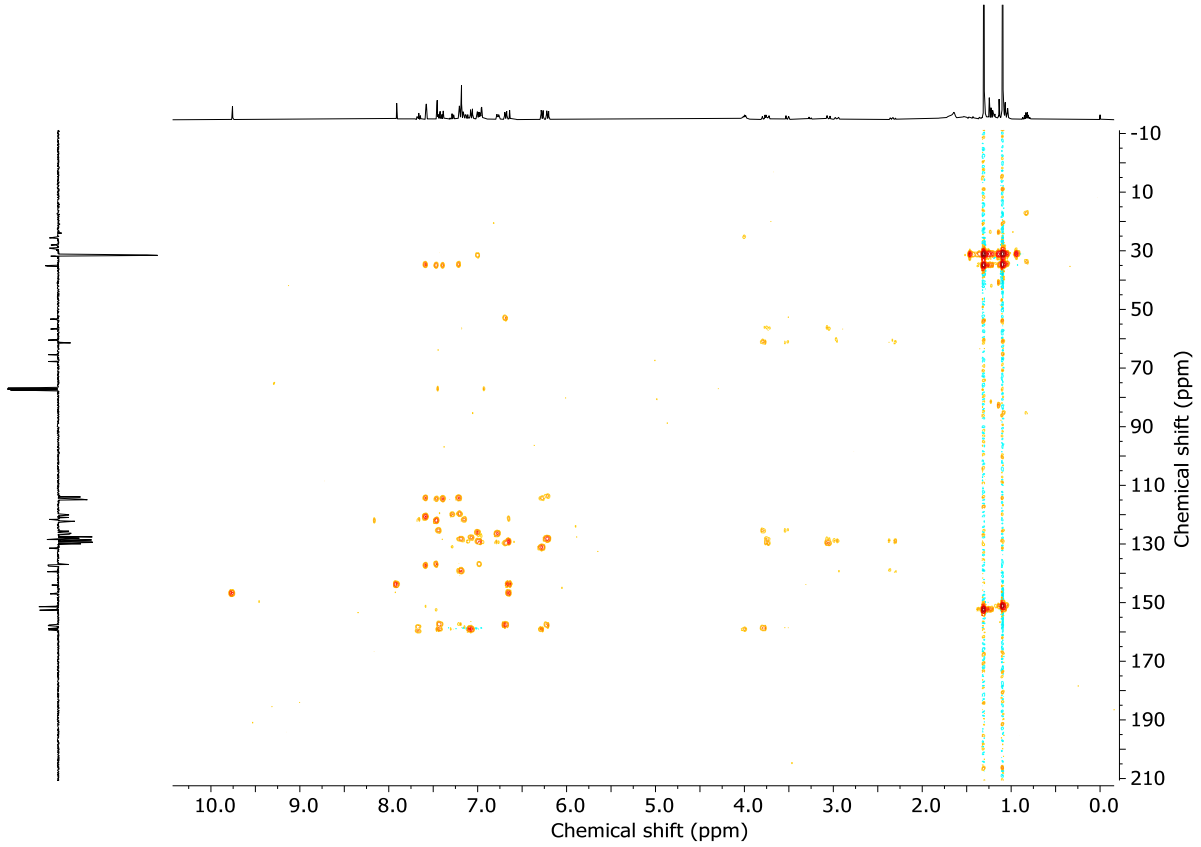

Figure 205: HMBC NMR ($CDCl_3$, 298 K) of (S,R_{mp},$E_{co\text{-}c}$)-**S34**.

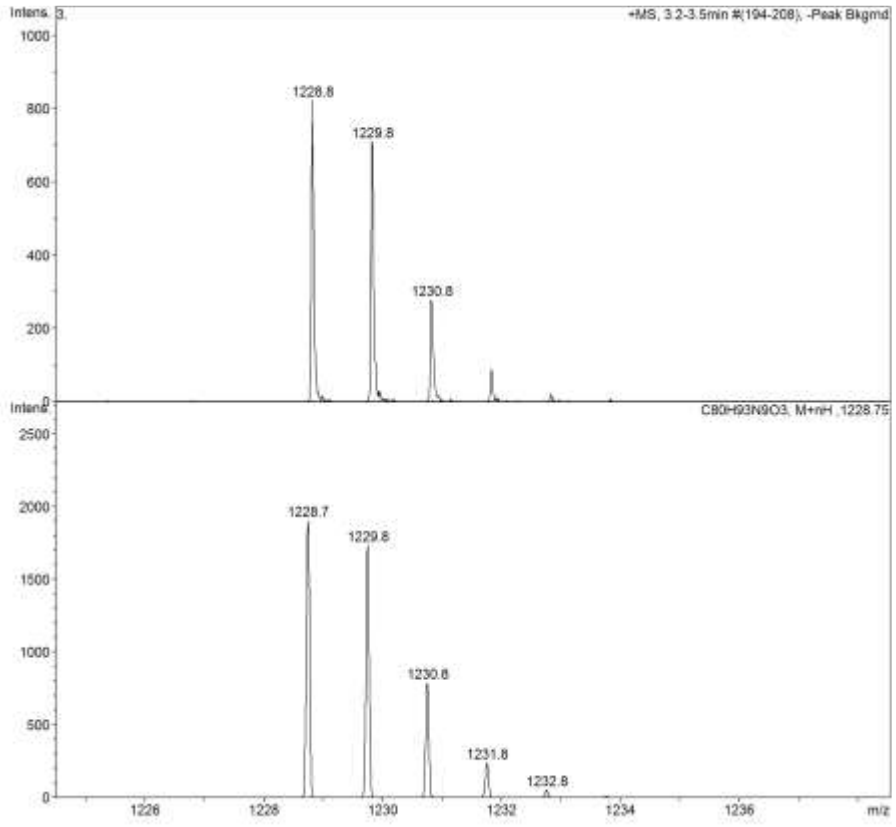

Figure 206: LRMS - Observed (top) and calculated (bottom) isotopic pattern for (S,R_{mp},$E_{co\text{-}c}$)-**S34** $C_{80}H_{93}N_9O_3$.

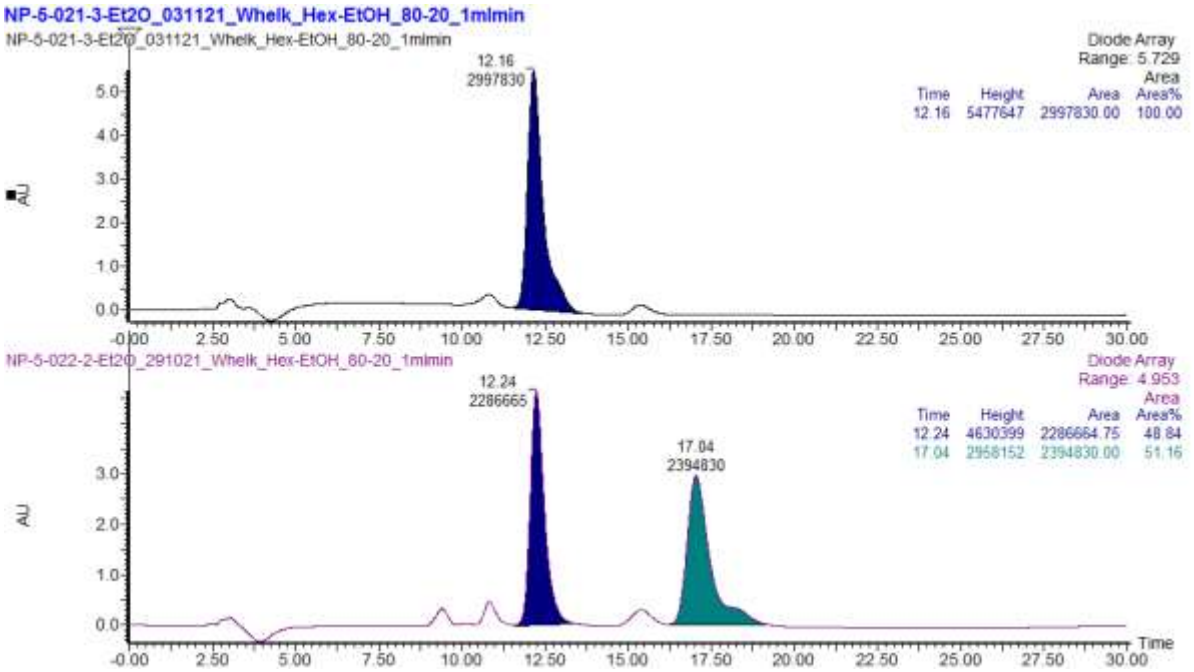

Figure 207: CSP-HPLC of (S,S_{mp},$E_{co\text{-}c}$)-**S34** (loaded in Et_2O). SSWhelk, ^{n}hexane-EtOH 80 : 20, flowrate 1 mLmin-1. (Top) (S,R_{mp},$E_{co\text{-}c}$)-**S34** (12.16 min, > 99.9%); (Middle) *rac*-(S,R_{mp},$E_{co\text{-}c}$)-**S34 :** (S,R_{mp},$E_{co\text{-}c}$)-**S34** (12.22 min, 48.8%), (R,S_{mp},$E_{co\text{-}c}$)-**S34** (17.02 min, 51.2%).

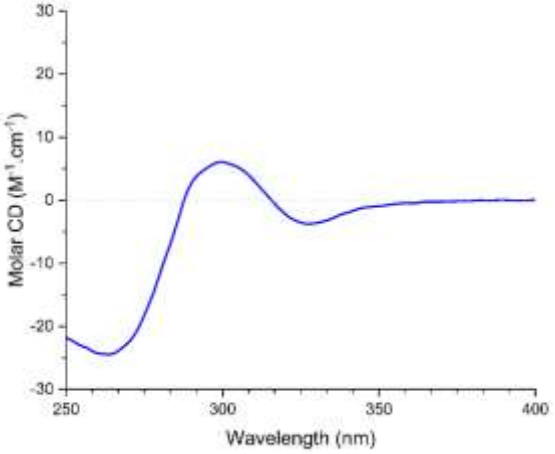

Figure 208: Circular dichroism spectra (27.1 μM in $CHCl_3$, 298 K) of (S,R_{mp},$E_{co\text{-}c}$)-**S34.**

Rotaxane (R_{mp},$E_{co\text{-}c}$)-S36

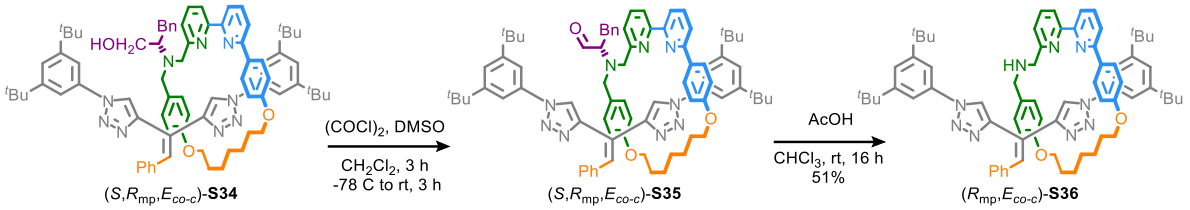

DMSO (0.12 mL, 1.7 mmol) was added dropwise to a solution of oxalyl chloride (0.07 mL 0.8 mmol) in CH_2Cl_2 (3.0 mL) at -78 °C and the reaction mixture was stirred for 10 min. An aliquot of this solution (1.0 mL) was added to rotaxane (S,R_{mp},$E_{co\text{-}c}$)-**S34** (84 mg, 0.26 mmol) was dissolved in CH_2Cl_2 (0.5 mL) at -78 °C followed by Et_3N (0.14 mL, 1.0 mmol) and the reaction mixture was stirred for 5 min before the flask was removed from the -78 °C bath. After 3 hours at rt, the reaction was diluted with CH_2Cl_2 (30 mL) and the organic layer washed with sat. $NaHCO_3$ (20 mL). The layers were separated, and the aqueous layer was extracted with CH_2Cl_2 (2 x 10 mL). The combined organic layers were dried (Na_2SO_4) and concentrated *in vacuo*. The residue, containing aldehyde rotaxane (S,R_{mp},$E_{co\text{-}c}$)-**S35**, was dissolved in $CHCl_3$ (10 mL) and glacial AcOH (1.0 mL) was added. The reaction mixture was stirred overnight at rt then diluted with CH_2Cl_2 (20 mL), washed with $NaHCO_{3(sat.)}$ (20 mL), and the aqueous layer extracted with CH_2Cl_2 (2 x 10 mL). The combined organic layers were dried (Na_2SO_4) and concentrated *in vacuo*. Two rounds of chromatography (1st: petrol-acetone 95 : 5 to 15 : 85; 2nd: ^{n}hexane-Et_2O 1 : 1 to 0 : 100) gave rotaxane (R_{mp},$E_{co\text{-}c}$)-**S36** as a pale yellow foam (38 mg, 51%).

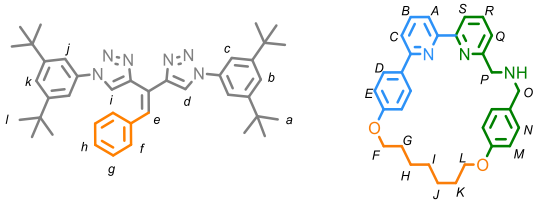

^{1}H NMR (400 MHz, $CDCl_3$) δ 9.72 (s, 1H, H_d), 7.71 (s, 1H, H_i), 7.55 – 7.50 (m, 4H, H_c, H_B, H_R), 7.48 (s, 1H, H_e), 7.39 (t, J = 1.7, 1H, H_k), 7.33 – 7.28 (m, 2H, H_C, H_Q), 7.19 (dd, J = 7.9, 1.0, 1H, H_S), 7.18 – 7.10 (m, 8H, H_b, H_f, H_g, H_h, H_j), 7.09 (dd, J = 7.8, 0.9, 1H, H_A), 7.04 (d, J = 8.6, 2H, H_D), 6.72 (d, J = 8.5, 2H, H_N), 6.40 (d, J = 8.7, 2H, H_E), 6.28 (d, J = 8.5, 2H, H_M), 4.26 – 4.16 (m, 2H, 1 of H_F, 1 of H_L), 4.08 (dt, J = 10.1, 6.1, 1H, 1 of H_F), 3.97 (dt, J = 9.3, 4.9, 1H, 1 of H_L), 3.72 (d, J = 13.6, 1H, 1 of H_O), 3.59 (d, J = 14.5, 1H, 1 of H_P), 3.56 (d, J = 14.5, 1H, 1 of H_P), 3.51 (d, J = 13.6, 1H, 1 of H_O), 2.16 – 1.56 (m, 10H, H_G, H_H, H_I, H_J, H_K,), 1.30 (s, 18H, H_l), 1.12 (s, 18H, H_a).

^{13}C NMR (101 MHz, $CDCl_3$) δ 160.6, 159.9, 159.3, 157.8, 157.3, 156.8, 152.3, 151.1, 147.1, 144.4, 137.2, 137.1, 137.1, 136.7, 136.5, 131.6, 130.2, 129.5, 129.3, 129.2, 128.1, 128.0, 127.0, 123.2, 123.1, 122.4, 121.5, 121.1, 120.4, 120.3, 120.2, 119.9, 114.6, 114.3, 113.9, 113.8, 67.7, 65.6, 54.1, 54.0, 35.2, 35.0, 31.5, 31.4, 29.4, 29.2, 28.2, 25.7 (x2).

LR-ESI-MS (+ve): m/z = 1094.7 $[M + H]^+$ calc. for $C_{71}H_{83}N_9O_2$ 1094.7.

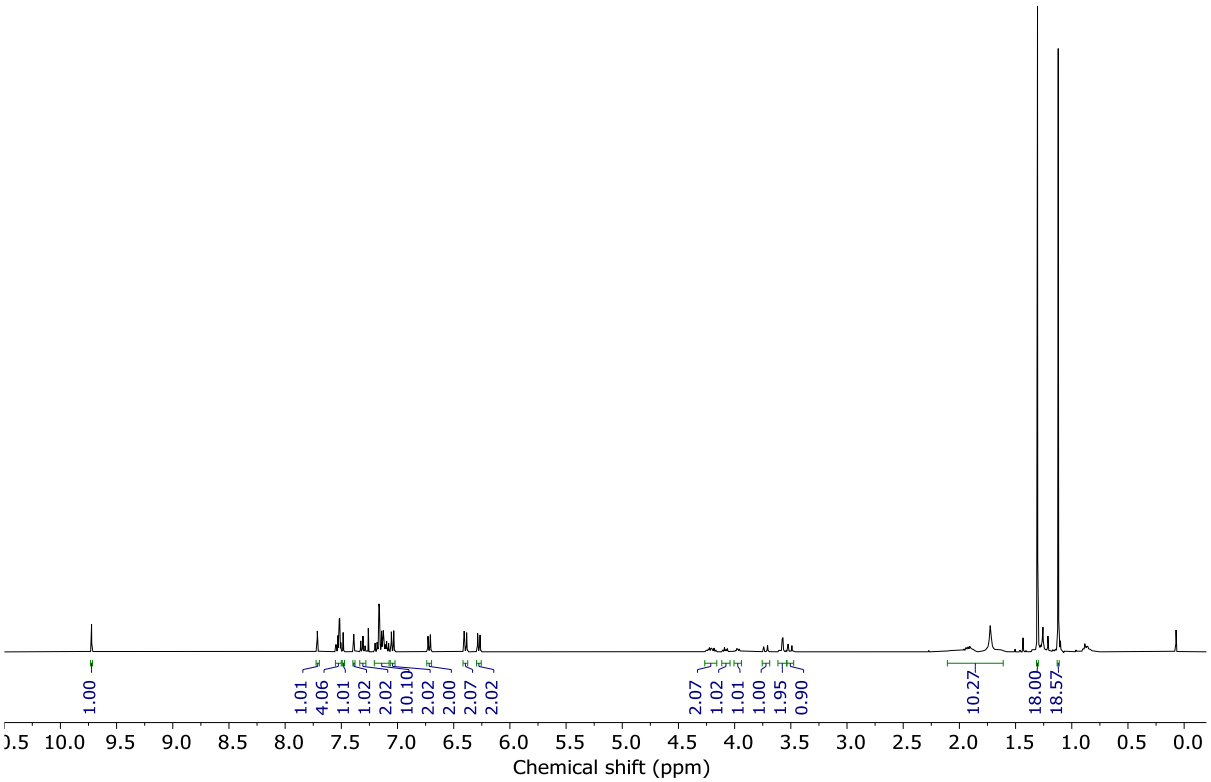

Figure 209: ^{1}H NMR ($CDCl_3$, 400 MHz, 298 K) of (R_{mp},$E_{co\text{-}c}$)-**S36**.

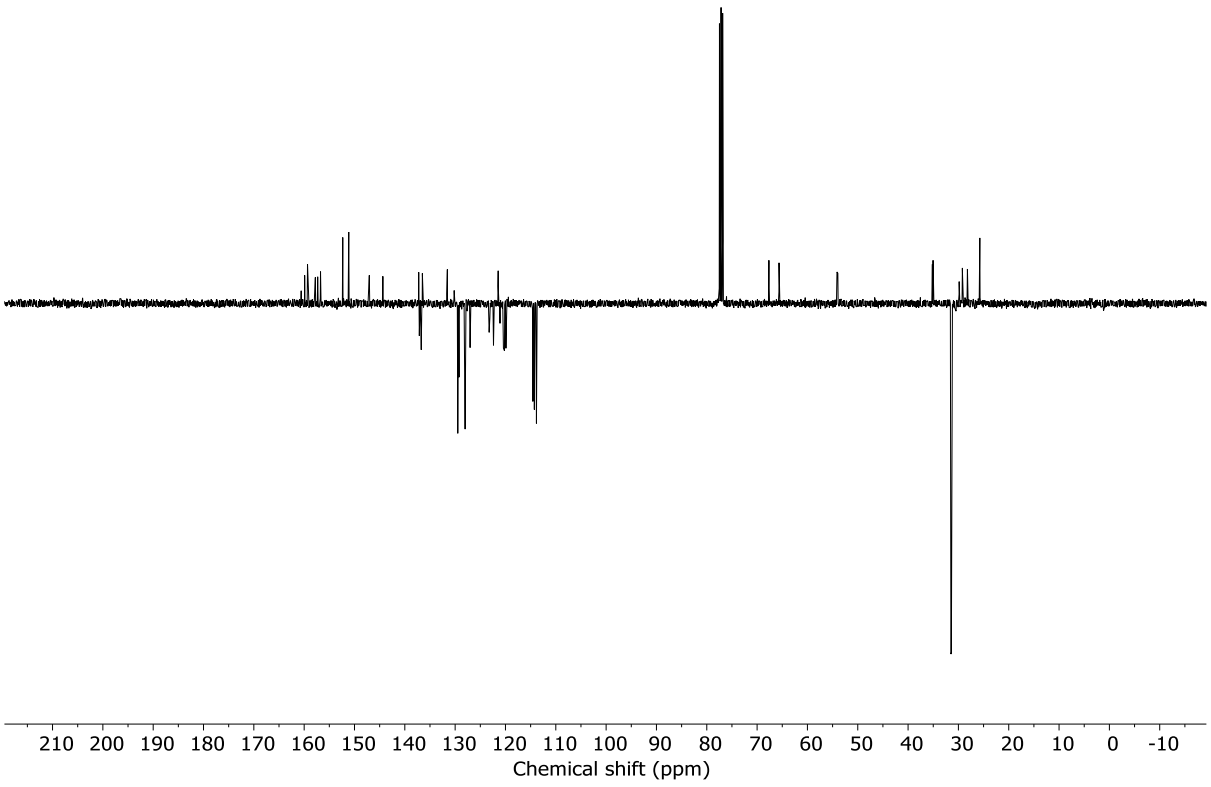

Figure 210: JMOD NMR ($CDCl_3$, 101 MHz, 298 K) of (R_{mp},$E_{co\text{-}c}$)-**S36**.

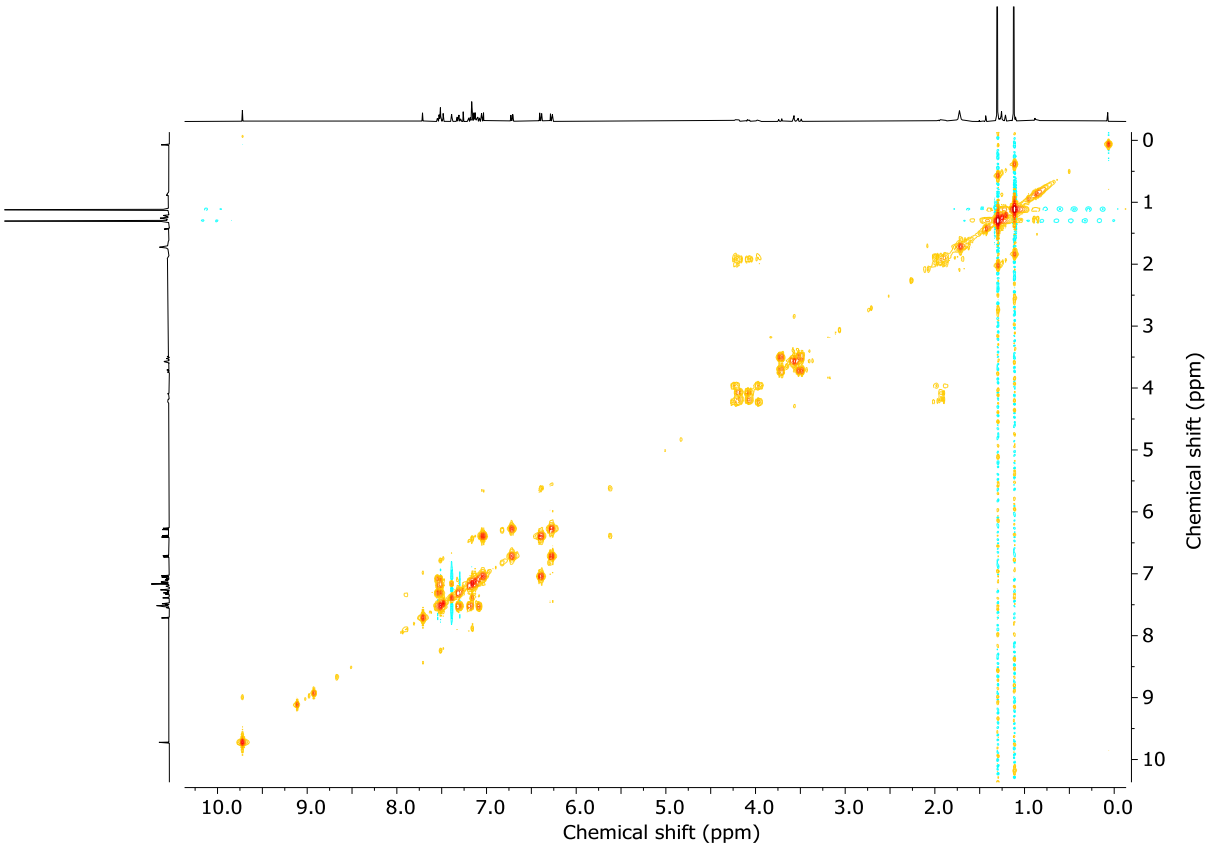

Figure 211: COSY NMR ($CDCl_3$, 298 K) of (R_{mp},$E_{co\text{-}c}$)-**S36**.

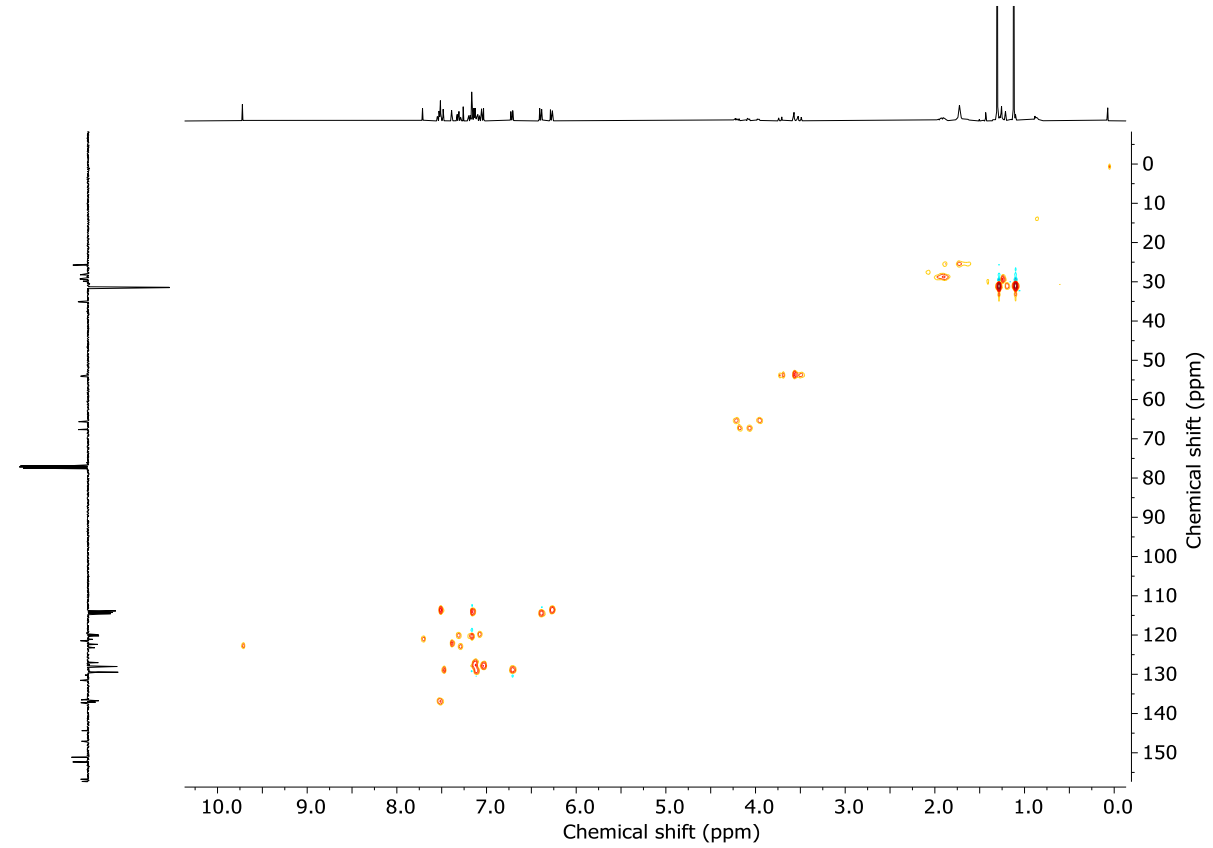

Figure 212: HSQC NMR ($CDCl_3$, 298 K) of (R_{mp},$E_{co\text{-}c}$)-**S36**.

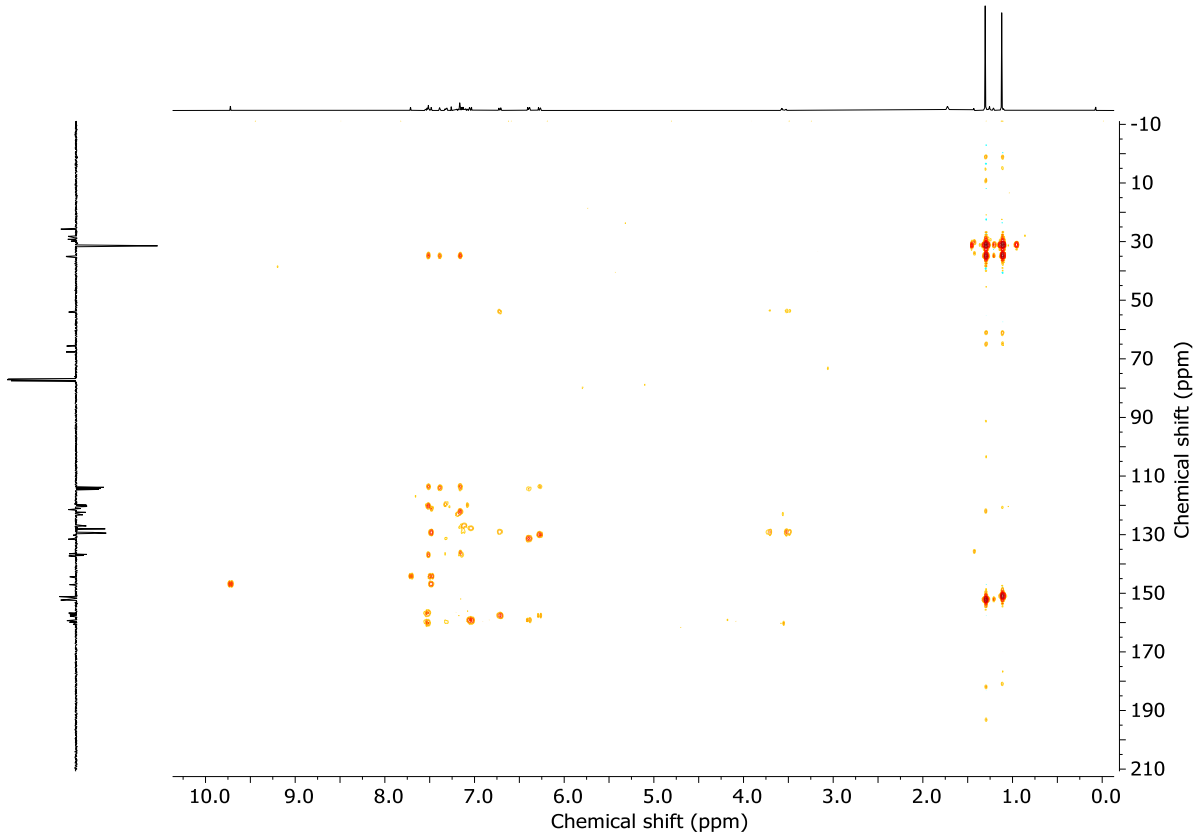

Figure 213: HMBC NMR ($CDCl_3$, 298 K) of (R_{mp},$E_{co\text{-}c}$)-**S36**.

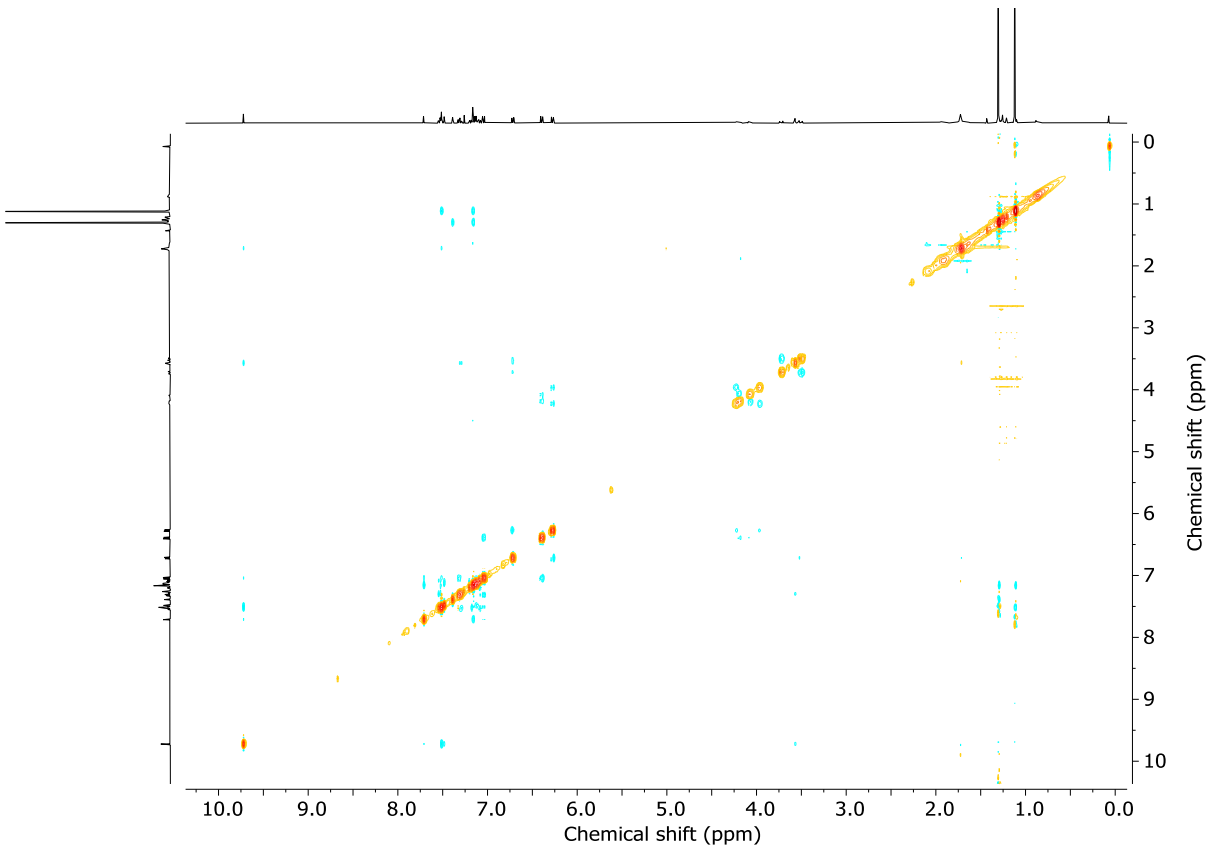

Figure 214: NOESY NMR ($CDCl_3$, 298 K) of (R_{mp},$E_{co\text{-}c}$)-**S36**.

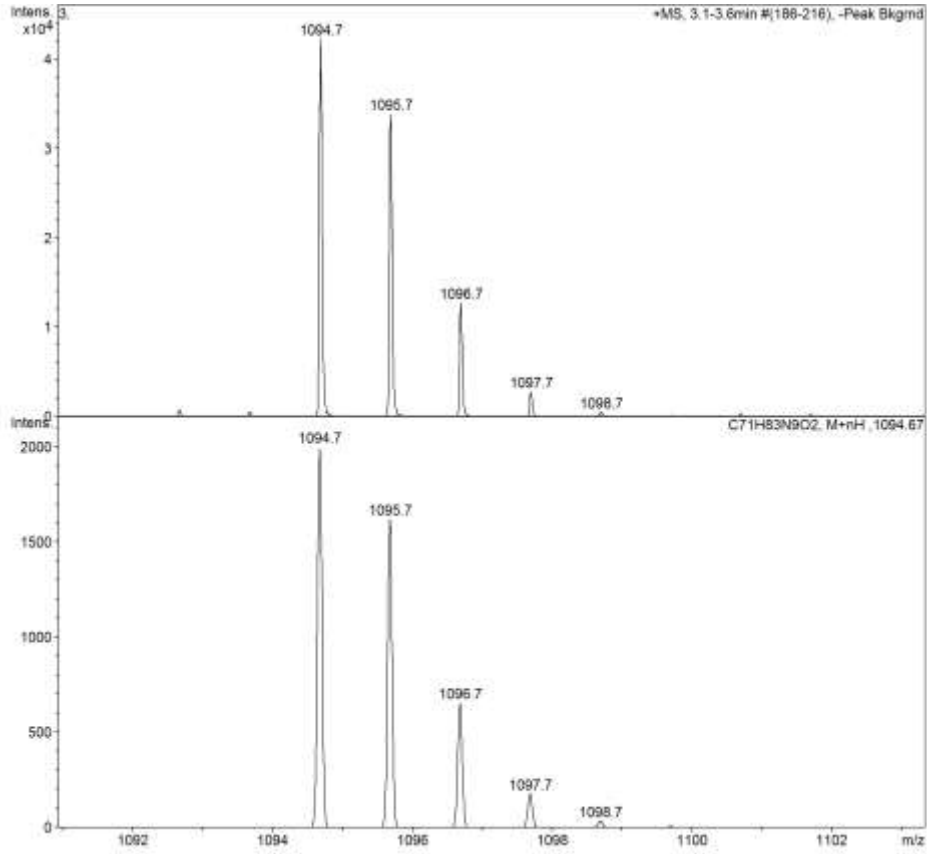

Figure 215: LRMS - Observed (top) and calculated (bottom) isotopic pattern for (R_{mp},$E_{co\text{-}c}$)-**S36** $C_{71}H_{83}N_9O_2$.

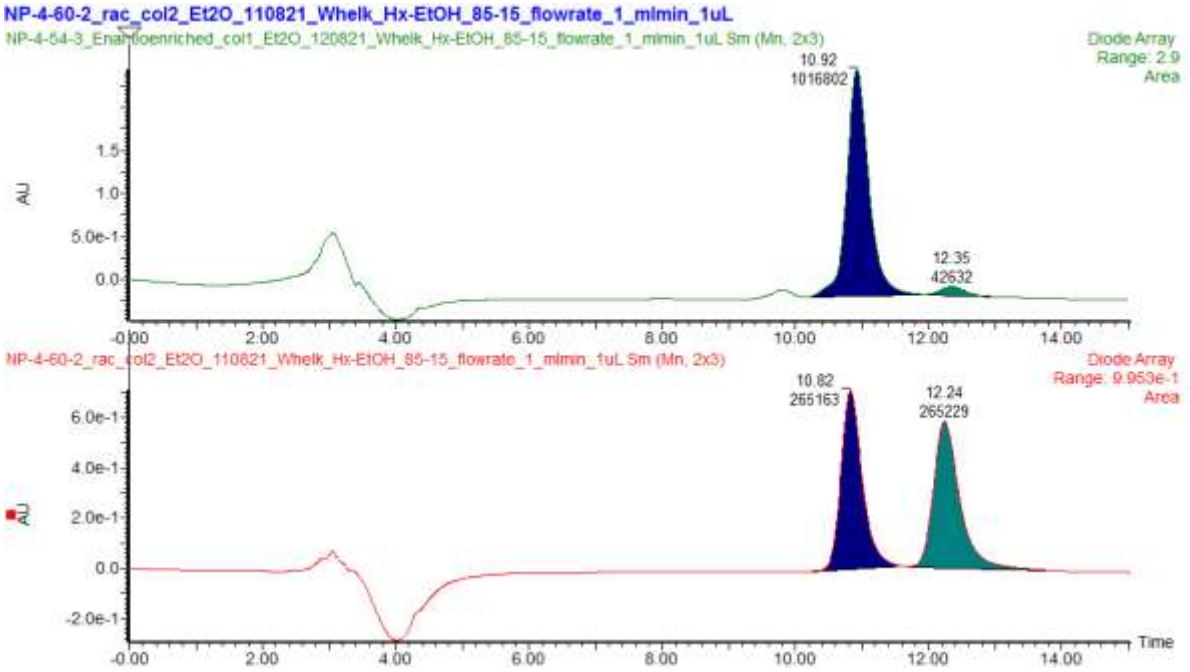

Figure 216: CSP-HPLC of **S36** (loaded in Et_2O). SSWhelk, ^{n}hexane-EtOH 85 : 15, flowrate 1 mLmin-1. (top) (R_{mp},$E_{co\text{-}c}$)-**S36** (10.92 min, 96.0%); (bottom) (*Rac*)-(R_{mp},$E_{co\text{-}c}$)-**S36:** (R_{mp},$E_{co\text{-}c}$)-**S36** (10.82 min, 50.0%), (S_{mp},$E_{co\text{-}c}$)-**S36** (12.24 min, 50.0%).

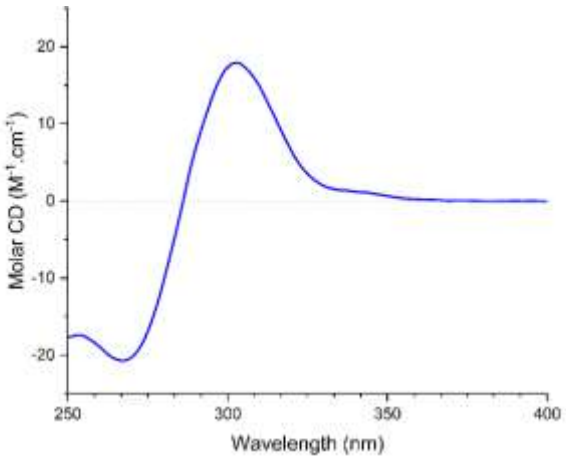

Figure 217: Circular dichroism spectra (26.7 µM in $CHCl_3$, 298 K) of (R_{mp},$E_{co\text{-}c}$)-**S36** (96 : 4 e.r.).

***rac*-(R_{mp},$E_{co\text{-}c}$)-S36**

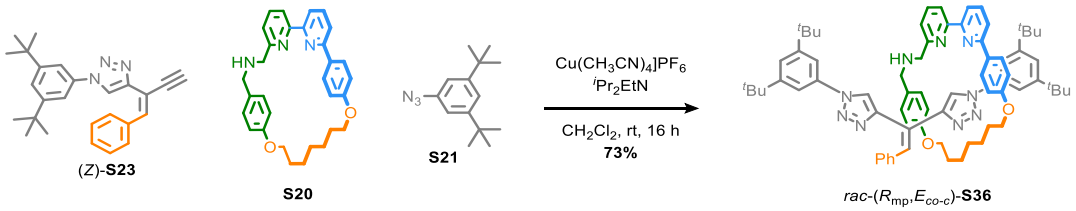

Macrocycle **S20** (18 mg, 0.037 mmol), alkyne (*Z*)-**S23** (15 mg, 0.039 mmol) and $[Cu(CH_3CN)_4]PF_6$ (13 mg, 0.034 mmol) were dissolved in CH_2Cl_2 (0.5 mL). Azide **S21** (10 mg, 0.043 mmol) was added as a solution in CH_2Cl_2 (1.0 mL), followed by N^iPr_2Et (31.0 µL, 0.178 mmol). The dark red solution was stirred overnight at rt then sat. EDTA-$NH_{3(aq.)}$ (2 mL) was added and the mixture stirred under air for 3 h. The reaction mixture was diluted with H_2O (20 mL), the phases separated and the aqueous layer extracted with CH_2Cl_2 (3 x 10 mL). The combined organic layers were dried (Na_2SO_4) and concentrated *in vacuo*. Chromatography (CH_2Cl_2-MeOH 100 : 0 to 9 : 1) gave *rac*-(R_{mp},$E_{co\text{-}c}$)-**S36** as pale yellow powder (29 mg, 73%). All analytical data (with the exception of CSP-HPLC) were identical to those obtained for (R_{mp},$E_{co\text{-}c}$)-**S36**.

8. Single Crystal X-ray Diffraction Analysis of Catenane *rac*-(*S*,S_{MP},$E_{co\text{-}c}$)-4 and Rotaxane S36

8.1. Catenane *rac*-(*S*,S_{mp},$E_{co\text{-}c}$)-4

Suitable single crystals of *rac*-(*S*,S_{mp},$E_{co\text{-}c}$)-**4** were grown by slow evaporation of a Et_2O solution in the fridge. Data were collected at 100 K using a Rigaku 007HF diffractometer with Arc)Sec VHF Varimax confocal mirrors, a UG2 goniometer and HyPix 6000HE detector. Cell determination, data collection, data reduction, cell refinement and absorption correction were performed with CrysAlisPro. The crystal structure was solved using Olex2[11] with SHELXT[12] dual methods and refined against F^2 with SHELXL[13] refinement package using anisotropic thermal displacement parameters for all non-hydrogen atoms. H atoms were placed in calculated position and refined using a riding model. Data Intensity fell off sharply at higher angles and so data were processed with a 0.88Å resolution limit.

Responses to A and B alerts raised by CheckCIF (also embedded in the CIF file):

PROBLEM (A alert): Solvent accessible void(s) in structure.

RESPONSE: The void was investigated but no significant electron density was found.

PROBLEM (B alert): The value of sine(theta_max)/wavelength is less than 0.575.

RESPONSE: The diffraction intensity fell off sharply with increasing resolution and so the max data resolution was cut to F^2/sigma F^2 > 2 during data processing.

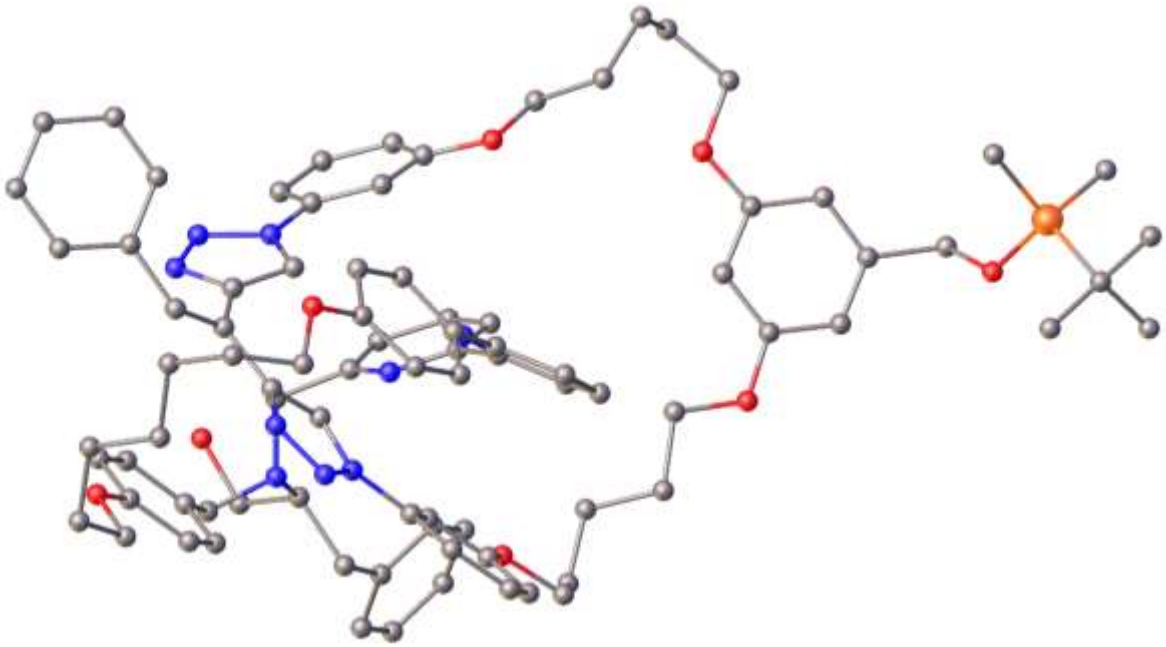

Figure S218: Solid state structure of catenane *rac*-(*S*,S_{mp},$E_{co\text{-}c}$)-4. shown as ball and stick mode with H-atoms omitted for clarity.

Compound	(S,S_{mp},$E_{co\text{-}c}$)-**4**
Empirical formula	$C_{87}H_{99}N_9O_8Si$
Formula weight	1426.84
Temperature/K	100(2)
Crystal system	trigonal
Space group	*R-3*
a/Å	56.6971(14)
b/Å	56.6971(14)
c/Å	12.7862(3)
α/°	90
β/°	90
γ/°	120
Volume/Å^3	35595.5(19)
Z	18
ρ_{calc}/g cm^{-3}	1.198
μ/mm^{-1}	0.751
F(000)	13716.0
Crystal size/mm^3	0.05 × 0.02 × 0.005
Radiation	CuK_α (λ = 1.54178)
2Θ range for data collection/°	5.400 to 122.278
Index ranges	-64 ≤ h ≤ 50, -64 ≤ k ≤ 64, -143 ≤ l ≤ 14
Reflections collected	47912
Independent reflections	12150 [Rint = 0.1147, Rsigma = 0.0795]
Data/restraints/parameters	12150/0/952
Goodness-of-fit on F^2	1.028
Final *R* indexes [I>=2σ (I)]	R_1 = 0.0683, wR_2 = 0.1668
Final *R* indexes [all data]	R_1 = 0.1218, wR_2 = 0.1980
Largest diff. peak/hole / e Å^{-3}	0.440/-0.550
CCDC Deposition Number	2207578

8.2. Crystals grown from *rac*-(*S*,R_{mp},$E_{co\text{-}c}$)-S34

Single crystals were grown by slow diffusion of ^{n}hexane into 9 : 1 CH_2Cl_2-MeOH solution of *rac*-(*S*,R_{mp},$E_{co\text{-}c}$)-**S34** at rt. Data were collected at 100 K using a Rigaku 007HF diffractometer with HF Varimax confocal mirrors, a UG2 goniometer and HyPix 6000HE detector. Cell determination, data collection, data reduction, cell refinement and absorption correction were performed with CrysAlisPro. The crystal structure was solved using Olex2[11] with SHELXT[12] dual methods and refined against F^2 with SHELXL[13] refinement package using anisotropic thermal displacement parameters for all non-hydrogen atoms. H atoms were placed in calculated position and refined using a riding model. Two tBu groups are disordered over two positions (ca.64:36 and ca. 62:38). Thermal restraints have been applied to all disorder components and 1,2 and 1,3 equal distance geometric restraints have been applied to all equivalent atom pairs of the disorder components. Solvent masking was applied to eliminate the electronic contribution equivalent to two solvent pentane per asymmetric unit.

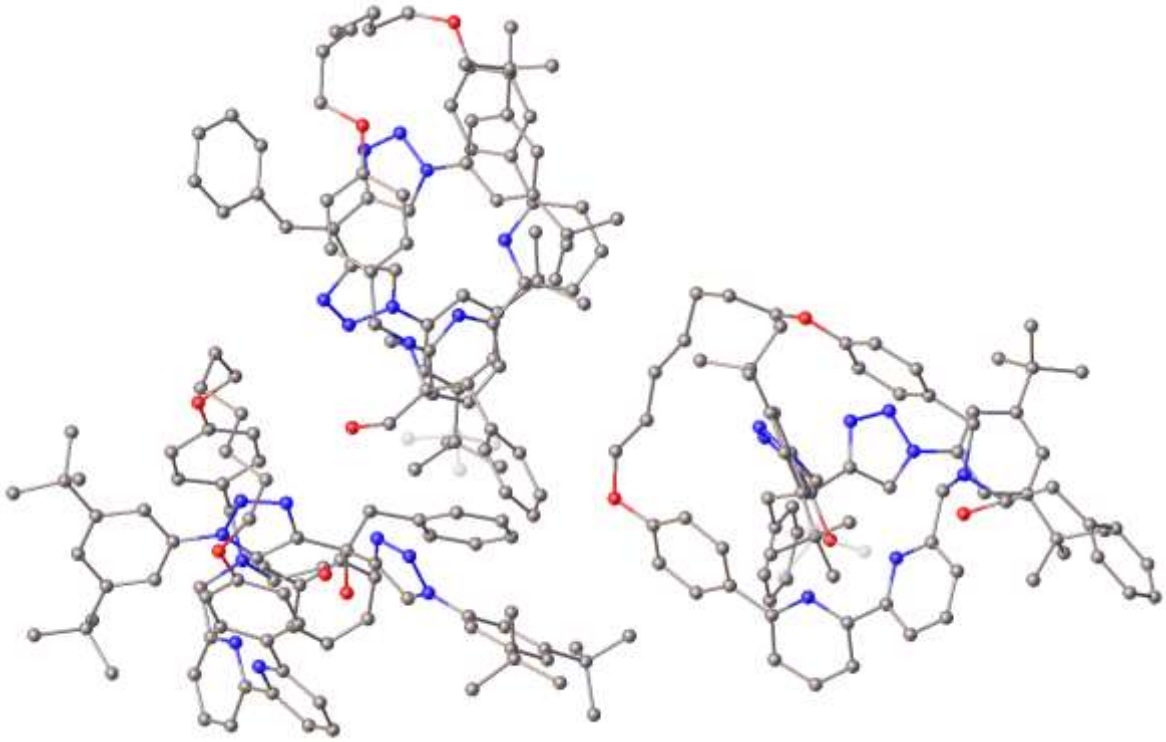

Figure S219: Solid state structure of the asymmetric unit obtained, shown as ball and stick mode with H-atoms and solvent pentane omitted and minor disorder components 'ghosted' for clarity.

The solid-state structure did not contain *rac*-(*S*,R_{mp},$E_{co\text{-}c}$)-**S34**. Instead, the asymmetric unit contains one molecule of (*S*,S_{mp},$Z_{co\text{-}c}$)-**S34**, the product of double bond isomerisation of (*S*,R_{mp},$E_{co\text{-}c}$)-**S34** (Figure S220, note that double bond isomerisation inverts both mechanical stereolabels), one molecule of (*S*,$R_{co\text{-}c}$,$S_{co\text{-}mp}$)-**S39**, the product of hydration of (*S*,R_{mp},$E_{co\text{-}c}$)-**S34** (Figure S221) and one molecule of (*R*,$S_{co\text{-}c}$,$R_{co\text{-}mp}$)-**S39**, the product of hydration of (*R*,S_{mp},$E_{co\text{-}c}$)-**S34** (Figure S222). The unit cell contains the enantiomeric structure, giving rise to a racemic crystal.

Responses to A and B alerts raised by CheckCIF (also embedded in the CIF file):

PROBLEM (B alert): Large reported max. (positive) residual density = 0.87 eA-3

RESPONSE: This arises due to unmodelled minor disorder of the macrocycle linker.

PROBLEM (B alert): Short inter D-H..H-D - H00N..H00S = 1.96.

RESPONSE: This arises from intra- and inter-molecular H-bonded hydroxyl groups of a single rotaxane of the structure which are geometrically close.

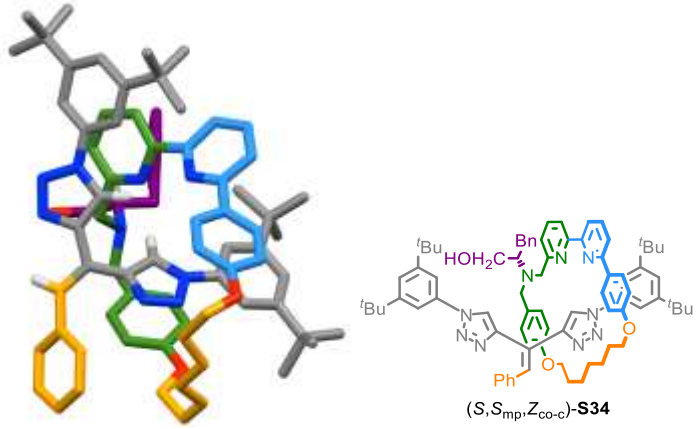

($S,S_{mp},Z_{co\text{-}c}$)-**S34**

Figure S220: The structure of ($S,S_{mp},Z_{co\text{-}c}$)-**S34** observed in the asymmetric unit.

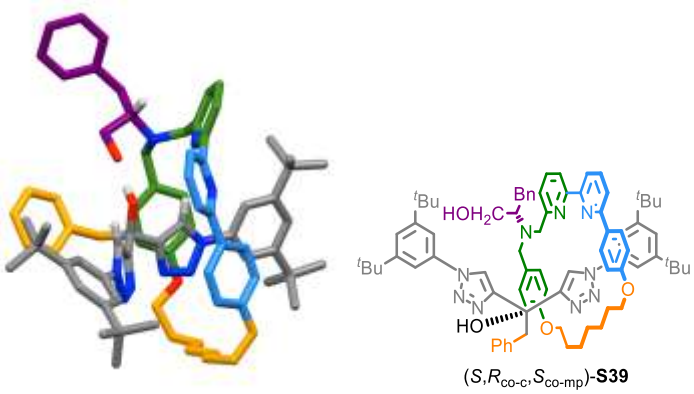

($S,R_{co\text{-}c},S_{co\text{-}mp}$)-**S39**

Figure S221: The structure of ($S,R_{co\text{-}c},S_{co\text{-}mp}$)-**S39** observed in the asymmetric unit.

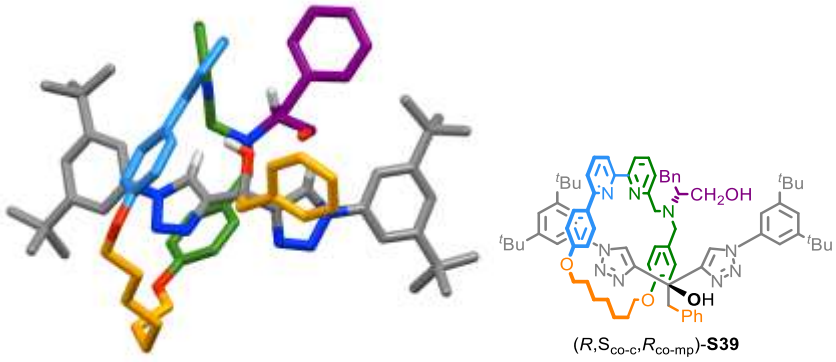

($R,S_{co\text{-}c},R_{co\text{-}mp}$)-**S39**

Figure S222: The structure of ($R,S_{co\text{-}c},R_{co\text{-}mp}$)-**S39** observed in the asymmetric unit.

Compound	*Rac*-(S_{mp},$E_{co\text{-}c}$)-S36
Empirical formula	$C_{264}H_{339}N_{27}O_{11}$
Formula weight	4066.60
Temperature/K	100(2)
Crystal system	Triclinic
Space group	*P*-1
a/Å	23.4801(3)
b/Å	23.6834(2)
c/Å	24.6001(3)
α/°	75.3860(10)
β/°	70.3060(10)
γ/°	67.9000(10)
Volume/Å^3	11809.2(3)
Z	2
ρ_{calc}/g cm^{-3}	1.144
μ/mm^{-1}	0.541
F(000)	4400.0
Crystal size/mm^3	0.25×0.20×0.15
Radiation	CuK_α (λ = 1.54178)
2Θ range for data collection/°	6.438 to 154.070
Index ranges	-29 ≤ h ≤ 29, -28 ≤ k ≤ 22, -30 ≤ l ≤ 30
Reflections collected	209037
Independent reflections	46453 [Rint = 0.0399, Rsigma = 0.024]
Data/restraints/parameters	46453/49/2727
Goodness-of-fit on F^2	1.015
Final *R* indexes [I>=2σ (I)]	R_1 = 0.0617, wR_2 = 0.1679
Final *R* indexes [all data]	R_1 = 0.0726, wR_2 = 0.1787
Largest diff. peak/hole / e Å^{-3}	0.874/-0.638
CCDC Deposition Number	2207579

9. PROPOSED METHOD FOR ASSIGNING STEREOCHEMISTRY OF THE MECHANICAL BOND.

Methods to assign the absolute stereochemistry of interlocked molecules are still in development. However, we have previously proposed methods[14] for the assignment of absolute stereochemistry in mechanically planar chiral catenanes and chiral rotaxanes by using Cahn-Ingold-Prelog-derived atom priorities to assign the orientation of the covalent subcomponents:

1) Following to the Cahn-Ingold-Prelog (CIP) rules, identify the highest priority atom on one ring and label it as "A"

2) Moving outward from A determine the highest priority atom (CIP) that can be used to define an orientation of the ring (typically a ligand of A) and label it as "B". The orientation of the ring is defined by the vector A → B, which, where relevant, passes through the intervening atoms (*i.e.*, follows the bonds).

3) Repeat the process on the second subcomponent to identity its orientation.

4) Orient the assembly with the A → B vector of the axle (rotaxanes) or either ring for (catenanes) passing through the cavity of the other ring away from the observer.

5) The direction of the A → B vector of the ring parallel to the plane of the observer defines the stereolabel: clockwise = R_{mp}, counterclockwise = S_{mp}. The "mp" subscript is included to indicate that the stereodescriptor refers to a mechanically planar stereogenic unit.

9.1. Catenane 3

Catenane **3** contains three stereogenic units which are fixed by the method of synthesis as shown (Figure 223a) and whose configuration could be determined by single crystal x-ray diffraction analysis of catenane **4** by making use of the known configuration of the fixed covalent stereogenic centre (Section 3).

The most obvious source of stereochemistry is the covalent stereogenic unit of the bipyridine macrocycle. Given that this is fixed in the starting material, (*S*)-**2** gives rise to catenane **3** which contains an *S*-configured covalent stereogenic centre. Less obvious (and more unusual) [15] is the co-conformational covalent geometric stereogenic unit. The double bond in triazole-containing macrocycle has no defined configuration when considered in isolation but in catenane **3** the position of the bipyridine macrocycle can desymmetrize the double bond, giving rise to co-conformational geometric isomerism. Catenane **3** is formed as a single geometric isomer as bipyridine ring is installed on one side of the double bond due to the structure of (*Z*)-**1** and it cannot move between the two triazole-containing compartments. However, a second isomer is technically possible (Figure 223b). As with co-conformational point stereochemistry,[16] we assign the geometry of the double bond in catenane **3** by considering the bipyridine macrocycle to be an additional substituent of the atoms in the compartment it encircles. Thus, the $E_{co\text{-}c}$ isomer is produced from (*Z*)-**1**, where the "co-c" subscript highlights that the configuration of this covalent stereogenic unit relies on the co-conformation of the molecule.

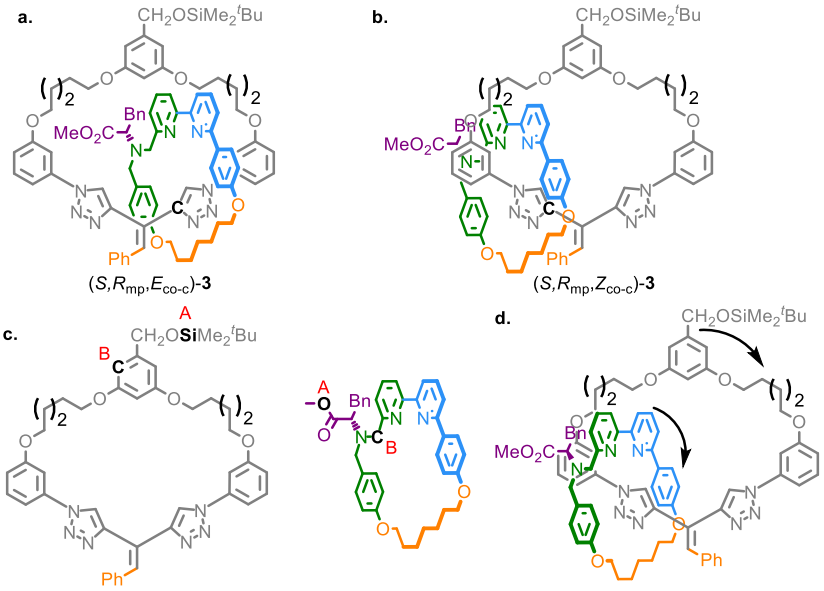

Figure 223: a. the structure of catenane (S,R_{mp},$E_{co\text{-}c}$)-**3** produced from the reaction of (Z)-**1** and (S)-**2** as depicted in the manuscript with the highest priority alkene substituent indicated in bold. b. The (S,R_{mp},$Z_{co\text{-}c}$)-**3** co-conformational covalent geometric isomer of **3** with the highest priority alkene substituent indicated in bold. c. The components of **3** with atoms A and B labelled. d. Catenane **3** redrawn such that the A→B vector of the bipyridine ring passes through the triazole ring away from the observer, confirming that the stereochemistry of **3** produced from (S)-**2** is R_{mp}.

To assign the mechanical planar stereogenic unit we apply the rules outlined above. This approach results in the atom priorities shown (Figure 223c). We note that the assignment of atom B in the triazole-containing ring is non-trivial. Exploring outwards from the Si atom (atom A), the first atoms that could allow us to assign direction in the macrocycle are the carbons *ortho* to the benzylic ether moiety. To differentiate between these two atoms, we explore outwards until we reach the quaternary triazole carbons. At this point we identify that, according to CIP, to differentiate between double bond substituents bonded to the same carbon we consider their relationship to the substituents on the other alkene carbon; the group that is arranged *cis* to the highest priority substituent of the other carbon is assigned a higher priority. Thus, the ortho C that leads to the triazole *cis* to the Ph substituent of the double bond is assigned higher priority, and so labelled as atom B. Finally, we orient catenane **3** so that the A→B vector of the bipyridine macrocycle passes through the triazole-containing macrocycle away from the observer (Figure 223d) and note that the A→B vector associated with the triazole-containing macrocycle is oriented in a clockwise direction, leading to the assignment of the mechanical planar stereogenic unit as R_{mp} (the subscript identifies the origin of the stereochemistry.

Thus, we can assign the configuration of catenane **3** produced by reaction of (Z)-**1** and (S)-**2** to be (S,R_{mp},$E_{co\text{-}c}$)-**3**.

9.2. Catenane 4

Based on the arguments presented above, (*S*,R_{mp},$E_{co\text{-}c}$)-**3** leads to a product (Figure 224a) with *S* covalent configuration and $E_{co\text{-}c}$ co-conformational configuration (neither are affected by the reduction of the ester). The mechanical planar stereogenic unit is assigned as above but reduction of the ester moiety of the bipyridine macrocycle leads to a change in atom priorities (Figure 224b) such that the A→B vector of the bipyridine macrocycle is inverted compared with catenane **3**. Thus, although the relative orientation of the triazole and bipyridine macrocycles is unchanged, when viewed with the A→B vector of the bipyridine ring passing through the triazole macrocycle away from the observer, the A→B vector of the triazole macrocycle is oriented in an anticlockwise direction (Figure 224c), resulting in an S_{mp} stereolabel. Thus, we can assign the configuration of catenane **4** produced from (*S*,R_{mp},$E_{co\text{-}c}$)-**3** to be (*S*,S_{mp},$E_{co\text{-}c}$)-**4**.

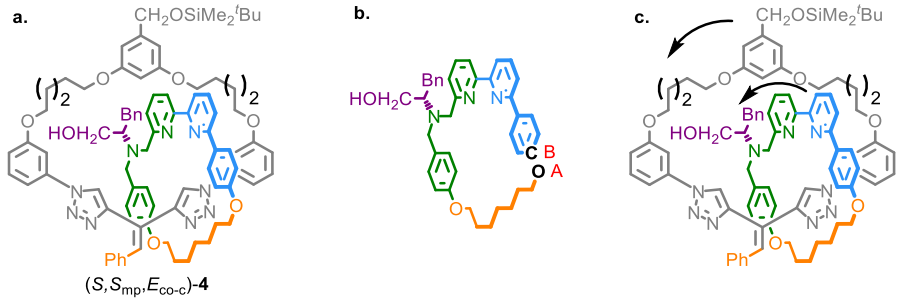

Figure 224: a. the structure of catenane (*S*,S_{mp},$E_{co\text{-}c}$)-**4** produced from (*S*)-**2** as depicted in the manuscript. b. The bipyridine macrocycle with atoms A and B labelled. d. Catenane **4** with the A→B vector of the bipyridine ring passing through the triazole ring away from the observer, confirming that the stereochemistry of **4** produced from (*S*)-**2** is S_{mp}.

9.1. Catenane S16

Catenane **S16** is assigned exactly as for catenane **4** (Figure 225). Thus, we can assign the configuration of catenane **S16** produced from (*S*,S_{mp},$E_{co\text{-}c}$)-**4** to be (*S*,S_{mp},$E_{co\text{-}c}$)-**S16**.

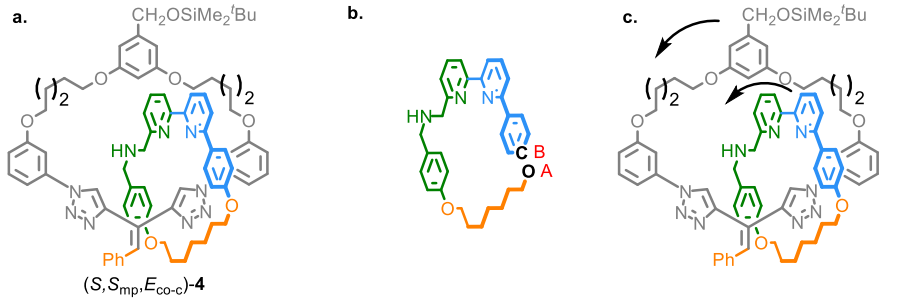

Figure 225: a. the structure of catenane (*S*,S_{mp},$E_{co\text{-}c}$)-**S16** produced from (*S*)-**2** as depicted in the manuscript. b. The bipyridine macrocycle with atoms A and B labelled. d. Catenane **S16** with the A→B vector of the bipyridine ring passing through the triazole ring away from the observer, confirming that the stereochemistry of **S16** produced from (*S*)-**2** is S_{mp}.

9.2. Catenane 5

Unlike catenanes **3** and **4**, the bipyridine macrocycle of catenane **5** can move between the two triazole containing compartments, giving rise to a dynamic mixture of $E_{co\text{-}c}$ (shown in Figure 226b) and $Z_{co\text{-}c}$ co-conformations (see section 5), whose double bond configuration is defined as described above. There is also no fixed covalent stereogenic unit. Thus, the only fixed stereogenic unit of catenane **5** arises due to the mechanical planar unit. Removal of the silyl group from the triazole-containing macrocycle results in a

change in atom priorities (Figure 226b). Using these atom priorities (Figure 226c), we can assign the product of (S,S_{mp},$E_{co\text{-}c}$)-**4** as (R_{mp})-**5** which preferentially adopts the (R_{mp},$E_{co\text{-}c}$)-**5** co-conformation (see section 5).

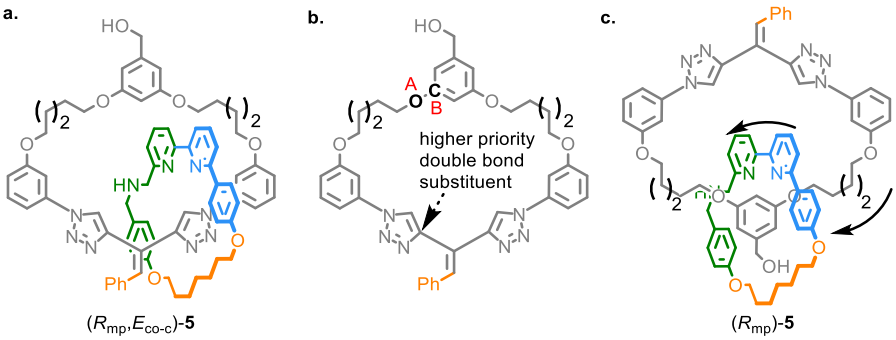

Figure 226: a. the structure of catenane (S,S_{mp},$E_{co\text{-}c}$)-**4** produced from (S)-**2** as depicted in the manuscript. b. The bipyridine macrocycle with atoms A and B labelled. d. Catenane **3** with the A→B vector of the bipyridine ring passing through the triazole ring away from the observer, confirming that the stereochemistry of **3** produced from (S)-**2** is S_{mp}.

9.3. Rotaxane S28

Rotaxane **S28** (Figure 227) contains a covalent stereogenic unit (the double bond) and the mechanical stereogenic unit that arises due to the relative orientation of the axle and macrocycle. It was synthesised as a racemate (hence referred to as *rac*-(E)-**S28** above) but we thought it would be useful to demonstrate its stereochemical assignment, particularly in light of the additional complications faced when assigning the stereochemistry of S29.

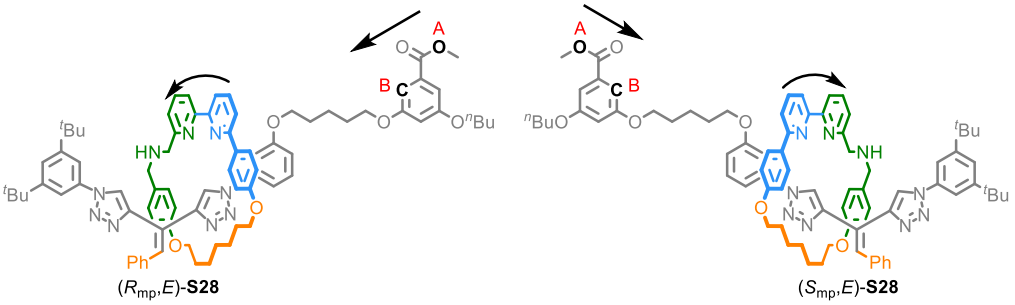

Figure 227: The structure of the enantiomers of rotaxane (E)-**S28** produced in equal quantities from **S20** including the axle atom labels and vectors used for stereochemical assignment.

9.4. Pseudo-rotaxane S29

Reduction of rotaxane **S28** (Figure 228) gives rise to pseudo-rotaxane **S29**, which slowly dethreads to give the corresponding non-interlocked components. Although **S29** is not mechanically interlocked, it is kinetically quite stable, requiring several days to completely dethread. Although **S29** is formed as racemic mixture, it would be helpful to be able to assign its stereochemistry. This can be done using the methods used for rotaxane **S29**, although it should be noted that, because **S29** is not permanently interlocked, the "mp" suffix, is not particularly appropriate and so we have prefixed the label with "co-" to indicate it depends on co-conformation.

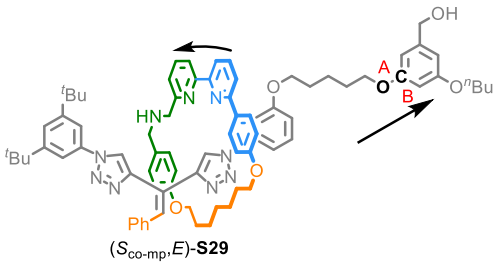

($S_{co\text{-}mp}$,E)-**S29**

Figure 228: The structure of pseudo-rotaxane (R_{mp},E)-**S29** produced from (R_{mp},E)-**S28** including the axle atom labels and vectors used for stereochemical assignment.

9.5. Rotaxane S33

Rotaxane **S33** (Figure 229) was synthesised using macrocycle (*S*)-**2** in high stereopurity. If we assume that the relative orientation of the azide and alkyne components of the axle and macrocycle are as in catenane **4**, and by taking note that the quaternary triazole C *cis* to the Ph group has higher priority than that *cis* to the H atom, we can assign the major stereoisomer as (S,S_{mp},$E_{co\text{-}c}$)-**S34**.

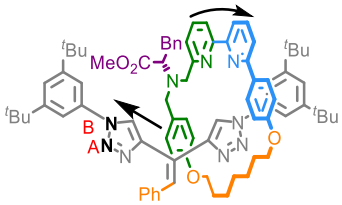

(S,S_{mp},$E_{co\text{-}c}$)-**S33**

Figure 229: The structure of rotaxane **S33** including the axle atom labels used for stereochemical assignment.

9.6. Rotaxane S34

Rotaxane **S34** (Figure 230) was produced by reduction of the ester moiety of rotaxane **S33**. This changes the atom priorities in the macrocycle, resulting in the product being assigned as (S,R_{mp},$E_{co\text{-}c}$)-**S34**.

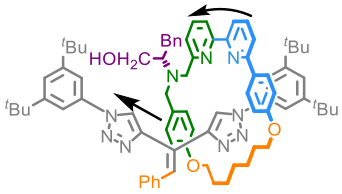

(S,R_{mp},$E_{co\text{-}c}$)-**S34**

Figure 230: The structure of rotaxane **S34** indicating the vectors used for stereochemical assignment.

9.7. Rotaxane S36

Removal of the auxiliary unit from **S34** to generate **S36** (Figure 231) does not change the atom priorities and thus (S,R_{mp},$E_{co\text{-}c}$)-**S34** is converted to (R_{mp},$E_{co\text{-}c}$)-**S36**.

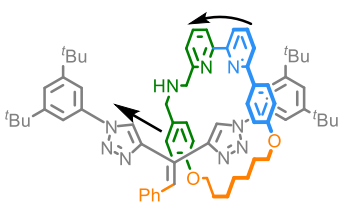

(R_{mp},$E_{co\text{-}c}$)-**S36**

Figure 231: The structure of rotaxane **S36** indicating the vectors used for stereochemical assignment.

9.8. Rotaxane S39

Hydration of the double bond of rotaxane **S34**, as observed during attempts to grow crystals for SCXRD analysis, removes the covalent orientation of the axle and so the mechanical planar chiral stereogenic unit is converted to a co-conformational mechanical planar chiral stereogenic unit in **S39** (i.e., the stereochemistry relies on the position of the macrocycle along the axle. For similar reasons, the hydration reaction introduces a co-conformational covalent stereogenic unit as the OH can be added to either face of the axle. Both are fixed due to the steric bulk of the benzyl group. To assign the axle orientation of **S39**, we consider the macrocycle as a substituent of all of the atoms in the compartment of the axle it occupies. This leads to the atom priorities shown, and thus the R_{mp} isomer of **S34** is converted stereospecifically to the $S_{co\text{-}mp}$ isomer of **S39**, whereas the co-conformational covalent stereogenic unit can be formed as either $R_{co\text{-}mp}$ or $S_{co\text{-}mp}$ (shown as undefined), depending on which face of the alkene the water approaches from.

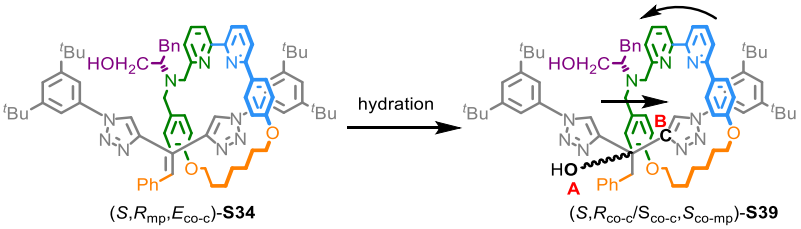

Figure 232: The structure of rotaxane **S39** indicating the vectors used for stereochemical assignment.

10. REFERENCES

1 Pigorsch, A. & Köckerling, M. The Crystallization of Extended Niobium-Cluster Framework Compounds: A Novel Approach Using Ionic Liquids. *Cryst. Growth Des.* **16**, 4240-4246 (2016).

2 Zhang, S., Rodríguez-Rubio, A., Saady, A., Tizzard, G. & Goldup, S. A Chiral Macrocycle for the Synthesis of Both Mechanically Planar Chiral Rotaxanes and Catenanes in Excellent Enantiopurity. ChemRxiv (2022). doi:10.26434/chemrxiv-2022-3f8zm This content is a preprint and has not been peer-reviewed.

3 Lopez, F., Castedo, L. & Mascarenas, J. L. Practical asymmetric approach to medium-sized carbocycles based on the combination of two ru-catalyzed transformations and a lewis Acid-induced cyclization. *Org. Lett.* **7**, 287-290 (2005).

4 Yamauchi, Y. *et al.* Ruthenium-catalyzed vinylic substitution reactions with nucleophiles via butatrienylidene intermediates. *J. Am. Chem. Soc.* **130**, 2908-2909 (2008).

5 Lewis, J. E. M., Modicom, F. & Goldup, S. M. Efficient Multicomponent Active Template Synthesis of Catenanes. *J. Am. Chem. Soc.* **140**, 4787-4791 (2018).

6 Zhu, J., Beugelmans, R., Bourdet, S., Chastanet, J. & Roussi, G. A Convergent Synthesis of 14-Membered F-O-G Ring Analogs of the Teicoplanin Binding Pocket via Intramolecular SNAr Reaction. *J. Org. Chem.* **60**, 6389-6396 (2002).

7 Juríček, M. *et al.* Triazole–pyridineligands: a novel approach to chromophoric iridium arrays. *J. Mater. Chem.* **21**, 2104-2111 (2011).

8 Heindl, S. *et al.* Chemoselective gamma-Oxidation of beta,gamma-Unsaturated Amides with TEMPO. *Angew. Chem. Int. Ed.* **60**, 19123-19127 (2021).

9 Alvarez, S. G. & Alvarez, M. T. A Practical Procedure for the Synthesis of Alkyl Azides at Ambient Temperature in Dimethyl Sulfoxide in High Purity and Yield. *Synthesis* **1997**, 413-414 (1997).

10 Post, E. A. J. & Fletcher, S. P. Controlling the Kinetics of Self-Reproducing Micelles by Catalyst Compartmentalization in a Biphasic System. *J. Org. Chem.* **84**, 2741-2755 (2019).

[11] Dolomanov, O. V., Bourhis, L. J., Gildea, R. J., Howard, J. A. K. & Puschmann, H. OLEX2: a complete structure solution, refinement and analysis program. *Journal of Applied Crystallography* **42**, 339-341 (2009).

[12] Sheldrick, G. M. SHELXT - integrated space-group and crystal-structure determination. *Acta. Cryst.* **A71**, 3-8 (2015).

[13] Sheldrick, G. M. Crystal structure refinement with SHELXL. *Acta. Cryst.* **C71**, 3-8 (2015).

14 Jamieson, E. M. G., Modicom, F. & Goldup, S. M. Chirality in rotaxanes and catenanes. *Chem. Soc. Rev.* **47**, 5266-5311 (2018).

15 Corra, S., de Vet, C., Baroncini, M., Credi, A. & Silvi, S. Stereodynamics of E/Z isomerization in rotaxanes through mechanical shuttling and covalent bond rotation. *Chem* **7**, 2137-2150 (2021).

16 Alvarez-Perez, M., Goldup, S. M., Leigh, D. A. & Slawin, A. M. A chemically-driven molecular information ratchet. *J. Am. Chem. Soc.* **130**, 1836-1838 (2008).